NB. Blank pages inserted for double sided printing

Gifford and Partners Ltd

Mersey Gateway - Phase II Modelling Study

Date: November 2005

Project Ref: R/3411/1

Report No: R.1151

ABP mer
marine environmental research

Gifford and Partners Ltd

New Mersey Crossing - Phase II Modelling Study

Date: November 2005

Project Ref: R/3411/1

Report No: R.1151

© ABP Marine Environmental Research Ltd

Version	Details of Change	Authorised By	Date
1	Draft for Comment	J M Harris	03/11/04
2	2nd Draft for Comment	J M Harris	08/03/05
3	Final	J M Harris	07/11/05

Document Authorisation		Signature	Date
Project Manager:	J M Harris	John Harris	7th Nov 2005
Quality Manager:	R H Swift	RH Swift	7 Nov 2005
Project Director:	W S Cooper	W. Cooper	7-11-5

ABP Marine Environmental Research Ltd
Suite B, Waterside House
Town Quay
SOUTHAMPTON
Hampshire
SO14 2AQ

Tel: +44(0)23 8071 1840
Fax: +44(0)23 8071 1841
Web: www.abpmer.co.uk
Email: enquires@abpmer.co.uk

INVESTOR IN PEOPLE

Summary

This report describes the numerical modelling study undertaken to investigate the preferred route option (Route 3A) for the proposed new bridge crossing over the Mersey Estuary. The preferred bridge layout is located a few kilometres upstream of Runcorn Gap. The modelling was carried out under Phase II of the Mersey Gateway Study and has involved building a high-resolution model. Under Phase I of the study a comparative modelling study of five route options was undertaken using a coarser grid model.

Under Phase II the initial model run investigated the original Route 3A alignment (Drawing No. B4027/2/B/361). Following this test a modified pier/tower alignment was tested (Drawing No. B4027/3/H/G/3). A further three bridge scheme options have also been tested. These additional runs correspond to the Route 3A medium span layout as shown in Drawing No. B4027/3/B/300, the Route 3A Short span layout as shown in Drawing No. B4027/3/B301 and the revised Route 3A medium 3 Tower layout as shown in Drawing No. B4027/3/B/300 Rev. A. For the modified medium span layout shown in drawings B4027/3/B/300 and B4027/3/B/300 Rev. A the number of towers have been reduced from 4 to 3 and pier alignments have been modified. Below are listed the model runs undertaken:

- Baseline:
  - Spring-neap cycle
  - High fluvial flow (1:200 year event) and spring tide
  - High fluvial (1:200 year event) and corresponding 1:200 year surge event.

- Route 3A Medium Span original alignment (Drawing No. B4027/2/B/361):
  - Spring-neap cycle

- Route 3A Medium Span modified alignment (Drawing No. B4027/3/H/G/3):
  - Spring-neap cycle
  - High fluvial flow (1:200 year event) and spring tide
  - High fluvial (1:200 year event) and corresponding 1:200 year surge event.

- Route 3A Medium Span 3 Tower alignment (Drawing No. B4027/3/B/300):
  - Spring-neap cycle

- Route 3A Medium Span Revised 3 Tower alignment (Drawing No. B4027/3/B/300 Rev. A):
  - Spring-neap cycle
  - High fluvial (1:200 year event) and corresponding 1:200 year surge event.
  - Recovery
  - 2005 bathymetry

- Route 3A Short Span (Drawing No. B4027/3/B/301):
  - Spring-neap cycle

The key hydrodynamic processes that have been investigated in this part of the study are water level, bed shear stress and velocity. In addition to this a morphological model has been run. The detailed hydrodynamic and morphological results are shown in Appendices C and D, respectively. Based on the results of the study the following key points have been made.

- The two schemes that show the least impact are the Route 3A Medium span Modified alignment and the Route 3A Medium 3 Tower revised alignment. Of these two schemes, the revised alignment for the Route 3A medium span 3 towers option shows the least impact in terms of extent of change across the upper estuary but a greater magnitude of change local to the tower structure in the north channel.

- The modelling has demonstrated that the careful placement of the bridge piers and towers outside of the existing channels may assist the performance in the short-term. However, in the long-term, movement of the position of the channels results in different patterns of change particularly local to the structures. However, the modelling suggests that for different channel configurations the impact of the proposed crossing will lead to no significant variation in change over those predicted to date from all the modelling undertaken in terms of the extent and magnitude of the change.

- Comparison of the Short Span scenario against the other scheme layouts shows the greatest impact in terms of sediment distribution within the upper Mersey Estuary. The short span leads to accelerated flows through the piers on the flood tide leading to increased erosion upstream of the proposed crossing. This implies that the bridge structures cause a restriction across the channel leading to a build up in the hydraulic head of water at the bridge (backwater effect) and this is observed in the water level results. It is recommended that this scheme is not progressed further.

- Based on the morphological modelling the immediate change as a result of placing the bridge structures within the channel dissipates after about a year and then the changes become insignificant as the system appears to reach a new equilibrium. The model results suggest that the system responds rapidly to the removal of the temporary structures and appears to be capable of returning to a condition predicted under normal water levels and fresh water discharges.

- For the Route 3A Medium span Modified alignment and the Route 3A Medium 3 Tower revised alignment the impact of the bridge during extreme events appears relatively small. Based on the scenarios undertaken, the impact of the extreme events appears to be far more significant than that of the disturbance caused by placing bridge towers within the estuary.

- It is considered that the bridge towers do not represent a significant blockage effect across the upper estuary and, therefore, should not lead to a detrimental change in the behaviour of the system. However, the upper estuary is highly dynamic and this has implications for scouring around the tower and pier structures. The use of scour countermeasures may require extensive coverage, which may in turn have a greater effect on channel movement than the structures themselves. Careful design of the structures and their foundations will be required and it is recommended that physical model tests be carried out at the design stage to assess scouring round the structures.

- Additional modelling (ABPmer, 2005) has demonstrated that the impact of the construction stage of the bridge is more significant on the hydrodynamics and morphology of the upper estuary than the operational phase.

Acknowledgements

We would like to thank Dr. John Ridgway, British Geological Survey, for supplying us with a copy of the sediment PSA dataset for the Mersey Estuary and Paul Williams, Environment Agency, for supplying us with bathymetric data for the Mersey Estuary.

Mersey Gateway - Phase II Modelling Study

Contents

Page

Summary i

Acknowledgements iv

1. Background 1

2. Physical Processes 2
   - 2.1 Introduction 2
   - 2.2 Tidal Flow 2
   - 2.3 Tidal Asymmetry 2
   - 2.4 Residual Circulation 4
   - 2.5 Fluvial Flow 5
   - 2.6 Seasonal Variations 6
   - 2.7 Sediment Transport 6

3. Modelling Results 10
   - 3.1 Previous Modelling - Phase I 11
   - 3.2 Detailed Modelling Phase II 12
     - 3.2.1 Introduction 12
     - 3.2.2 Water Level Changes 13
     - 3.2.3 Speed Changes 13
     - 3.2.4 Morphological Changes 19

4. Discussion 29

5. Conclusions 31

6. References 32

Appendices

A. Hydrodynamic Model
B. Fluvial Flows and Tidal Surges
C. Detailed Hydrodynamic Assessment
D. Morphological Modelling

Tables

1. Tidal height variation along the Mersey Estuary 2
2. Results of analysis of water surface distortion 3
3. Predicted return events 5
4. Construction works resulting in a reduction in tidal capacity of the Upper Estuary 8
5. Average yearly sediment influx in the Mersey Estuary 9
6. Summary of cross-sectional bed level changes for the various schemes. Description of changes compared against the existing 'baseline' condition 26
7. Summary of cross-sectional bed level changes for the extreme schemes. Description of changes compared against the existing condition (without bridge structures) 27
8. Summary of cross-sectional bed level changes for the Route 3A 3 Tower revised alignment for an extreme fluvial and surge event. Description of changes compared against the corresponding existing condition (without bridge structures) 27
9. Summary of cross-sectional bed level changes for the Route 3A 3 Tower revised alignment recovery scenario. Description of changes compared against the corresponding existing condition (without bridge structures) 28
10. Summary of cross-sectional bed level changes for the Route 3A 3 Tower revised alignment – 2005 bathymetry. Description of changes compared against the corresponding existing condition (without bridge structures) 28

Figures

1. Plan of the Mersey Estuary
2. Figure showing the bathymetry as derived from data collected by the Environment Agency, 2002
3. Figure showing the changes in water elevation along the Mersey Estuary (A) together with water levels and near-bed speed at Widnes for a spring and neap tide (B)
4. Positions of the navigation channel in the Inner Estuary from 1825 - 1880 (A) and 1881 -1900 (B). Figures reproduced from Cashin (1949)
5. Positions of the navigation channel in the Inner Estuary from 1901 - 1926 (A) and a figure showing the stability of the main channel from Hale Head to Runcorn Bridge between 1867 - 1936. Figures reproduced from Cashin (1949)
6. The difference in water level (m) between Route 3A Short Span revised and the baseline case around peak flood on a spring tide (A). Difference in near-surface speed (m/s) between the proposed bridge scheme Route 3A Medium and the baseline case peak flood (B) on a spring tide
7. Plot of bed shear stress across the study area showing the threshold of sediment motion for 150mm grain size over spring (A) and neap (B) tides
8. Bathymetry within the upper estuary; 2002 survey (A) 2005 survey (B)

9 Figure A shows locations of various positions in the study area. Figure B shows the near-surface speed at position (54,23) for baseline, extreme fluvial and extreme surge and fluvial events

10. Near-surface speed at positions (168,47) (A) and (246,118) (B) for baseline, extreme fluvial and extreme surge and fluvial events
11. Figure shows cross – Sections C and L for the existing condition and for extreme fluvial and combined extreme surge and fluvial events

1. Background

Halton Borough Council wishes to relieve the congestion at the existing road crossing, the Silver Jubilee Bridge, carrying the A557 across the Mersey at Runcorn, through the construction of a new bridge crossing over the estuary. ABP Marine Environmental Research Ltd. (ABPmer) was commissioned by Gifford & Partners on behalf of Halton Borough Council to carry out fieldwork and undertake a numerical modelling study. In Phase I of the study five possible route options were assessed, including different span designs. Eleven options were tested in total, excluding the baseline case (existing conditions). Under Phase II of the study, the preferred scheme was modelled in detail using a high resolution model scheme.

The Mersey Estuary is located in the north west of the UK. The outer estuary forms Liverpool Bay, a generally shallow region containing large areas of sandbanks that are exposed at low water. Liverpool Bay is bounded to the east by the Lancashire coast, from Seaforth to Formby Point; and to the south by the Wirral Peninsula, from Hilbre Point at the mouth of the Dee Estuary, to New Brighton at the mouth of the River Mersey. At New Brighton the width of the Mersey is 1.5km, approximately, and at Pier Head the river narrows to about half this width (Figure 1). Beyond the Narrows is a large tidal basin, classified as the inner estuary, which widens to a maximum width of about 5.5km. The upper estuary extends for a distance of about 42km from the Dingle to Howley Weir. At low water almost all the tidal basin dries out leaving three channels, Garston, Middle Deep and Eastham. In the area of the proposed new bridge crossing (Runcorn Gap - Fiddler's Ferry) the low-water channel meanders through large areas of sand and mud banks (Figure 2).

The Mersey has been classified as a coastal plain estuary formed during the Holocene transgression through the flooding of pre-existing valleys in both glaciated and unglaciated areas. Typical characteristics of such estuaries are large width to depth ratios (dependent on rock type), low river flows compared with the volume of the tidal prism and low fluvial sediment transport. The geological constraints that exist in the Mersey basin mean that the large width to depth ratio is not a characteristic of large parts of the estuary. McDowell (1964) described the tidal mouth of the Mersey as a tidal inlet since the inner basin between Hale Head and the Narrows was not formed by the action of the rivers that discharged into it.

The main report is divided into several sections. Section 2 of the report provides an overview of the main physical processes, which influence the estuary form based on previous studies. Section 3 summarises the main results from the numerical modelling study, which are discussed in more detail in the Appendices C and D. Section 4 presents a discussion of the findings and Section 5 the main conclusions from the study.

2. Physical Processes

2.1 Introduction

The form an estuary takes is influenced by a range of physical processes that operate over varying temporal and spatial scales. In terms of the morphology of an estuary, and in particular the sediment transport, the principal hydrodynamic forcing mechanisms are tidal flow, fluvial flow, waves and density driven circulation. In the present study, waves have been neglected due to the sheltered upstream position of the bridge crossing.

2.2 Tidal Flow

The Mersey Estuary is dominated by the tidal flows, being a macro-tidal estuary with variations in tidal elevation at the mouth of between 4 to 10m over the extremes of the neap-spring cycle. Maximum tidal currents through the narrows can exceed 3m/s (Halliwell and O'Connor, 1967). The M_2 semi-diurnal tide is the predominant tidal constituent.

Table 1. Tidal height variation along the Mersey Estuary

Place	Distance from Mouth (km)	Lat.	Long.	Height in m Above Chart Datum			
		N	W	MHWS	MHWN	MLWN	MLWS
Gladstone Dock	0	53°27'	3°01'	9.2	7.3	2.9	0.8
Liverpool (Alfred Dock)	4.5	53°24'	3°01'	9.3	7.4	2.9	0.9
Eastham	12	53°19'	2°57'	9.6	7.5	2.8	0.6
Hale Head	21	53°19'	2°48'	6.9	4.9	-	-
Widnes	26	53°21'	2°44'	5.1	3.0	0.4	0.6
Fiddlers Ferry	31	53°22'	2°39'	3.4	1.1	0.5	0.5

2.3 Tidal Asymmetry

As a tide propagates from the open ocean into shallow water it becomes distorted due to the non-linear growth of compound constituents and harmonics of the principal astronomical tidal components. Along the coastline of the UK the tides are dominated by the M_2 component, representing the semi-diurnal lunar tide. As a result of this M_2 dominance, the most significant overtide is the M_4 component. Friedrichs and Aubrey (1988) show that a direct measure of the non-linear distortion can be defined by the M_4 to M_2 water-surface amplitude ratio.

$$\frac{M_4}{M_2} = \frac{a_{M_4}}{a_{M_2}}$$

An undistorted tide has an M_4/M_2 amplitude ratio of zero. The water-surface phase of M_4 relative to M_2 is given by the expression:

$$2M_2 - M_4 = 2\theta_{M_2} - \theta_{M_4}$$

Assuming a linear relationship between M_4 and M_2, a flood-dominant system has a water-surface phase of 0°-180°. For an ebb-dominant system the surface phase is 180°-360°. Various hypotheses have been proposed to try and explain the existence of flood- and ebb-dominance in estuaries. In the absence of friction, flood dominance has been linked to the distortion of a non-reflected progressive wave (for example Dronkers, 1986). However, to provide a better explanation of flood dominance in shallow estuaries, friction must be included where non-linear frictional effects give rise to greater frictional damping in shallow water (Uncles, 1981).

Additionally, ebb dominance has been linked to inefficient water exchange around high water in estuaries with relatively deep channels and extensive intertidal water storage (Speer and Aubrey, 1985).

Table 2. Results of analysis of water surface distortion

Location	Ratio	Hydrographer of the Navy *			Model
		(1980)	(2000)	(2002)	(2002) Bathymetry
Liverpool (Alfred Dock)	M_4/M_2	0.069	0.062	0.059	0.074
	Relative water-surface phase	72	68	69	67
Eastham	M_4/M_2	0.077	0.075	0.075	0.080
	Relative water-surface phase	70	65	65	63
Widnes	M_4/M_2	-	-	-	0.516
	Relative water-surface phase	-	-	-	26
Fiddlers' Ferry	M_4/M_2	-	-	-	0.613
	Relative water-surface phase	-	-	-	21
* Note that the years correspond to the prediction periods not the publication dates (1979; 1999; 2001)					

In order to assess the flood or ebb dominance of the Mersey Estuary, tidal constituents published by the Hydrographer of the Navy (1979; 1999; 2001) were used to determine the water-surface amplitude and relative water-surface phase at Liverpool (Alfred Dock) and Eastham. In addition, harmonic analysis was undertaken on time-series of water level at several stations within the numerical model. From the harmonic analysis, the principal astronomical components were obtained for each station and used to assess the flood/ebb dominance along the estuary.

From the analysis of tidal currents it is evident that the Mersey Estuary is flood dominant. This can also be deduced from looking at the shape of the tidal curve along the estuary (Figure 3A). On a spring tide, the flood tide at Alfred Dock (Mersey Narrows) lasts about 5.5 hours, whilst the ebb tide has a duration of 7 hours, approximately. Assuming conservation of mass, the implication is that the same volume of water flows into the estuary over a shorter period, with higher velocities on the flood than the ebb tide, and that the Narrows is flood dominant. This agrees with previous studies, although there is evidence of the flood asymmetry reducing over time (Gifford & Partners, 2004).

In the upper estuary tidal asymmetry is clearly evident and the flood dominance can be clearly seen in the tidal curve at the various water level stations. At Widnes on a spring tide, the flood period lasts for about 2 hours, whilst the ebb lasts around 10 hours. Figure 3B shows a comparison of a typical spring and neap tide at Widnes together with the corresponding near-surface velocities. The observed lower low waters in the neap tides, in comparison with the spring tides, are considered to be due to the drainage capacity of the upper estuary. The result of this effect is an increase in mean water depth over the spring tidal cycle as a result of tidal pumping (see Section 2.4). At Fiddler's Ferry, the tidal curve shows the tide to be depth-limited at this location since both the spring and neap tides have the same low water positions.

2.4 Residual Circulation

Tidal currents are driven by water elevation changes and thus the same basic constituents that can be derived for water levels can be found in the analysis of long time-series of tidal current, although the amplitudes and phases will differ from those of the water elevations. Superimposed on the 'back-and-forth' tidal flow is a net, steady circulation, generally referred to as the residual circulation. This residual flow is obtained by averaging the velocity at each point in the estuary over a tidal cycle. However, the definition is somewhat vague since no tidal cycle is identical to the one preceding or following it. Therefore, the residual velocity field is in fact a slowly varying and poorly defined quantity.

In large estuaries one of the causes of the residual circulation is due to the Coriolis effect (the rotation of the Earth). Another cause is the interaction of the tidal flow with the bathymetry. This form of circulation is sometimes referred to as tidal pumping to differentiate it from other forms of residuals, such as freshwater run-off. Therefore, it should be remembered that this residual circulation is additional to any circulation driven by the wind, waves or density-driven flows.

Density gradients through the water column can have a significant impact on local net movement of water. Price and Kendrick (1963) built a physical model of the Mersey Estuary. Field measurements had demonstrated that there was a net landward movement of water near the channel bed whilst near to the surface the movement was seaward. Price and Kendrick only reproduced this effect in the model when they used

both fresh and saline waters. Additionally, Heaps (1972) showed that small density gradients found in the near-shore regions contribute to the net landward drift of near-bed water and sediment in Liverpool Bay.

Within the current modelling study vertical density differences have been ignored. This is based on previous modelling (ABPmer, 2003a), which suggested that in the upper estuary tidal residuals were dominated by geometric effects rather than density effects.

2.5 Fluvial Flow

Analysis of flow data from 6 gauging stations has been undertaken to assess return period flows into the Mersey Estuary. The records used correspond to the following stations:

- River Mersey at Irlam Weir
- River Mersey at Westy
- River Weaver at Pickerings Cut
- Sankey Brook at Causey Bridge
- Ditton Brook at Greens Bridge
- River Gowy at Picton

The flow data was obtained from the Environment Agency and the National Flow Archive.

A Gumbel distribution was used to determine return period flows for each station based on the annual maxima method (see Appendix B). From this analysis the values in Table 3 were obtained.

Table 3. Predicted return events

Location	Discharge (m^3/s)		
	1: 1	1: 200	1: 500
River Mersey (Irlam)	43.6	275.1	306.2
River Mersey (Westy)	94.9	228.9	246.9
River Weaver	32.6	239.5	267.4
Sankey Brook	7.6	46.1	51.2
Ditton Brook	2.9	19.9	22.1
River Gowy	2.9	30.0	33.6

The principal sources of freshwater into the Mersey, enter at Howley Weir (18.8m^3/s modal flow) and via the Manchester Ship Canal at the Weaver Sluices and at Eastham Locks in addition to various other minor tributaries (combined modal flow 15.2 m^3/s).

There can be a considerable variation in the freshwater flow into the Mersey. Prandle *et al.* (1990) calculate a mean flow ratio of 0.01, approximately. The ratio is calculated as (the freshwater flow x 12.42 hours)/(volume between high and low water). Flow ratios of less than 0.1 generally indicate a well-mixed estuary. However, over certain parts of the tidal cycle there are sections of the Mersey Estuary that are only partially-mixed. This may be as a result of the narrow entrance channel that opens up into a wide and shallow upper basin (Prandle *et al.*, 1990).

2.6 Seasonal Variations

Seasonal variations will affect various aspects of the physical processes in an estuary. Freshwater flows from the rivers will vary over a year. For example, in the summer period the amount of freshwater entering the estuary is usually reduced. This in turn will affect the density circulation.

Increases in temperature will lead to a reduction in the water viscosity and this will give rise to an increased rate of settling of sediment particles carried in suspension. Halliwell and O'Connor (1967) noted that a reduction in viscosity over the summer increases the flocculation of fine material, thus reducing any buoyancy effect that the fine sediment provides for the coarser fraction. Therefore, this implies that an increase in the settling rate will lead to increased sedimentation and allow for longer time for sediment to consolidate and, therefore, estuary deposits will have a greater shear strength.

Halliwell and O'Connor (1967) demonstrated this seasonal change for sediments in the Mersey, finding less material in suspension in the summer period than during the winter period.

Seasonal changes are observed in both the physical and biological conditions and this in turn will impact on sediment transport. ABPmer (2003a) reported on survey measurements of critical erosion threshold values across the study area. The results demonstrated the increase in critical threshold values when microalgae are present.

2.7 Sediment Transport

The Mersey Estuary is classified as a flood dominated system, i.e. there is a net movement of material into the estuary on the flood tide. As discussed in the section on residual currents this is, in part, due to the unique tidal signature. The existing bed sediment distribution within the Mersey has been classified by the British Geological Survey (BGS). In general their findings were:

- From Gladstone Docks to Albert Dock, the southern half of the Narrows is classified as being rock.

- With the exception of the estuary margins, the inner section of the estuary up to Runcorn, has been classified as being predominately sand interspersed with a small patch of gravely sand.

- The margins of the inner estuary up to Hale Head are a mix of sandy mud and mud.

- The upper sections are comprised of sand and mud deposits.

It is essential to identify the current morphological status of a river or estuary to enable a prediction of how any future development will impact upon the morphology. Morphological impacts are known to spread both upstream and downstream from the point of disturbance due to the process feedback mechanisms that operate within a fluvial/estuarine system. Of key importance to evaluating the future response of such a system is the understanding of how it responded to past alterations, both natural and manmade.

In the present study to assess the hydrodynamic and morphological impact of a new bridge crossing in the upper reaches of the Mersey Estuary the adopted approach has used both historical changes to the estuary as well as state-of-the-art numerical models to form an understanding of the likely changes. The following section describes the historical changes within the estuary and assesses their impact on the system as a whole as well as local to the scheme.

Changes in the tidal capacity of the Mersey Estuary can be generalized to be the result of three main causes:

(1) Natural changes due to erosion and accretion.
(2) Dredging.
(3) Construction.

The latter two causes could be classified under one heading as anthropogenic changes, but for current purposes they will be kept separate.

Cashin (1949) identified losses in tidal capacity as a result of engineering works (Table 4). From Table 4 it is seen that construction works in the Upper Estuary have accounted for a reduction in tidal capacity of 11.3 million cubic metres since 1861.

Price and Kendrick (1963) undertook a detailed investigation into the reasons for siltation in the Mersey Estuary. They looked at the contribution that the training works, low-water channel movements and dredging had exerted on siltation in the upper estuary. They identified the importance of the meandering of the low-water channels in the erosional processes in the Mersey, providing the mechanism by which accumulations of silt are kept under control and thus preventing a progressive deterioration in the tidal capacity.

Table 4. Construction works resulting in a reduction in tidal capacity of the Upper Estuary

Works	Date	Loss (x 10^6 m^3)
Manchester Ship Canal and	1887 - 1896	3.2
River Weaver diversion		2.0
Reclamation of Tranmere foreshore	1901 - 1906	1.4
Dingle embankment	1906 - 1931	1.5
Otterspool Promenade	1926 - 1931	2.8
Bromborough Dock	1921 - 1931	
Alterations to river walls and entrances		0.4

(Source: Cashin, 1949)

To a large extent this is the key morphological issue with regards to the placement of bridge piers within the upper estuary. Will the siting of such structures within the estuary inhibit the natural movement of the low water channels? From historical evidence it is possible to develop a picture of past channel movement and its response to anthropogenic impact.

In Cashin's (1949) paper he presents a series of figures showing the position of the navigation channel in the Inner Estuary from 1825 - 1926 (Figures 4 and 5). Whilst these figures do not cover the study area directly, they do reveal some potentially relevant patterns. Prior to the construction of the Manchester Ship Canal the navigation channel is seen to oscillate over the whole width of the estuary moving across both Ince and Frodsham banks. However, after the late 1880's the movement of the navigation channel becomes more restricted and is confined more to the northern side between Speke and Hale. In addition, the River Weaver diversion scheme, the construction of an embankment on the north side of the estuary and the construction of the bridge piers for the Runcorn transporter bridge (completed in about 1902) result in the navigation channel stabilizing and becoming 'locked' onto the north side of the estuary between Hale and Runcorn. It is not clear which of these had the greatest impact, however, the combined effect is to restrict the movement of the channel through the Runcorn Gap. It is considered that this effect is key in understanding the behaviour of the low water channels upstream of Runcorn.

Between 1932 and 1937 the Water Pollution Research Laboratory undertook an analysis of the low water channel movements. Based on this analysis it was concluded that the extent of the movement of the low water channel between Hale Head and Eastham was decreasing leading to a loss in the capacity of the upper estuary and an associated stabilization in the reach immediately upstream.

O'Connor (1987) undertook an assessment of both the short- and long-term changes in estuary capacity in the Mersey. He demonstrated that the principal source of sediment into the estuary was from sea and coastal sources in Liverpool Bay. This corresponded with the earlier study of Price and Kendrick (1963) who identified that the major source of material entering the Mersey was from Liverpool Bay and not from the

rivers or incoming solid sewage. O'Connor also suggested that the estuary did not appear to be in a state of dynamic equilibrium, although changes in the capacity were smaller in magnitude prior to 1906. This is in contrast to Price and Kendrick who considered that around 1900 the Mersey Estuary was in long-term equilibrium.

Halliwell and O'Connor (1968) and Al-Muttair (1974; cited O'Connor, 1987) used field measurements of sediment fluxes and detailed dredging information combined with hydrographic survey information for the period 1955 - 1965 to estimate values of the yearly sediment influx and capacity. In terms of the influx of material into the system the table below shows the estimated yearly values.

Table 5. Average yearly sediment influx in the Mersey Estuary

Item	Average Yearly Sediment Influx (Mm^3/year)
Sand influx, S_n (no dredging influence)	1.85
Silt influx, SS_n (no dredging influence)	2.43
River influx, S_r (fine silt/clay)	0.04

Based on these values it is clear that the sediment influx from the rivers represents only about 1% of the total sediment entering the system. Even within the study area the likely main source of sediment will be marine derived.

Construction of the training walls in Liverpool Bay were started in 1901 to fix the position of the main navigation channel to the Port of Liverpool. The outcome of this change was to suppress channel meandering, confining more of the ebb tide to the trained channel and leading to a strengthening of the flood tide along the Lancashire and North Wirral coastlines. Enhancement of the flood tide would have contributed to an increase in siltation in both the trained navigation channel and the estuary itself. On this basis, Price and Kendrick suggested that where meandering in the estuary is suppressed there is a resulting loss in volume. However, Inglis (1964) pointed out that channel stabilization only caused deterioration if it led to a loss of flow energy. In the case of the upper estuary the width far exceeded that required to provide an adequate meander belt. The regimen of the upper estuary was determined by the overall energy of the flow and the sediment entering through the Narrows.

The process of meandering of tidal channels is a relatively poorly studied subject despite the fact that meandering is a common feature of tidal environments. Solari *et al.* (2002) report that recent observational evidence suggests that meander wavelength scales with channel width, which would also imply that the process of meander formation must arise from the effect of secondary flows driven by some planimetric instability similar to that observed in rivers.

The construction of the Manchester Ship Canal and the diversion of the River Weaver may have brought about a reduction in the flushing capacity of the rivers causing a landward movement of the estuary's gravitational circulation to occur. Sediment trapping due to the gravitational circulation would have caused a permanent loss in estuary capacity (Price and Kendrick, 1963; O'Connor, 1987).

O'Connor (1987) suggested that the Mersey Estuary was over-deepened and over-widened in the last 10-20,000 years as a result of glacial and tidal action. In the absence of engineering works, the estuary capacity would probably have reduced at a relatively slow rate. However, the result of the engineering works has been to greatly accelerate this process.

The relative importance of the different sediment sources in an estuary can be represented in the form of a sediment balance. Dyer (1972) noted that there had been a 10% reduction over the last hundred years in the volume of the Mersey Estuary despite the significant amount of dredging undertaken (> 306 x 10^6 m^3 of material).

Pye and Van der Wal (2000) assessed the morphological change in the Mersey Estuary based on digitised charts for the years 1900, 1950 and 1980. From their sediment volume calculations they showed that in the outer estuary the total sediment volume increased between 1900 and 1950, although the intertidal sediment volume showed a decrease. In the inner estuary, during this period, both the total sediment volume and the intertidal sediment volume increased. Between 1950 and 1980 the total sediment volume in the outer estuary was maintained while the intertidal volume continued to decrease. During the same period in the inner estuary the total sediment volume was maintained. However, Pye and Van der Wal (2000) point to evidence that suggests that during the last few decades erosion has been taking place in the inner estuary.

Thomas (1999) also noted an infilling of the Mersey Estuary over the period 1936-1956 with erosion occurring between 1977-1997. Thomas highlights the broad divisions between the various sections of the estuary (Narrows; inner and upper) and suggests that morphological changes in the upper estuary may be due more to freshwater inputs than tidal influences.

3. Modelling Results

A detailed description of the numerical modelling results is presented in Appendices C and D. The aim of the Phase II study was to investigate the preferred Route 3A option in more detail. In order to undertake this work, two higher resolution models were constructed. The set up for the model grids and the calibration and validation of these models is described in Appendix A. The results of the calibration and validation exercise have shown the models to be capable of providing a good representation of the water levels and currents across the whole region of each model.

The main concerns to be addressed in the modelling study can be summarized within the following topics:

- Flood defence and intertidal habitats
- Channel morphology
- Scouring around bridge piers
- Potential impacts on the SSSI site downstream of Runcorn
- Potential impact on existing structures, in particular the Manchester Ship Canal

The use of two models was necessary to enable the morphological modelling calculations for longer-term changes to be undertaken within a reasonable time-scale. The hydrodynamic model set up is computationally intensive with calculations taking the order of weeks to run a simulation over a spring-neap cycle. Such time-scales are not practical for the morphological runs, particularly as the introduction of sediment into the hydrodynamics extends model run times.

The bridge piers and towers in the two models have been simulated using a combination of approaches. In general, where bridge piers and towers are the same size as the model grid cells the cells have been closed off as they are effectively blocked for the transmission of fluid flow. However, where the bridge piers are smaller than the grid cell size added friction terms have been used to represent the piers. In this manner there is an allowance for some flow transmission across the cell, even if that flow is low. Whilst the piers and towers are octagonal in shape their representation in the model when represented as solid structures is as squares. However, it is not considered that pier shape will have a significant impact on the results as flow separation and viscous effects are excluded from the model solution and only flow transmission effects as a result of blockage are simulated.

3.1 Previous Modelling - Phase I

Within the previous modelling study undertaken for Phase I a coarse grid model was used to provide a comparative assessment of several scheme options. The Route 3A scheme simulations were undertaken for short and medium span options and Table 3.1 summarizes the maximum and minimum differences obtained from the hydrodynamic simulations for the Route 3A option.

Whilst the general changes are of similar order the localized differences observed in the detailed modelling are not. This is due, primarily, to the representation of the structures in the model and the grid size (ABPmer, 2003b).

3.2 Detailed Modelling Phase II

3.2.1 Introduction

The detailed modelling has concentrated on investigating the impact of the Route 3A bridge alignment. The initial model run investigated the original Route 3A alignment (Drawing No. B4027/2/B/361). Following this test a modified pier/tower alignment was tested (Drawing No. B4027/3/H/G/3). A further three bridge scheme options have been tested. These additional runs correspond to the Route 3A medium span layout as shown in Drawing No. B4027/3/B/300, the Route 3A Short span layout as shown in Drawing No. B4027/3/B301 and the revised Route 3A medium 3 Tower layout as shown in Drawing No. B4027/3/B/300 Rev. A. For the modified medium span layout shown in drawings B4027/3/B/300 and B4027/3/B/300 Rev. A the number of towers have been reduced from 4 to 3 and pier alignments have been modified. Below are listed the model runs undertaken:

- Baseline:
  - Spring-neap cycle
  - High fluvial flow (1:200 year event) and spring tide
  - High fluvial (1:200 year event) and corresponding 1:200 year surge event.

- Route 3A Medium Span original alignment (Drawing No. B4027/2/B/361):
  - Spring-neap cycle

- Route 3A Medium Span modified alignment (Drawing No. B4027/3/H/G/3):
  - Spring-neap cycle
  - High fluvial flow (1:200 year event) and spring tide
  - High fluvial (1:200 year event) and corresponding 1:200 year surge event.

- Route 3A Medium Span 3 Tower alignment (Drawing No. B4027/3/B/300):
  - Spring-neap cycle

- Route 3A Medium Span Revised 3 Tower alignment (Drawing No. B4027/3/B/300 Rev. A):
  - Spring-neap cycle
  - High fluvial (1:200 year event) and corresponding 1:200 year surge event.
  - Recovery (morphology only)
  - 2005 bathymetry (morphology only)

- Route 3A Short Span (Drawing No. B4027/3/B/301):
  - Spring-neap cycle

The key hydrodynamic processes that have been investigated in this part of the study are water level, bed shear stress and velocity. Results have been presented as changes relative to a baseline case. The bed shear stress is the frictional force exerted on an area of seabed or riverbed by current flowing over it. Therefore, it is an important quantity in the study of sediment transport processes, because it represents the flow-induced force acting on the bed sediments. The detailed hydrodynamic and morphological results are shown in Appendices C and D, respectively.

3.2.2 Water Level Changes

Changes in water level can impact on the ability of the estuary to discharge flood waters effectively, may have implications for quay/river wall stability and may also affect intertidal habitats. Therefore, to assess any change in water levels as a result of the various Route 3A scheme options the various sets of results from the hydrodynamic model have been analysed.

Changes in water level are considered to be negligible in most of the schemes tested. The changes that exist are generally confined to the local area around the bridge piers and towers. Some of the observed differences are due to small phase changes as the tide propagates over the intertidal areas. All differences are less than 4cm.

The exception to this small change in water level is the Route 3A Short Span case (Drawing No. B4027/3/B/301). On the flooding tide the bridge piers cause a blockage within the main channels of the estuary. This is an artefact of the tidal asymmetry and the short flood tide period. Therefore, a large volume of water is entering the upper estuary within this period resulting in an increase in water level over a wide extent as a head of water is built up across the channel in the vicinity of the bridge. This effect is particularly evident in the north channel (Figure 6A). This build up of water is transient and has dissipated before the time of high water. However, the head of water will likely result in accelerated flows upstream of the bridge, which may impact on the channels and the shallower intertidal areas by increasing sediment erosion and in turn sediment deposition on the weaker but longer duration ebb tide.

Summary

For the Route 3A Medium Span original alignment, Route 3A Medium Span modified alignment, Route 3A Medium Span 3 Tower alignment and Route 3A Medium Span Revised 3 Tower alignment the changes in water level are considered to be insignificant. However, the Route 3A Short span option causes a blockage within the main channels of the estuary, although the magnitude of this is relatively small.

3.2.3 Speed Changes

Route 3A Medium Span Original Alignment

The greatest differences in speed occur around the tower structures with a maximum predicted increase of 1.0m/s, approximately, occurring around high water. However,

typical speed differences are between 0.02 - 0.05m/s. The positioning of the tower structures within the north and south channels generates increased speeds along the edge of the intertidal shorelines extending downstream of Old Quay Lock on the southern side of the estuary.

The maximum reduction in speed also occurs local to the bridge structures with changes in the order of 0.3 - 0.8m/s. Differences in speed observed along the front of the tidal wave as it propagates onto the intertidal banks are due to slight phase changes between the baseline case and the scheme (Figure 6B). However, these effects are transient and dissipate quickly as the banks are flooded.

Route 3A Medium Span Modified Alignment

The Route 3A Medium Span modified alignment involves moving the bridge towers away from the north and south channels. Typical differences in flow speed are between 0.02 - 0.05 m/s, whilst peak differences in flow speed are between 0.30 - 0.80 m/s for increased flows and 0.10 - 0.30 m/s for reduced flow speeds. These maximum and minimum differences remain local to the structures.

Comparing maximum changes in speed around the bridge piers/towers with those values obtained from the original Route 3A Medium span alignment shows a 20 - 40% reduction as a result of repositioning of the bridge towers. Also the extent of speed changes as a result of implementing the modified alignment are significantly reduced compared with the Route 3A Medium Span original alignment, demonstrating the importance of tower/pier placement within the estuary.

The Route 3A Medium Span modified alignment has also been investigated for extreme fluvial and extreme fluvial plus surge conditions. Over a spring tide with a 1:200 year fluvial event typical differences in flow speeds are between 0.02 - 0.05 m/s. Peak increases in flow speed are between 0.20 - 0.40 m/s and maximum deceleration in flow is between 0.40 - 0.60m/s. These maximum and minimum differences remain local to the bridge structures. The increased freshwater flow appears to reduce the impact of the scheme within the estuary at peak times while increasing the impact around low water.

Under a combined fluvial and surge event (1:200 years return period) typical differences in flow speeds are between 0.02 - 0.05 m/s. Maximum differences in flow speed are between ±0.20 - 0.50 m/s. In general, these maximum and minimum differences are found adjacent to the bridge structures. Around high water there is some interaction between the central piers and a radiating flow pattern is observed. There is also interaction with the first set of pier footings on the upper intertidal area. However, overall, the bridge appears to have a limited impact on the estuary during an extreme fluvial and surge event.

Route 3A Medium Span 3 Tower Alignment

For this modified version of Route 3A Medium Span operational case the number of towers is reduced to 3 and the pier alignments have been modified. The greatest changes in speed are local to the bridge structures with maximum increases in near-surface flow speed between 0.06 - 0.11 m/s whilst the maximum reduction in flow speeds are of the order of 0.20 m/s. These show a considerable reduction (up to 90%, approximately) in observed changes in speed over those observed for the Route 3A Medium span option - original and modified alignments (4 towers). On the southern bank the positioning of the twin pier structure on the edge of the channel leads to some impact on flow speeds along the edge of the southern channel and intertidal area. In addition, the position of the central tower is such that under the existing channel alignment it is only exposed to flow around the time of high water on spring tides. This again demonstrates the importance of the siting of the bridge piers in the short-term.

Route 3A Medium Span 3 Tower Revised Alignment

Around the time of peak flows the greatest changes in speed are local to the bridge structures with maximum increases in near-surface flow speed between 0.04 - 0.16 m/s whilst the maximum reduction in flow speeds are of the order of 0.60m/s. Again these results show a considerable reduction (up to 94%, approximately) in observed changes in speed over those observed for the Route 3A Medium span option - original and modified alignments (4 towers). As previously, this demonstrates the importance of the siting of the bridge piers in the short term. In addition, as with the previous 3 tower alignment (Drawing No. B4027/3/B/300) the position of the central tower is such that under the existing channel alignment it is only exposed to flow around the time of high water on spring tides.

On the southern bank the twin pier structure closest to the southern-most tower is now positioned away from the edge of the channel and, therefore, changes in flow speeds are limited to the three tower structures.

Under a combined fluvial and surge event (1:200 years return period) typical differences in flow speeds are between 0.02 - 0.05 m/s. Maximum changes in flow speed around the bridge structures are between 0.07 - 0.82 m/s, with minimum changes between 0.55 – 1.19m/s. During the high water period there is some interaction between the central piers generating a radiating flow pattern. There is also interaction with the first set of pier footings on the upper intertidal area. However, overall, the bridge appears to have a limited impact on the estuary during an extreme fluvial and surge event.

The 1:200 year surge event leads to flows over the intertidal area and parts of Wigg Island. Similar order of increases in speed around low water are observed in the combined extreme surge and fluvial scenario as observed in the 1:200 years fluvial scenario. This would indicate that this is primarily due to the increased fluvial flow in the low water channels leading to high water levels and greater velocities rather than due to increased tidal velocities as a result of the surge.

Route 3A Short Span

The maximum increase in flow speed local to the bridge piers are of the order of 0.08 - 0.20 m/s. However, around peak flood there is a larger change in flow speed within the channels than compared with any of the other schemes tested (0.2m/s). The largest extent of flow change is within the south channel around peak flood, with increased flows along much of the intertidal foreshore of Wigg Island.

Over the ebbing tide the bridge structures lead to increased flow speeds along much of the north bank along the intertidal area local to the bridge as well as along the south bank downstream of Old Quay lock.

Around the time of high water there is a general change in flow speed across the whole width of the estuary due to the number of piers present. This effect is reduced on neap tides (not shown) due to the lower water levels. However, the short span option shows the greatest impact within the study area in terms of extent, although the magnitude of the change is often less than observed for some of the schemes using towers.

Summary

- Of all the schemes tested the Route 3A Medium Span modified alignment and Route 3A Medium Span Revised 3 Tower alignment show the least impact. The short span option shows the greatest impact within the study area in terms of extent, although the magnitude of the change is often less than observed for some of the schemes using towers.

- Differences in speed observed along the front of the tidal wave as it propagates onto the intertidal banks are due to slight phase changes between the baseline case and the scheme. However, these effects are transient and dissipate quickly as the banks are flooded. Such effects are observed in all the schemes tested.

- In general, the greatest differences in speed occur around the tower/pier structures as a result of the changes in flow transmission due to the presence of the structure.

- The Route 3A Medium Span modified alignment and Route 3A Medium Span Revised 3 Tower alignment demonstrate the importance of the positioning of the bridge towers/piers within the estuary, at least within the short-term.

Bed Shear Stresses Changes

The bed shear stress is the frictional force exerted on an area of seabed or riverbed by current flowing over it. Therefore, it is an important quantity in the study of sediment transport processes, because it represents the flow-induced force acting on the bed sediments. The importance of looking at the predicted changes in the context of the baseline case is demonstrated in Figure 7, which shows the threshold of sediment

motion for 150μm grain size over a spring and neap tide. Clearly for almost all states of the tide the sediment is in motion, therefore, even quite large changes in bed shear stress may not result in any substantial increase in sediment transport.

Route 3A Medium Span Original Alignment

The greatest changes observed are local to the bridge piers, with maximum increases of the order of 1.2 - 3.6N/m^2 and maximum reduction in bed shear stress of between 1.3 - 3.5N/m^2. At peak flows there is a predicted change along the shoreface of the intertidal areas, which stretches along a significant extent of this area both upstream and downstream of the structures.

Route 3A Medium Span Modified Alignment

The greatest changes observed are local to the bridge piers, with maximum increases of around 1.7 - 2.2N/m^2 and maximum reduction in bed shear stress of around 0.4 - 2.1N/m^2. These large values correspond to positions adjacent to the pier/tower structures where changes due to reductions in flow transmission are likely to be a maximum.

In general, at peak flows there is no significant increase in bed shear stress along the shoreface of the intertidal areas, unlike the Route 3A Medium Span Original Alignment Typical changes in bed shear stress are between 0.04 - 0.06 N/m^2.

For extreme fluvial flow the greatest changes observed are local to the bridge towers/piers, with maximum increases of around 2.4 - 4.3N/m^2 and maximum reduction in bed shear stress of around 1.8 - 3.2N/m^2. Around High water the model results indicate changes across much of the upper estuary to be limited to around the bridge piers/towers and along the edge of the intertidal area with the greatest extent of change of less than 0.04N/m^2. At other states of the tide the changes are generally confined to the locality of the bridge structures.

For extreme surge and fluvial conditions the greatest changes observed are also local to the bridge piers, with maximum increases of around 2.2 - 5.5N/m^2 and maximum reduction in bed shear stress of around 0.9 - 1.5N/m^2. Around High water the model results indicate changes over a larger extent of the upper estuary both upstream and downstream of the proposed crossing. This is a function of the intertidal area being flooded on the extreme tide over the high water period. At other states of the tide the changes are generally confined to the locality of the bridge structures.

Although the model results indicate large changes in bed shear stress along the intertidal, these areas are limited in extent and are also considered to be caused by changes in the flow propagation rather than absolute increases as a result of the bridge scheme.

Route 3A Medium Span 3 Tower Alignment

There is no observed change in bed shear stress around low water due to the bridge towers and pier positions being outside the low water flow channels. In general, changes are confined to the immediate locality of the bridge structures with the greatest observed impact occurring around the time of peak flood with maximum increases of around 0.2 - 1.5N/m^2 and maximum reduction in bed shear stress of around 0.8 - 2.9N/m^2.

Route 3A Medium Span 3 Tower Revised Alignment

The proposed Route 3A Medium - 3 Tower Option revised alignment also shows no change in bed shear stress around low water due to the bridge towers and pier positions being outside the low water flow channels. The greatest changes observed are local to the bridge piers and show maximum increases of around 0.8 - 2.7N/m^2 and maximum reduction in bed shear stress of around 0.7 - 5.0N/m^2. In general, changes are confined to the immediate locality of the bridge structures with the greatest observed impact occurring around the time of peak flood.

For extreme surge and fluvial conditions the greatest changes observed are also local to the bridge piers, with maximum increases of around 0.4 - 1.6N/m^2 and maximum reduction in bed shear stress of around 1.1 - 3.7N/m^2. Around High water the model results indicate changes over a larger extent of the upper estuary both upstream and downstream of the proposed crossing. This is a function of the intertidal area being flooded on the extreme tide over the high water period. At other states of the tide the changes are generally confined to the locality of the bridge structures.

The majority of changes in bed shear stress have been shown to be an artefact of the representation of intertidal flooding and drying in the numerical model and are, therefore, of no significance (for example the speckled areas in Figures C69 and C70). Across much of the study area the changes are less than 10%.

Route 3A Short Span

In general, the largest changes are confined to the immediate locality of the bridge structures with maximum increases of around 0.3 - 5.0N/m^2 and maximum reduction in bed shear stress of around 0.6 - 5.7N/m^2. Around peak flood there is a general increase in bed shear stress in both the north and south channels.

Although the results indicate large changes in bed shear stress along the intertidal (up to 8.2N/m^2) many of these changes are due to the positional change in bed shear stress as a result of a change in the flow propagation. However, some of these large changes are real and are caused by the obstruction across the channel that this scheme represents.

Summary

- From the modelling the Route 3A Medium Span modified alignment and Route 3A Medium Span Revised 3 Tower alignment show the least impact. However, the bed shear stress results for the Route 3A Medium Span Revised 3 Tower alignment would suggest a higher level of accretion around the bridge structures, though the extent of the changes is lower.

- For all schemes tested the greatest changes observed are local to the bridge structures, in general.

- Some of the predicted changes in bed shear stress along the intertidal are large in value. However, these areas are limited in extent and in many instances are considered to be caused by changes in the flow propagation and hence represent a shift in phase rather than an absolute increase. In the case of the Route 3A short span option some of these large changes are real and are caused by the obstruction across the channel that this scheme represents.

3.2.4 Morphological Changes

Appendix D presents the results of the morphological modelling. The bed shear stress values described above and quoted in detail in Appendix C represent maximum changes of the instantaneous stress and may not be sustained for any length of time. The bed shear stresses give an indication of potential change in erosion/accretion based on the hydrodynamic equations. Changes in sedimentation patterns can be identified from the morphological modelling.

For riverbeds consisting of sands (non-cohesive sediments) the movement of these particles depends on the physical properties of the individual grains, such as size shape and density. For riverbeds made up of silty and muddy materials, the cohesive forces between the sediment particles become important, leading to a significant increase in sediment resistance to erosion. Flocculation of sediment particles is the result of particles adhering together as they come into contact with each other and the resulting aggregations are called flocs. Biological activity at the bed may also influence the critical shear stress values required to initiate sediment movement (ABPmer, 2003a). Seasonal variations in sedimentation are considered sufficiently small to be masked by the variances arising from the acknowledged limitations of sediment transport models.

The other important factor relating to the erodibility of cohesive sediments is the consolidation rate. Mud recently deposited consists of low-density mud flocs possessing a relatively loose structure. The cohesive forces in this deposit are not very strong at this early stage. If the deposit is not eroded again, then the density will increase gradually, as the interstitial water (water between the flocs) is expelled from the deposit as a result of its own weight. As the deposit is compacted so its resistance to erosion increases.

Whilst changes to the hydrodynamic regime are important, what is most important to the intertidal areas is erosion and deposition. The following discussion will concentrate on results from the morphological modelling. Based on the complexity of sediments as discussed above, the results from the morphological model need to be interpreted with care, taking into account the various factors affecting sediment transport, and considering the effects of processes not included as parameters within the model (for example biological activity. The morphological modelling of the Mersey Estuary has been undertaken using the predominant sediment type found across the study area (sand d_{50} = 150 μm).

Route 3A Medium Option - Original Alignment

For the Route 3A Medium Option the following highlight the key changes in the sedimentation patterns:

- In the vicinity of the proposed bridge crossing material is eroded from around the bridge tower adjacent to the main South Channel (maximum depth of erosion -0.75m). There is a zone of accretion slightly upstream of this area of erosion, which extends into a zone of erosion (0.05 - 0.10m).

- The largest extent of deposition occurs along the margins of the South Channel and upstream of the pier structures, located towards the margins of the South Channel. Upstream of the proposed bridge crossing an increase in sedimentation of approximately 10-20cm is predicted along the side slopes of the South Channel (Maximum Accretion 1.82m).

- Along the north bank adjacent the existing bridge, and along the quay wall, there is a predicted increase in sediment deposition of less then 0.05m. The morphological modelling predicts an increase in bed elevation of approximately 0.5m adjacent the pier in the North Channel.

- A general pattern of increased sedimentation is predicted within the area of the proposed bridge crossing. The pattern of erosion and sedimentation suggests that the placement of the piers has led to an increase in erosion along the margins of the South Channel downstream of the proposed pier positions. The overall pattern upstream of the proposed crossing is of an increase in sediment. This is most likely a result of the reduced transmission of flows caused by the 'blockage effect' of the structures and the weaker ebb currents.

- The modelling shows no change in sediment distribution downstream of Runcorn and upstream of Fiddlers Ferry.

Route 3A Medium Option - Modified Alignment

For the Route 3A Medium span Modified alignment the main changes in the sedimentation pattern are:

- There is an area of deposition along the North Channel adjacent to the proposed bridge tower placements (maximum deposition 0.73 m). The modelling shows deposition of sediment occurring between the tower structure and the intertidal area. Upstream and downstream of this deposition are patches of erosion typically 0.05m or less in depth with maximum erosion of 0.15m indicated.

- Along the southern side of the channel there is a general increase in sedimentation of less than 0.05m. Immediately adjacent to the bridge tower the morphological model predicts erosion to a depth of 0.7m, approximately and maximum accretion of 1.32m.

- The modelling shows no change in sediment distribution downstream of Runcorn and upstream of Fiddlers Ferry.

- Overall the Route 3A Medium span modified alignment shows a significant improvement in the amount of impact the scheme is causing within the estuary compared to that predicted to occur due to the Route 3A Medium span - original alignment.

In addition, the Route 3A Medium span Modified alignment has been tested for two extreme events: an extreme fluvial event with a 1:200 years return period and a surge with an extreme fluvial event both with 1:200 years return periods. The main findings for the fluvial event are:

- The morphological model suggests that the greatest extent of change occurs within the north channel during an extreme fluvial event. In general there is deposition of sediment upstream and downstream of the tower in the north channel with values of less than 0.05m typically, although there are a couple of patches of deposition up to 0.10m.

- Within the south channel the change in sedimentation remains local to the bridge structure with some erosion occurring between the tower and the intertidal area.

- The placement of sediment is predominantly downstream of the structures suggesting that there is more ebb dominance in the system as a result of the significantly increased fluvial flows.

For the combined surge and fluvial event the key changes in the sedimentation patterns are:

- The greatest extent of change occurs within the north channel. However, downstream of the bridge structures the higher tidal flows appear to suppress changes in sedimentation compared with the extreme fluvial event. In addition, the higher water levels as a result of the surge lead to changes in sedimentation across the upper areas of the intertidal banks in the vicinity of the two central bridge towers with typical values of deposition less than 0.05m.

- Within the north channel the greatest changes occur local to the bridge tower with maximum erosion and deposition of -0.67m and 0.45m, respectively. Along the southern side of the estuary most changes are local to the bridge tower situated towards the south channel. However, the higher water levels result in small changes along the intertidal suggesting that sediment will be deposited (less than 0.05m).

- The changes local to the tower in the south channel show maximum deposition of 0.27m and maximum erosion of 0.49m. As observed in the extreme fluvial event, the placement of sediment is still predominantly downstream of the structures suggesting that there is more ebb dominance in the system. This would suggest that the increased fluvial flows are still dominating the time-averaged hydrodynamics in the upper estuary despite the significant tidal event.

Route 3A Medium - 3 Tower Option

For the Route 3A Medium span 3 Tower alignment the main findings from the morphological model are:

- The main areas of erosion and deposition are observed immediately adjacent to the bridge structures located in the proximity of the north and south channels (maximum erosion 1.46m, maximum accretion 1.79m). The extent of erosion is approximately 70-100m either side of the bridge towers and piers.

- Along the northern side of the estuary upstream of the proposed bridge structures there is a predicted increase in erosion of between 0.05 - 0.25m. This erosion occurs both along the shoreline and over the intertidal banks. Downstream of the bridge structures deposition of sediment is shown to occur (less than 0.05m) except for a few small patches of erosion close to Spike Island (< 0.05m).

- Along the southern bank, the morphological model predicts accretion to be occurring both upstream and downstream of the bridge structures along the intertidal area adjacent Wigg Island (typically < 0.05m). Although the bridge tower adjacent to the south channel is away from this channel, the location of the bridge piers on the edge of the intertidal/channel area influence the sediment patterns along the intertidal area.

- Compared with the Route 3A Medium Option Modified Alignment (4 tower) the Route 3A Medium span 3 tower option performs less well. Despite the reduction in the number of towers placed within the estuary the scenario demonstrates that poor placement of the bridge structures has a significant impact on the morphological change, at least in the short-term.

Route 3A Medium - 3 Tower Option - Revised Alignment

For the Route 3A Medium 3 Tower revised alignment the following highlight the key changes in the sedimentation patterns:

- In general, the changes are local to the tower structures. Moving the position of the towers and piers away from the channels has significantly reduced the impact of the proposed crossing on the system

- Away from the bridge structures morphological changes as a result of the scheme are less than ±0.05m. The maximum changes local to the bridge tower adjacent to the south channel are erosion of -0.1m and deposition of 0.29m. Adjacent to the tower situated close to the north channel the maximum deposition is 0.33m and the maximum erosion is 1.38m.

- The revised alignment for the Route 3A medium span 3 towers option shows the least impact in terms of extent of change across the upper estuary.

For the combined surge and fluvial event the key changes in the sedimentation patterns are:

- In general, the changes are local to the tower structures. The area around the north tower shows the greatest extent of erosion extending 500m, approximately either side of the tower. The maximum erosion (≈ 1.8m) is predicted to occur adjacent to the north tower, whilst the largest accretion of sediment (1.2m) occurs either side of the north tower

- Some changes are seen upstream and downstream of the proposed bridge crossing. However, these changes are less than 0.5m and only occur within isolated sections of the study area.

For the morphological simulation undertaken to assess the 'recovery' of the system post construction for the Route 3A medium span 3 towers option revised alignment the key changes in the sedimentation patterns are:

- In general, the changes are local to the tower structures. Away from the bridge structures morphological changes as a result of the scheme are less than ±0.05m. The maximum changes local to the bridge tower adjacent to the north channel are erosion of 1.37m and deposition of 0.33m.

- The results obtained from the recovery scenario are comparable to the revised alignment for the Route 3A medium span 3 towers option (Figures D11a and D11b). The pattern of sediment distribution is very similar with no significant difference in bed elevation.

- The recovery scenario has demonstrated that from an initial bed elevation, which has been subjected to an extreme event, the system appears to be capable of returning quickly to a condition predicted under normal water levels and fresh water discharges.

For the morphological simulation undertaken to assess the morphological response of the system to the proposed bridge with a completely different channel configuration (2005 bathymetry - Figure 8) the key changes in the sedimentation patterns are:

- The different channel configuration has created a south channel dominance over that observed for the 2002 bathymetry, which was dominated by flows through the north channel. The greatest extent of change is upstream of the proposed crossing, with accretion predicted to occur along the intertidal shoreline and banks. Downstream of the proposed bridge there is some erosion along the intertidal area adjacent the south bank.

- Within the south channel the greatest changes occur local to the bridge tower with maximum erosion and deposition of -1.54m and 0.65m, respectively. Changes within the north channel are limited to the location of the bridge tower and piers.

- In general the channel configuration leads to a slight increase in bed elevation downstream of the proposed bridge crossing, this increase is localised to the margins of the north channel.

Route 3A Short Option

For the Route 3A Short span alignment the main changes in the sedimentation pattern are:

- Downstream of the bridge structures the model shows sediment to be eroded along the intertidal area of Wigg Island and downstream of Old Quay Lock (typical changes < 0.15m). Through Runcorn Gap there are patches of erosion and deposition with maximum changes less than 0.20m. Downstream of Runcorn Gap the predicted morphological changes become insignificant.

- Upstream of the bridge structures the model shows deposition, predominantly, with maximum changes over the intertidal banks of less than 0.20m. Along the intertidal shorelines on the south and north channels the maximum deposition is 0.39m and 1.71m, respectively.

- Adjacent to the bridge piers located within or close to the channels the maximum predicted deposition is 1.79m whilst the maximum erosion is 1.48m. In general, the short span option suggests that flows are accelerated between the piers on the flood tide leading to increased erosion local to the proposed crossing. The bridge causes a restriction across the channel leading to a build up in the hydraulic head of water at the bridge (backwater effect). This is likely caused by the asymmetry in the tidal curve with a very rapid flood tide (1.5 hours, approximately). This increases deposition as a result of higher water levels and delay in tidal propagation.

- Although the short span option has not been run for any extreme events it is likely that on surge events in particular, this design option will provide an increased restriction to the propagation of the flood tide. Comparison of the Short Span scenario against the other scheme layouts shows the greatest impact in terms of sediment distribution within the upper Mersey Estuary and it is recommended that this scheme is not progressed further.

Summary

Tables 6 - 10 summarise the results from the cross-section analysis. Based on the results of the morphological modelling the two schemes which show the least impact are the Route 3A Medium span Modified alignment and the Route 3A Medium 3 Tower revised alignment. Of these two schemes, the revised alignment for the Route 3A medium span 3 towers option shows the least impact in terms of extent of change across the upper estuary but a greater magnitude of change local to the tower structure in the north channel. Running the Route 3A Medium 3 Tower revised alignment for a range of different scenarios including an extreme event, a system recovery scenario and a new channel configuration (2005 bathymetry) shows different patterns of change, particularly local to the structures. However, the magnitude and extent of the change is of a similar order to other scenarios run and is a reflection of some of the inherent system variability.

Table 6. Summary of cross-sectional bed level changes for the various schemes. Description of changes compared against the existing 'baseline' condition

Cross-Section	Scenario				
	Route 3A Medium - Modified	Route 3A Medium - Original	Route 3A Medium - 3 Tower	Route 3A Short	Route 3A Medium 3 Tower Revised
A	No change	No change	No change	No change	No change
B	No change	No change	No change	No Change	No Change
C	Minor changes in elevation over cross-section (max ≈ 0.04m)	Minor changes in elevation over cross-section (max ≈ 0.01m)	Minor changes in elevation over cross-section (max ≈ 0.02m)	Minor changes in elevation over cross-section (max ≈ 0.01m)	Some deposition in south channel (max ≈ 0.07m) and erosion over bank (max ≈ 0.18m).
D	Some minor deposition over cross-section (max ≈ 0.03m)	Minor changes in elevation over cross-section (max ≈ 0.02m)	Minor changes in elevation over cross-section (max ≈ 0.02m)	Minor changes in elevation over cross-section (max ≈ 0.01m).	Some erosion in south channel (max ≈ 0.09m) and deposition within north channel (max ≈ 0.03m)
E	Deposition in south channel (max ≈ 1.82m) and north channel (max ≈ 0.60m)	Minor erosion in south channel (max ≈ 0.01m) and deposition within north channel (max ≈ 0.05m)	Some erosion in south channel (max ≈ 0.03m) and erosion (max ≈ 0.19m) and deposition (max ≈ 0.13m) in north channel	Minor changes in elevation over cross-section (max ≈ 0.02m)	Erosion in south channel (max ≈ 0.07m) and deposition within north channel (max ≈ 0.08m)
F	Erosion in south channel (max ≈ 0.13m) deposition in north channel (max ≈ 0.05m)	Minor erosion in south channel (max ≈ 0.02m) and deposition within north channel (max ≈ 0.04m)	Significant erosion and deposition in north channel, max ≈ 1.46m and 0.34m, respectively.	Significant erosion and deposition in north channel, max ≈ 1.38m and 0.29m, respectively.	Significant erosion and deposition in north channel, max ≈ 1.10m and 0.34m, respectively.
G	Some erosion in south channel (max ≈ 0.31m) deposition in north channel (max ≈ 0.09m)	Some erosion in south channel (max ≈ 0.03m) deposition in north channel (max ≈ 0.10m)	Some erosion in south channel (max ≈ 0.07m) deposition in north channel (max ≈ 0.32m)	Deposition in north channel (max ≈ 0.06m)	Erosion in south channel (max ≈ 0.18m) Erosion and deposition in north channel max ≈ 0.43m and 0.36m, respectively.
H	Erosion in south channel (max ≈ 0.11m) and deposition on sides of channel (max ≈ 0.28m). Deposition in north channel (max ≈ 0.06m)	Erosion in south channel (max ≈ 0.08m) and deposition on sides of channel (max ≈ 0.02m). Deposition in north channel (max ≈ 0.07m)	Erosion in south channel and on sides of channel (max ≈ 0.44m). Deposition in north channel (max ≈ 0.18m)	Erosion and deposition on sides of channel max ≈ 0.29m and 0.09m, respectively.	Erosion and deposition on sides of channel max ≈ 0.45m and 0.28m, respectively. Deposition in north channel (max ≈ 0.20m)
I	Erosion and deposition on southern side of channel max ≈ 0.22m and 0.05m, respectively.	General deposition over cross-section (max ≈ 0.06m)	General deposition over cross-section (max ≈ 0.13m)	General deposition over cross-section (max ≈ 0.06m)	Erosion and deposition on southern side of channel max ≈ 0.14m and 0.88m, respectively. Deposition in north channel (max ≈ 0.27m)
J	Erosion and deposition in south channel max ≈ 0.16m and 0.17m, respectively. Over remaining section erosion and deposition (max ≈ 0.08m)	General deposition over cross-section (max ≈ 0.06m). Some erosion over central banks (max ≈ 0.05m)	Generally deposition over cross-section (max ≈ 0.14m) with some erosion over sides of central bank (max ≈ 0.03m)	General deposition over cross-section (max ≈ 0.04m). Some erosion over central banks (max ≈ 0.03m)	Erosion and deposition on southern side of channel max ≈ 0.20m and 0.45m, respectively. Deposition in north channel (max ≈ 0.20m)
K	Erosion and deposition over central banks max ≈ 0.02m and 0.15m, respectively. Deposition in north channel (max ≈ 0.02m)	Deposition in north channel (max ≈ 0.02m)	Generally deposition over cross-section (max ≈ 0.07m) with some erosion over sides of central bank (max ≈ 0.03m)	Generally deposition over cross-section (max ≈ 0.03m) with some localized erosion over sides banks (max ≈ 0.01m)	Erosion and deposition in south channel max ≈ 0.11m and 0.35m, respectively. General deposition over remaining cross-section (max ≈ 0.27m)
L	Deposition over central banks and north channel (max ≈ 0.07m)	Some minor deposition and erosion on north side of channel (max ≈ 0.01m)	Generally deposition over cross-section (max ≈ 0.03m) with some erosion over sides of central bank (max ≈ 0.01m)	Minor changes in elevation over cross-section (max ≈ 0.01m)	General deposition over cross-section (max ≈ 0.09m).

Table 7. Summary of cross-sectional bed level changes for the extreme schemes. Description of changes compared against the existing condition (without bridge structures)

Cross-Section	Scenario	
	Route 3A Medium Modified Alignment - Fluvial with Surge	Route 3A Medium Modified Alignment - Fluvial
A	No Change	No Change
B	No Change	No Change
C	No Change	No Change
D	No Change	No Change
E	No Change	No Change
F	Slight increase in erosion along the margin of the south channel.	No Change
G	No Change	No Change
H	No Change	No Change
I	No Change	No Change
J	No Change	No Change
K	No Change	No Change
L	No Change	No Change

Table 8. Summary of cross-sectional bed level changes for the Route 3A 3 Tower revised alignment for an extreme fluvial and surge event. Description of changes compared against the corresponding existing condition (without bridge structures)

Cross-Section	Scenario
	Route 3A Medium 3 Tower Revised Alignment - Fluvial with Surge
A	No change
B	Erosion in bottom of central channel (max ≈ 0.04m). Erosion on shoulder of bank towards northern side (max ≈ 0.03m).
C	Some deposition (max ≈ 0.02m) and erosion (max ≈ 0.06m) over central part of channel.
D	Slight erosion in southern channel (max ≈ 0.01m) and deposition on side of intertidal bank (max ≈ 0.05m). Erosion in northern channel (max ≈ 0.04m) as well as some deposition (max ≈ 0.02m).
E	Minor changes in southern channel, deposition (max ≈ 0.01m). In northern channel some erosion on side of intertidal bank (max ≈ 0.08m) and deposition within channel (max ≈ 0.23m).
F	Minor changes in southern channel deposition (max ≈ 0.01m). In northern channel both erosion (max ≈ 1.79m) and deposition (max ≈ 0.86m).
G	Slight erosion (max ≈ 0.03m) and deposition within southern channel. Within northern channel both erosion (max ≈ 0.01m – 0.48m) and deposition (max ≈ 0.01m – 0.59m).
H	Erosion and deposition within southern channel (max ≈ ±0.02m). Some deposition on southern side of intertidal bank (max ≈ 0.04m). Erosion (max ≈ 0.07m) and deposition (max ≈ 0.11m) on shoulder of intertidal bank. In northern channel some erosion (max ≈ 0.08m) and deposition (max = 0.03m).
I	Some erosion and accretion in southern channel (max ≈ ±0.02m). Slight erosion and deposition over central intertidal banks (max ≈ ±0.01m). Towards northern channel areas of erosion (max ≈ 0.04m) and deposition (max ≈ 0.03m).
J	Minor erosion (max ≈ 0.01m) and some deposition (max ≈ 0.02m) in southern channel. Some erosion (max ≈ 0.01m) and deposition (max ≈ 0.02m) over central intertidal banks. Some accretion (max ≈ 0.01m) and erosion (max ≈ 0.02m) towards the northern channel.
K	Within the southern channel there is some erosion (max ≈ 0.01m) and deposition (max ≈ 0.02m). Some deposition (max ≈ 0.01m) across the central channel and banks. Towards the northern bank there is some erosion and deposition (max ≈ ±0.01m).
L	Some erosion and deposition within southern channel (max ≈ ±0.02m). Over central banks and channels there is some erosion and deposition (max ≈ ±0.02m). Towards the northen channel there is erosion (max ≈ 0.02m) and deposition (max ≈ 0.01m).

Table 9. Summary of cross-sectional bed level changes for the Route 3A 3 Tower revised alignment recovery scenario. Description of changes compared against the corresponding existing condition (without bridge structures)

Cross-Section	Scenario
	Route 3A Medium 3 Tower Revised Alignment - Recovery
A	No change
B	No change
C	Some erosion and deposition (max ≈ ±0.01m) over intertidal banks.
D	Towards northern channel some erosion and deposition over intertidal banks (max ≈ ±0.01m). Within the northern channel there is some deposition (max ≈ 0.03m).
E	Limited changes within southern channel with some minor erosion (max ≈ 0.01m). Within the northern channel there is some erosion and deposition (max ≈ ±0.02m).
F	Changes limited to northern channel, with both erosion (max ≈ 1.37m) and deposition (max ≈ 0.29m).
G	Some changes in southern channel and over central intertidal banks (max ≈ ±0.01m). Within the northern channel some deposition (max ≈ 0.06m) and some erosion (max ≈ 0.01m).
H	Some deposition in southern channel (max ≈ 0.02m). Some erosion (max ≈ 0.29m) and deposition (max ≈ 0.09m) on shoulder of intertidal bank. In north channel some erosion and deposition (max ≈ ±0.03m).
I	Some deposition in southern channel (max ≈ 0.01m). Deposition over central area (max ≈ 0.06m) together with some erosion (max ≈ 0.01m). Deposition within northern channel (max ≈ 0.03m).
J	Some erosion and deposition within southern channel and on adjacent intertidal bank (max ≈ ±0.01m). Within central bank area there is some erosion (max ≈ 0.03m) and deposition (max ≈ 0.02m). Within the northern channel there is deposition (max ≈ 0.04m).
K	Some erosion and deposition within southern channel (max ≈ ±0.01m) and on adjacent intertidal bank (max deposition ≈ 0.02m; max erosion ≈ 0.01m). Towards northern side of estuary some erosion (max ≈ 0.01m) and deposition (max ≈ 0.03m).
L	Little change over whole cross-section. Some erosion towards southern side (max ≈ 0.01m) and both deposition and erosion towards northern side (max ≈ ±0.01m).

Table 10. Summary of cross-sectional bed level changes for the Route 3A 3 Tower revised alignment – 2005 bathymetry. Description of changes compared against the corresponding existing condition (without bridge structures)

Cross-Section	Scenario
	Route 3A Medium 3 Tower Revised Alignment – 2005 bathymetry
A	No change
B	Some deposition on southern bank (max ≈ 0.01m). Erosion in central channel (max ≈ 0.01m). Some erosion towards northern side.
C	Deposition in southern channel (max ≈ 0.01m). Erosion over intertidal bank (max ≈ 0.01m). Some deposition towards north bank (max ≈ 0.01m).
D	No change
E	Deposition in southern channel (max ≈ 0.03m) together with some erosion (max ≈ 0.01m). Some deposition on intertidal bank (max ≈ 0.01m). Deposition (max ≈ 0.05m) and erosion (max ≈ 0.04m) in northern channel.
F	Erosion and deposition in southern channel (max ≈ ±0.02m). Erosion and deposition over intertidal bank (max ≈ ±0.02m). Within northern channel there is deposition (max ≈ 0.35m) and erosion (max ≈ 1.01m).
G	Erosion in southern channel on side closest to intertidal bank (max ≈ 0.04m). Some deposition on 'hump' bisecting channel (max ≈ 0.01m) with erosion on other side of channel (max ≈ 0.06m). Erosion (max ≈ 0.36m) and deposition (max ≈ 0.21m) over intertidal bank. Deposition in northern channel (max ≈ 0.11m).
H	Erosion (max ≈ 0.06m) and deposition (max ≈ 0.04m) in southern channel. Erosion (max ≈ 1.39m) and deposition (max ≈ 0.58m) on side of intertidal bank. Over top of bank there is some erosion (max ≈ 0.04m). There is erosion in northern channel (max ≈ 0.04m).
I	Erosion (max ≈ 0.10m) and deposition (max ≈ 0.18m) in south channel. Erosion (max ≈ 0.26m) and deposition (max ≈ 0.20m) over southern side of intertidal bank. Some erosion in northern channel (max ≈ 0.03m).
J	Erosion (max ≈ 0.04m) and deposition (max ≈ 0.29m) in southern channel. Over southern side of intertidal bank there is erosion (max ≈ 0.04m) and deposition (max ≈ 0.14m). Some erosion and deposition in northern channel (max ≈ ±0.01m).
K	Deposition in southern channel (max ≈ 0.09m). Some erosion (max ≈ 0.01m) and deposition (max ≈ 0.13m) over southern side of intertidal bank. Some deposition in northern channel (max ≈ 0.01m).
L	Deposition in southern channel (max ≈ 0.18m). Deposition over southern side of intertidal bank (max ≈ 0.07m). Some erosion and deposition in north channel (max ≈ ±0.01m) .

4. Discussion

A range of variants on the Route 3A scheme option have been tested. The variations have involved tower and pier realignment, reducing the number of tower structures from 4 to 3 and looking at a viaduct design (short span). The impact of the various scheme options has been assessed using both a hydrodynamic and morphological model. Whilst the morphological model allows for the updating of the riverbed through time the model has not been used to try and simulate historic channel movement. However, it is possible to combine both the modelling and observed historic change to suggest more long-term outcomes of channel movement.

One of the more general findings to come out of the study is the influence of extreme fluvial flows on the average long-term hydrodynamics of the upper estuary. Figures 9B and 10 show the variation in near-surface speed at 3 points within the upper estuary (Figure 9A) during a normal spring neap cycle and during an extreme fluvial event and a combined surge and extreme fluvial event. The figures show that the flow speed is sustained at an almost constant value throughout the whole of the ebb tide period until the onset of the next flood tide. In addition, this constant value can be of significant magnitude, greater than 1m/s and it is suggested that this is the dominant mechanism for significant channel movement in the upper estuary. Figure 11 shows the variation in channel cross-sections at C and L (see Appendix D for positions) between the existing baseline case and for an extreme fluvial event and a combined surge and extreme fluvial event. There is clearly a significant difference in channel configuration between the two extreme events and the existing baseline. Therefore, it is likely that the dominance between the north and the south channels is dictated by the fluvial flows.

However, in terms of the historic channel movement the studies of Cashin (1949) and Price and Kendrick (1963) have shown that anthropogenic changes in the estuary have already altered the ability of the channel to meander freely. Figures 4 and 5 demonstrate that prior to the construction of the Manchester Ship Canal the navigation channel in the inner estuary was free to oscillate over the whole width of the estuary moving across both Ince and Frodsham banks. However, after the late 1880's the movement of the navigation channel became more restricted and was confined more to the northern side between Speke and Hale. In addition, the River Weaver diversion scheme, the construction of an embankment on the north side of the estuary and the construction of the bridge piers for the Runcorn transporter bridge (completed in about 1902) resulted in the navigation channel stabilizing and becoming 'locked' onto the north side of the estuary between Hale and Runcorn. It is not clear which of these had the greatest impact, however, the combined effect is to restrict the movement of the channel through the Runcorn Gap. Therefore, it is suggested that the channels immediately upstream of Runcorn do not have the same ability to meander as perhaps suggested by the early studies of the low water channel movement. Clearly, from more recent studies (Gifford & Partners, 2002) there is still a significant amount of movement of the channel in the upper estuary, however, the variability in channel movement does

not appear to extend to the immediate area (perhaps 1km - 2km) upstream of the Runcorn Gap.

Based on the morphological modelling the immediate change as a result of placing the bridge structures within the channel dissipates after about a year and then the changes become insignificant as the system appears to reach a new equilibrium. For the Route 3A Medium span Modified alignment the impact of the bridge during extreme events appears relatively small. However, this is the only scheme layout to be tested for extreme events. Based on this though, the impact of the extreme events appears to be far more significant than that of the disturbance caused by placing bridge towers within the estuary. It is considered that the bridge towers do not represent a significant blockage effect across the upper estuary and, therefore, should not lead to a detrimental change in the behaviour of the system. However, the upper estuary is highly dynamic and this has implications for scouring around the tower and pier structures. The use of scour countermeasures may require extensive coverage, which may in turn have a greater effect on channel movement than the structures themselves. Careful design of the structures and their foundations will be required and it is recommended that physical model tests be carried out at the design stage to assess scouring round the structures in more detail.

The results of the modelling for the construction phase are presented in ABPmer (2005). They demonstrate that the impact of the construction stage of the bridge is more significant on the hydrodynamics and morphology of the upper estuary than the operational phase. The recovery scenario was undertaken to assess the 'recovery' of the system post construction for the Route 3A medium span 3 towers option revised alignment. The simulation assumes that an aligned jetty approach has been adopted for construction purposes (see ABPmer, 2005). The morphological simulation was run with the construction scheme in place for an extreme fluvial and surge event. At the end of this period the temporary structures related to the construction phase, (for example cofferdams, piles etc) were removed from the model set up and the model then run for a spring-neap-spring cycle scaled to represent one year. The model response to this suggests that the system responds rapidly to the removal of the temporary structures and appears to be capable of returning to a condition predicted under normal water levels and fresh water discharges.

The use of a new channel configuration based on one of the 2005 surveys results in different patterns of change particularly local to the structures. However, the magnitude and extent of the change is of a similar order to that observed using the 2002 bathymetry. This is an important result, since it suggests that for different channel configurations the impact of the proposed crossing will lead to no significant variation in change over those predicted to date from all the modelling undertaken in terms of the extent and magnitude of the change.

5. Conclusions

A detailed numerical modelling study has been undertaken to assess the Route 3A scheme. Five scheme variants have been tested in total as detailed below:

- Route 3A Medium Span original alignment (Drawing No. B4027/2/B/361):
  - Spring-neap cycle

- Route 3A Medium Span modified alignment (Drawing No. B4027/3/H/G/3):
  - Spring-neap cycle
  - High fluvial flow (1:200 year event) and spring tide
  - High fluvial (1:200 year event) and corresponding 1:200 year surge event.

- Route 3A Medium Span 3 Tower alignment (Drawing No. B4027/3/B/300):
  - Spring-neap cycle

- Route 3A Medium Span Revised 3 Tower alignment (Drawing No. B4027/3/B/300 Rev. A):
  - Spring-neap cycle
  - High fluvial (1:200 year event) and corresponding 1:200 year surge event.
  - Recovery
  - 2005 bathymetry

- Route 3A Short Span (Drawing No. B4027/3/B/301):
  - Spring-neap cycle

Based on the results of the hydrodynamic and morphological modelling the two schemes which show the least impact are the Route 3A Medium span Modified alignment and the Route 3A Medium 3 Tower revised alignment. Of these two schemes, the revised alignment for the Route 3A medium span 3 towers option shows the least impact in terms of extent of change across the upper estuary but a greater magnitude of change local to the tower structure in the north channel. If the revised alignment for the Route 3A medium span 3 towers option is taken forward it is recommended that further sensitivity tests are undertaken for this scheme.

The model results suggests that the system responds rapidly to the removal of the temporary structures and appears to be capable of returning to a condition predicted under normal water levels and fresh water discharges.

The modelling has demonstrated that the careful placement of the bridge piers and towers outside of the existing channels may assist the performance in the short-term. However, in the long-term, movement of the position of the channels results in different patterns of change particularly local to the structures. However, the modelling suggests

that for different channel configurations the impact of the proposed crossing will lead to no significant variation in change over those predicted to date from all the modelling undertaken in terms of the extent and magnitude of the change.

Comparison of the Short Span scenario against the other scheme layouts shows the greatest impact in terms of sediment distribution within the upper Mersey Estuary. The short span leads to accelerated flows through the piers on the flood tide leading to increased erosion upstream of the proposed crossing. This implies that the bridge causes a restriction across the channel leading to a build up in the hydraulic head of water at the bridge (backwater effect) and this is observed in the water level results. It is recommended that this scheme is not progressed further.

6. References

ABPmer (2003a). New Mersey Crossing. May, Rep. No. R.1007.

ABPmer (2003b). New Mersey Crossing. Nov., Rep. No. R.1034.

ABPmer (2005). The Mersey Gateway – A New Mersey Crossing Phase II Modelling: Construction Options. July, Rep. No. R1180.

Dronkers, J.J. (1986). Tidal asymmetry and estuarine morphology. Netherlands Journal of Sea Res., Vol. 20, pp 117-131.

Dyer, K.R. (1972). Sedimentation in Estuaries. In: The Estuarine Environment. Eds. Barnes, R.S.K and Green, J., Applied Science Publishers, 133pp.

Friedrichs, C.T. and Aubrey, D.G. (1988). Non-linear tidal distortion in shallow well-mixed estuaries: a synthesis. Estuarine, Coastal and Shelf Science, Vol. 27, pp. 521-545.

Gifford & Partners (2004). New Mersey Crossing: Morphological Desk Study. Revision, March Report No. B4027/011/01.

Halliwell, A.R. and O'Connor B.A. (1967). Suspended sediment in a tidal estuary. In: Proc. of 10th Conference on Coastal Engng., Tokyo, Japan, Sept. 1966, ASCE, Vol 1., Chap. 20, pp 687-706.

Heaps, N.S. (1972). Estimation of density currents in the Liverpool Bay area of the Irish Sea. Geophys. J. R. astr. Soc., Vol. 30, pp. 415 - 432.

Hydrographer of the Navy (1979; 1999; 2001). Admiralty Tide Tables. Vol.1, the UK Hydrographic Office, Taunton.

Inglis, C. (1964). In: Field and model investigation into the reasons for siltation in the Mersey estuary, Price, W.A. and Kendrick M.P., Reply to the Discussions, Proc. Inst. Of Civil Engrs., Vol. 27, March, pp. 613-647.

McDowell, D.M. (1964) In: Field and model investigation into the reasons for siltation in the Mersey estuary, Price, W.A. and Kendrick M.P., Reply to the Discussions, Proc. Inst. Of Civil Engrs., Vol. 27, March, pp. 613-647.

O'Connor, B. A. (1987). Short and long term changes in estuary capacity. J. of Geological Soc., London, Vol. 144, pp. 187 - 195.

Prandle, D., Murray, A. and Johnson, R. (1990). Analysis of flux measurements in the River Mersey. In: Coastal and Estuarine Studies Residual currents and long-term transport processes in shallow estuaries and bays. (ed.) Cheng, R.T., Vol. 38, Springer-verlag, pp. 413 - 430.

Price, W.A. and Kendrick, M.P. (1963). Field and model investigation into the reasons for siltation in the Mersey Estuary. Proc. Inst. Civil Engrs., April, Vol 24, pp 473-518.

Pye, K. and Van der Wal, D. (2000). Historical trend analysis (HTA) as a tool for long-term morphological prediction in estuaries. In: EMPHASYS Consortium Phase 1B - Modelling Results, Interim Report, October.

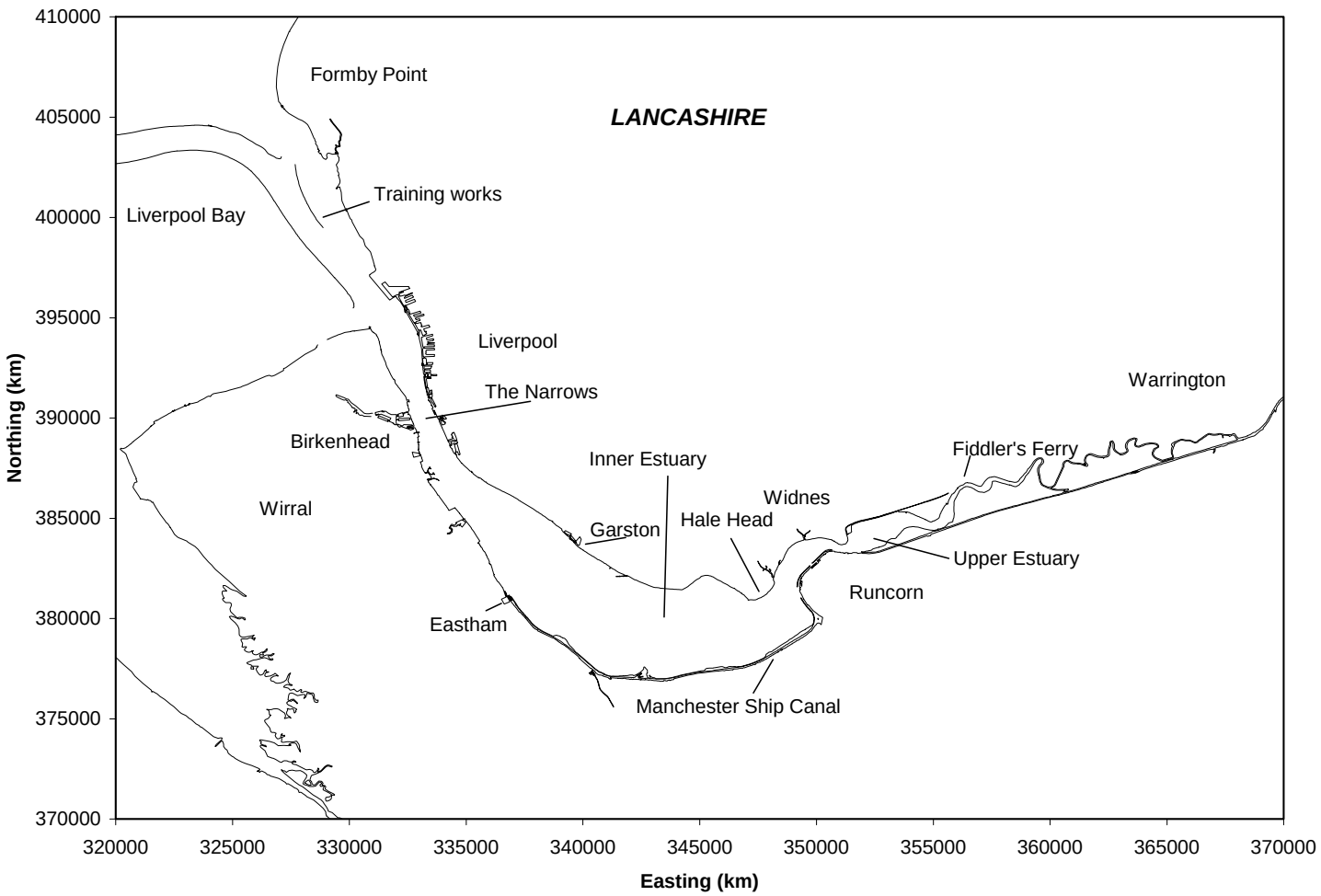
Thomas, C. (1999). Analysis of bathymetric surveys of the Mersey Estuary. HR Wallingford, Report IT 469, October, 18pp. + Figures.

Solari, L., Seminara, G., Lanzoni, S., Marani, M. and Rinaldo, A. (2002). Sand bars in tidal channels Part 2. Tidal meanders. J. Fluid Mech., Vol. 451, pp. 203 - 238.

Speer, P.E. and Aubrey, D.G. (1985). A study of non-linear propagation in shallow inlet/estuarine systems. Part II; theory. Estuarine, Coastal and Shelf Science, Vol. 21, pp. 207-224.

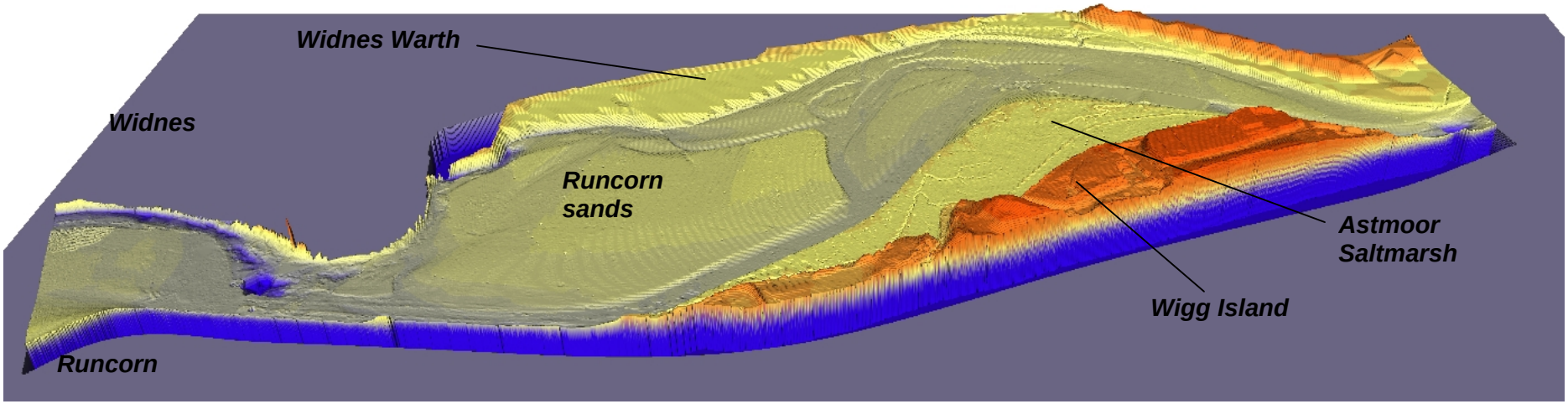
Uncles, R.J. (1981). A note on tidal asymmetry in the Severn Estuary. Estuarine, Coastal and Shelf Science, Vol. 13, pp. 419-432.

Figures



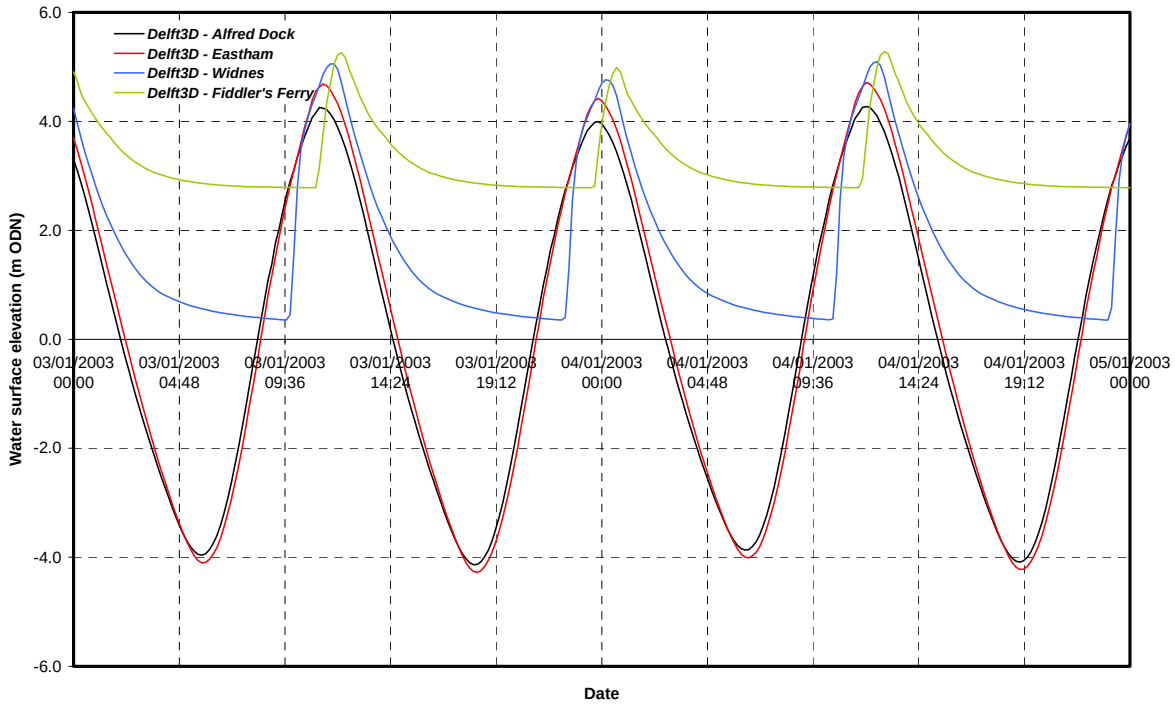
Plan of the Mersey Estuary

Figure 1

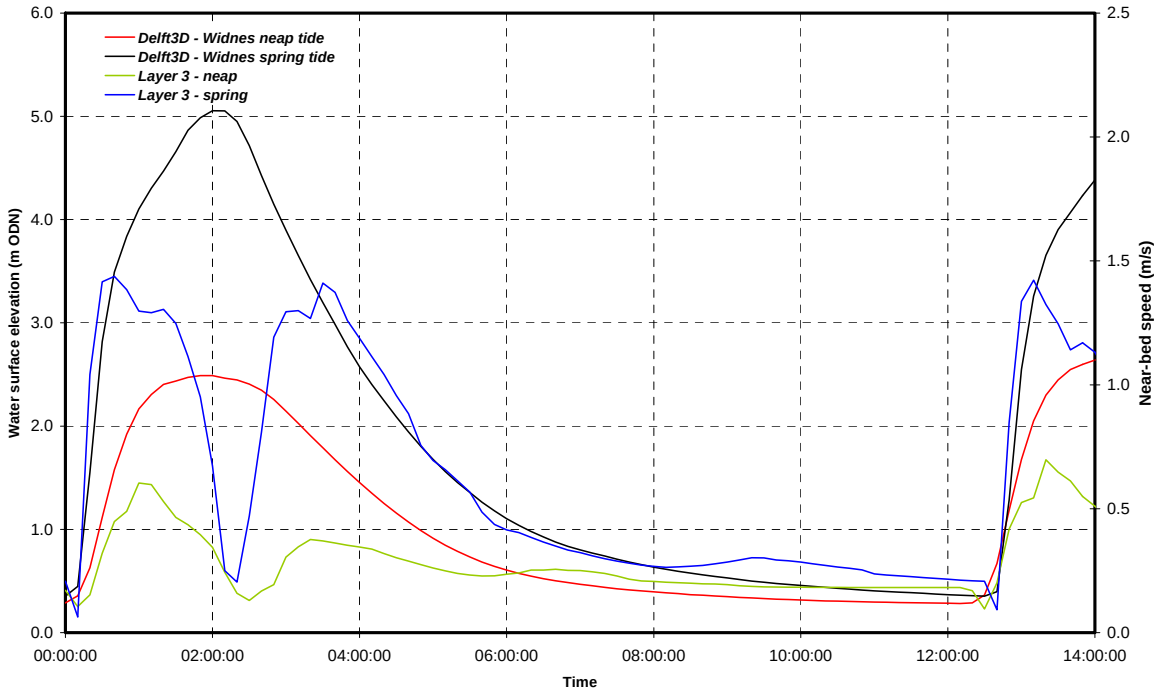


ABP mer marine environmental research	Figure showing the bathymetry as derived from data collected by the Environment Agency, 2002	Figure 2

A.



B.

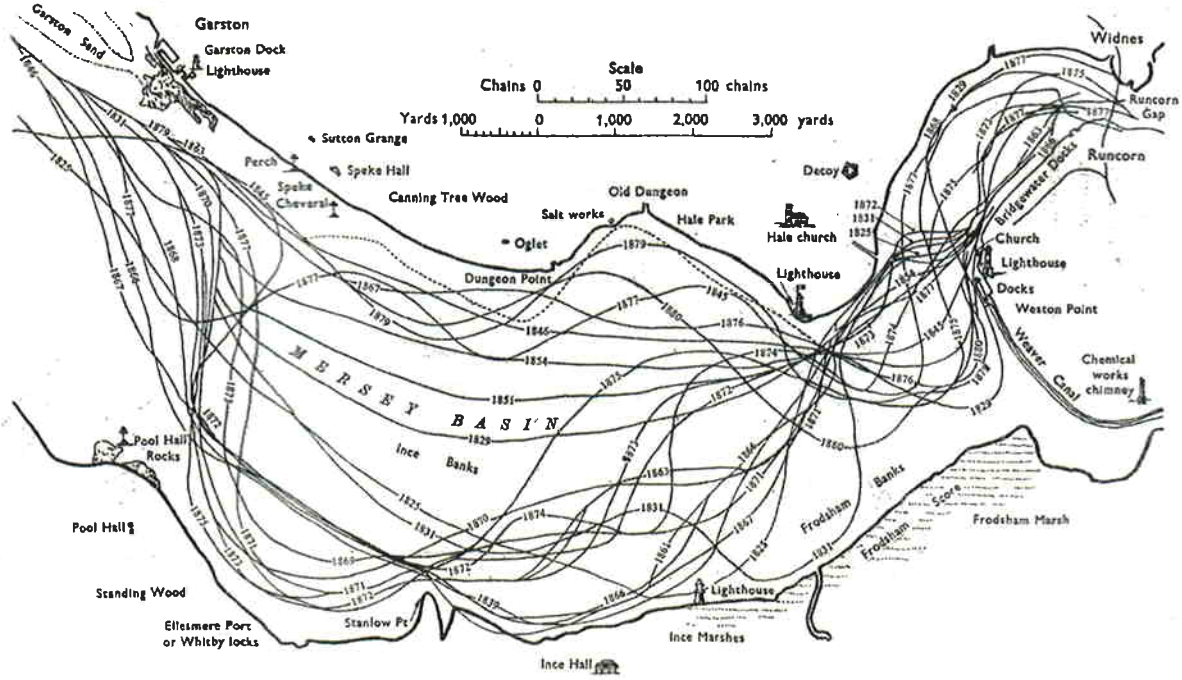


ABP mer marine environmental research

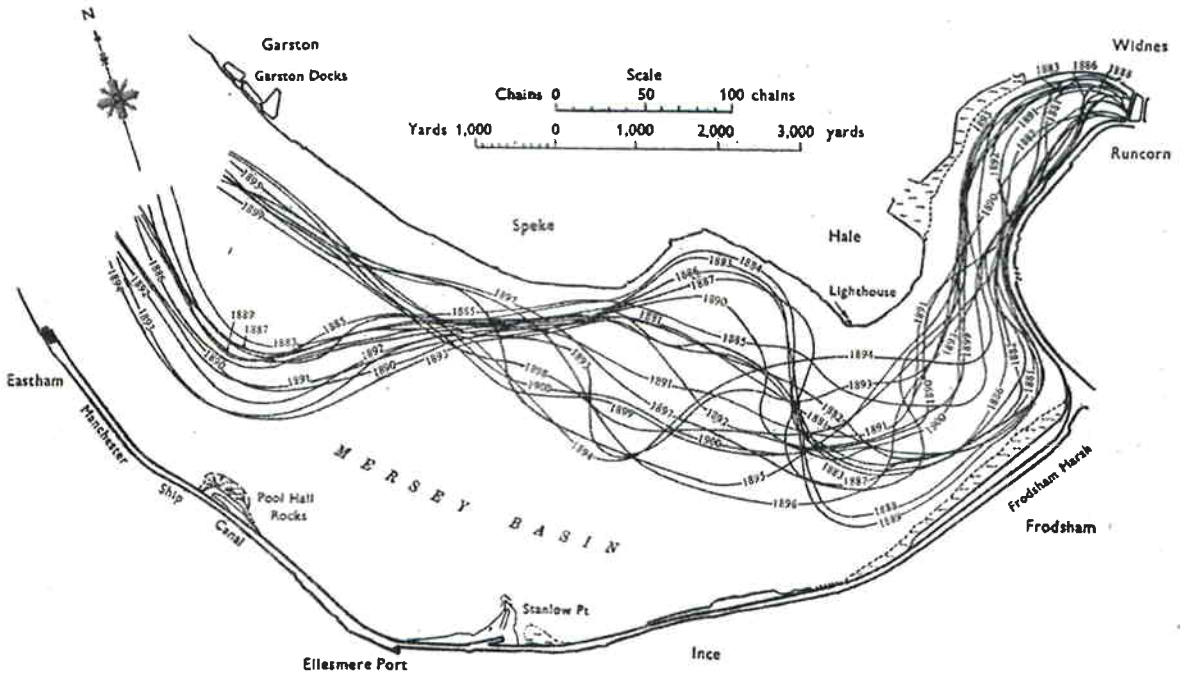
Figure showing the changes in water elevation along the Mersey Estuary (A) together with water levels and near-bed speed at Widnes for a spring and neap tide (B)

Figure 3

A.

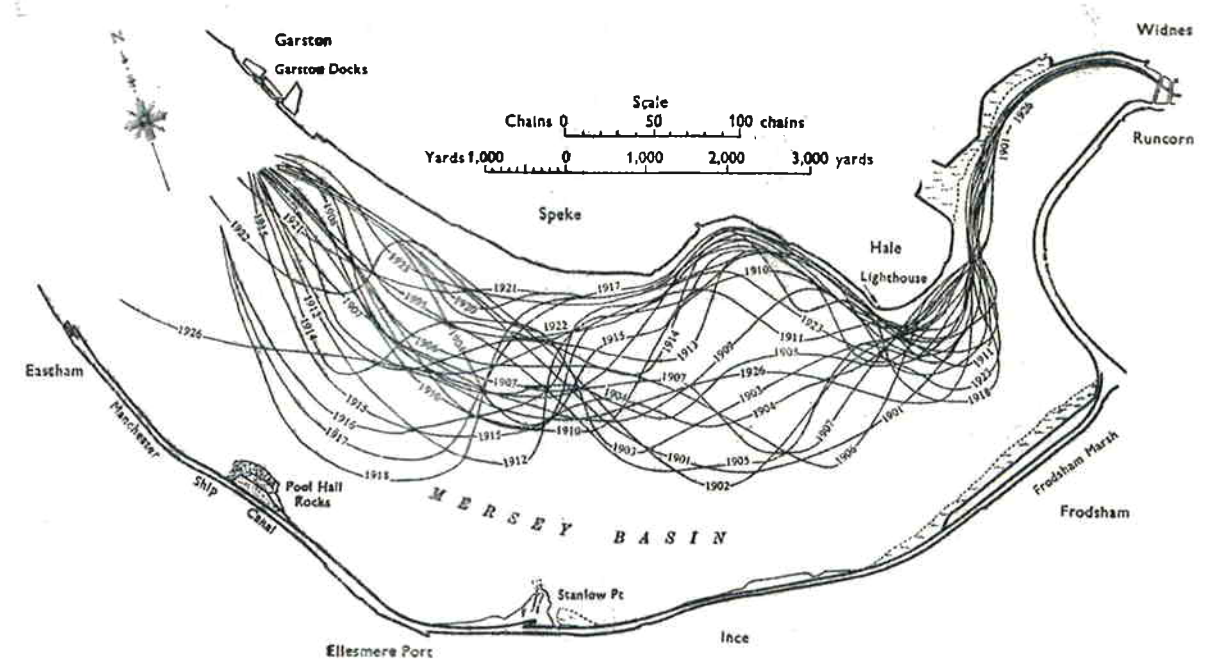


B.

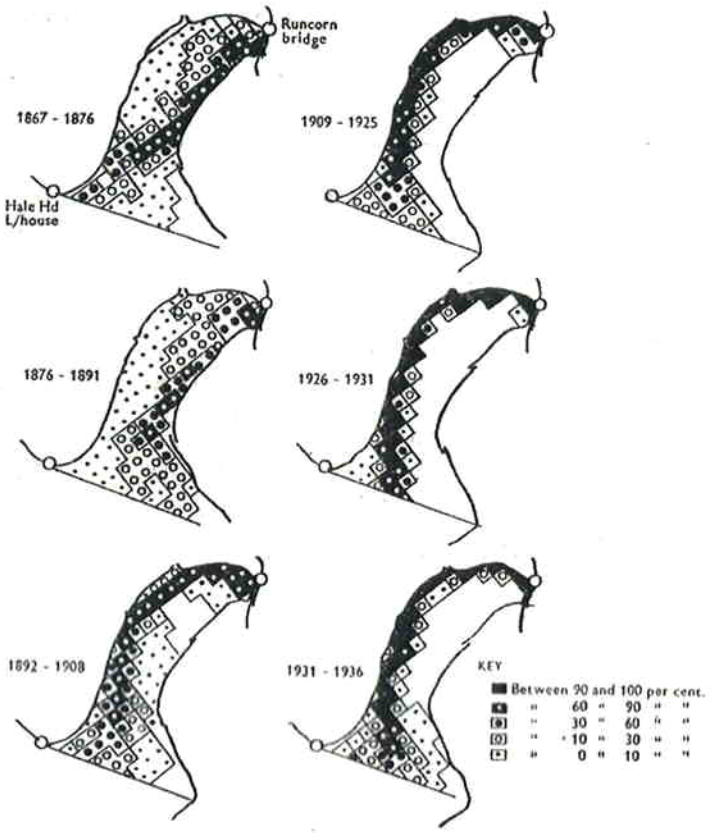


ABP mer marine environmental research	**Positions of the navigation channel in the Inner Estuary from 1825 – 1880 (A) and 1881 –1900 (B). Figures reproduced from Cashin (1949)**	**Figure 4**

A.



B.

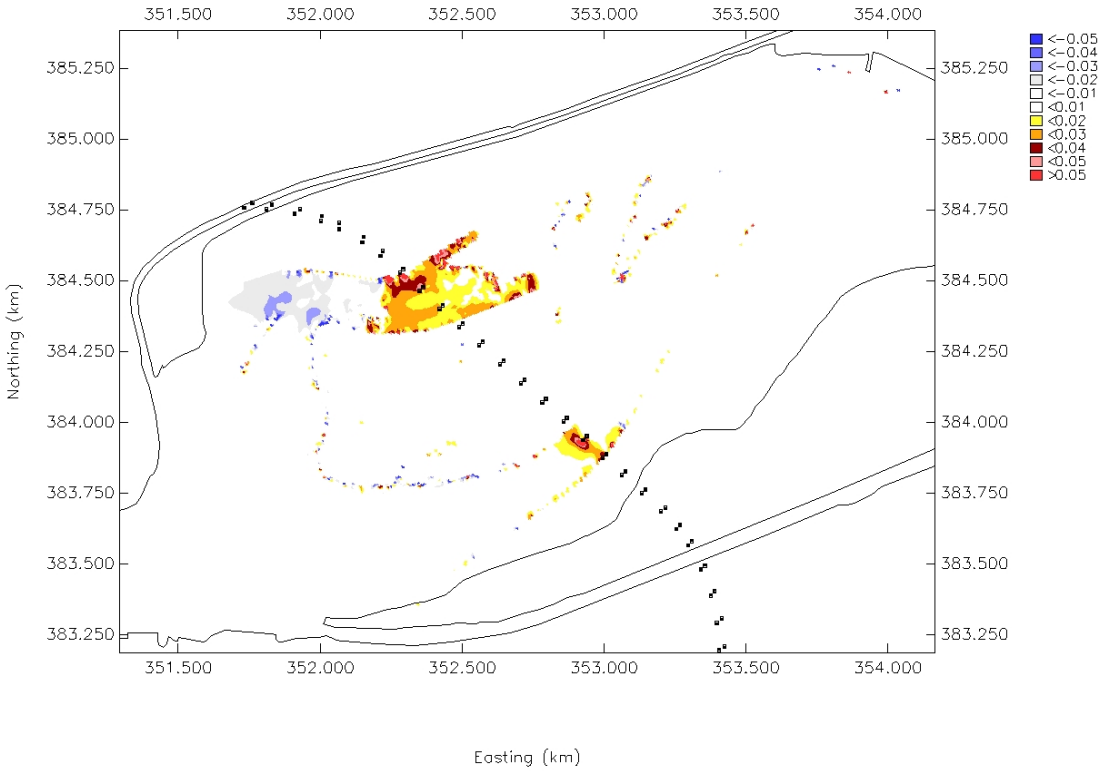


ABP mer marine environmental research

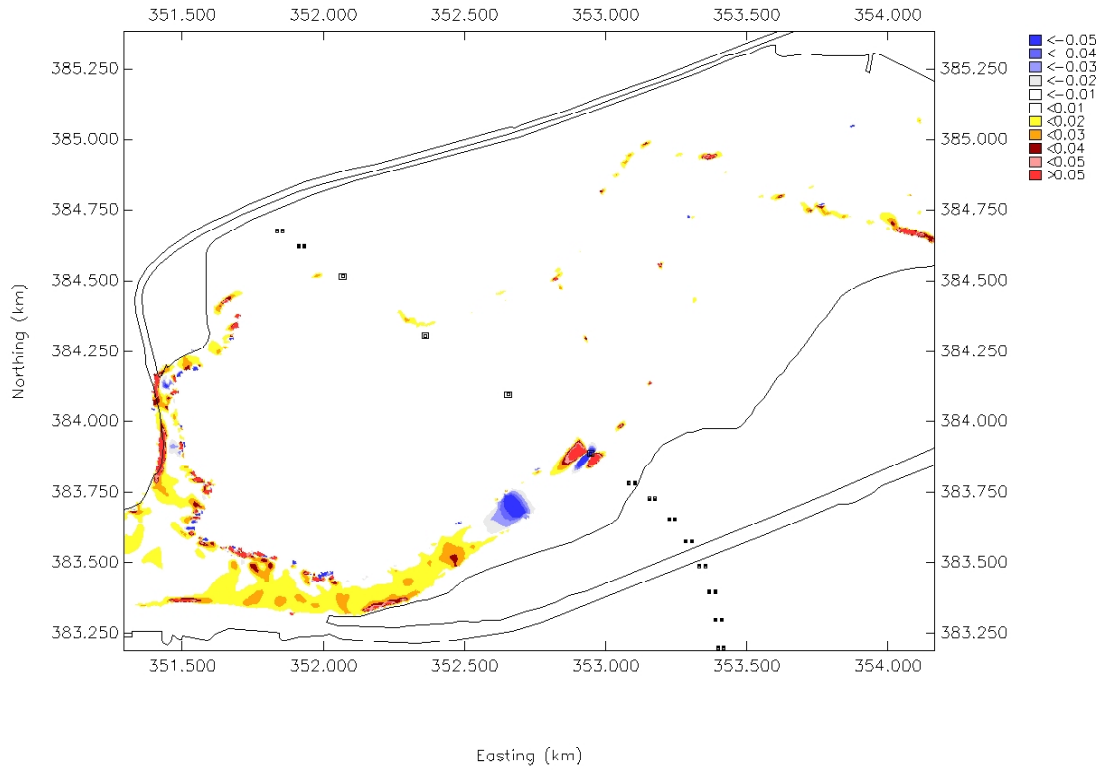
Positions of the navigation channel in the Inner Estuary from 1901 – 1926 (A) and a figure showing the stability of the main channel from Hale Head to Runcorn Bridge between 1867 – 1936. Figures reproduced from Cashin (1949)

Figure 5

A.



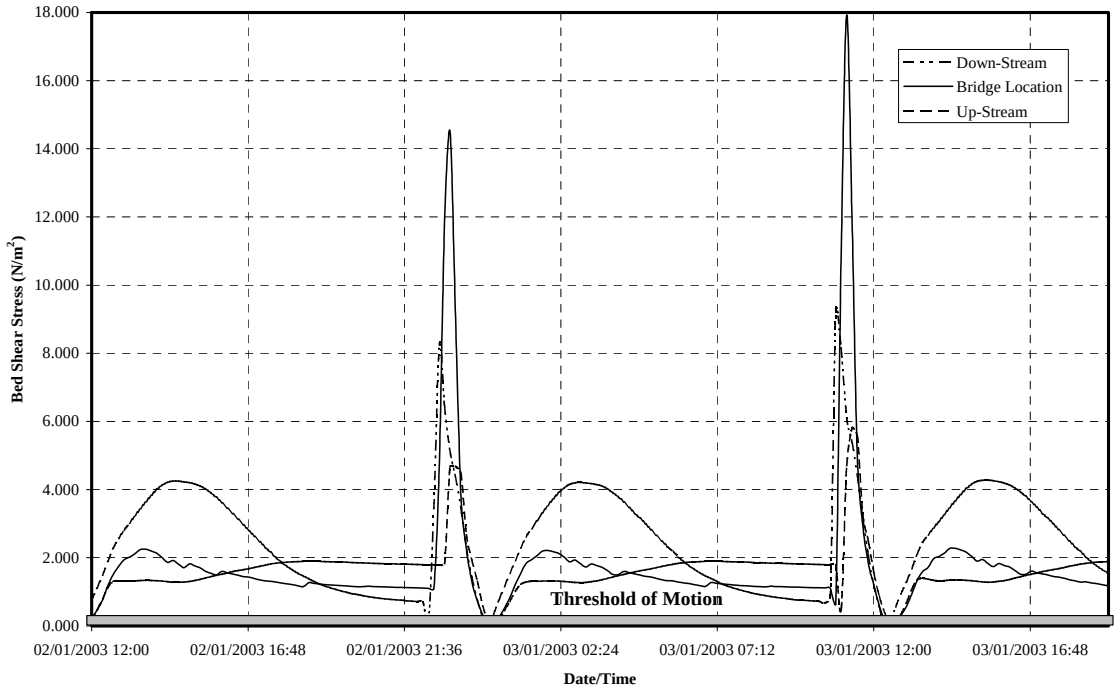
B.



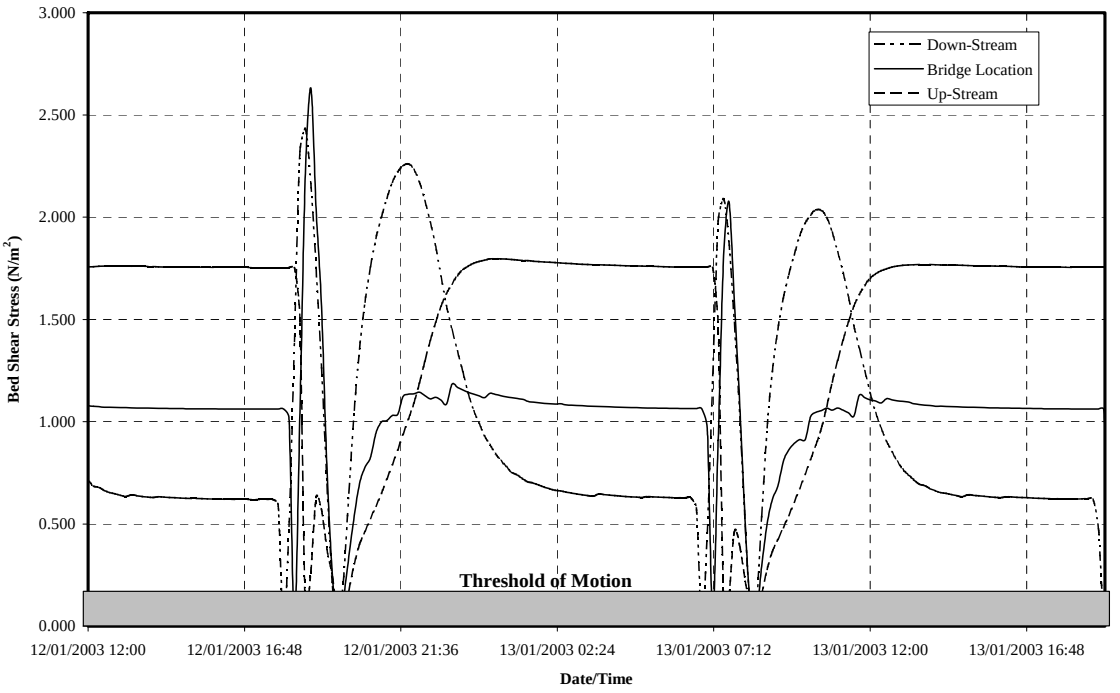
The difference in water level (m) between Route 3A Short Span revised and the baseline case around peak flood on a spring tide (A). Difference in near-surface speed (m/s) between the proposed bridge scheme Route 3A Medium and the baseline case peak flood (B) on a spring tide

Figure 6

A.

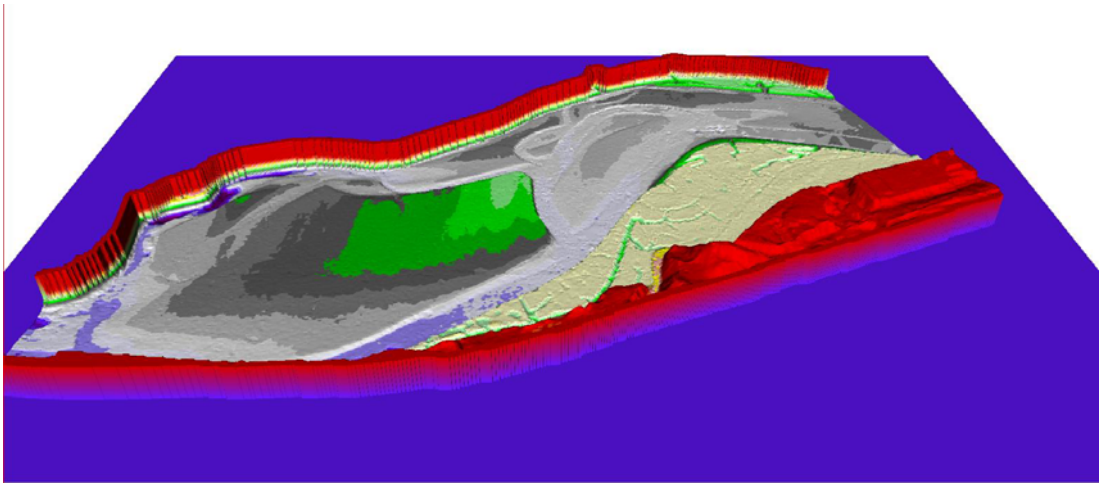


B.

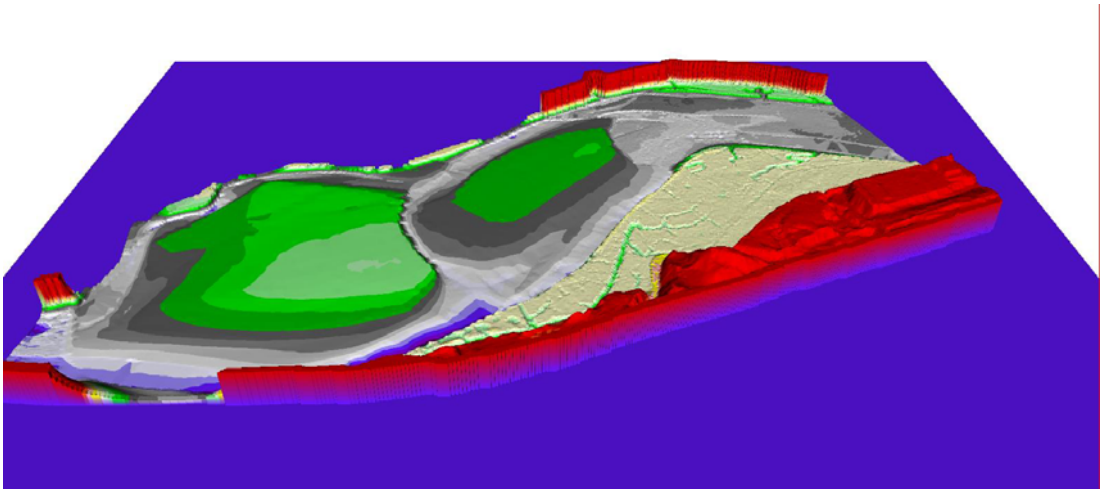


ABP mer marine environmental research	Plot of bed shear stress across the study area showing the threshold of sediment motion for 150μm grain size over spring (A) and neap (B) tides	Figure 7

A.

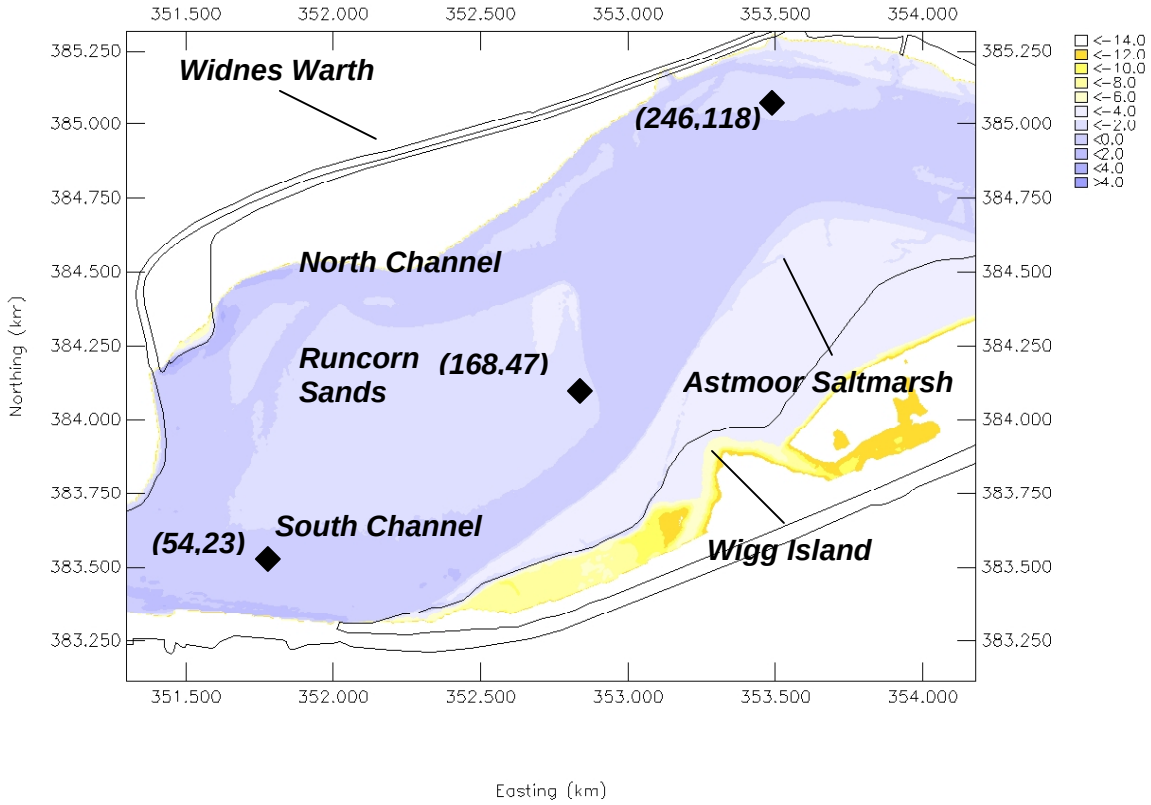


B.

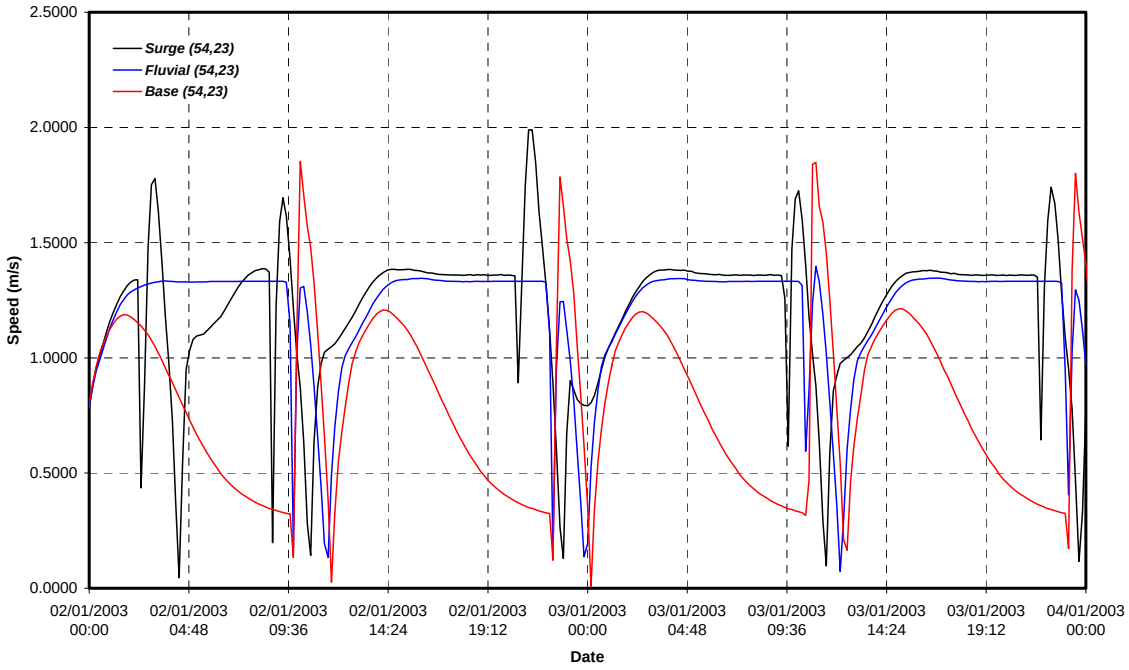


ABP mer marine environmental research	Bathymetry within the upper estuary; 2002 survey (A) 2005 survey (B)	Figure 8

A.

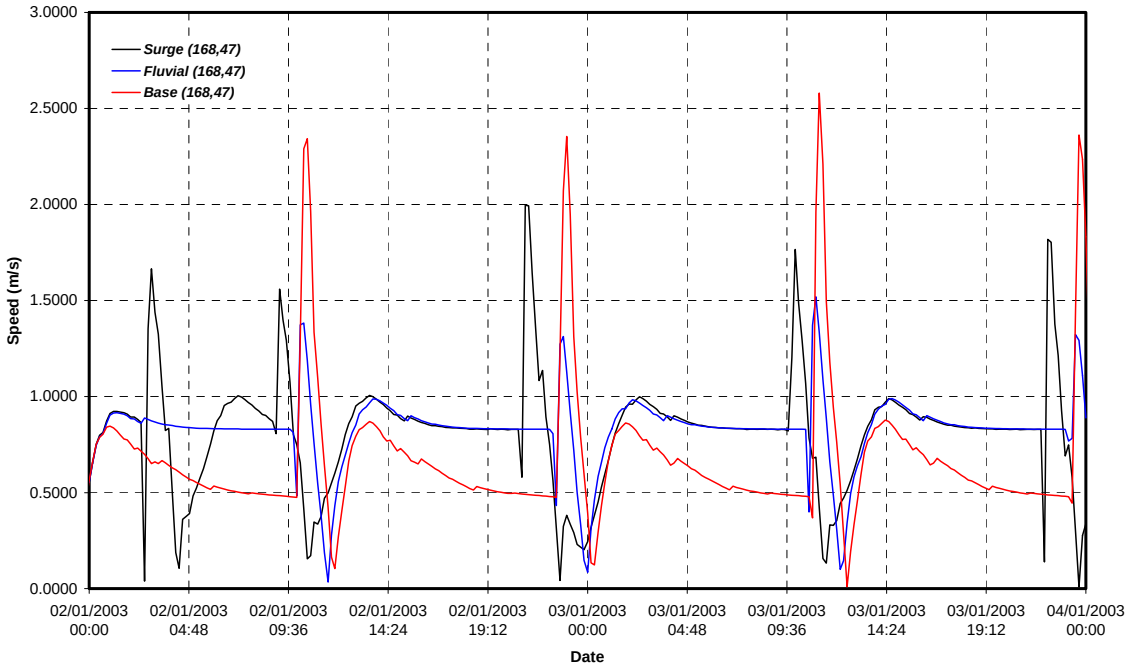


B.

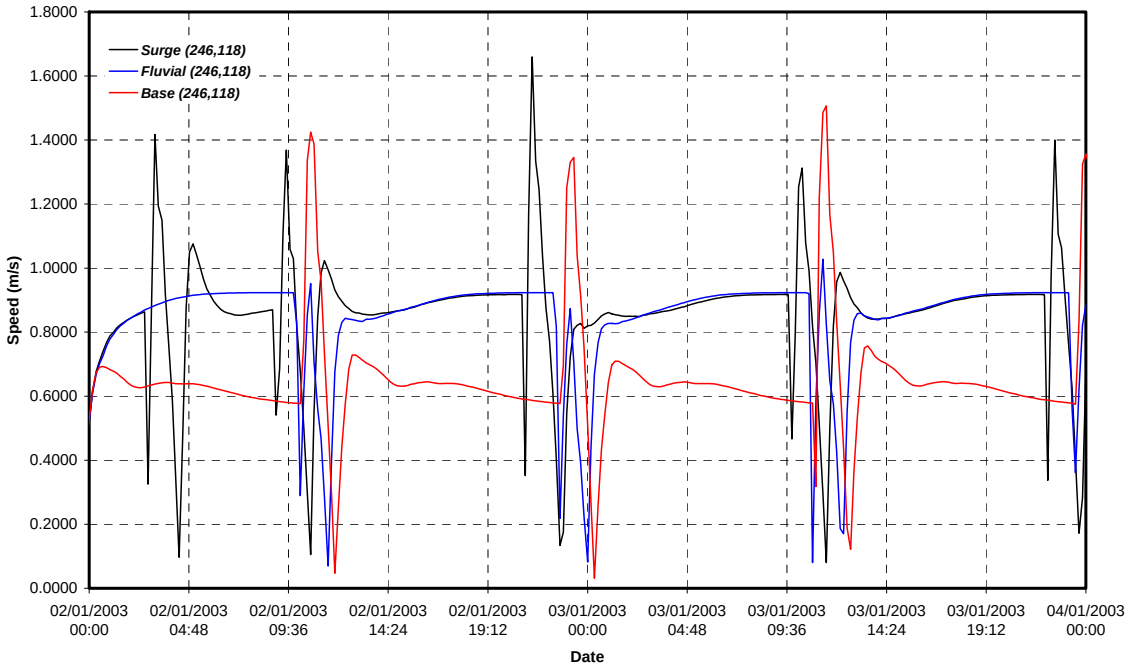


ABP mer marine environmental research	Figure A shows locations of various positions in the study area. Figure B shows the near-surface speed at position (54,23) for baseline, extreme fluvial and extreme surge and fluvial events	Figure 9

A.



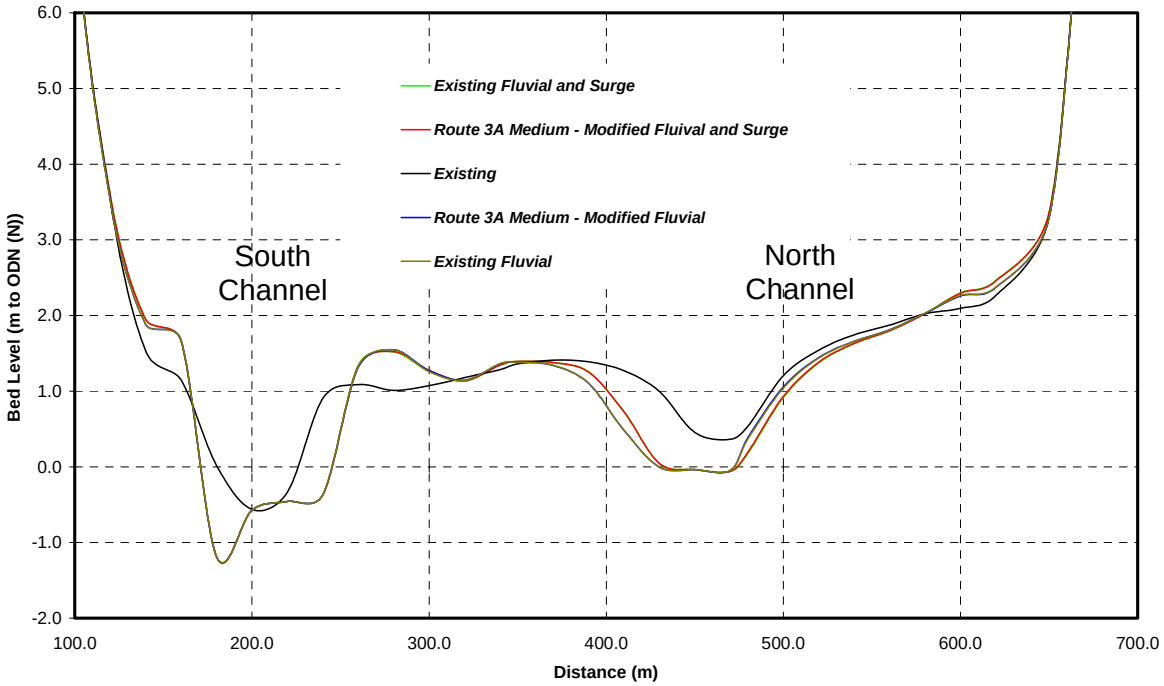
B.

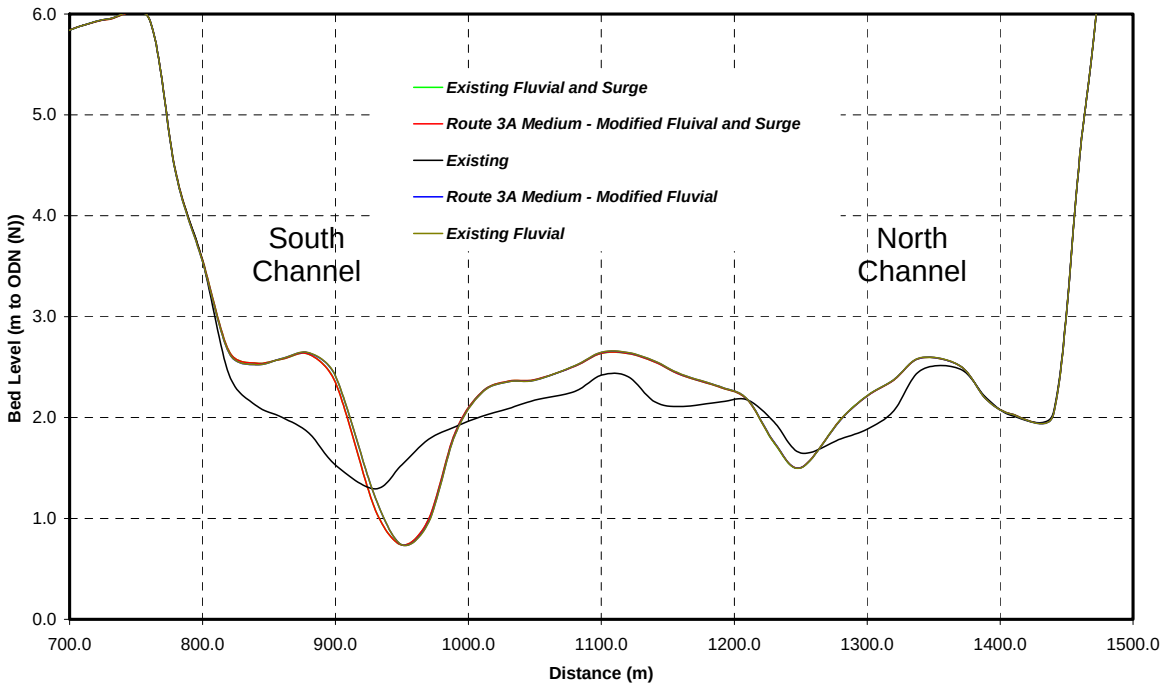


ABP mer marine environmental research

Near-surface speed at positions (168,47) (A) and (246,118) (B) for baseline, extreme fluvial and extreme surge and fluvial events

Figure 10





ABP mer marine environmental research	Figure shows cross – Sections C and L for the existing condition and for extreme fluvial and combined extreme surge and fluvial events	Figure 11

Appendices

Appendix A

Hydrodynamic Model

Appendix A. Hydrodynamic Model

A1. Introduction

As part of the Phase II studies for the New Mersey Crossing Project two detailed hydrodynamic models of the Mersey Estuary have been configured, calibrated and validated. The most detailed of these models consists of 5 dynamically linked model grids that provide a varying level of resolution across the whole model area. The other detailed model consists of 3 dynamically linked model grids also providing a varying level of resolution across the whole model area. The most detailed model has been used for the hydrodynamic simulations whereas the 3 grid model has been used for the morphological modelling. This has been necessary to enable long-term morphological simulations to be undertaken within a sensible time-scale.

During Phase I of the project a single grid Delft-3D model of the Mersey Estuary was configured, calibrated and validated to provide a means of assessing the local hydrodynamic regime and any significant changes to this regime brought about by the proposed bridge crossing. This model consisted of a curvilinear grid with an open tidal boundary across the estuary in the vicinity of Gladstone Dock (Figure A1) and the upstream end of the model finishing at Howley Weir. In Phase II of the study this model was adapted to provide two high-resolution models in the area of the proposed crossing. Figures A2 and A3 show the layout of the two new models and their grids. The boundaries of the new models remain unchanged with those used previously.

A2. Physical Processes to be Described

The form an estuary takes is influenced by a range of physical processes that operate over varying temporal and spatial scales. The hydrodynamic regime is defined here as the behaviour of bulk water movements driven by the action of tides and non-tidal influences such as river flows and meteorological conditions (e.g. winds, atmospheric pressure and storm events). The Mersey Estuary is dominated by the tidal flows, with variations in tidal elevation at the mouth of between 4 to 10m over the extremes of the neap-spring cycle. Maximum tidal currents through the narrows can exceed 3m/s (Halliwell and O'Connor, 1967).

A3. Model Type

The present study has adopted a 3-D description of the estuary with 5 - 10 layers through the vertical. The number of layers and grid resolution dictates the computational speed of the simulations. Having more vertical layers enables more accurate sediment transport predictions to be made. The reproduction of helical flow

around the bends is reproduced in a 3-D model description. Within the 5 grid model the outer part of the estuary is described with only 5 layers in the vertical in order to reduce the computational run times. However, in the area of interest 10 vertical layers have been used. Within the 3 grid model 8 layers have been used throughout.

The models use the domain decomposition module of Delft3D allowing a model grid to be subdivided into several smaller model domains (sub-domains). The sub-division is based on the horizontal and vertical model resolution required for adequately simulating the key physical processes under consideration. Domain decomposition allows for local grid refinement in both the horizontal and vertical directions.

A4. Data Requirements

In order to set up the numerical model various data inputs are required. The following data inputs have been used in the current study:

- Land boundary
- Bathymetric data
- Boundary conditions:
  - Seaward tidal boundary conditions (harmonic tidal constituents)
  - Freshwater discharge information
- Calibration and Verification data
- Water levels
- Flow speeds and directions

A5. Model Design

The computational grids have been set up to include the inner part of the Mersey Estuary up to the tidal limit at Howley Weir. Fluvial flows are described by internal boundaries set up within the estuary and described with line discharges. Figures A2 and A3 show the curvilinear model grids. Delft-3D uses a curvilinear grid system allowing for the more accurate representation of the boundaries of a natural system compared to a rectilinear grid. This enables the model to provide greater resolution in the areas requiring more detail, for example around river bends/meanders. The grid design has been significantly refined in the area of interest in the vicinity of Widnes to Fiddler's Ferry. Within the 5 grid model the resolution of the grid in this area is in the order of 3m to 10m, typically. For the less refined 3 grid model the cell sizes are typically between 20m - 30m. The outer extents of the model were dictated primarily by the requirement to have a boundary far enough away not to influence the numerical solution in the area of interest and to provide good boundary conditions.

The water depth information (bathymetry) used within the numerical model was based on 2002 survey data provided by the Environment Agency. The data were collected using both LIDAR and conventional sonar surveys.

A6. Model Boundary Conditions

The model boundary conditions applied within the Mersey Estuary were derived from water level time-series obtained from the tide gauge at Gladstone Dock. Harmonic analysis of the time-series data was undertaken to provide astronomical tidal constituents at the boundary. A total of 57 tidal constituents were used to generate the boundary conditions.

A7. Representation of Bridge Piers in the Model

In Phase I of the study the representation of the bridge piers in the model was through the addition of a quadratic friction term to the momentum equations. This additional friction term influences the horizontal flow distribution and, therefore, indirectly the turbulent mixing (ABPmer 2003). Using this friction term it is possible to represent the effect of piles in the model.

The horizontal forces due to flow on a vertical section, Δz of a single pile are given by the equations:

$$F_u = \frac{\rho C_D D}{2} U_{Eff} \left| \langle U_{Eff} \rangle \right| \Delta z$$

$$F_v = \frac{\rho C_D D}{2} V_{Eff} \left| \langle U_{Eff} \rangle \right| \Delta z$$

Where:

F_u = The drag force on the pile in the u co-ordinate direction - inline force
F_v = The drag force on the pile in the v co-ordinate direction - transverse force
C_D = The drag coefficient ($\approx$ 1 in tidal flow regime)
ρ = Density of water
$\langle U_{Eff} \rangle$ = Effective approach velocity vector
$\left| \langle U_{Eff} \rangle \right|$ = Magnitude of the effective approach velocity vector
D = Pier diameter
Δz = Length of vertical section of pier
V_{Eff} = Effective transverse flow velocity

It is assumed that the piers under consideration do not lie in each other's wake. The effective approach velocity is determined from the flow velocity using the wet cross-sectional area that is not blocked by the pier(s).

$$\langle U_{Eff} \rangle = \langle U \rangle \left\{ \frac{A_{Total}}{A_{Eff}} \right\} = \langle U \rangle a$$

where:

A_{Total} =Total cross-sectional area

A_{Eff} = Effective wet cross-sectional area (A_{Total} - area blocked by pier(s))

$a = \left\{ \frac{A_{Total}}{A_{Eff}} \right\}$

Therefore, the total force on the flow due to the piers can be written as:

$$F_{Total,u} = N \frac{\rho C_D D}{2} U_{Eff} \left| \langle U_{Eff} \rangle \right| \Delta z$$

$$F_{Total,v} = N \frac{\rho C_D D}{2} V_{Eff} \left| \langle U_{Eff} \rangle \right| \Delta z$$

Where:

N = The number of piers in the model grid cell

F_{Total} = Total resistance force

Since the additional friction is applied as a loss term in the equations, it is possible to describe the loss coefficients in the *u* and *v* co-ordinate directions by the equations:

$$C_{Loss,u} = N \frac{C_D D}{2 \Delta y} a^2$$

$$C_{Loss,v} = N \frac{C_D D}{2 \Delta x} a^2$$

It is these terms that are determined for input into the model. The added friction term is applied to all of a cell, therefore, in instances where adjacent cells contain this additional friction term the results are likely to be conservative. The drag coefficients were calculated for each scenario using the pier dimensions and shape for each respective scheme.

However, in the current modelling for the Phase II stage the bridge piers and towers in the two models have been simulated using a combination of approaches. Where bridge piers and towers are the same size as the model grid cells the cells have been closed off as they are effectively blocked for the transmission of fluid flow. However, where the bridge piers are smaller than the grid cell size added friction terms have been used to represent the piers. In this manner there is an allowance for some flow transmission across the cell, even if that flow is low.

Whilst the piers and towers are octagonal in shape their representation in the model when represented as solid structures is as squares. However, it is not considered that pier shape will have a significant impact on the results as flow separation and viscous effects are excluded from the model solution and only flow transmission effects as a result of blockage are simulated.

A8. Model Calibration and Validation

To provide a measure of confidence in a modelling scheme a calibration and validation exercise is required. Model calibration allows the adjustment of certain model parameters in order to optimise the simulation of reality against a set of measurements. The model is calibrated against measured tide levels at various tidal gauging stations along the length of the estuary to ensure the model reproduces the correct water levels. In addition, tidal current measurements are used to calibrate the flow vectors determined by the model results at selected sites along the estuary. For quality control in the numerical model ABPmer use the guidelines laid down by the Environment Agency (Bartlett, 1998).

The validation exercise determines whether a model is 'fit for purpose'. The model is applied to a new set of measurements with no alteration or further calibration. The ability of the model to reproduce these new data is used to assess the model's performance. For estuaries typical performance criteria can be expressed in percentage terms as:

- Speeds to within ±10-20% of observed speeds
- Levels to within 15% of spring tidal ranges or 20% of neap tidal ranges.

The validation exercise is similar to the calibration exercise subject to inherent variability of the real world. The model has been calibrated against a series of spring tides and validated against a series of neap tides. A constant freshwater discharge was applied at the tidal limit (Howley Weir) based on a 1: 1 year return period (Appendix B) and this was applied to both the calibration and validation runs.

A8.1 Hydrodynamic Model (5 Grids)

The initial calibration exercise has been undertaken using tidal stream data obtained from predicted water levels determined using the UK Hydrographic Office TotalTide software package. Some of the results for the 5 grid high resolution model are shown in Figures A5-A7.

Tables A1 and A2 show the results of a comparison of root-mean-square (RMS) error values of flow speed and direction and water surface elevation over a 6 days period. Also shown are the mean values over the same 6 days period.

Table A1a. Calibration of model flow speeds against tidal stream data

Tidal Diamond	TotalTide u_{mean} (m/s)	Model u_{mean} (m/s)	TotalTide u_{rms} (m/s)	Model u_{rms} (m/s)	rms % Difference
SN045L	1.27	1.45	0.698	0.648	7.16
SN045M	1.23	1.50	0.736	0.689	6.39
SN045N	1.02	1.32	0.616	0.619	0.45

Table A1b. Calibration of model flow directions against tidal stream data

Tidal Diamond	TotalTide θ_{mean} (degrees)	Model θ_{mean} (degrees)	TotalTide θ_{rms} (degrees)	Model θ_{rms} (degrees)	rms % Difference
SN045L	270.29	267.16	90.04	95.65	-6.23
SN045M	258.62	260.51	79.19	84.41	-6.59
SN045N	243.75	232.98	81.42	90.64	-11.32

Table A2a. Calibration of model against water levels determined using TotalTide

Gauge Station	TotalTide/Field h_{mean} (m)	Model h_{mean} (m)	TotalTide/Field h_{RMS} (m)	Model h_{RMS} (m)	% Difference
Alfred Dock	0.04	-0.03	2.731	2.678	1.94
Eastham	0.09	0.09	2.853	2.799	1.89
Widnes	2.49	1.64	1.527	1.412	7.53

Phase differences in the timing of high water at the three tidal stations averaged over the simulation period for the spring tide are shown in Table A2b.

Results from the calibration run compare favourably with the TotalTide predictions. The differences observed between the model prediction and the TotalTide prediction on moving upstream from Eastham are an artefact of TotalTide failing to reproduce the non-linear shallow water effects in the tidal signature, for example in the predicted tidal signal at Widnes (Figure A5). Therefore, the TotalTide prediction is not representative of the shape of the actual tidal curve. The calibration results show RMS differences in the mean water levels at the various water level stations to be in the range of 6-11%.

A comparison of the model against tidal stream data (Figures A6-A7) also shows good agreement, with rms errors in directions within 11% and speeds within 7%.

Table A2b. Calibration of model against timings of high and low waters at the tide gauge stations as determined using TotalTide

Gauge Station	Mean Difference (min)
Alfred Dock	3.43
Eastham	4.00
Widnes	13.27

Results of the validation exercise are shown in Tables A3 and A4. In addition, some of the results are shown in Figures A8-A11. The RMS values have been calculated over a 6 days period during a neap part of the tidal cycle. The flow speeds are reasonably well reproduced and are within the Environment Agency guidelines (Bartlett, 1998) of between ±10-20%. The general direction of flow is well represented with a RMS error of, typically, between ±6 - 11%.

Table A3a. Validation of model flow speeds against tidal stream data

Tidal Diamond	TotalTide u_{mean} (m/s)	Model u_{mean} (m/s)	TotalTide u_{rms} (m/s)	Model u_{rms} (m/s)	rms % Difference
SN045L	0.91	0.97	0.519	0.481	7.32
SN045M	0.96	0.99	0.589	0.493	16.30
SN045N	0.80	0.89	0.494	0.438	11.34

Table A3b. Validation of model flow directions against tidal stream data

Tidal Diamond	TotalTide θ_{mean} (degrees)	Model θ_{mean} (degrees)	TotalTide θ_{rms} (degrees)	Model θ_{rms} (degrees)	rms % Difference
SN045L	268.80	262.86	86.96	97.06	-11.61
SN045M	257.72	253.96	79.58	85.00	-6.81
SN045N	243.30	227.84	81.70	89.19	-9.17

A comparison of RMS values of water levels at the tidal gauge stations over the same 6 days period show good agreement with tidal amplitude (less than ±8%). The rms error calculated for Fiddler's Ferry is misleading as TotalTide ignores the non-linear shallow water effects in its prediction, as stated previously, and predicts low water values that are below the bed level at that position in the estuary. The numerical model is performing well within the target values stated in Environment Agency guidelines (Bartlett, 1998).

Table A4a. Validation of model against water levels determined using TotalTide and measurements†

Gauge Station	TotalTide h_{mean} (m)	Model h_{mean} (m)	TotalTide h_{RMS} (m)	Model h_{RMS} (m)	% Difference
Alfred Dock	0.04	0.03	1.898	1.734	8.64
Eastham	0.06	0.09	1.918	1.816	5.32
Widnes	1.74	1.07	1.180	0.968	17.97
Old Quay Lock†	1.19	1.31	0.791	0.667	15.68
Wigg Island†	2.30	2.20	0.330	0.217	34.24

Table A4b. Validation of model against timings of high water at the tide gauge stations as determined using TotalTide and measurements†

Gauge Station	Mean Difference (min)
Alfred Dock	5.62
Eastham	10.41
Widnes	14.17
Old Quay Lock†*	10.68
Wigg Island†*	10.81
* Calculated using high-water values only	

A8.2 Morphological Model (3 Grids)

The tabulated results for the morphological model are given in Tables A5 - A8. Figures A12 and A13 show example output from the model. As previously, the initial calibration exercise has been undertaken using tidal stream data obtained from predicted water levels determined using the UK Hydrographic Office TotalTide software package.

Results from the calibration run compare favourably with the TotalTide predictions and the measured field data. The calibration results show RMS errors in the water levels at the various stations to be typically, in the range of 5-7%.

Table A5a. Calibration of model flow speeds against tidal stream data

Tidal Diamond	TotalTide u_{mean} (m/s)	Model u_{mean} (m/s)	TotalTide u_{rms} (m/s)	Model u_{rms} (m/s)	rms % Difference
SN045L	1.27	1.41	0.698	0.652	6.59
SN045M	1.23	1.49	0.736	0.685	6.92
SN045N	1.02	1.27	0.616	0.615	0.16

Table A5b. Calibration of model flow directions against tidal stream data

Tidal Diamond	TotalTide θ_{mean} (degrees)	Model θ_{mean} (degrees)	TotalTide θ_{rms} (degrees)	Model θ_{rms} (degrees)	rms % Difference
SN045L	270.29	268.01	90.04	95.05	-5.56
SN045M	258.62	261.09	79.19	84.54	-6.76
SN045N	243.75	233.35	81.42	90.02	-10.56

Table A6a. Calibration of model against water levels determined using TotalTide

Gauge Station	TotalTide/Field h_{mean} (m)	Model h_{mean} (m)	TotalTide/Field h_{RMS} (m)	Model h_{RMS} (m)	% Difference
Alfred Dock	0.04	-0.23	2.731	2.572	5.82
Eastham	0.09	-0.19	2.853	2.687	5.82
Widnes	2.49	1.56	1.527	1.421	6.94

Phase differences in the timing of high water at the three tidal stations averaged over the simulation period for the spring tide are shown in Table A6b.

A comparison of the model against tidal stream data also shows good agreement, with RMS errors in directions within 10% and speeds within 7%.

Table A6b. Calibration of model against timings of high and low waters at the tide gauge stations as determined using TotalTide and measurements†

Gauge Station	Mean Difference (min)
Alfred Dock	5.52
Eastham	4.90
Widnes	11.81

Results of the validation exercise are shown in Tables A7 and A8. In addition, Figure A13 shows a comparison of the model against tidal stream data at station SN045M. The RMS values have been calculated over a 6 days period during a neap part of the tidal cycle. The flow speeds are reasonably well reproduced and are within the Environment Agency guidelines (Bartlett, 1998) of between ±10-20%. The general direction of flow is well represented with a RMS error of, typically, less than ±8%.

Table A7a. Validation of model flow speeds against tidal stream data

Tidal Diamond	TotalTide u_{mean} (m/s)	Model u_{mean} (m/s)	TotalTide u_{rms} (m/s)	Model u_{rms} (m/s)	rms % Difference
SN045L	0.91	1.02	0.519	0.492	5.20
SN045M	0.96	1.07	0.589	0.541	8.15
SN045N	0.80	0.85	0.494	0.443	10.32

Table A7b. Validation of model flow directions against tidal stream data

Tidal Diamond	TotalTide θ_{mean} (degrees)	Model θ_{mean} (degrees)	TotalTide θ_{rms} (degrees)	Model θ_{rms} (degrees)	rms % Difference
SN045L	268.80	260.12	86.96	94.51	-8.68
SN045M	257.72	250.22	79.58	85.29	-7.18
SN045N	243.30	234.15	81.70	87.24	-6.78

A comparison of RMS values of water levels at the tidal gauge stations over the same 6 days period show reasonable agreement with tidal amplitude. Overall, the numerical model is performing well within the target values stated in Environment Agency guidelines (Bartlett, 1998).

Table A8a. Validation of model against water levels determined using TotalTide and measurements†

Gauge Station	TotalTide h_{mean} (m)	Model h_{mean} (m)	TotalTide h_{RMS} (m)	Model h_{RMS} (m)	% Difference
Alfred Dock	0.04	0.02	1.898	1.744	8.11
Eastham	0.06	0.07	1.918	1.810	5.63
Widnes	1.74	1.15	1.180	0.974	17.46
Old Quay Lock†	1.19	1.24	0.791	0.671	15.17
Wigg Island†	2.30	2.23	0.330	0.228	30.90

Table A8b. Validation of model against timings of high water at the tide gauge stations as determined using TotalTide and measurements†

Gauge Station	Mean Difference (min)
Alfred Dock	5.52
Eastham	10.90
Widnes	16.48
Old Quay Lock†*	11.71
Wigg Island†*	10.90
* Calculated using high-water values only	

A9. Conclusions

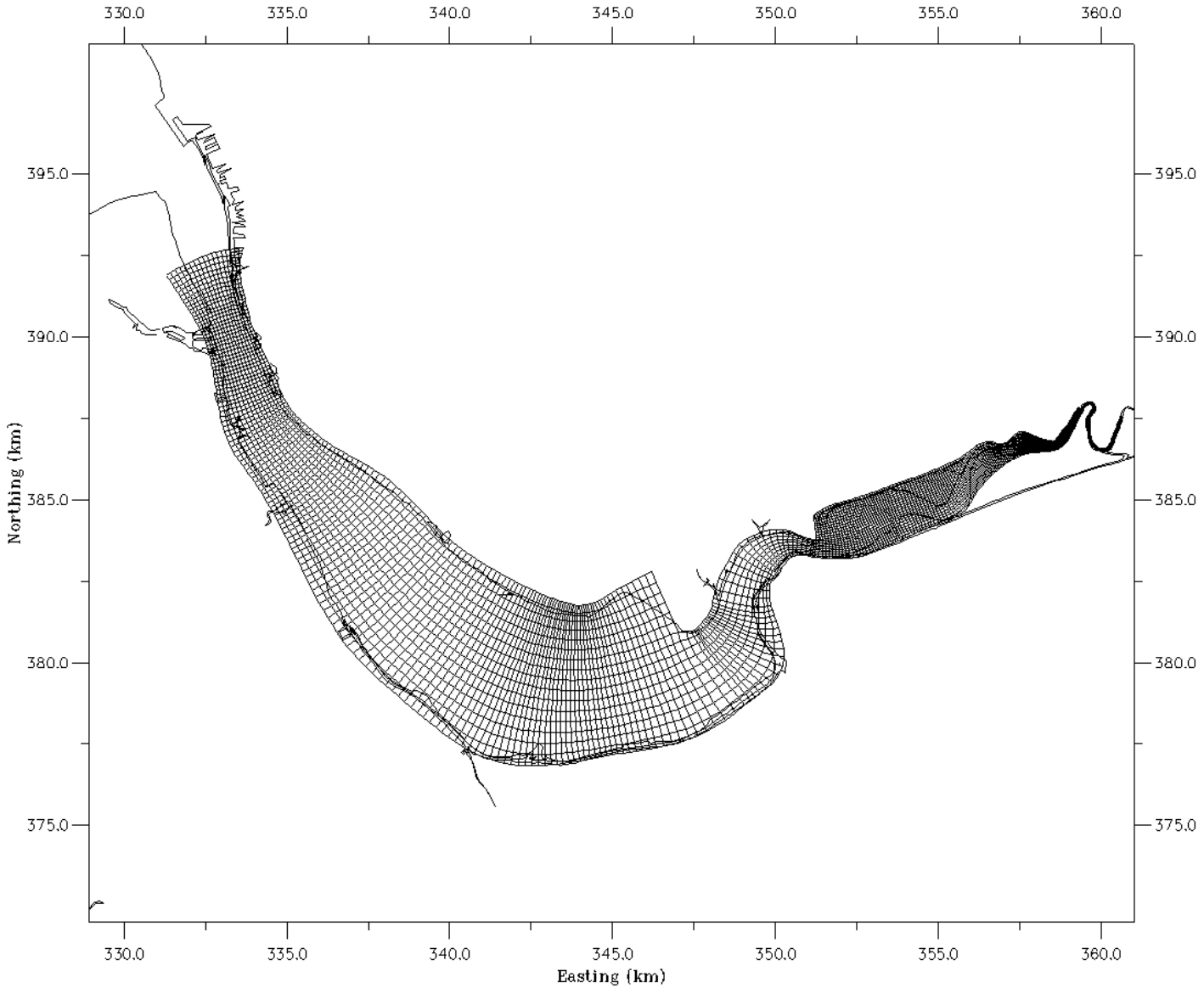
The models can be considered as meeting the initial requirements of this calibration/validation exercise. The comparison of water level data obtained from field measurements at sites close to Old Quay Lock and Wigg Island show the model to be performing reasonably well. There will always be variations between the model and reality since the model does not account for meteorological forcing, which can have a significant impact on water levels. Changes in model bathymetry can also be important and in estuaries that have particularly mobile morphology (as in the study area) the model should use as recent a bathymetric survey as is available to ensure reasonable reproduction of the main seabed/riverbed features.

A10. References

ABPmer (2003). New Mersey Crossing. May, Rep. No. R.1007.

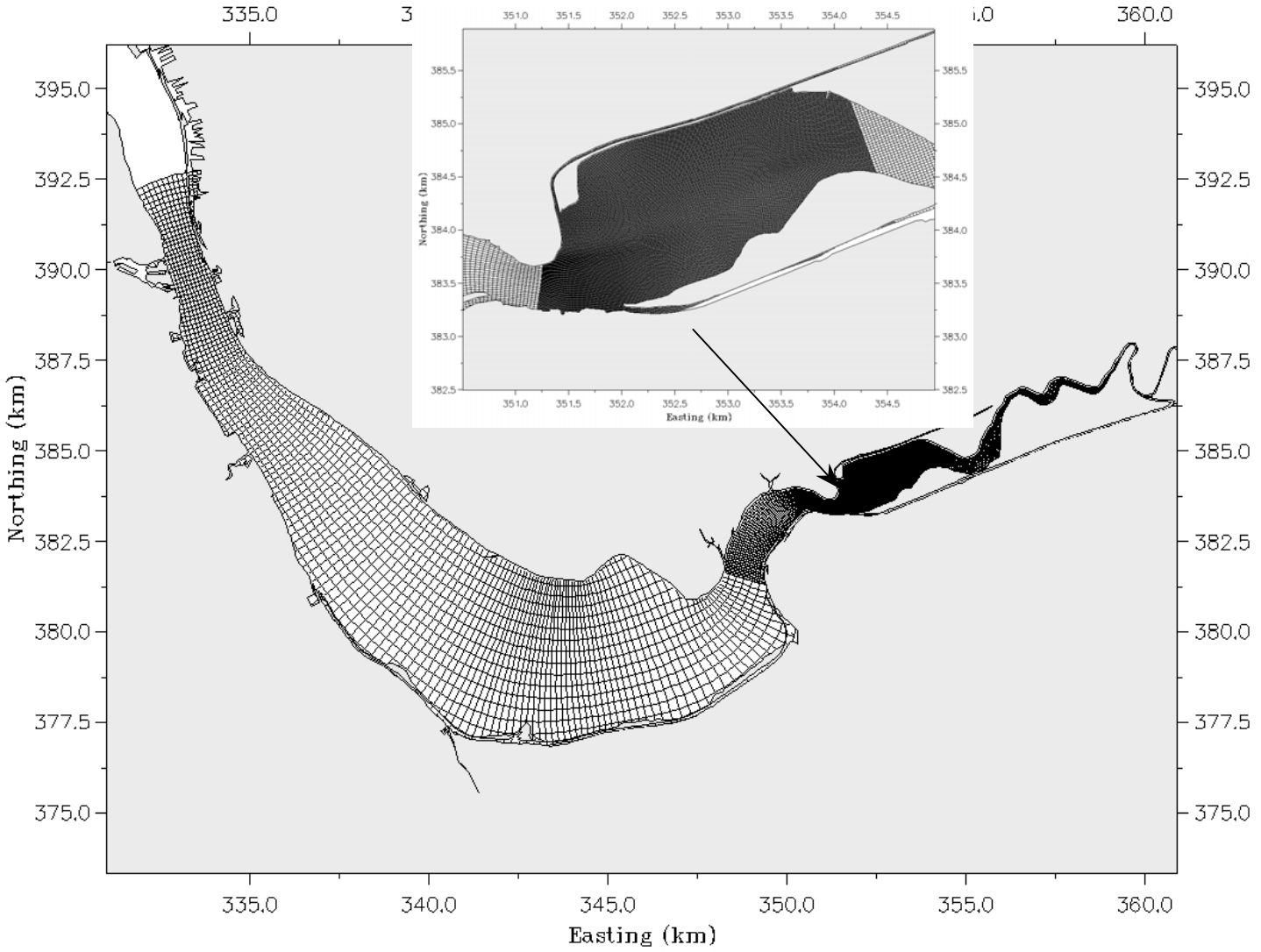
Bartlett, J.M. (1998). *Quality Control Manual for Computational Estuarine Modelling*. Environment Agency, R&D Technical Report W113, 80pp + appendix.

Halliwell, A.R. and O'Connor B.A. (1967). Suspended sediment in a tidal estuary. In: *Proc. of 10th Conference on Coastal Engng.,* Tokyo, Japan, Sept. 1966, ASCE, Vol 1., Chap. 20, pp 687-706.



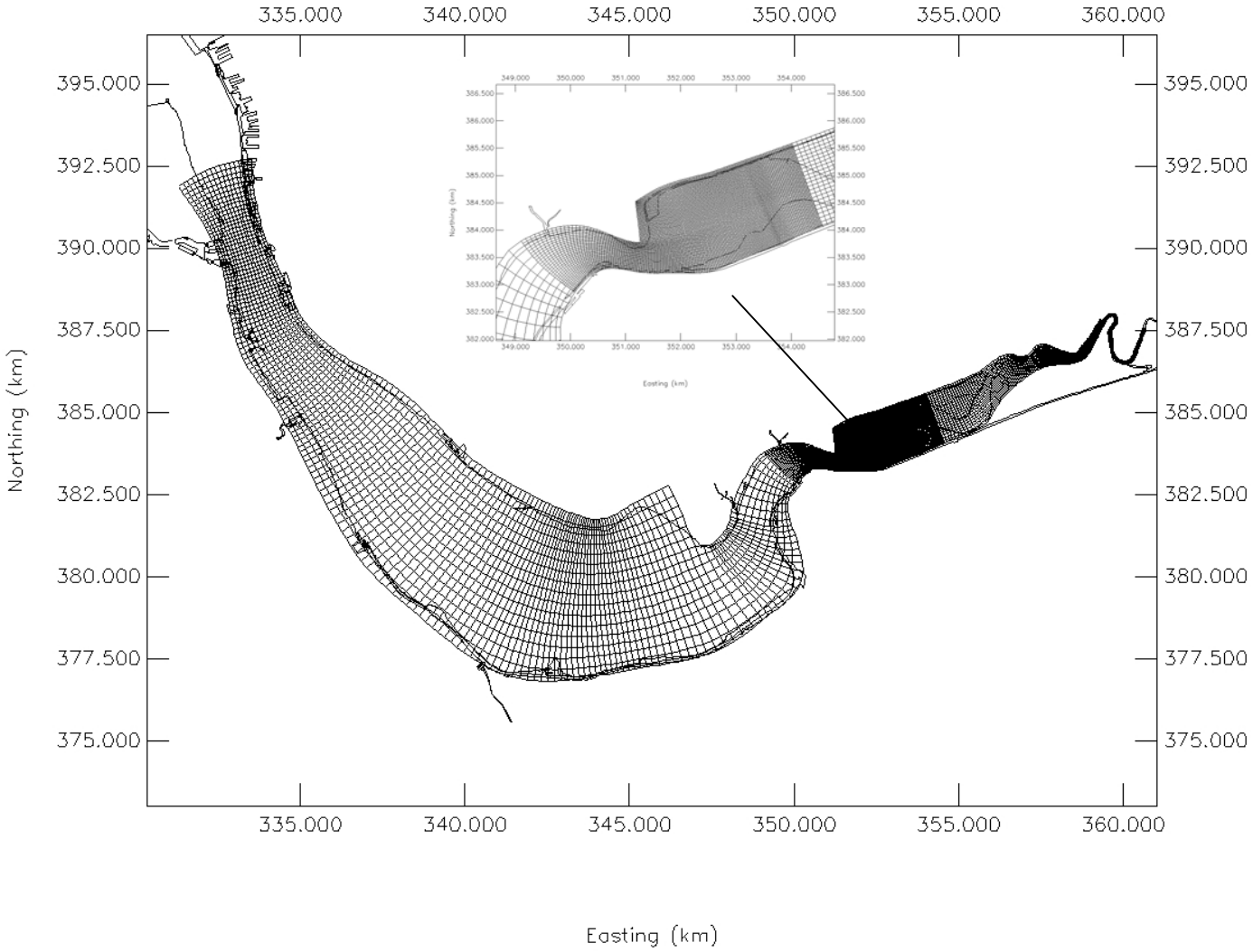
Curvilinear model grid for the Mersey Estuary Phase I modelling study

Figure A1



High resolution curvilinear model grids for the Mersey Estuary Phase II modelling study.
Inset shows grid resolution in area of proposed crossing.

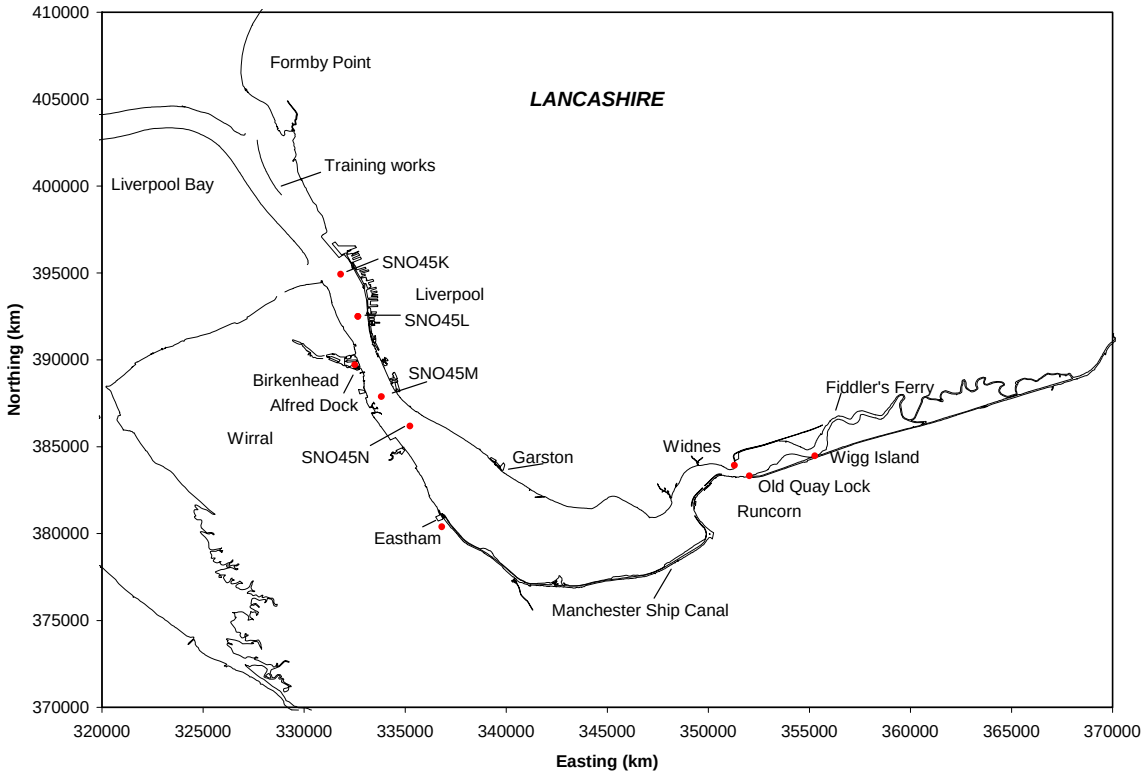
Figure A2



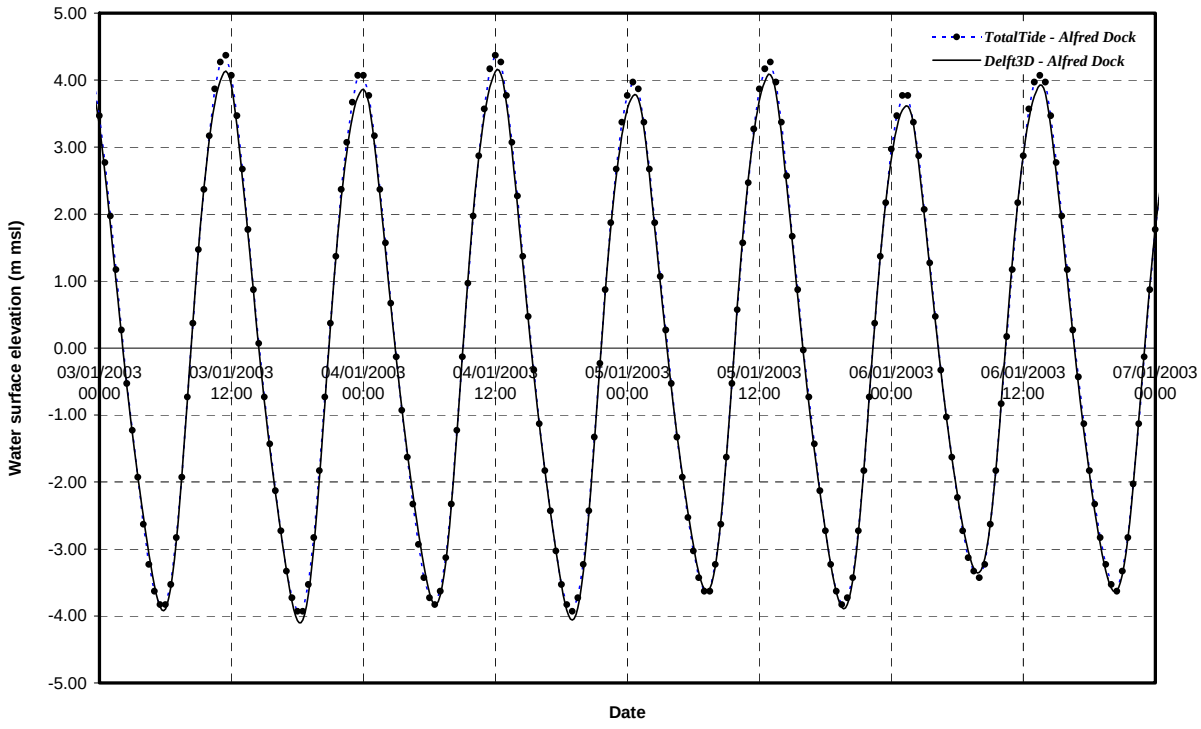
Morphological curvilinear model grids for the Mersey Estuary Phase II modelling study.
Inset shows grid resolution in area of proposed crossing.

Figure A3

A.



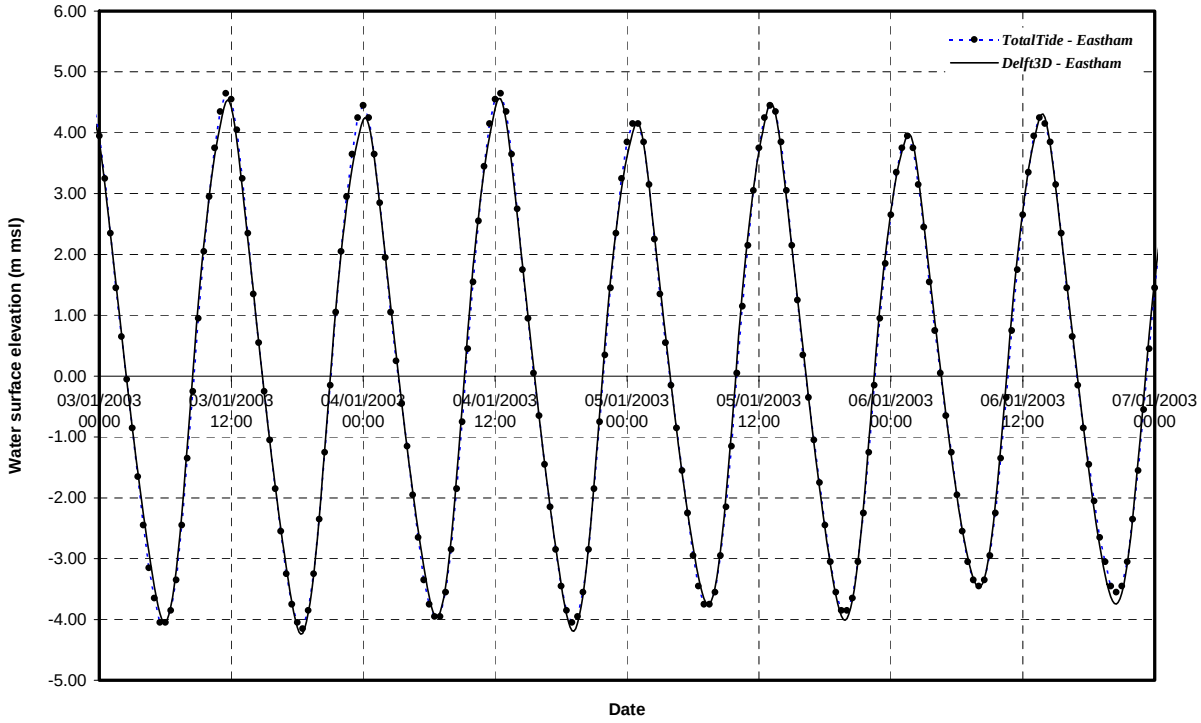
B.



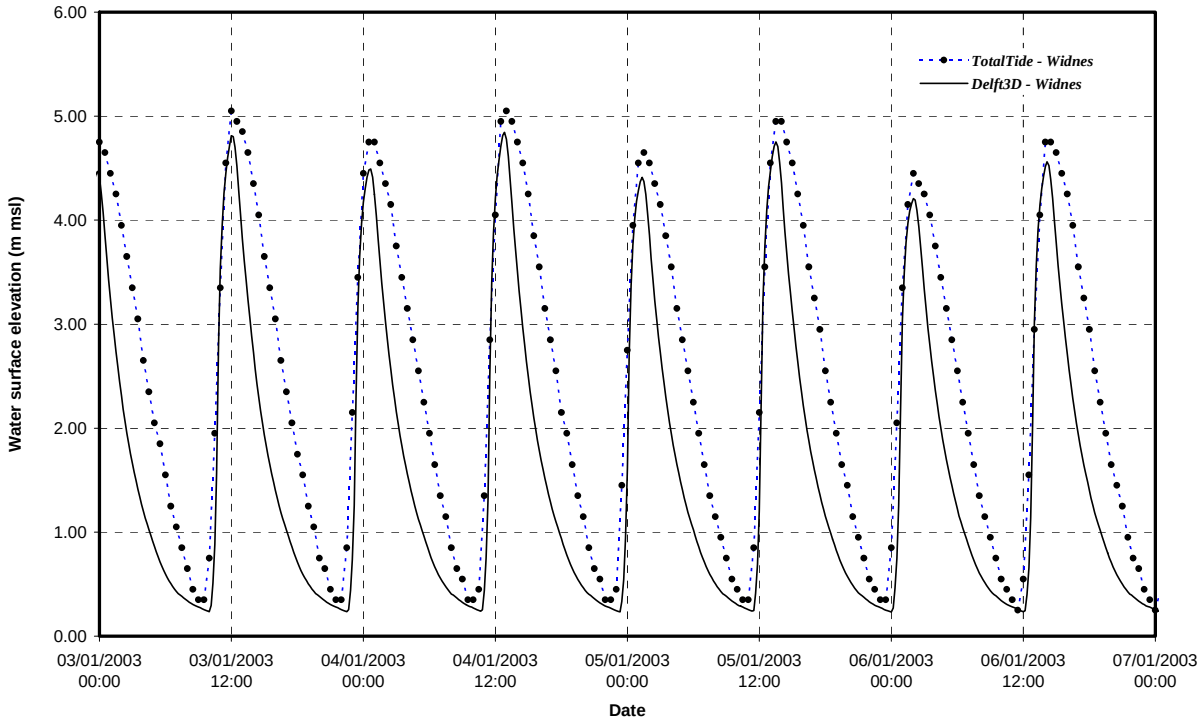
Position of monitoring stations (A). Comparison of water levels at Alfred Dock (B). Calibration results obtained from Delft3D model and UKHO tidal prediction package TotalTide

Figure A4

A.



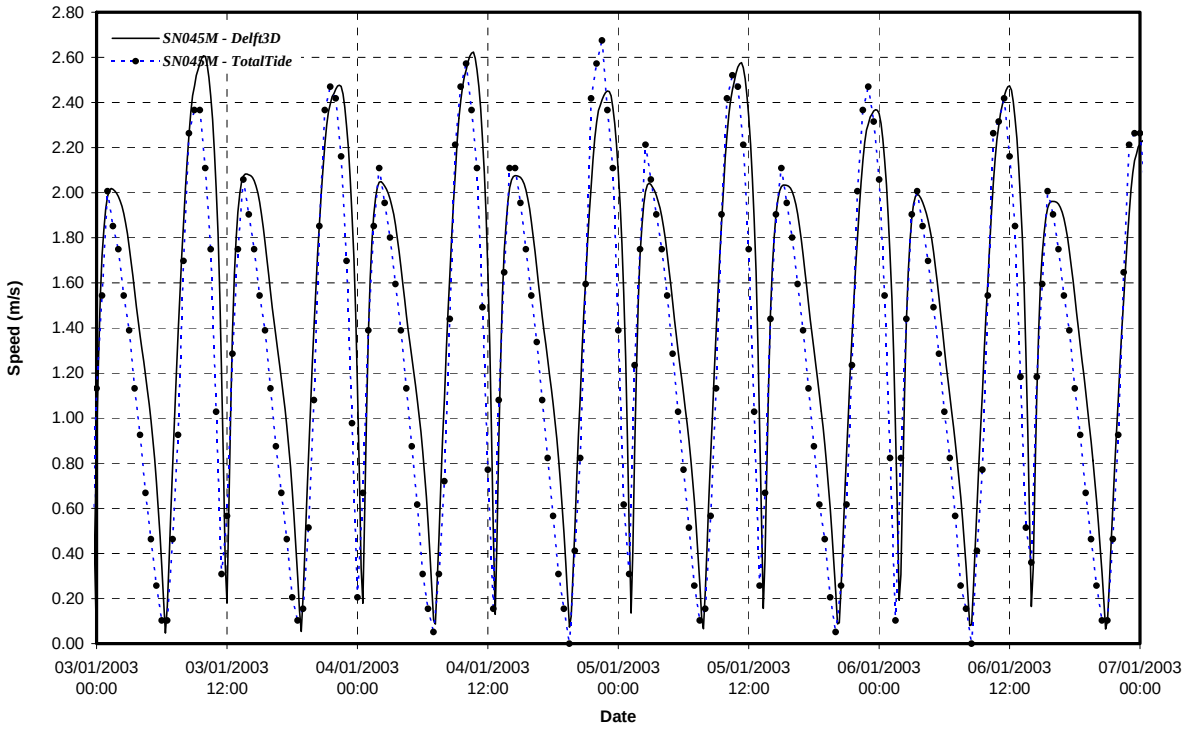
B.



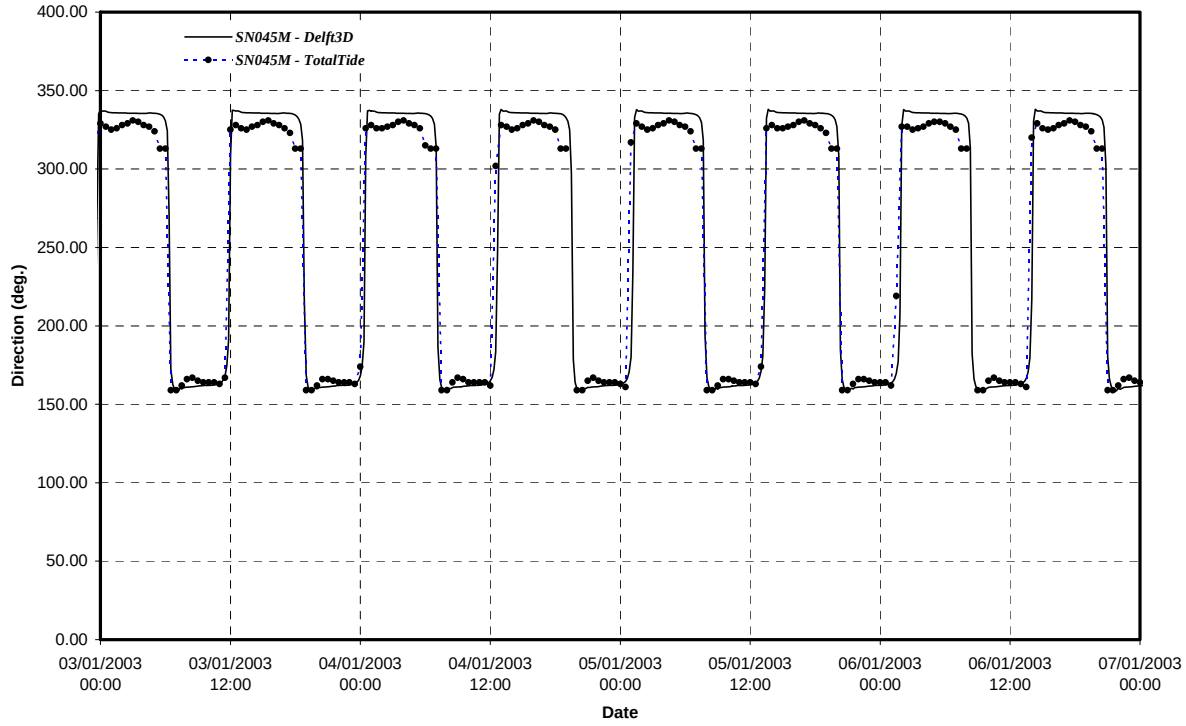
Comparison of water levels at Eastham (A) and Widnes (B). Calibration results obtained from Delft3D model and UKHO tidal prediction package TotalTide

Figure A5

A.



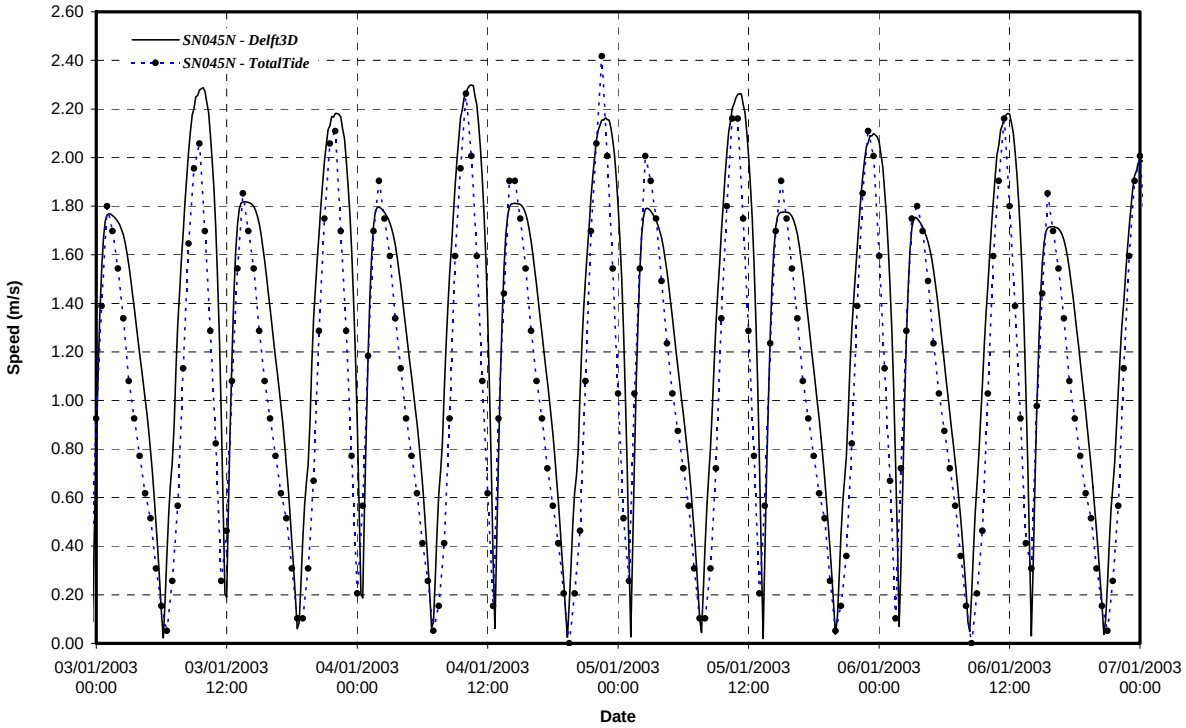
B.



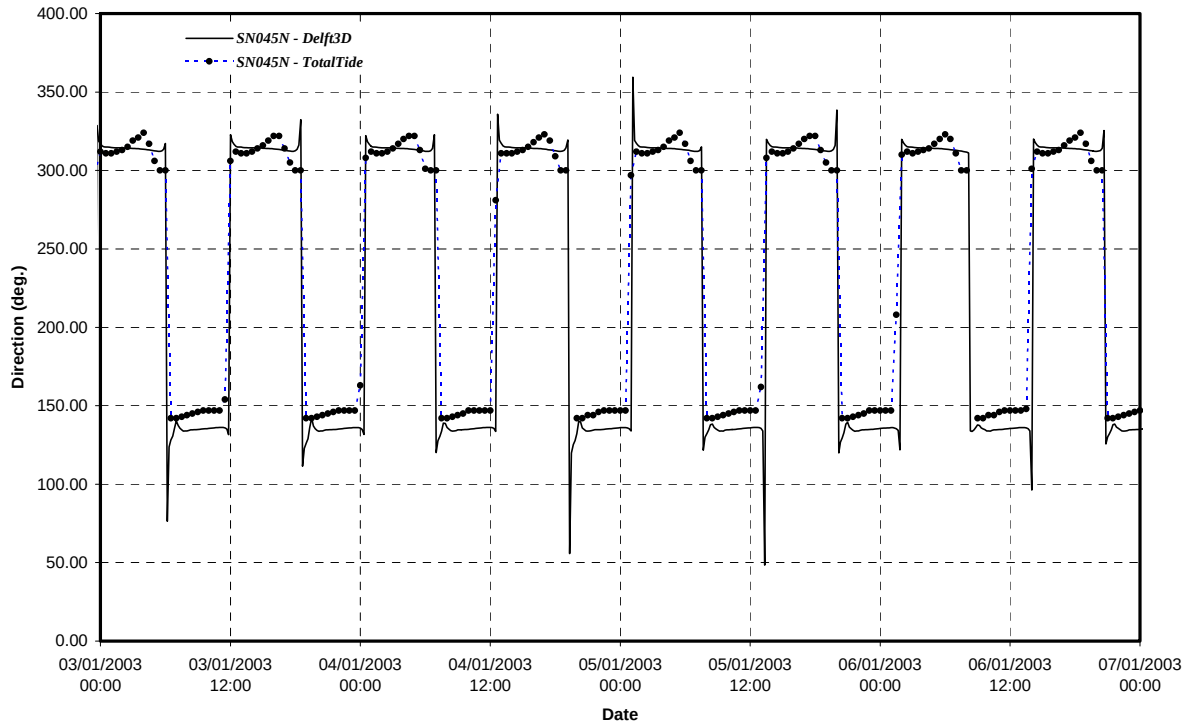
Comparison of tidal stream data at UKHO position SN045M. Figure shows speed (A) and direction (B) results obtained from Delft3D model and UKHO tidal prediction package TotalTide

Figure A6

A.



B.

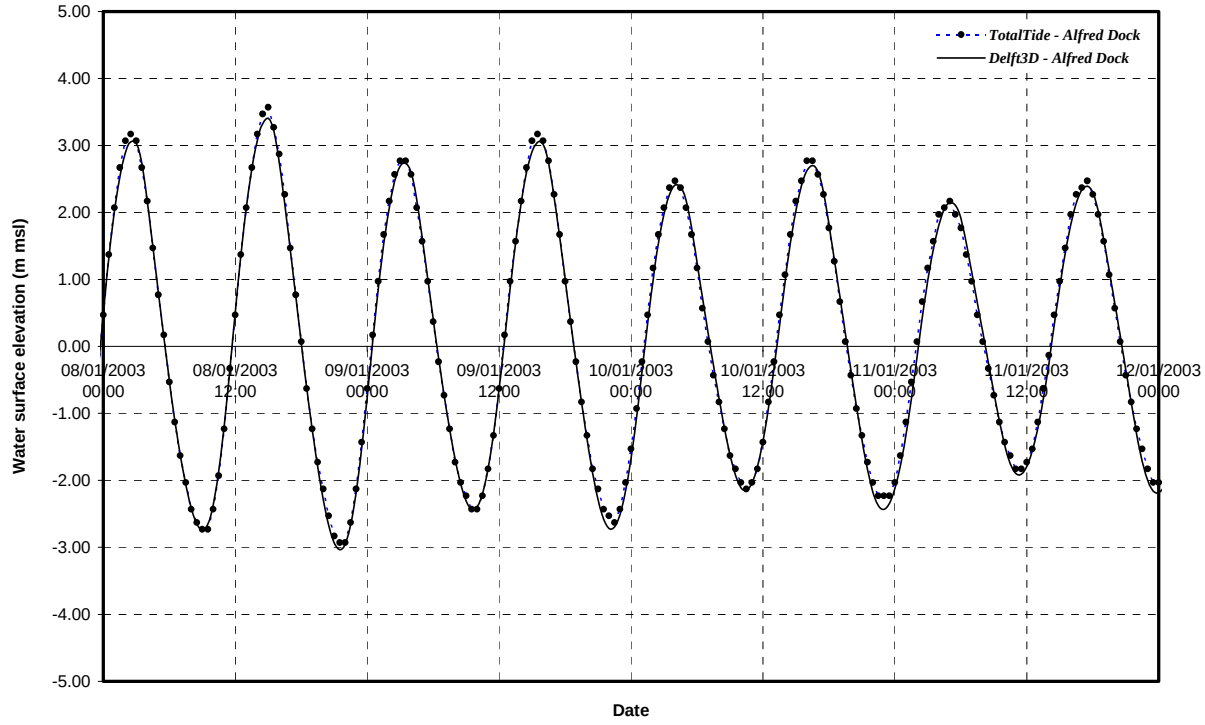


ABP mer marine environmental research

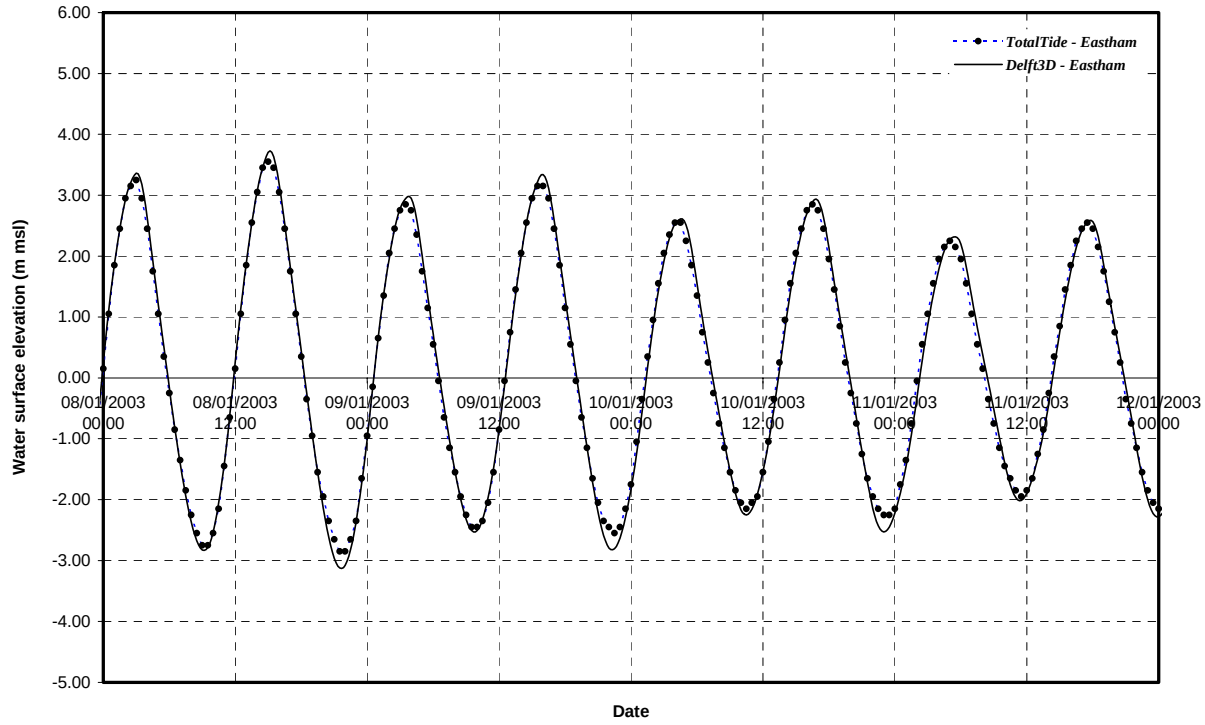
Comparison of tidal stream data at UKHO position SN045N. Figure shows speed (A) and direction (B) results obtained from Delft3D model and UKHO tidal prediction package TotalTide

Figure A7

A.

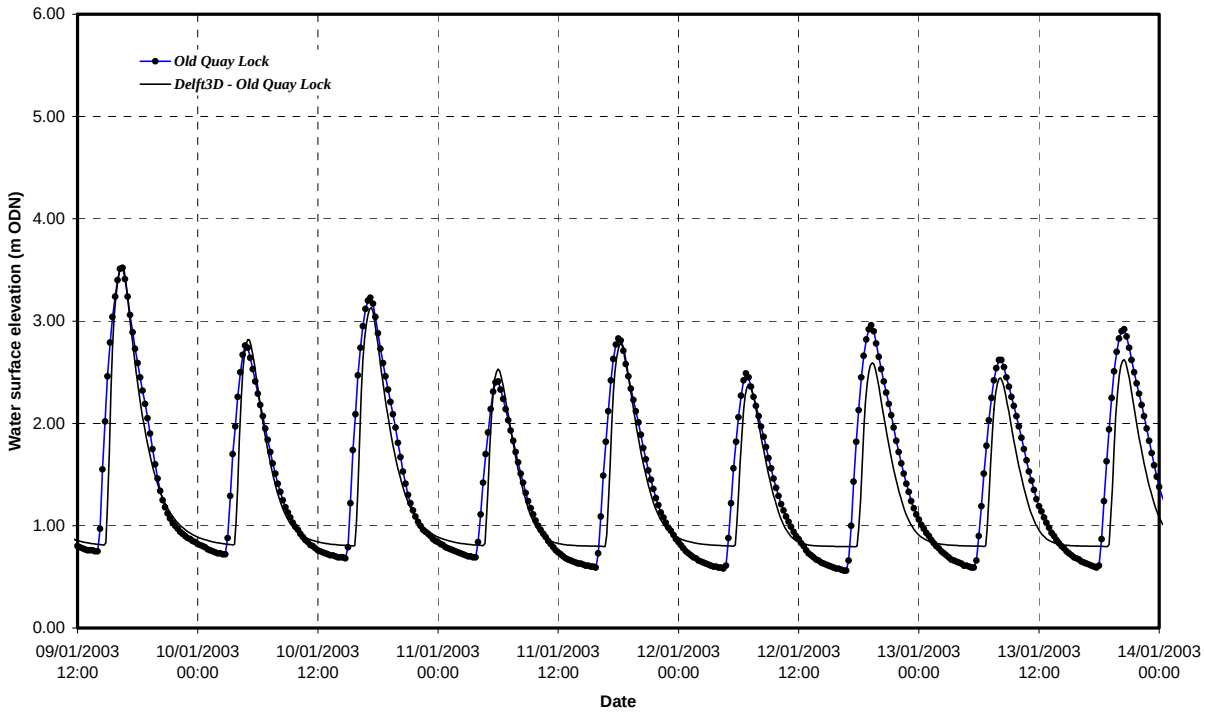


B.

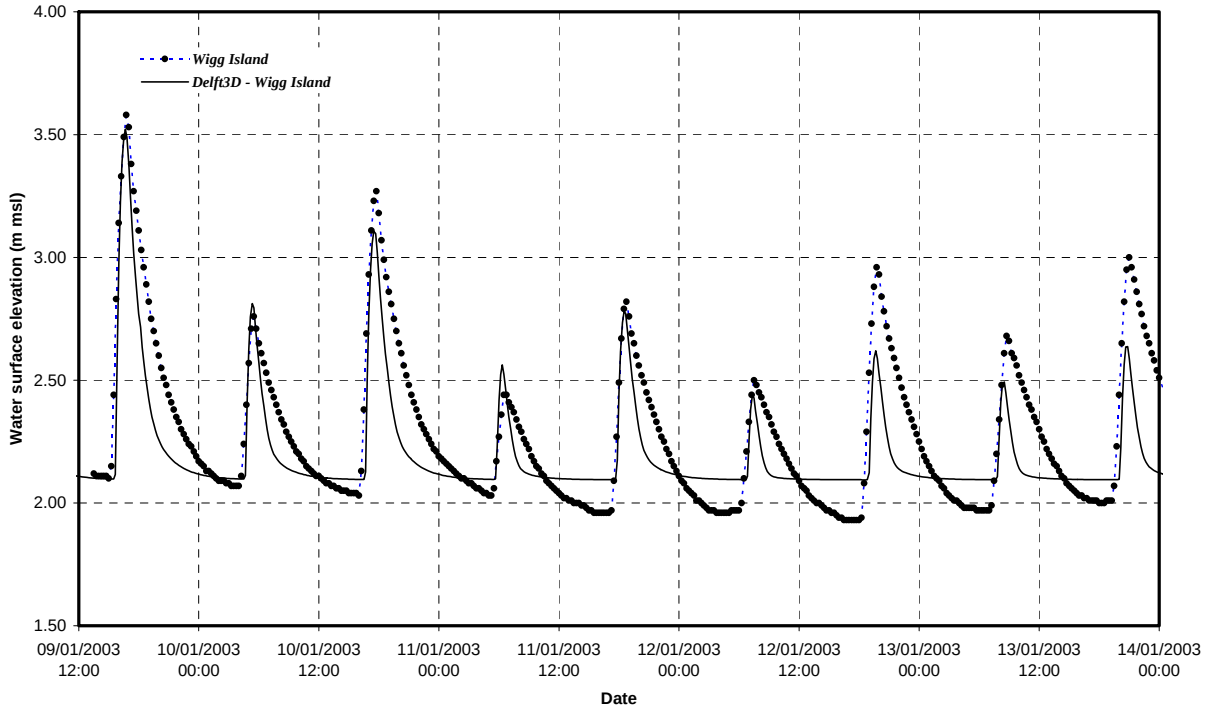


ABP mer marine environmental research	Comparison of water levels at Eastham (A) and Widnes (B). Validation results obtained from Delft3D model and UKHO tidal prediction package TotalTide	Figure A8

A.

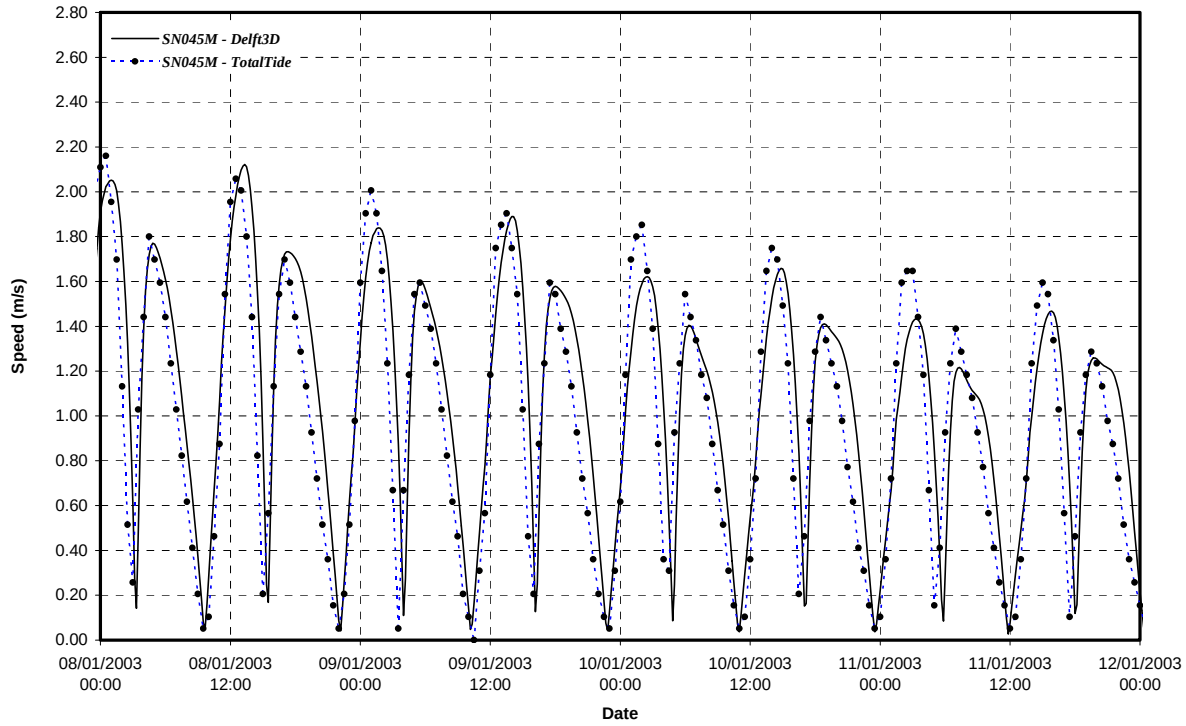


B.

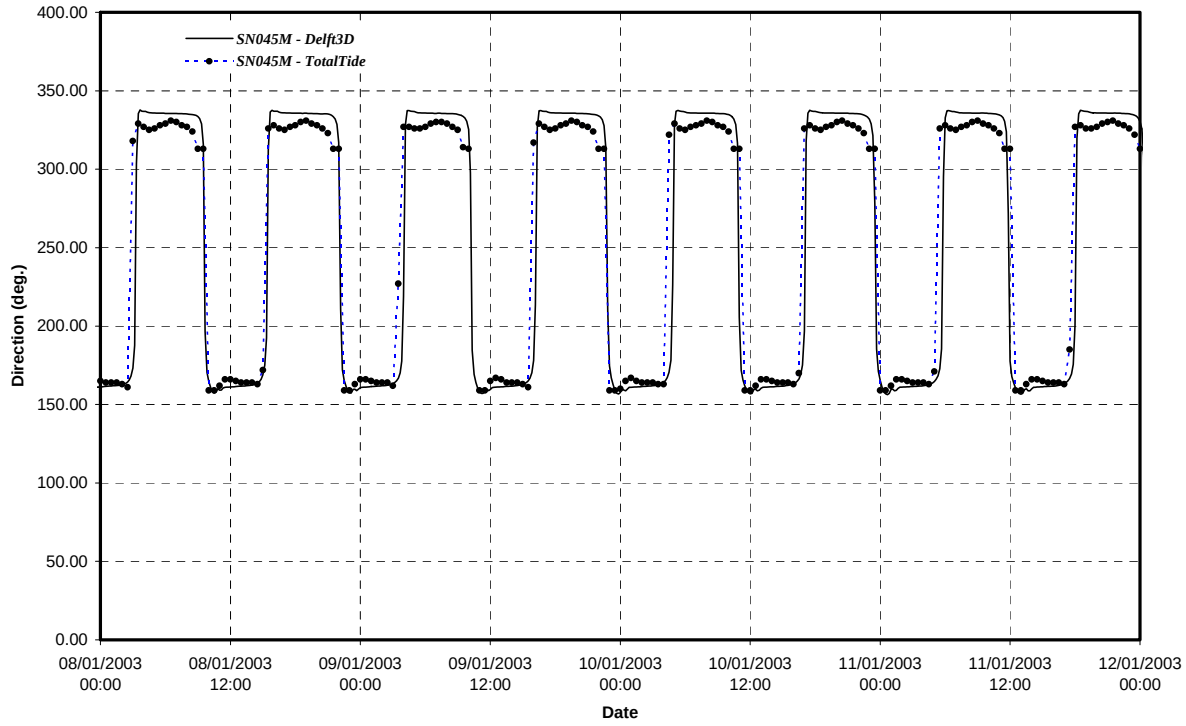


ABP mer marine environmental research	Comparison of water levels at Old Quay Lock (A) and Wigg Island (B). Validation results obtained from Delft3D model and field measurements	Figure A9

A.

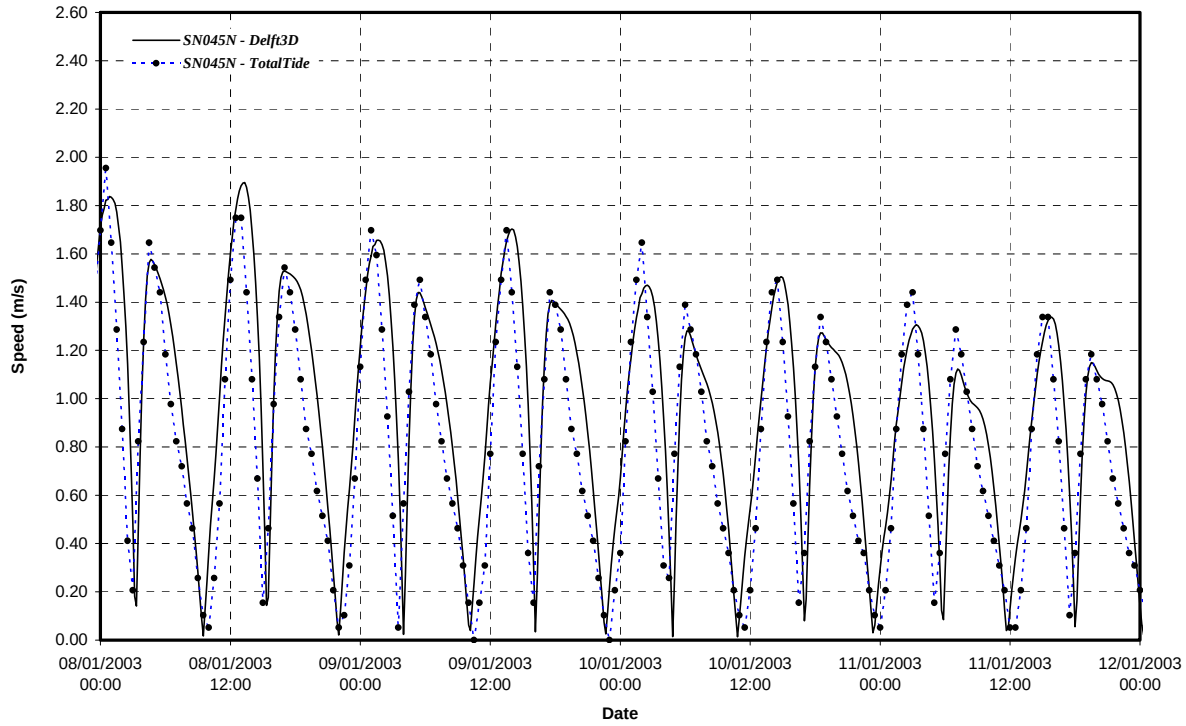


B.

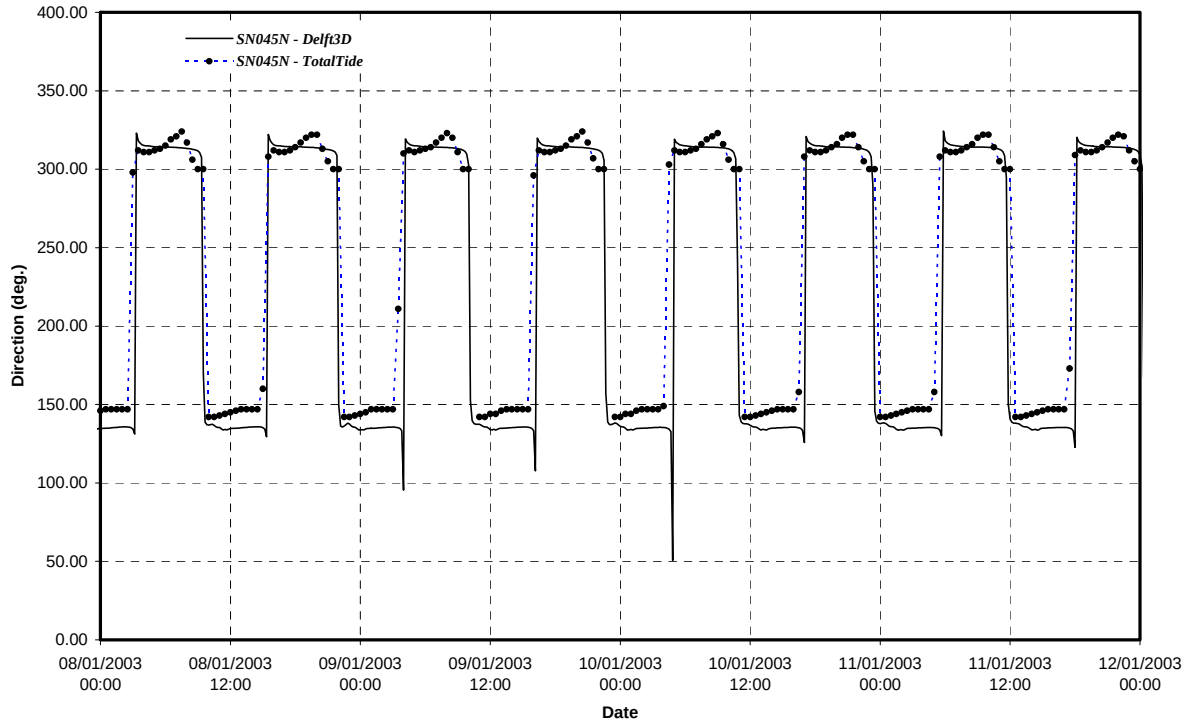


ABP mer marine environmental research	Comparison of tidal stream data at UKHO position SN045M. Figure shows speed (A) and direction (B) results obtained from Delft3D model and UKHO tidal prediction package TotalTide	Figure A10

A.

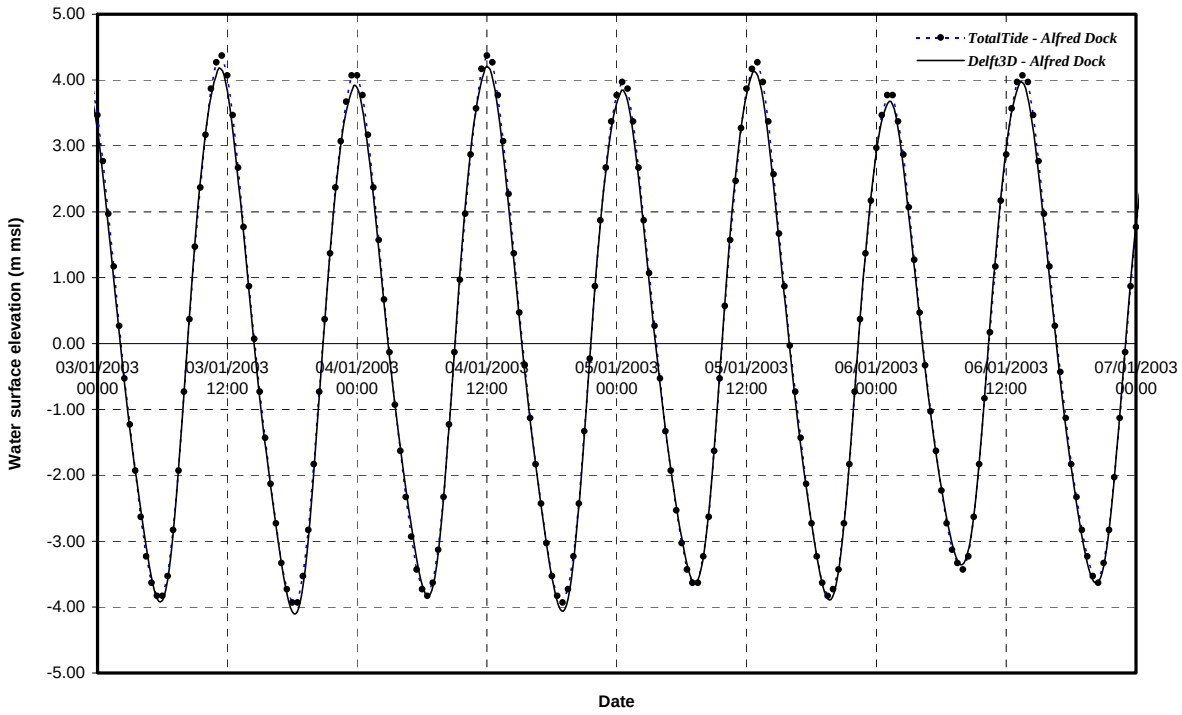


B.

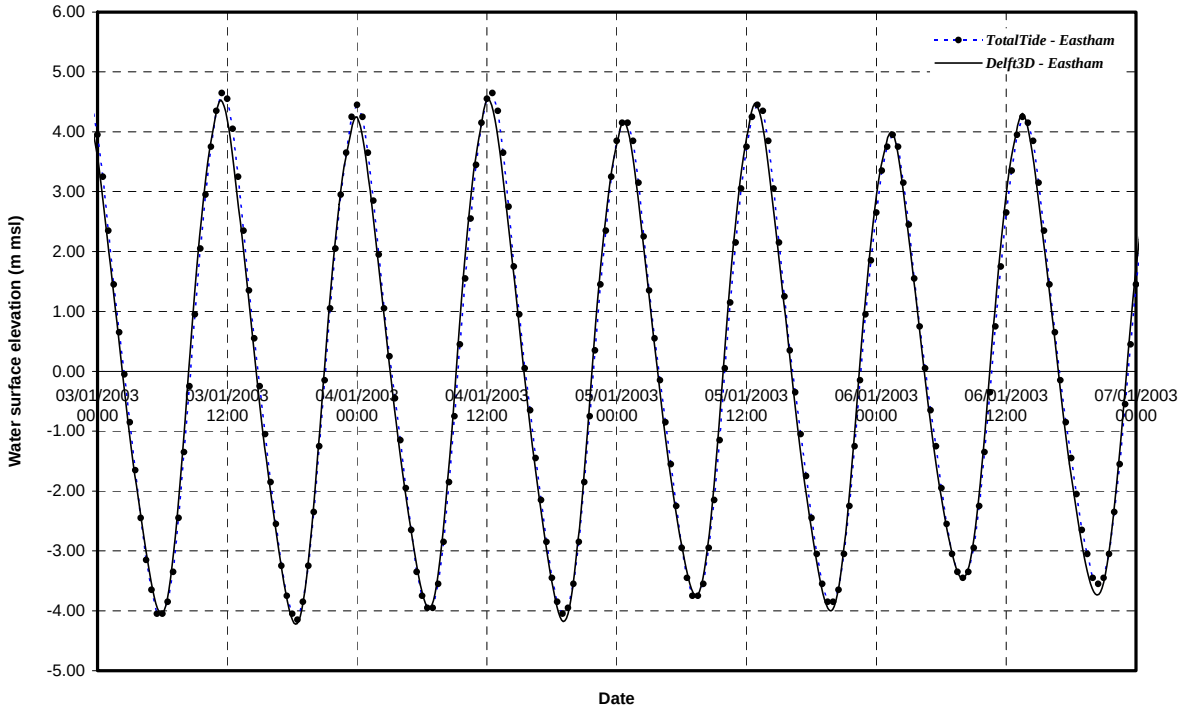


ABP mer marine environmental research	Comparison of tidal stream data at UKHO position SN045N. Figure shows speed (A) and direction (B) results obtained from Delft3D model and UKHO tidal prediction package TotalTide	Figure A11

A.



B.

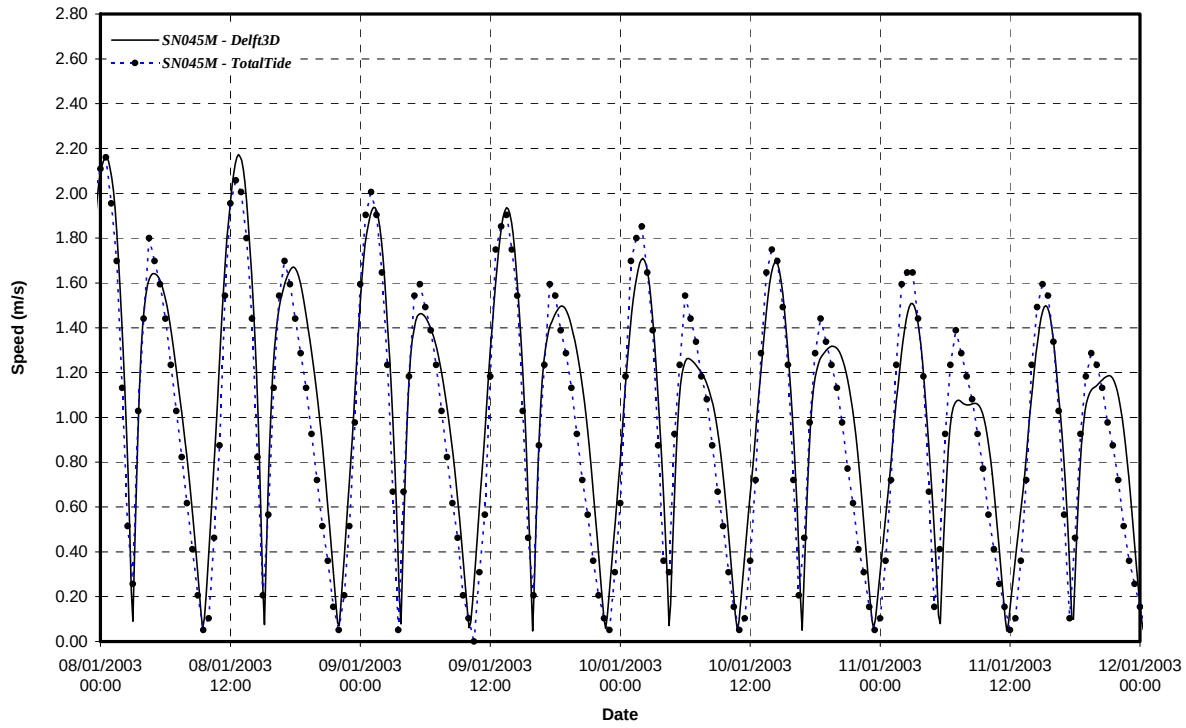


ABP mer
marine environmental research

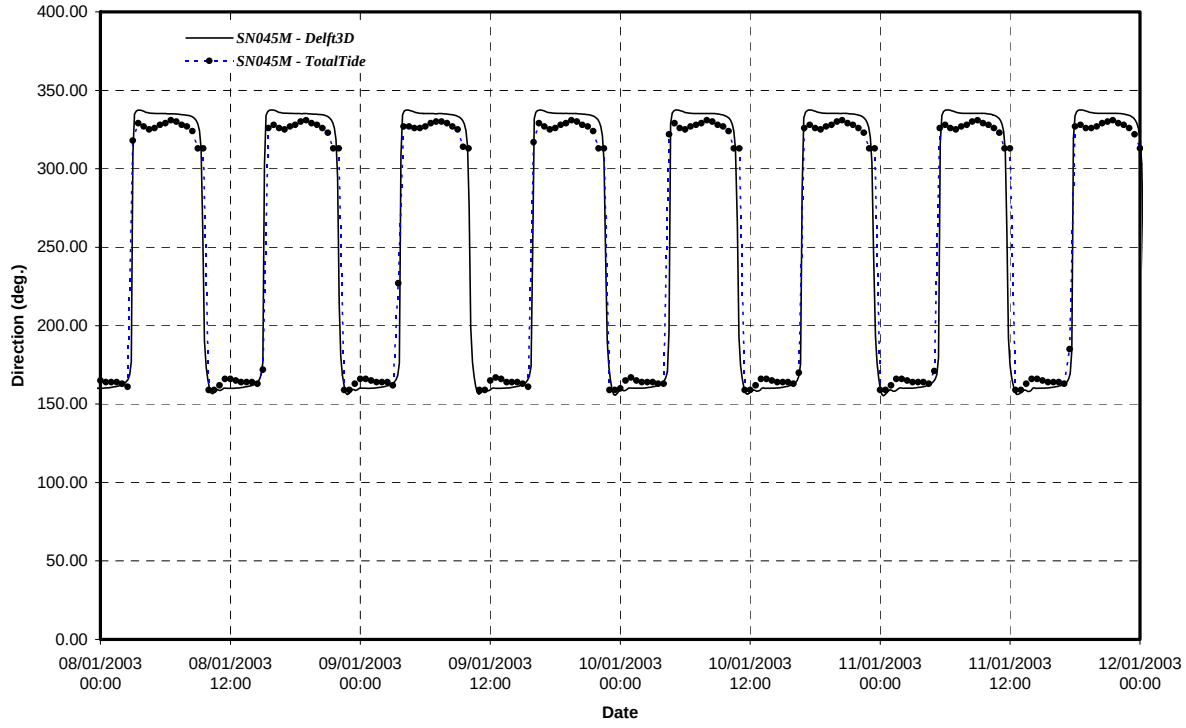
Comparison of water levels at Alfred Dock (A) and Eastham (B). Calibration results obtained from Delft3D morphological model and UKHO tidal prediction package TotalTide

Figure A12

A.



B.



ABP mer marine environmental research	Comparison of tidal stream data at UKHO position SN045M. Figure shows speed (A) and direction (B). Validation results obtained from Delft3D morphological model and UKHO tidal prediction package TotalTide	Figure A13

Appendix B

Fluvial Flows and Tidal Surges

Appendix B. Fluvial Flows and Tidal Surges

B1. Introduction

Freshwater flow data were obtained from the Environment Agency and the National Flow Archive for 6 gauging stations for rivers draining into the Mersey Estuary. The records used correspond to the following stations:

- River Gowy at Picton (1949-1976)
- River Weaver at Pickerings Cut (1993-2001), but no 1998-9 data
- River Mersey at Irlam Weir (1921,1934-1978)
- Sankey Brook at Causey Bridge (1977-2001)
- Ditton Brook at Greens Bridge (1974-2001), but no 1975,1990-2 data
- River Mersey at Westy (1986-2001)

A Gumbel distribution was calculated for the annual maxima for each station to determine return period flows.

The Gumbel distribution was determined using the following:

$$P(q) = \Pr ob[Q \geq q] = 1 - \exp\{-\exp[-\alpha(q-u)]\}_i = \frac{1}{T_r} \qquad \text{B1.}$$

$$\overline{Q}_m = u + \frac{0.5772}{\alpha} \qquad \text{B2.}$$

$$\sigma = \frac{\pi}{\sqrt{6}\alpha} \qquad \text{B3.}$$

It is assumed that $\overline{Q}_m$ is approximated by $\overline{Q}$ and σ is approximated by *s*, where $\overline{Q}$ is the mean value of discharge from n data values of *Q*, *s* is an estimate of the standard deviation and T_r is the return period. Extensive analysis of historic flow records shows the Gumbel distribution to yield a better description of the peak river discharges than the Gaussian distribution. Table B1 shows the predicted discharge values for the 6 gauging stations for return period events of 1: 1 year, 1: 100 years and 1: 500 years.

Table B1. Predicted return events

Location	Discharge (m^3/s)		
	1: 1	1: 200	1: 500
River Mersey (Irlam)	43.62	275.09	306.22
River Mersey (Westy)	94.86	228.89	246.90
River Weaver	32.62	239.54	267.37
Sankey Brook	7.57	46.06	51.23
Ditton Brook	2.85	19.85	22.14
River Gowy	2.90	29.96	33.60

The 1: 1 year return values for the Mersey at Irlam and Westy do not correspond (Irlam is upstream of Westy) and this is most likely due to the short record for the gauging station at Westy. Based on the ratio of the 1: 200 and 1: 500 years events the discharge at Westy should be closer to 35-37m^3/s. The results of the analysis show the considerable variation in flows between 1: 1 year events and the more extreme flows, of the order of 7-8 times for a 1: 500 years scenario. Figures B1-B3 show the Gumbel distributions for the 6 stations.

Based on this analysis a 1: 1 year return period was used to represent the flow at the tidal limit at Howley Weir. A value of 36m^3/s was applied at this location, the value being determined on the basis of the data for Westy and Irlam.

Fluvial extremes were represented in the model using a 1: 200 years return period event.

B2. Tidal Surges

The term 'storm surge' is generally reserved for excess sea levels generated by a severe storm. When the weather acts in such a way as to increase the water level above the astronomical tide these are called positive surges. Negative surges are when the water level is lower than predicted.

Surges are caused by two main features of the atmosphere acting on the ocean surface. Atmospheric pressure changes result in variations in the vertical forces acting on the sea surface and these propagate throughout the depth. Secondly, forces due to wind stresses acting parallel to the water surface are transferred down through the water column.

The character of surges on the west coast of the UK is different to those observed in the North Sea. The most effective wind direction for producing large surges is from the south and southeast, which corresponds with the Ekman transport theory with motion to the right of the wind and the resulting build up of coastal sea levels. No two surge

events are identical due to the small variations in weather patterns which can result in significant differences in the response of the water body.

The extreme tidal levels at Gladstone Dock were obtained from an Environment Agency (North West Region) report (Environment Agency, 1998) of extreme sea level predictions. Several different methods were applied, however, the most reliable was considered to be the General Extreme Value distribution fitted by the Maximum Likelihood (MLE) approach. From the report the following return period levels were obtained.

Table B2. Return period levels

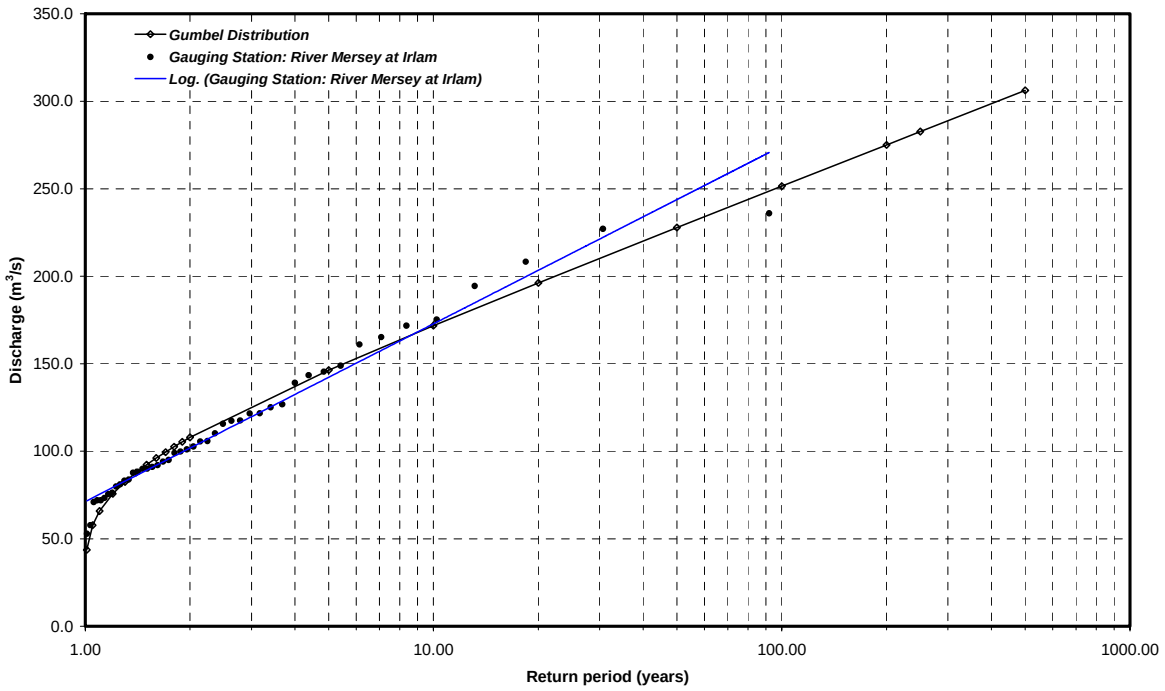
Location	Level (m)		
	1: 1	1: 200	1: 500
Gladstone Dock	4.70	6.20	6.30

The shape of the tidal curve applied in the numerical model was determined from a recorded surge event at Gladstone Dock. Whilst this event was lower than the required 1: 200 years return period the shape of the curve was used to construct the required extreme event.

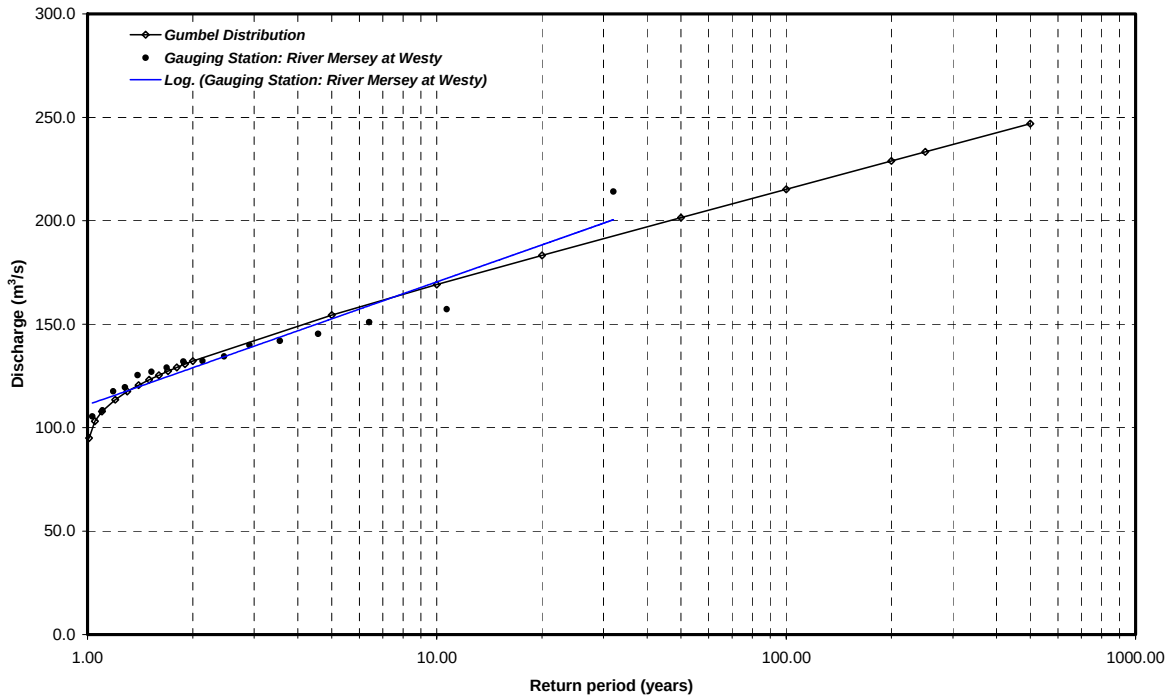
B3. Reference

Environment Agency (1998). *Extreme Sea levels for Section 105 Surveys*. Final report, JBA Ltd., July, 9pp (+Tables and Figures).

A.

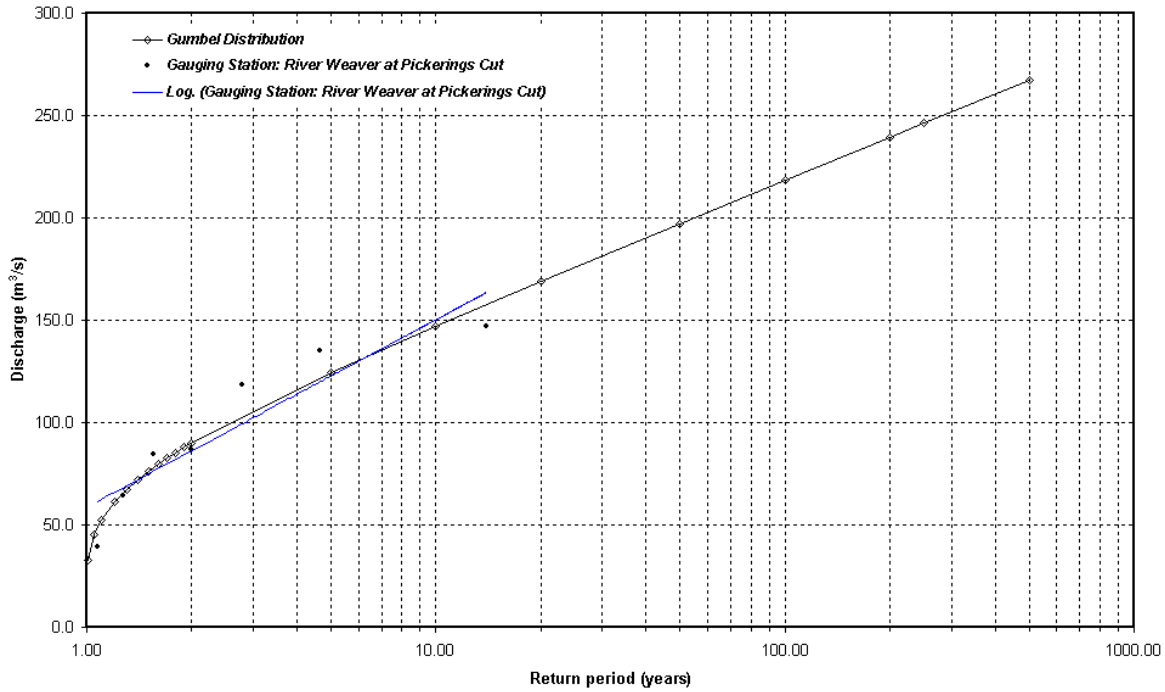


B.

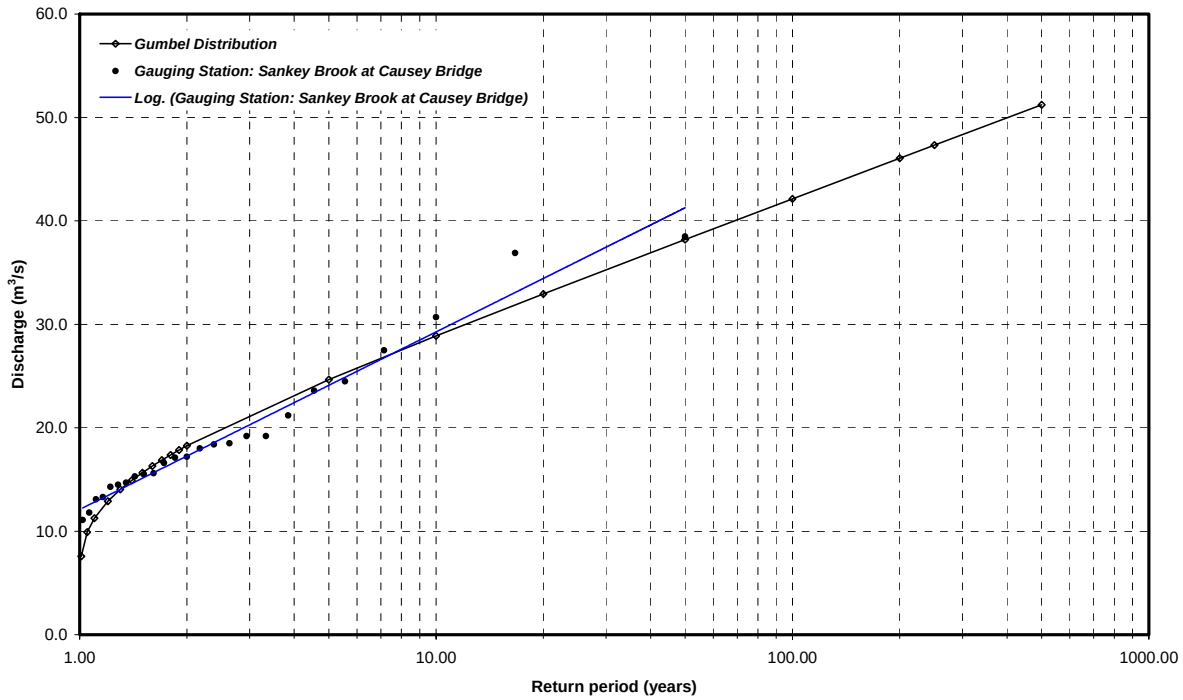


ABP mer marine environmental research	Gumbel distribution applied to annual maxima discharge recorded at gauging stations at Irlam (A) and Westy (B) on the River Mersey. Also shown is a logarithmic fit to the data values	Figure B1

A.

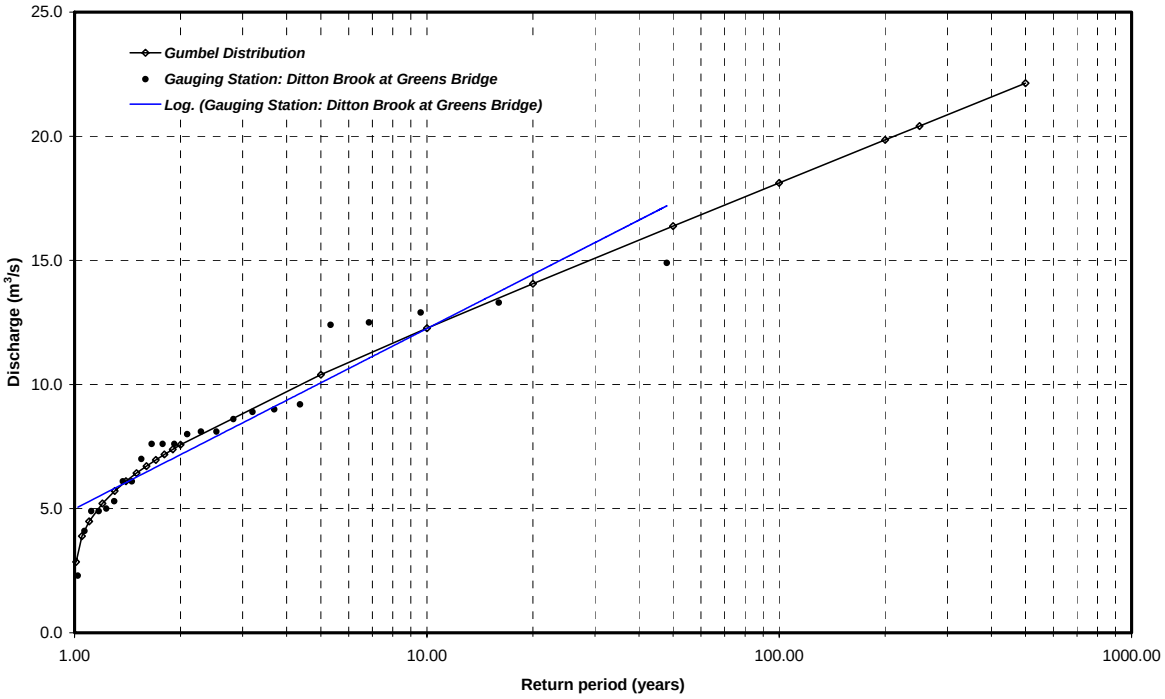


B.

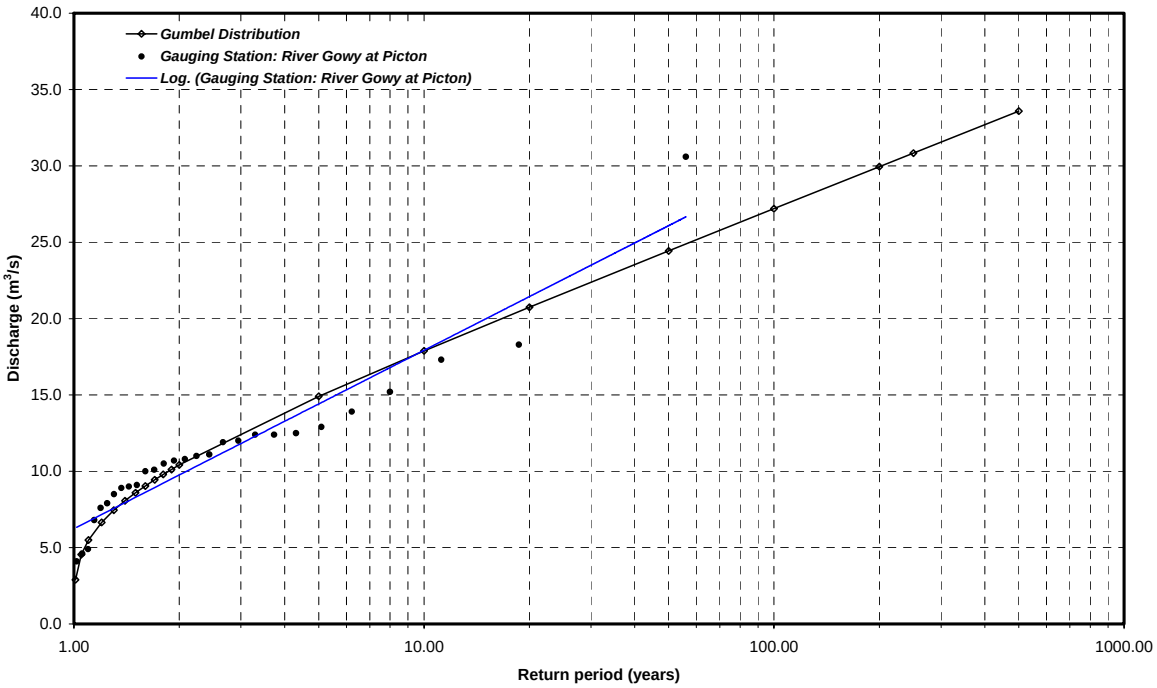


ABP mer marine environmental research	Gumbel distribution applied to annual maxima discharge recorded at gauging stations on the River Weaver (A) and Sankey Brook (B). Also shown is a logarithmic fit to the data values	Figure B2

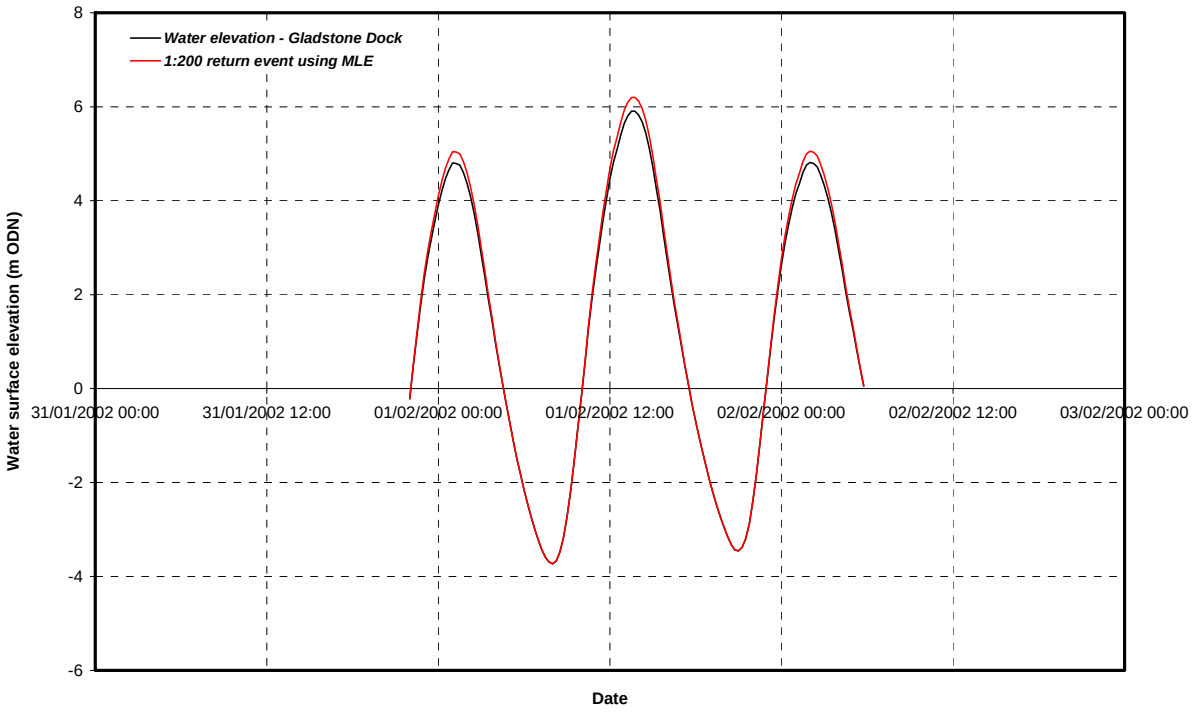
A.



B.



ABP mer marine environmental research	Gumbel distribution applied to annual maxima discharge recorded at gauging stations on the Ditton Brook (A) and the River Gowy (B). Also shown is a logarithmic fit to the data values	Figure B3



ABP mer marine environmental research	Modelled 1: 200 years return period extreme water level event	Figure B4

Appendix C

Detailed Hydrodynamic Assessment

Appendix C. Detailed Hydrodynamic Assessment

C1. Introduction

This appendix presents the results from the detailed hydrodynamic numerical modelling undertaken to assess the impact of the preferred scheme option Route 3A. During the course of the work several alternative pier/tower layout and alignment schemes have been tested.

The detailed modelling has concentrated on investigating the impact of the Route 3A bridge alignment. The initial model run investigated the original Route 3A alignment (Drawing No. B4027/2/B/361). Following this test a modified pier/tower alignment was tested (Drawing No. B4027/3/H/G/3) and this modified scheme has been the focus of much of the subsequent modelling. A further three bridge scheme options have been tested. These additional runs correspond to the Route 3A medium span layout as shown in Drawing No. B4027/3/B/300, the Route 3A Short span layout as shown in Drawing No. B4027/3/B301 and the revised Route 3A medium 3 Tower layout as shown in Drawing No. B4027/3/B/300 Rev. A. For the modified medium span layout shown in drawings B4027/3/B/300 and B4027/3/B/300 Rev. A, the number of towers have been reduced from 4 to 3 and pier alignments have been modified. Below are listed the model runs undertaken:

- Baseline:
  - Spring-neap cycle
  - High fluvial flow (1:200 year event) and spring tide
  - High fluvial (1:200 year event) and corresponding 1:200 year surge event.

- Route 3A Medium Span original alignment (Drawing No. B4027/2/B/361):
  - Spring-neap cycle

- Route 3A Medium Span modified alignment (Drawing No. B4027/3/H/G/3):
  - Spring-neap cycle
  - High fluvial flow (1:200 year event) and spring tide
  - High fluvial (1:200 year event) and corresponding 1:200 year surge event.

- Route 3A Medium Span 3 Tower alignment (Drawing No. B4027/3/B/300):
  - Spring-neap cycle

- Route 3A Medium Span Revised 3 Tower alignment (Drawing No. B4027/3/B/300 Rev. A):
  - Spring-neap cycle
  - High fluvial (1:200 year event) and corresponding 1:200 year surge event.
- Route 3A Short Span (Drawing No. B4027/3/B/301):
  - Spring-neap cycle

The previous modelling study undertaken in Phase I of the work used an additional quadratic friction term in the momentum equations to represent the effect of bridge piers in the model. Further details on this approach are given in Appendix A and ABPmer (2003a). In the current modelling bridge piers have been simulated using a combination of approaches. Where bridge piers and towers are the same size as the model grid cells the cells have been closed off as they are effectively blocked for the transmission of fluid flow. However, were the bridge piers are smaller than the grid cell size added friction terms have been used to represent the piers. In this manner there is an allowance for some flow transmission across the cell, even if that flow is low. Appendix A describes the calibration and validation of the hydrodynamic and morphological models.

The key hydrodynamic processes that have been investigated in this part of the study are water level, bed shear stress and velocity. Results are presented as changes relative to a baseline case. The bed shear stress is the frictional force exerted on an area of seabed or riverbed by current flowing over it. Therefore, it is an important quantity in the study of sediment transport processes, because it represents the flow-induced force acting on the bed sediments.

For the various schemes the results are shown in the figures as a difference between the scenario and the baseline case. Therefore, an increase in a quantity appears as a positive value whilst negative values represent a reduction. Changes in water level of less than $\pm$0.01m are considered to represent no change. Similarly, changes in speed of less than $\pm$0.01m/s and bed shear stress of $\pm$0.02N/m^2 are considered insignificant.

The vertical direction in the numerical model uses a scaled co-ordinate system called σ-co-ordinates. The σ-co-ordinate system is boundary fitted both to the bottom and to the moving free surface. The numbers of vertical layers used in the model are defined as a percentage of the total depth. Therefore, the actual value of the total depth that each of these layers represents varies through any given tidal cycle. The near-surface speed represents the uppermost layer in the model and provides an indication of the speeds likely to impact on shallow drafted vessels, whilst the near-bed speeds are more representative of the forces acting on the riverbed/seabed.

Tables C1.1 and C1.2 provide a schedule of the model runs undertaken for each scenario with their respective figure numbers for high water and peak ebb (Table C1.1) and low water and peak flood (Table C1.2).

Table C1.1 Schedule of scenario model runs for high water and peak ebb of the spring tide

	High Water Spring					Peak Ebb Spring				
	Water Levels	Near-Surface Speed	Near-Bed Speed	Bed Shear Stress	% Bed Shear Stress	Water Levels	Near-Surface Speed	Near-Bed Speed	Bed Shear Stress	% Bed Shear Stress
Medium Span - Original	C2A	C4A	C6A	C8A	C10A	C2B	C4B	C6B	C8B	C10B
Medium Span - modified	C12A	C14A	C16A	C18A	C20A	C12B	C14B	C16B	C18B	C20B
Medium Span 3 Towers	C42A	C44A	C46A	C48A	C50A	C42B	C44B	C46B	C48B	C50B
Medium Span 3 Towers revised	C52A	C54A	C56A	C58A	C60A	C52B	C54B	C56B	C58B	C60B
Short Span	C72A	C74A	C76A	C78A	C80A	C72B	C74B	C76B	C78B	C80B
	High Water Spring + 200 Year Fluvial Event					Peak Ebb Spring + 200 year Fluvial Event				
Medium Span - modified	C22A	C24A	C26A	C28A	C30A	C22B	C24B	C26B	C28B	C30B
	High Water Spring + 200 year Surge and Fluvial Event					Peak Ebb Spring + 200 year Surge and Fluvial Event				
Medium Span - modified	C32A	C34A	C36A	C38A	C40A	C32B	C34B	C36B	C38B	C40B
Medium Span 3 Towers revised	C62A	C64A	C66A	C68A	C70A	C62B	C64B	C66B	C68B	C70B

Table C1.2 Schedule of scenario model runs for low water and peak flood of the spring tide

	Low Water Spring					Peak Flood Spring				
	Water levels	Near-surface speed	Near-bed speed	Bed shear stress	% bed shear stress	Water levels	Near-surface speed	Near-bed speed	Bed shear stress	% bed shear stress
Medium Span - Original	C1A	C3A	C5A	C7A	C9A	C1B	C3B	C5B	C7B	C9B
Medium Span - modified	C11A	C13A	C15A	C17A	C19A	C11B	C13B	C15B	C17B	C19B
Medium Span 3 Towers	C41A	C43A	C45A	C47A	C49A	C41B	C43B	C45B	C47B	C49B
Medium Span 3 Towers revised	C51A	C53A	C55A	C57A	C59A	C51B	C53B	C55B	C57B	C59B
Short Span	C71A	C73A	C75A	C77A	C79A	C71B	C73B	C75B	C77B	C79B
	High Water Spring + 200 Year Fluvial Event					Peak Ebb Spring + 200 year Fluvial Event				
Medium Span - modified	C21A	C23A	C25A	C27A	C29A	C21B	C23B	C25B	C27B	C29B
	High Water Spring + 200 Year Surge and Fluvial Event					Peak Ebb Spring + 200 Year Surge and Fluvial Event				
Medium Span - modified	C31A	C33A	C35A	C37A	C39A	C31B	C33B	C35B	C37B	C39B
Medium Span 3 Towers revised	C61A	C63A	C65A	C67A	C69A	C61B	C63B	C65B	C67B	C69B

C2. Route 3A Medium Option - Original Alignment:

This section describes the hydrodynamic simulation undertaken for the Route 3A medium span layout as shown in Drawing No. B4027/2/B/361. This bridge configuration and alignment had previously been tested in the coarser grid model and the results reported in ABPmer (2003b). For the Route 3A Medium Span operational case there are 3 sets of piers and 4 towers with footings in the estuary (Plate C1). The pier groups are located on the intertidal area with the remaining structures within the main channel. The bridge piers are octagonal (5m x 5m) and the towers are also octagonal (10m x 10m).

Plate C1. Route 3A Medium Option - Original Alignment



C2.1 Water Level

Figures C1-C2 show differences in water level between the baseline case and the Route 3A scenario over a spring tide. The figures show that changes in water level as a result of the bridge are negligible. Some of the observed differences are due to small phase changes as the tide propagates over the intertidal areas. Changes in water level local to the tower structures are also negligible (< 0.03m) although at low water the maximum change around the piers is 0.15m. However, around low water minor changes in flow propagation may manifest themselves as apparent large differences. Similarly, as the flooding or ebbing tide moves onto the intertidal areas large differences can be manifested along the edge of the tidal wave. These differences do

not provide a real indication of change as they are an artefact of phase differences in the propagation of the front of the tidal wave (see Figure C1B). In addition, changes in water level observed on areas of intertidal which are dry at that particular state of the tide are caused by the inability of the model to resolve the small drainage channels (< 1m in width) in these areas leading to 'ponding' of water which in reality would be able to drain away. Comparison with the values reported in the previous Phase I modelling study were similar in magnitude, although the extent of the changes were larger. However, this is an artefact of running the simulation using a coarser grid resolution.

C2.2 Speed

Figures C3 - C6 show differences in near-surface and near-bed speed between the baseline case and the Route 3A scenario over a spring tide. The figures clearly show the acceleration of the flow around the bridge towers where the footings are exposed to the flow with flow deceleration directly behind and in front of the structures. At peak ebb the strongest currents are located within the north and south channels, with increased flows, as a result of the proposed scheme, along the edge of the intertidal area of the north bank (typical values between 0.02 - 0.05 m/s). Along the south bank there are increased speeds downstream of Old Quay Lock (again, typical values between 0.02 - 0.05 m/s) in an area, which is already undergoing some erosion.

Around peak flood (Figure C3B) the strongest currents are located within the south channel. There is an increase in speed along the edge of the intertidal area due to the acceleration of flow around the tower structure in the channel and this change stretches along much of the bankline of Wigg Island (typical values between 0.02 - 0.05 m/s). Along the north bank there is also an observed increase in speed between the baseline case and the proposed scheme. Though these differences are generally confined to upstream of the tower structure in the north channel with values again in the order of 0.02 - 0.05 m/s.

The position of the bridge tower in the north channel is such that it acts to push the flow to the left when looking downstream towards the structure (Figure C4A). This is due to the channel being relatively narrow and the tower footing being towards the bank-side edge of the channel. Figure C3B shows small differences in speed along the front of the tidal wave as it propagates onto the intertidal banks. This is considered to be due to a slight phase change between the baseline case and scheme caused by the interaction of the strong incoming tide and the weak ebbing tide. This effect dissipates quickly as the intertidal banks are flooded.

The greatest increase and reduction in speed occurs local to the bridge structures with peak increases in speed of between 0.50 - 1.00 m/s. The maximum decreases in flow speeds are of the order of 0.30 - 0.80 m/s.

C2.3 Bed Shear Stress

Figures C7 - C10 show differences in bed shear stress between the proposed Route 3A Medium span - original alignment and the baseline case. The greatest changes observed are local to the bridge piers, with maximum increases of the order of 1.2 - 3.6N/m^2 and maximum reduction in bed shear stress of between 1.3 - 3.5 N/m^2. At peak flows there is a predicted change along the shoreface of the intertidal areas, which stretches along a significant extent of this area both upstream and downstream of the structures. Some of these changes appear large from Table C2.1. However, again these changes should not be taken on face value as they represent changes in propagation rather than absolute increases as a result of the bridge scheme. This is an artefact of the rate of increase of the flood tide levels and their timing with respect to ebbing tide within the upper estuary. In addition, the background bed shear stresses are already high enough to mobilise sediment across the study area, therefore, even large changes may not represent a significant increase in sediment transport.

Figures C9 and C10 show percentage differences between the proposed Route 3A Medium span - original alignment and the baseline case. The velocity vectors corresponding to the state of the tide shown, demonstrate that the majority of changes shown are an artefact of the representation of intertidal flooding and drying in the numerical model and are, therefore, of no significance (the speckled areas). Across much of the study area the changes are less than 10% (note that the percentage values in the key are shown as 1 representing 100% and 0.1 representing 10%).

Table C2.1 Maximum and minimum changes for Route 3A medium option - original alignment

		Low Water		Peak Flood		High Water		Peak Ebb	
		max	min	max	min	max	min	max	min
Water level (m)	Piers	0.15	-0.22	-	-	-	-	0.02	-
	Channels	0.04	-0.07	0.04	-0.05	-	-	0.03	-
	Intertidal	0.17	-0.09	0.10	-0.36	0.06	-0.13	0.20	-0.05
Near- surface speed (m/s)	Piers	0.15	-0.17	0.16	-0.22	1.06	-0.82	0.70	-0.36
	Channels	0.08	-0.07	0.09	-0.06	0.10	-0.08	0.04	-0.05
	Intertidal	0.17	-0.11	0.16	-0.12	0.82	-0.16	0.36	-0.15
Near-bed speed (m/s)	Piers	0.17	-0.14	0.17	-0.14	0.77	-0.67	0.55	-0.30
	Channels	0.02	-0.06	0.06	-0.04	0.14	-0.07	0.02	-0.03
	Intertidal	0.09	-0.10	0.12	-0.18	0.14	-0.11	0.21	-0.09
Bed shear stress (N/m^2)	Piers	1.19	-1.25	1.57	-1.35	3.56	-3.47	3.06	-2.58
	Channels	0.44	-0.25	0.32	-0.29	0.31	-0.40	0.25	-0.33
	Intertidal	0.90	-1.02	2.01	-1.42	3.85	-4.51	3.29	-0.62

C3. Route 3A Medium Option - Modified Alignment

This section describes the hydrodynamic simulation undertaken for the Route 3A medium span layout as shown in Drawing No. B4027/3/H/G/3. For this modified version of Route 3A Medium Span operational case there are still 3 sets of piers and 4 towers with footings in the estuary (Plate C2). The pier groups are located on the intertidal area with the remaining structures within the main channel. The bridge piers are octagonal (5m x 5m) and the towers are also octagonal (10m x 10m). However, there is some minor alignment change with the bridge towers being moved away from the north and south channels.

Plate C2. Route 3A Medium Option - Modified Alignment



C3.1 Water Level

Figures C11-C12 show differences in water level between the baseline case and the modified Route 3A scenario over a spring tide. The figures show that changes in water level as a result of the proposed bridge are negligible. Some of the observed differences are due to small phase changes as the tide propagates over the intertidal areas and as observed with the Route 3A Medium Option original alignment the revised alignment shows minor phase changes along the front of the approaching flood tide as it meets with the weak ebb tide upstream of Runcorn Gap. Typical changes in water level over a spring tide are < 0.03 m, although there are locations adjacent to the bridge piers where this value is exceeded (see Table C2.1). As stated previously,

changes in water level observed on areas of intertidal which are dry at that particular state of the tide are caused by the inability of the model to resolve the small drainage channels in these areas leading to 'ponding' of water which in reality would be able to drain away.

C3.2 Speed

Figures C13- C16 show differences in near-surface and near-bed speed between the baseline case and the revised Route 3A scenario over a spring tide. Again the results clearly show the division of the flow around the tower structures as a result of blocked transmission of flow. However, what is of greater interest in the results from this bridge alignment option is the significant reduction in impact along the face of the intertidal area when compared with the original Route 3A alignment. Clearly, in the short-term there is a significant benefit in moving the bridge structures away from the main flow channels. Whether this will remain the case in the longer-term is more difficult to predict. Typical differences in flow speeds are between 0.02 - 0.05 m/s, whilst peak differences in flow speed are between 0.30 - 0.80 m/s for increased flows and 0.10 - 0.30 m/s for reduced flow speeds. These maximum and minimum differences remain local to the structures.

Figures C13B and C15B show differences in speed along the front of the tidal wave as it propagates onto the intertidal banks. As mentioned previously, this is considered to be due to a slight phase change between the baseline case and scheme and represents a positional change in flow speed rather than an absolute increase. This effect dissipates quickly as the intertidal banks are flooded. Comparing maximum changes in speed around the bridge piers/towers with those values obtained from the original Route 3A Medium span alignment there is 20 - 40% reduction as a result of repositioning of the bridge towers.

C3.3 Bed Shear Stress

Figures C17 - C20 show differences in bed shear stress between the modified Route 3A over a spring tide. The greatest changes observed are local to the bridge piers, with maximum increases of around 1.7 - 2.2N/m^2 and maximum reduction in bed shear stress of around 0.4 - 2.1N/m^2. These large values correspond to positions adjacent to the pier/tower structures where changes due to scour are likely to be a maximum.

In general, at peak flows there is no significant increase in bed shear stress along the shoreface of the intertidal areas, unlike the Route 3A Medium Span Original Alignment (compare Figures C8A and B with Figures C18A and B). Typical changes in bed shear stress are between 0.04 - 0.06 N/m^2 although some of these changes appear large from Table C2.1. However, again these changes should not be taken on face value as they represent changes in the flow propagation rather than absolute increases as a result of the bridge scheme.

Figures C19 and C20 show percentage differences between the proposed Route 3A Medium span - modified alignment and the baseline case. The velocity vectors corresponding to the state of the tide shown, demonstrate that the majority of changes shown are an artefact of the representation of intertidal flooding and drying in the numerical model and are, therefore, of no significance (the speckled areas). Across much of the study area the changes are less than 10% (note that the percentage values in the key are shown as 1 representing 100% and 0.1 representing 10%). In addition, compared with the Route 3A Medium Span Original Alignment the figures show that the modified alignment reduces the impact of the scheme on the area reducing both the magnitude and extent of any observed change.

Table C3.1 Maximum and minimum changes for Route 3a medium option - modified alignment

		Low Water		Peak Flood		High Water		Peak Ebb	
		max	min	max	min	max	min	max	min
Water level (m)	Piers	-	-	-	-	0.07	-	0.02	-
	Channels	-	-	-	-	-	-	0	-
	Intertidal	-	-	0.09	-0.11	0.01	-	0.01	-0.01
Near-surface speed (m/s)	Piers	0.06	-0.14	0.07	-0.13	0.78	-0.07	0.60	-0.11
	Channels	-	-	0.08	-0.09	0.01	-0.06	0.07	-0.03
	Intertidal	-	-0.01	0.33	-0.30	0.05	-0.18	0.27	-0.03
Near-bed speed (m/s)	Piers	0.06	-0.09	0.03	-0.06	0.56	-0.07	0.34	-0.21
	Channels	-	-0.01	0.01	-0.03	0.01	-0.01	0.07	-0.02
	Intertidal	-	-0.01	0.26	-0.21	0.04	-0.09	0.24	-0.03
Bed shear stress (N/m^2)	Piers	0.14	-0.40	0.11	-0.36	1.70	-2.08	2.22	-1.68
	Channels	0.01	-0.03	0.04	-0.02	0.03	-0.05	0.04	-0.01
	Intertidal	-	-	2.05	-1.96	1.73	-1.29	2.10	-0.39

C4. Route 3A Medium Option - Modified Alignment: Extreme Fluvial Event - 1:200 Return Period

The model set-up was modified to account for an extreme fluvial event using a 1: 200 years return period. The return period values were calculated from freshwater flow data obtained from the Environment Agency and the National Flow Archive. A Gumbel distribution was used to determine the return period flows using the annual maxima for each station. The following stations were used in the analysis:

- River Gowy
- River Weaver
- River Mersey
- Sankey Brook
- Ditton Brook

For further details see Appendix B.

It was assumed that the extreme flow events occurred over a spring tide.

C4.1 Water Level

Figures C21 - C22 show differences in water level between the baseline case and the extreme fluvial event. There are no significant changes within the main estuary with increases being confined to areas adjacent to the bridge piers/towers (maximum and minimum changes of 0.06m and -0.05m, respectively). The largest changes are indicated to occur over the intertidal area. However, some of these observed differences are due to small phase changes as the tide propagates over the intertidal areas and others are caused by the inability of the model to resolve drainage from the intertidal areas leading to 'ponding'.

C4.2 Speed

Figures C23 - C26 show differences in near-surface and near-bed speed between the baseline case and the revised Route 3A scenario over a spring tide with a 1:200 year fluvial event. Typical differences in flow speeds are between 0.02 - 0.05 m/s, whilst peak increases in flow speed are between 0.20 - 0.40 m/s and maximum deceleration in flow is between 0.40 - 0.60m/s (see Table C4.1). These maximum and minimum differences remain local to the bridge structures. The increased freshwater flow appears to reduce the impact of the scheme within the estuary at peak times while increasing the impact around low water. This is likely to be due to the increased fluvial flow in the low water channels leading to high water levels and greater velocities.

Figures C23B and C25B show the same differences in speed along the front of the tidal wave as it propagates onto the intertidal banks as observed in the previous scenarios tested. Again, this effect is considered to be caused by a slight phase change between the baseline case and scheme and represents a positional change in flow speed rather than an absolute increase.

C4.3 Bed Shear Stress

Figures C27 - C30 show differences in bed shear stress between the modified Route 3A over a spring tide with a 1:200 year fluvial event. The greatest changes observed are local to the bridge piers, with maximum increases of around 2.4 - 4.3N/m^2 and maximum reduction in bed shear stress of around 1.8 - 3.2N/m^2. Around High water the model results indicate changes across much of the upper estuary to be limited to around the bridge piers/towers and along the edge of the intertidal area with the greatest extent of change of less than 0.04N/m^2. At other states of the tide the changes are generally confined to the locality of the bridge structures.

The large increases in bed shear stress indicated in Table C4.1 should be viewed in context of the background values of bed shear stresses which are already high enough to mobilise sediment across the study area, therefore, even large changes may not represent a significant increase in sediment transport.

Figures C29 and C30 show percentage differences between the proposed Route 3A Medium Option - Modified Alignment with a 1:200 years fluvial event against the baseline case. The velocity vectors corresponding to the state of the tide shown, demonstrate that the majority of changes shown are an artefact of the representation of intertidal flooding and drying in the numerical model and are, therefore, of no significance (the speckled areas). Across much of the study area the changes are less than 10%

Table C4.1 Maximum and minimum changes for Route 3a medium option - modified alignment: extreme fluvial event - 1:200 return period

		Low Water		Peak Flood		High Water		Peak Ebb	
		max	min	max	min	max	min	max	min
Water level (m)	Piers	0.06	-0.04	0.04	-0.05	0.01	-0.01	0.02	-0.05
	Channels	-	-	-	-	-	-	-	-
	Intertidal	0.07	-0.04	0.07	-0.12	0.14	-0.22	0.07	-0.05
Near-surface speed (m/s)	Piers	0.25	-0.38	0.38	-0.42	0.02	-0.09	0.23	-0.44
	Channels	-	-	0.02	-0.03	0.02	-	-	-
	Intertidal	0.04	-0.01	0.31	-0.20	0.40	-0.27	0.12	-0.04
Near-bed speed (m/s)	Piers	0.24	-0.37	0.44	-0.57	0.03	-0.07	0.26	-0.44
	Channels	-	-	0.03	-0.02	0.02	-	-	-
	Intertidal	0.07	-0.06	0.32	-0.25	0.30	-0.18	0.11	-0.02
Bed shear stress (N/m^2)	Piers	2.35	-1.84	4.26	-3.21	0.05	-0.19	2.43	-2.07
	Channels	-	-	0.14	-0.08	0.02	-	0.04	-
	Intertidal	0.33	-0.36	2.21	-1.63	0.31	-0.25	0.46	-0.05

C5. Route 3A Medium Option - Modified Alignment: Extreme Fluvial and Surge Event - 1:200 return period

The model set-up was modified to account for an extreme fluvial and surge event using a 1:200 years return period. The return period values for the freshwater flow were calculated as described above. The extreme surge was determined from an Environment Agency - North West Region report (Environment Agency, 1998). The shape of the surge tide was determined from a surge event recorded at Gladstone Dock. The recorded tidal curve was 'stretched' to fit the 1:200 year return event. A synthetic tidal time-series was then generated and used to provide the driving tidal boundary conditions in the model. Further details are given in Appendix B.

C5.1 Water Level

Figures C31 - C32 show differences in water level between the baseline case and the extreme fluvial and surge event. There are no significant changes within the main estuary, although around high water the surge tide has covered the intertidal area. The surge tide is high enough to cover parts of Wigg Island, though in general differences in water level are confined to the local vicinity of the bridge piers (maximum increase

0.04m; maximum reduction -0.08m). There is no indication that the tower/piers structures cause any significant blockage across the estuary with typical changes in water level of 0.02 m, approximately.

As the flooding or ebbing tide moves onto the intertidal areas large differences (Table C5.1) can be manifested along the edge of the tidal wave. These differences do not provide a real indication of absolute change as they are an artefact of phase differences in the propagation of the front of the tidal wave and represent a positional change in water level (for example Figure C31).

C5.2 Speed

Figures C33- C36 show differences in near-surface and near-bed speed between the baseline case and the revised Route 3A scenario over an extreme fluvial and surge event. In general, differences are limited to the immediate area around the bridge structures, with typical differences in flow speeds are between 0.02 - 0.05 m/s. Maximum differences in flow speed are between $\pm$0.20 - 0.50 m/s. In general, these maximum and minimum differences are found adjacent to the bridge structures. Around high water there is some interaction between the central piers generating a radiating flow pattern. There is also interaction with the first set of pier footings on the upper intertidal area. However, overall, the bridge appears to have a limited impact on the estuary during an extreme fluvial and surge event.

The 1:200 year surge event leads to flows over the intertidal area and parts of Wigg Island. From Table C5.1 some of the changes along the intertidal areas would appear large. However, this is considered to be due to a slight phase change between the baseline case and scheme and represents a positional change in flow speed rather than an absolute increase (for example see Figure C33B).

Similar order of increases in speed around low water are observed in the combined extreme surge and fluvial scenario as observed in the 1:200 years fluvial scenario. This would indicate that this is primarily due to the increased fluvial flow in the low water channels leading to high water levels and greater velocities rather than due to increased tidal velocities as a result of the surge.

C5.3 Bed Shear Stress

Figures C37 - C40 show differences in bed shear stress between the modified Route 3A over an extreme fluvial and surge event. The greatest changes observed are local to the bridge piers, with maximum increases of around 2.2 - 5.5N/m^2 and maximum reduction in bed shear stress of around 0.9 - 1.5N/m^2. Around High water the model results indicate changes over a larger extent of the upper estuary both upstream and downstream of the proposed crossing. This is a function of the intertidal area being flooded on the extreme tide over the high water period. At other states of the tide the changes are generally confined to the locality of the bridge structures.

Although Table C5.1 indicates large changes in bed shear stress along the intertidal, these areas are limited in extent and are also considered to be caused by changes in the flow propagation rather than absolute increases as a result of the bridge scheme. This is demonstrated by comparing the difference plots of bed shear stress with the percentage difference plots of bed shear stress (for example compare Figure C38A with Figure C40A).

Figures C39 and C40 show percentage differences between the proposed Route 3A Medium Option - Modified Alignment with a 1:200 year surge and fluvial event against the baseline case. The velocity vectors corresponding to the state of the tide shown, demonstrate that the majority of changes shown are an artefact of the representation of intertidal flooding and drying in the numerical model and are, therefore, of no significance (the speckled areas). Across much of the study area the changes are less than 10%.

Table C5.1 Maximum and minimum changes for Route 3a medium option - modified alignment: extreme fluvial and surge event - 1:200 return period

		Low Water		Peak Flood		High Water		Peak Ebb	
		max	min	max	min	max	min	max	min
Water level (m)	Piers	0.02	-0.03	0.04	-0.08	0.02	-0.01	0.01	-0.02
	Channels	-	-	-	-	-	-	-	-
	Intertidal	0.17	-0.08	0.55	-0.12	0.41	-0.29	0.21	-0.14
Near-surface speed (m/s)	Piers	0.25	-0.38	0.37	-0.45	0.07	-0.34	0.09	-0.36
	Channels	0.03	-0.03	0.01	-0.02	0.04	-0.01	0.02	-0.03
	Intertidal	0.32	-0.27	0.42	-0.25	0.07	-0.36	0.08	-0.12
Near-bed speed (m/s)	Piers	0.24	-0.36	0.45	-0.23	0.07	-0.33	0.12	-0.30
	Channels	0.02	-0.01	0.01	-0.01	0.04	-0.01	0.01	-0.02
	Intertidal	0.29	-0.22	0.24	-0.19	0.07	-0.35	0.10	-0.18
Bed shear stress (N/m^2)	Piers	2.24	-1.77	5.48	-2.81	0.27	-1.09	0.64	-1.32
	Channels	0.23	-0.01	0.12	-0.11	0.15	-0.20	0.04	-0.04
	Intertidal	1.89	-1.45	1.84	-0.91	0.70	-0.99	0.26	-0.39

C6. Route 3A Medium - 3 Tower Option

This section describes the hydrodynamic simulation undertaken for the Route 3A medium span layout as shown in Drawing No. B4027/3/B/300. For this modified version of Route 3A Medium Span operational case the number of towers is reduced to 3 and the pier alignments have been modified (Plate C3). The bridge piers are octagonal (5m x 5m) and the towers are also octagonal (10m x 10m). The towers are all located with the main body of the upper estuary whilst the pier groups are located either on or above the intertidal area.

Plate C3. Route 3A Medium - 3 Tower Option



C6.1 Water Levels

Figures C41-C42 show differences in water level between the proposed Route 3A Medium - 3 Tower Option and the baseline case over a spring tide. The model results show that the proposed scheme has a negligible impact on water levels with any observed changes typically being of the order of < 0.02m. Around low water there is almost no discernible effect on water levels since all the bridge structures are outside the low water flow channels.

Peak changes in water level occur on the front of the tidal wave as it propagates onto the intertidal areas (see Table C6.1). However, such changes are considered to be insignificant, as they are very short in duration (seconds) and affect a very limited area. In addition, such changes are considered to represent a positional change in value rather than an absolute change.

C6.2 Speed

Figures C43 - C46 show differences in near-bed and near-surface flow speeds between the proposed scheme and the baseline case over a spring tide. Around low water there is no observed impact on flow speeds due to the bridge towers and pier positions being outside the low water flow channels.

Around the time of peak flows the greatest changes in speed are local to the bridge structures. Maximum increases in near-surface flow speed are between 0.06 - 0.11 m/s. For near-bed flows the maximum increases are of the order of 0.10 m/s whilst the maximum reduction in flow speeds are of the order of 0.20 m/s. (see Table C6.1). These show a considerable reduction (up to 90%, approximately) in observed changes in speed over those observed for the Route 3A Medium span option - original and modified alignments (4 towers). This again demonstrates the importance of the siting of the bridge piers in the short term. In addition, the position of the central tower is such that under the existing channel alignment it is only exposed to flow around the time of high water on spring tides.

On the southern bank the twin pier structure closest to the southern-most tower is positioned on the edge of the channel and, therefore, leads to some impact on flow speeds along the edge of the southern channel and intertidal area. Although Table C6.1 indicates larger changes in speed along the intertidal regions, these areas are limited in extent and are also considered to be caused by changes in the flow propagation rather than absolute increases as a result of the bridge scheme.

C6.3 Bed Shear Stress

Figures C47-C50 show differences in bed shear stress between the proposed Route 3A Medium - 3 Tower Option and the baseline case over a spring tide. As with the flow speeds, there is no observed change in bed shear stress around low water due to the bridge towers and pier positions being outside the low water flow channels. In general, changes are confined to the immediate locality of the bridge structures with the greatest observed impact occurring around the time of peak flood. There is a wide band of increased bed shear stress (0.04-0.06 N/m^2) along the southern bank in the vicinity of Wigg Island and upstream of the bridge structure around peak flood due to interaction between the southern-most tower and the nearest pier structures. The greatest changes observed local to the bridge piers show maximum increases of around 0.2-1.5N/m^2 and maximum reduction in bed shear stress of around 0.8-2.9N/m^2.

Figures C49 and C50 show percentage differences between the proposed Route 3A Medium 3 Tower Option against the baseline case. The velocity vectors corresponding to the state of the tide shown, demonstrate that the majority of changes shown are an artefact of the representation of intertidal flooding and drying in the numerical model and are, therefore, of no significance (the speckled areas). Across much of the study area the changes are less than 10%.

Table C6.1 Maximum and minimum changes for Route 3a medium - 3 tower option

		Low Water		Peak Flood		High Water		Peak Ebb	
		max	min	max	min	max	min	max	min
Water level (m)	Piers	-	-	0.30	-0.06	-	-	-	-
	Channels	0.12	-	-	-	-	-	-	-
	Intertidal	-	-	-	-	0.02	-0.03	0.07	0.11
Near-surface speed (m/s)	Piers	-	-	0.11	-0.11	0.10	-0.23	0.06	-0.13
	Channels	-	-	0.12	-0.09	0.02	-0.02	-	-
	Intertidal	-	-	0.23	-0.08	0.03	-0.03	0.11	-0.13
Near-bed speed (m/s)	Piers	-	-	0.09	-0.07	0.08	-0.20	0.05	-0.09
	Channels	-	-	0.12	-0.09	0.01	-0.01	-	-
	Intertidal	-	-	0.23	-0.08	0.17	-0.04	0.13	-0.09
Bed shear stress (N/m^2)	Piers	No change	No change	1.50	-2.87	0.41	-0.80	0.22	-0.21
	Channels			0.52	-0.62	1.40	-0.54	-	-
	Intertidal			1.80	-0.40	0.06	-	0.18	-0.10

C7. Route 3A Medium - 3 Tower Option - Revised Alignment

This section describes the hydrodynamic simulation undertaken for the Route 3A medium span layout as shown in Drawing No. B4027/3/B/300 Rev A.

Plate C4.. Route 3A Medium - 3 Tower Option - Revised Alignment



For this modified version of Route 3A Medium Span operational case the number of towers is reduced to 3 and the pier alignments have been modified (Plate C4). The bridge piers are octagonal (5m x 5m) and the towers are also octagonal (10m x 10m). As with the previous 3 Tower alignment (Drawing No. B4027/3/B/300) the towers are all located within the main body of the upper estuary whilst the pier groups are located either on or above the intertidal area.

C7.1 Water Levels

Figures C51-C52 show differences in water level between the proposed Route 3A Medium - 3 Tower Option and the baseline case over a spring tide. The model results show that the proposed scheme has a negligible impact on water levels with any observed changes typically being of the order of < 0.02m. Around low water there is almost no discernible effect on water levels since all the bridge structures are outside the low water flow channels. Also, around the time of high water there is no real discernible effect due to the bridge.

Changes in water level local to the tower structures are also negligible (< 0.03m) although at low water and peak ebb the maximum change around the piers is 0.08m. However, this is not considered significant due to its very limited extent and also because of the state of the tide.

Maximum changes in water level occur on the front of the tidal wave as it propagates onto the intertidal areas (see Table C7.1). However, such changes are considered to be insignificant, as they are very short in duration (seconds) and affect a very limited area. In addition, such changes are considered to represent a positional change in value rather than an absolute change.

C7.2 Speed

Figures C53 - C56 show differences in near-bed and near-surface flow speeds between the proposed scheme and the baseline case over a spring tide. Around low water there is no observed impact on flow speeds due to the bridge towers and pier positions being outside the low water flow channels.

Around the time of peak flows the greatest changes in speed are local to the bridge structures. Maximum increases in near-surface flow speed are between 0.04 - 0.16 m/s. For near-bed flows the maximum increases are of the order of 0.04 - 0.18 m/s whilst the maximum reduction in flow speeds are of the order of 0.60 and 0.50 m/s for near-surface and near-bed flows, respectively (see Table C6.1). Again these results show a considerable reduction (up to 94%, approximately) in observed changes in speed over those observed for the Route 3A Medium span option - original and modified alignments (4 towers). As previously, this demonstrates the importance of the siting of the bridge piers in the short term. In addition, as with the previous 3 tower alignment (Drawing No. B4027/3/B/300) the position of the central tower is such that

under the existing channel alignment it is only exposed to flow around the time of high water on spring tides.

On the southern bank the twin pier structure closest to the southern-most tower is now positioned away from the edge of the channel and, therefore, changes in flow speeds are limited to the three tower structures. Table C7.1 indicates similar order of changes in speed along the intertidal regions as observed in the previous 3 towers alignment scheme. These areas of change are limited in extent and the changes are also considered to represent an alteration in the flow propagation rather than absolute increase in speed.

C7.3 Bed Shear Stress

Figures C57 - C60 show differences in bed shear stress between the proposed Route 3A Medium - 3 Tower Option revised alignment and the baseline case over a spring tide. As with the flow speeds, there is no observed change in bed shear stress around low water due to the bridge towers and pier positions being outside the low water flow channels. In general, changes are confined to the immediate locality of the bridge structures with the greatest observed impact occurring around the time of peak flood. The greatest changes observed local to the bridge piers show maximum increases of around 0.8 - 2.7N/m^2 and maximum reduction in bed shear stress of around 0.7 - 5.0N/m^2.

Figure C57B shows the difference in bed shear stress along the front of the tidal wave as it propagates onto the intertidal banks as observed in the previous scenarios tested. Again, this effect is considered to represent a phase change between the baseline case and scheme and shows a positional change in bed shear stress rather than an absolute increase.

Table C7.1 Maximum and minimum changes for Route 3a medium - 3 tower option revised alignment

		Low Water		Peak Flood		High Water		Peak Ebb	
		max	min	max	min	max	min	max	min
Water level (m)	Piers	0.08	-	0.02	-0.07	0.01	-0.02	0.08	-0.07
	Channels	-	-	-	-0.03	-	-	-	-
	Intertidal	0.14	-0.09	0.12	-0.10	-	-0.02	0.08	0.06
Near-surface speed (m/s)	Piers	-	-	0.16	-0.21	0.10	-0.63	0.04	-0.23
	Channels	-	-	0.04	-0.06	0.02	-	-	-
	Intertidal	-	-	0.25	-0.28	0.03	-0.08	-	-
Near-bed speed (m/s)	Piers	-	-	0.18	-0.40	0.12	-0.46	0.06	-0.21
	Channels	-	-	0.01	-0.02	0.02	-	-	-
	Intertidal	-	-	0.21	-0.21	0.03	-0.07	-	-
Bed shear stress (N/m^2)	Piers	-	-	2.68	-4.95	0.82	-2.02	0.28	-0.67
	Channels	-	-	0.17	-0.12	0.09	-0.02	-	-
	Intertidal	-	-	0.84	-0.72	0.14	-0.09	-	-

Figures C59 and C60 show percentage differences between the proposed Route 3A Medium 3 Tower Option revised alignment against the baseline case. The velocity vectors corresponding to the state of the tide shown, demonstrate that the majority of changes shown are an artefact of the representation of intertidal flooding and drying in the numerical model and are, therefore, of no significance (the speckled areas). Across the majority of the study area they represent a change in bed shear stress of less than 10%.

C8. Route 3A 3 Tower Option - Revised Alignment: Extreme Fluvial and Surge Event - 1:200 return period

Similarly to the modified 4 tower option the revised alignment 3 tower option was set-up to account for an extreme fluvial and surge event using a 1:200 years return period. The return period values for the freshwater flow were calculated as described above. The extreme surge was determined from an Environment Agency - North West Region report (Environment Agency, 1998) with the shape of the surge tide being determined from a surge event recorded at Gladstone Dock. Further details are given in Appendix B.

C8.1 Water Level

Figures C61 – C62 show differences in water level between the baseline case and the extreme fluvial and surge event. At low water there are no observed changes within the estuary and around peak flood most of the predicted changes are associated with phase-induced changes as a result of minor differences in the propagation of the flood tide. Around high water the results show a reduction in water level in the area of the proposed crossing (typically less than 0.02m). However, there is no indication that the tower/piers structures cause any significant blockage across the estuary with typical changes in water level of 0.02 m, approximately.

As the flooding tide moves onto the intertidal areas differences (Table C8.1) can be manifested along the edge of the tidal wave. These differences do not provide a real indication of absolute change as they are an artefact of phase differences in the propagation of the front of the tidal wave and represent a positional change in water level (for example Figure C61).

C8.2 Speed

Figures C63- C66 show differences in near-surface and near-bed speed between the baseline case and the revised Route 3A scenario over an extreme fluvial and surge event. In general, differences are limited to the immediate area around the bridge structures, with typical differences in flow speeds between 0.02 - 0.05 m/s. Maximum changes in flow speed around the bridge structures are between 0.07 - 0.82 m/s, with

minimum changes between 0.55 – 1.19 m/s. Around high water there is some interaction between the central piers generating a radiating flow pattern. There is also interaction with the first set of pier footings on the upper intertidal area. However, overall, the bridge appears to have a limited impact on the estuary during an extreme fluvial and surge event.

The 1:200 year surge event leads to flows over the intertidal area and parts of Wigg Island. From Table C5.1 some of the changes along the intertidal areas would appear large. However, this is considered to be due to a slight phase change between the baseline case and scheme and represents a positional change in flow speed rather than an absolute increase (for example see Figure C63B).

Similar order of increases in speed around low water are observed in the combined extreme surge and fluvial scenario as observed in the 1:200 years fluvial scenario. This would indicate that this is primarily due to the increased fluvial flow in the low water channels leading to high water levels and greater velocities rather than due to increased tidal velocities as a result of the surge.

C8.3 Bed Shear Stress

Figures C67 – C70 show differences in bed shear stress between the modified Route 3A over an extreme fluvial and surge event. The greatest changes observed are local to the bridge piers, with maximum increases of around 0.36 - 1.56N/m^2 and maximum reduction in bed shear stress of around 1.12 - 3.69N/m^2. Around High water the model results indicate changes over a larger extent of the upper estuary both upstream and downstream of the proposed crossing. This is a function of the intertidal area being flooded on the extreme tide over the high water period. At other states of the tide the changes are generally confined to the locality of the bridge structures.

Although Table C8.1 indicates changes in bed shear stress along the intertidal, these areas are limited in extent and some are considered to be caused by changes in the flow propagation rather than absolute increases as a result of the bridge scheme. This is demonstrated by comparing the difference plots of bed shear stress with the percentage difference plots of bed shear stress (for example compare Figure C68A with Figure C70A).

Figures C69 and C70 show percentage differences between the proposed Route 3A Medium Option - Modified Alignment with a 1:200 year surge and fluvial event against the baseline case. The velocity vectors corresponding to the state of the tide shown, demonstrate that the majority of changes shown are an artefact of the representation of intertidal flooding and drying in the numerical model and are, therefore, of no significance (the speckled areas). Across much of the study area the changes are less than 10%.

Table C8.1 Maximum and minimum changes for Route 3a 3 Tower Option - Revised Alignment: extreme fluvial and surge event - 1:200 return period

		Low Water		Peak Flood		High Water		Peak Ebb	
		max	min	max	min	max	min	max	min
Water level (m)	Piers	0.01	-	0.02	-	-	-0.03	0.01	-
	Channels	-	-	-	-	-	-0.02	-	-
	Intertidal	0.03	-	0.01	-0.02	-	-0.05	0.02	-
Near-surface speed (m/s)	Piers	0.07	-0.55	0.82	-1.19	0.09	-0.77	0.12	-0.85
	Channels	-	-	-	-	0.02	-0.05	0.02	-0.05
	Intertidal	0.02	-	0.04	-0.04	0.06	-0.07	0.01	-
Near-bed speed (m/s)	Piers	0.07	-0.34	0.53	-0.77	0.09	-0.56	0.15	-0.59
	Channels	-	-	-	-	0.01	-0.04	0.02	-0.03
	Intertidal	0.03	-	0.03	-0.04	0.02	-0.04	0.01	-
Bed shear stress (N/m^2)	Piers	0.36	-1.12	1.56	-3.69	0.39	-1.14	0.43	-1.43
	Channels	-	-	-	-	0.05	-0.25	0.08	-0.11
	Intertidal	0.12	-	0.25	-0.31	0.26	-0.23	0.25	-0.36

C9. Route 3A Short Option

Plate C5. Route 3A Short Option



This section describes the hydrodynamic simulation undertaken for the Route 3A Short span layout as shown in Drawing No. B4027/3/B/301. The Route 3A Short Span operational case has modified pier alignments compared to the version tested in Phase I of the modelling study (Plate C5). The bridge piers are octagonal (5m x 5m) and are placed in pairs. There are 11 sets of piers within the channel and intertidal area.

C9.1 Water Levels

Figures C71 – C72 show differences in water level between the proposed bridge scheme and the baseline case over a spring tide. The model results show that around peak flood (Figure C71B) the Short Span Option shows a general elevation of water levels in both the south and north channels. The extent of this blockage effect is greatest in the north channel. This backwater effect is limited to the flood tide and is caused by the strong asymmetry in the tidal curve with a very short flood period (≈1.5 hours) and a much longer ebb period (≈11 hours). The maximum change around the piers is 0.08 m and within the channel this reduces to 0.03 m (Table C9.1).

The observed blockage effect of the Short Span Scheme was demonstrated in the previous coarse grid model (Phase I) but the extent of those changes was greater. This is considered to be an artefact of the grid scale and the use of additional friction terms to represent the bridge piers in the coarse model leading to a conservative solution.

C9.2 Speed

Figures C73 – C76 show differences in near-bed and near-surface flow speeds between the proposed scheme and the baseline case over a spring tide. At peak flood the model shows the short span option to accelerate the flows speeds along the intertidal areas of the north and south channels. The maximum increase in flow speed local to the bridge piers are of the order of 0.08 - 0.20 m/s. However, around peak flood there is larger change in flow speed within the channels than compared with any of the other schemes tested (0.2m/s). The largest extent of flow change is within the south channel around peak flood, with increased flows along much of the intertidal foreshore of Wigg Island.

Over the ebbing tide the bridge structures lead to increased flow speeds along much of the north bank along the intertidal area local to the bridge as well as along the south bank downstream of Old Quay lock.

Around the time of high water there is a general change in flow speed across the whole width of the estuary due to the number of piers present. This effect is reduced on neap tides (not shown) due to the lower water levels, however, the short span option shows the greatest impact within the study area in terms of extent, although the magnitude of the change is often less then observed for some of the schemes using towers.

Maximum changes in speed along the intertidal tend to occur on the front of the tidal wave as it propagates onto the intertidal areas (see Table C9.1 and Figure C73B). However, as previously, where these observed changes occur along the edge of the propagating wave such changes are considered to be insignificant, as they are very short in duration (seconds) and affect a very limited area. In addition, such changes are considered to represent a positional change in value rather than an absolute change.

C9.3 Bed Shear Stress

Figures C77 – C80 show differences in bed shear stress between the proposed Route 3A Short Option and the baseline case over a spring tide. Figure C77B shows the difference in bed shear stress around peak flood with a general increase in both the north and south channels. In general, the largest changes are confined to the immediate locality of the bridge structures with maximum increases of around 0.3 - 5.0N/m^2 and maximum reduction in bed shear stress of around 0.6 - 5.7N/m^2.

Figure C77B also shows the difference in bed shear stress along the front of the tidal wave as it propagates onto the intertidal banks as observed in the previous scenarios tested. Again, this effect is considered to be represent a phase change between the baseline case and scheme and shows a positional change in bed shear stress rather than an absolute increase.

Although Table C9.1 indicates large changes in bed shear stress along the intertidal (up to 8.2N/m^2) many of these changes are due to the positional change in bed shear stress as a result of a change in the flow propagation. However, Figure C79B also reveals that some of these large changes are real and are caused by the obstruction across the channel that this scheme represents.

Table C9.1 Maximum and minimum changes for Route 3a short option

		Low Water		Peak Flood		High Water		Peak Ebb	
		max	min	max	min	max	min	max	min
Water level (m)	Piers	-	-	0.08	-0.01	-	-	-	-
	Channels	0.14	-0.08	0.03	-0.08	-	-	0.07	-0.10
	Intertidal	0.07	-0.08	0.07	-0.05	0.03	-0.03	0.03	-
Near-surface speed (m/s)	Piers	0.02	-0.06	0.21	-0.21	0.12	-0.17	0.08	-0.15
	Channels	0.06	-0.04	0.20	-0.19	0.02	-0.03	0.09	-0.08
	Intertidal	0.08	-0.07	0.39	-0.04	0.09	-0.25	0.37	-0.05
Near-bed speed (m/s)	Piers	-	-0.04	0.34	-0.24	0.07	-0.14	0.05	-0.13
	Channels	0.03	-0.10	0.09	-0.13	0.07	-	0.11	-0.04
	Intertidal	0.08	-0.06	0.43	-0.11	0.06	-0.11	0.26	-0.09
Bed shear stress (N/m^2)	Piers	0.10	-0.28	5.04	-5.67	0.21	-0.62	0.30	-1.36
	Channels	0.23	-0.22	0.87	-0.77	0.06	-0.16	1.43	-0.36
	Intertidal	1.23	-	8.15	-0.40	0.42	-1.35	2.42	-0.17

Figures C79 and C80 show percentage differences between the proposed Route 3A Short Span Option against the baseline case. The velocity vectors corresponding to the state of the tide shown, demonstrate that the majority of changes shown are an artefact of the representation of intertidal flooding and drying in the numerical model and are, therefore, of no significance (the speckled areas). Figure C79B reinforces the observed impact of the short span case around peak flood with large changes indicated along the edge of the channel (> 50%).

C10. Baseline

Figures C71 - C78 show the actual values for water level, speed and bed shear stress for the baseline case. These are provided to place the differences into context with the background values. Table C9.1 tabulates the maximum and minimum values for speed and bed shear stress across the study domain as represented by the area shown in the figures. It is clear from both the table and the figures that peak flows and bed stresses are high across the area. Therefore, as an example, a change of 1 N/m^2 when the background value is 12 N/m^2, approximately, only represents an 8% increase in bed shear stress.

Table C10.1 Maximum and minimum values baseline case

	Low Water		Peak Flood		High Water		Peak Ebb	
	max	min	max	min	max	min	max	min
Near-surface speed (m/s)	0.69	-1.23	2.32	-2.01	2.00	-0.48	1.52	-1.66
Near-bed speed (m/s)	0.43	-0.82	1.77	-1.37	1.54	-0.38	1.09	-1.15
Bed shear stress (N/m^2)	3.31	-11.45	11.99	-11.20	11.98	-3.52	10.86	-11.96

C.11 Bridge Scour Assessment

C11.1 Introduction

Whilst the theory behind the structural design of bridges is well founded, the mechanisms for flow and erosion in channels consisting of mobile sediments is not well defined. This makes the river boundary changes that occur at a bridge, due to a given flow condition, difficult to estimate with confidence.

In the context of the current report, scour is defined as the lowering of a riverbed by erosion due to water turbulence such that there is a tendency to expose the bridge foundations. The extent of this reduction in the natural level of the riverbed is the scour depth or depth of scour. The natural level of the bed is generally considered to be the level of the riverbed prior to the onset of scour. The types of scour that can occur at a bridge crossing are normally referred to as general scour, contraction scour and local

scour. These different types of scour may occur simultaneously, in combination or separately. In addition, in tidal estuaries scour development will take place in two directions due to the ebbing and flooding of the tide.

General scour occurs irrespective of the bridge being located within the river and can take place as long-term or short-term scour. Long-term scour is typically of the order of several years or longer, whilst short-term scour can occur over a single flood event. Long-term scour results in progressive degradation and lateral bank erosion. Progressive degradation is the general lowering of the riverbed due to geomorphological changes, anthropogenic changes, or hydrometeorological changes.

Contraction scour and local scour are a direct consequence of the bridge being located in the riverbed. The flow at a bridge usually converges as it approaches the bridge due to the bridge or the approach roads causing a constriction of the flow. As the flow contracts within the opening it accelerates. This accelerated flow induces scour across the contracted section of river and is, thus, termed contraction scour.

Local scour is caused by the interference of the bridge piers and abutments with the flow and manifests itself by the formation of scour holes immediately around these structures. Localized scour can occur either as clear-water scour or live-bed scour. Clear-water scour occurs when the bed sediment upstream of the areas of scour is at rest. Live-bed scour occurs when there is general sediment transport within the river. The maximum local scour depth is achieved when the flow is no longer able to remove bed material from the area of scour. The equilibrium scour depth occurs when the time-averaged transport of bed material into the scour hole equals that removed from it. Melville and Coleman (2000) give a detailed review of bridge scour.

The local scour around bridge piers is largely dependent on their geometry and, generally, will occur quite rapidly. Therefore, of most import is the maximum scour depth developed within the equilibrium phase.

The flow pattern near a bridge pier is quite complex, for example, Breusers and Raudkivi (1991), Melville and Coleman (2000). The principal features of scour round a circular pier are well defined, the downflow at the upstream face of the pier, the horseshoe vortex at the base of the pier, a surface roller (or bow wave) at the upstream face of the pier and wake vortices downstream of the pier (Figure C89).

The downflow is a result of flow deceleration in front of the pier. The associated stagnation pressures on the face of the pier are greatest near the surface, where the deceleration is largest, and decrease downwards. This resulting downwards pressure gradient at the face of the pier leads to the downflow. This downflow impinges on the bed, acting like a vertical jet and eroding a groove immediately adjacent to the pier face. The creation of the groove undermines the scour hole slope above and this slope then collapses bringing sediment into the erosion zone. The development of the scour hole around the pier creates a lee eddy, known as the horseshoe vortex. The

horseshoe vortex develops as a result of separation flow at the upstream rim of the scour hole and is, therefore, a consequence of the scour not the cause of it. The horseshoe vortex is effective at transporting sediment away from the scour hole. It is the downflow and horseshoe vortex that are the primary mechanisms in the scour hole development.

The wake vortices are a consequence of flow separation at the sides of the pier. These vortices travel downstream due to the mean flow. Raudkivi (1991) describes these cast-off vortices as having vertical low pressure centres lifting sediment from the bed like miniature tornados. Melville and Coleman (2000) describe the vortices as acting like vacuum cleaners sucking sediment from the bed as well as transporting sediment entrained by the downflow and horseshoe vortex.

C11.2 Timescale

Scour around bridge piers can be divided into several stages (Hoffmans and Verheij, 1997): the initial phase, development phase, stabilization phase and equilibrium phase. The initial phase of the scour process can be characterized as the period in which the erosion capacity is greatest. The development phase is represented by a significant increase in the scour depth, whilst the shape of the scour hole remains the same. During the equilibrium phase the rate of development of the maximum scour depth reduces. In addition, the erosion capacity in the deepest part of the scour hole is small compared to the erosion capacity downstream of the point of reattachment. This leads to a greater increase in the longitudinal dimensions of the scour hole than in the vertical depth. The equilibrium phase is defined as the period during which the dimensions of the scour hole remain significantly unaltered.

Under live-bed conditions, the equilibrium depth is reached more quickly than under clear-water scour conditions. Thereafter, the scour depth will fluctuate due to the movement of sediment/bedforms past the pier.

C11.3 Effect of Flow Depth

Melville and Coleman (2000) define flow shallowness as representing the effect of flow depth relative to the pier width. For deep flows, that is, for narrow piers, the scour depth increases proportionately with foundation size and is independent of flow depth. Whereas, for shallow flows, relative to the pier size, the scour depth increases proportionately with flow depth and is independent of pier width. While for intermediate flow depths the depth of scour is dependent on both. In addition, the depth of the bed material is also important as this may limit the scour development.

C11.4 Effect of Tidal Flow

Relatively little work has been undertaken to investigate flow at bridges in tidal rivers in comparison to studies undertaken for unidirectional flow. Since the flow reverses

direction with the tide consequently the scour development will take place in two directions. The local scour depth can be estimated using the same equations as for unidirectional river flow, although scour development is typically reduced due to sediment eroded during the first phase of the tide being deposited on the reversing part of the tidal cycle. Breusers (1966) suggested the following equation for local scour depth at piers.

$$d_s = 1.4b$$

Where

b is the pier width.

The equation was developed using measurements of scour depths in tidal estuaries. In addition to the astronomical variation of the tide, other factors that may affect local scour in tidal estuaries are meteorological effects such as storm surges and the relative magnitudes of the fluvial and tidal flows.

Numerous equations have been proposed for the estimation of the depth of local scour at bridge piers (Melville and Coleman, 2000), however, in the current study only the formulas of Breusers (1966), Breusers *et al.* (1977), Johnson (1992) and Richardson and Davis (2001) have been used for comparison purposes.

$$d_s = 1.5K_i b \tanh\left(\frac{h_0}{b}\right) \qquad \text{(Breusers } et\ al.,\ 1977\text{)}$$

$$d_s = 2.02K_i h_0 F_r^{0.21} \sigma_d^{-0.24} \left(\frac{b}{h_0}\right)^{0.98} \qquad \text{(Johnson, 1992)}$$

$$d_s = 2.0K_1K_2K_3K_4 h_0 F_r^{0.43} \left(\frac{b}{h_0}\right)^{0.65} \qquad \text{(Richardson and Davis, 2001)}$$

in which:

b = the pier width (m)
h_0 = flow depth (m)
K_i = correction factor
K_1 = correction factor for pier nose shape
K_2 = correction factor for angle of attack of flow
K_3 = correction factor for bed condition
K_4 = correction factor for size of bed material
F_r = Froude number
d_s = equilibrium scour depth

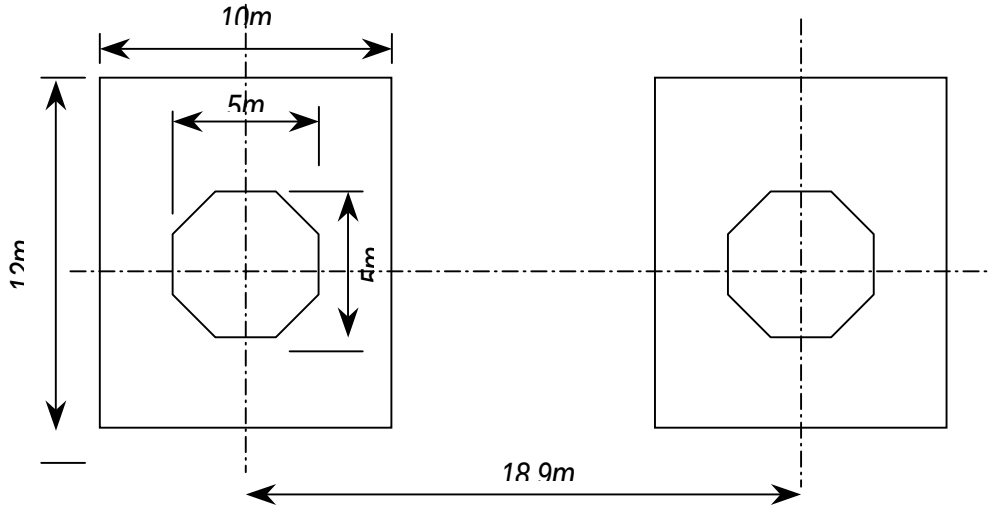


Diagram C1. Layout of Pier Base

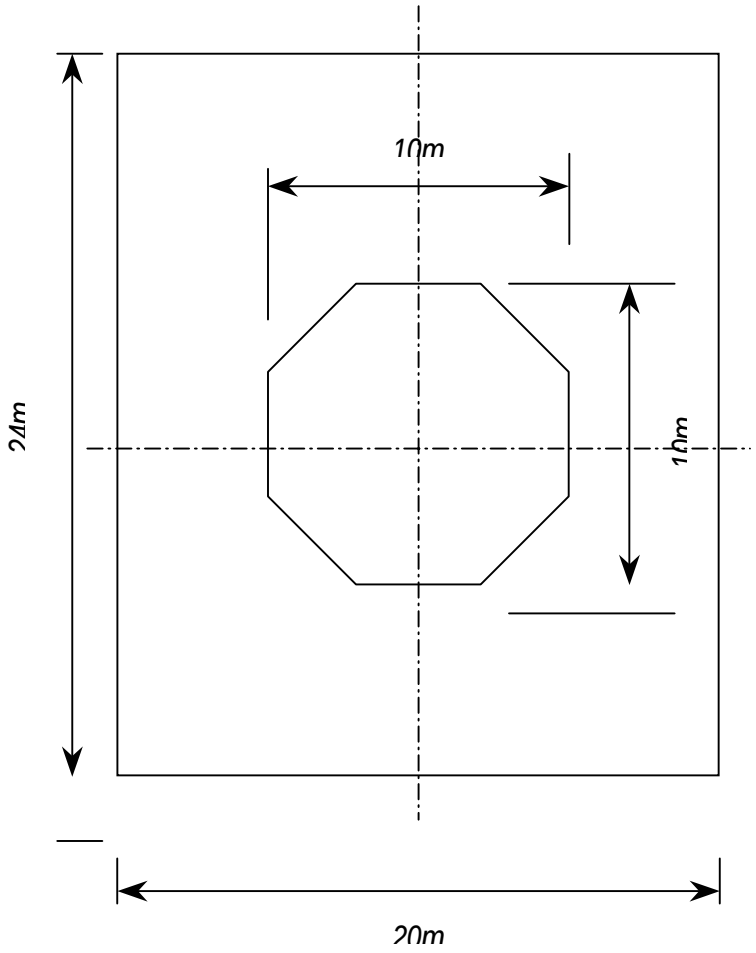


Diagram C2. Layout of Tower Base

As stated previously under tidal flow the scour development is typically reduced due to sediment eroded during the first phase of the tide being deposited on the reversing part of the tidal cycle. Therefore, assuming that the depth of scour with time, *d(t)*, can be defined by the following formula (Sumer and Fredsøe, 2002):

$$d(t) = d_S\left[1 - \exp\left(-\frac{t}{T}\right)\right]$$

Figure C90 shows the predicted scour depth through time for the Route 3A medium span original alignment (4 Tower layout) as shown in Drawing No. B4027/2/B/361. The prediction makes use of Richardson and Davis (2001) expression to calculate the equilibrium scour depth. The Richardson and Davis (2001) expression has a tendency to over-predict scour depth. However, it is likely that based on the calculation the depth of scour around the bridge piers/towers can be expected to reach the order of metres unless scour countermeasures are applied. The width of the scour hole can be approximated to 3 - 4 times the width of the structure. Therefore, for the tower structures the width will be between 30 and 40m.

The scour analysis undertaken is based on recognised empirical relationships, but remains simplistic in its approach and is based on calculated time-series of depths and speeds found at the various proposed bridge crossing locations. It assumes that the flow is aligned to the pier. For the present case more detailed analysis should be undertaken at the design stage. The layout of the piers and tower are shown in Diagrams C1 and C2.

C12 Discussion

The model has been set-up and run for a range of schemes, in addition to the baseline case, as listed below:

- Route 3A Medium Span - Original Configuration
- Route 3A Medium Span - Modified Alignment
- Route 3A Medium Span - 3 Towers Configuration
- Route 3A Medium Span - 3 Towers Revised Configuration
- Route 3A Short Span

In addition, the Route 3A Medium Span - Modified Alignment has been run for two extreme flow conditions:

- High fluvial flow (1:200 year event) and spring tide
- High fluvial (1:200 year event) and corresponding 1:200 year surge event.

From the detailed hydrodynamic model results, there are several issues common to all of the scenarios tested. Firstly, the largest changes across the study area are generally limited to the immediate area around the bridge piers. In addition, as the flooding or ebbing tide moves onto the intertidal areas large differences can be manifested along the edge of the tidal wave. These differences do not provide a real indication of absolute change as they are an artefact of phase differences in the propagation of the front of the tidal wave and represent a positional change in water level, and thus speed and bed shear stress. For example, the strong asymmetry in the tidal curve with a very short flood period (≈1.5 hours) and a much longer ebb period (≈11 hours) means that a slight delay in the tidal propagation on the flood may appear as a large change in water level (> 1m) when viewed as a difference between the existing case and a given scenario when in fact it only represents a change in phase. Such differences can exist under normal conditions as a result of the natural variability in the system due to meteorological drivers such as wind and rainfall.

On balance, the greatest impact on the estuary is caused by the Short Span Option. This is primarily due to the blockage effect that is caused by the scheme on the flooding tide. Whilst, the general increases in flow around the bridge structures for this scheme are smaller than for the medium span options tested, there is a greater impact within the channel as a whole during the rapid flood. The observed blockage effect of the Short Span Scheme was demonstrated in the previous coarse grid model (Phase I) but the extent of those changes was greater. This is considered to be an artefact of the grid scale and the use of additional friction terms to represent the bridge piers in the coarse model leading to a conservative solution.

Although the extreme events have only been run for the Route 3A Medium Span 4 Tower - modified alignment and the Route 3A Medium Span 3 Tower – revised alignment, the results show that the bridge does not cause any blockage in water levels and in general changes in flow speed are limited to the area around the tower/pier structures. Figures C91B and C92 show the variation in flow speed at three points within the study area. It is interesting to note the variation in the shape of the speed curves between the baseline case under normal spring-neap conditions and that for the baseline case under both extreme fluvial and extreme surge and fluvial events (1:200 years return period). The stronger fluvial flow suppresses the current speed on the flood tide and, more interesting, maintains the current on the ebb tide. Clearly, the extreme fluvial events provide an important mechanism for morphological change within the upper estuary. The sustained ebb current would allow for more material to be brought down from the upper reaches of the estuary and would appear to change the system from being flood dominant to ebb dominance. Such changes may well provide the key driver for channel switching. The impact of the surge event is to enhance the flood current beyond that observed in the baseline case, but the fluvial flows still dominate over the ebbing tide.

The importance of looking at the predicted changes in the context of the baseline system is demonstrated in Figure C93, which shows the threshold of sediment motion for 150μm grain size over a spring and neap tide. Clearly for almost all states of the tide the sediment is in motion, therefore, even quite large changes in bed shear stress may not result in any substantial increase in sediment transport. However, the empirical scour analysis undertaken for the Route 3A Medium Span Original Alignment demonstrates the potential for substantial scour around structures placed in the north and south channels, although the Richardson and Davis (2001) expression used to calculate the scour has a tendency to over-predict equilibrium scour depths.

A comparison between the Route 3A Medium Span Original Alignment, the Route 3A Medium Span modified Alignment and both of the Route 3A Medium Span - 3 Towers arrangements demonstrate the importance of pier/tower positioning within the estuary over the short term. Based on analysis of the hydrodynamic results the Route 3A Medium Span - 3 Towers revised alignment has the least impact.

C13 References

Breusers, H.N.C. (1966). Conformity and time scale in two-dimensional local scour. *Proc. Symp. On Model and Prototype Conformity.* Poona, pp. 1 - 8.

Breusers, H.N.C, Nicollet, G. and Shen, H.W. (1977). Local scour around cylindrical piers. *J. of Hydraulic Res.,* IAHR, Vol 15, No. 3, pp. 211-252.

Breusers, H.N.C. and Raudkivi, A.J. (1991). *Scouring*. IAHR Hydraulic structures design manual (2), A.A. Balkema, Rotterdam, 143pp.

Environment Agency (1998). *Extreme Sea levels for Section 105 Surveys*. Final report, JBA Ltd., July, 9pp (+Tables and Figures).

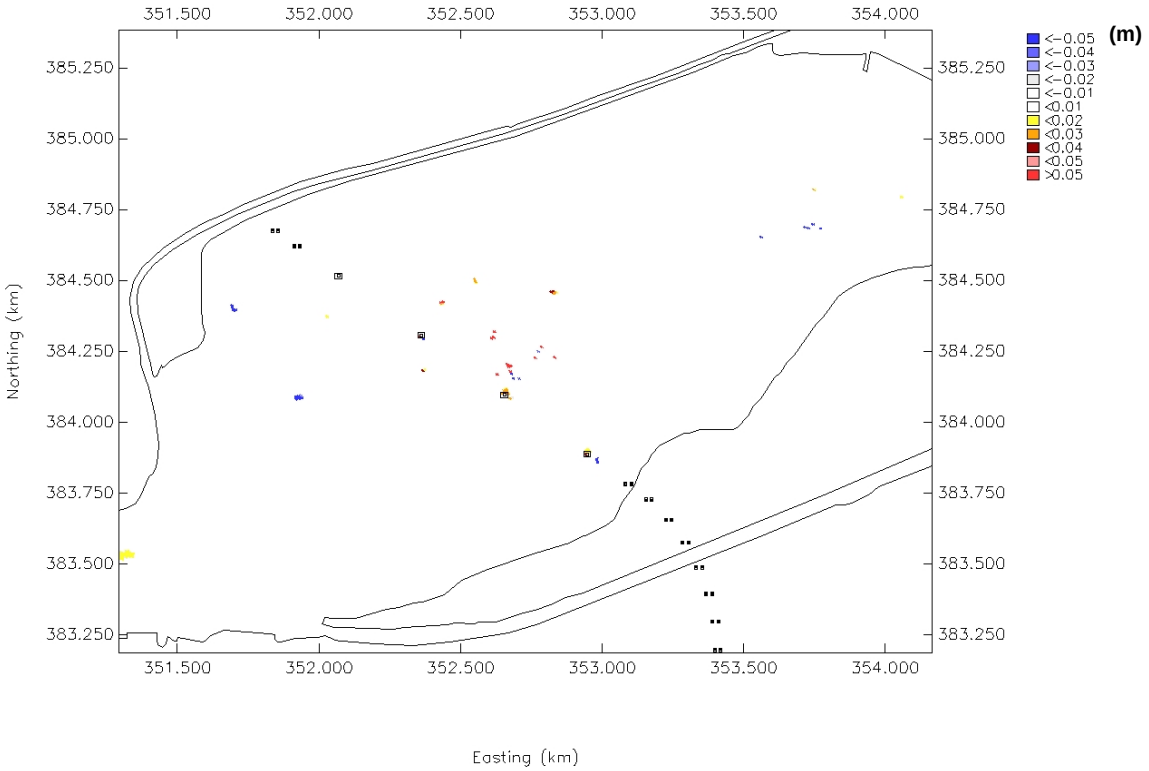
Richardson, E.V. and Davis, S.R. (2001). *Evaluating Scour at Bridges*. Hydr. Engng. Circular No. 18, US Department of Transport, Federal Highway Administration, Pub. No. FHWA NHI 01-001.

Johnson, P.A. (1992). Reliability-based pier scour engineering. *J. of Hydr. Engng.*, ASCE, Vol. 118, HY8, pp. 626-629.

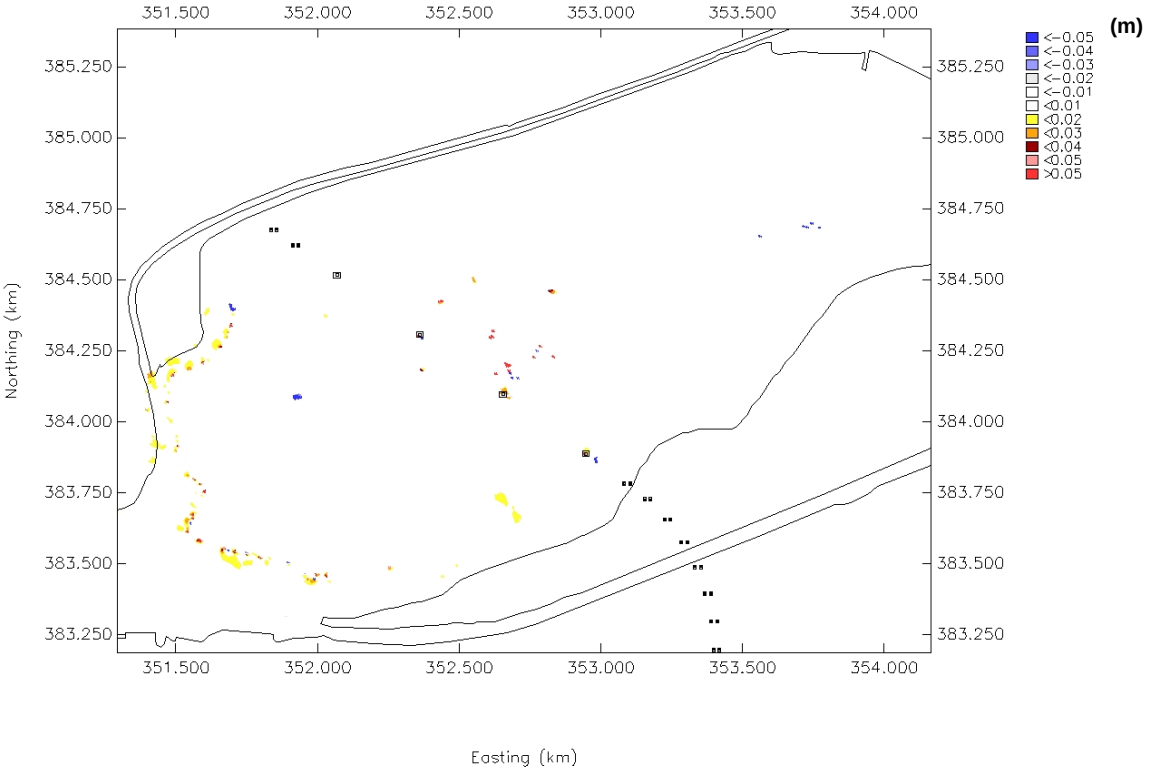
Melville, B.W. and Coleman, S.E. (2000). *Bridge Scour*. Water Resources Publications, LLC, Colorado, USA, 550 pp.

Sumer, B.M. & Fredsøe, J., 2002. *The mechanics of scour in the marine environment*. Advanced series in Ocean Engineering - Volume 17, pp536.

A.

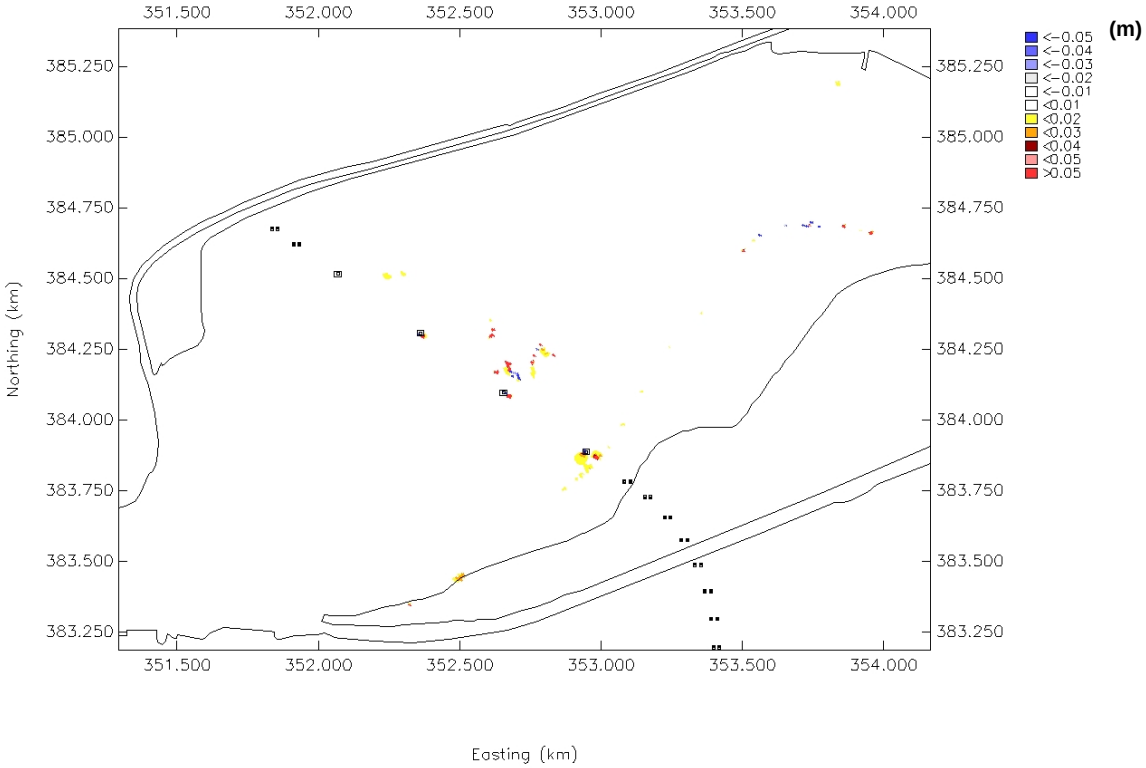


B.

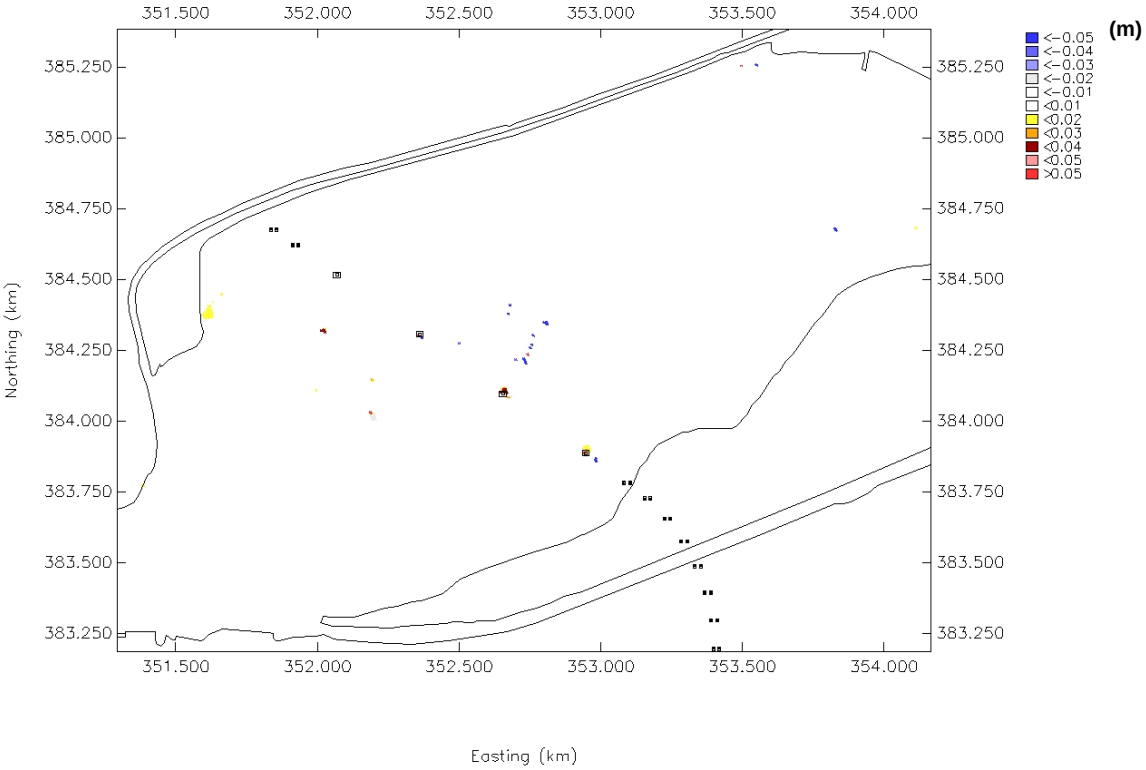


ABP mer marine environmental research	Differences in water level (m) between the proposed bridge scheme Route 3A Medium and the baseline case for low water (A) and peak flood (B) on a spring tide.	Figure C1

A.



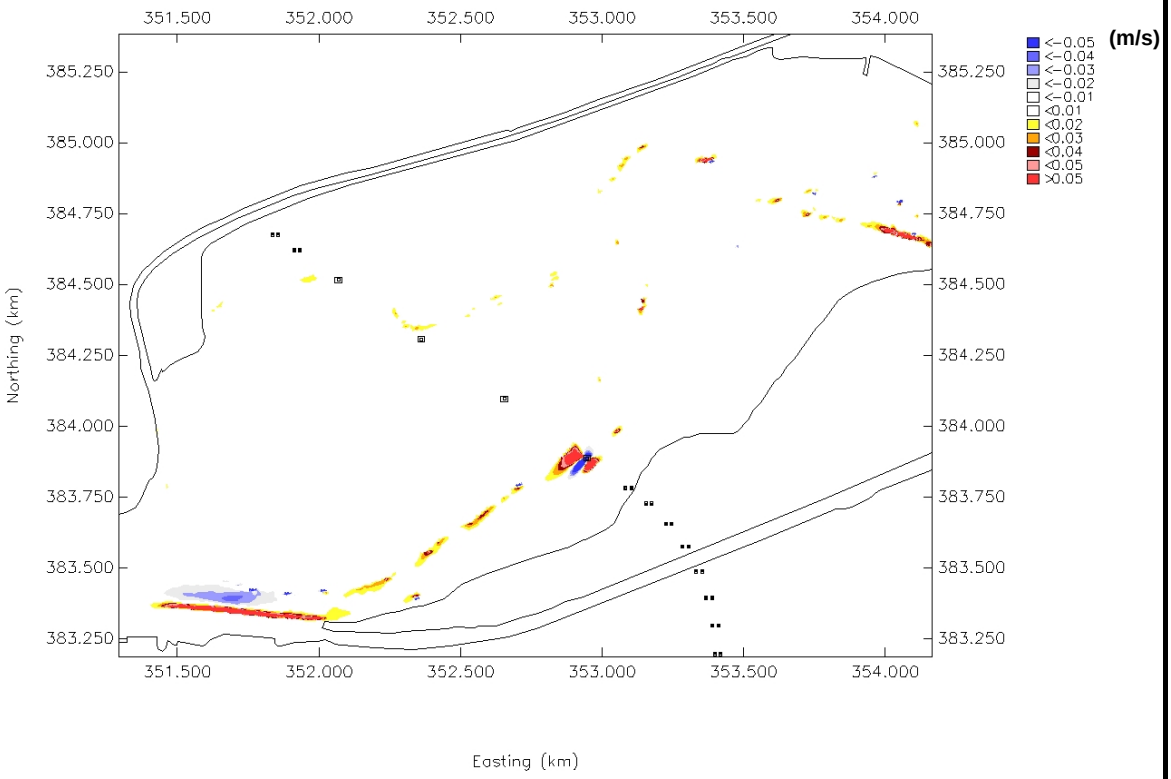
B.



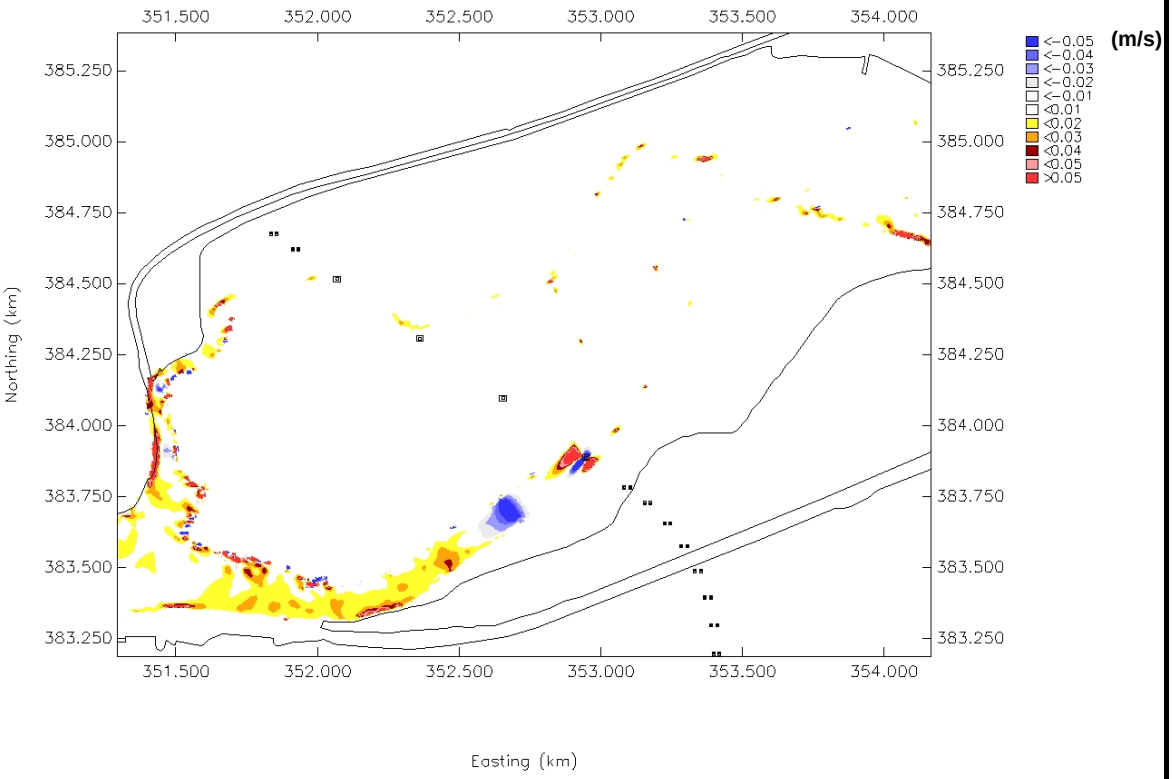
Differences in water level (m) between the proposed bridge scheme Route 3A Medium and the baseline case for high water (A) and peak ebb (B) on a spring tide.

Figure C2

A.

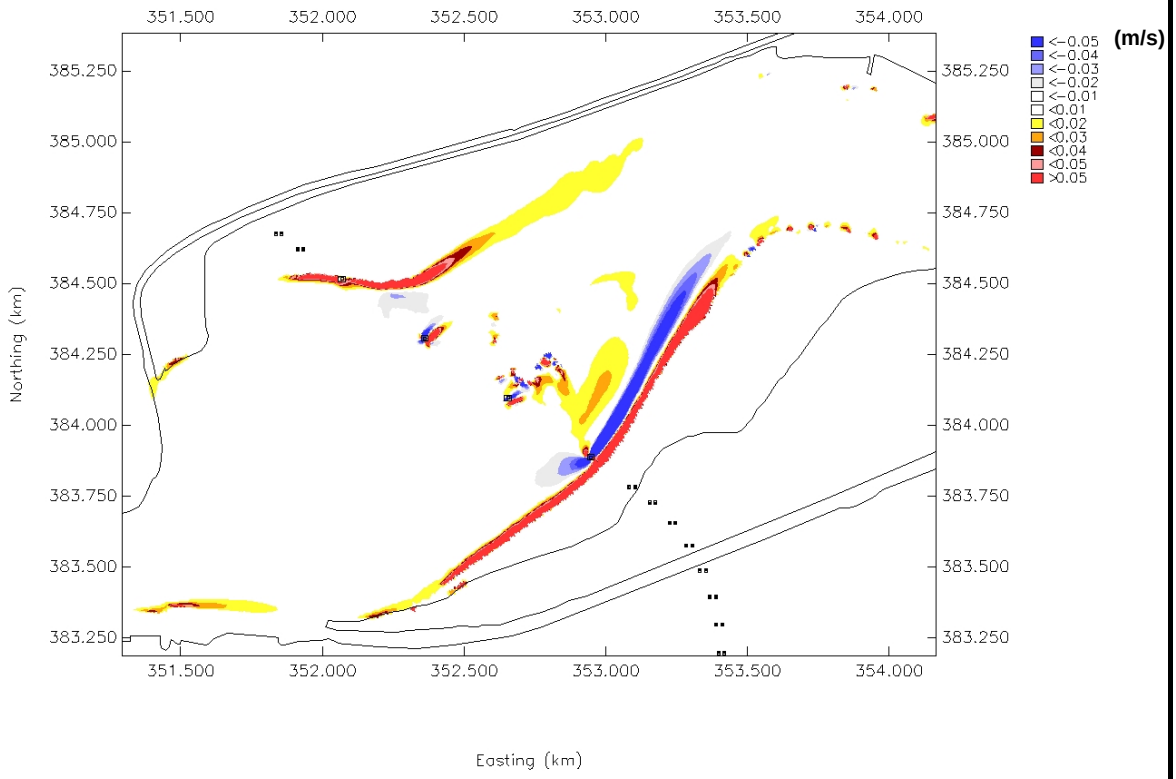


B.

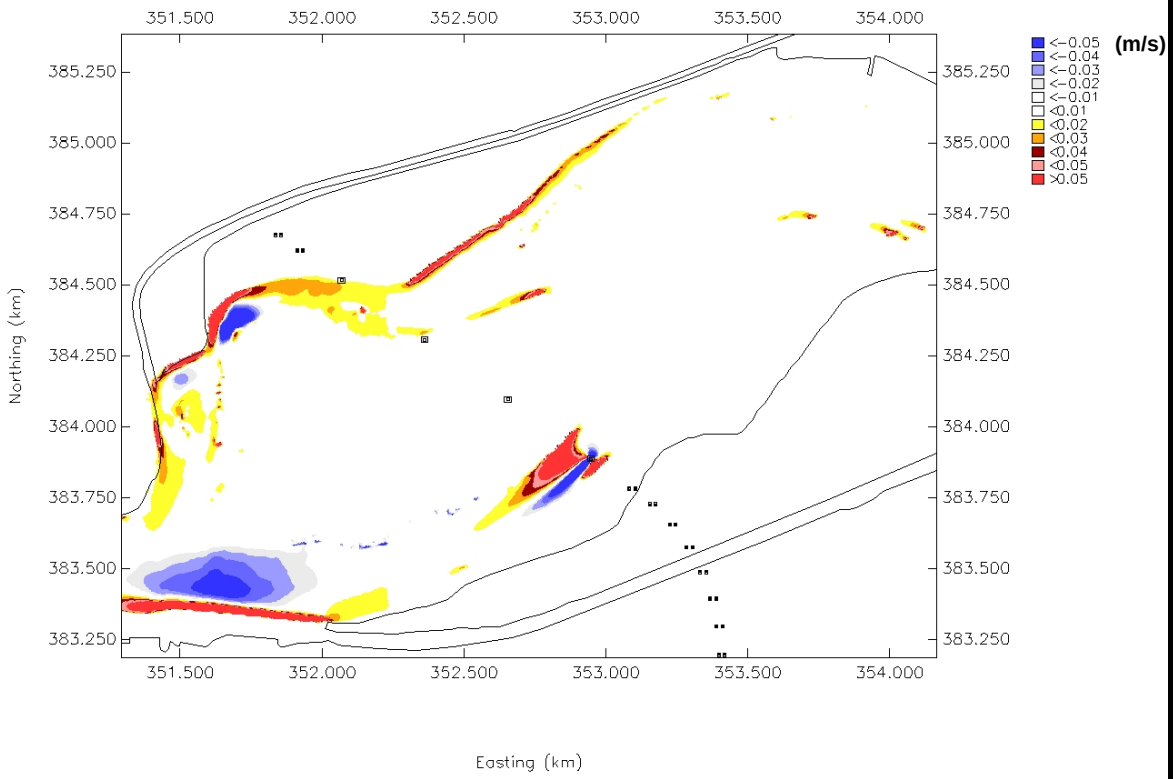


ABP mer marine environmental research	Differences in near-surface speed (m/s) between the proposed bridge scheme Route 3A Medium and the baseline case for low water (A) and peak flood (B) on a spring tide.	Figure C3

A.

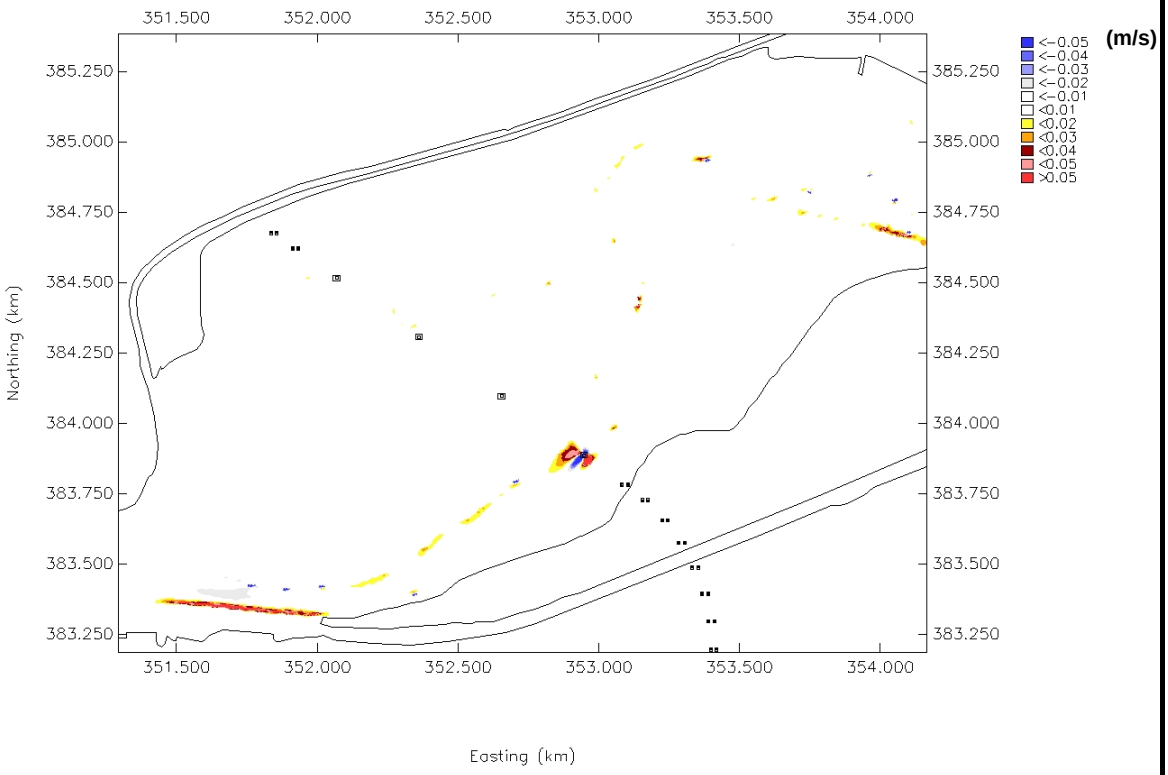


B.

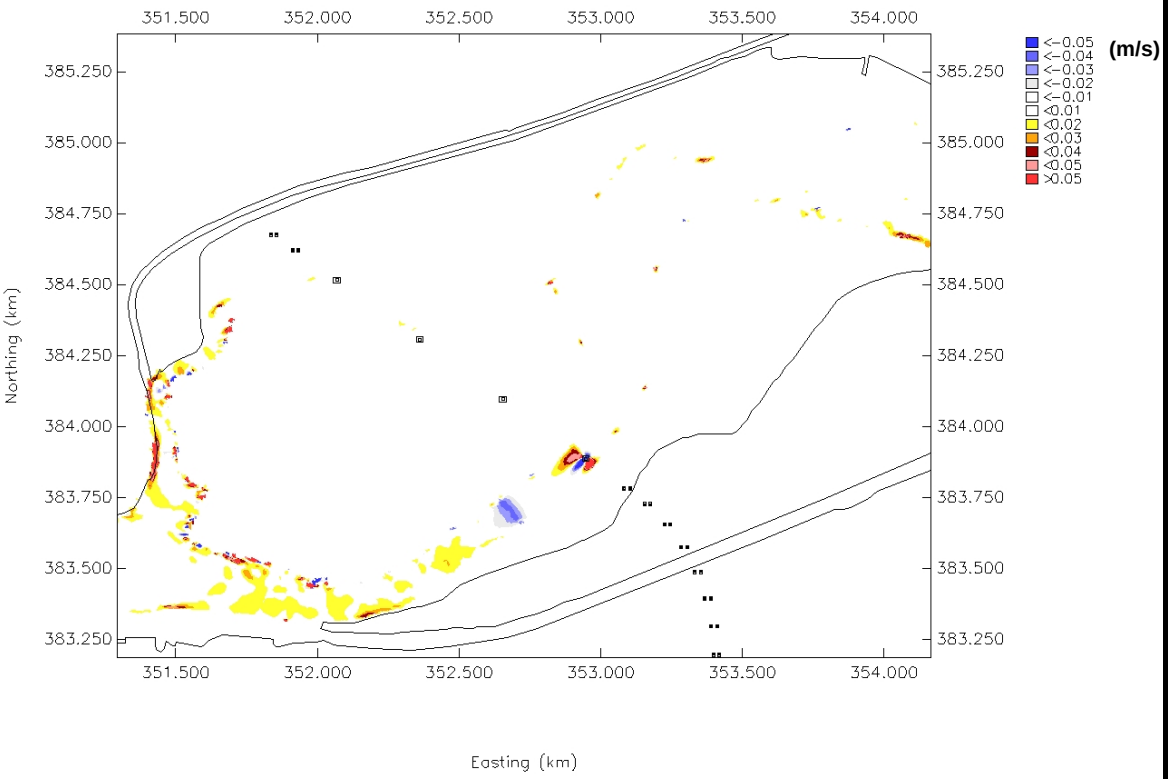


ABP mer marine environmental research	Differences in near-surface speed (m/s) between the proposed bridge scheme Route 3A Medium and the baseline case for high water (A) and peak ebb (B) on a spring tide.	Figure C4

A.

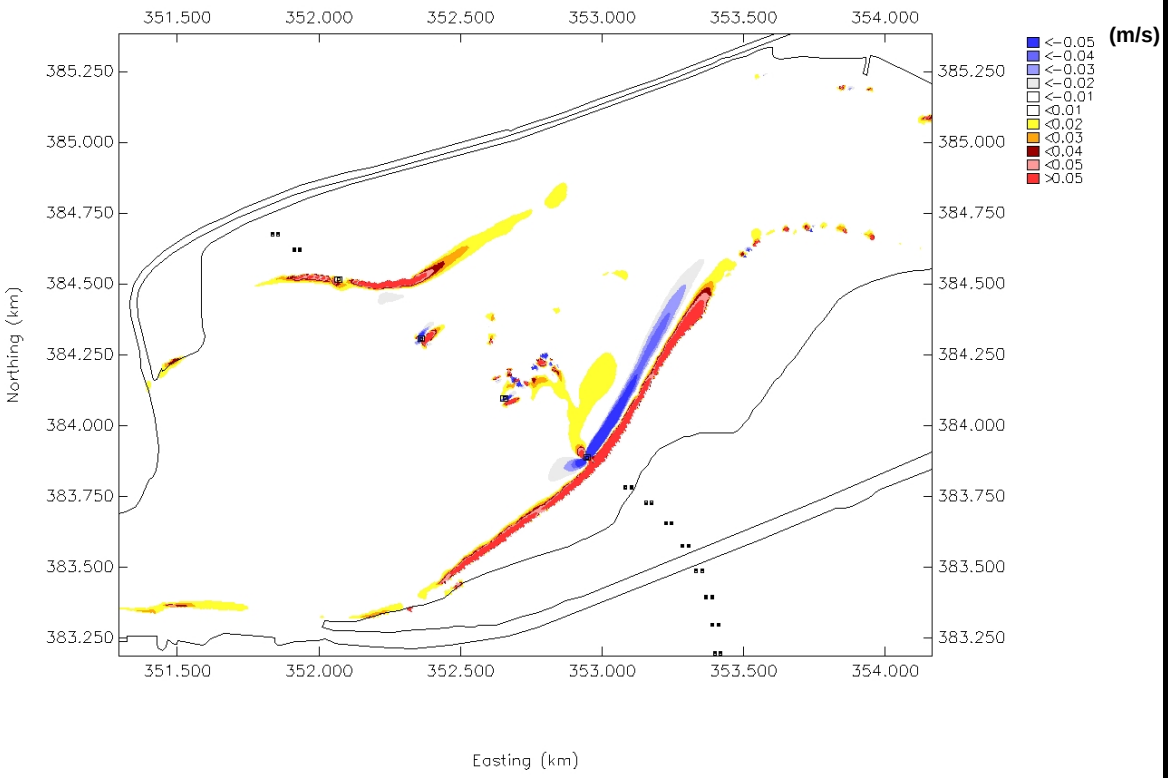


B.

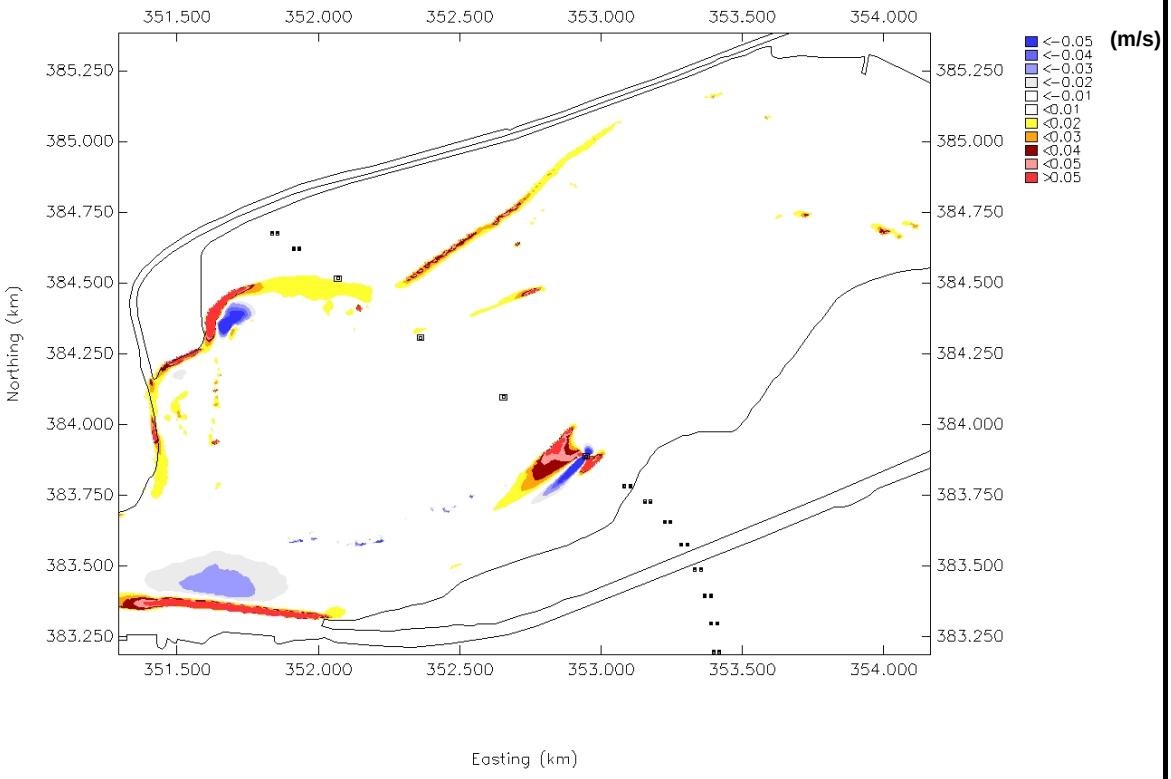


ABP mer marine environmental research	Differences in near-bed speed (m/s) between the proposed bridge scheme Route 3A Medium and the baseline case for low water (A) and peak flood (B) on a spring tide.	Figure C5

A.

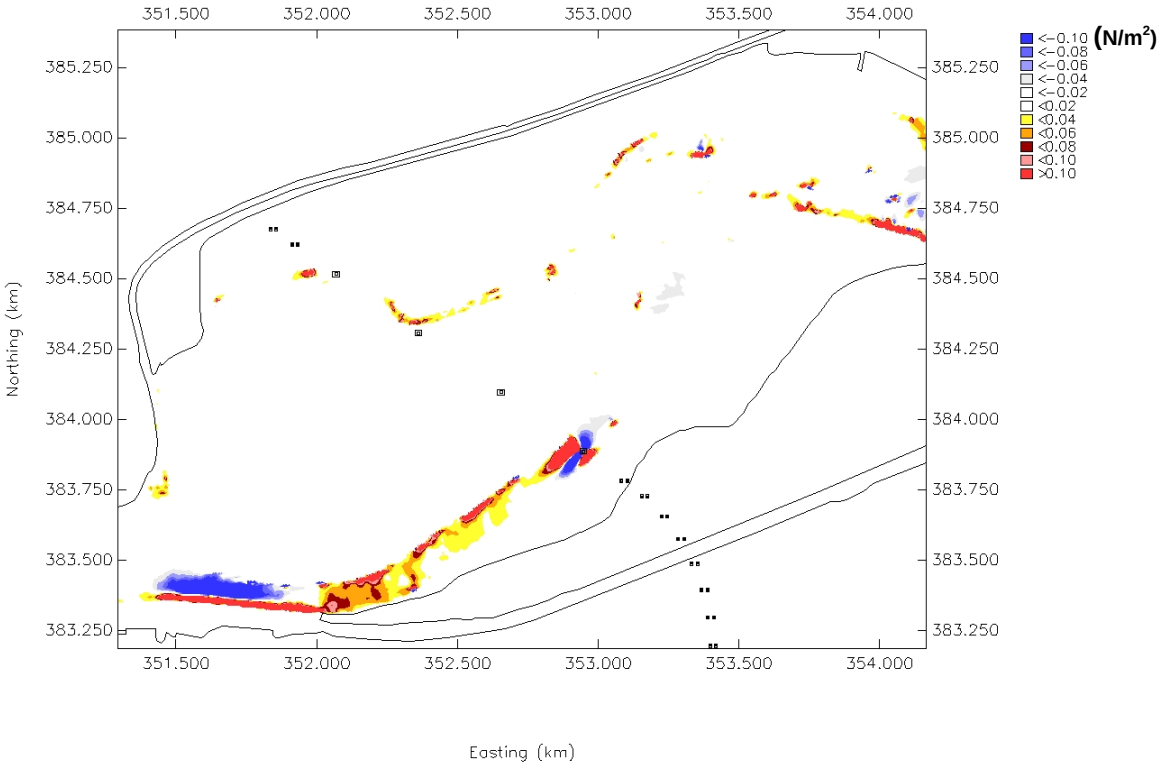


B.

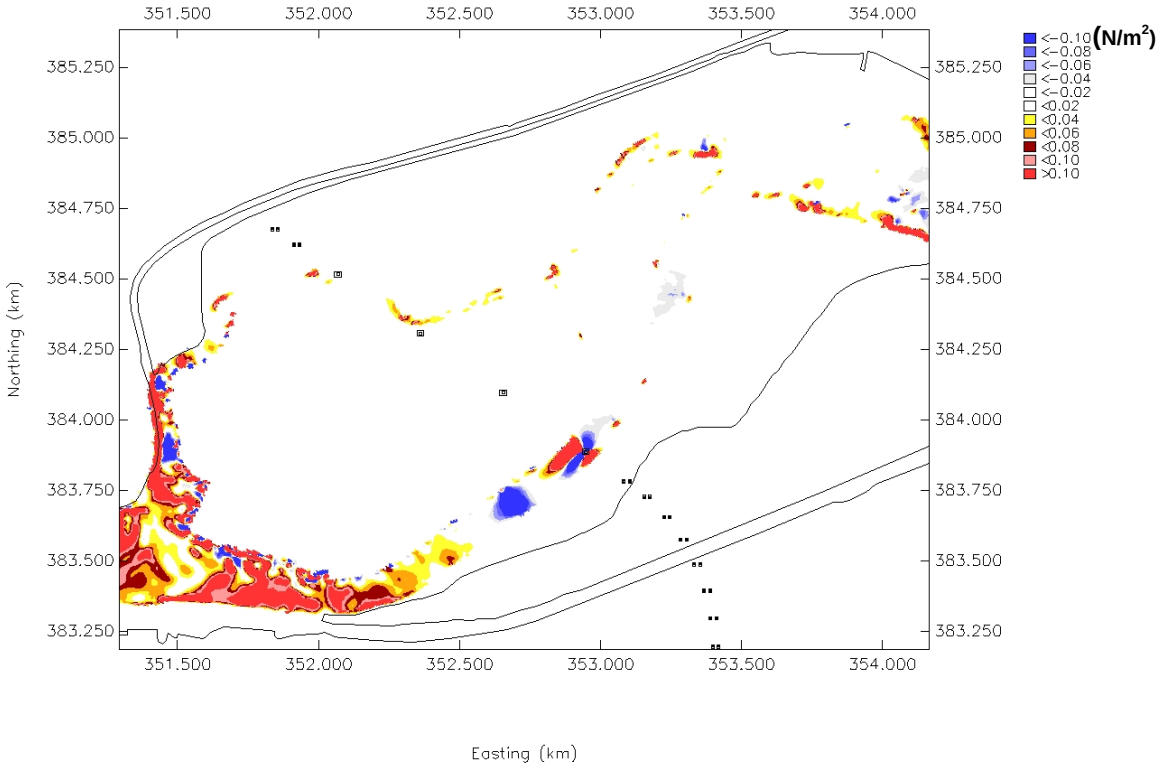


ABP mer marine environmental research	Differences in near-bed speed (m/s) between the proposed bridge scheme Route 3A Medium and the baseline case for high water (A) and peak ebb (B) on a spring tide.	Figure C6

A.

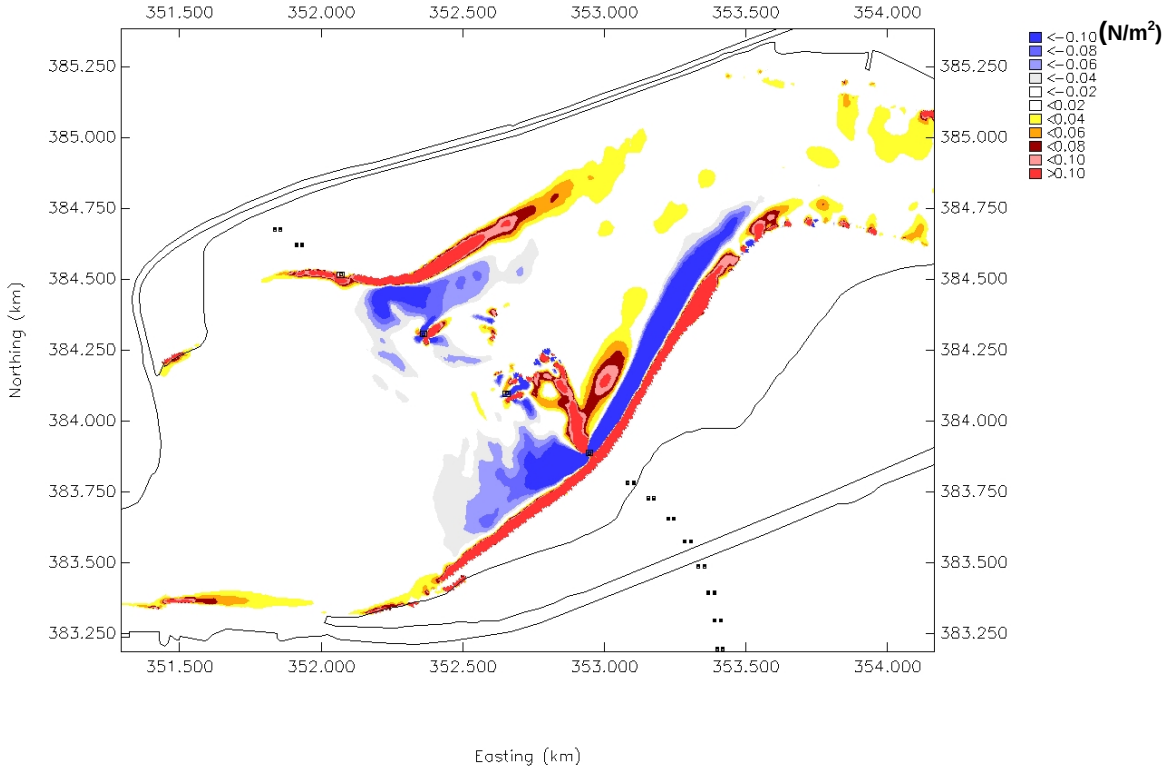


B.

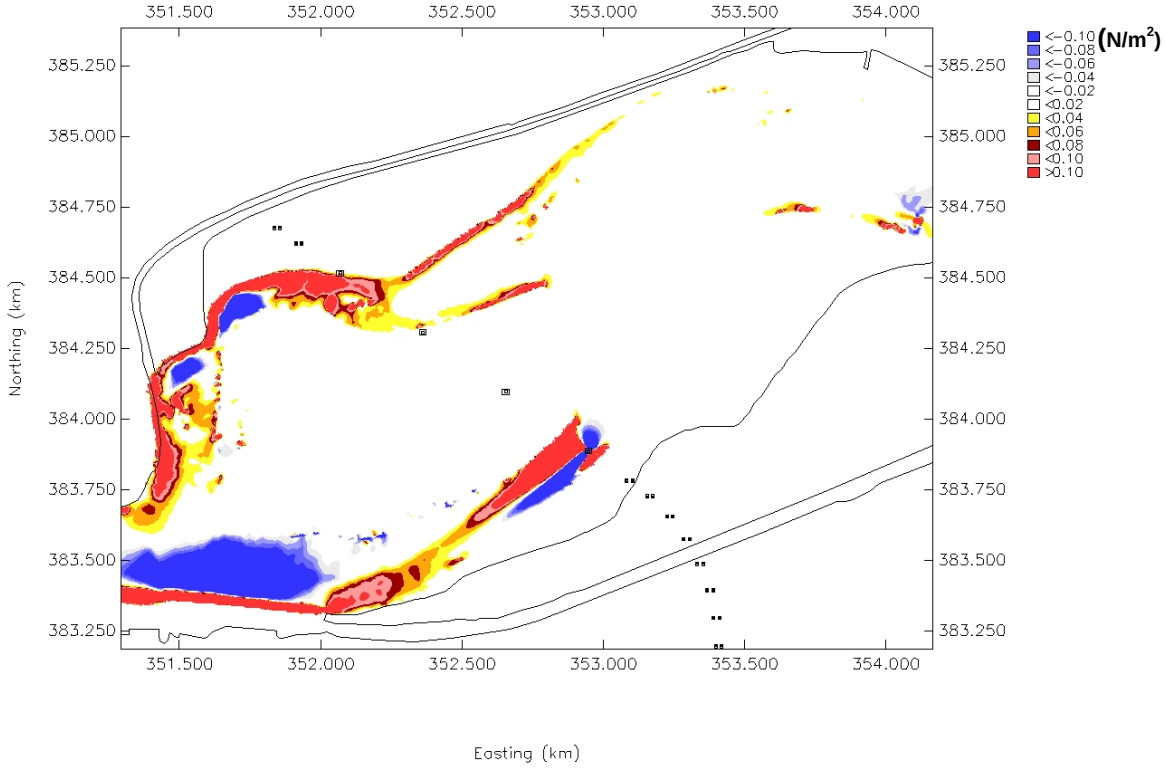


ABP mer marine environmental research	Differences in bed shear stress (N/m²) between the proposed bridge scheme Route 3A Medium and the baseline case for low water (A) and peak flood (B) on a spring tide.	Figure C7

A.



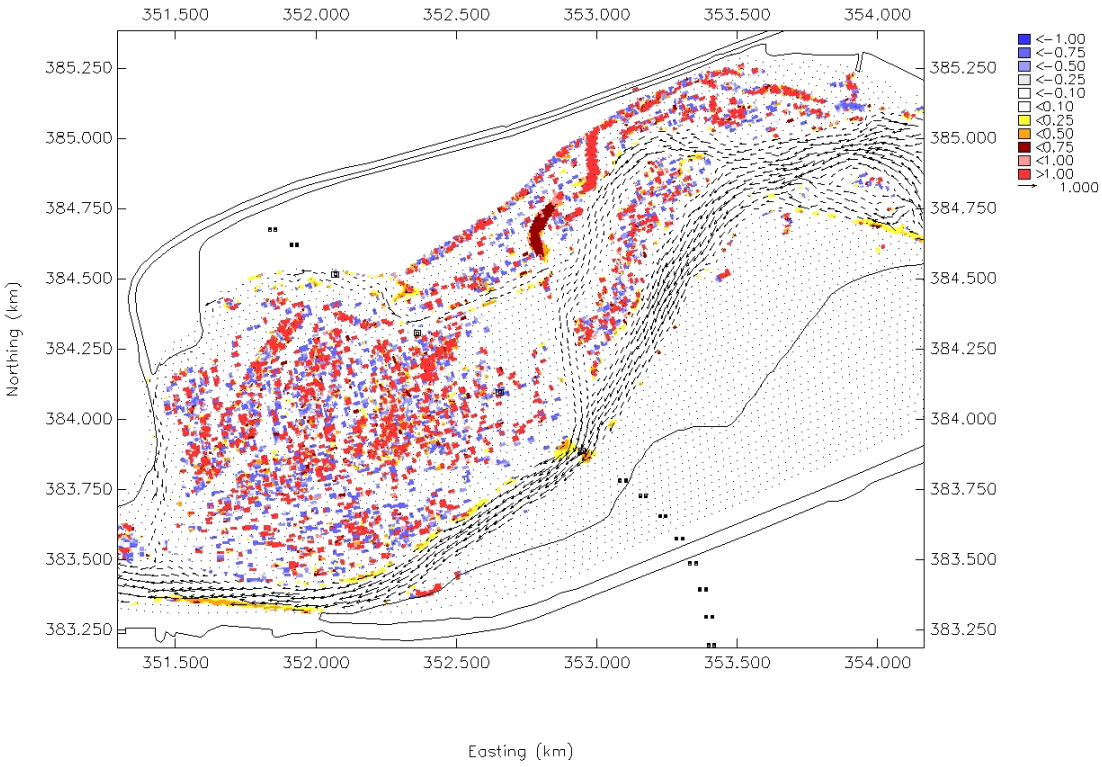
B.



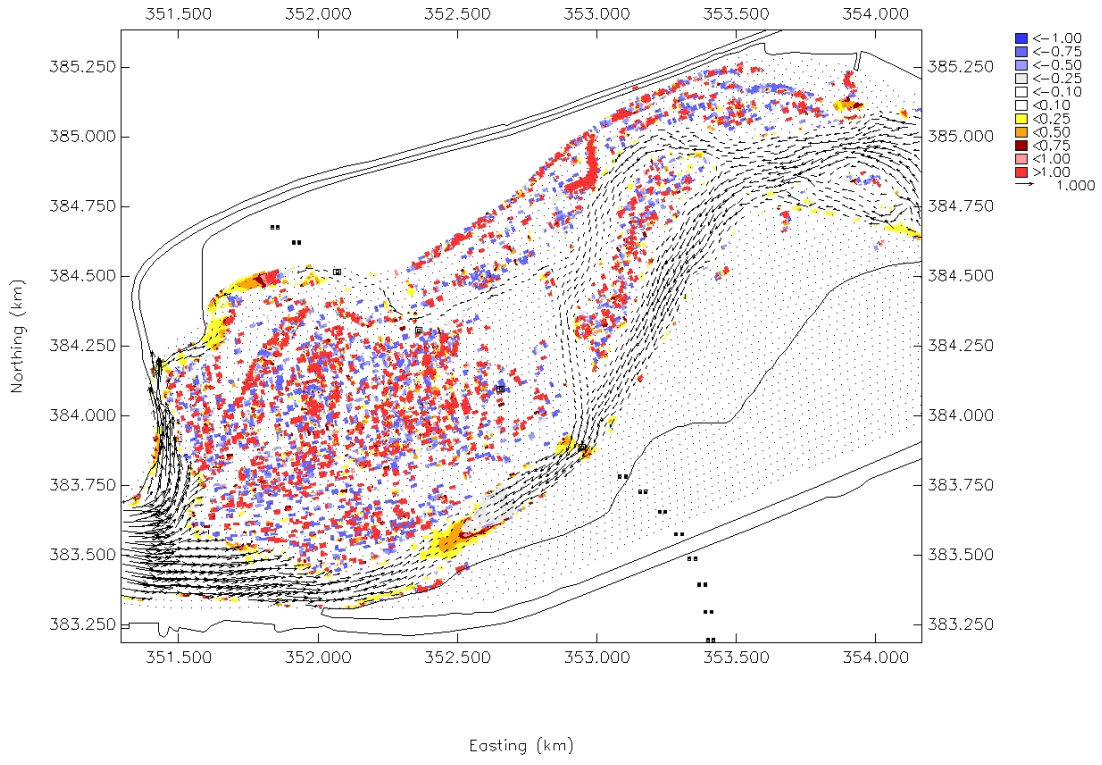
Differences in bed shear stress (N/m²) between the proposed bridge scheme Route 3A Medium and the baseline case for high water (A) and peak ebb (B) on a spring tide.

Figure C8

A.



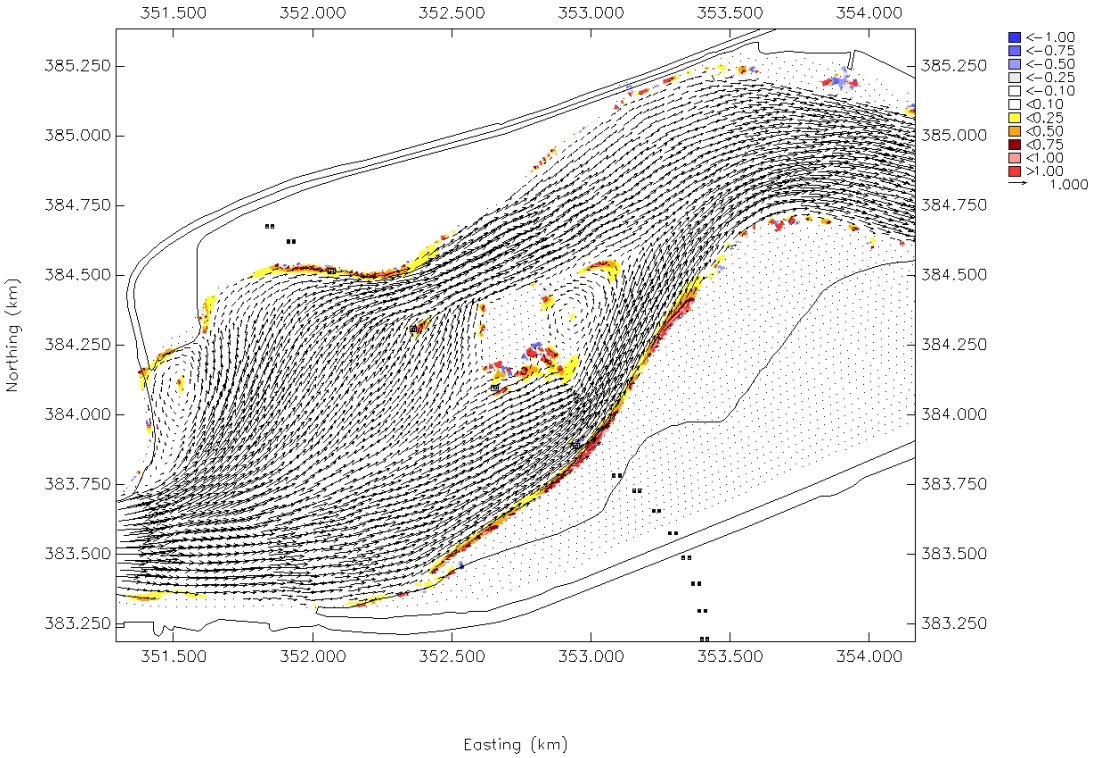
B.



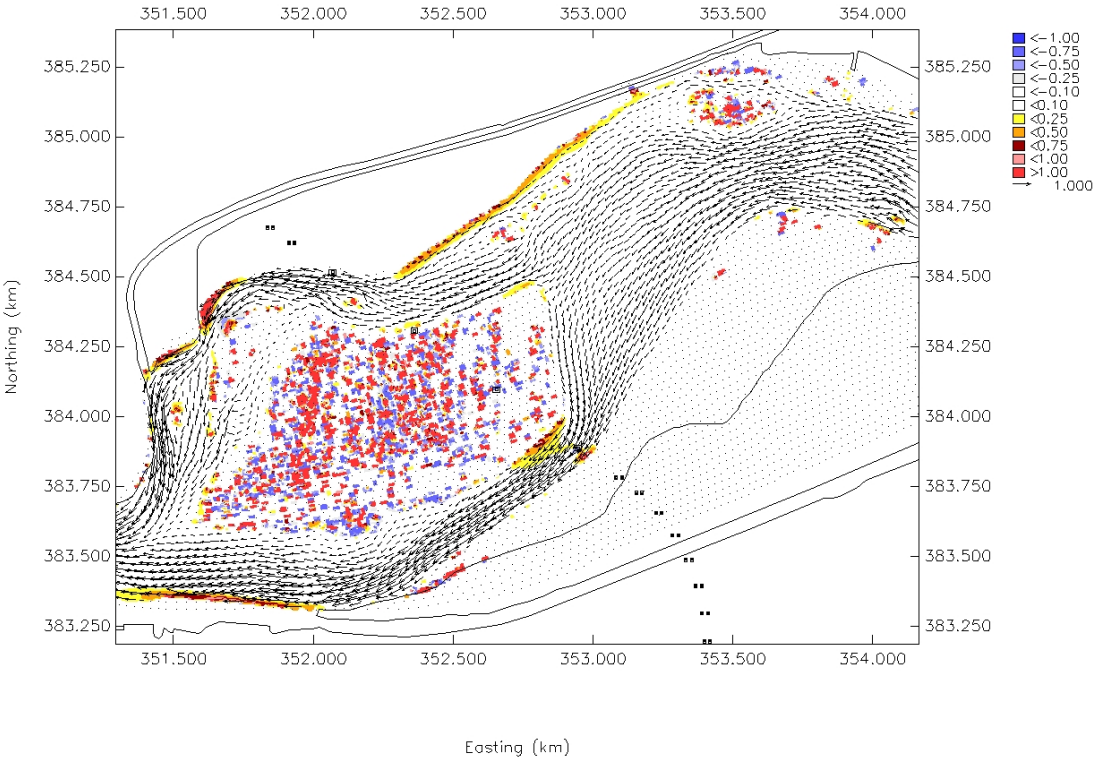
Percentage differences in bed shear stress between the proposed bridge scheme Route 3A Medium and the baseline case for low water (A) and peak flood (B) on a spring tide. (1 = 100% ; 0.1 = 10%).

Figure C9

A.



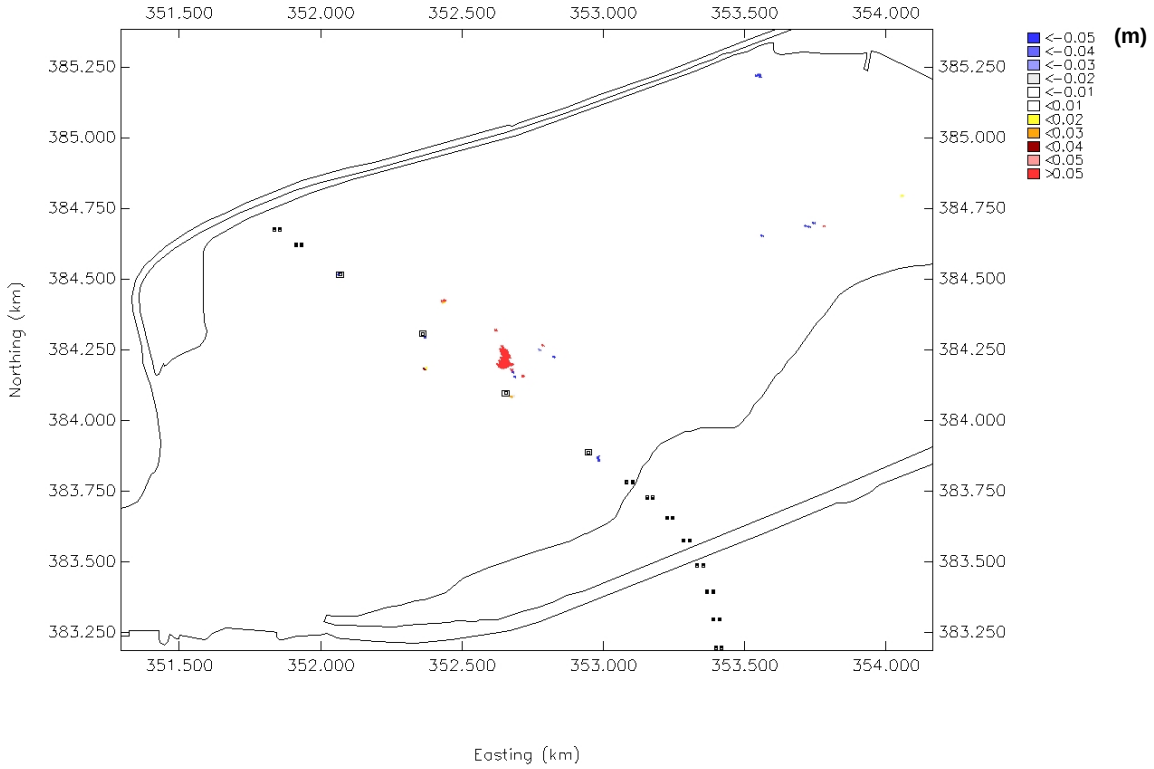
B.



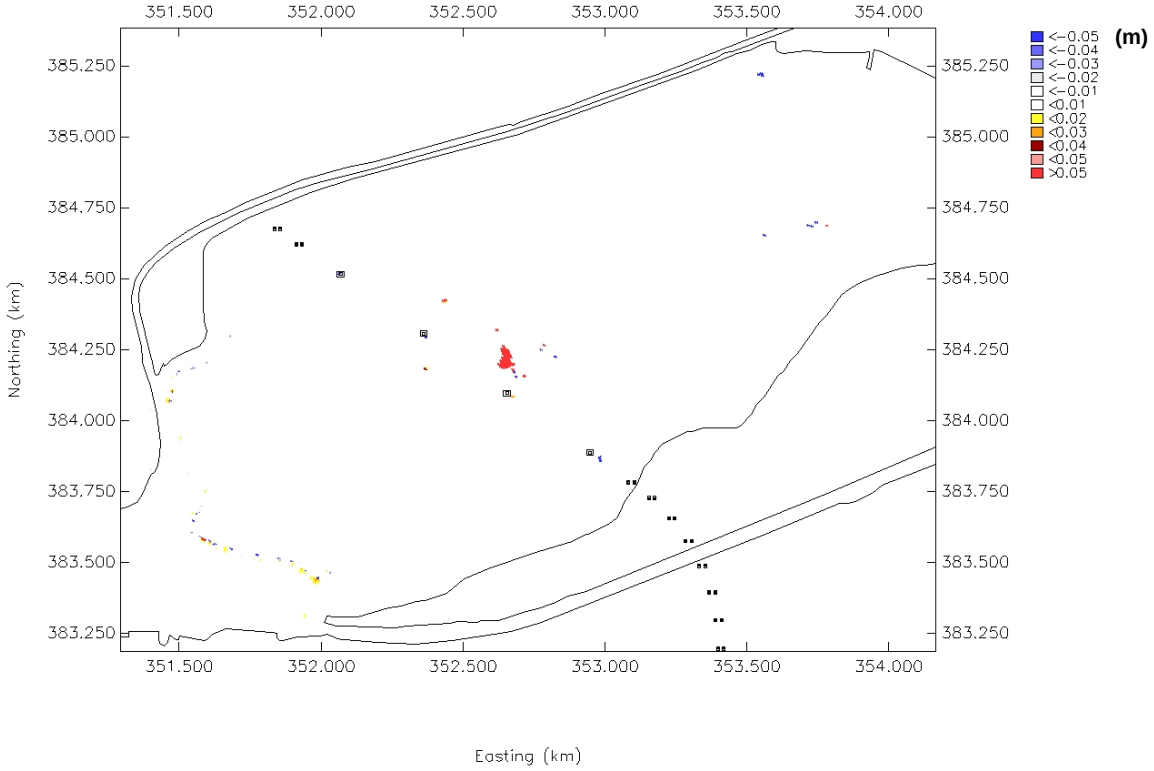
Percentage differences in bed shear stress between the proposed bridge scheme Route 3A Medium and the baseline case for high water (A) and peak ebb (B) on a spring tide. (1 = 100% ; 0.1 = 10%).

Figure C10

A.



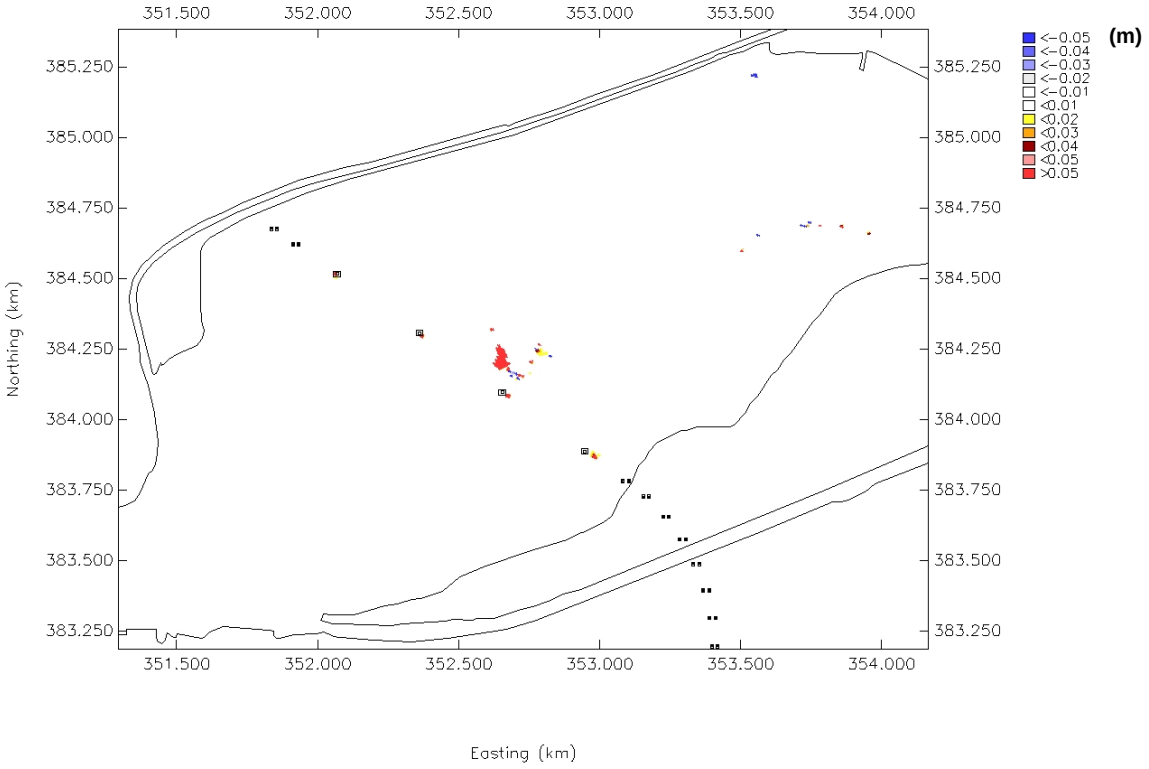
B.



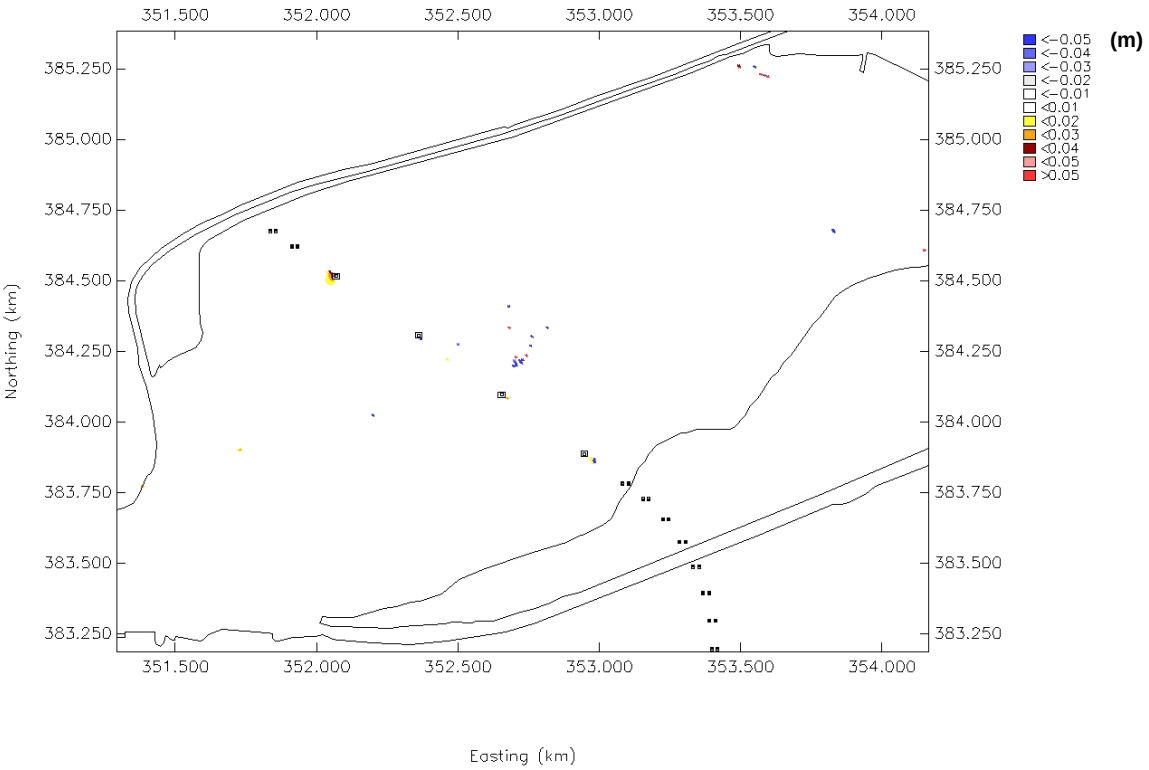
Differences in water level (m) between the proposed bridge scheme Route 3A Medium modified and the baseline case for low water (A) and peak flood (B) on a spring tide.

Figure C11

A.



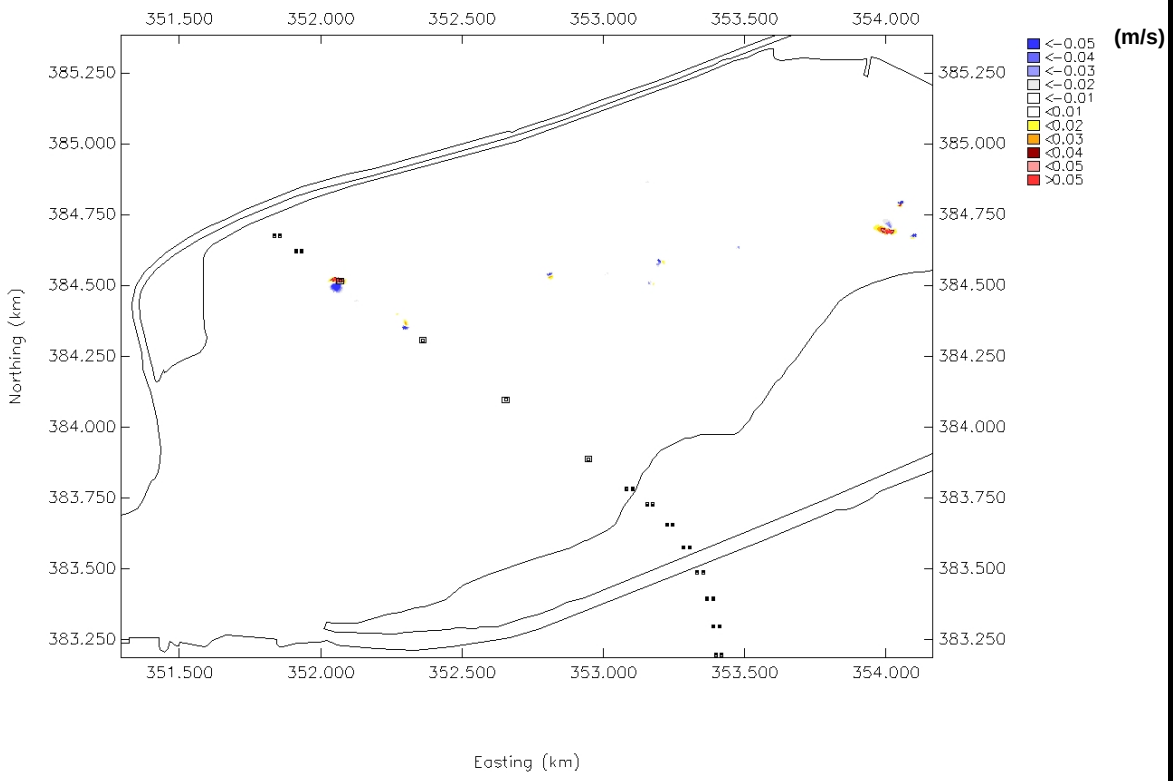
B.



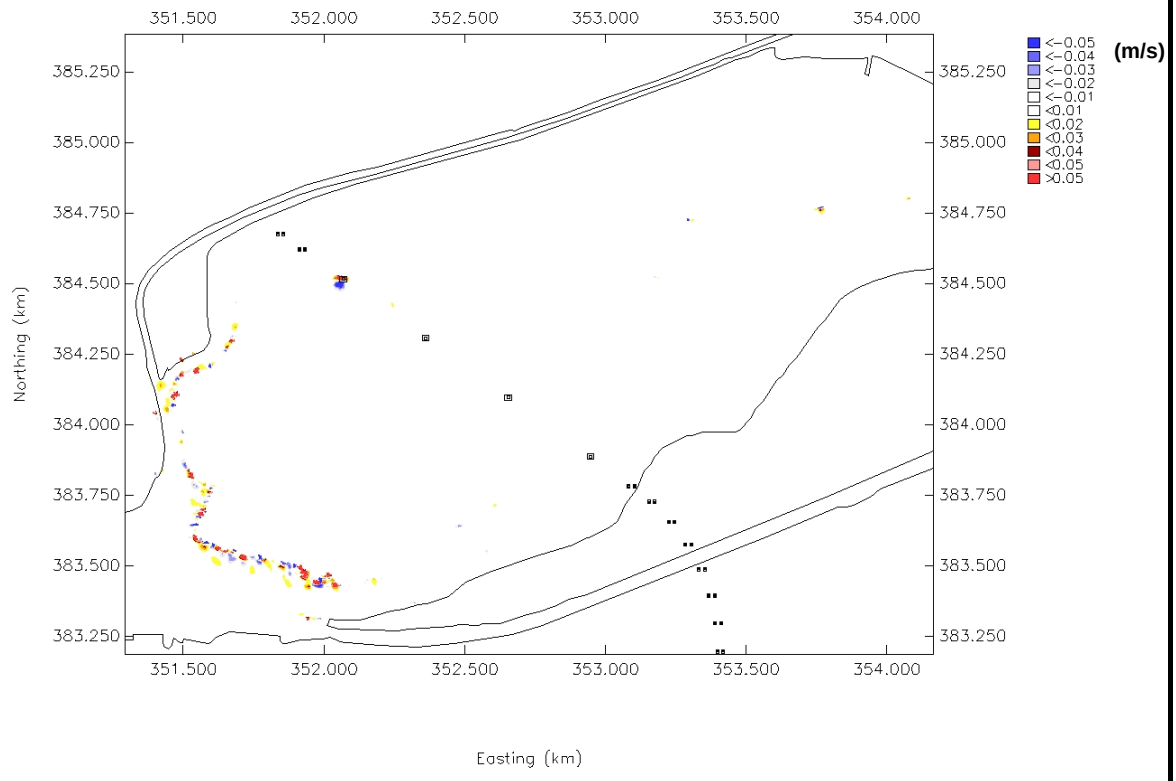
Differences in water level (m) between the proposed bridge scheme Route 3A Medium modified and the baseline case for high water (A) and peak ebb (B) on a spring tide.

Figure C12

A.



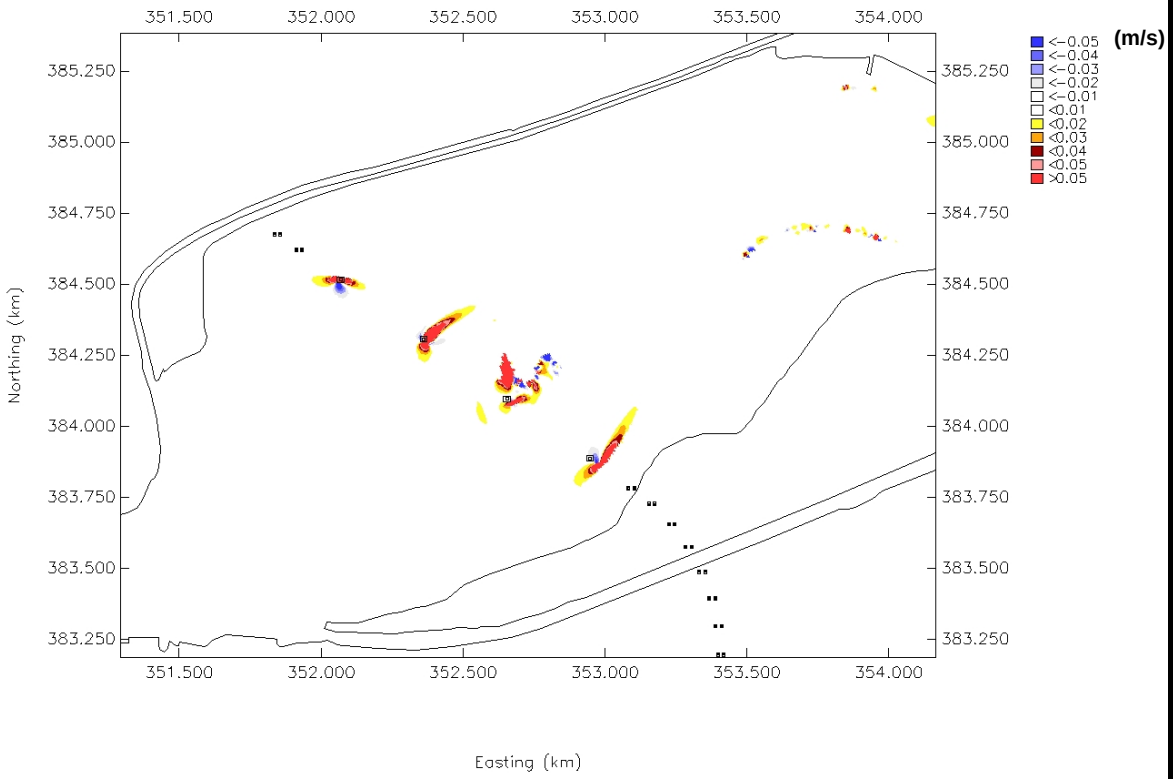
B.



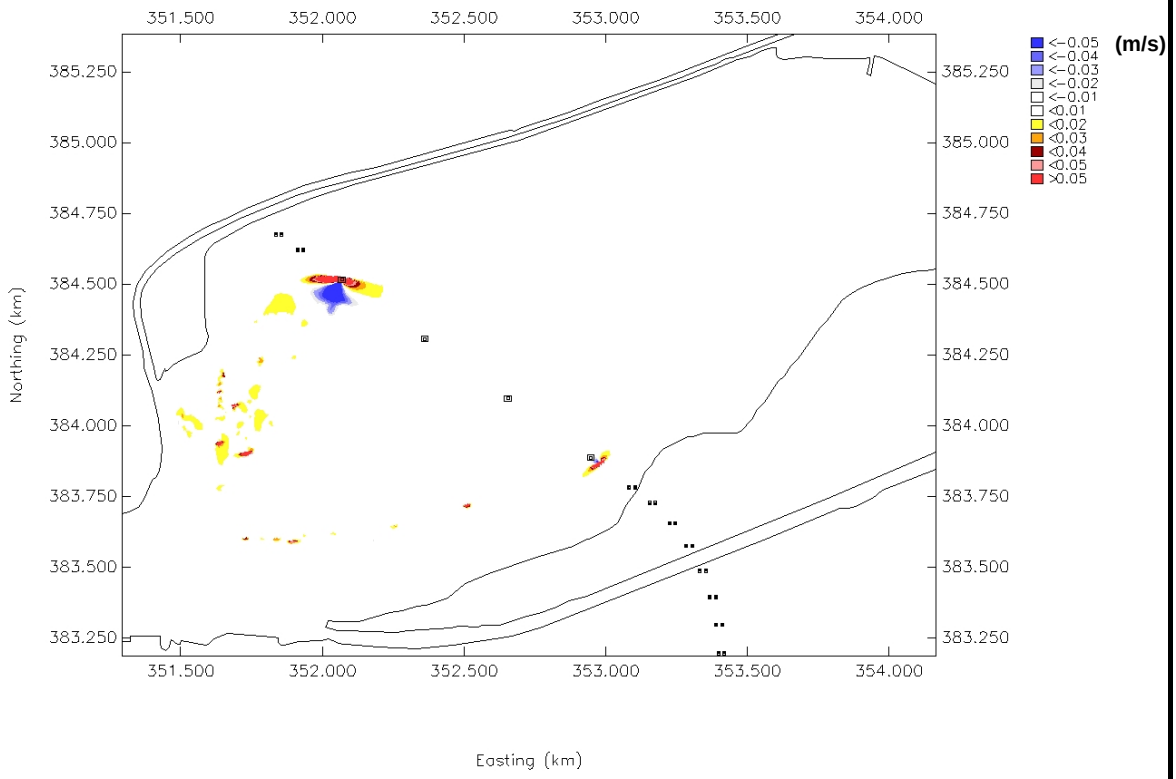
Differences in near-surface speed (m/s) between the proposed bridge scheme Route 3A Medium modified and the baseline case for low water (A) and peak flood (B) on a spring tide.

Figure C13

A.

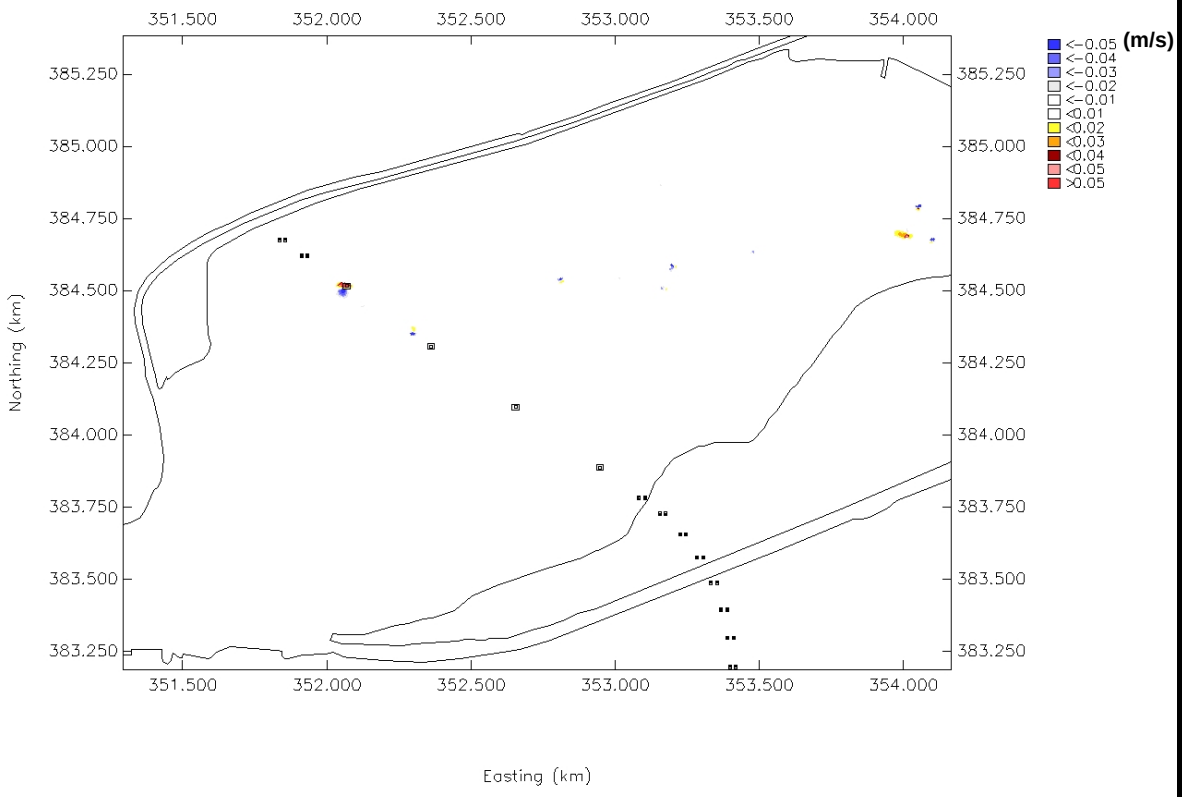


B.

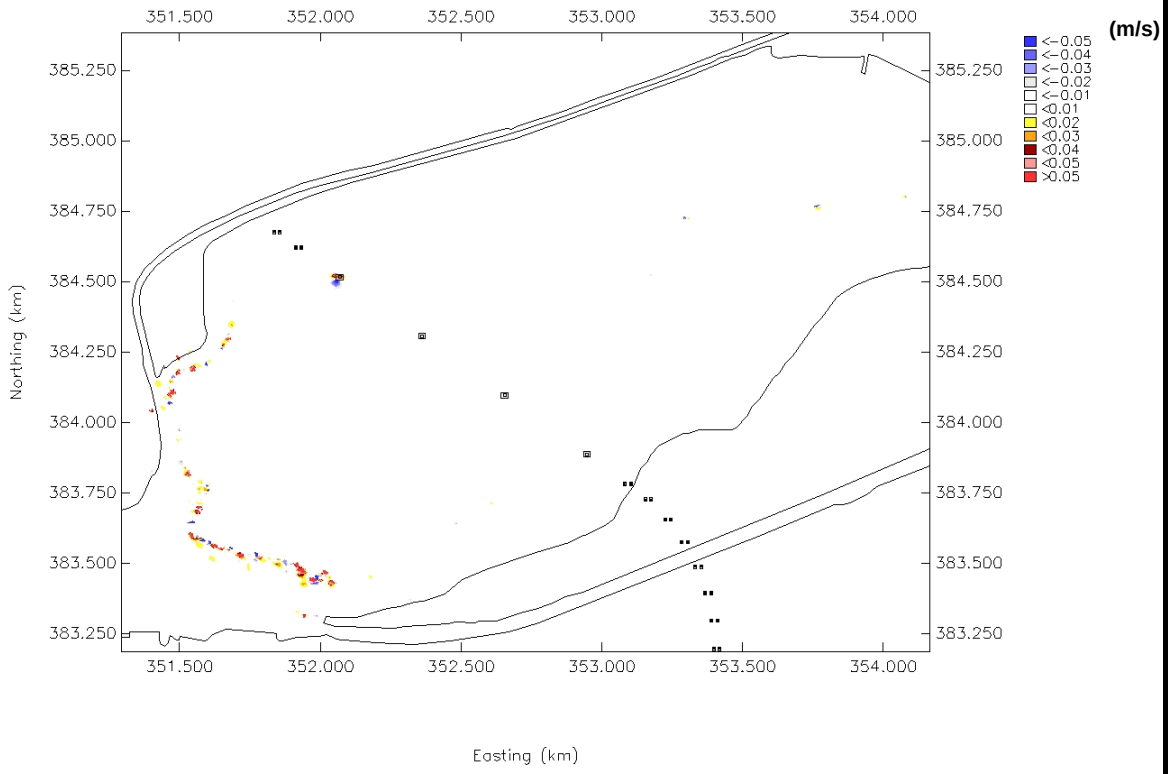


ABP mer marine environmental research	Differences in near-surface speed (m/s) between the proposed bridge scheme Route 3A Medium modified and the baseline case for high water (A) and peak ebb (B) on a spring tide.	Figure C14

A.

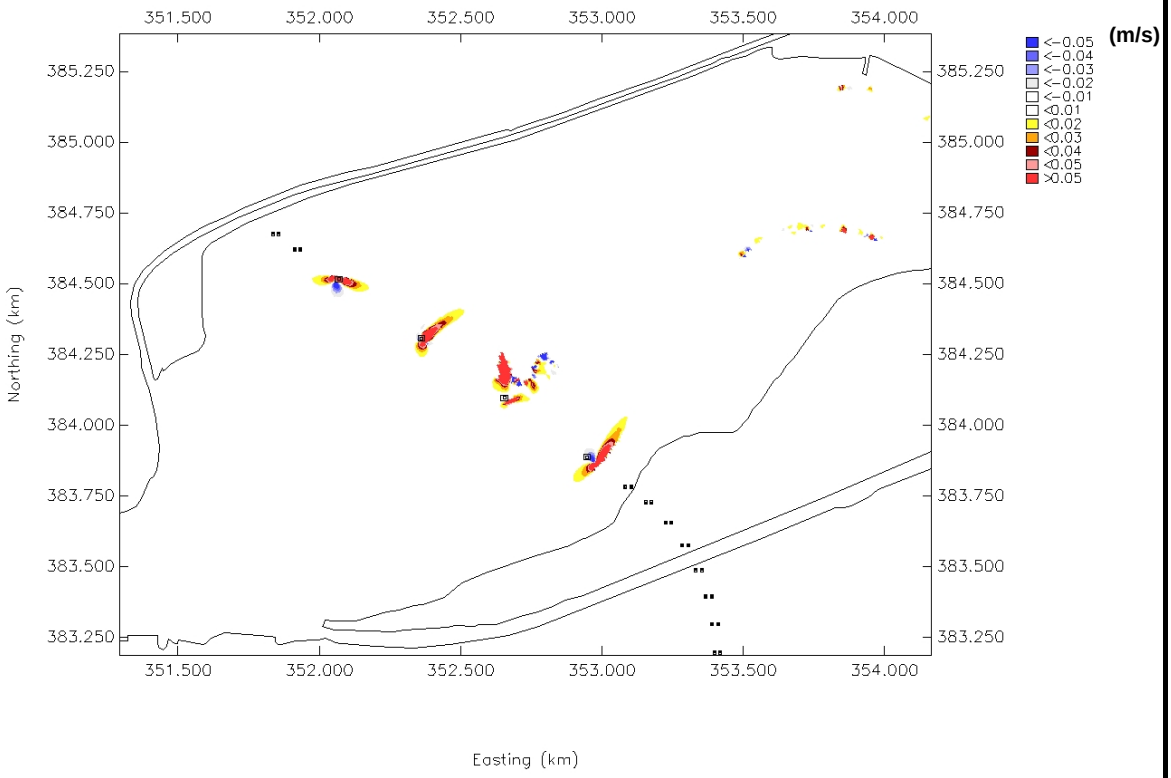


B.

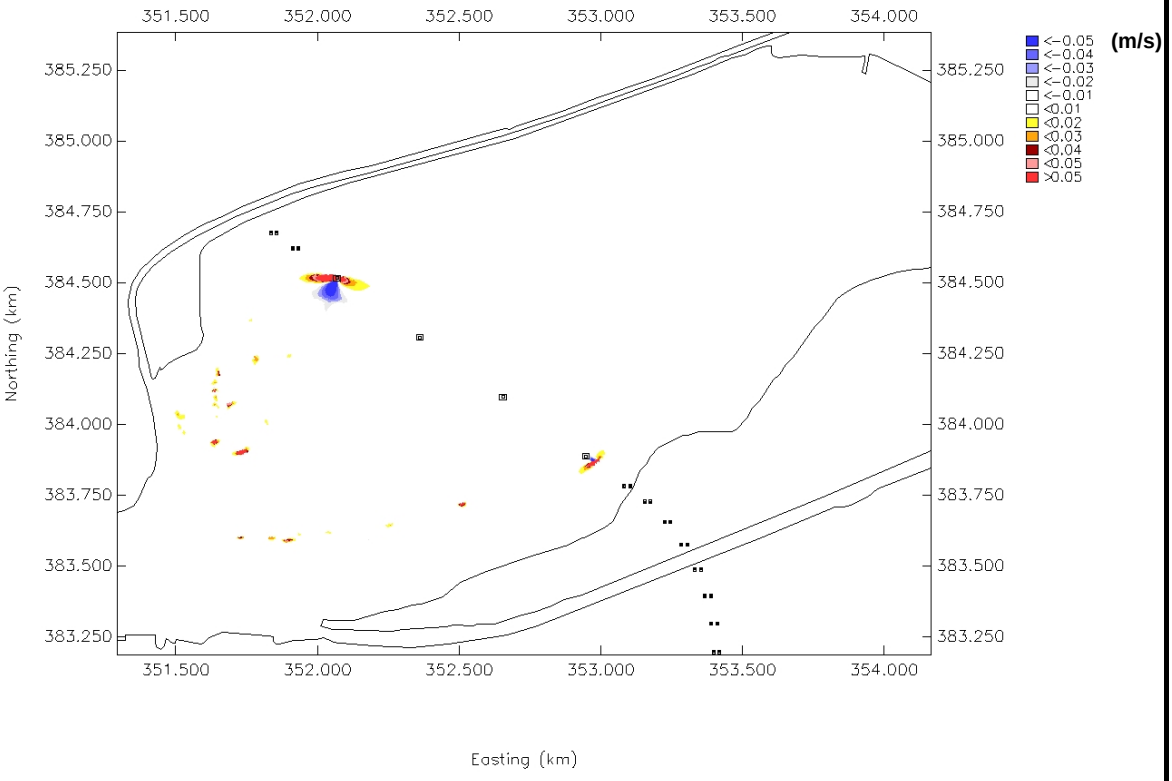


ABP mer marine environmental research	Differences in near-bed speed (m/s) between the proposed bridge scheme Route 3A Medium modified and the baseline case for low water (A) and peak flood (B) on a spring tide.	Figure C15

A.

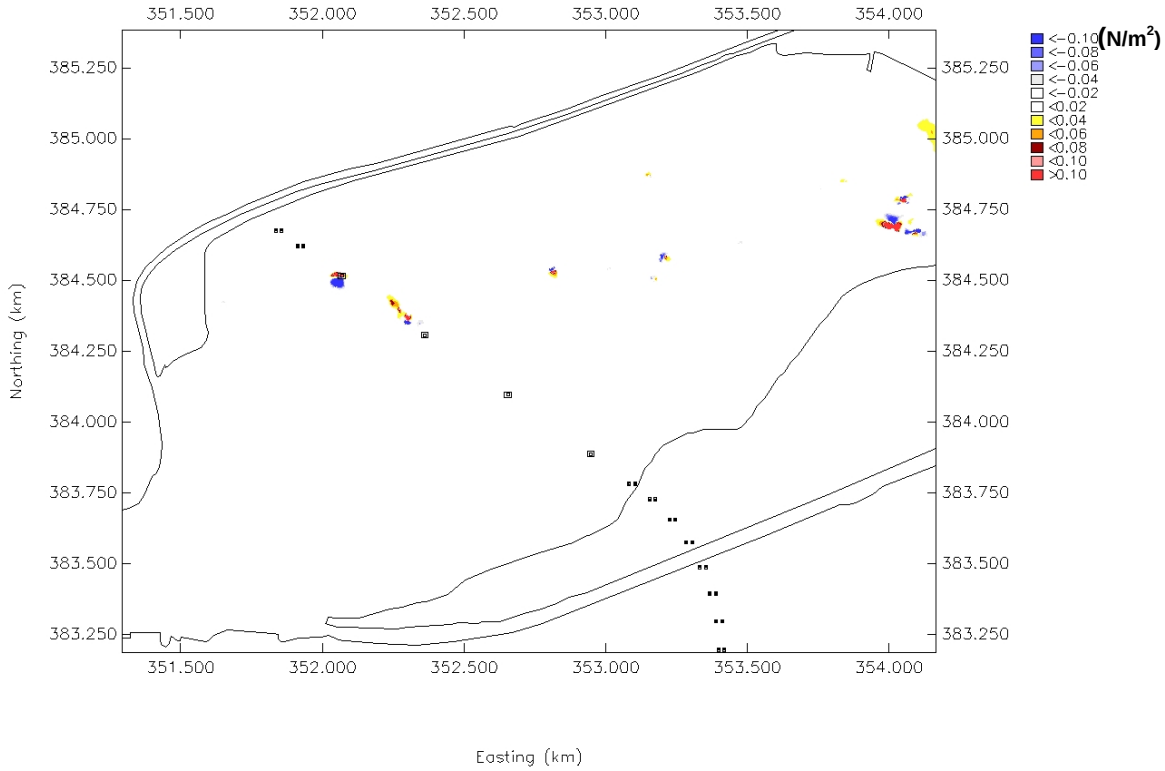


B.

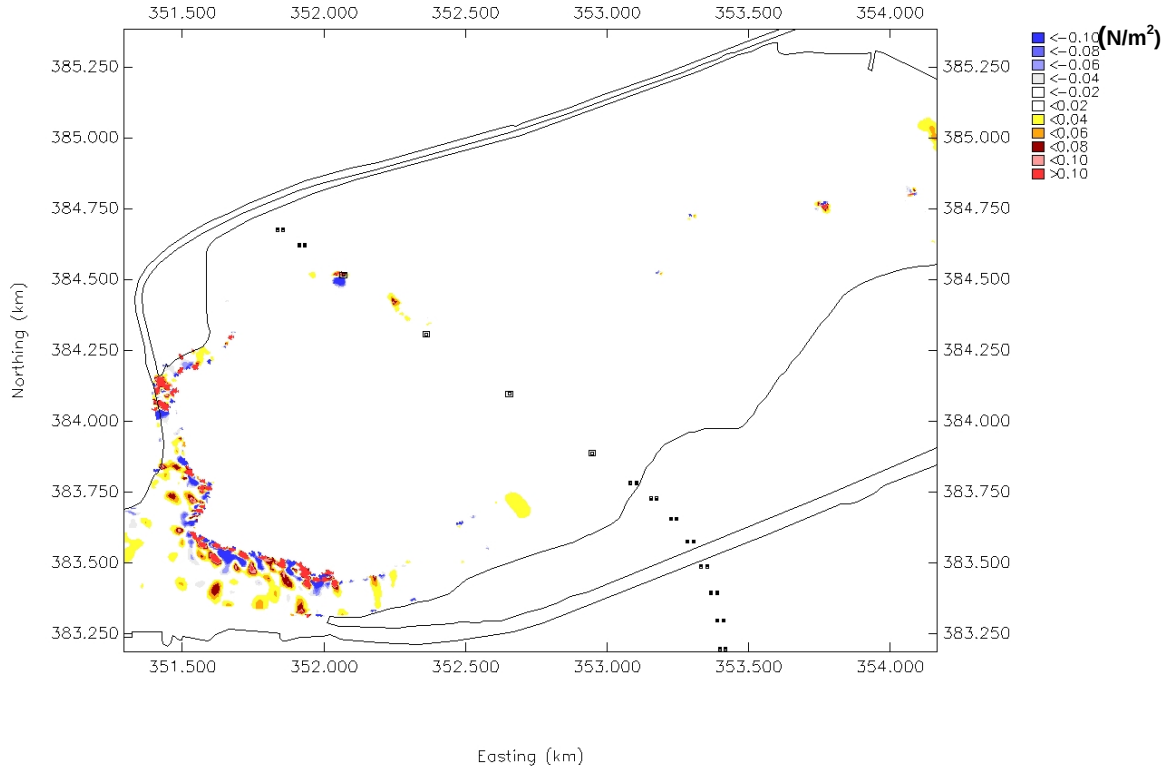


ABP mer marine environmental research	Differences in near-bed speed (m/s) between the proposed bridge scheme Route 3A Medium modified and the baseline case for high water (A) and peak ebb (B) on a spring tide.	Figure C16

A.



B.

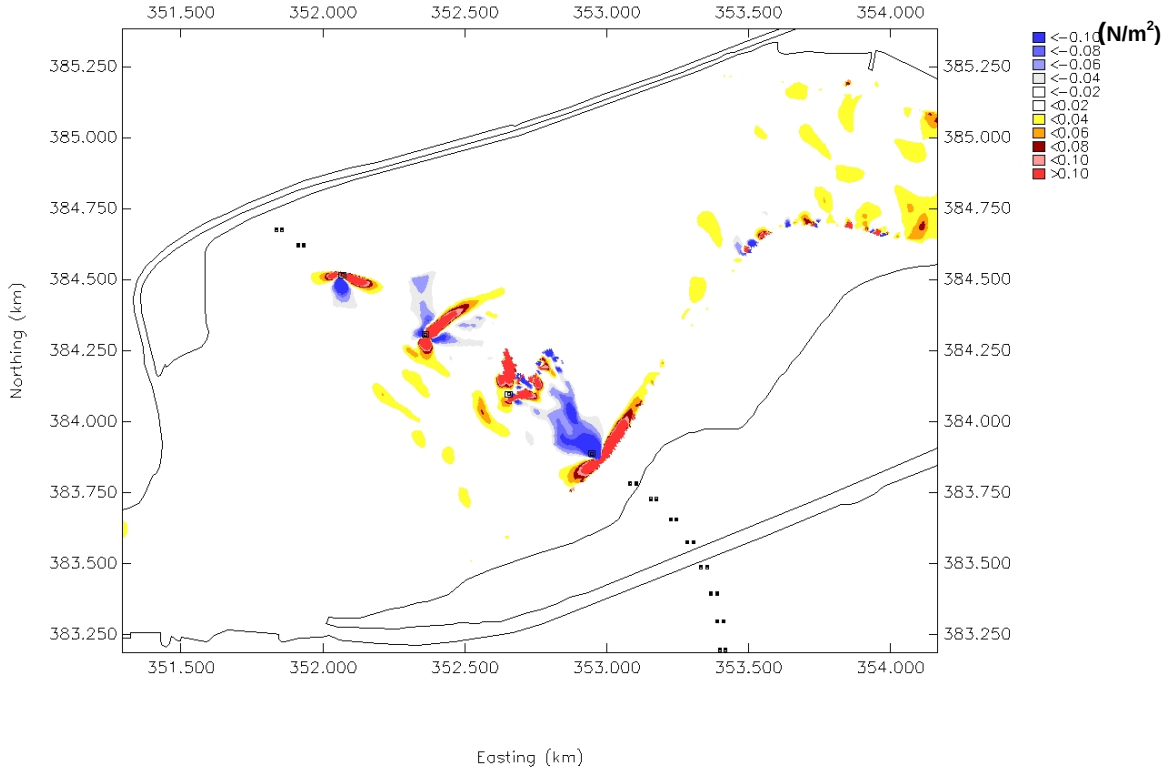


ABP mer marine environmental research

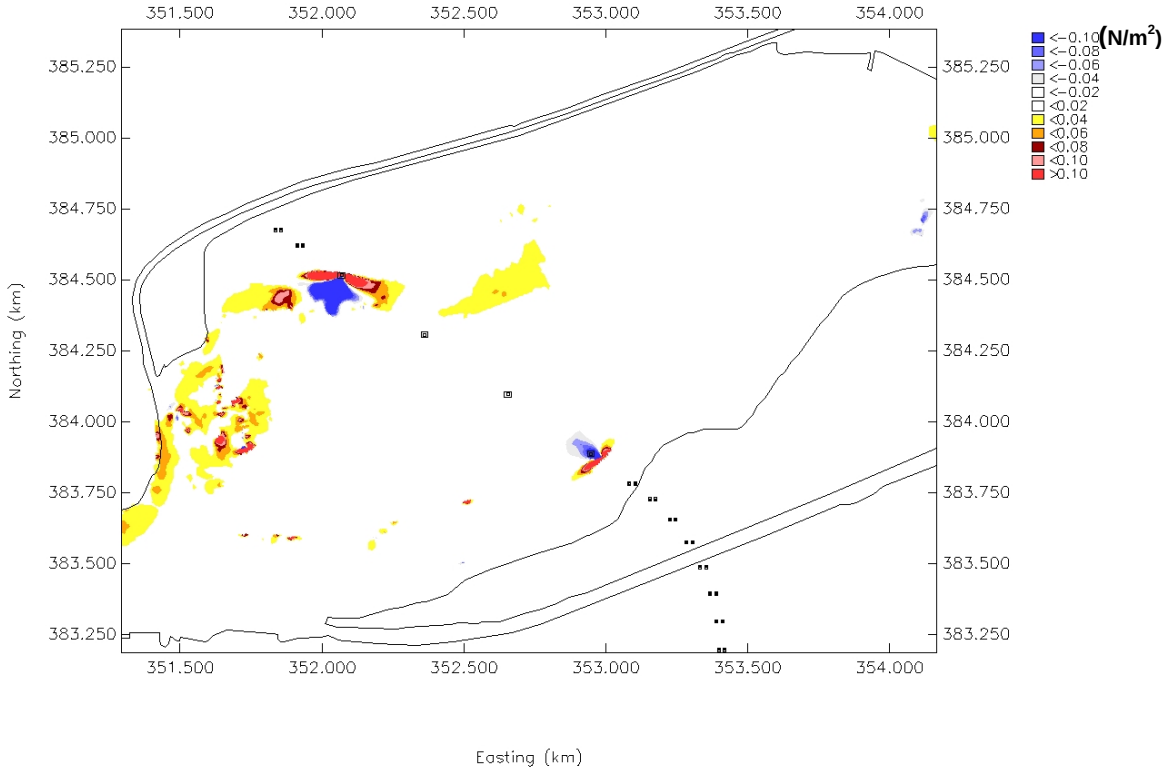
Differences in bed shear stress (N/m²) between the proposed bridge scheme Route 3A Medium modified and the baseline case for low water (A) and peak flood (B) on a spring tide.

Figure C17

A.



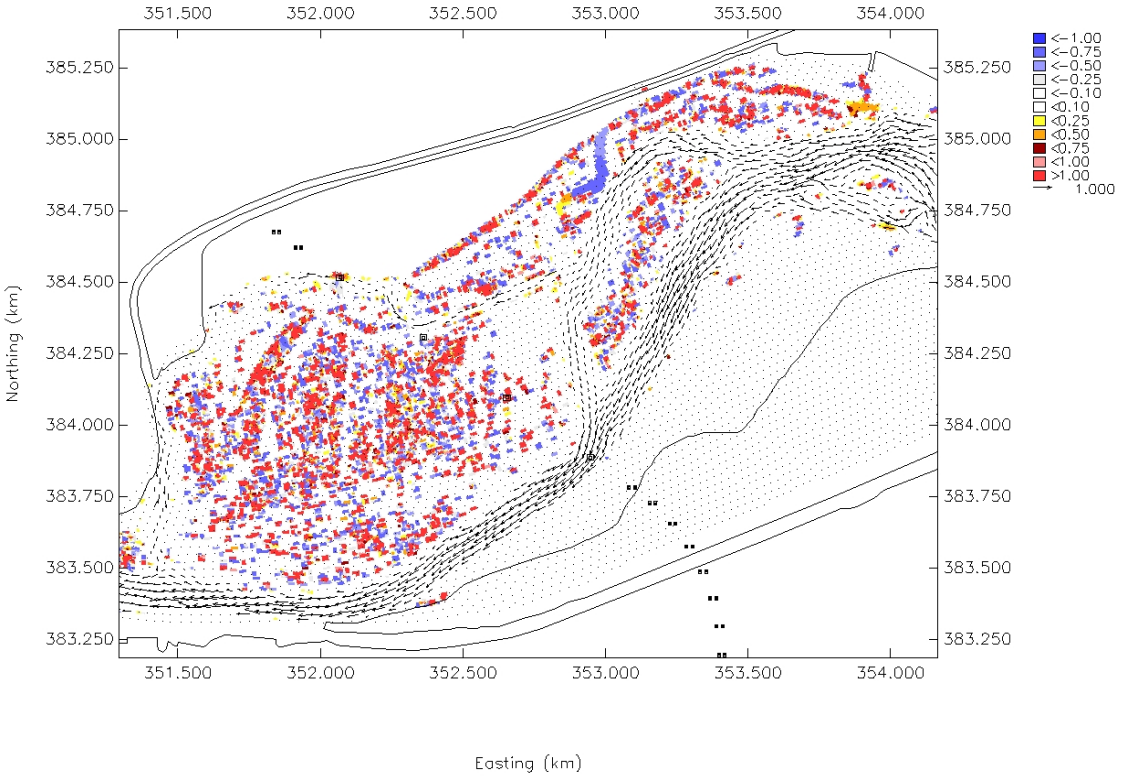
B.



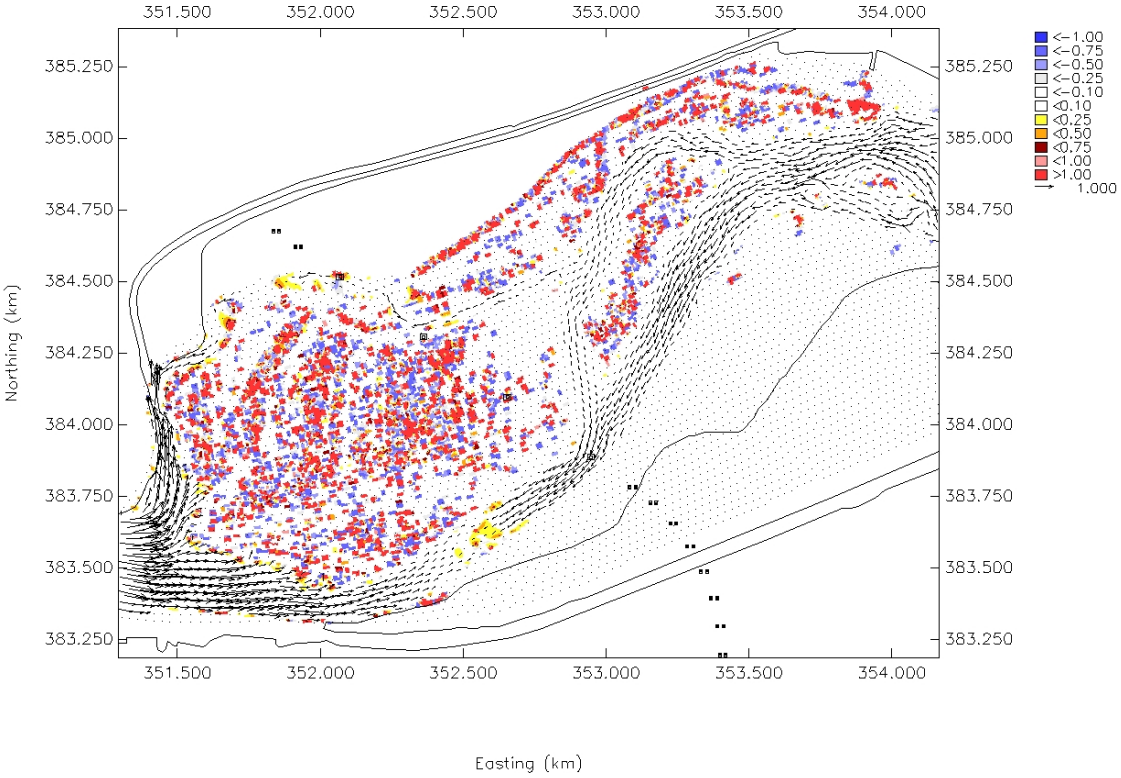
Differences in bed shear stress (N/m²) between the proposed bridge scheme Route 3A Medium modified and the baseline case for high water (A) and peak ebb (B) on a spring tide.

Figure C18

A.

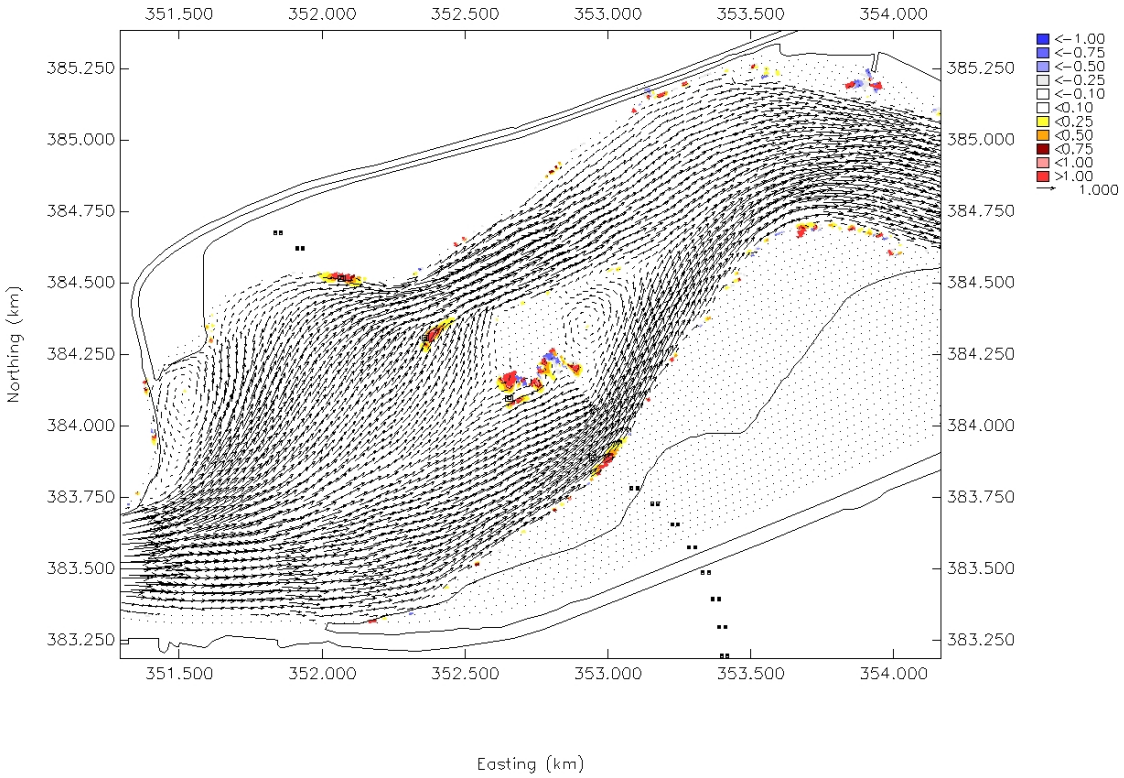


B.

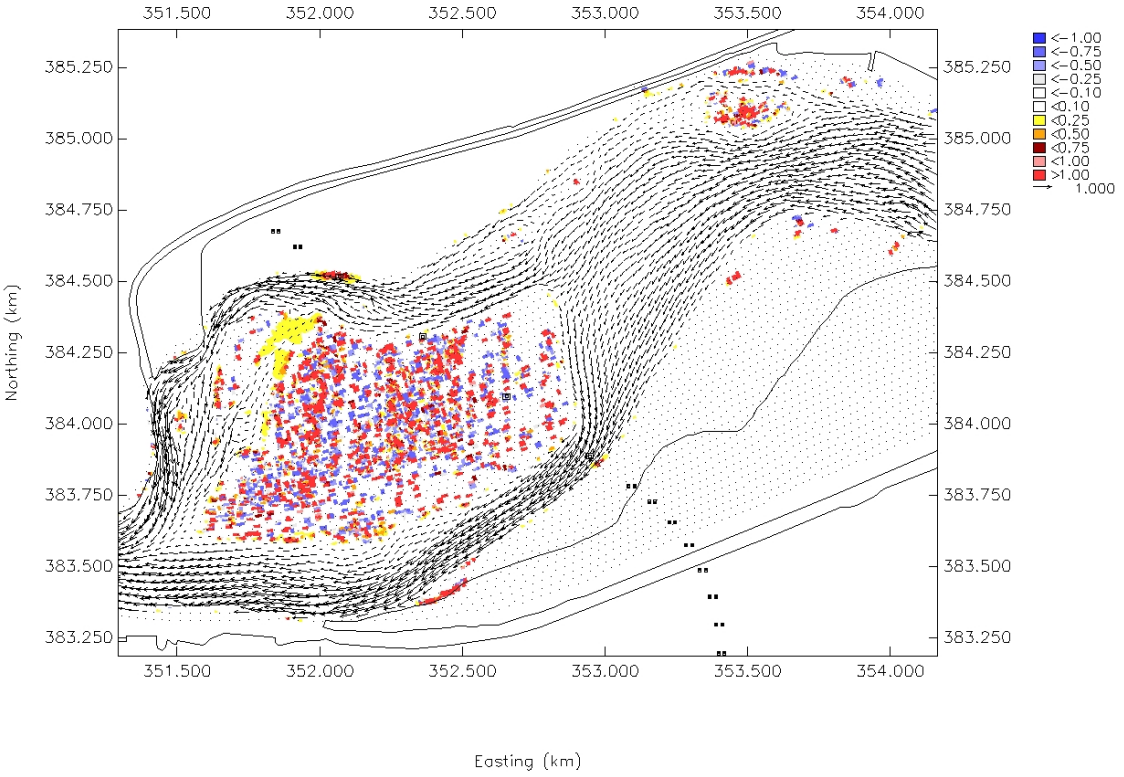


ABP mer marine environmental research	Percentage differences in bed shear stress between the proposed bridge scheme Route 3A Medium modified and the baseline case for low water (A) and peak flood (B) on a spring tide. (1 = 100% ; 0.1 = 10%).	Figure C19

A.



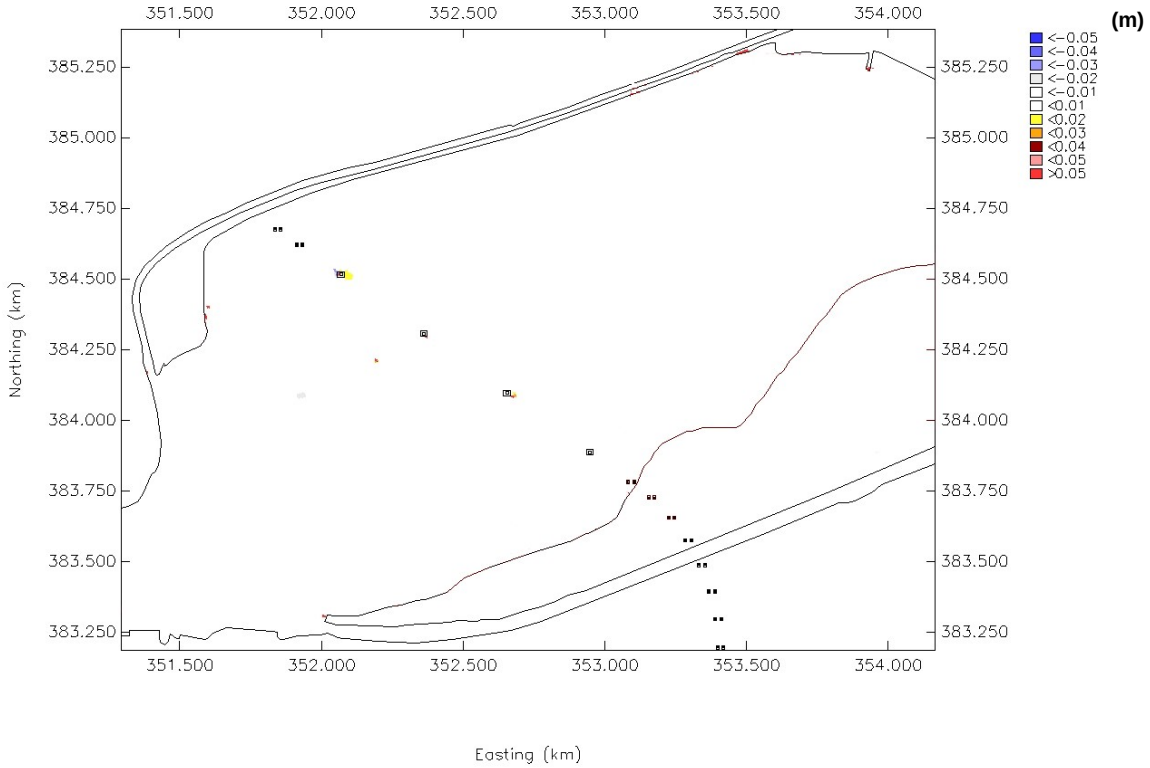
B.



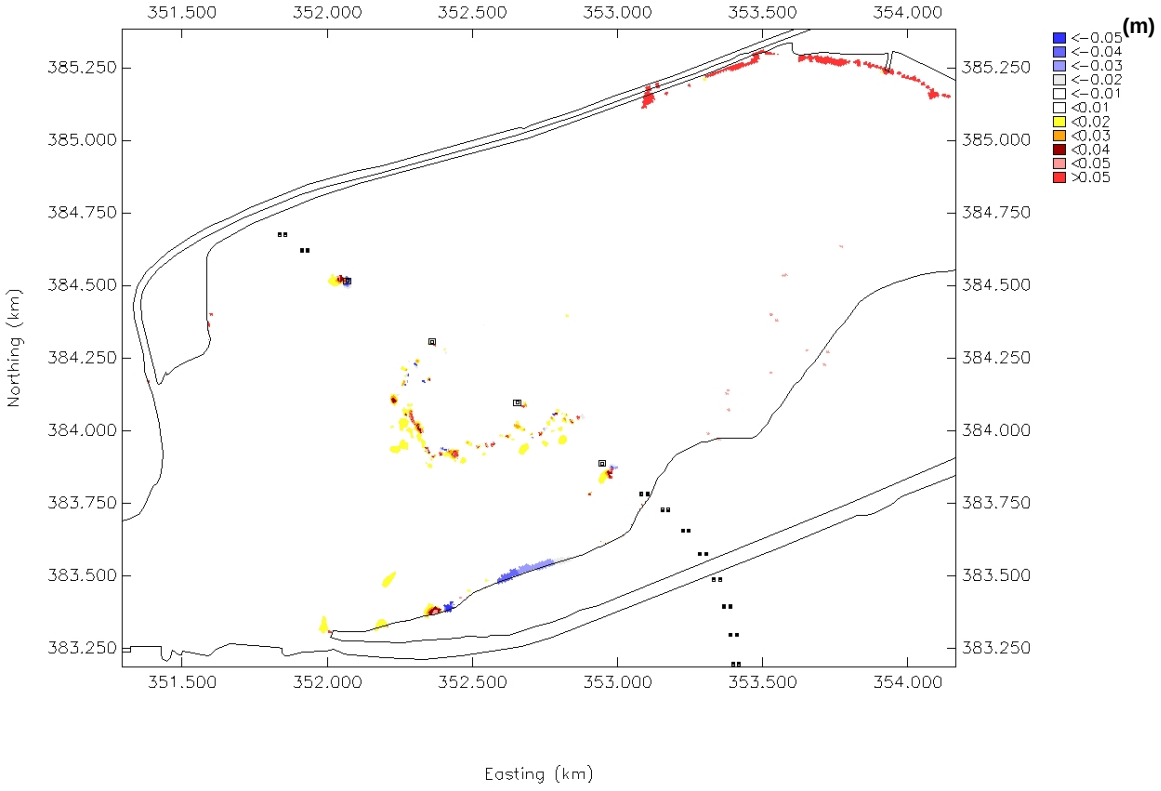
Percentage differences in bed shear stress between the proposed bridge scheme Route 3A Medium modified and the baseline case for high water (A) and peak ebb (B) on a spring tide. (1 = 100% ; 0.1 = 10%).

Figure C20

A.

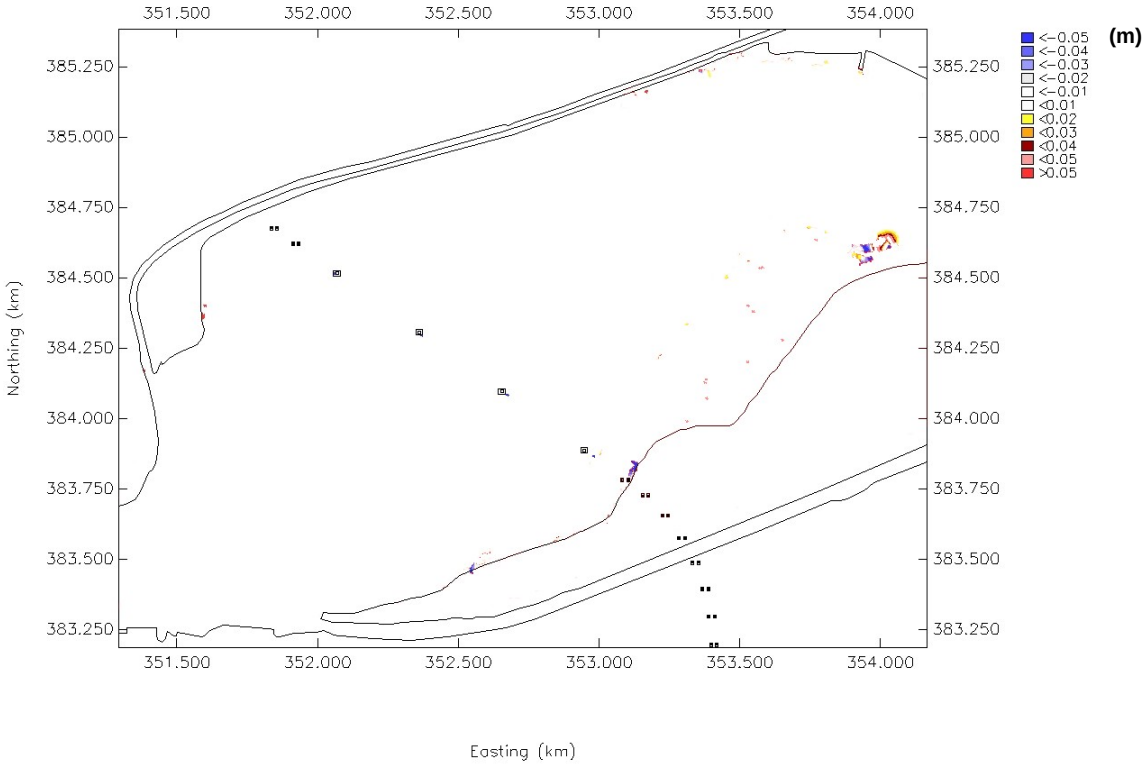


B.

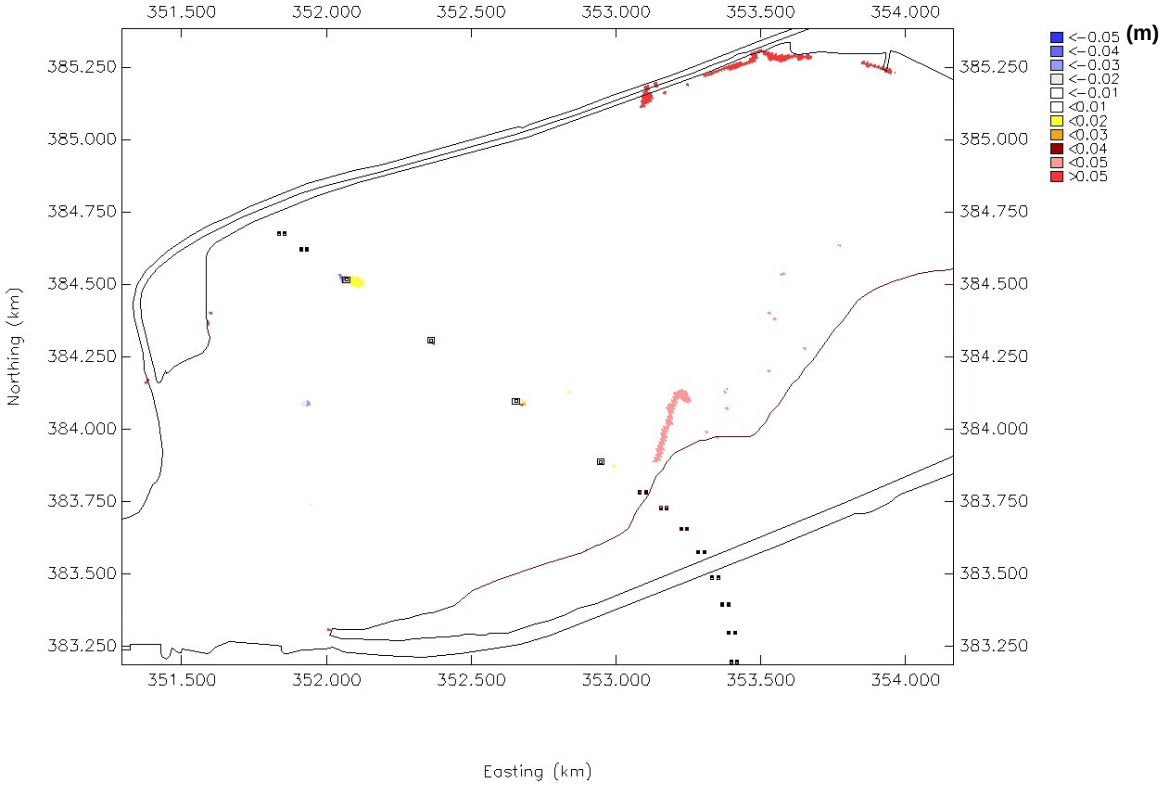


ABP mer marine environmental research	Differences in water level (m) between the proposed bridge scheme Route 3A Medium modified and the baseline case for low water (A) and peak flood (B) on a spring tide and 1:200 fluvial event.	Figure C21

A.



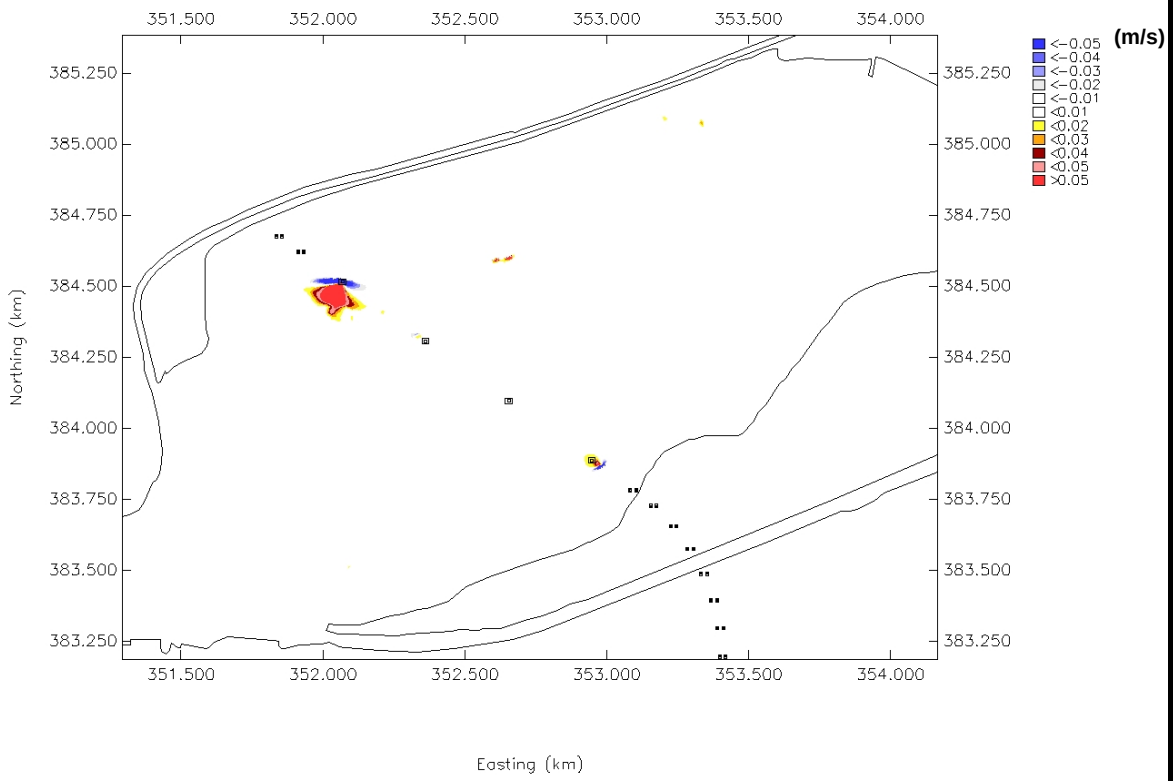
B.



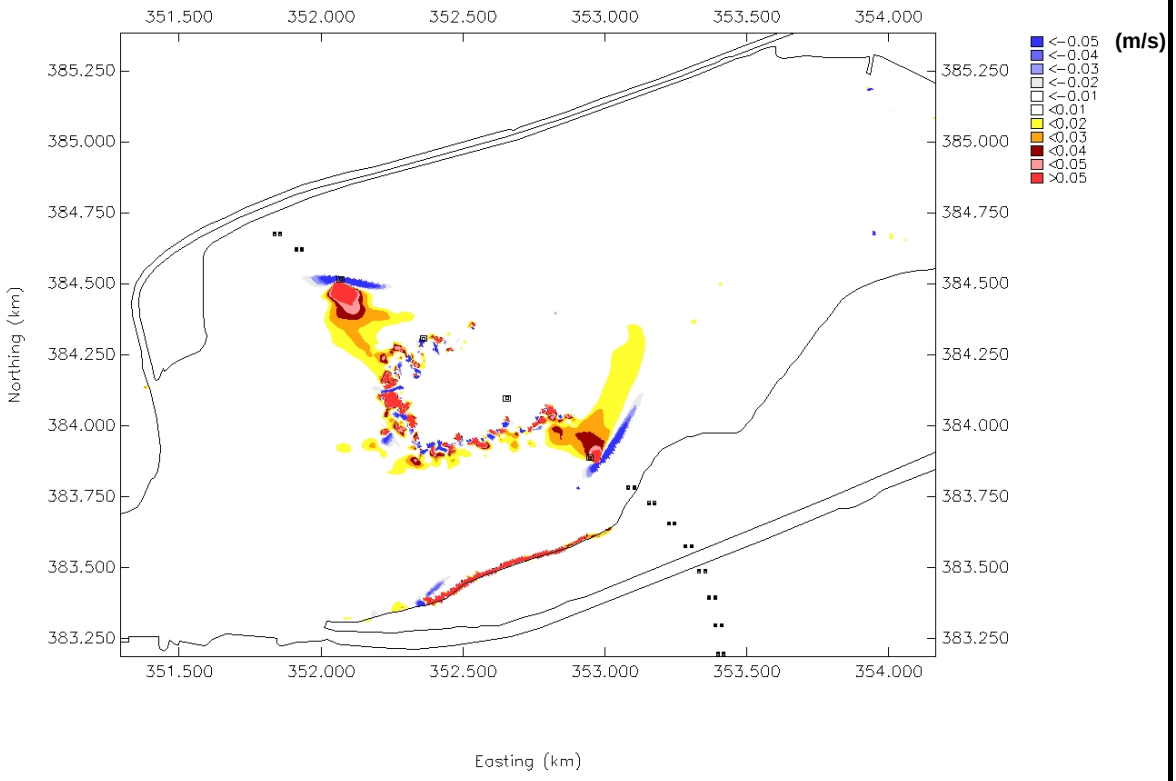
Differences in water level (m) between the proposed bridge scheme Route 3A Medium modified and the baseline case for high water (A) and peak ebb (B) on a spring tide and 1:200 fluvial event.

Figure C22

A.

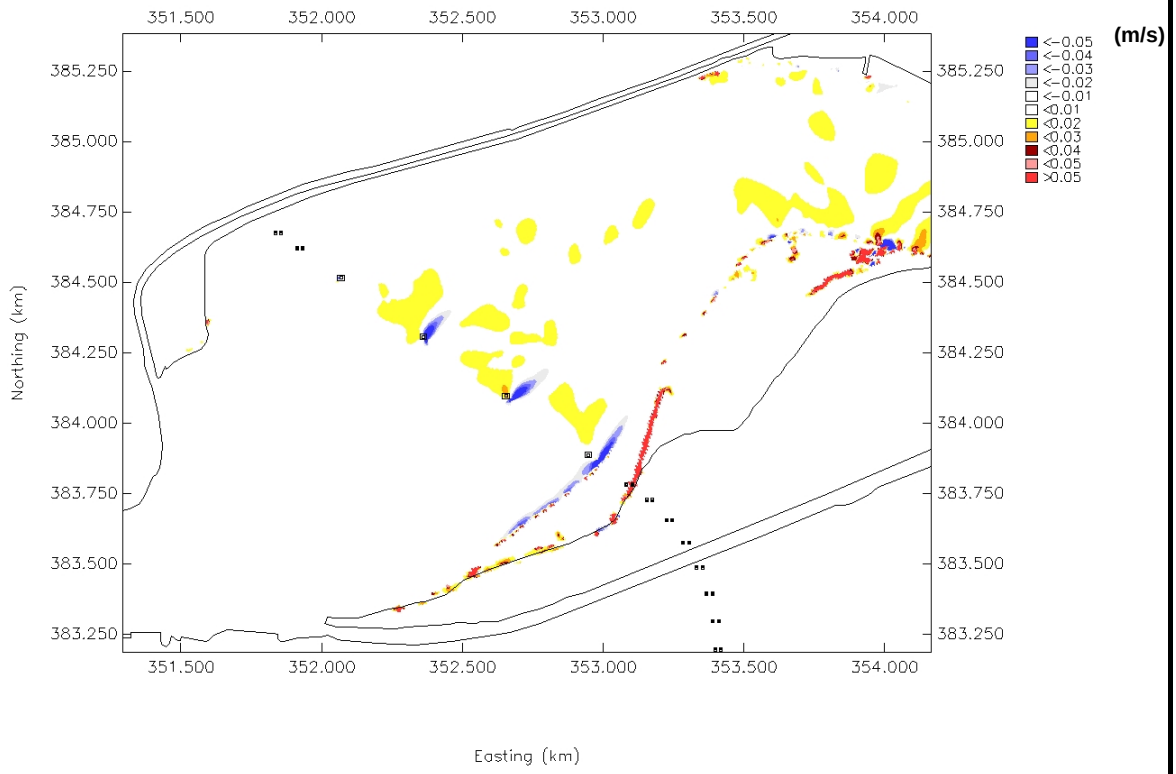


B.

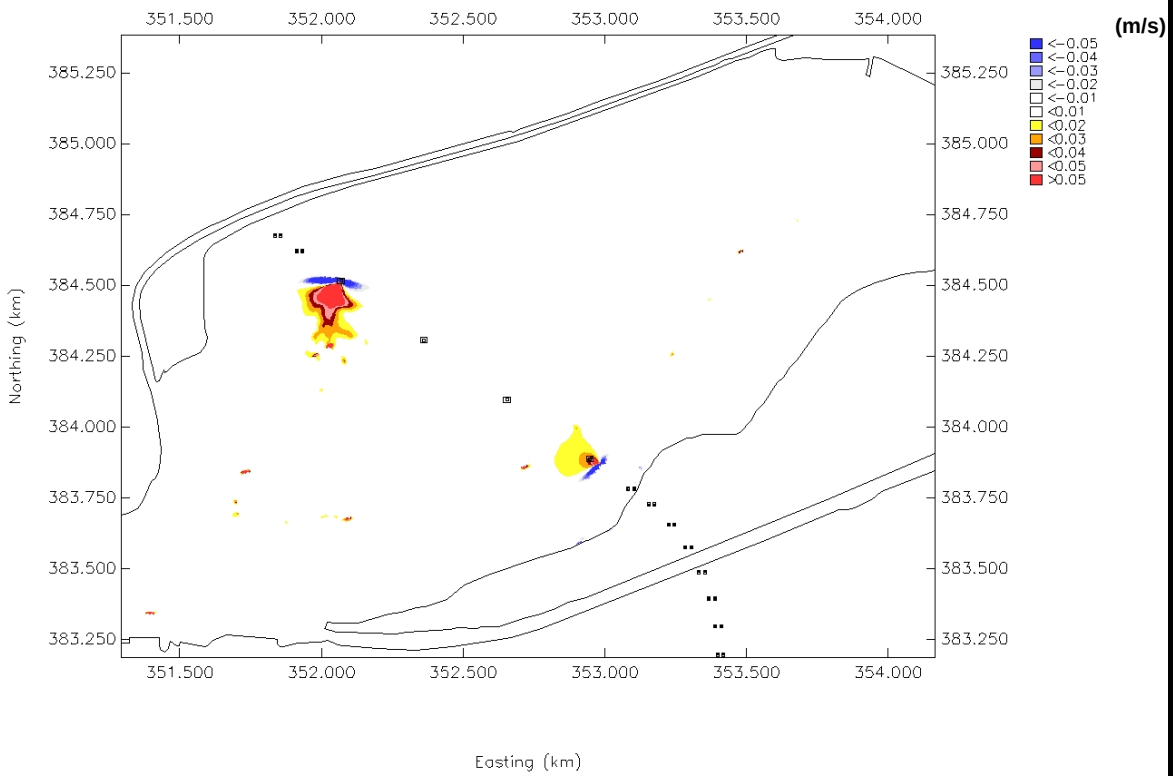


ABP mer marine environmental research	Differences in near-surface speed (m/s) between the proposed bridge scheme Route 3A Medium modified and the baseline case for low water (A) and peak flood (B) on a spring tide and 1:200 fluvial event.	Figure C23

A.



B.

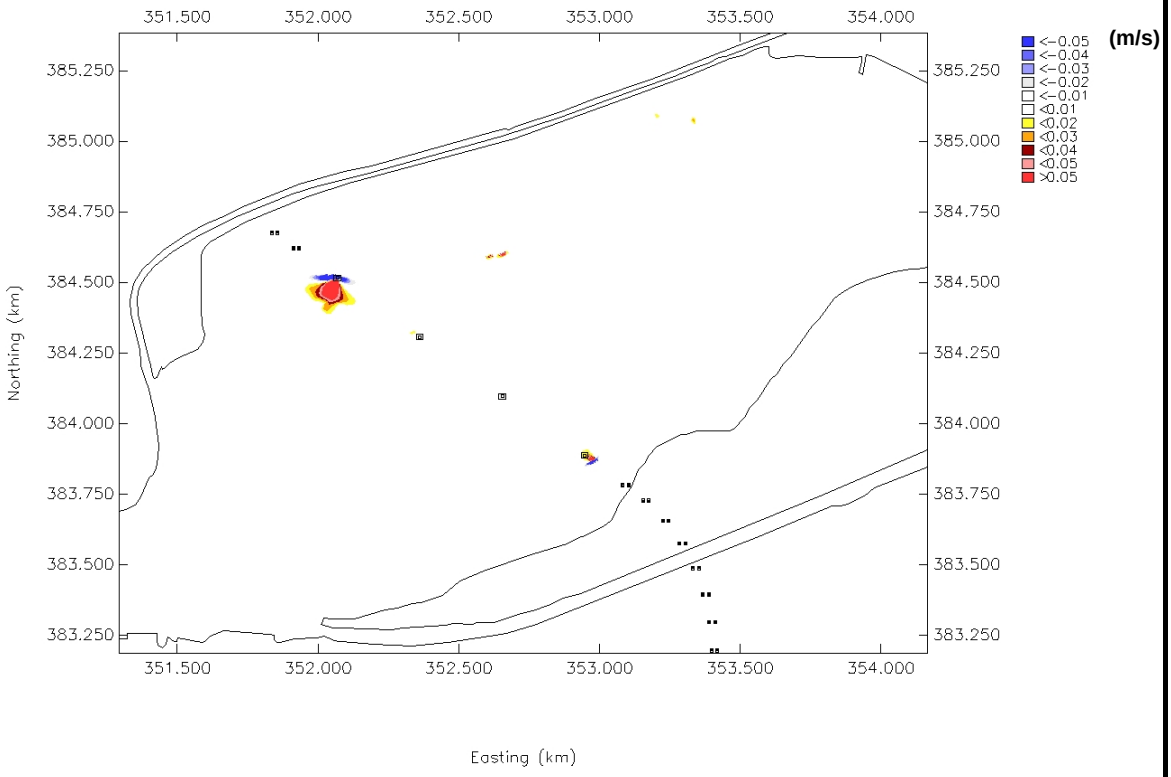


ABP mer marine environmental research

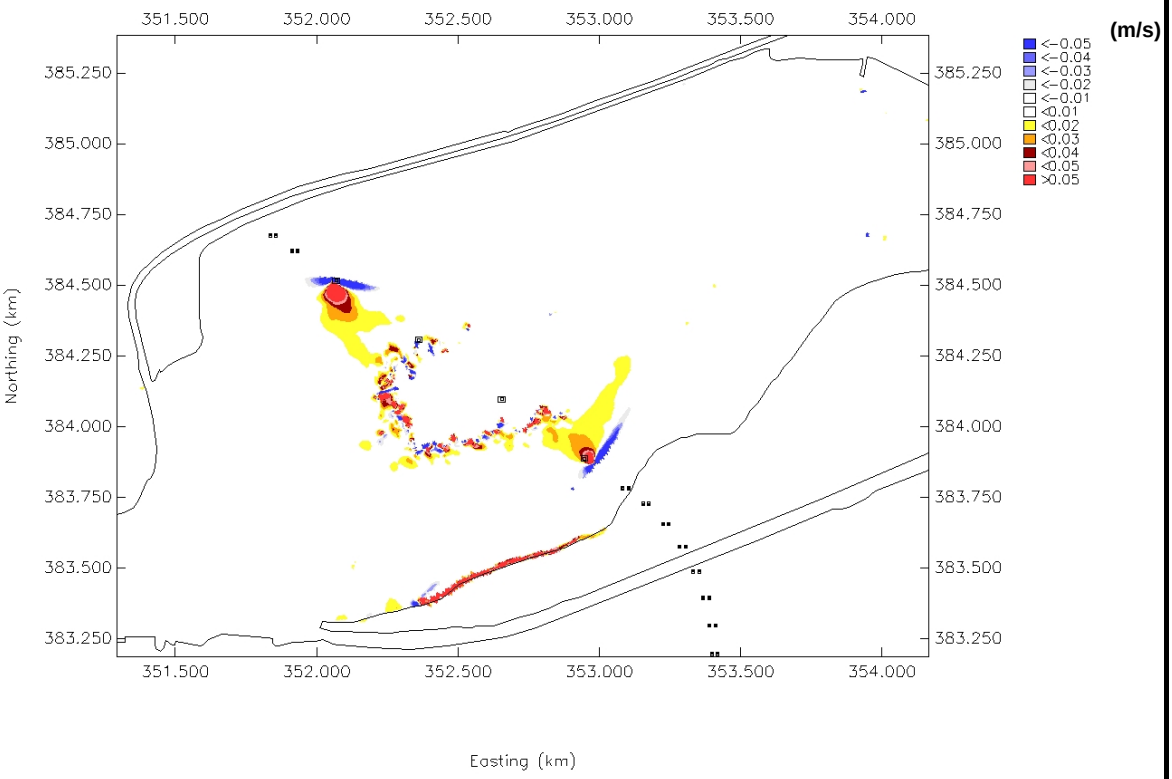
Differences in near-surface speed (m/s) between the proposed bridge scheme Route 3A Medium modified and the baseline case for high water (A) and peak ebb (B) on a spring tide and 1:200 fluvial event.

Figure C24

A.

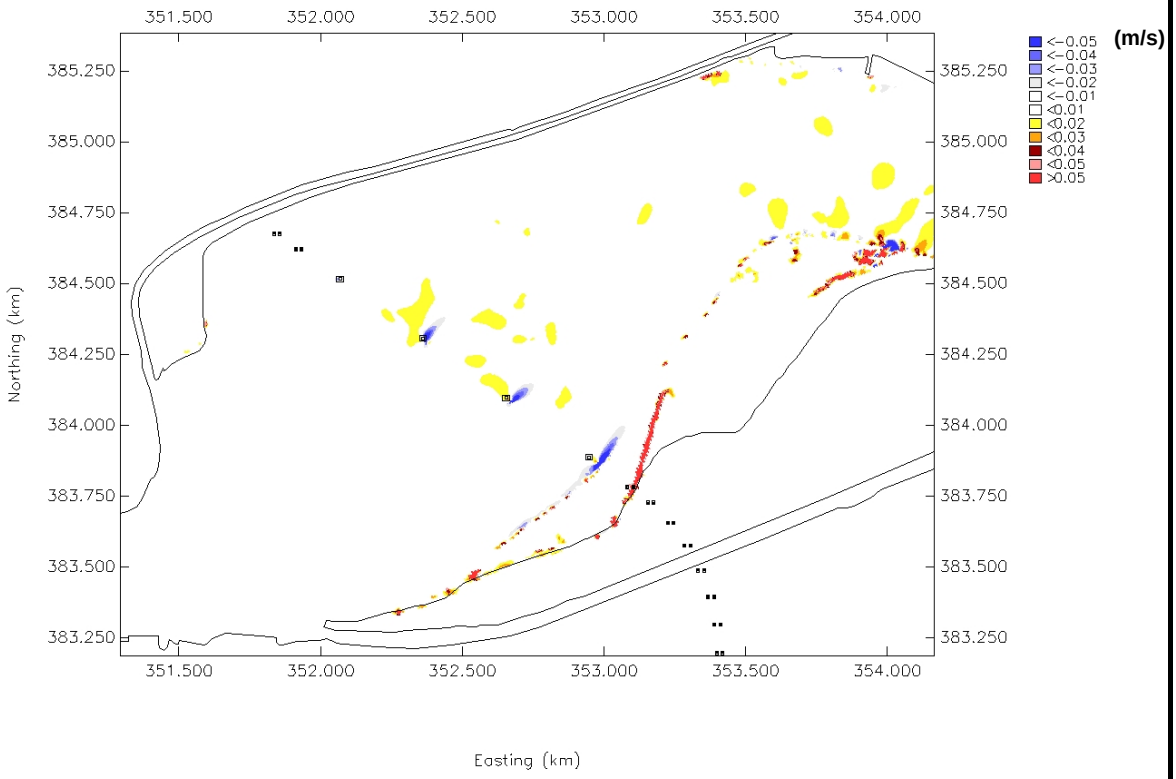


B.

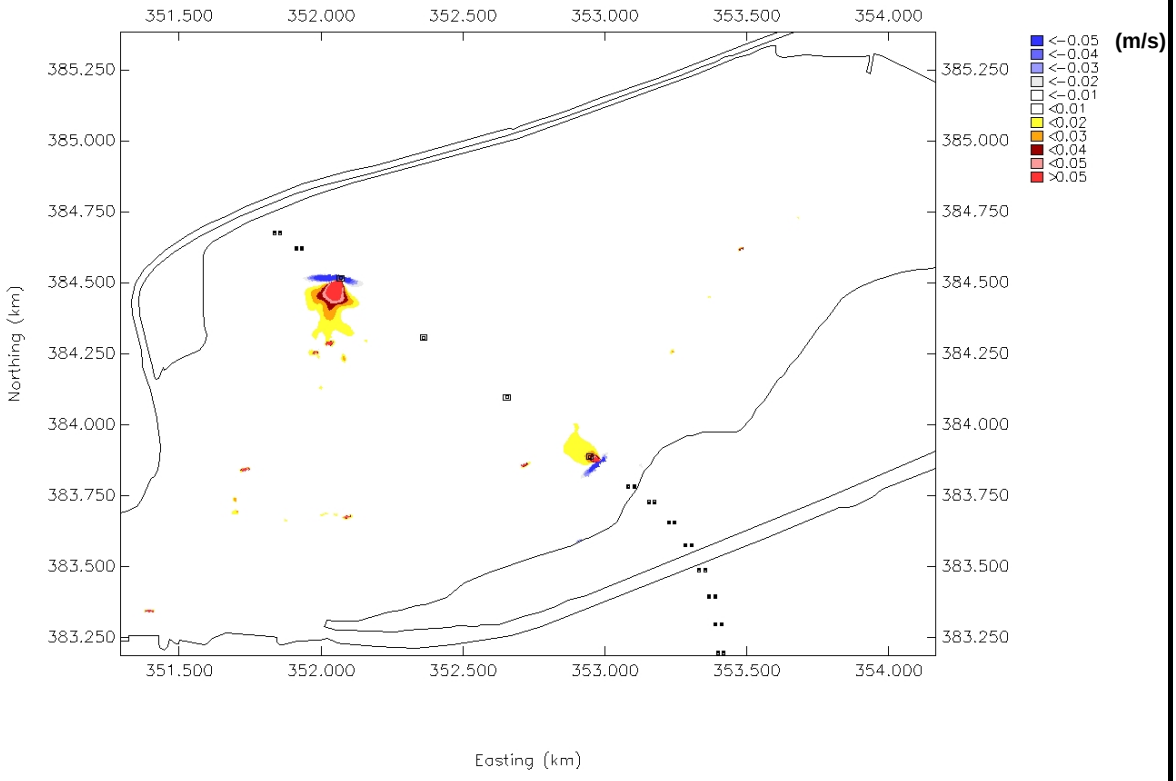


ABP mer marine environmental research	Differences in near-bed speed (m/s) between the proposed bridge scheme Route 3A Medium modified and the baseline case for low water (A) and peak flood (B) on a spring tide and 1:200 fluvial event.	Figure C25

A.



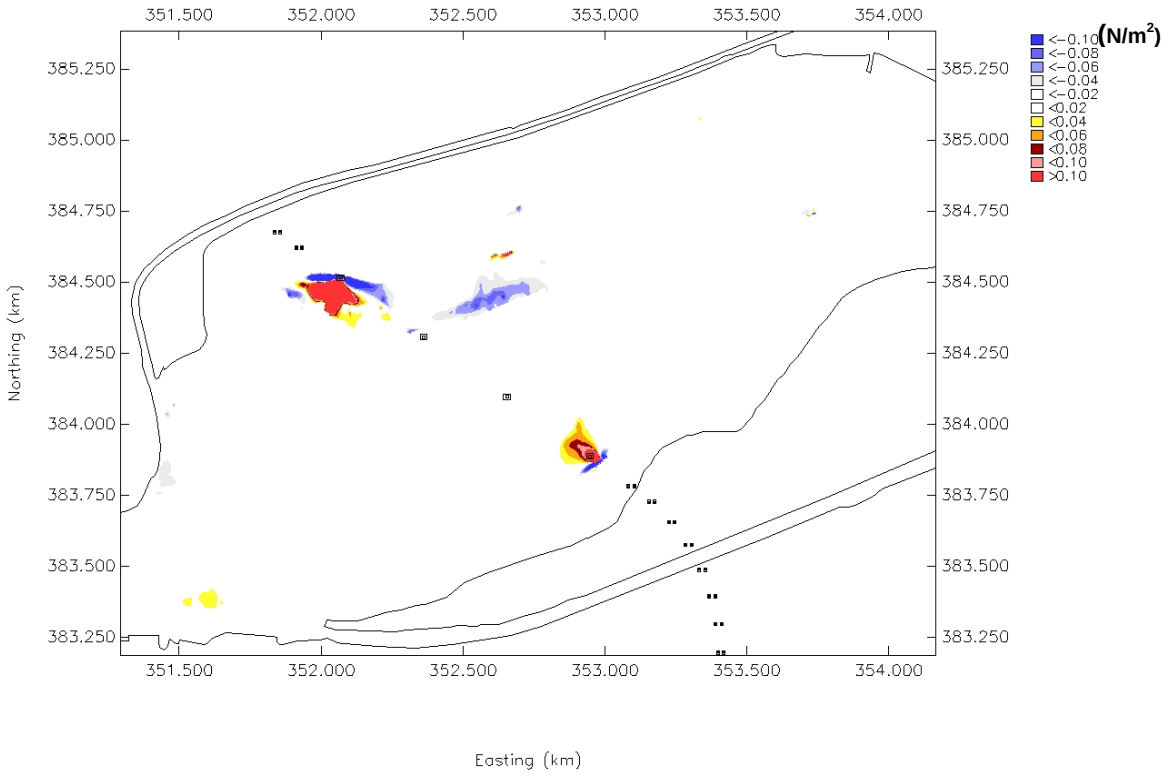
B.



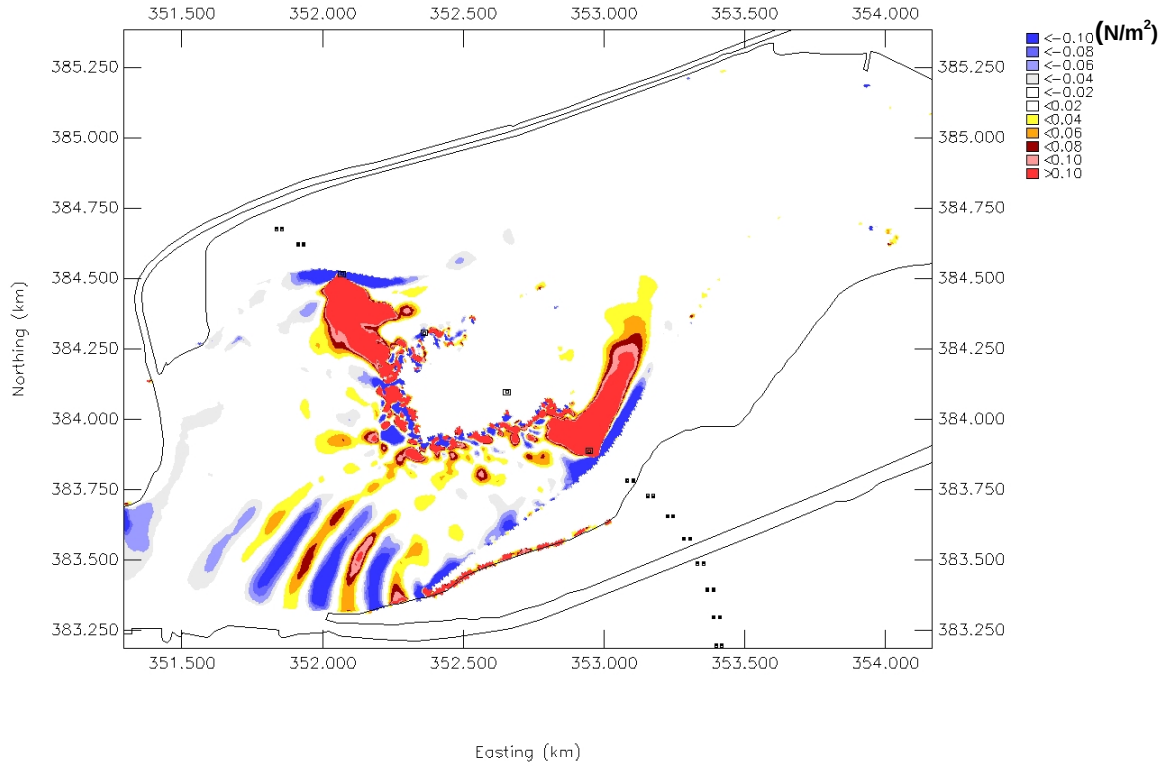
Differences in near-bed speed (m/s) between the proposed bridge scheme Route 3A Medium modified and the baseline case for high water (A) and peak ebb (B) on a spring tide and 1:200 fluvial event.

Figure C26

A.



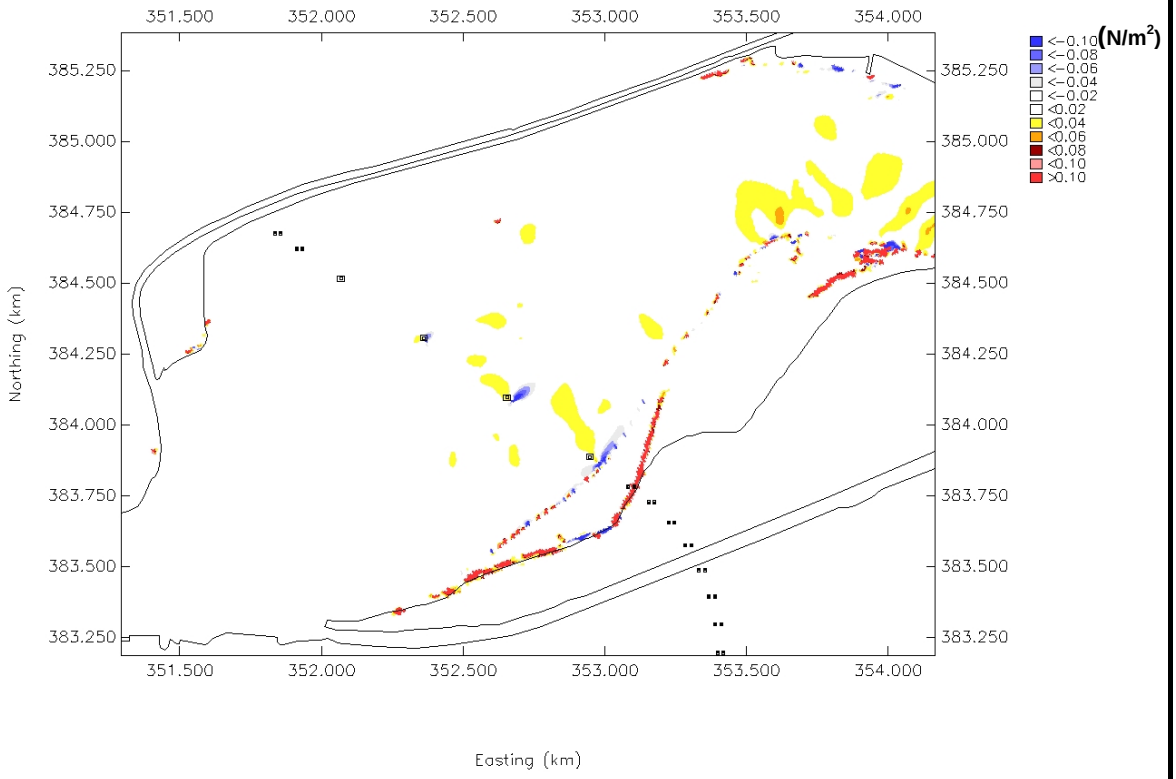
B.



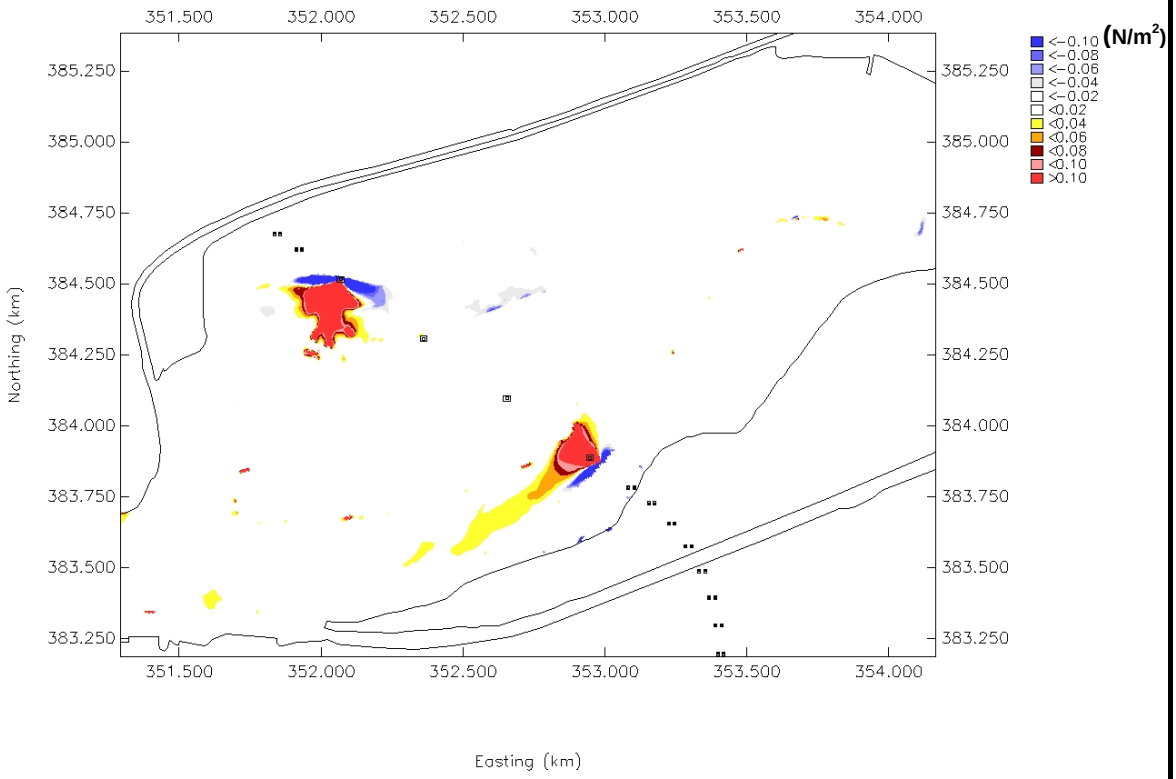
Differences in bed shear stress (N/m²) between the proposed bridge scheme Route 3A Medium modified and the baseline case for low water (A) and peak flood (B) on a spring tide and 1:200 fluvial event.

Figure C27

A.



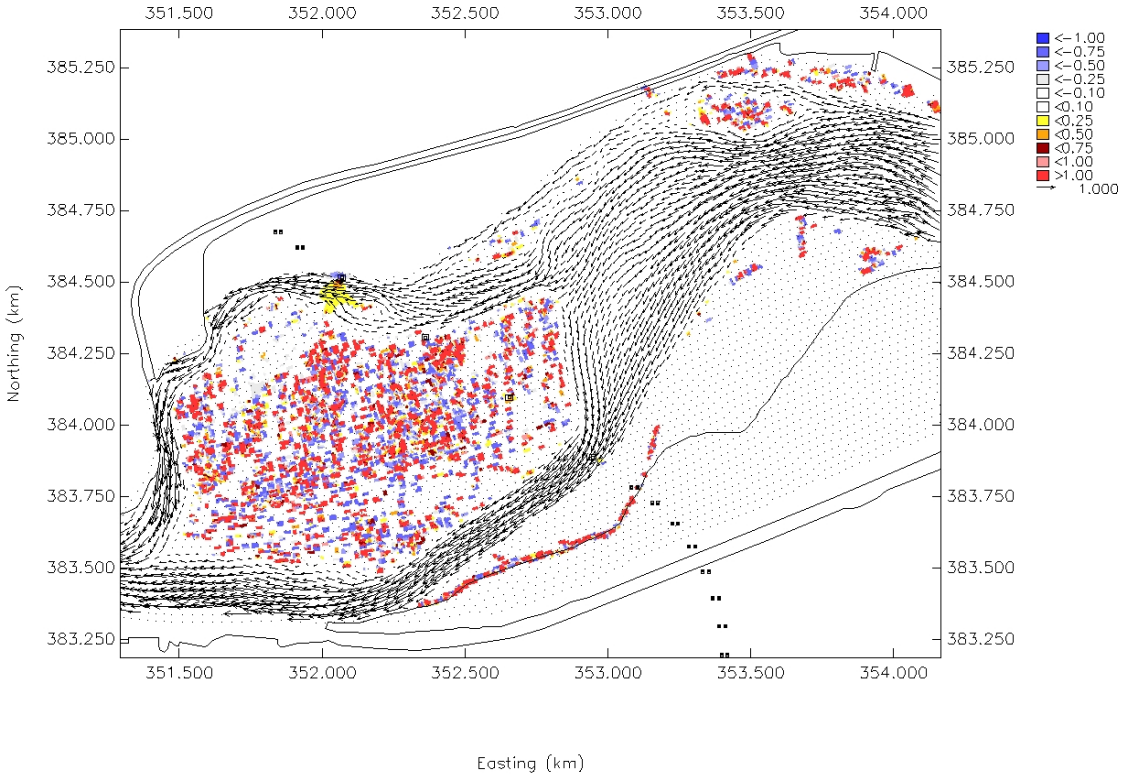
B.



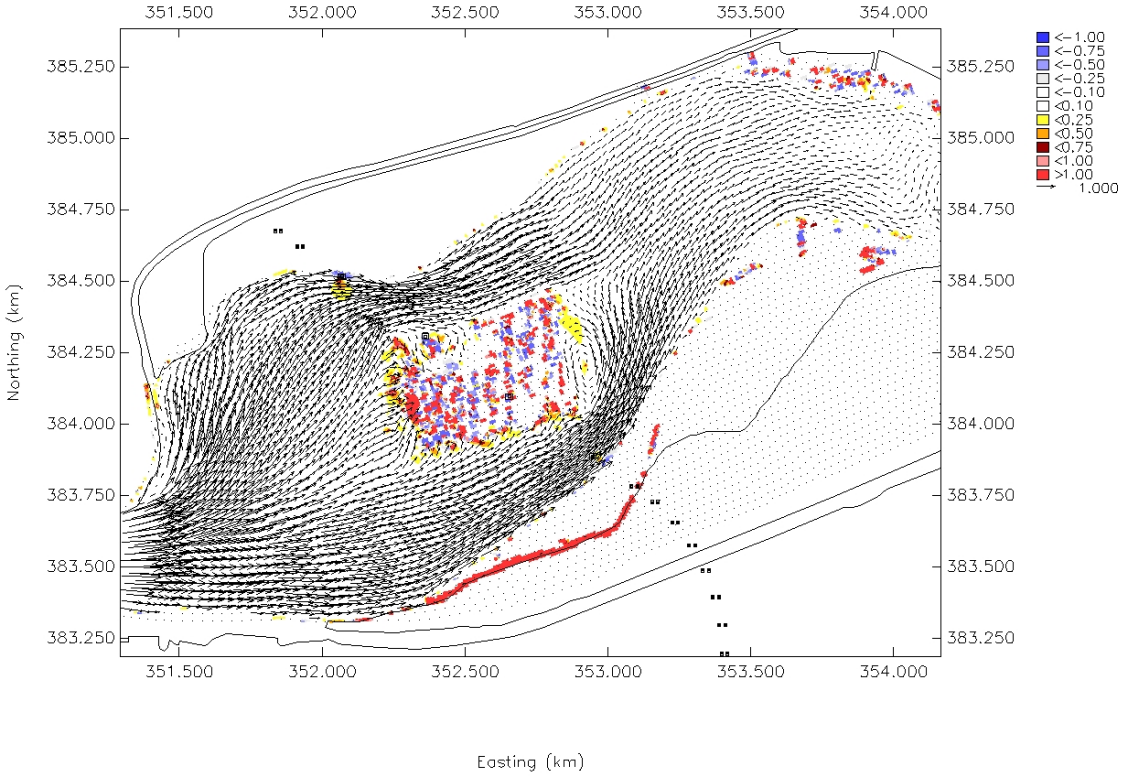
Differences in bed shear stress (N/m²) between the proposed bridge scheme Route 3A Medium modified and the baseline case for high water (A) and peak ebb (B) on a spring tide and 1:200 fluvial event.

Figure C28

A.

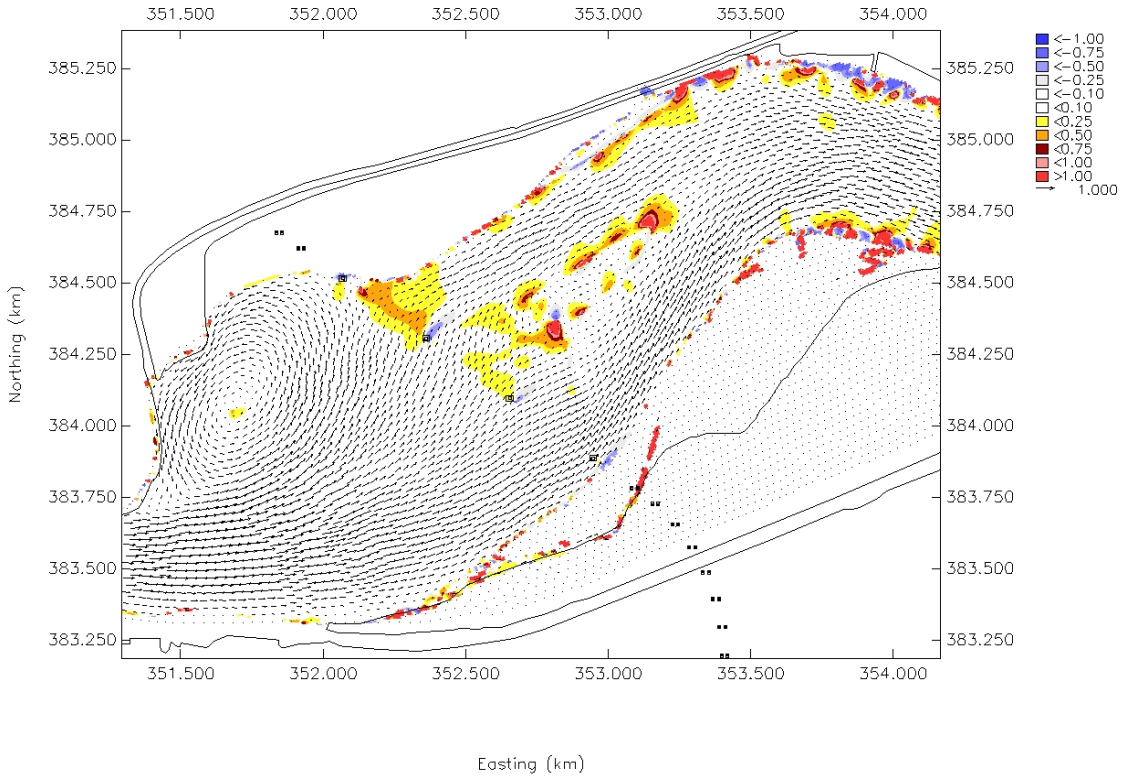


B.

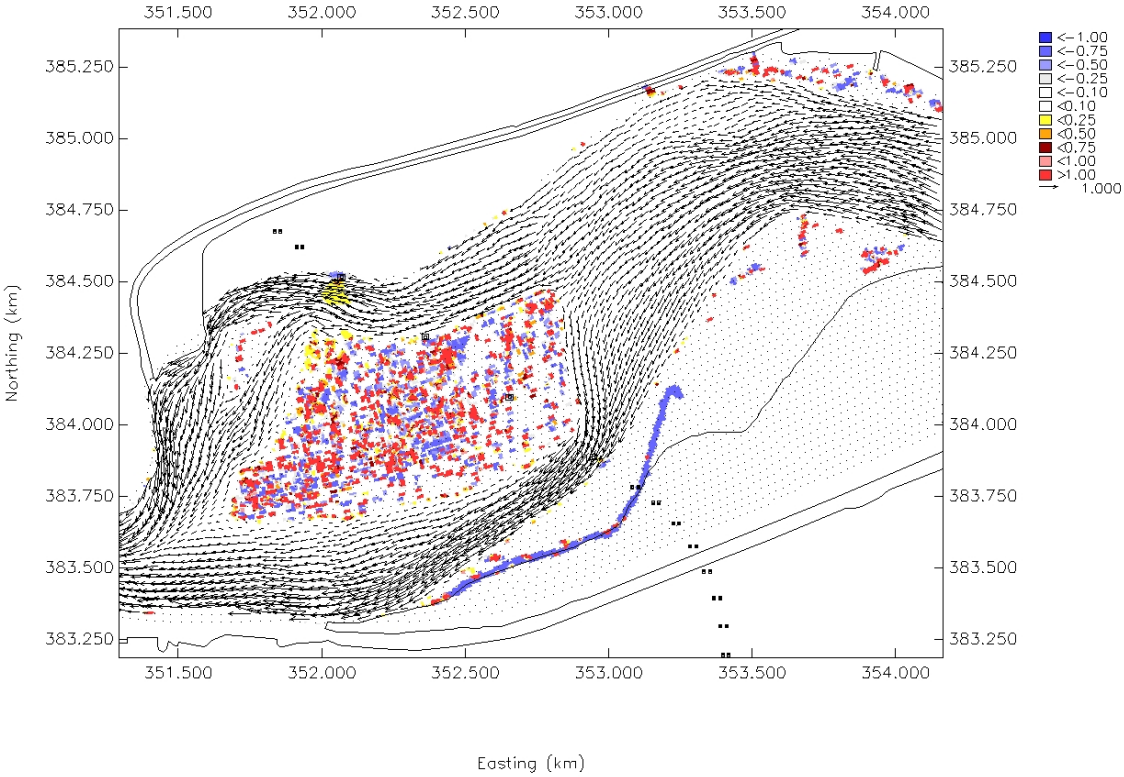


ABP mer marine environmental research	Percentage differences in bed shear stress between the proposed bridge scheme Route 3A Medium modified and the baseline case for low water (A) and peak flood (B) on a spring tide and 1:200 fluvial event. (1 = 100% ; 0.1 = 10%).	Figure C29

A.

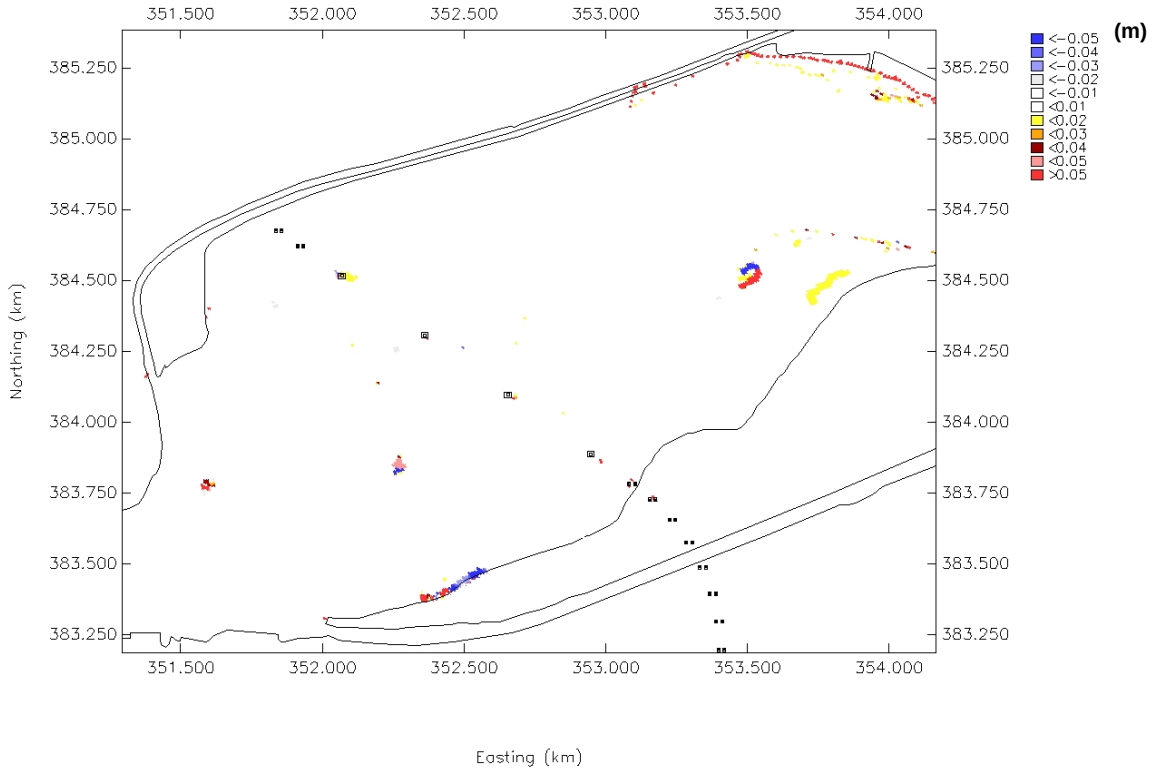


B.

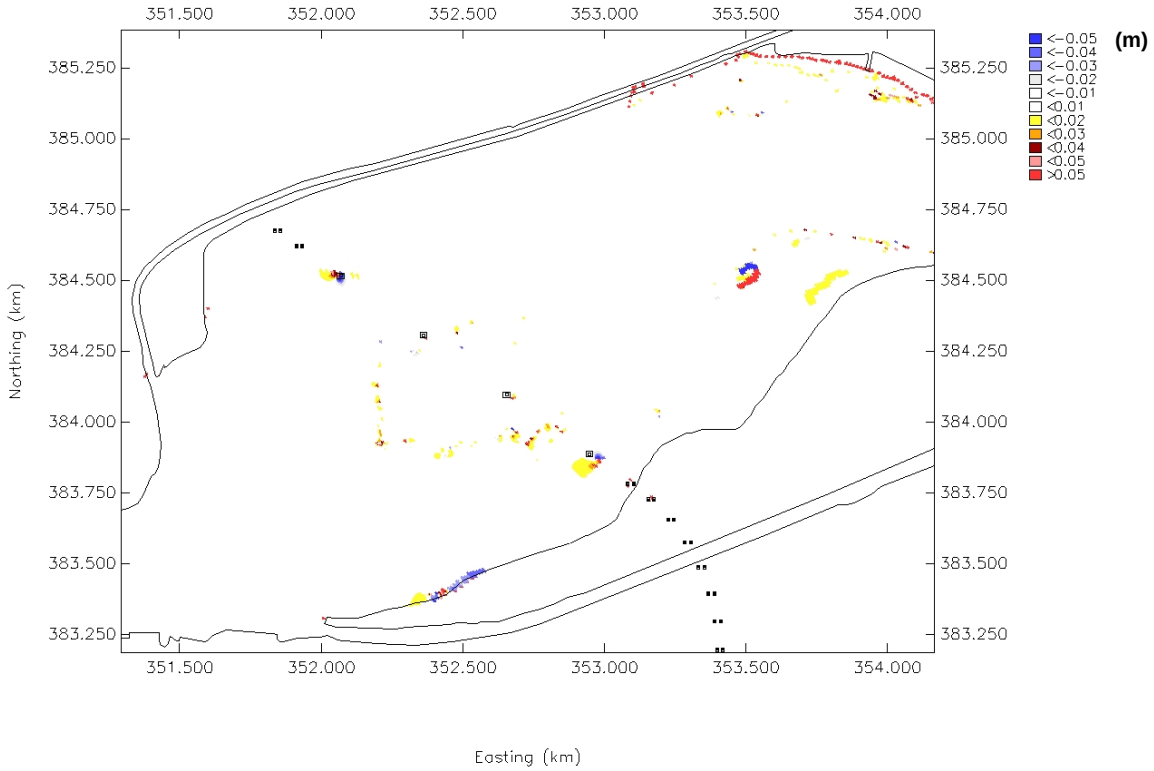


ABP mer marine environmental research	Percentage differences in bed shear stress between the proposed bridge scheme Route 3A Medium modified and the baseline case for high water (A) and peak ebb (B) on a spring tide and 1:200 fluvial event. (1 = 100% ; 0.1 = 10%).	Figure C30

A.



B.

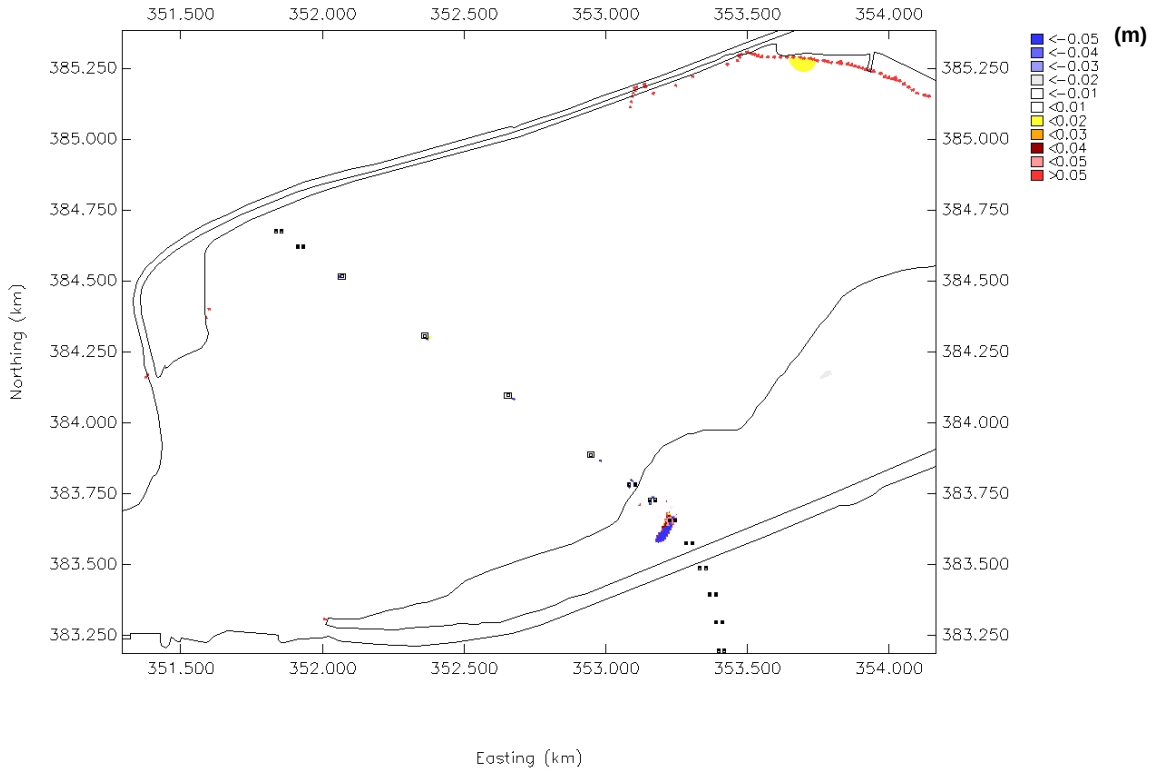


ABP mer marine environmental research

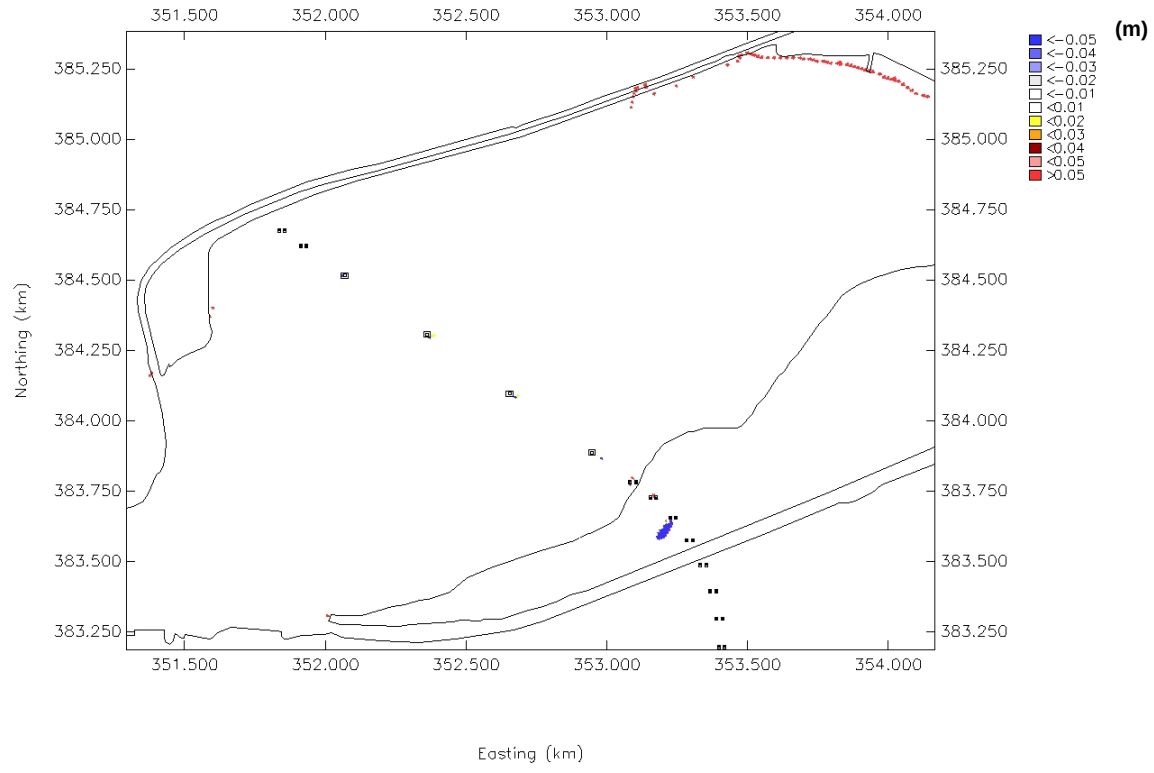
Differences in water level (m) between the proposed bridge scheme Route 3A Medium modified and the baseline case for low water (A) and peak flood (B) on a 1:200 surge tide and 1:200 fluvial event.

Figure C31

A.



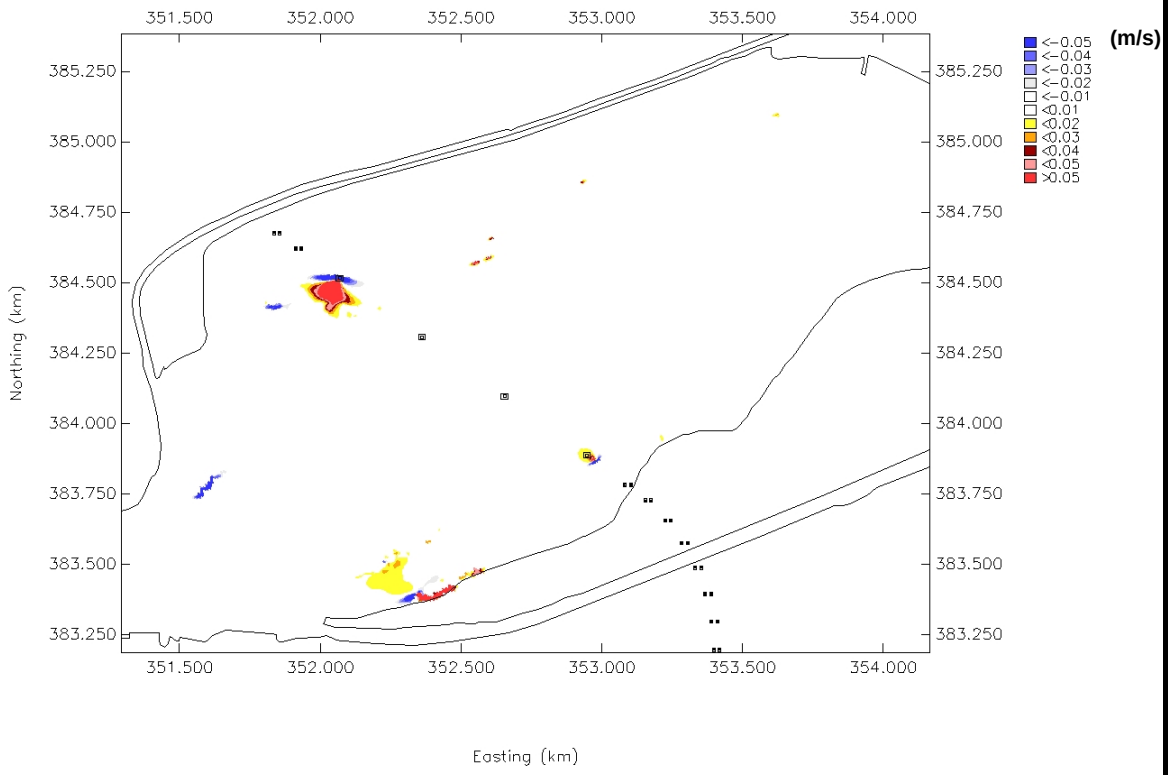
B.



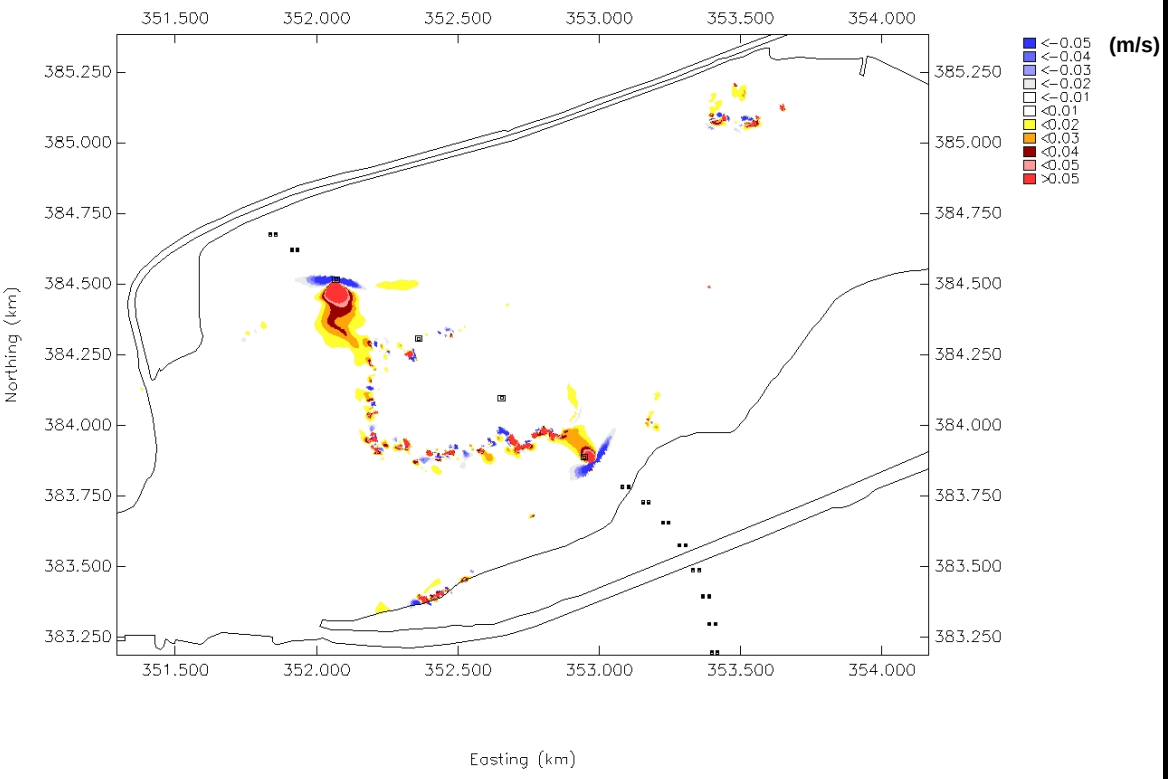
Differences in water level (m) between the proposed bridge scheme Route 3A Medium modified and the baseline case for high water (A) and peak ebb (B) on a 1:200 surge tide and 1:200 fluvial event.

Figure C32

A.

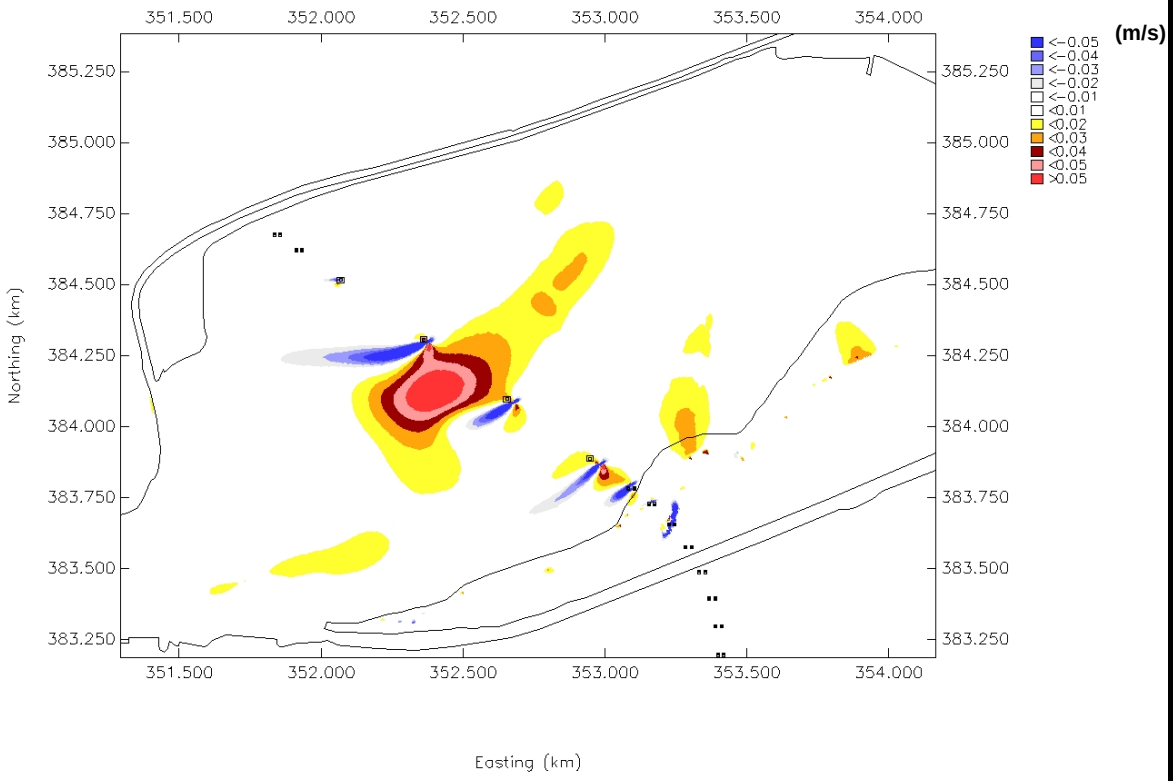


B.

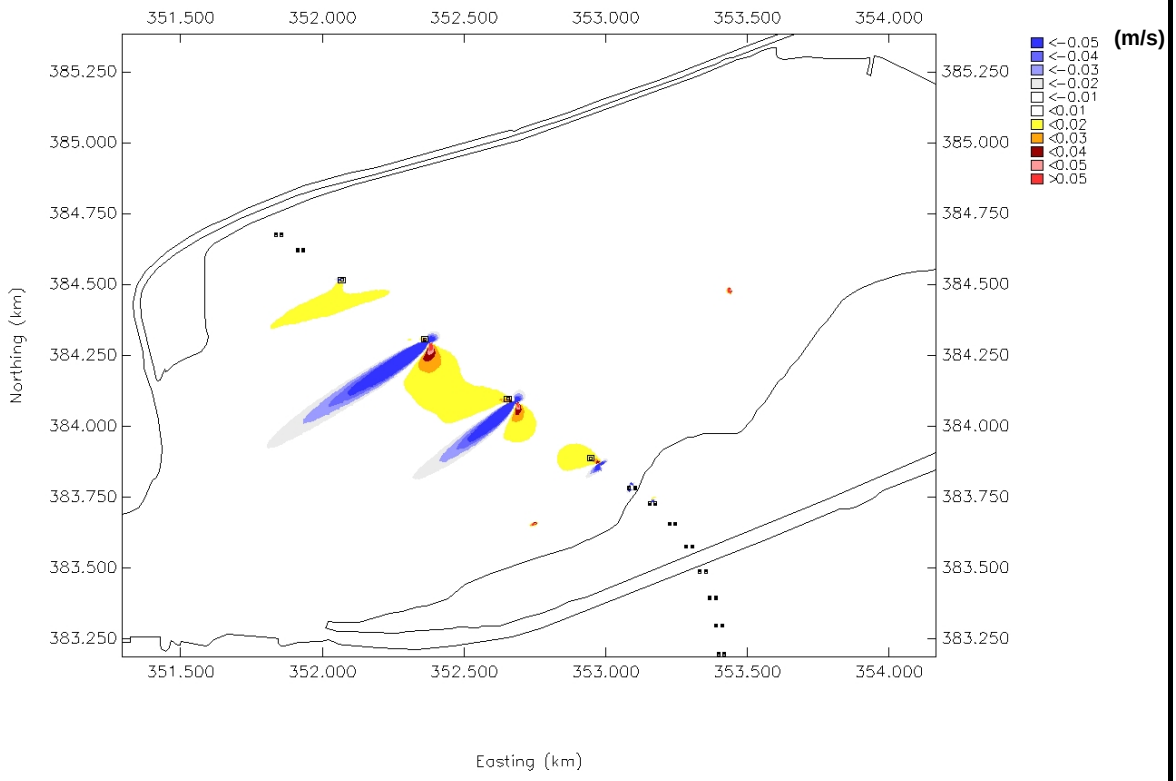


ABP mer marine environmental research	Differences in near-surface speed (m/s) between the proposed bridge scheme Route 3A Medium modified and the baseline case for low water (A) and peak flood (B) on a 1:200 surge tide and 1:200 fluvial event.	Figure C33

A.



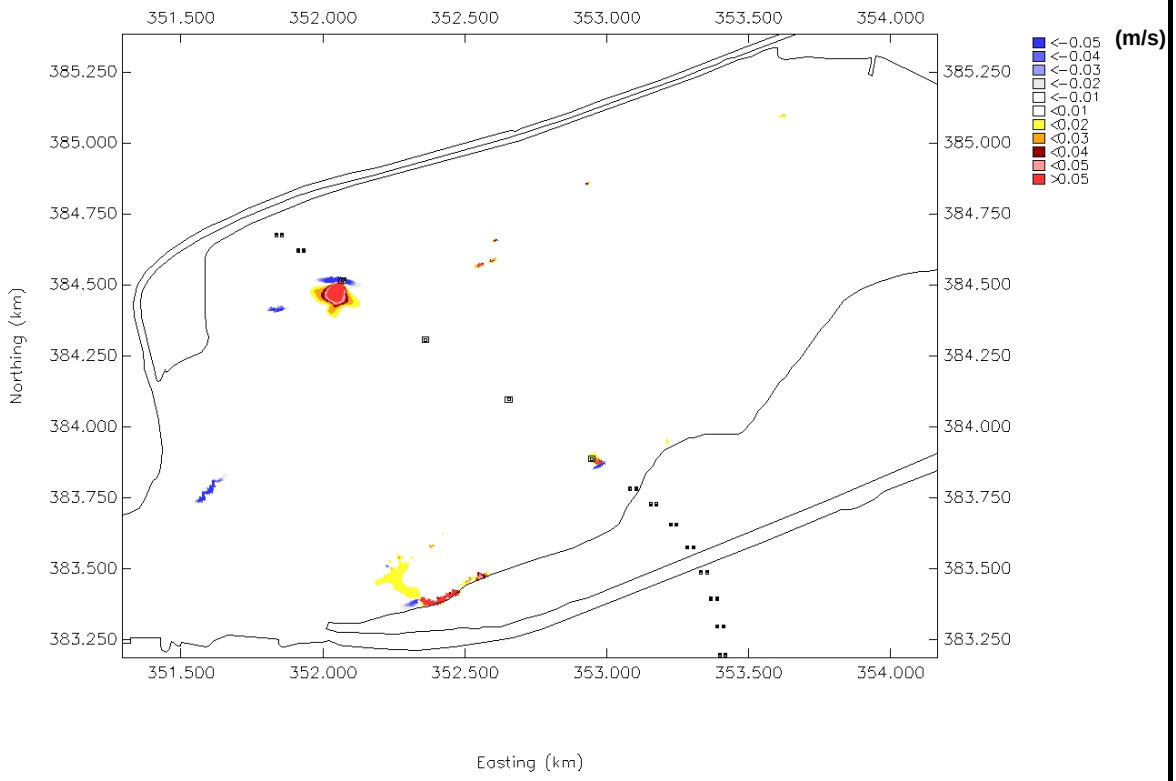
B.



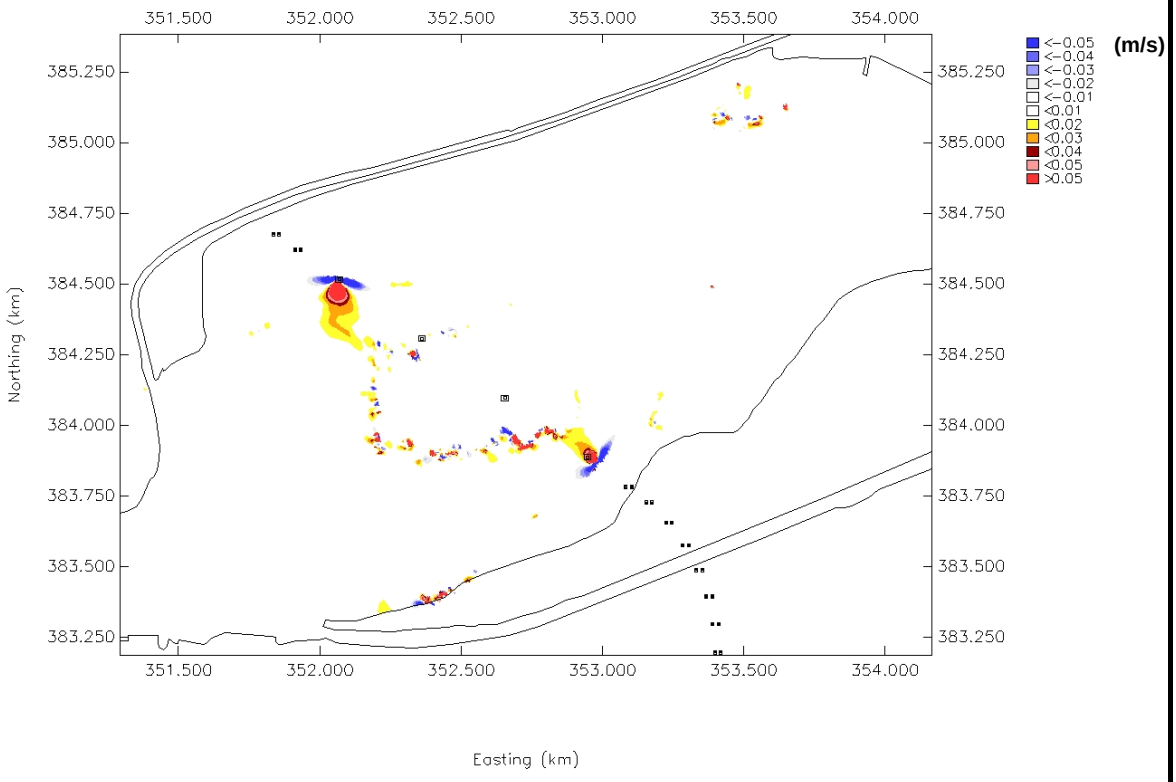
Differences in near-surface speed (m/s) between the proposed bridge scheme Route 3A Medium modified and the baseline case for high water (A) and peak ebb (B) on a 1:200 surge tide and 1:200 fluvial event.

Figure C34

A.

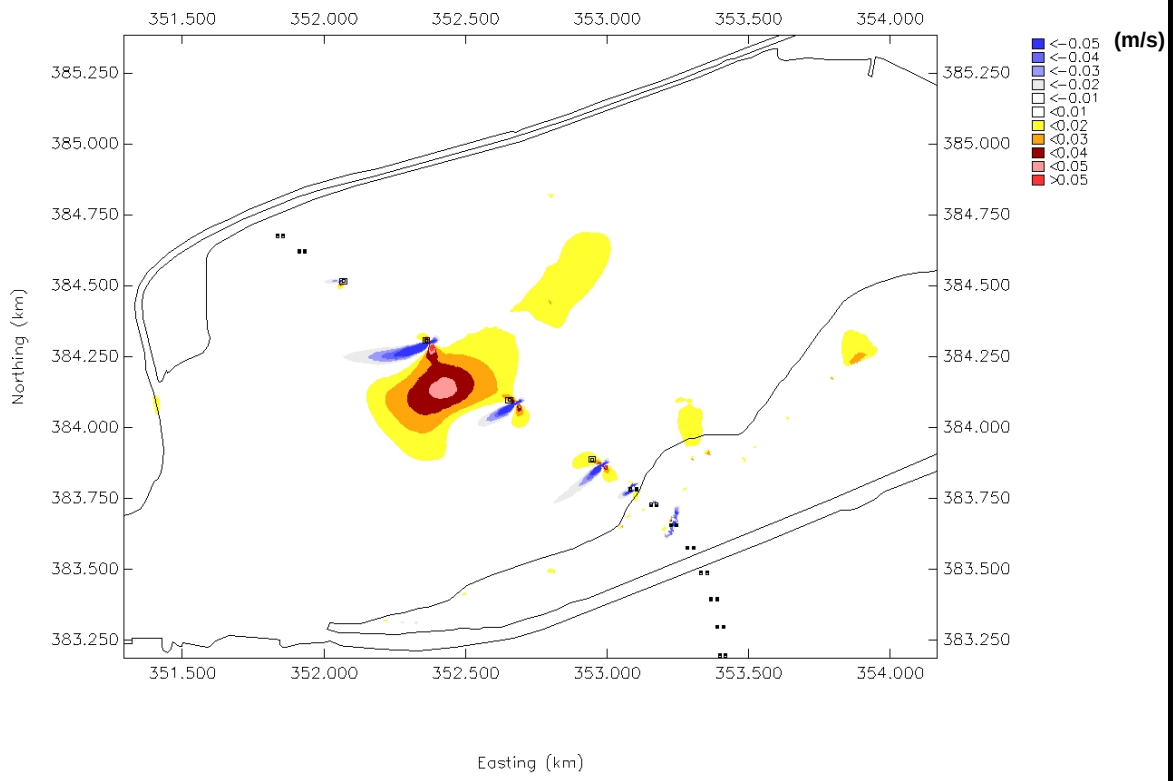


B.

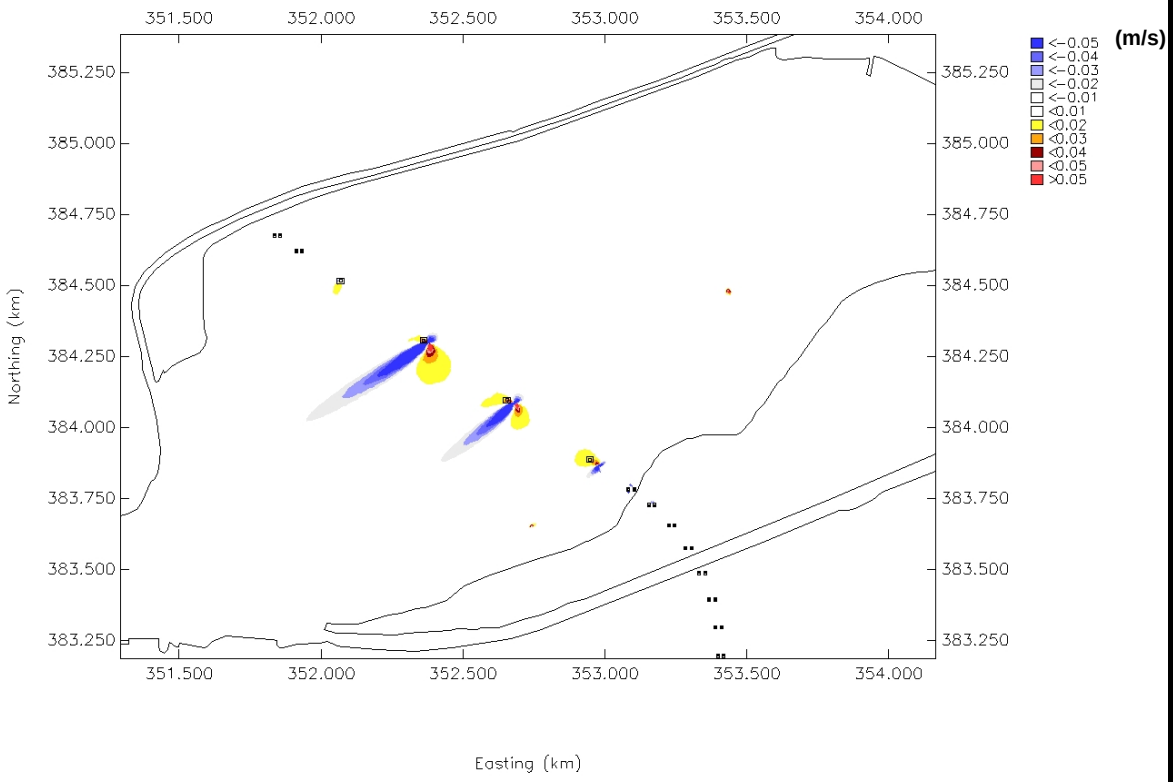


ABP mer marine environmental research	Differences in near-bed speed (m/s) between the proposed bridge scheme Route 3A Medium modified and the baseline case for low water (A) and peak flood (B) on a 1:200 surge tide and 1:200 fluvial event.	Figure C35

A.

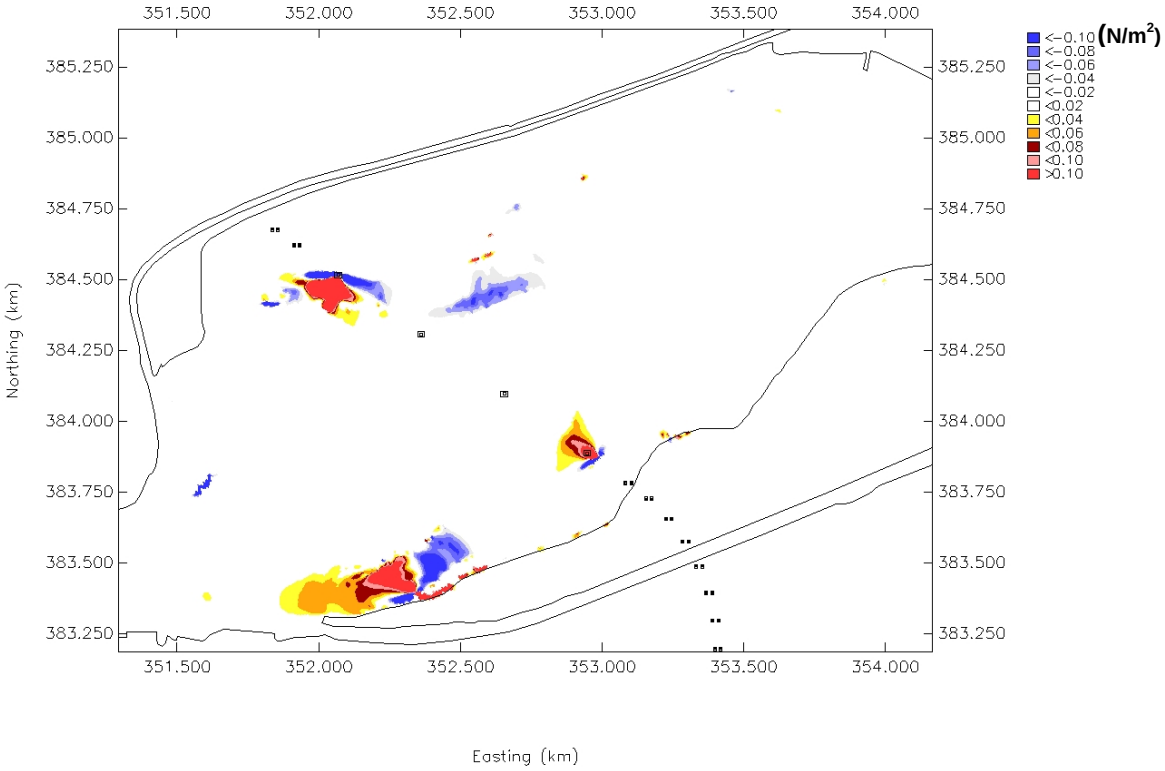


B.

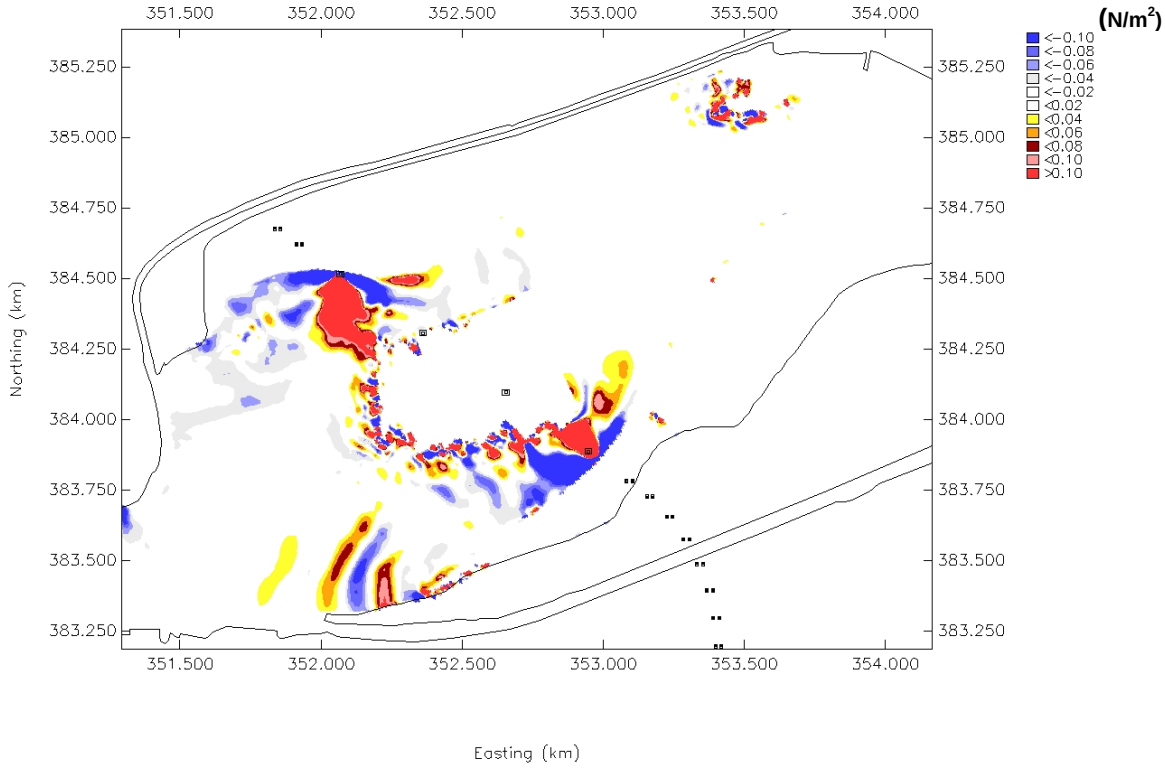


ABP mer marine environmental research	Differences in near-bed speed (m/s) between the proposed bridge scheme Route 3A Medium modified and the baseline case for high water (A) and peak ebb (B) on a 1:200 surge tide and 1:200 fluvial event.	Figure C36

A.



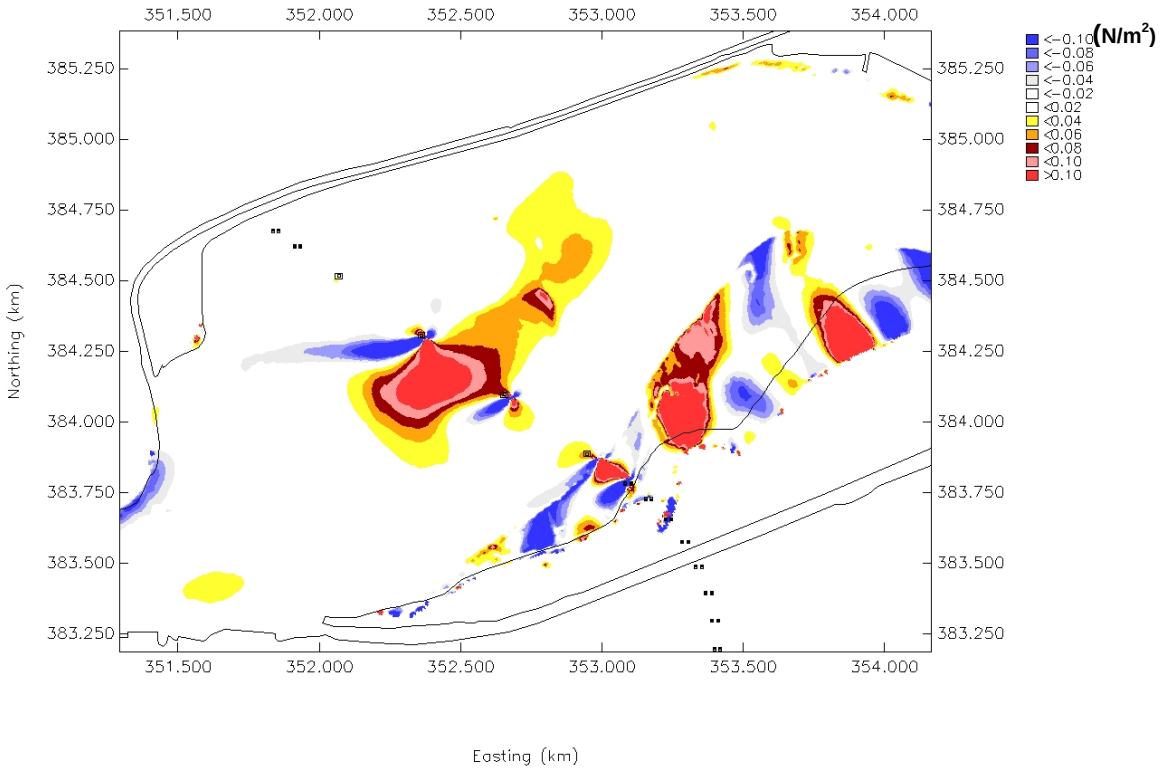
B.



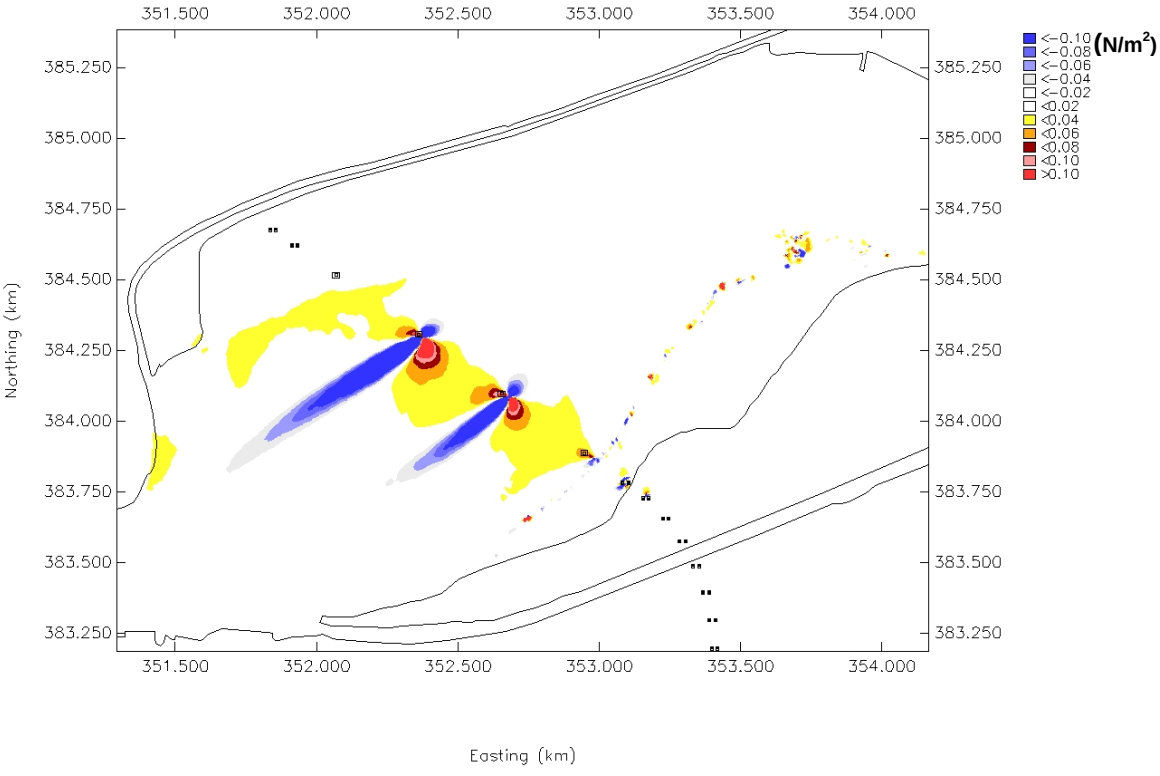
Differences in bed shear stress (N/m²) between the proposed bridge scheme Route 3A Medium modified and the baseline case for low water (A) and peak flood (B) on a 1:200 surge tide and 1:200 fluvial event.

Figure C37

A.



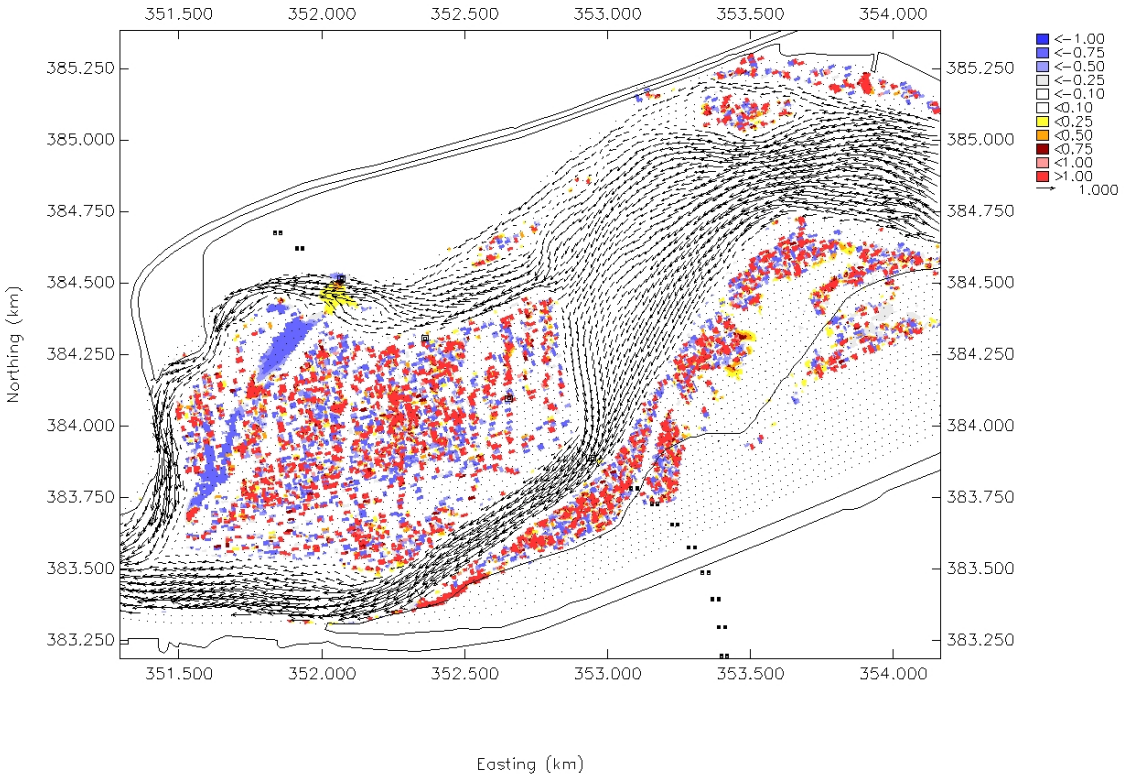
B.



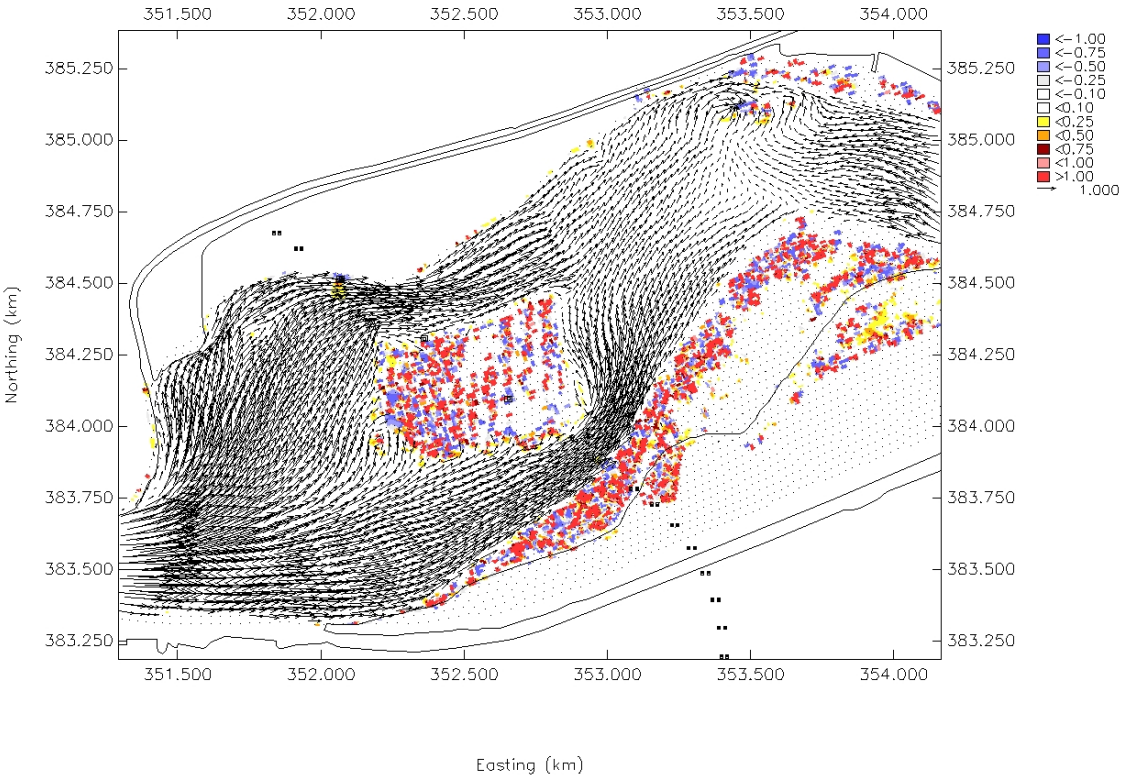
Differences in bed shear stress (N/m²) between the proposed bridge scheme Route 3A Medium modified and the baseline case for high water (A) and peak ebb (B) on a 1:200 surge tide and 1:200 fluvial event.

Figure C38

A.

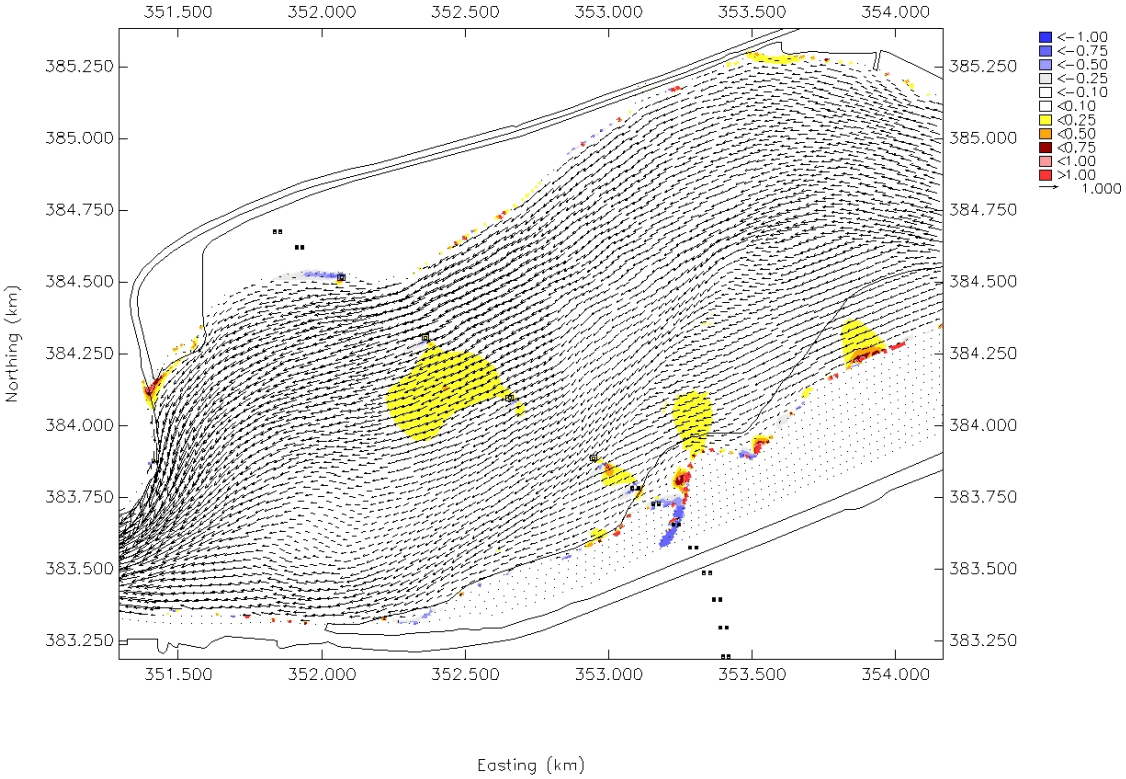


B.

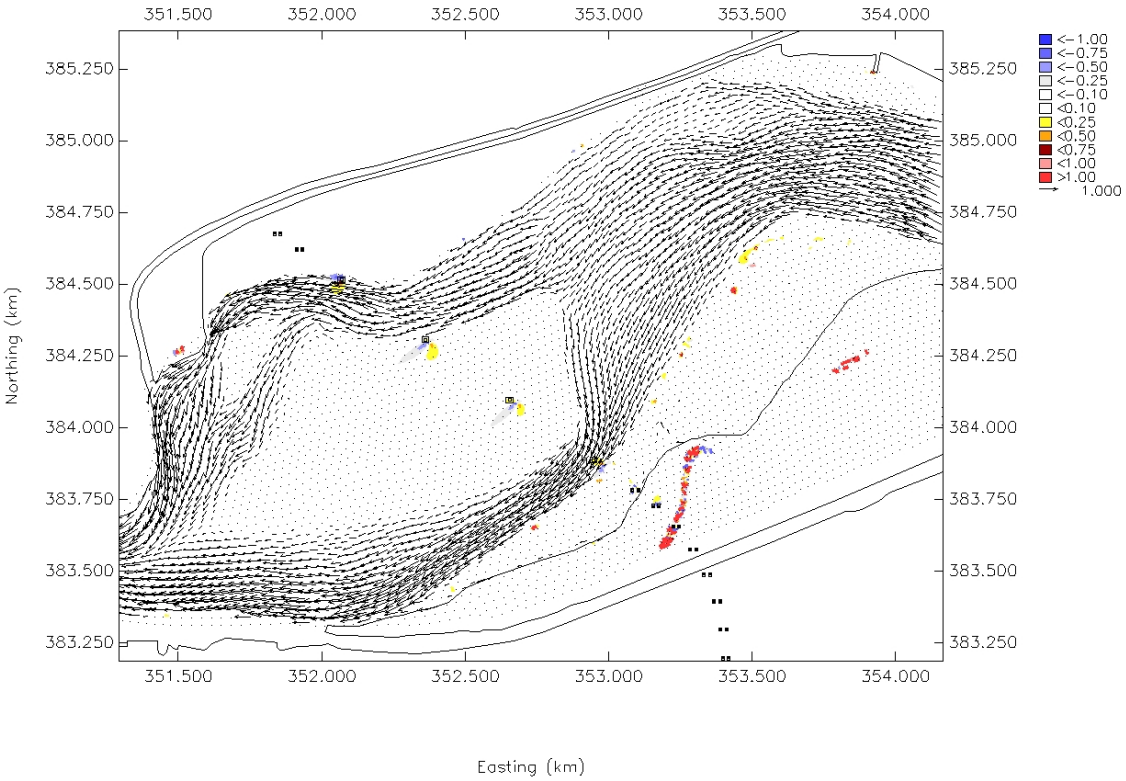


ABP mer marine environmental research	Percentage differences in bed shear stress between the proposed bridge scheme Route 3A Medium modified and the baseline case for low water (A) and peak flood (B) on a 1:200 surge tide and 1:200 fluvial event. (1 = 100% ; 0.1 = 10%).	Figure C39

A.

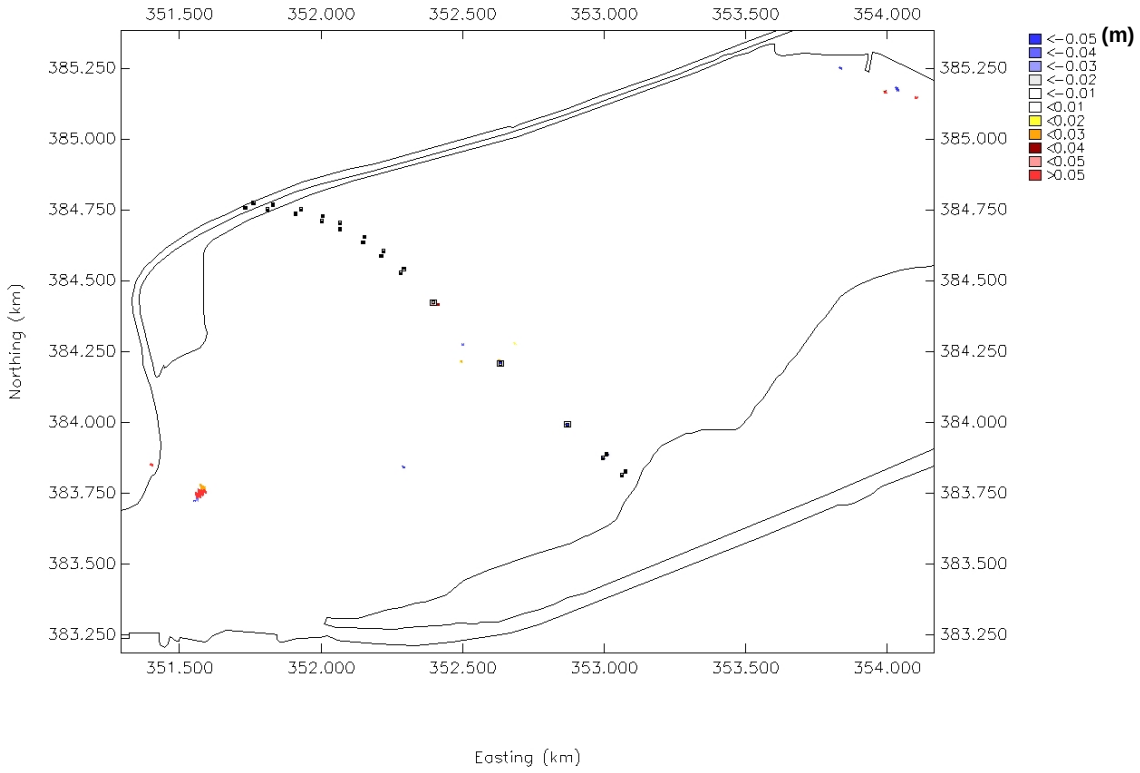


B.

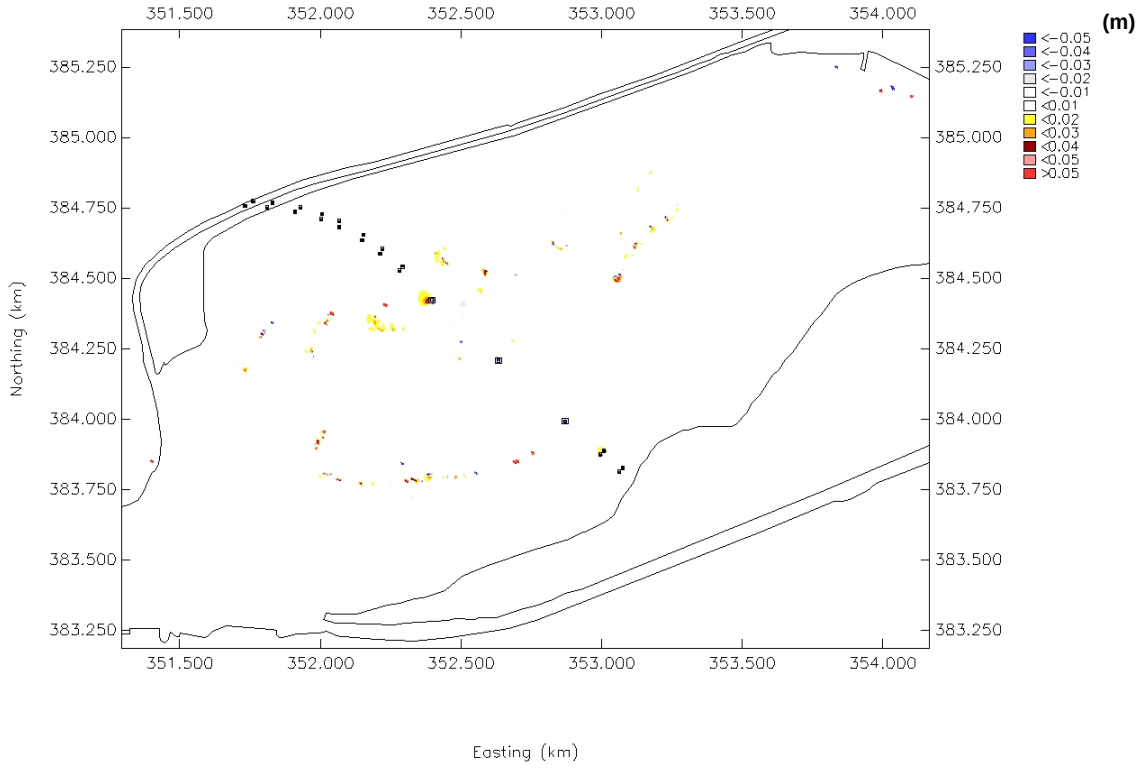


ABP mer marine environmental research	Percentage differences in bed shear stress between the proposed bridge scheme Route 3A Medium modified and the baseline case for high water (A) and peak ebb (B) on a 1:200 surge tide and 1:200 fluvial event. (1 = 100% ; 0.1 = 10%).	Figure C40

A.

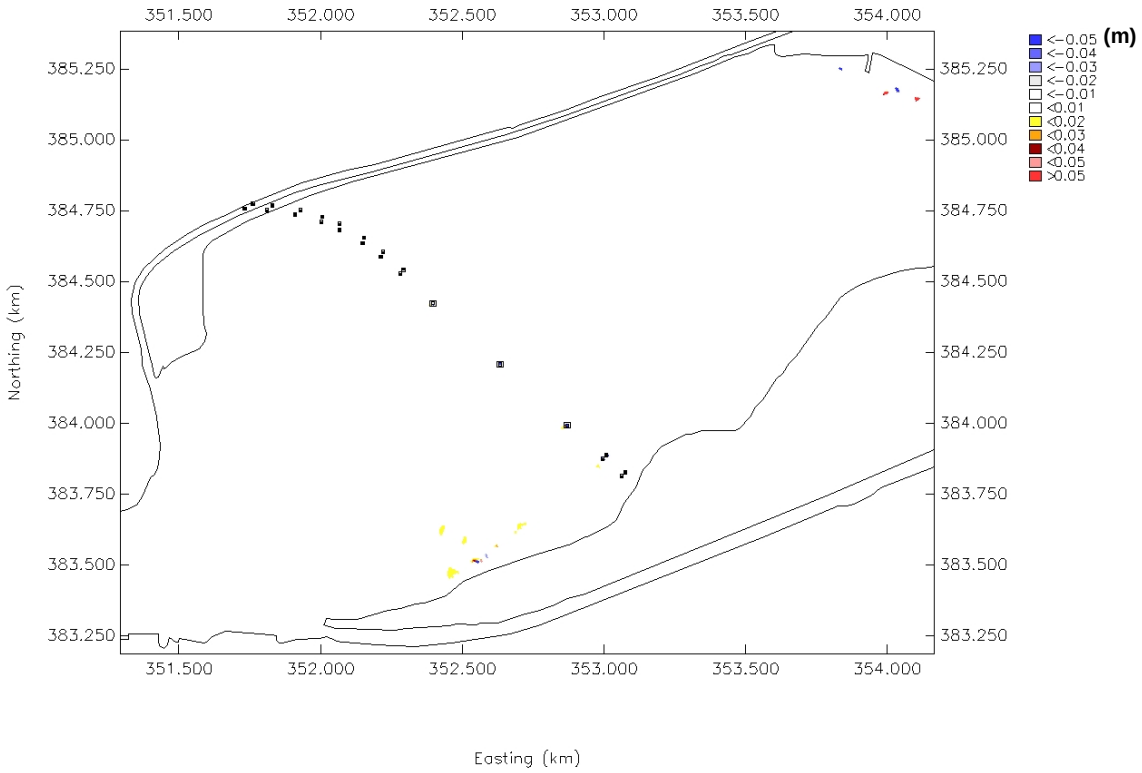


B.

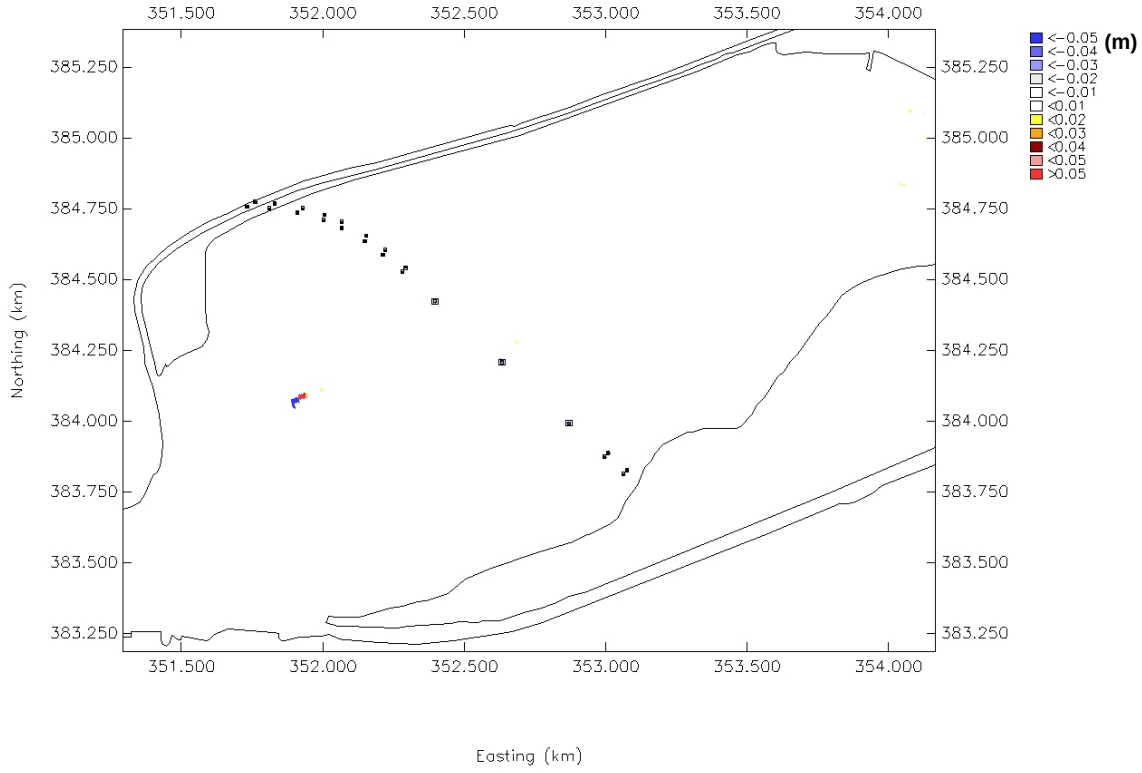


ABP mer marine environmental research	Differences in water level (m) between the proposed bridge scheme Route 3A Medium 3 Tower option and the baseline case for low water (A) and peak flood (B) on a spring tide.	Figure C41

A.

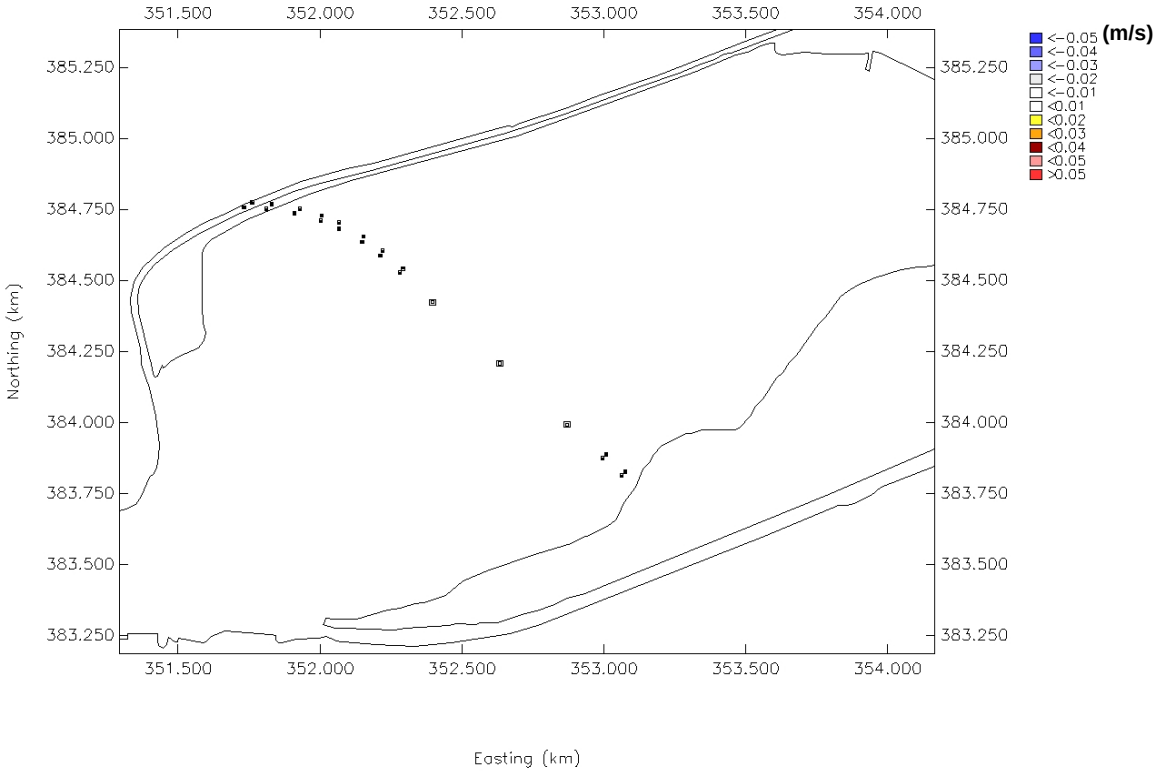


B.

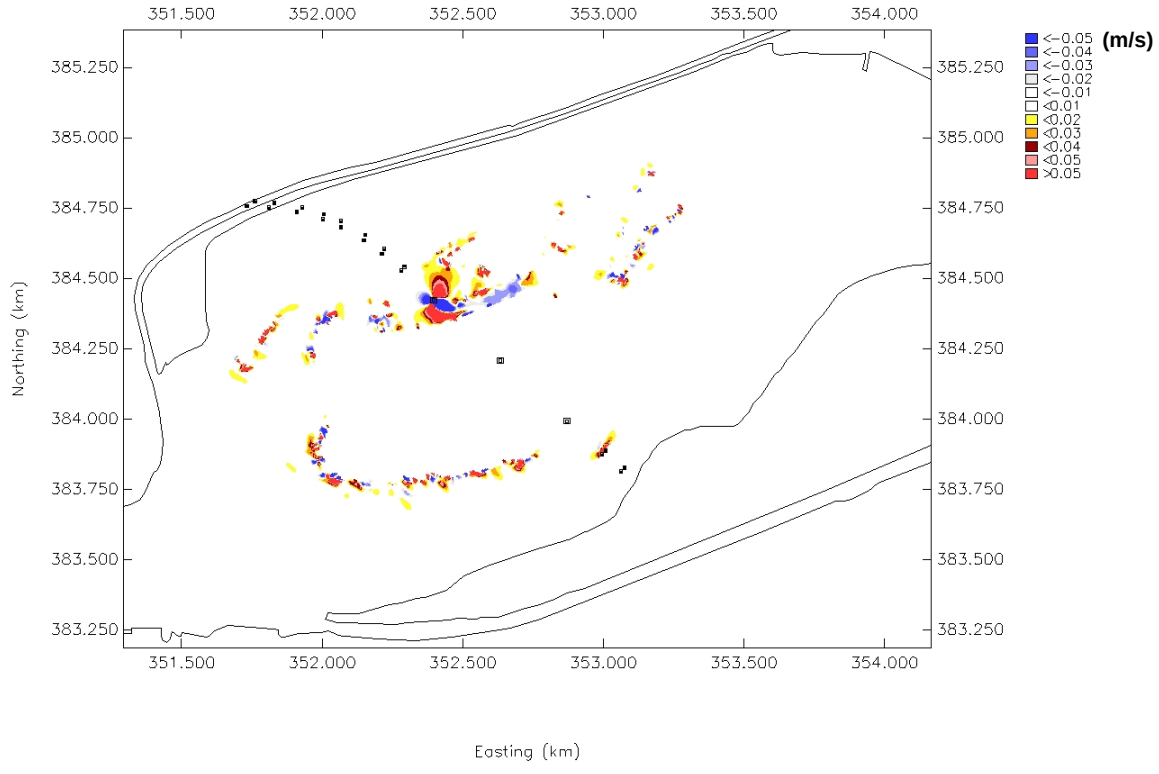


ABP mer marine environmental research	Differences in water level (m) between the proposed bridge scheme Route 3A Medium 3 Tower option and the baseline case for high water (A) and peak ebb (B) on a spring tide.	Figure C42

A.

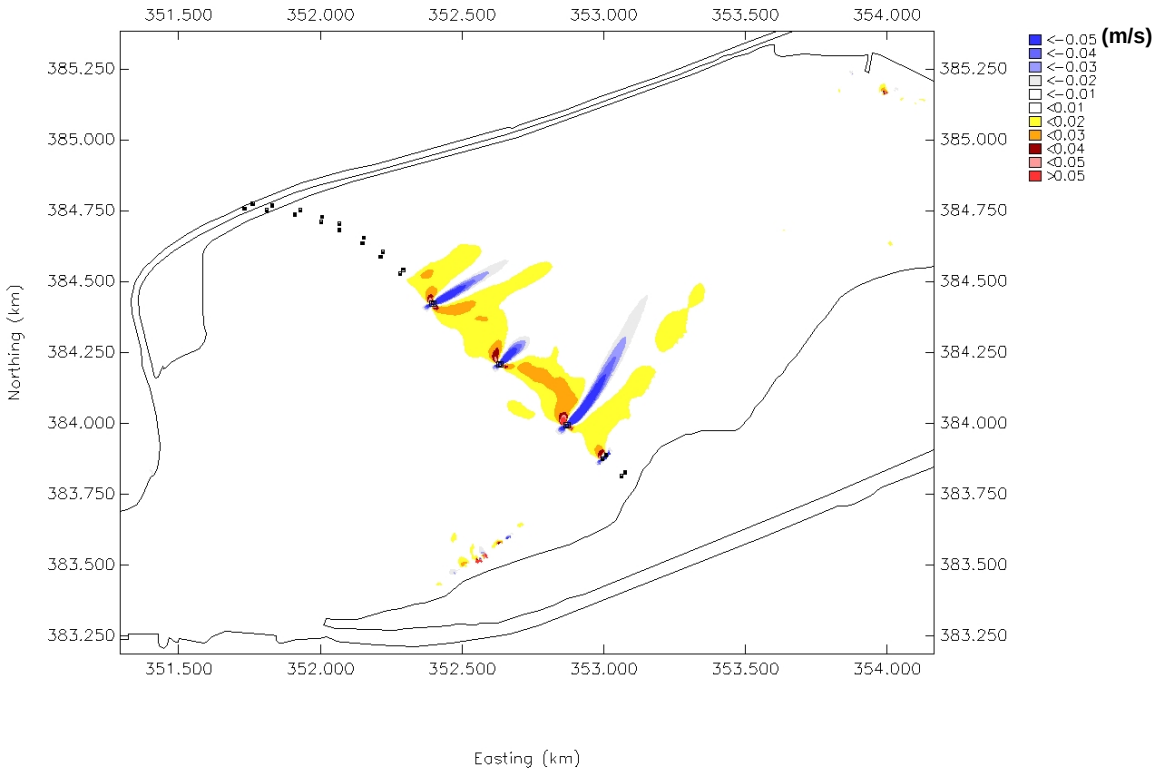


B.

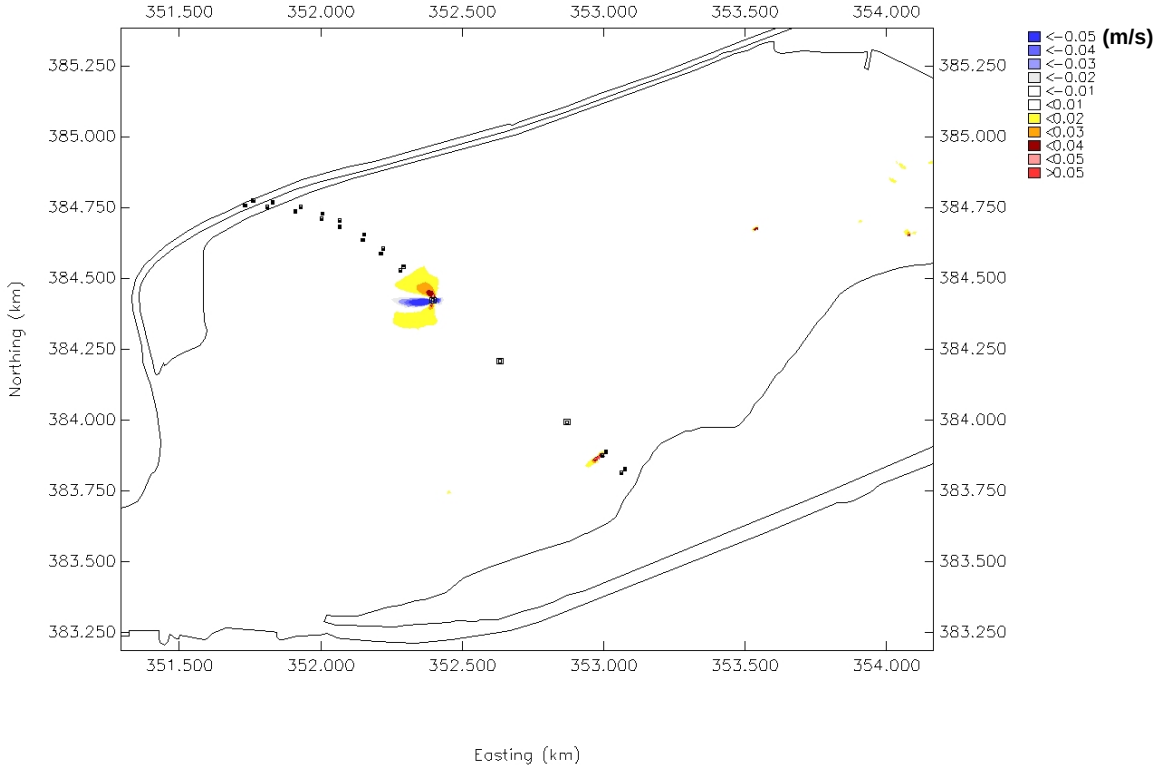


ABP mer marine environmental research	Differences in near-surface speed (m/s) between the proposed bridge scheme Route 3A Medium 3 Tower option and the baseline case for low water (A) and peak flood (B) on a spring tide.	Figure C43

A.

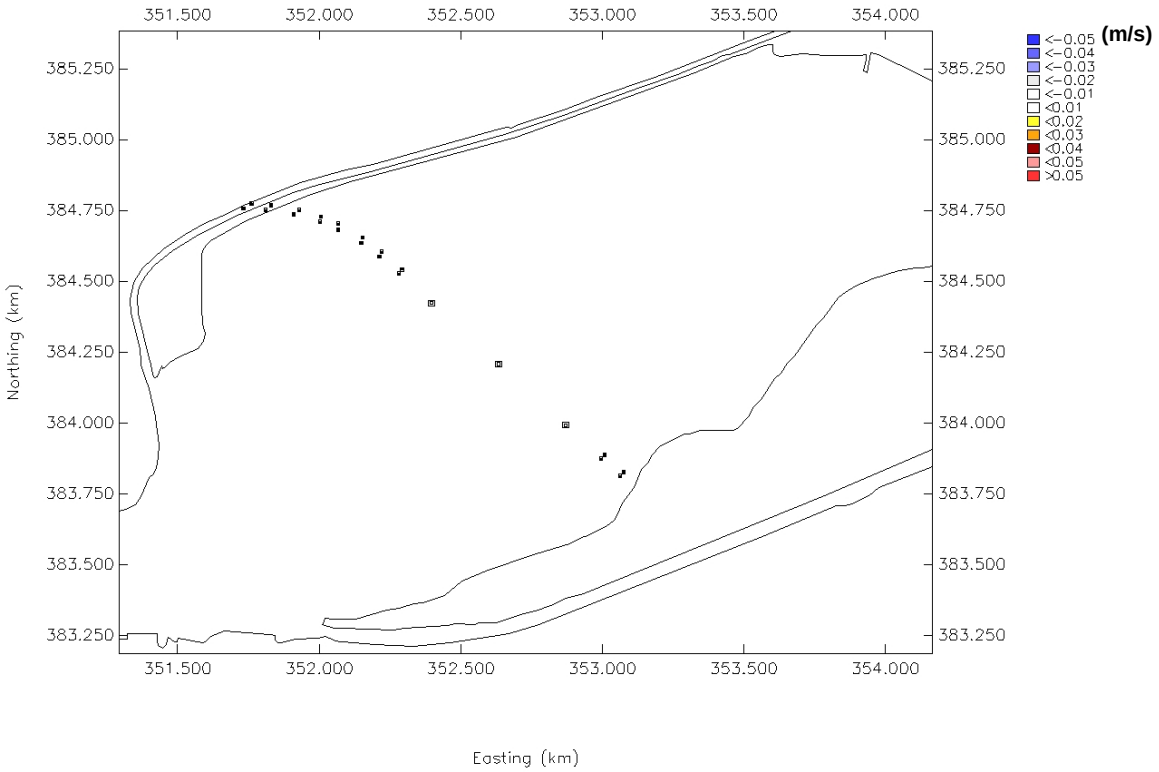


B.

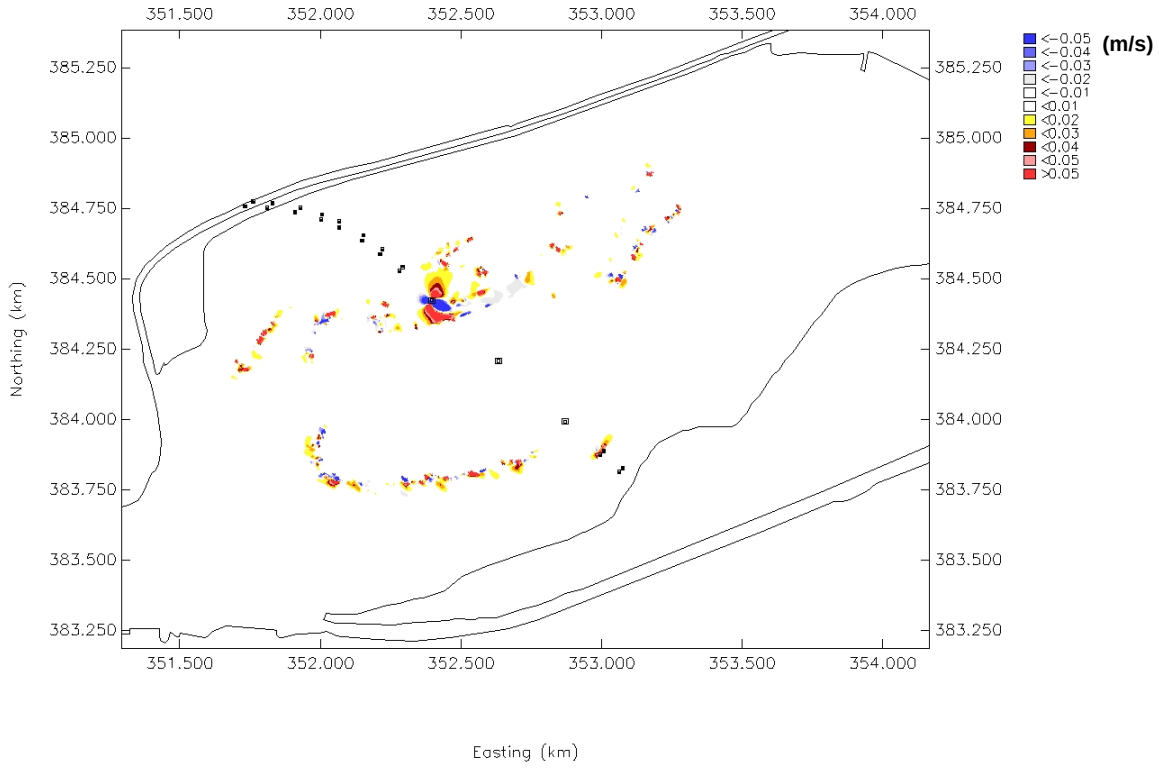


ABP mer marine environmental research	Differences in near-surface speed (m/s) between the proposed bridge scheme Route 3A Medium 3 Tower option and the baseline case for high water (A) and peak ebb (B) on a spring tide.	Figure C44

A.

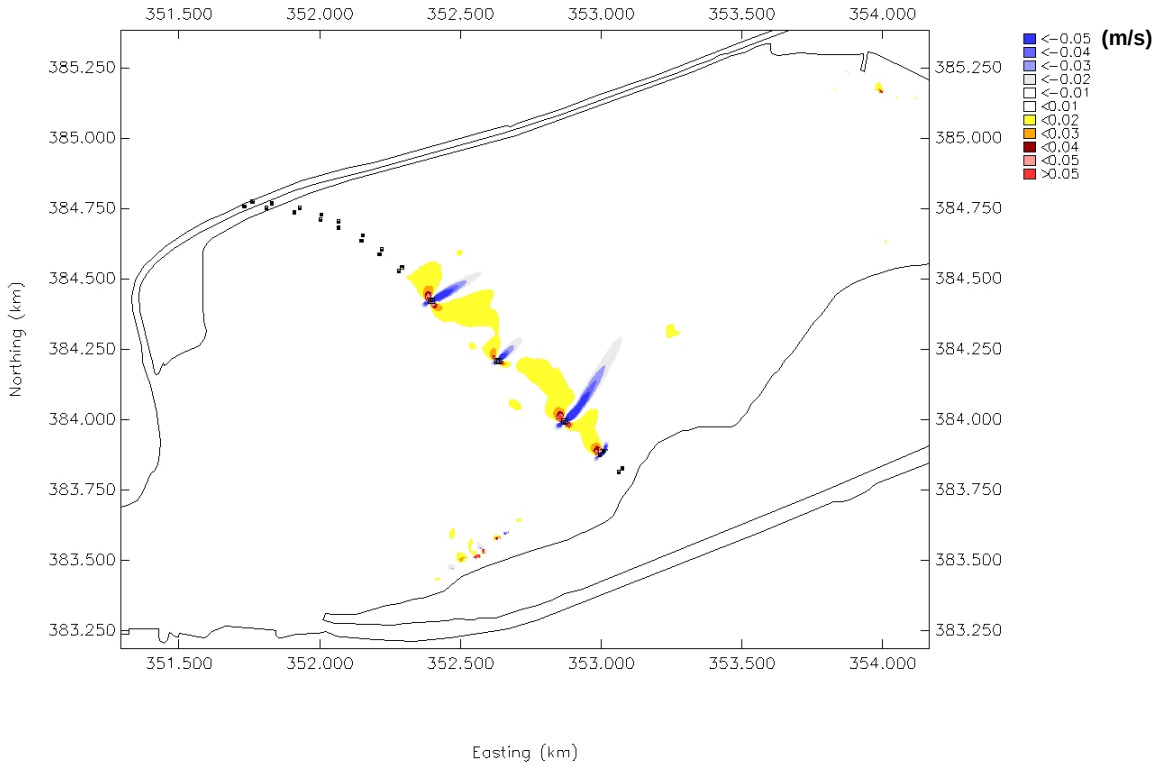


B.

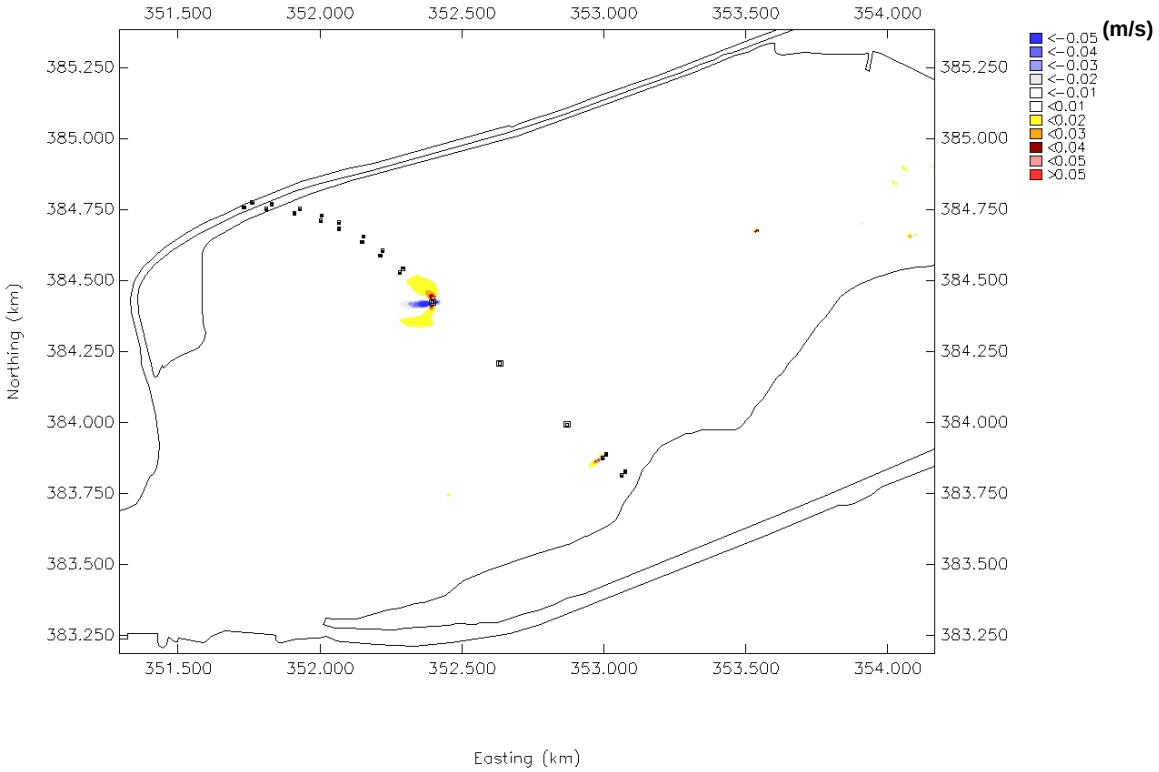


ABP mer marine environmental research	Differences in near-bed speed (m/s) between the proposed bridge scheme Route 3A Medium 3 Tower option and the baseline case for low water (A) and peak flood (B) on a spring tide.	Figure C45

A.

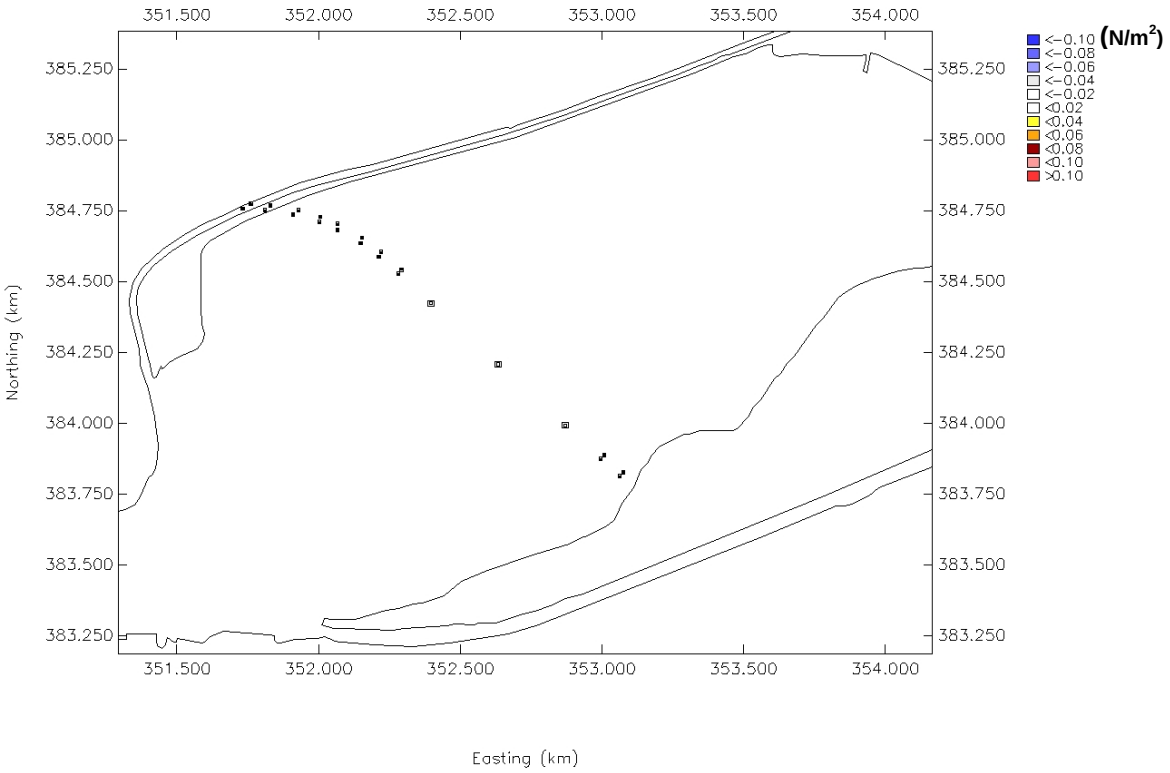


B.

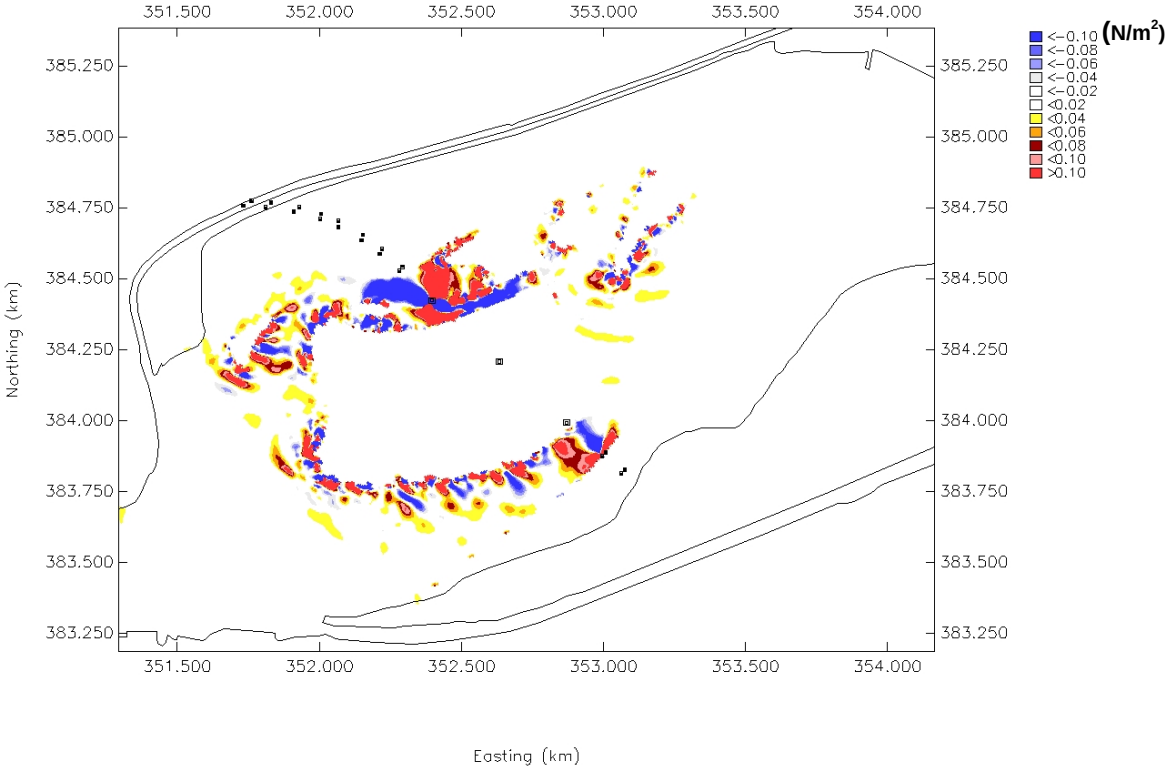


ABP mer marine environmental research	Differences in near-bed speed (m/s) between the proposed bridge scheme Route 3A Medium 3 Tower option and the baseline case for high water (A) and peak ebb (B) on a spring tide.	Figure C46

A.

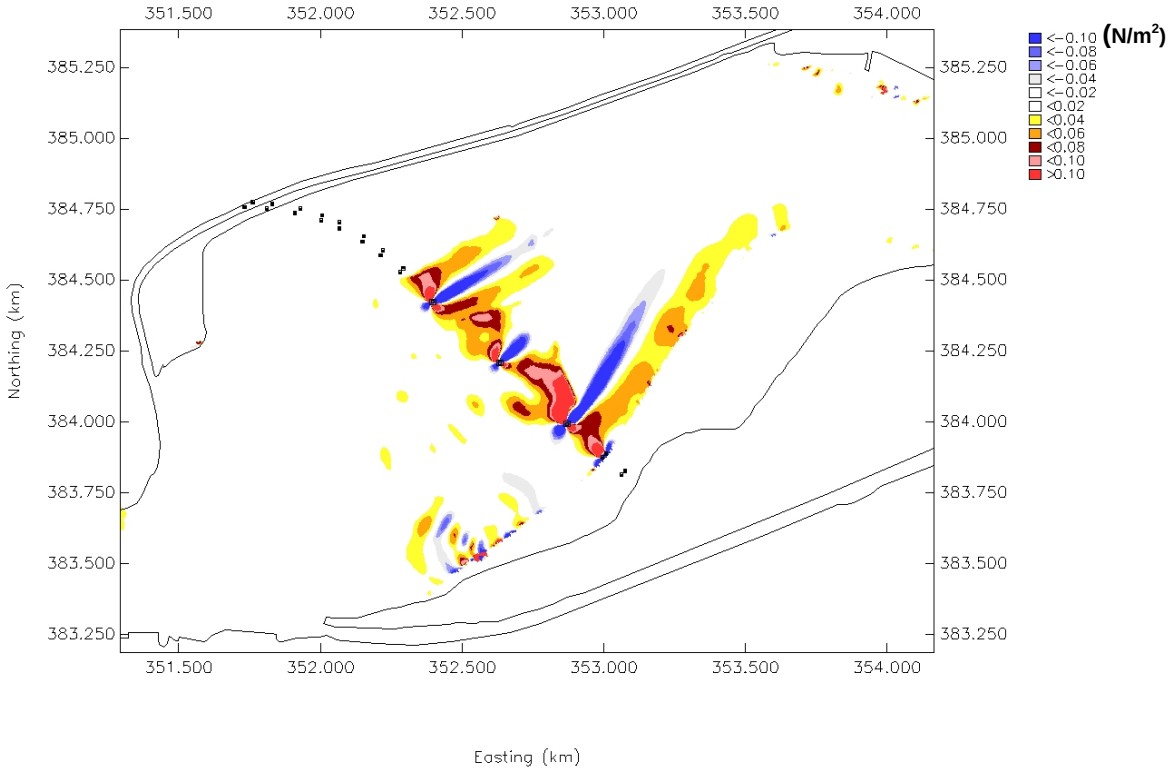


B.

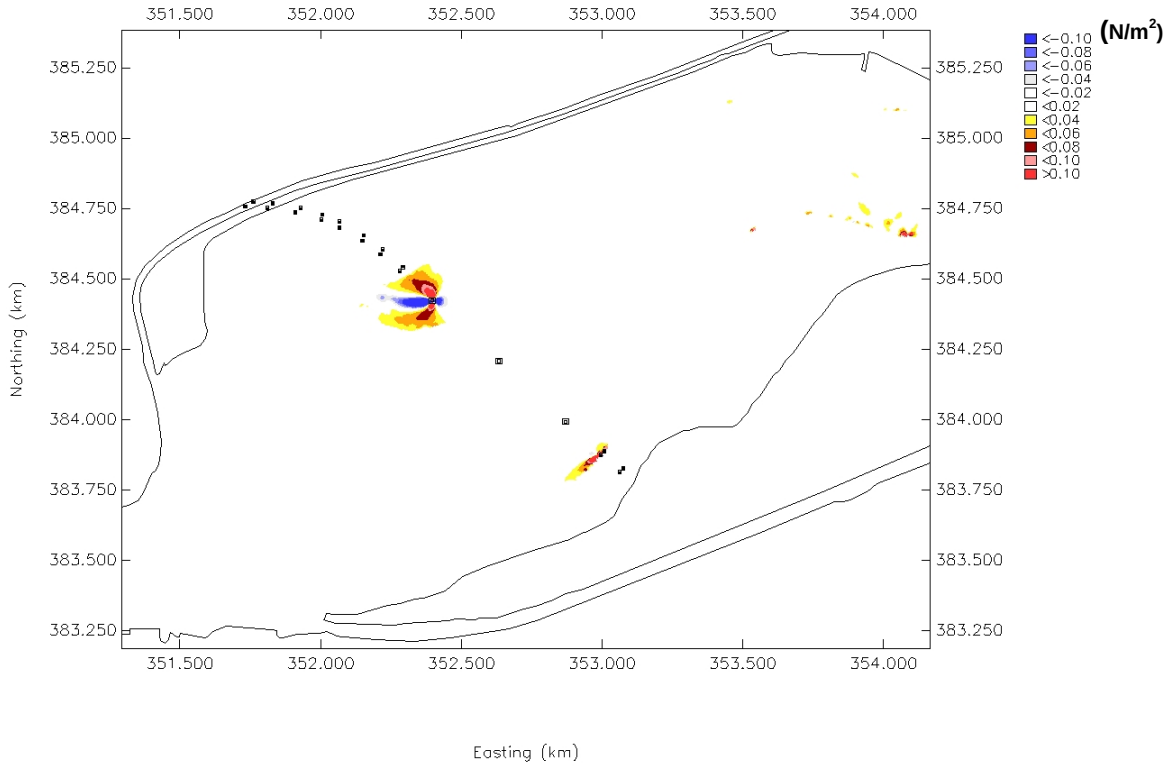


ABP mer marine environmental research	Differences in bed shear stress (N/m²) between the proposed bridge scheme Route 3A Medium 3 Tower option and the baseline case for low water (A) and peak flood (B) on a spring tide.	Figure C47

A.

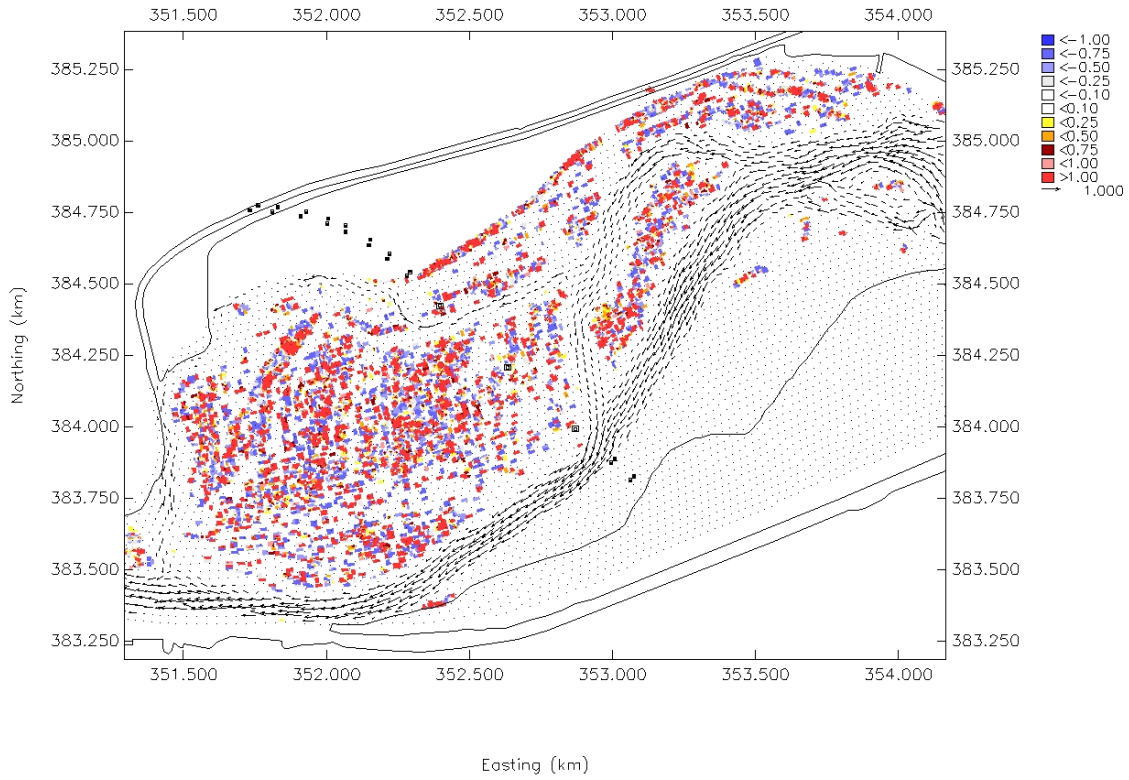


B.

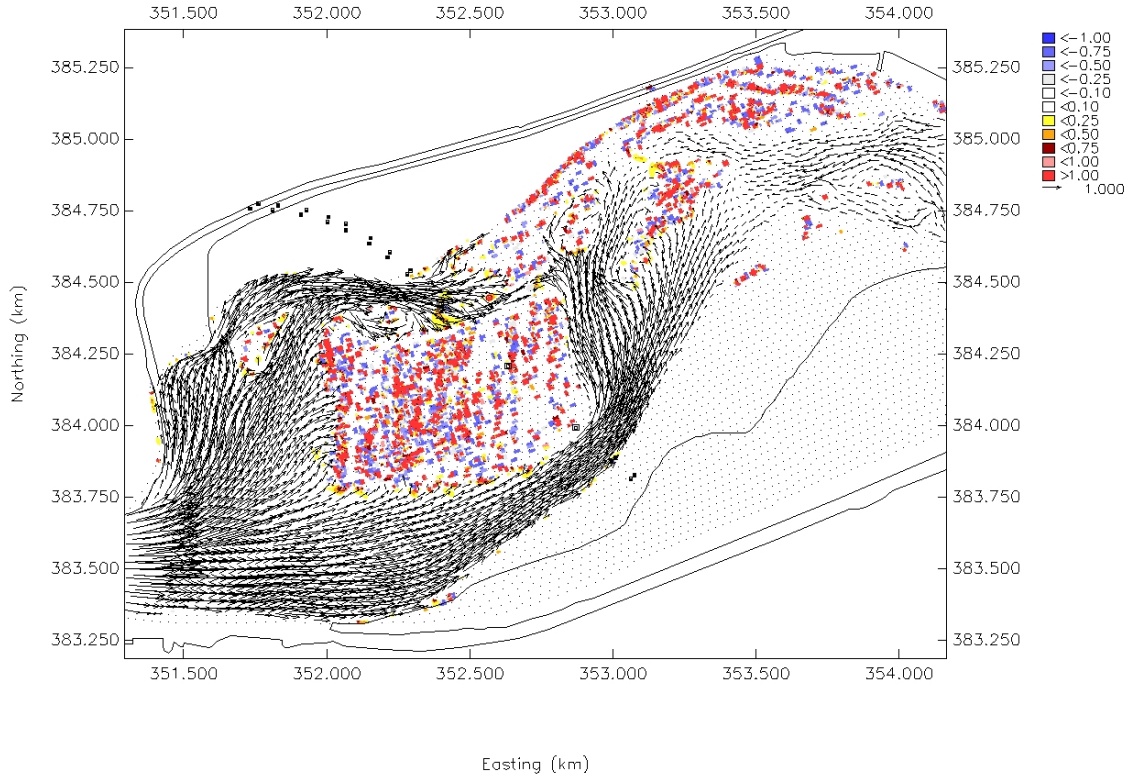


ABP mer marine environmental research	Differences in bed shear stress (N/m²) between the proposed bridge scheme Route 3A Medium 3 Tower option and the baseline case for high water (A) and peak ebb (B) on a spring tide.	Figure C48

A.

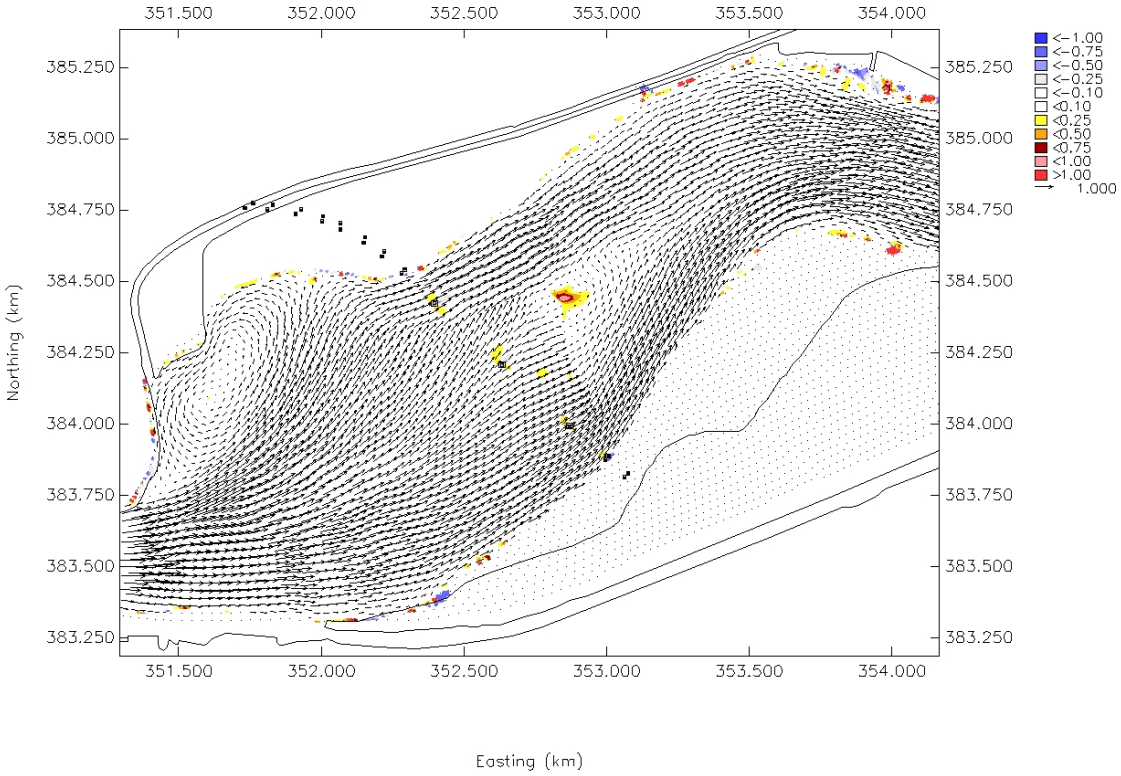


B.

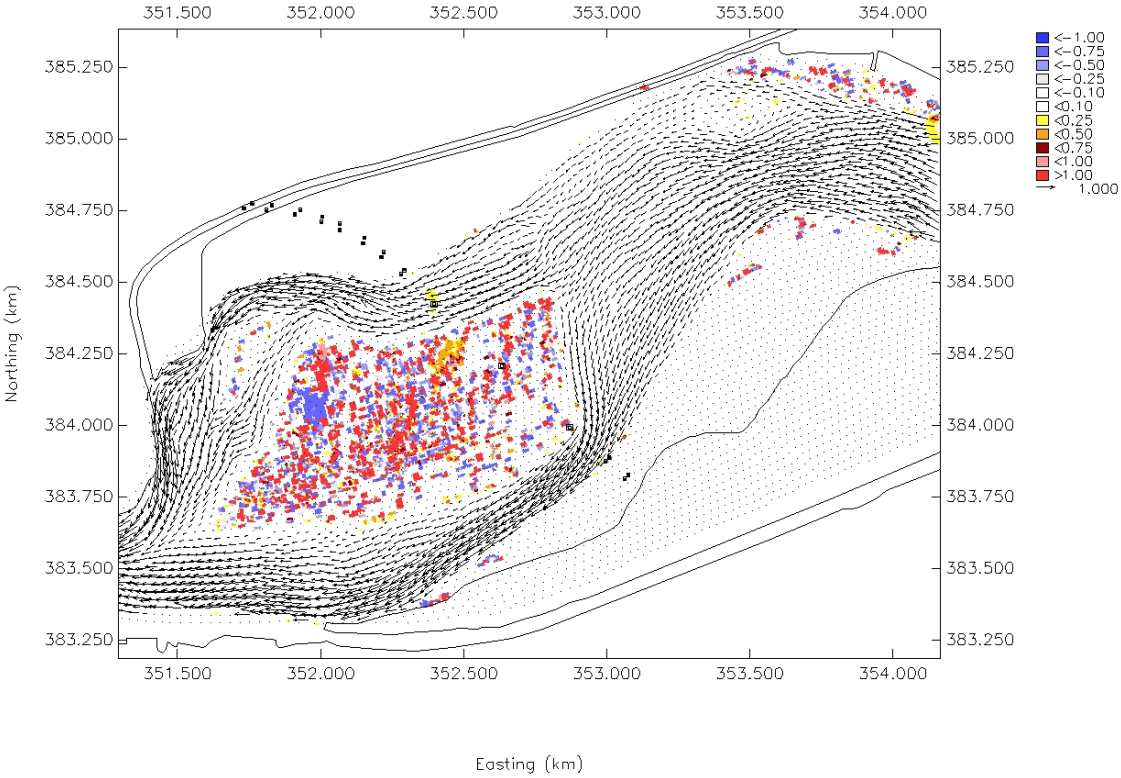


ABP mer marine environmental research	Percentage differences in bed shear stress between the proposed bridge scheme Route 3A Medium 3 Tower option and the baseline case for low water (A) and peak flood (B) on a spring tide. (1 = 100% ; 0.1 = 10%).	Figure C49

A.

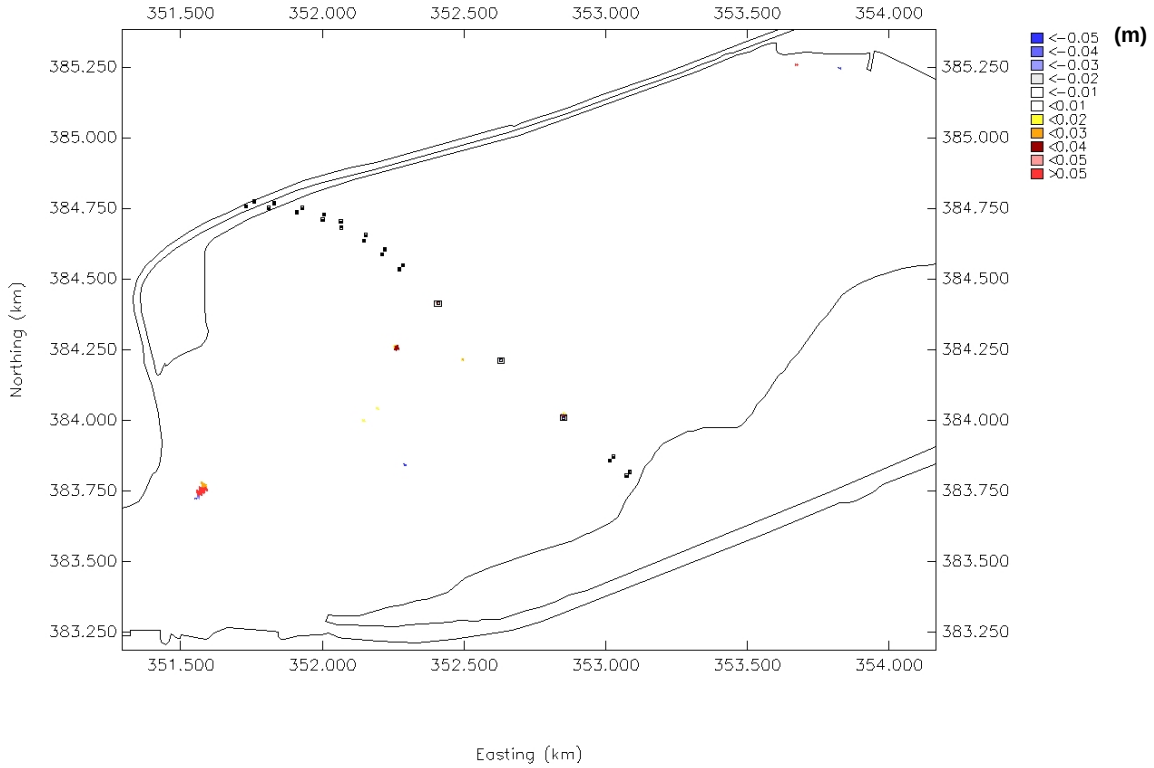


B.

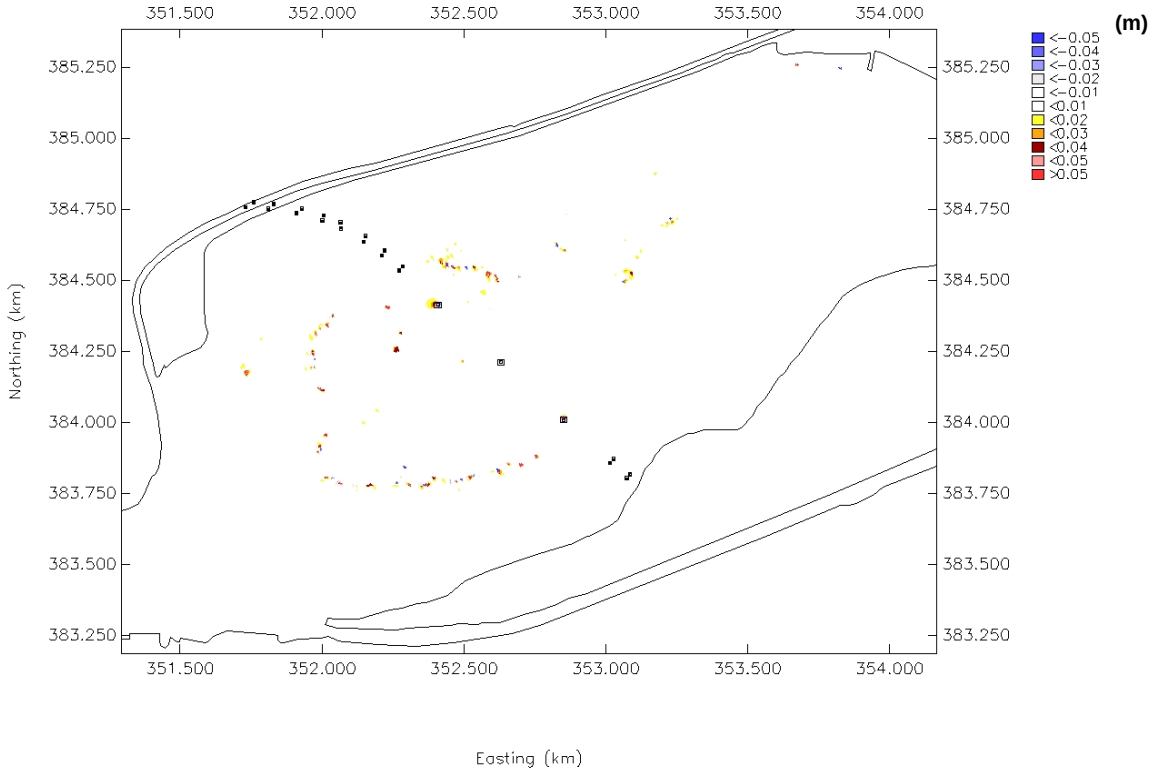


ABP mer marine environmental research	Percentage differences in bed shear stress between the proposed bridge scheme Route 3A Medium 3 Tower option and the baseline case for high water (A) and peak ebb (B) on a spring tide. (1 = 100% ; 0.1 = 10%).	Figure C50

A.

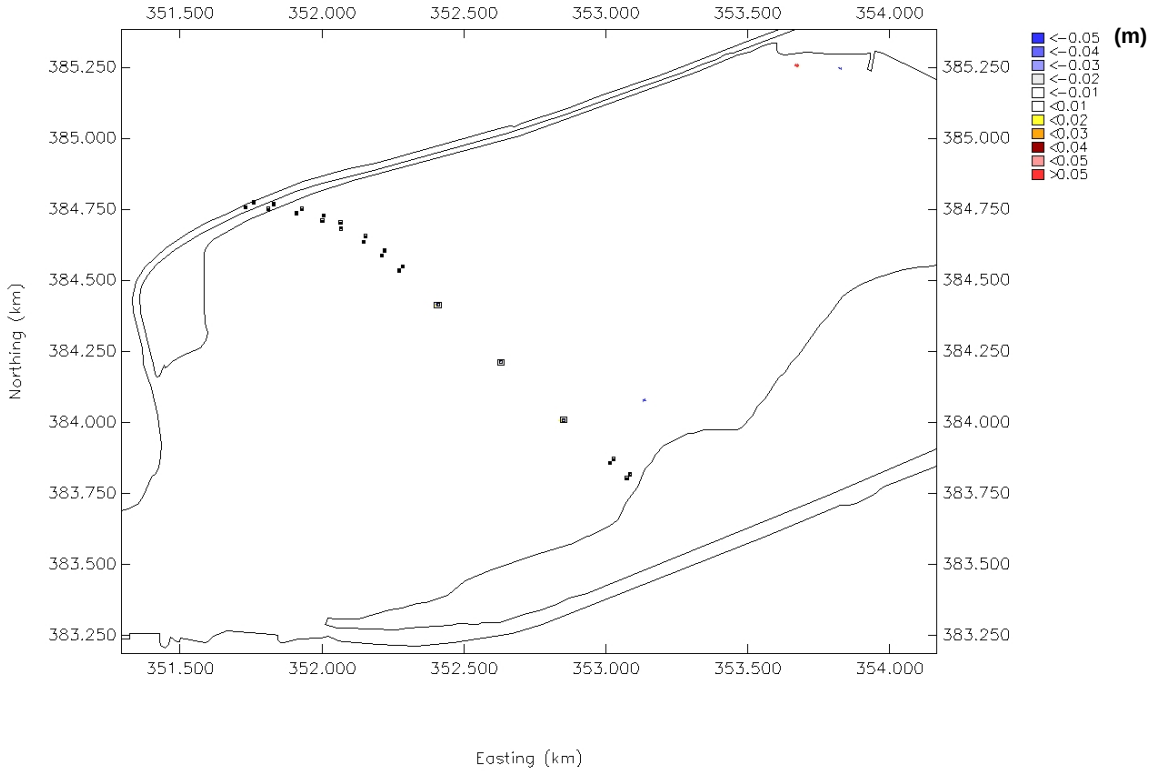


B.

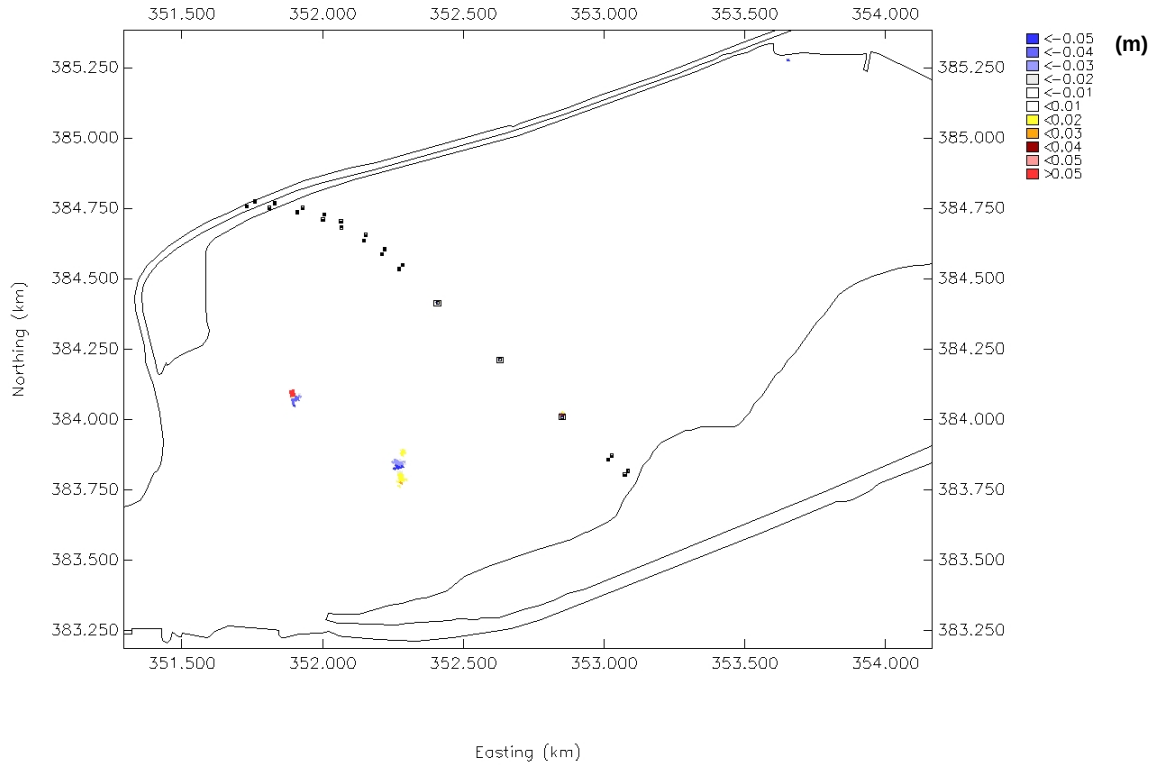


ABP mer marine environmental research	Differences in water level (m) between the proposed bridge scheme Route 3A Medium 3 Tower revised option and the baseline case for low water (A) and peak flood (B) on a spring tide.	Figure C51

A.



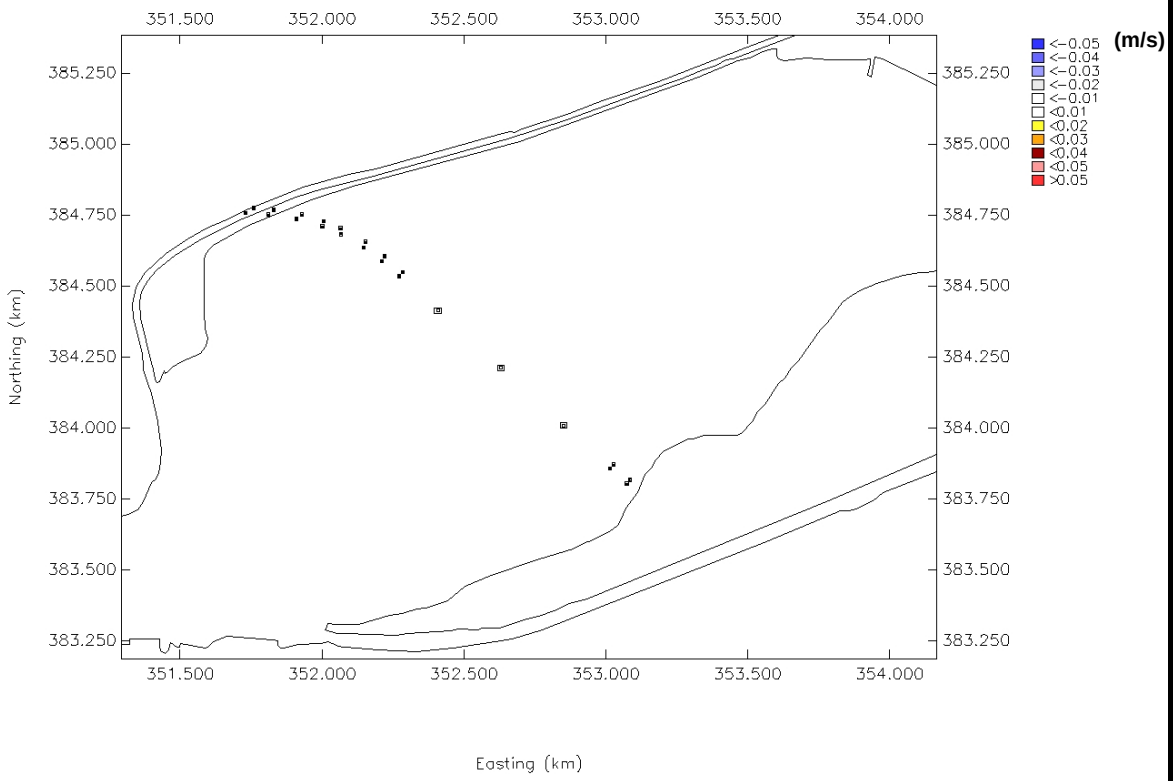
B.



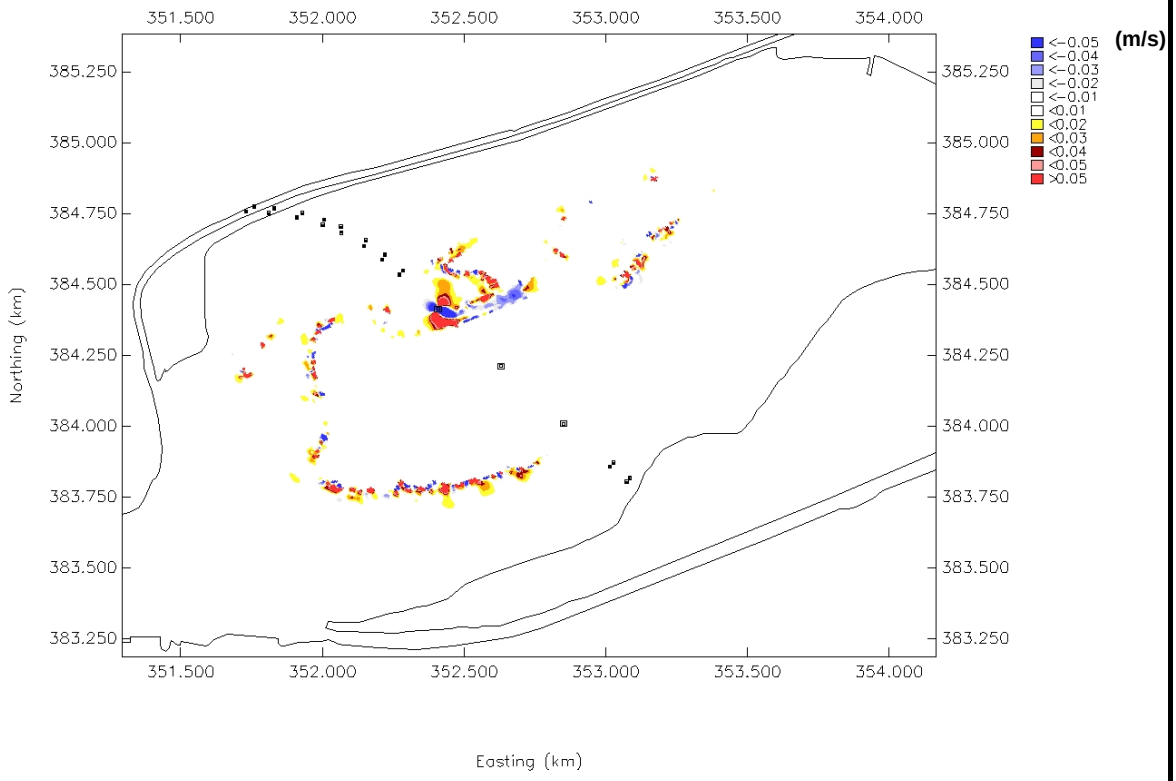
Differences in water level (m) between the proposed bridge scheme Route 3A Medium 3 Tower revised option and the baseline case for high water (A) and peak ebb (B) on a spring tide.

Figure C52

A.



B.

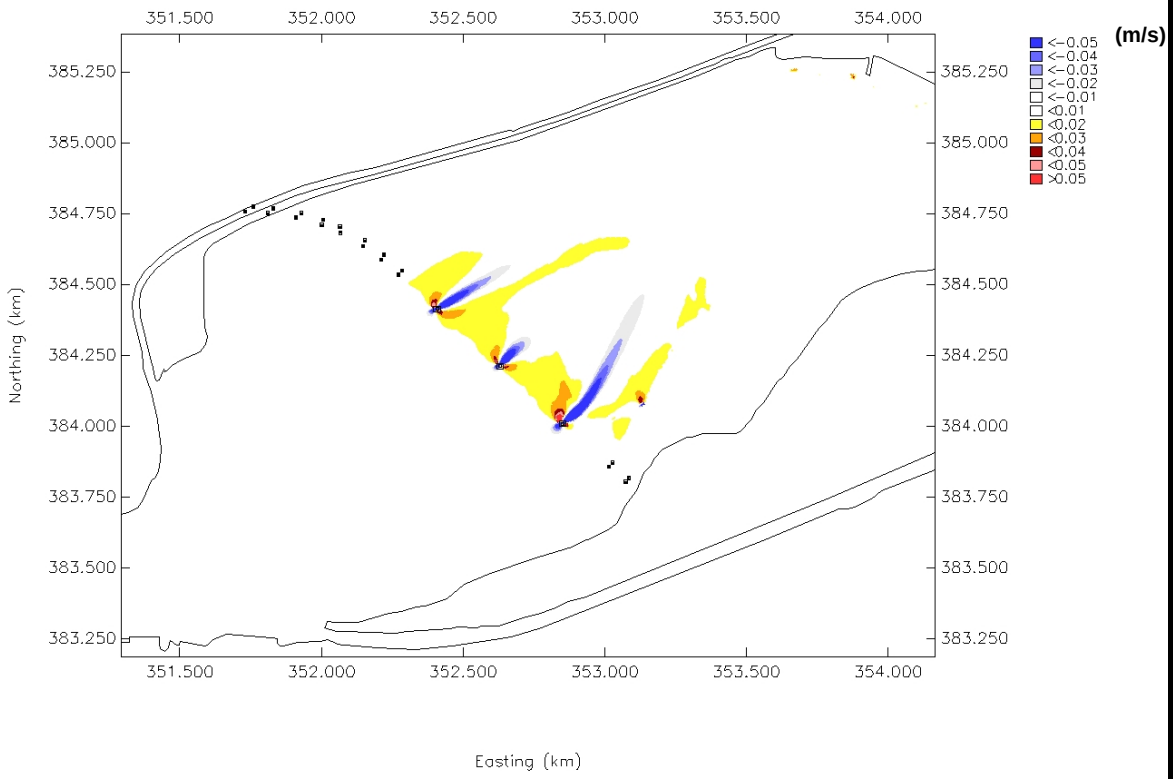


ABP mer marine environmental research

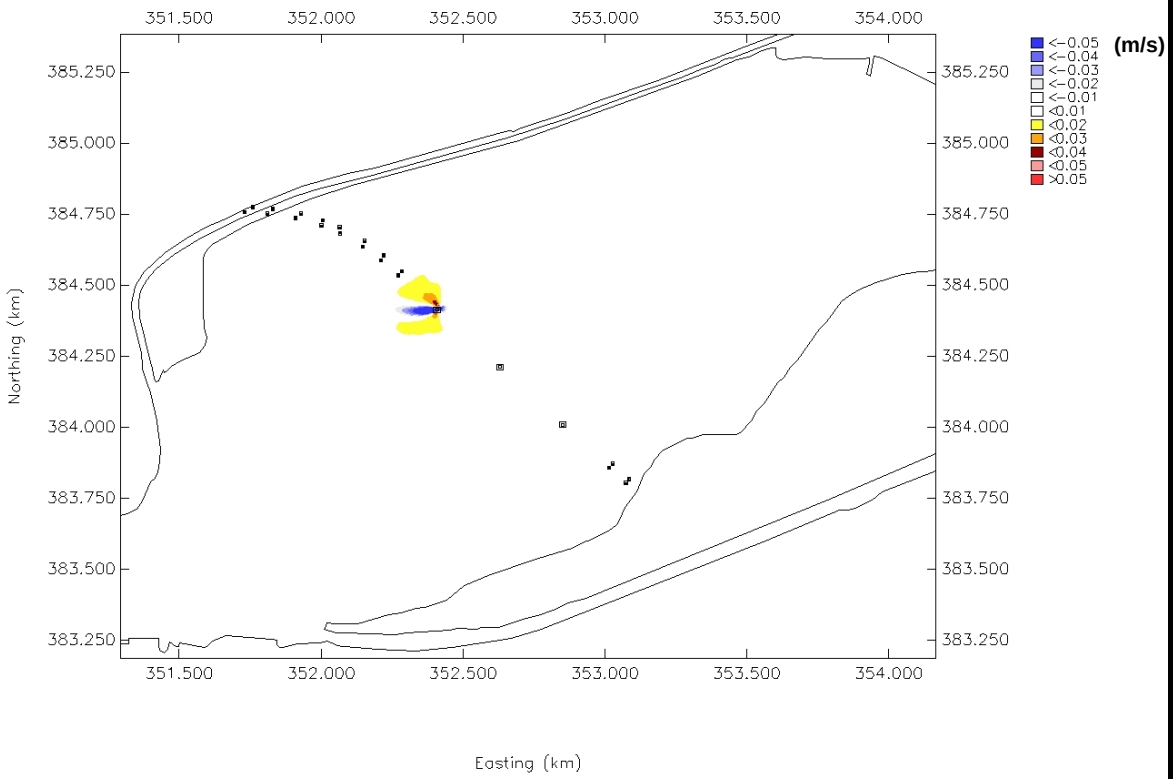
Differences in near-surface speed (m/s) between the proposed bridge scheme Route 3A Medium 3 Tower revised option and the baseline case for low water (A) and peak flood (B) on a spring tide.

Figure C53

A.



B.

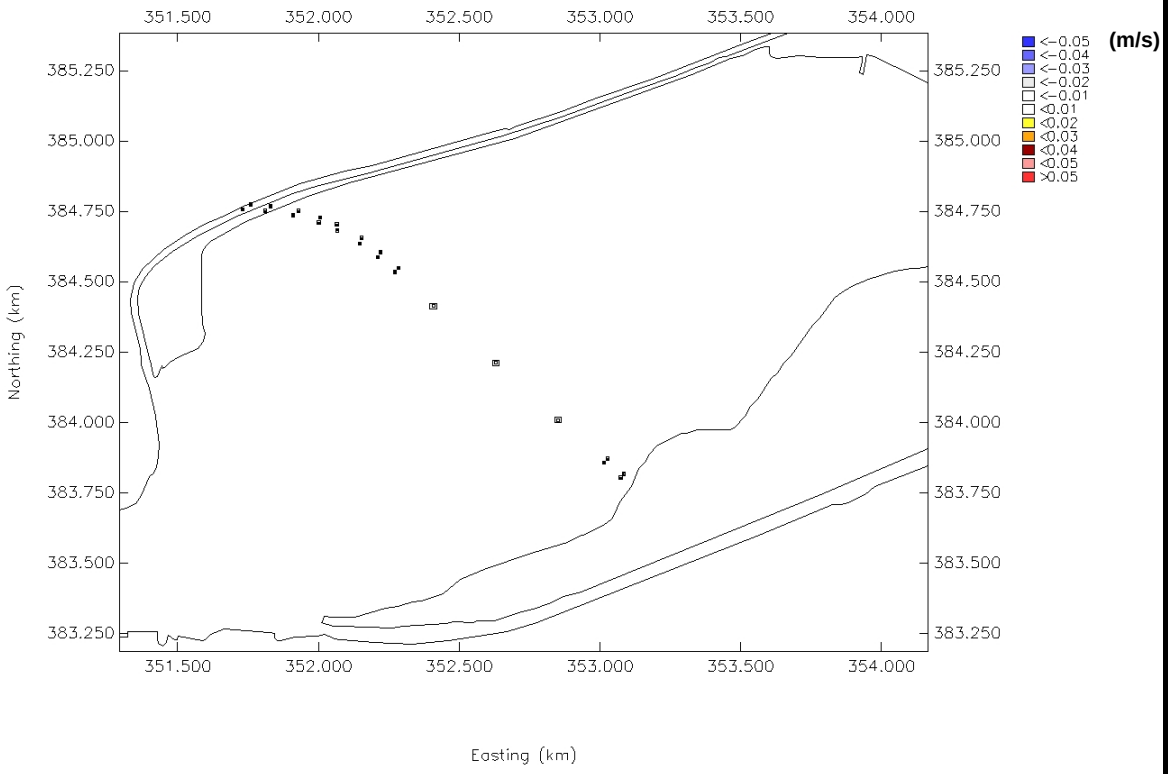


ABP mer marine environmental research

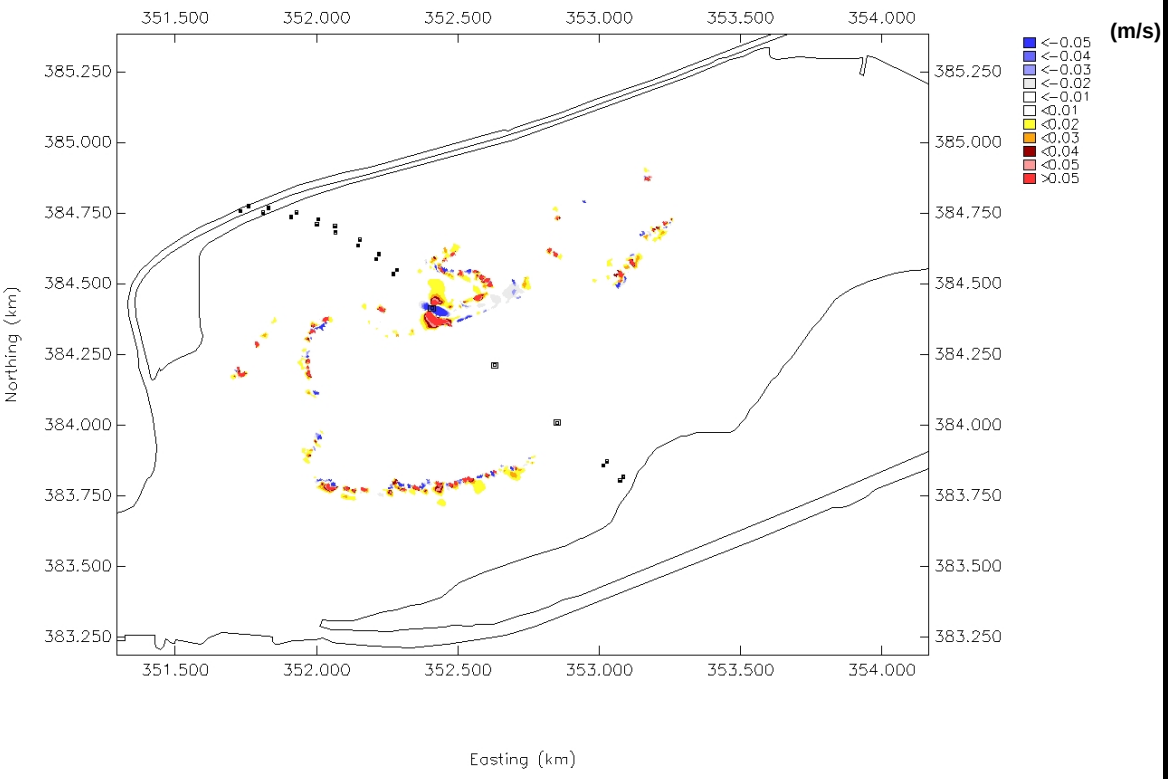
Differences in near-surface speed (m/s) between the proposed bridge scheme Route 3A Medium 3 Tower revised option and the baseline case for high water (A) and peak ebb (B) on a spring tide.

Figure C54

A.



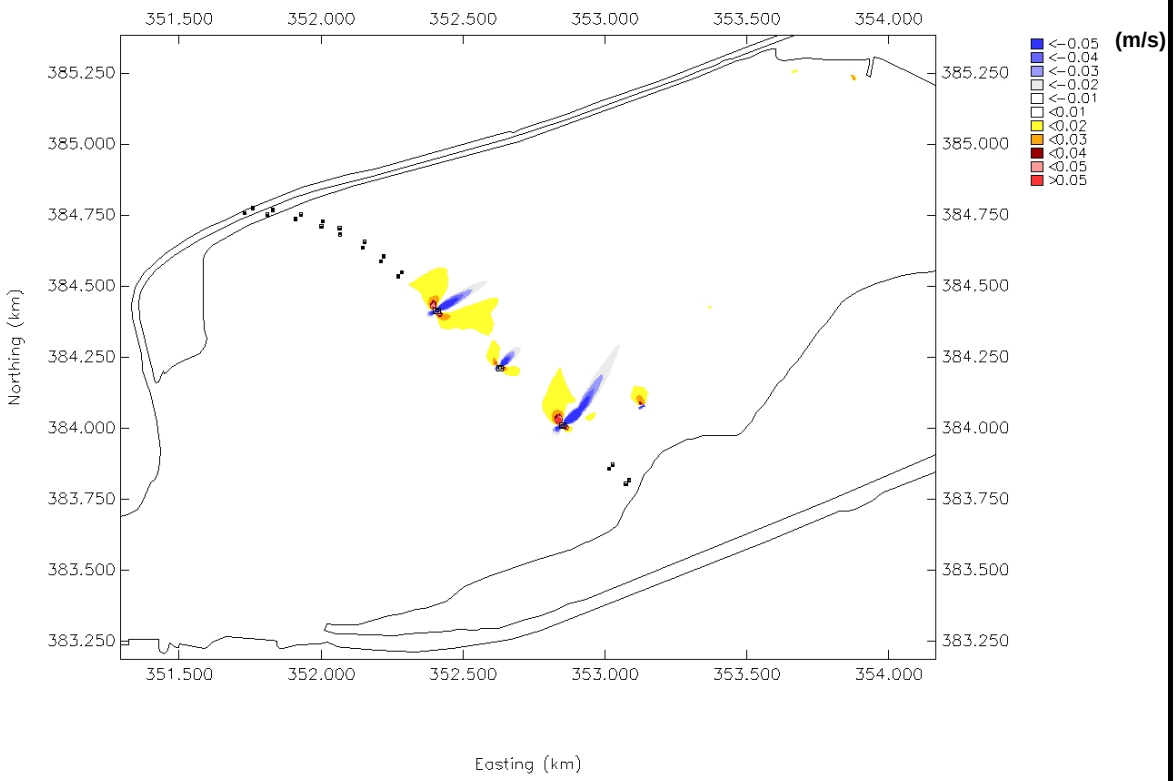
B.



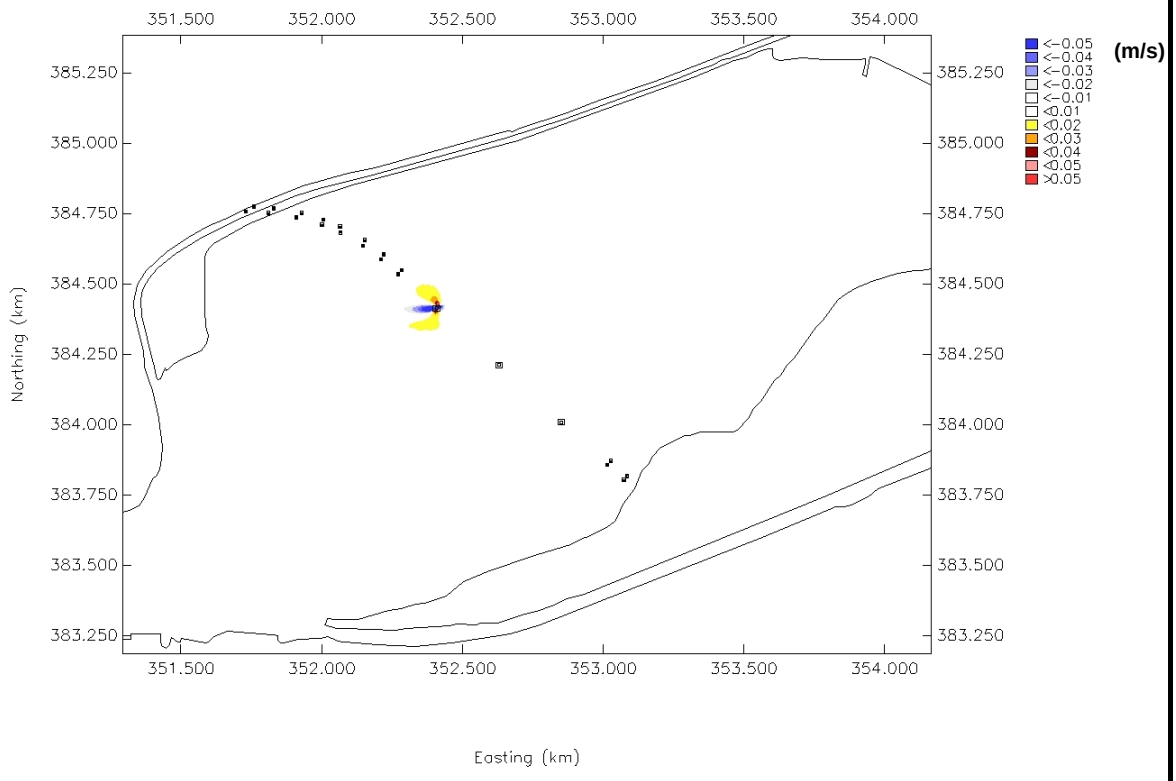
Differences in near-bed speed (m/s) between the proposed bridge scheme Route 3A Medium 3 Tower revised option and the baseline case for low water (A) and peak flood (B) on a spring tide.

Figure C55

A.



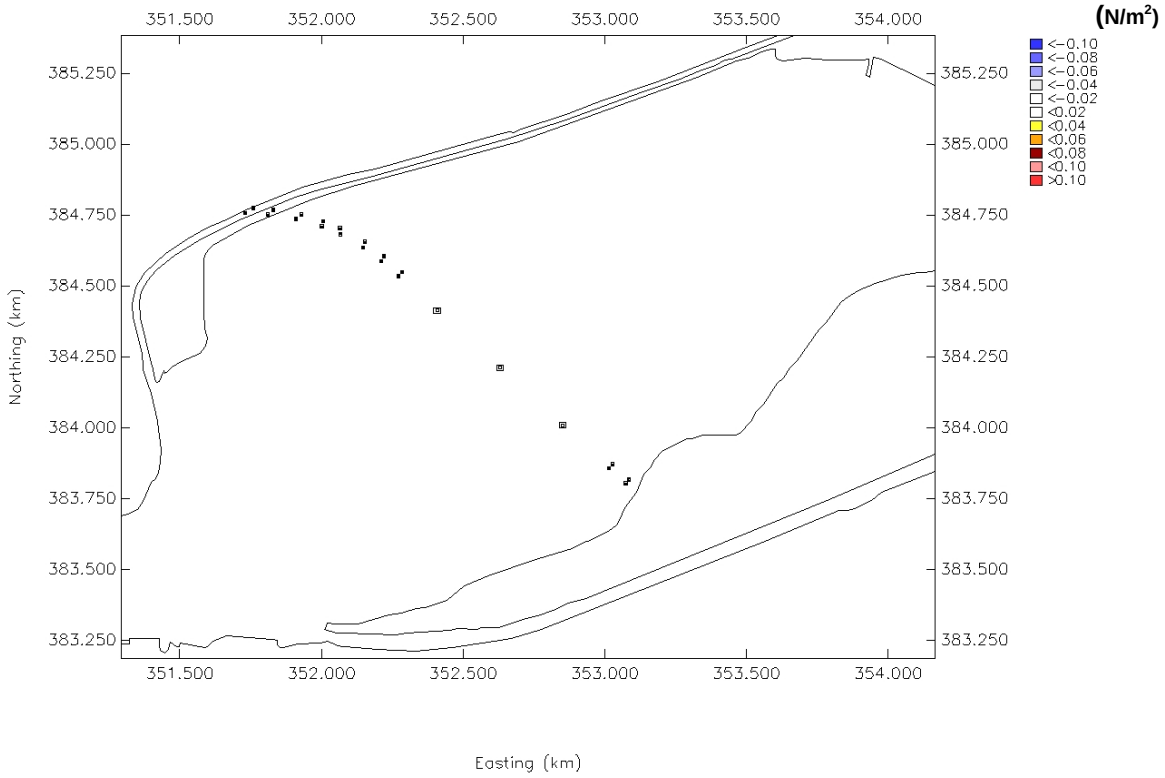
B.



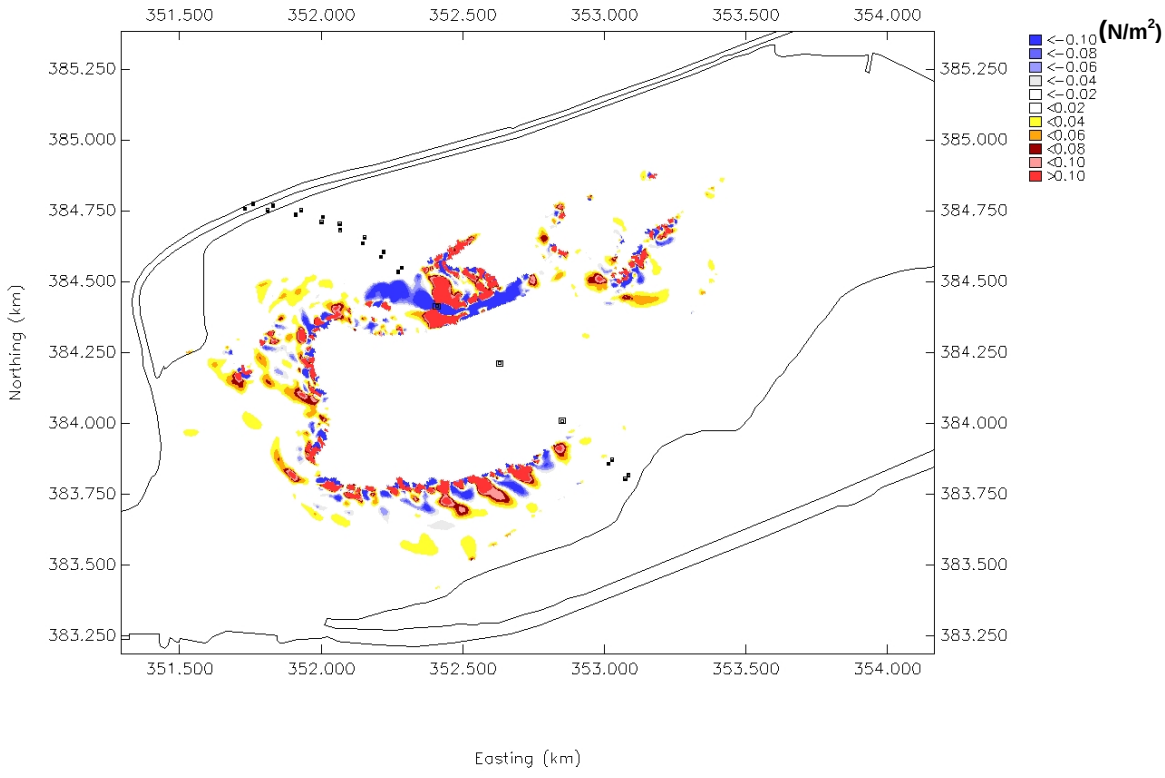
Differences in near-bed speed (m/s) between the proposed bridge scheme Route 3A Medium 3 Tower revised option and the baseline case for high water (A) and peak ebb (B) on a spring tide.

Figure C56

A.



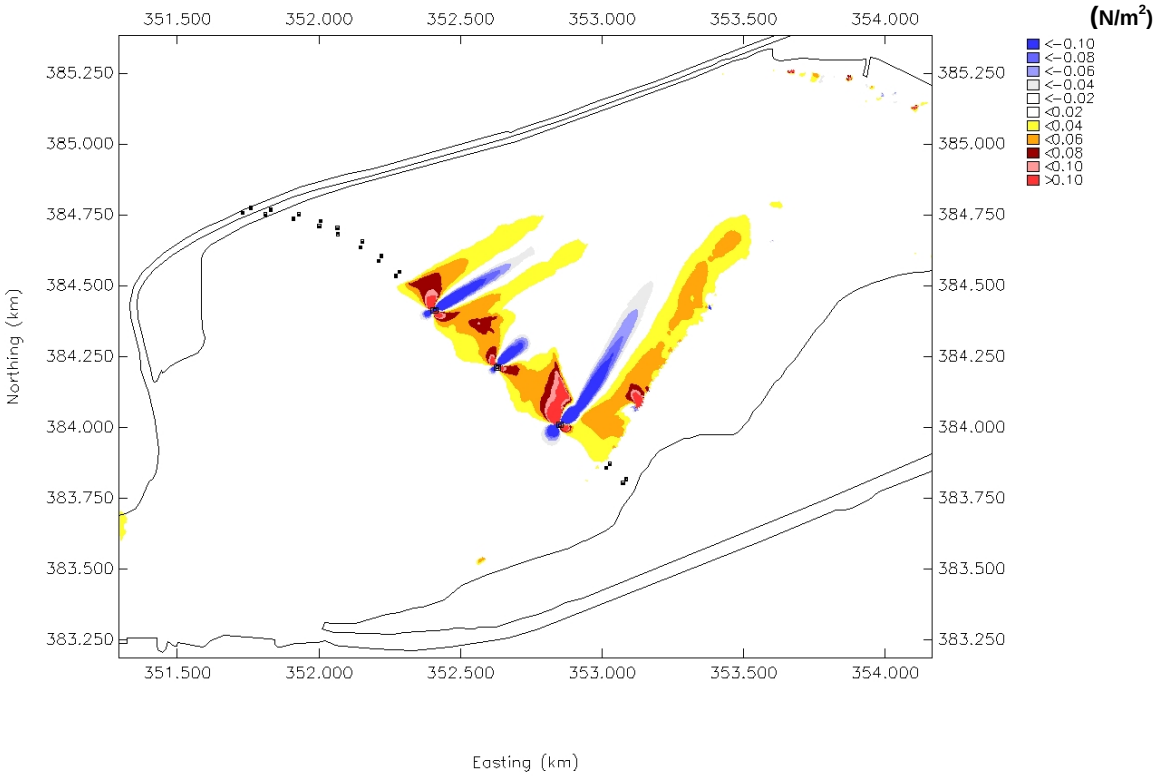
B.



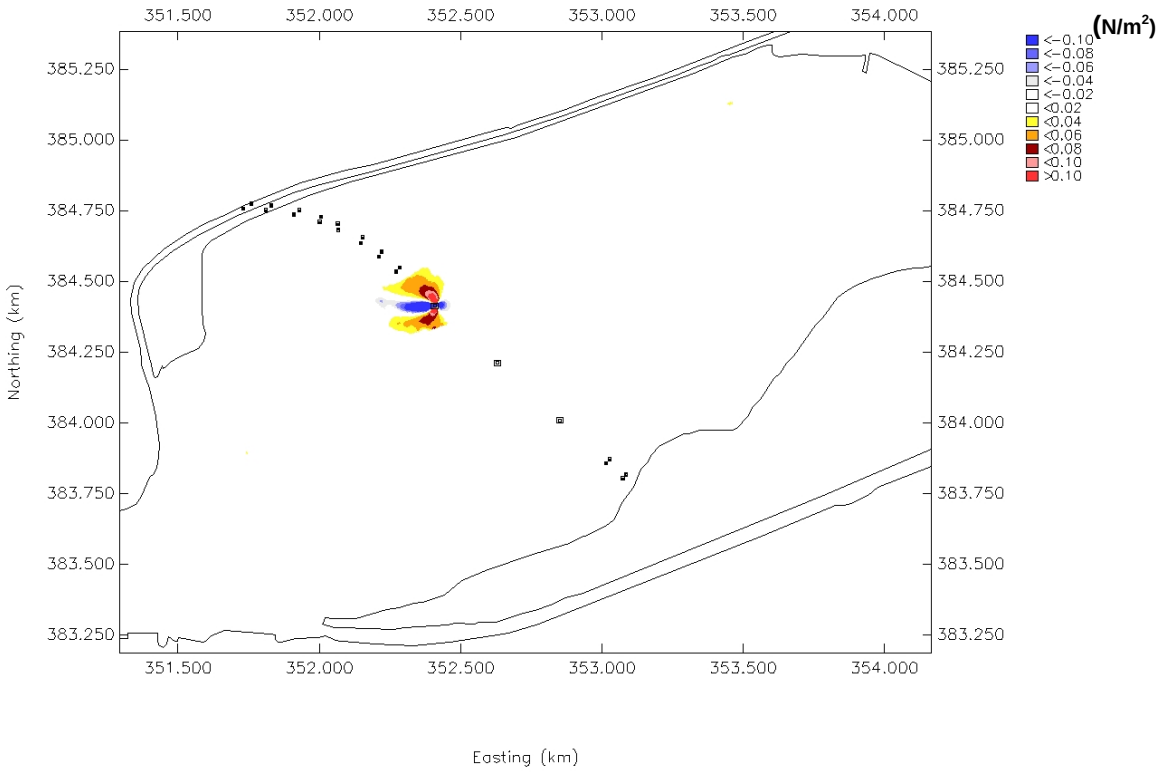
Differences in bed shear stress (N/m²) between the proposed bridge scheme Route 3A Medium 3 Tower revised option and the baseline case for low water (A) and peak flood (B) on a spring tide.

Figure C57

A.



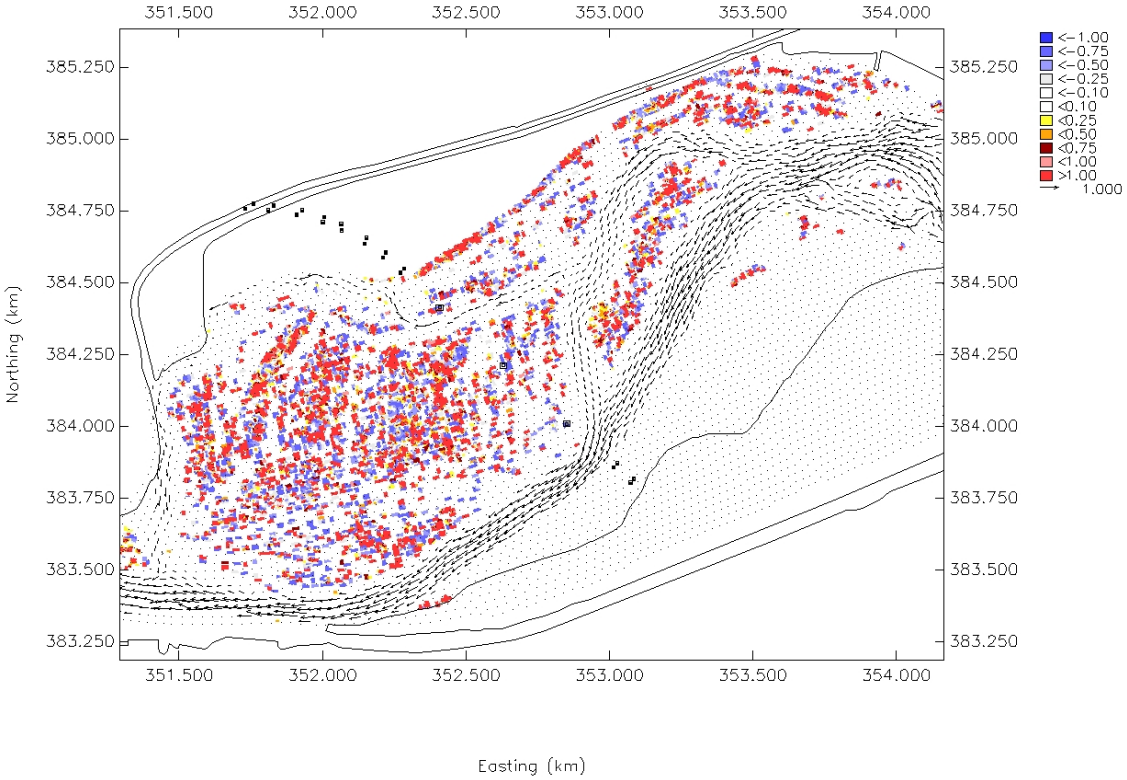
B.



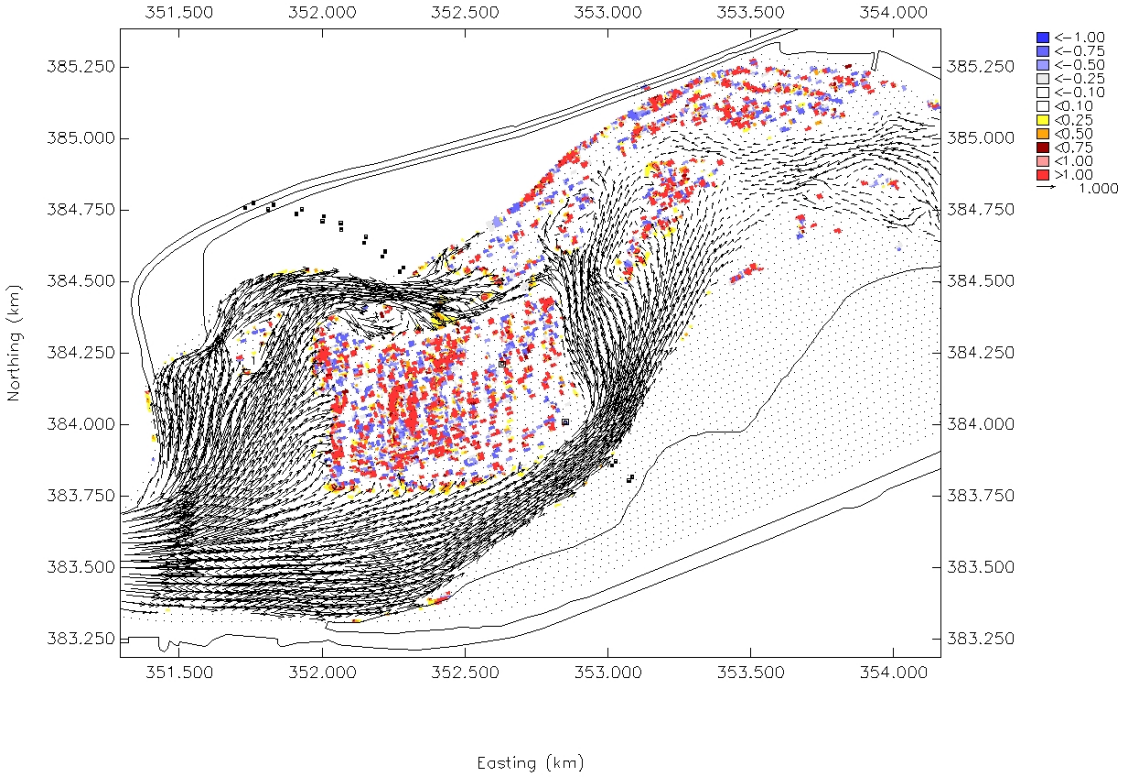
Differences in bed shear stress (N/m²) between the proposed bridge scheme Route 3A Medium 3 Tower revised option and the baseline case for high water (A) and peak ebb (B) on a spring tide.

Figure C58

A.

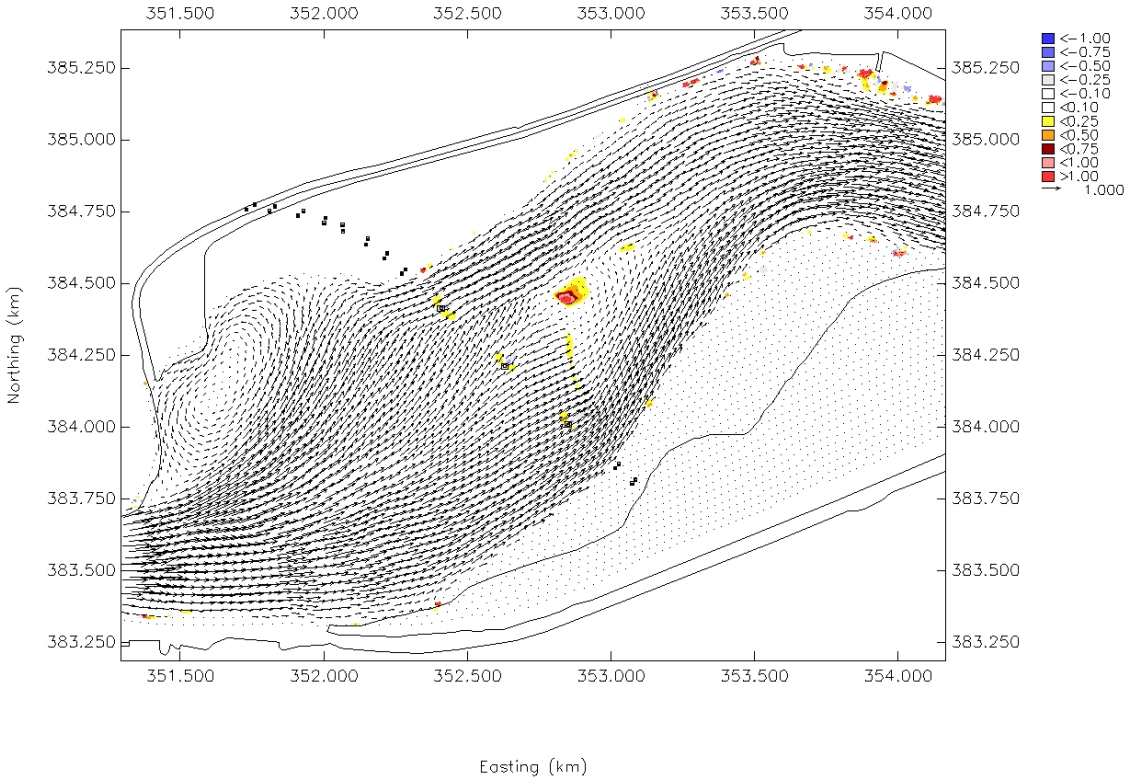


B.

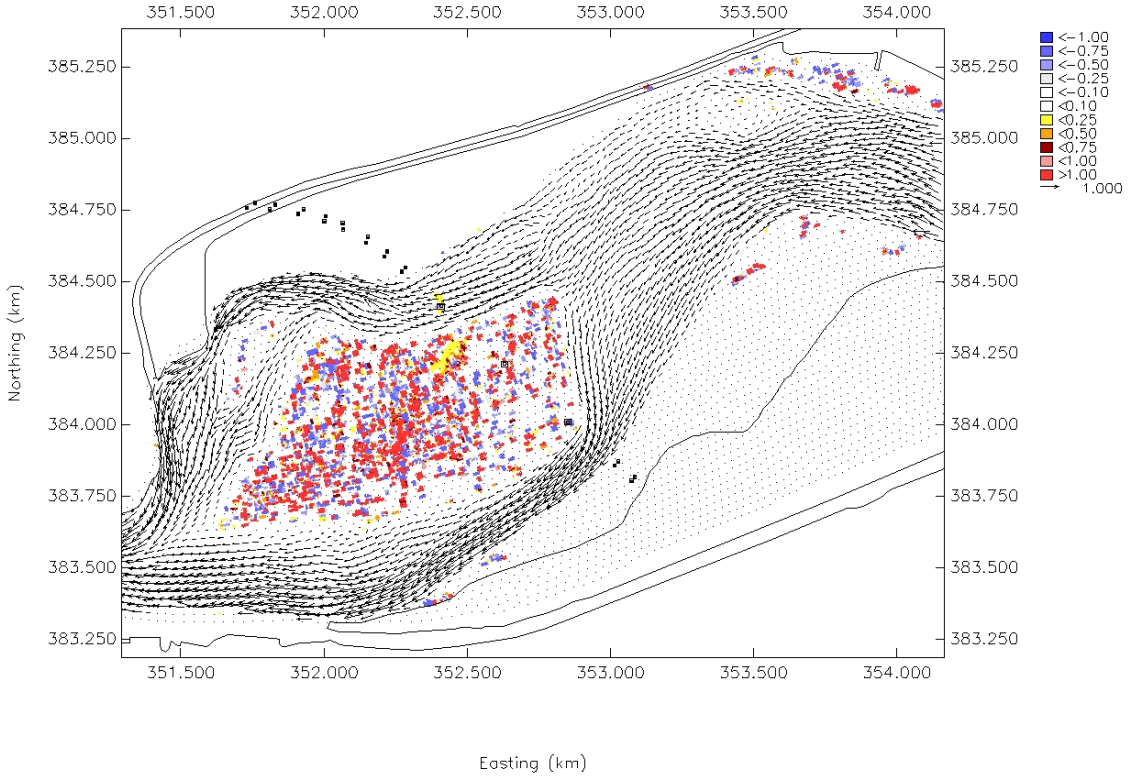


ABP mer marine environmental research	Percentage differences in bed shear stress between the proposed bridge scheme Route 3A Medium 3 Tower revised option and the baseline case for low water (A) and peak flood (B) on a spring tide. (1 = 100% ; 0.1 = 10%).	Figure C59

A.

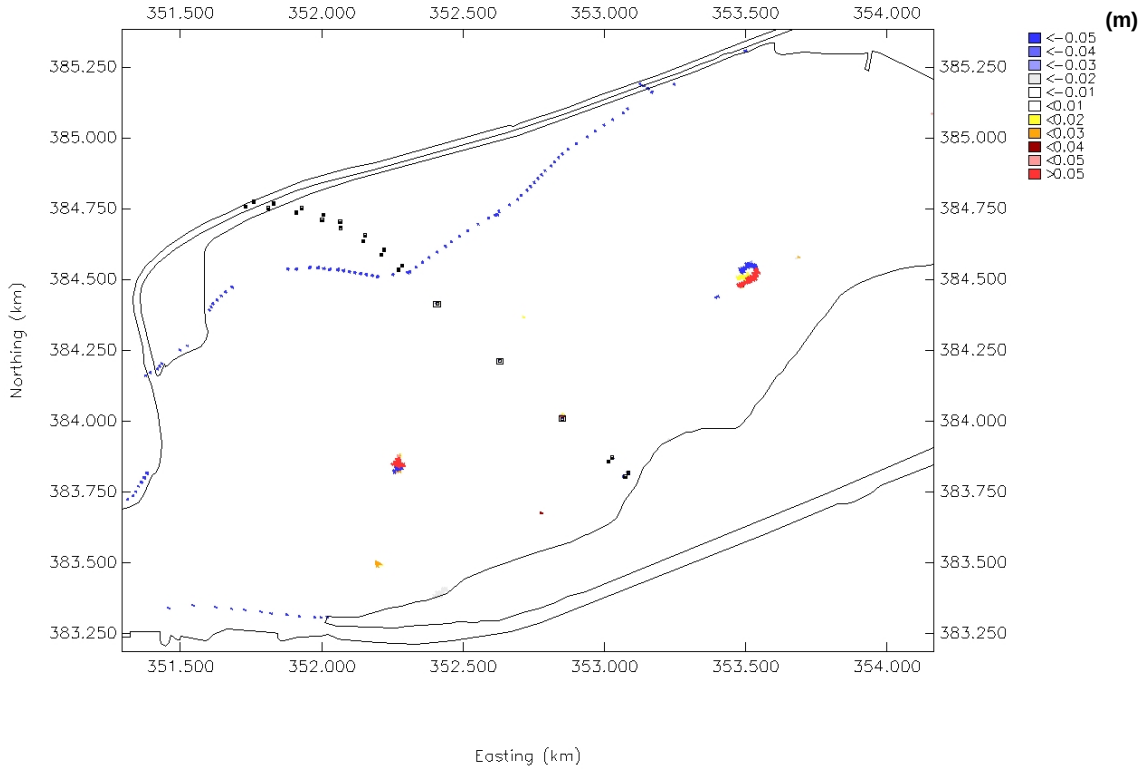


B.

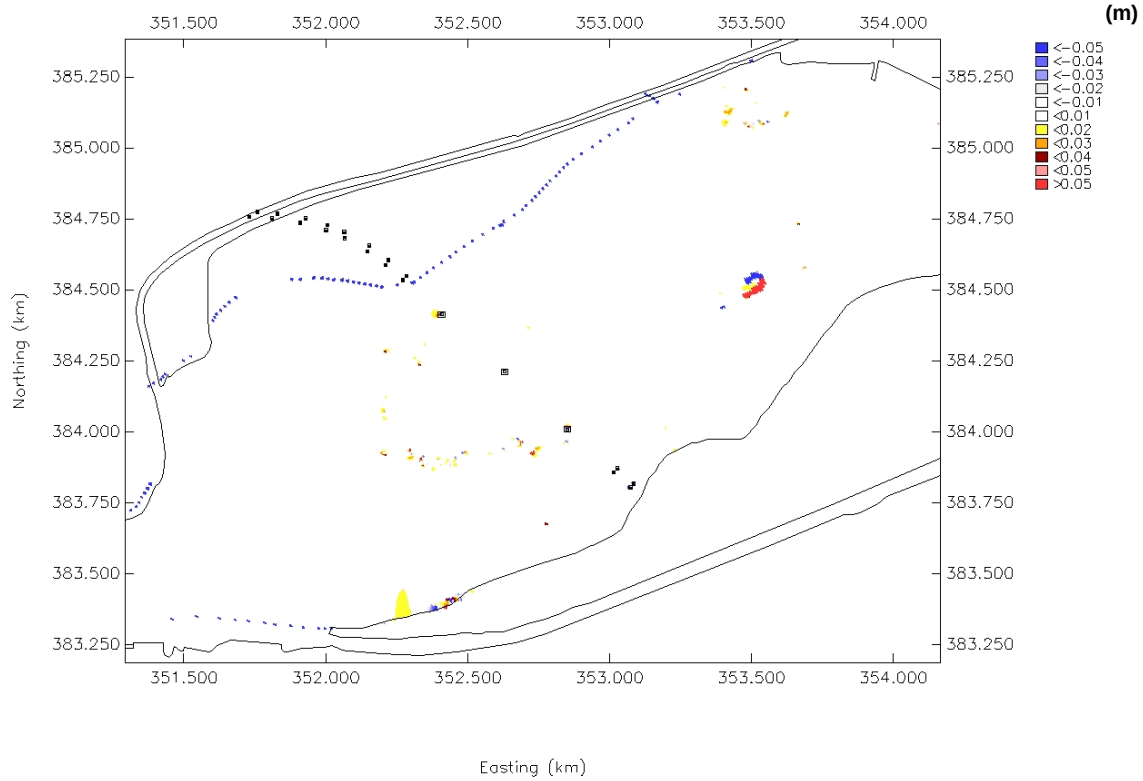


ABP mer marine environmental research	Percentage differences in bed shear stress between the proposed bridge scheme Route 3A Medium 3 Tower revised option and the baseline case for high water (A) and peak ebb (B) on a spring tide. (1 = 100%; 0.1 = 10%).	Figure C60

A.

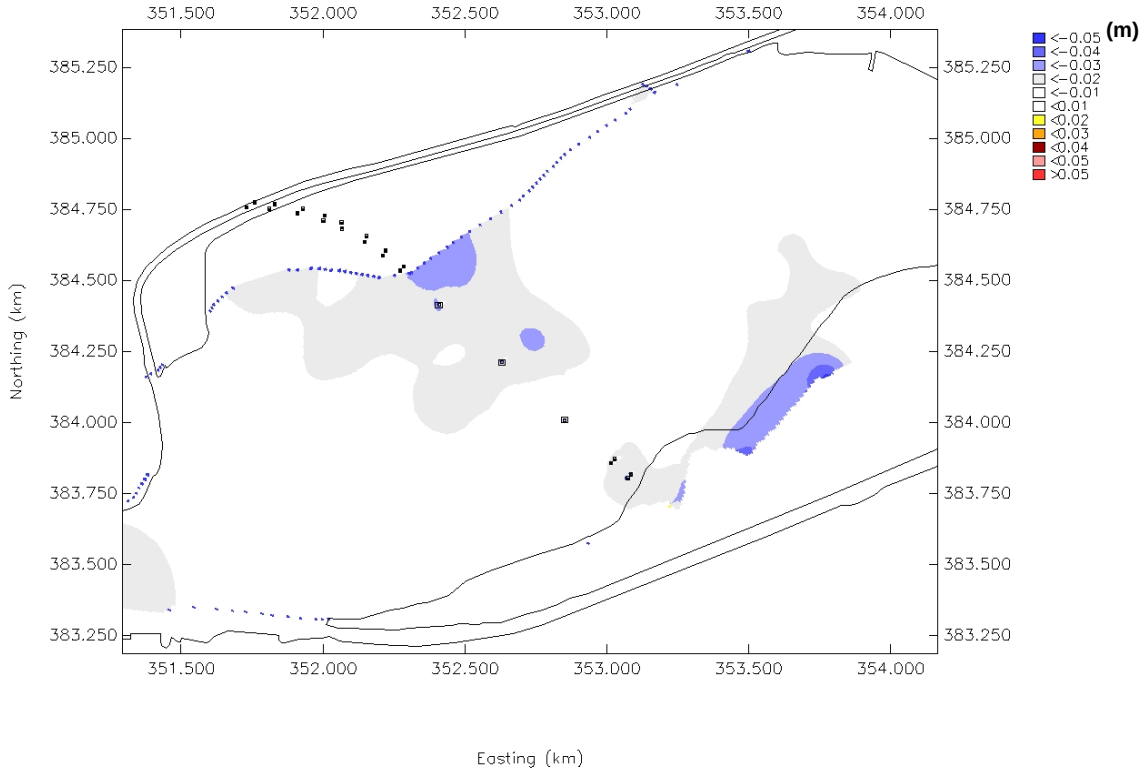


B.

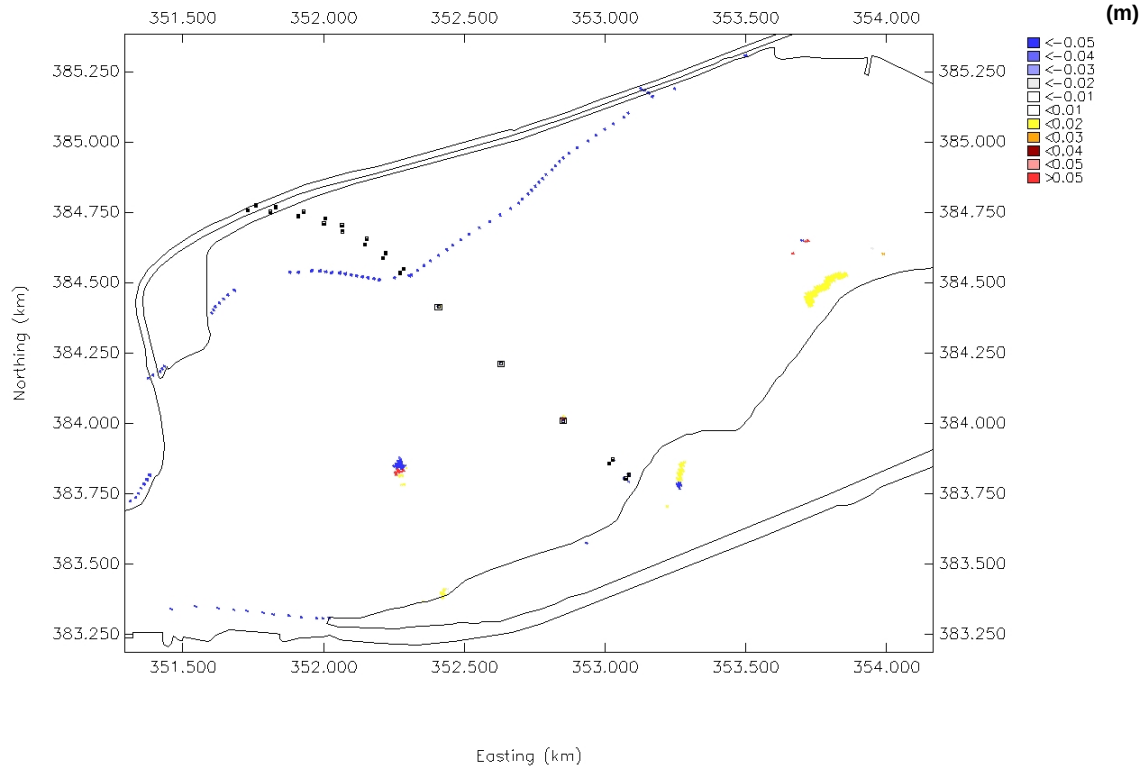


ABP mer marine environmental research	Differences in water level (m) between the proposed bridge scheme Route 3A Medium 3 Tower revised option and the baseline case for low water (A) and peak flood (B) on a 1:200 surge tide and 1:200 fluvial event.	Figure C61

A.



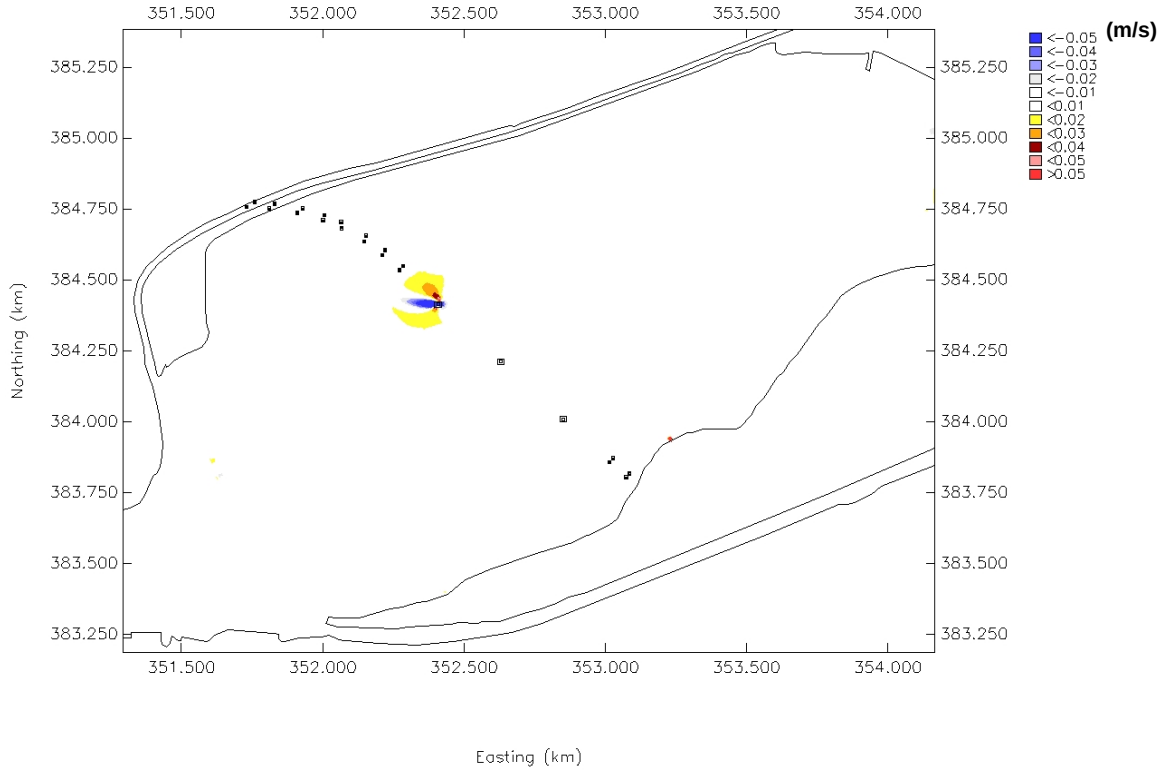
B.



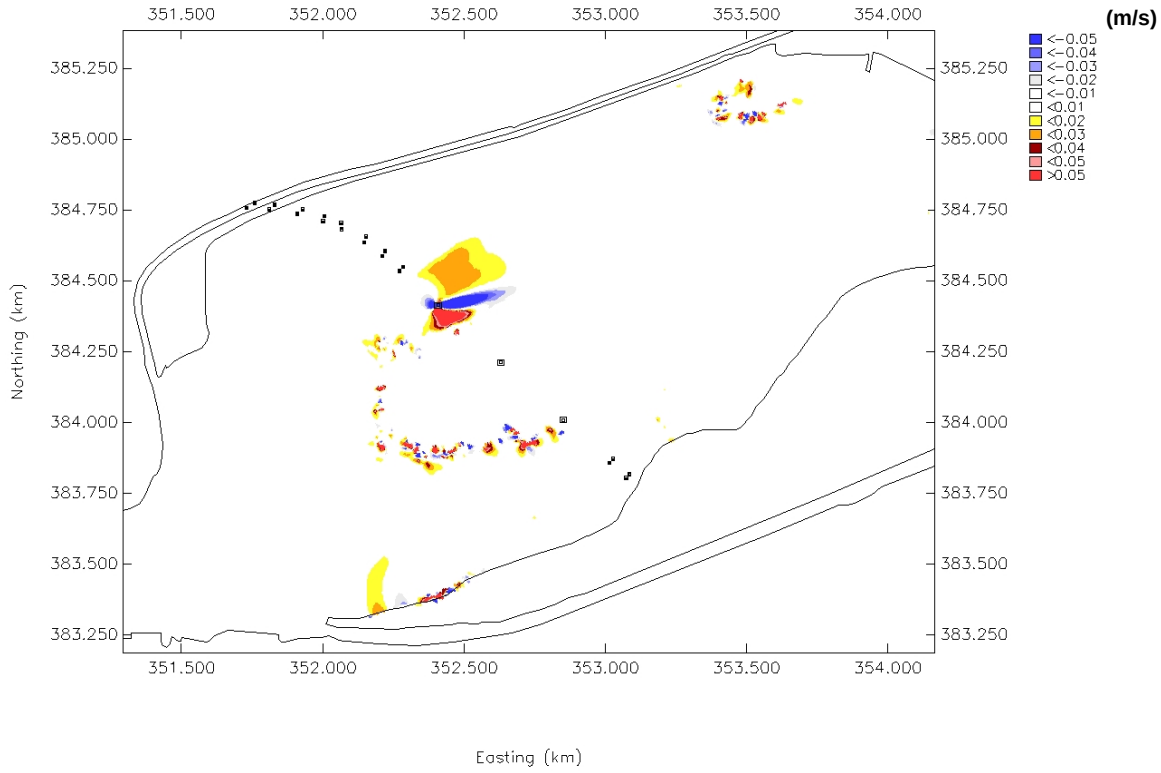
Differences in water level (m) between the proposed bridge scheme Route 3A Medium 3 Tower revised option and the baseline case for high water (A) and peak ebb (B) on a 1:200 surge tide and 1:200 fluvial event.

Figure C62

A.

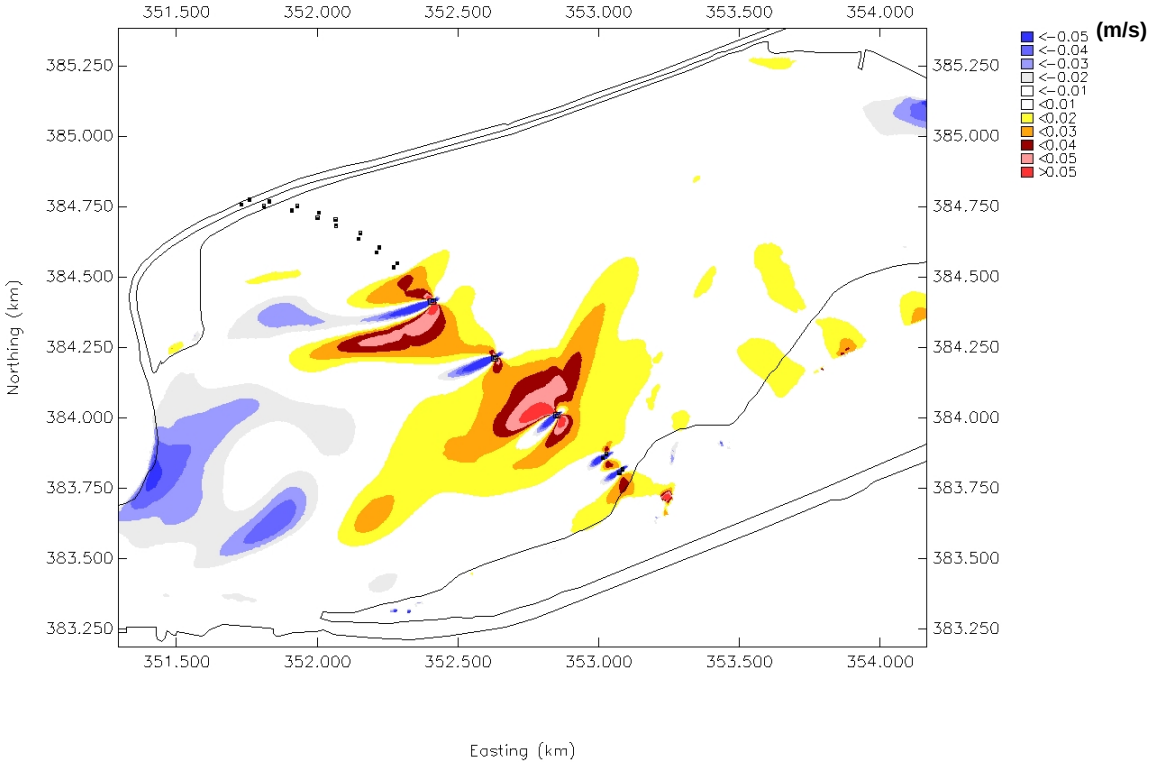


B.

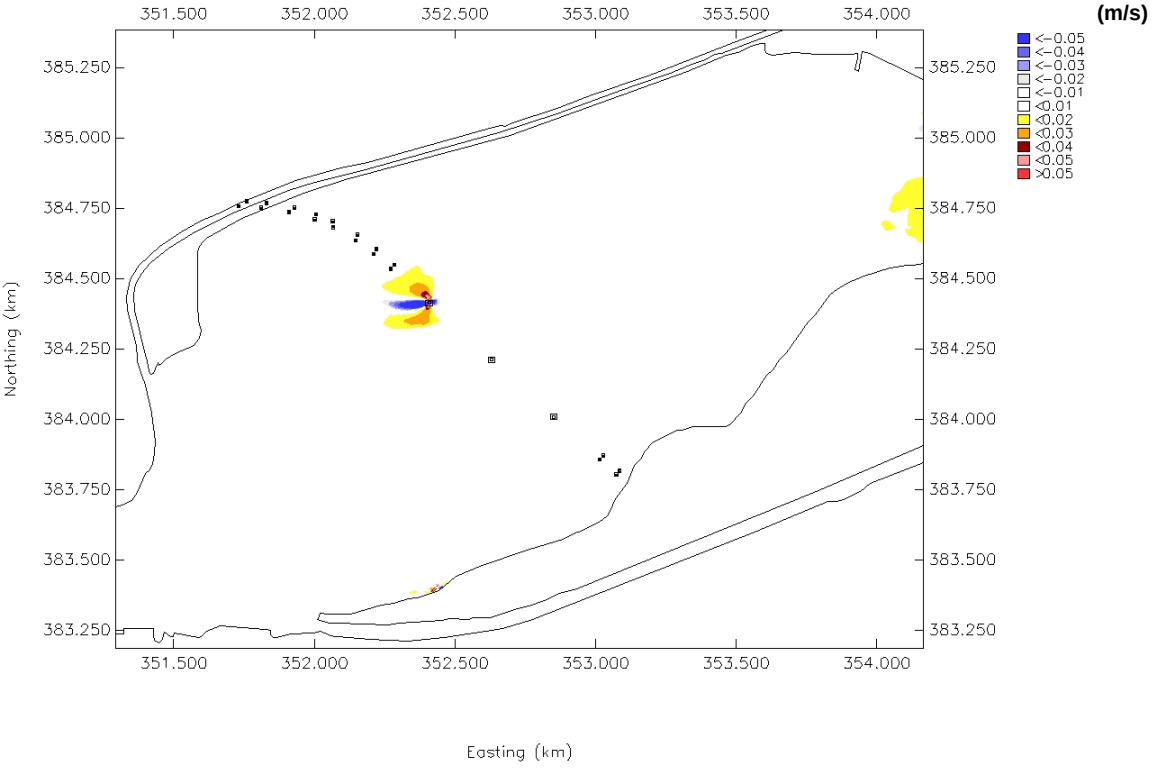


ABP mer marine environmental research	Differences in near-surface speed (m/s) between the proposed bridge scheme Route 3A Medium 3 Tower revised option and the baseline case for low water (A) and peak flood (B) on a 1:200 surge tide and 1:200 fluvial event.	Figure C63

A.

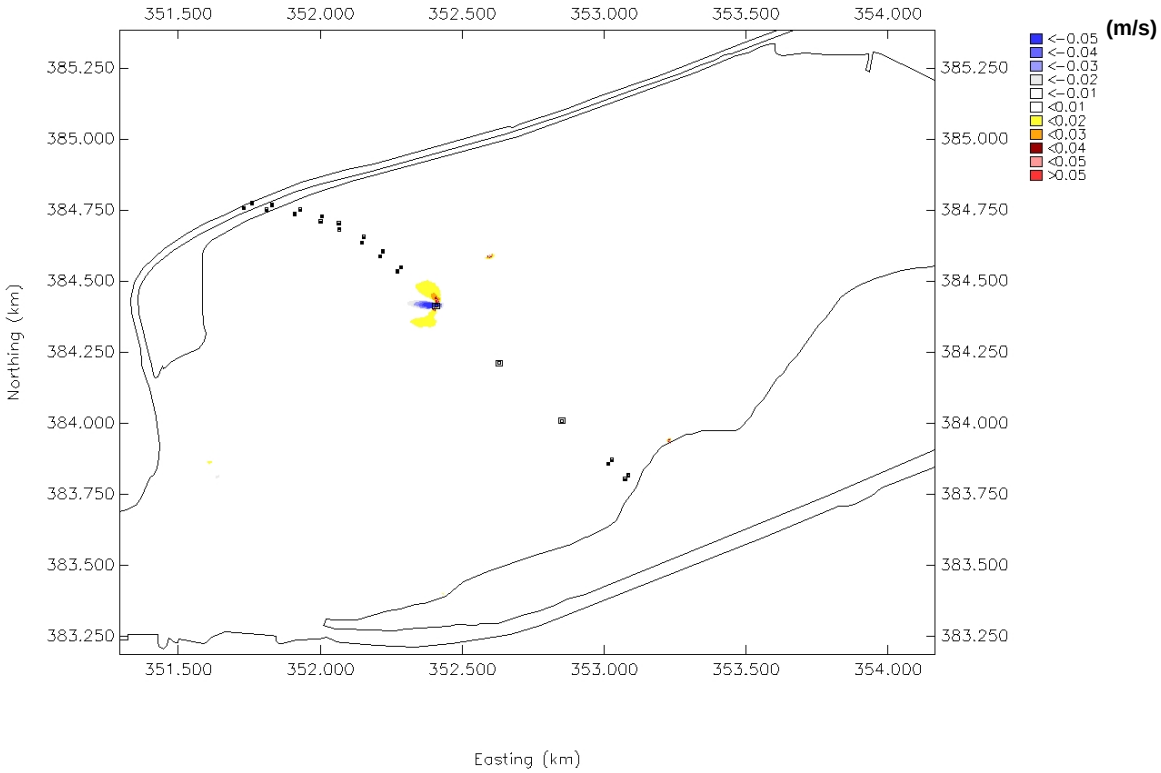


B.

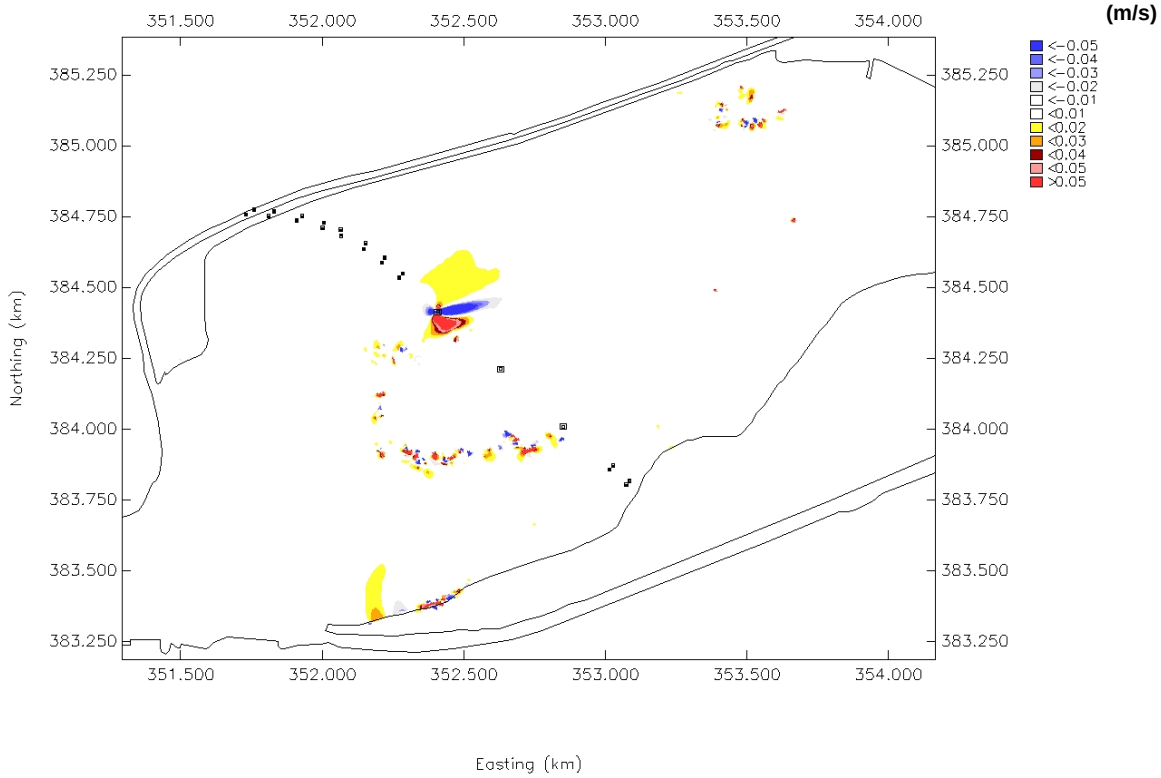


ABP mer marine environmental research	Differences in near-surface speed (m/s) between the proposed bridge scheme Route 3A Medium 3 Tower revised option and the baseline case for high water (A) and peak ebb (B) on a 1:200 surge tide and 1:200 fluvial event.	Figure C64

A.



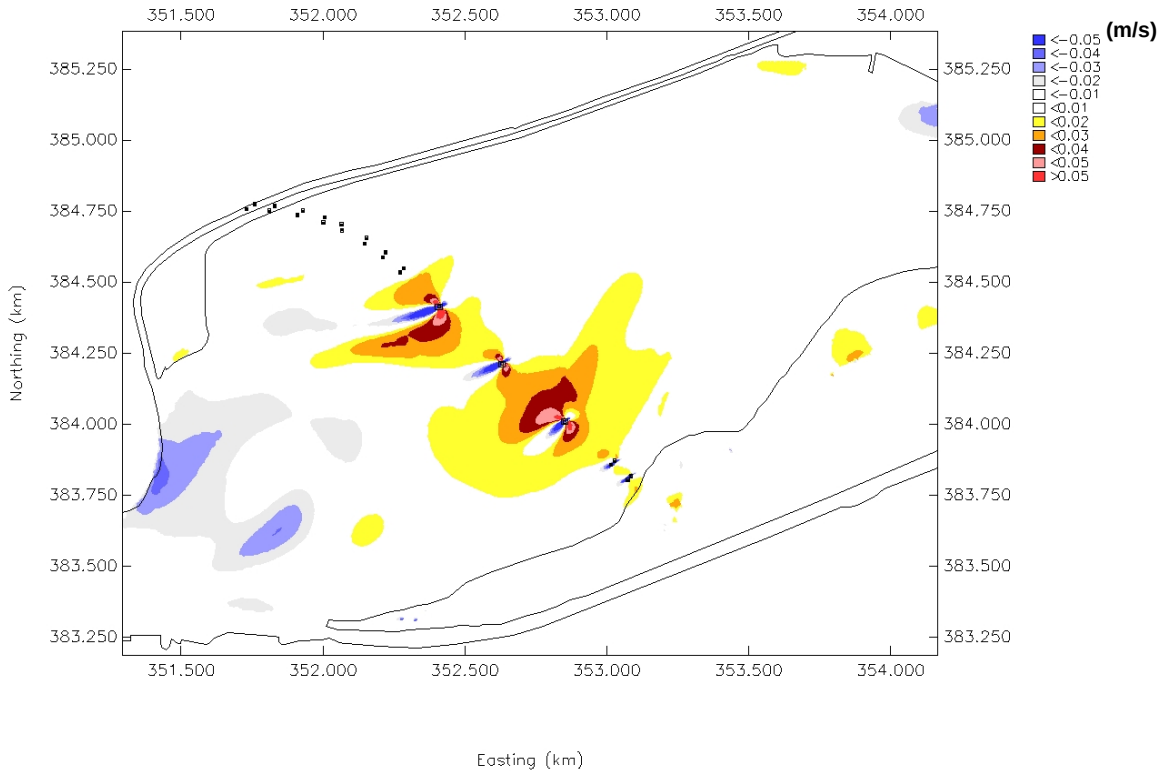
B.



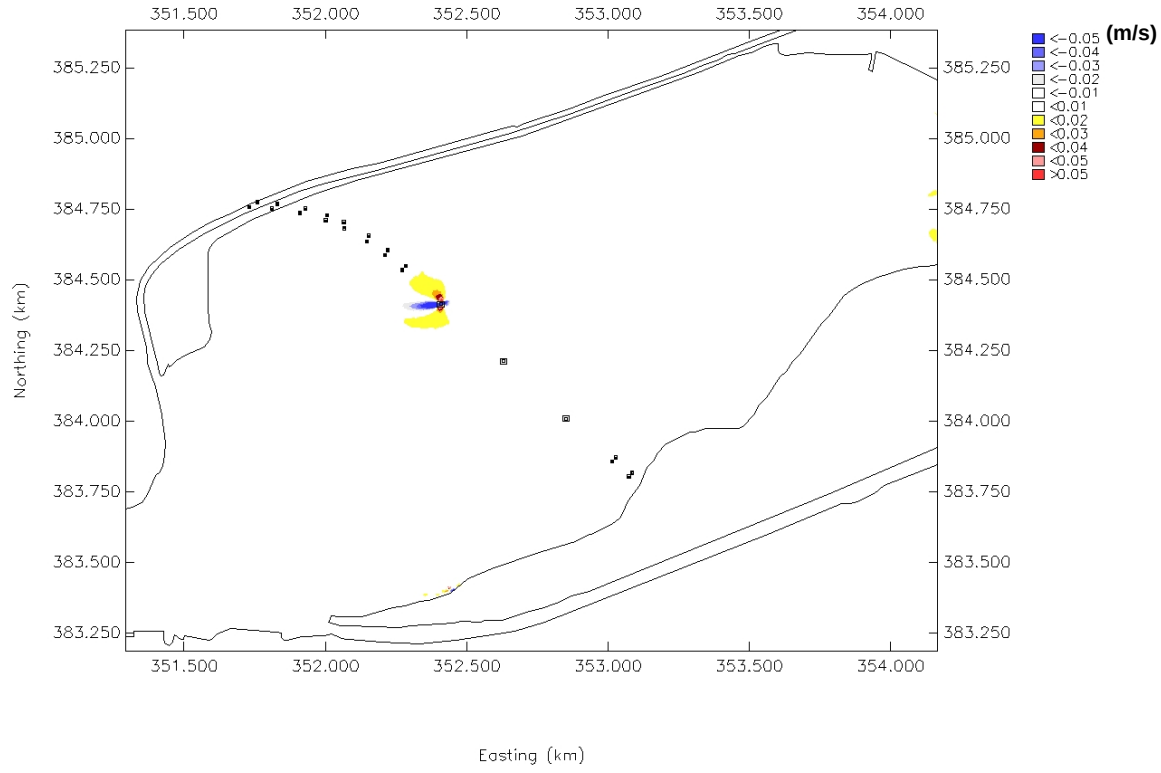
Differences in near-bed speed (m/s) between the proposed bridge scheme Route 3A Medium 3 Tower revised option and the baseline case for low water (A) and peak flood (B) on a 1:200 surge tide and 1:200 fluvial event.

Figure C65

A.



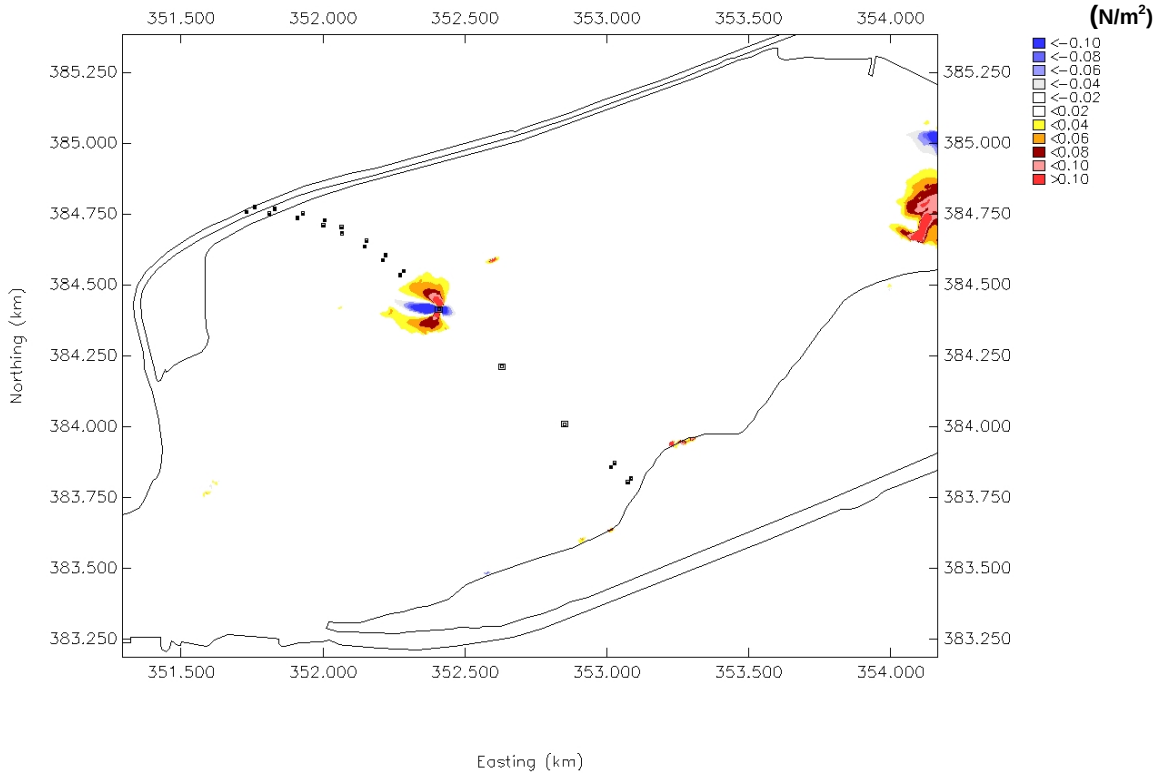
B.



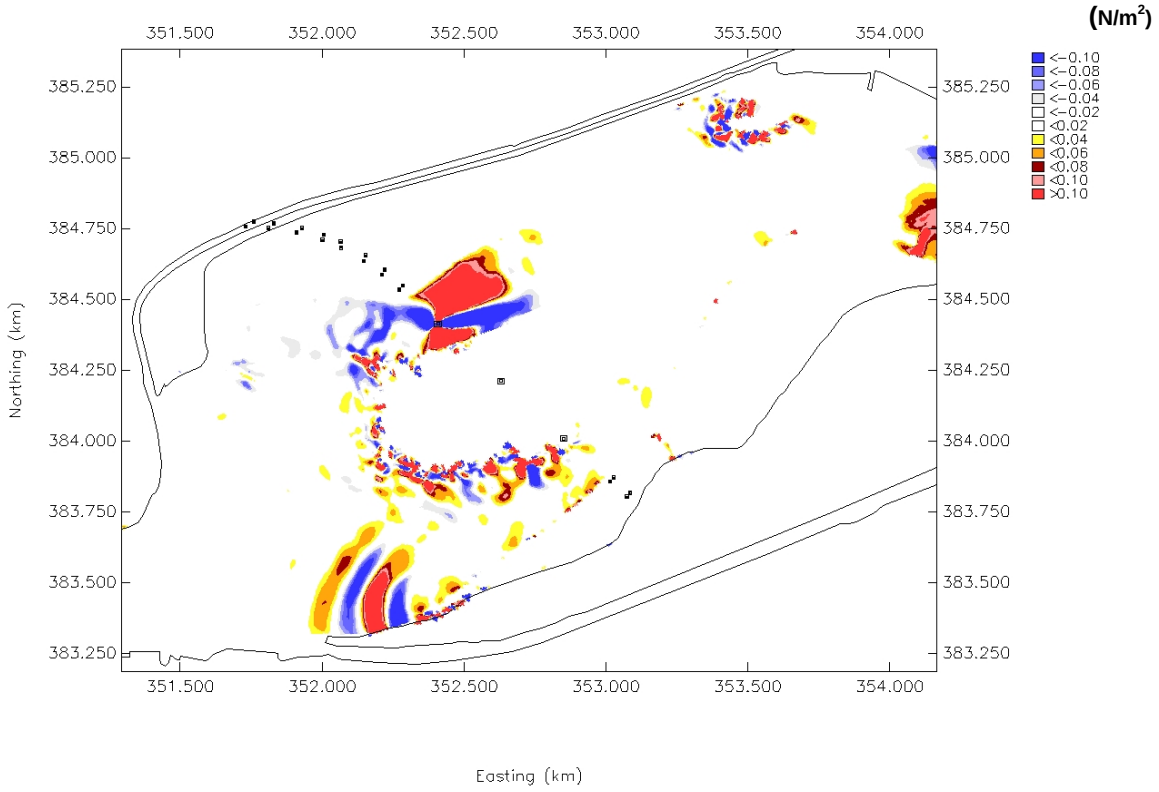
Differences in near-bed speed (m/s) between the proposed bridge scheme Route 3A Medium 3 Tower revised option and the baseline case for high water (A) and peak ebb (B) on a 1:200 surge tide and 1:200 fluvial event.

Figure C66

A.

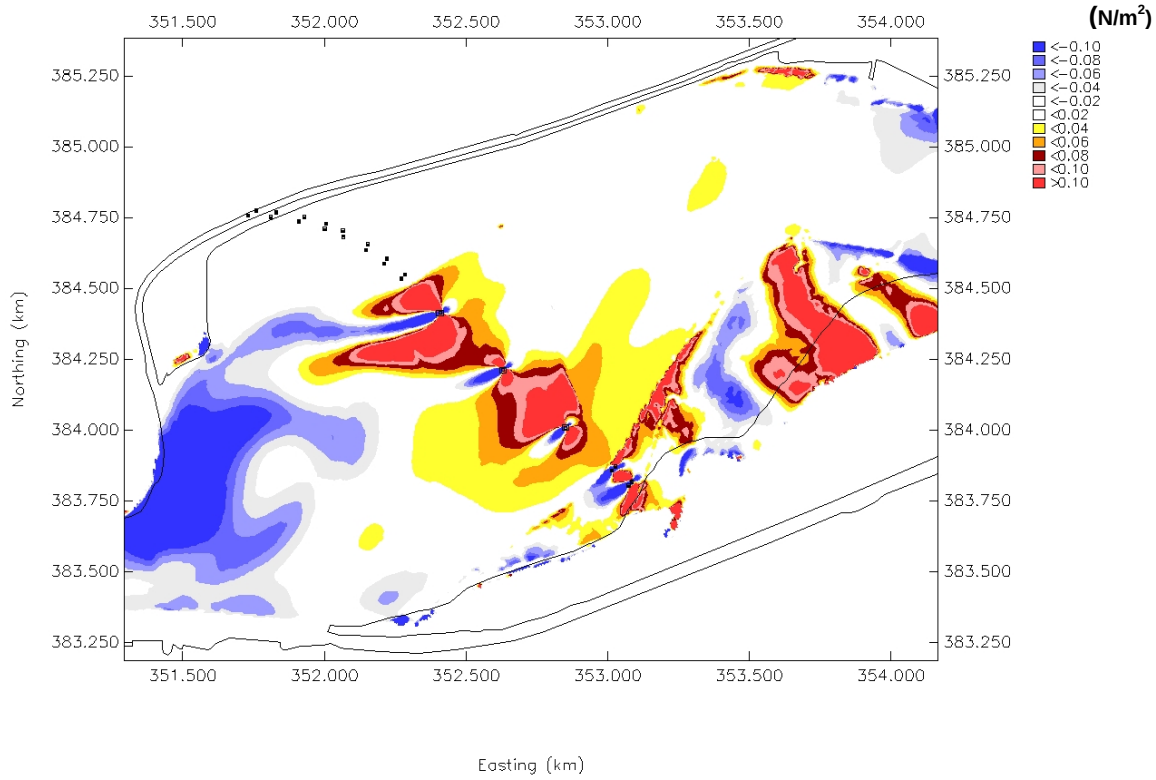


B.

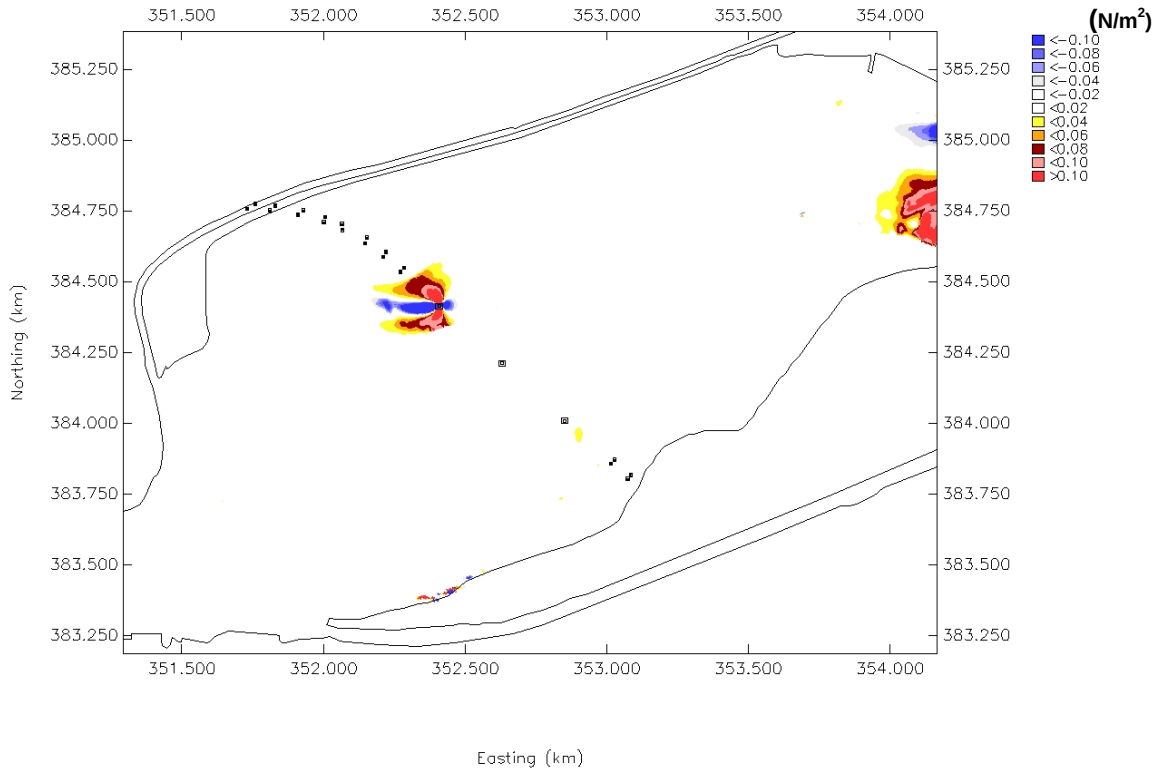


ABP mer marine environmental research	Differences in bed shear stress (N/m²) between the proposed bridge scheme Route 3A Medium 3 Tower revised option and the baseline case for low water (A) and peak flood (B) on a 1:200 surge tide and 1:200 fluvial event.	Figure C67

A.



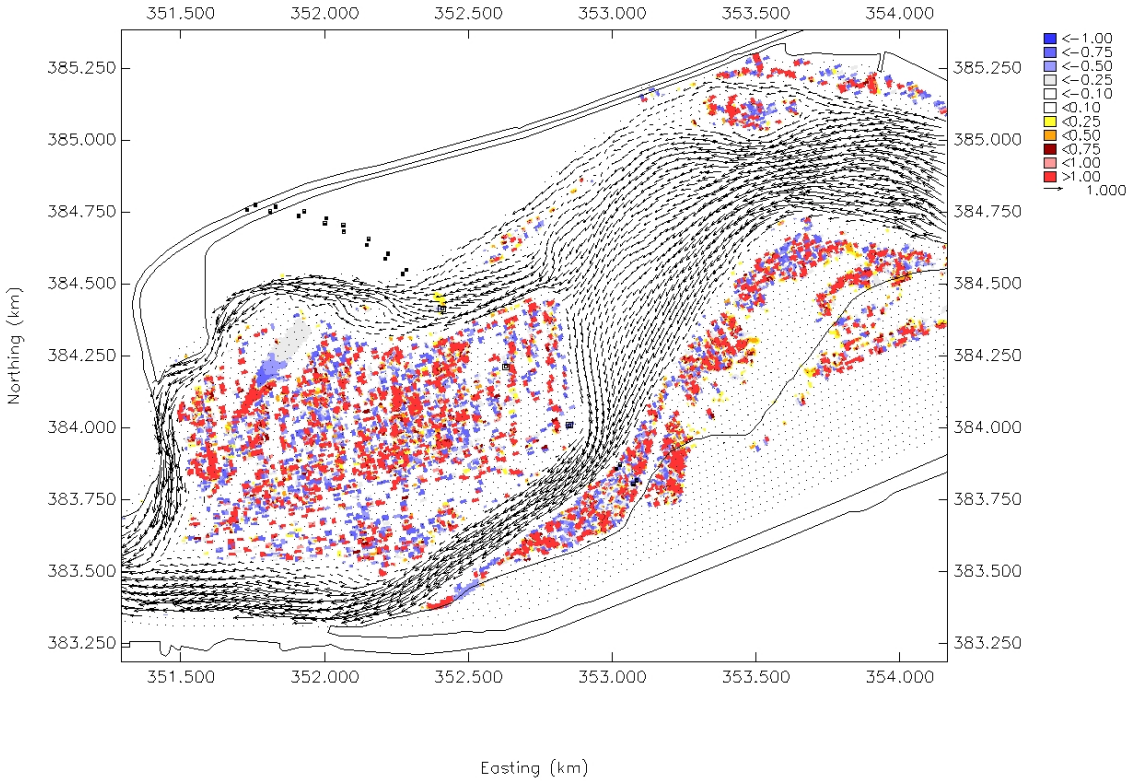
B.



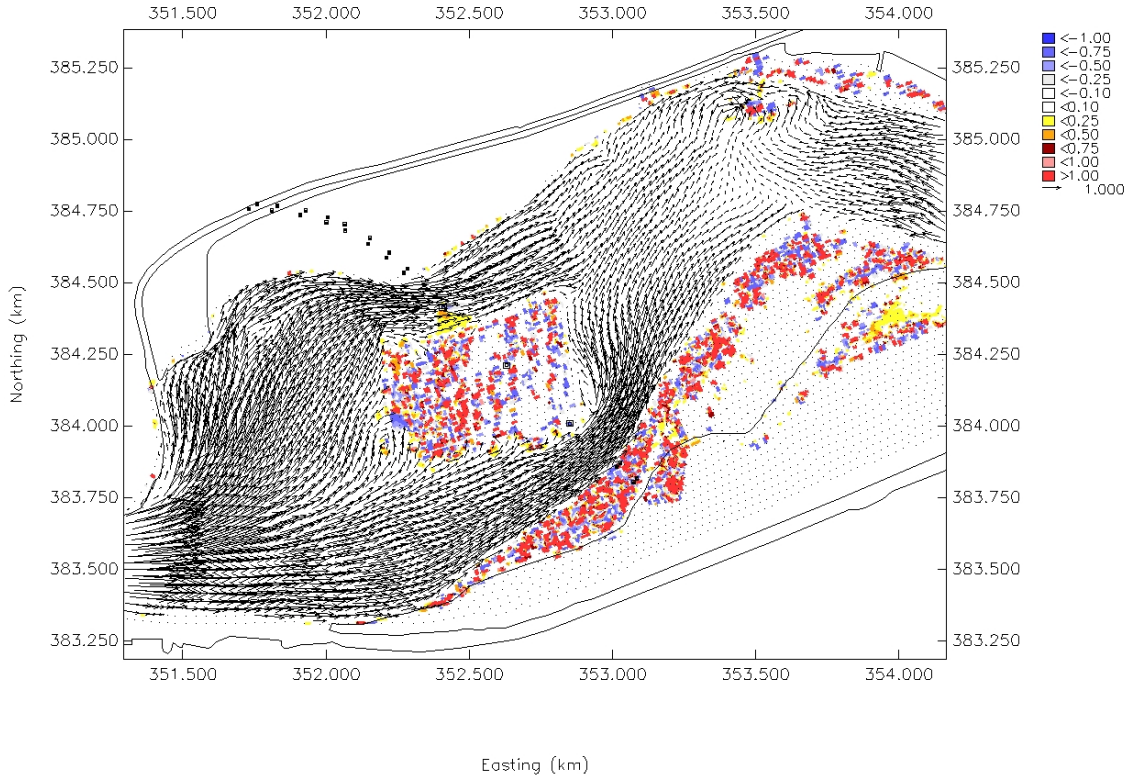
Differences in bed shear stress (N/m²) between the proposed bridge scheme Route 3A Medium 3 Tower revised option and the baseline case for high water (A) and peak ebb (B) on a 1:200 surge tide and 1:200 fluvial event.

Figure C68

A.



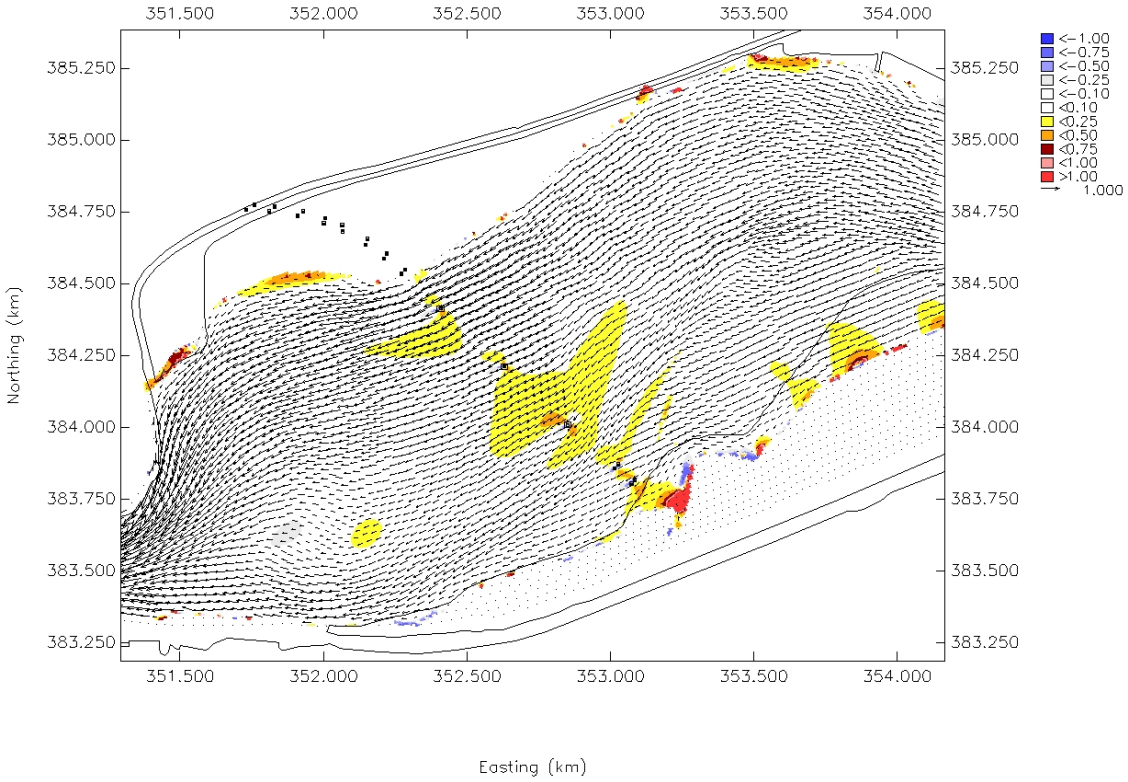
B.



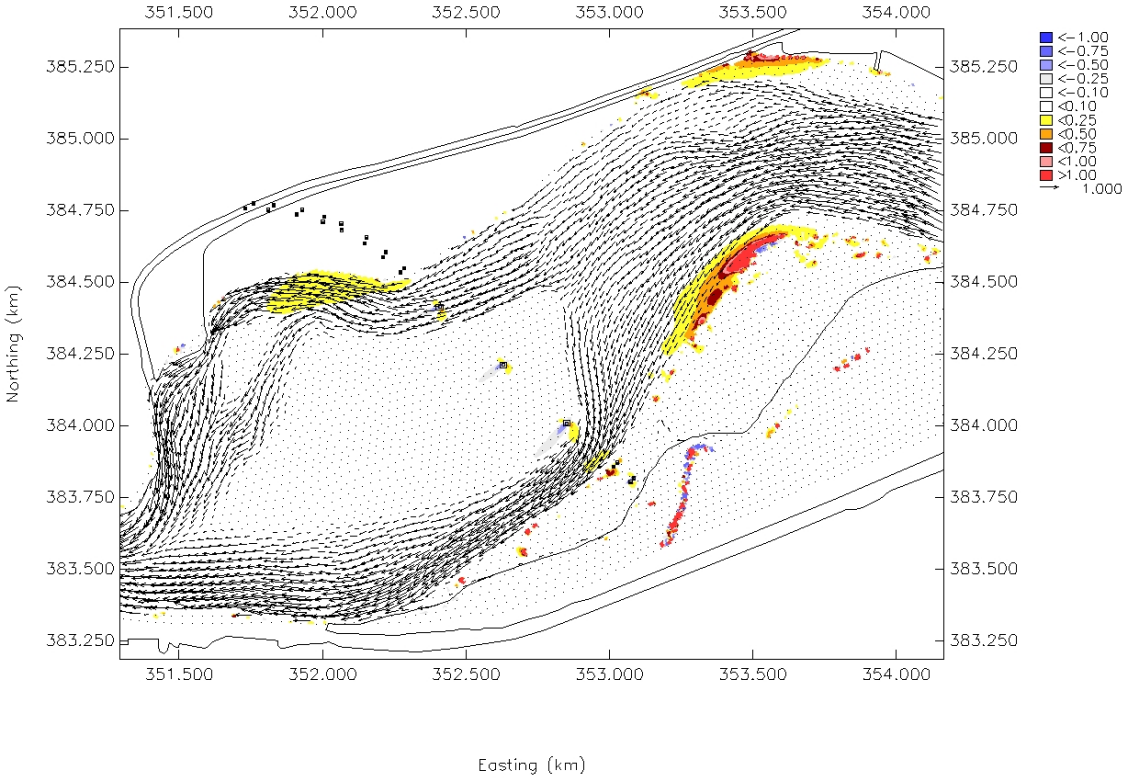
Percentage differences in bed shear stress between the proposed bridge scheme Route 3A Medium 3 Tower revised option and the baseline case for low water (A) and peak flood (B) on a 1:200 surge tide and 1:200 fluvial event. (1 = 100%; 0.1 = 10%).

Figure C69

A.

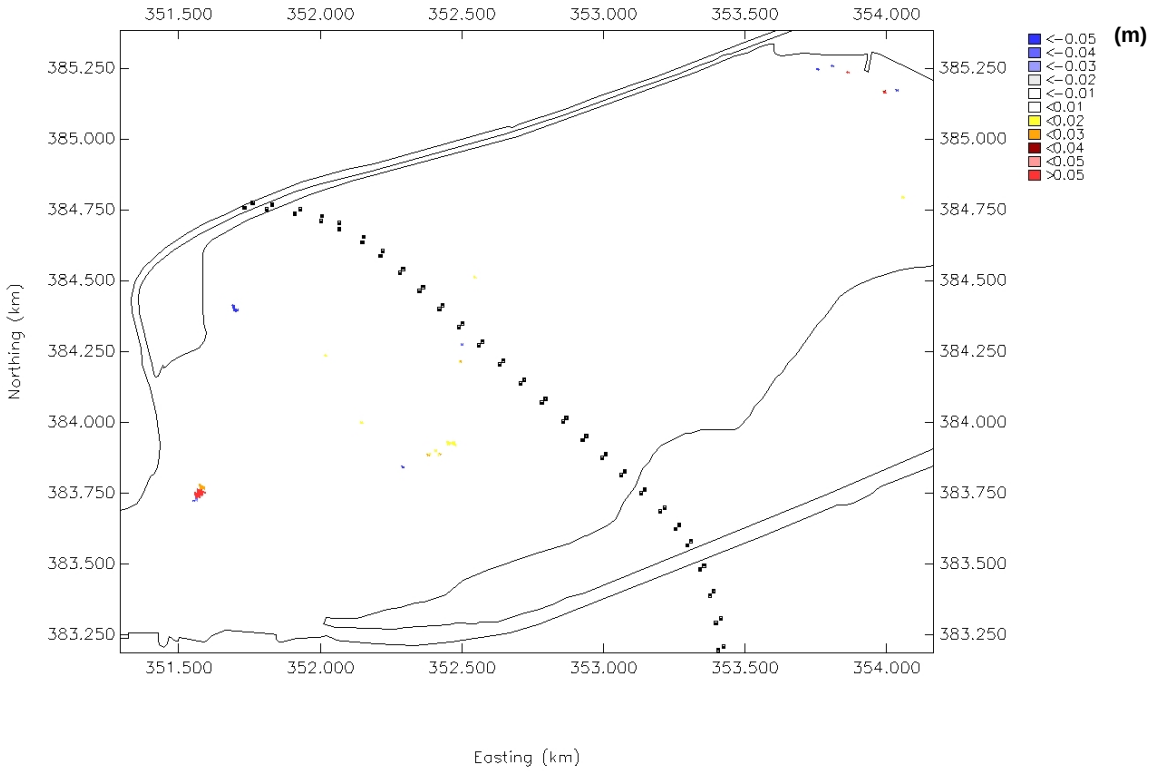


B.

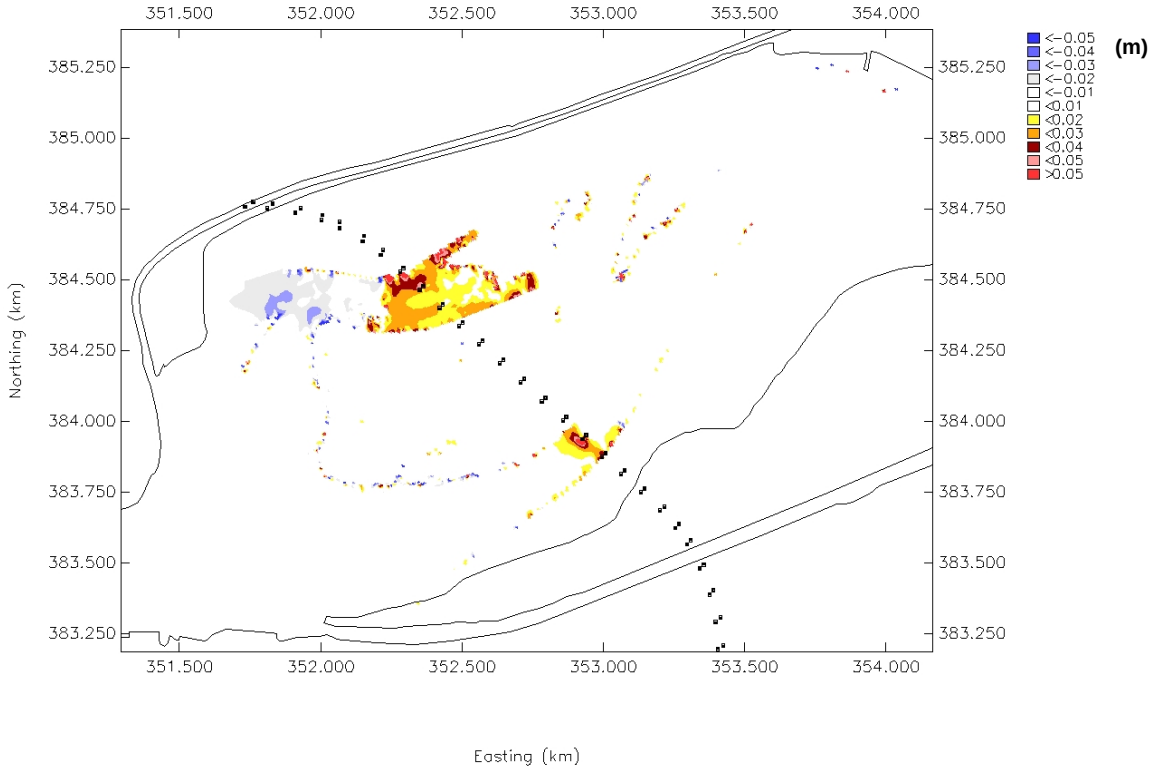


ABP mer marine environmental research	Percentage differences in bed shear stress between the proposed bridge scheme Route 3A Medium 3 Tower revised option and the baseline case for high water (A) and peak ebb (B) on a 1:200 surge tide and 1:200 fluvial event. (1 = 100%; 0.1 = 10%).	Figure C70

A.

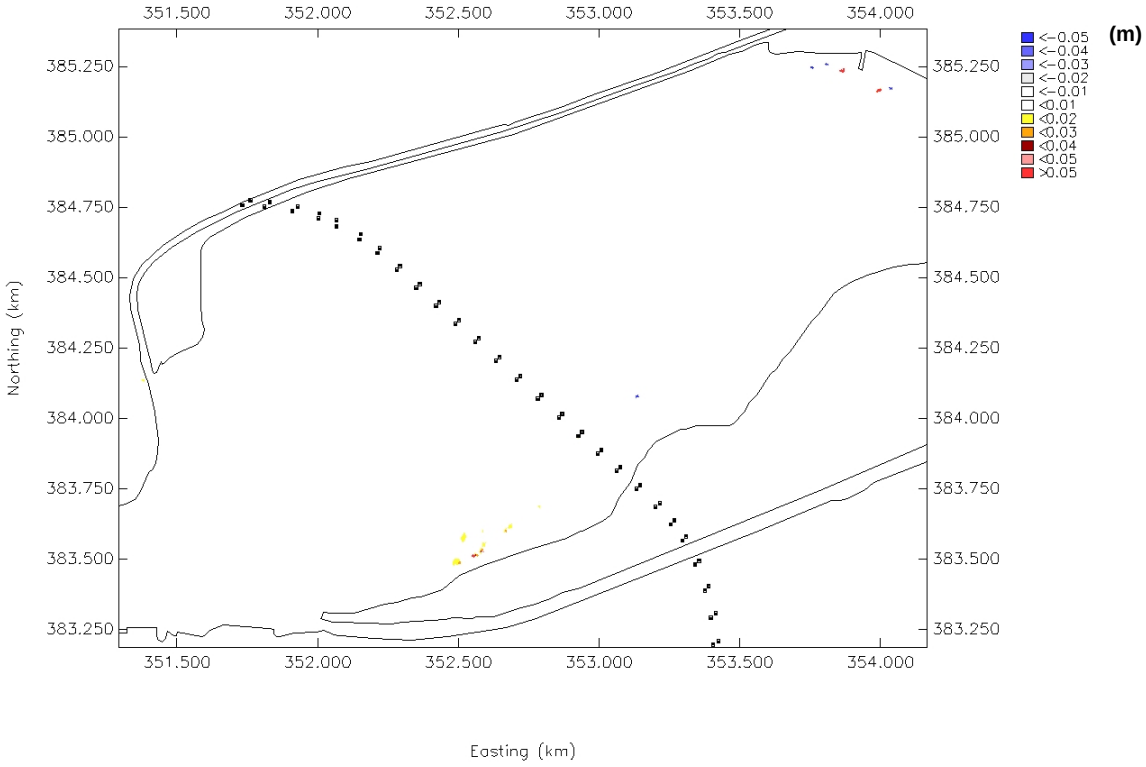


B.

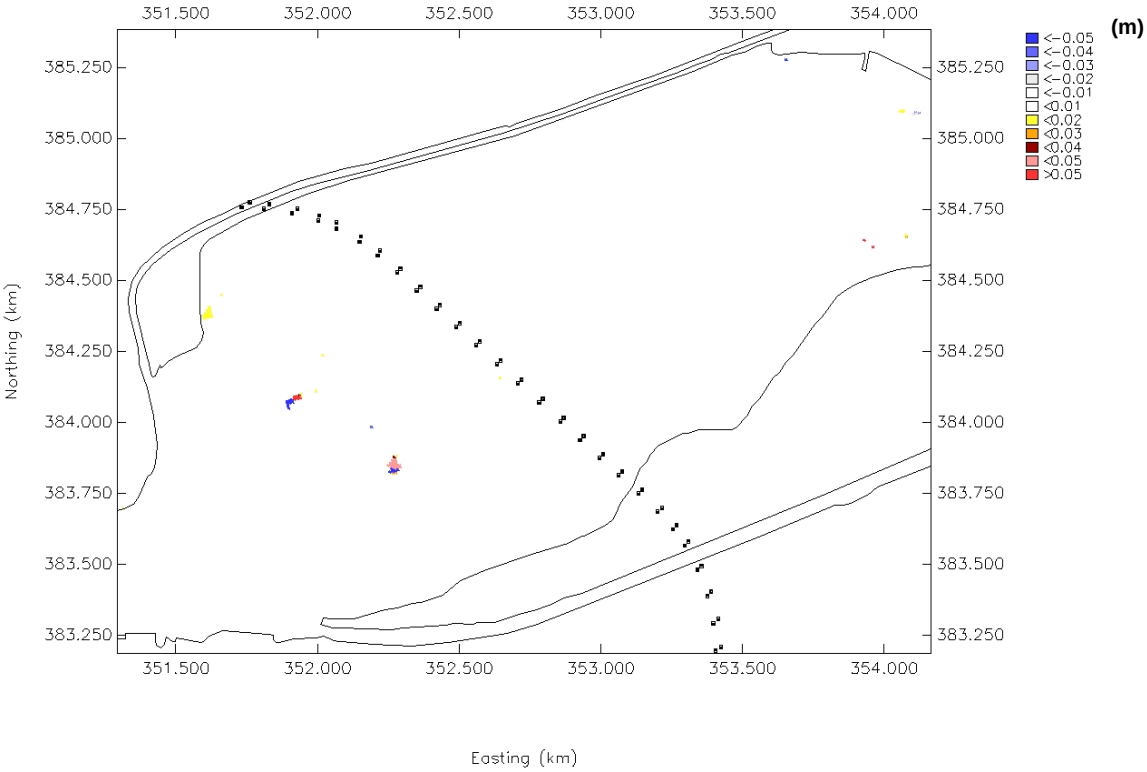


ABP mer marine environmental research	Differences in water level (m) between the proposed bridge scheme Route 3A Short Span revised and the baseline case for low water (A) and peak flood (B) on a spring tide.	Figure C71

A.

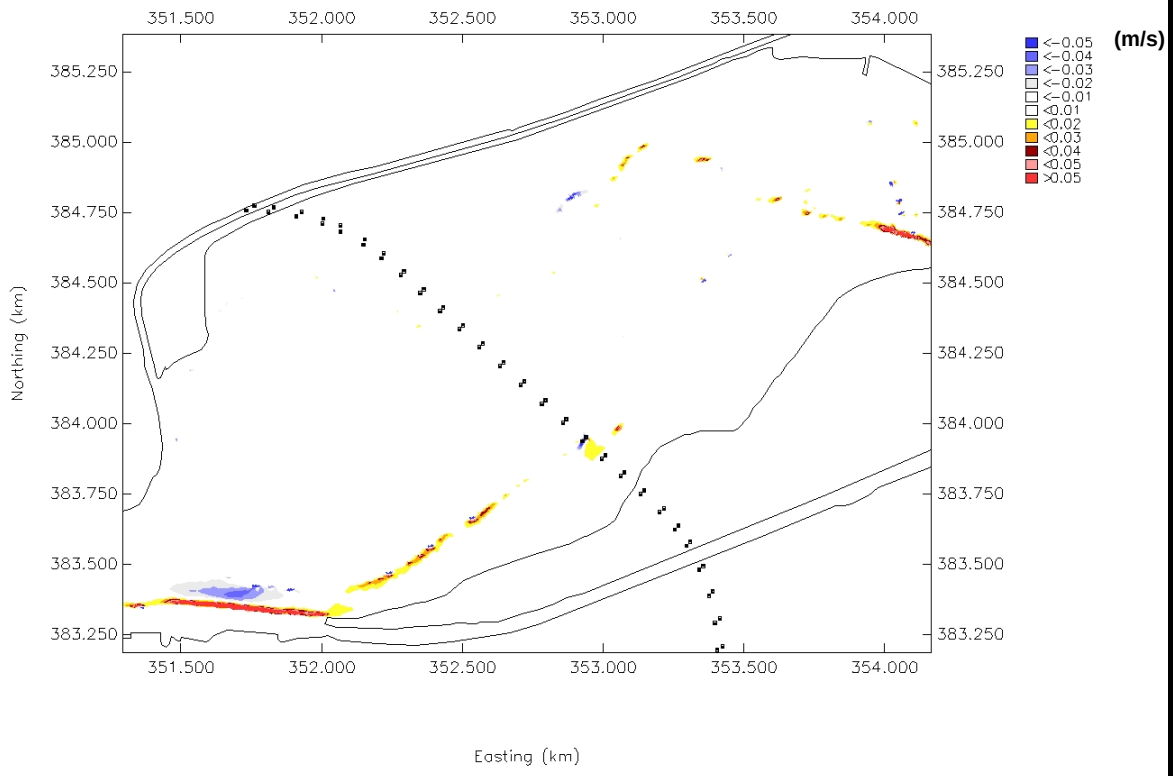


B.

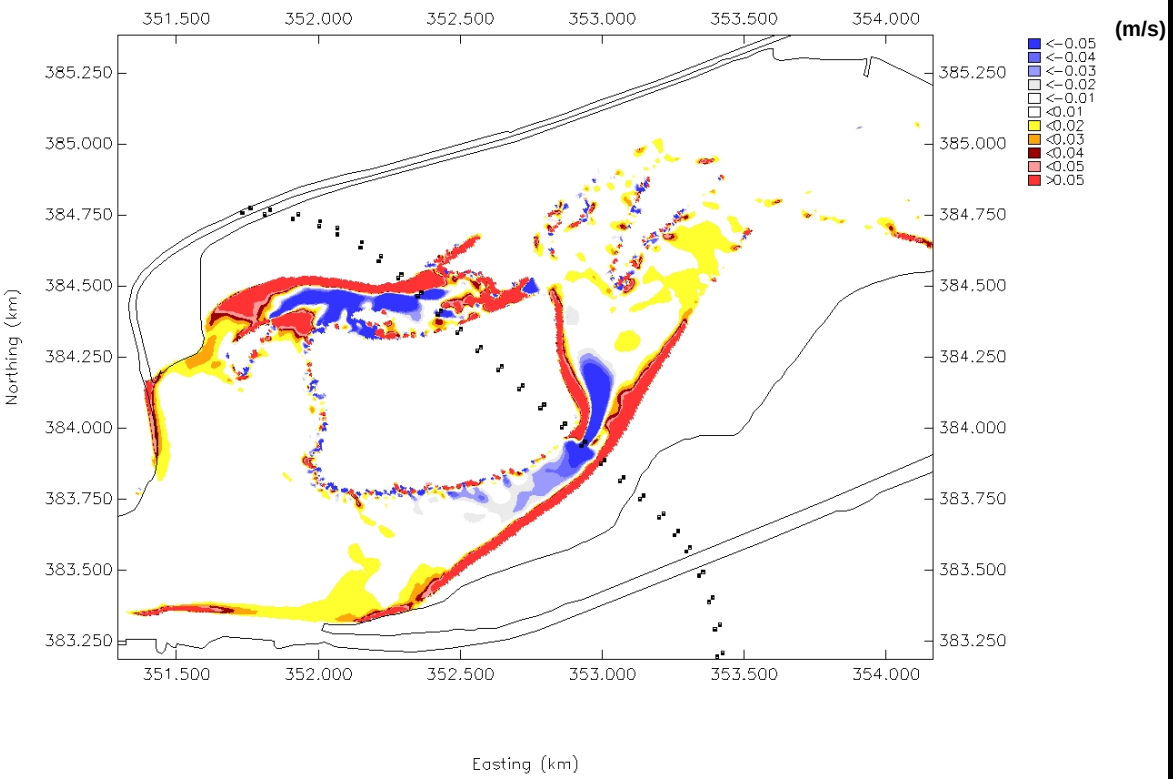


ABP mer marine environmental research	Differences in water level (m) between the proposed bridge scheme Route 3A Short Span revised and the baseline case for high water (A) and peak ebb (B) on a spring tide.	Figure C72

A.



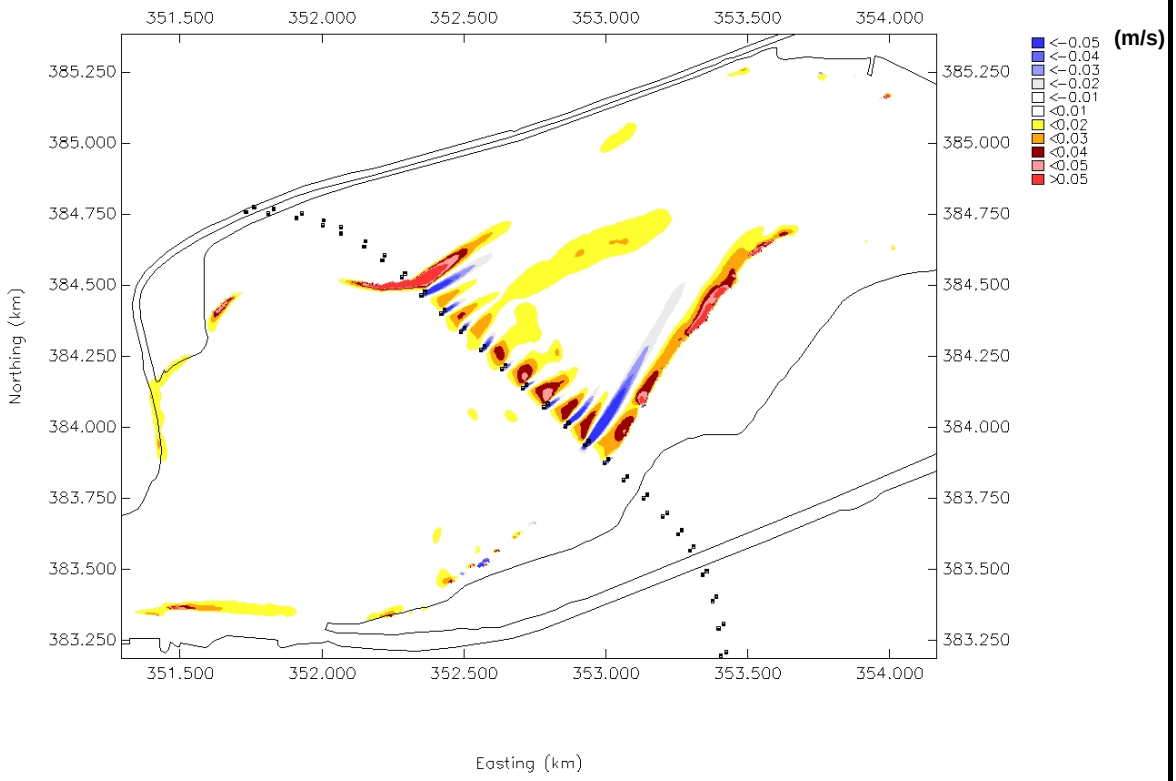
B.



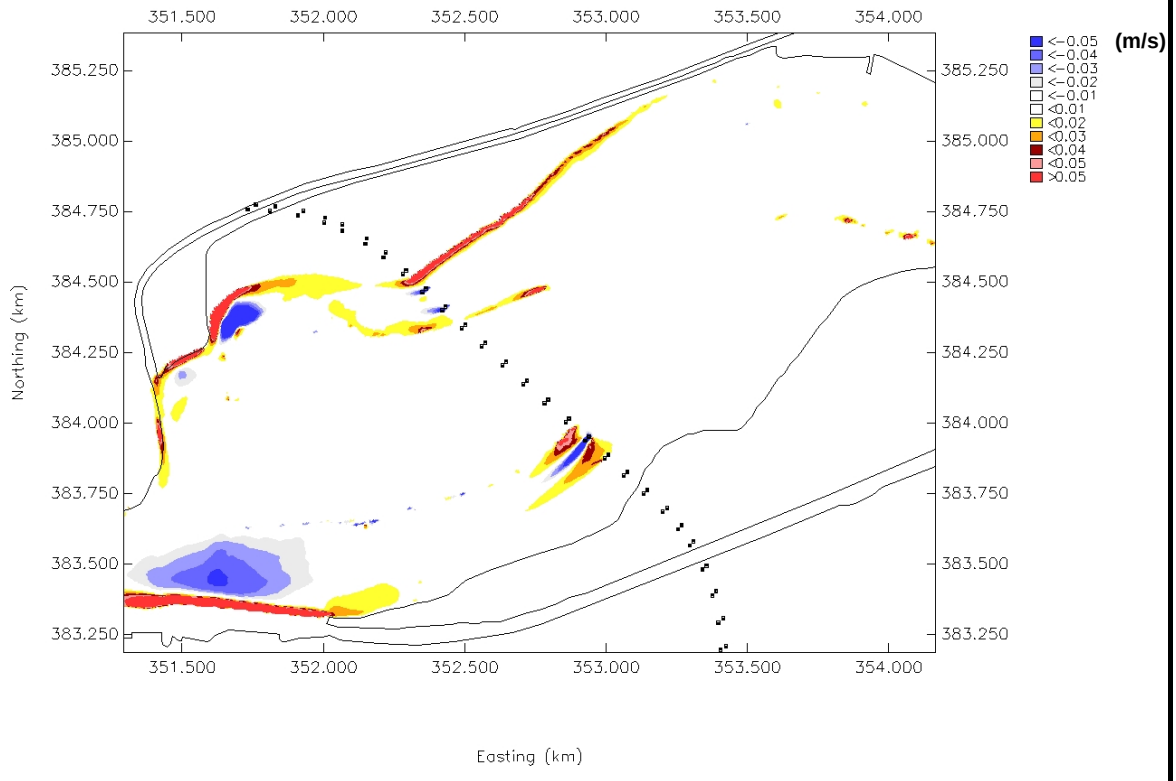
Differences in near-surface speed (m/s) between the proposed bridge scheme Route 3A Short Span revised and the baseline case for low water (A) and peak flood (B) on a spring tide.

Figure C73

A.

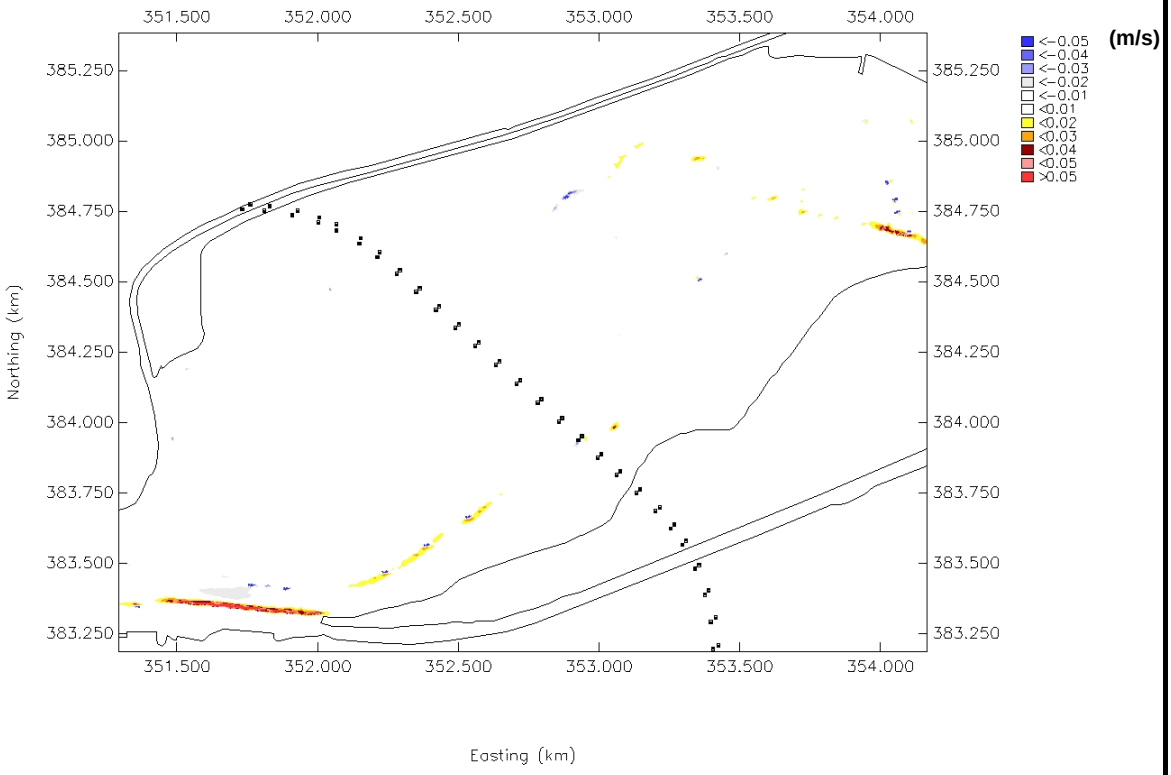


B.

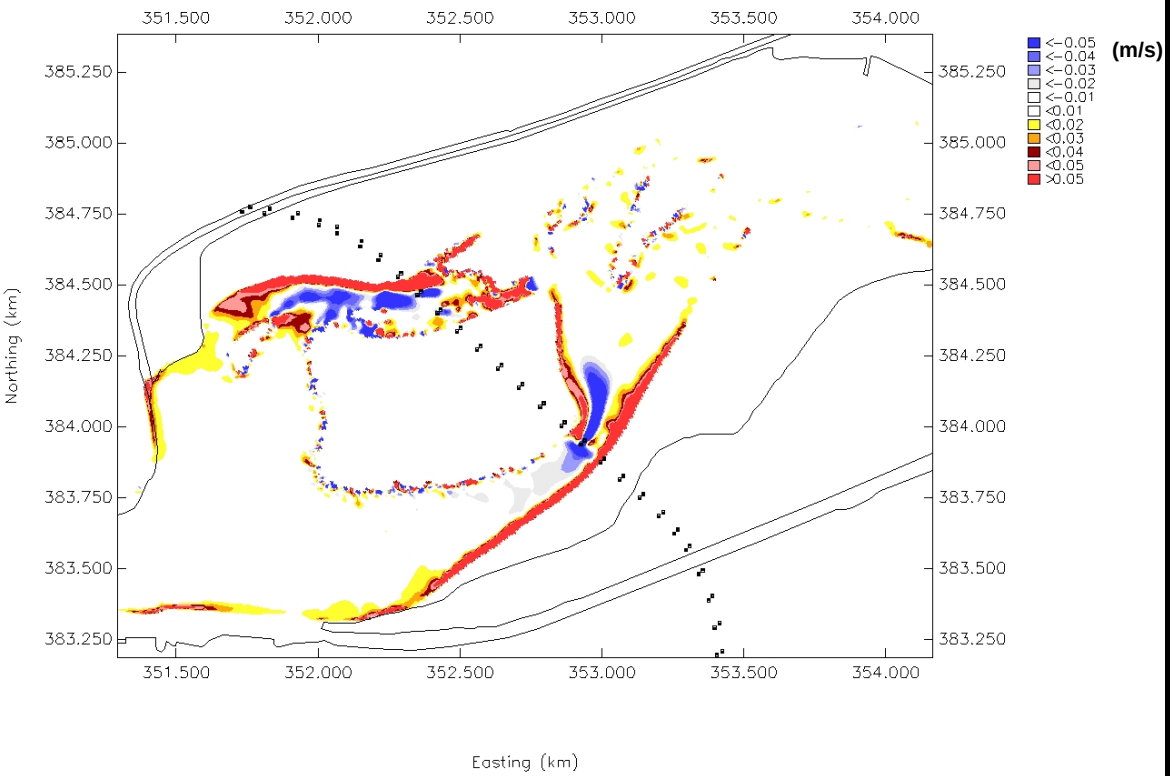


ABP mer marine environmental research	Differences in near-surface speed (m/s) between the proposed bridge scheme Route 3A Short Span revised and the baseline case for high water (A) and peak ebb (B) on a spring tide.	Figure C74

A.

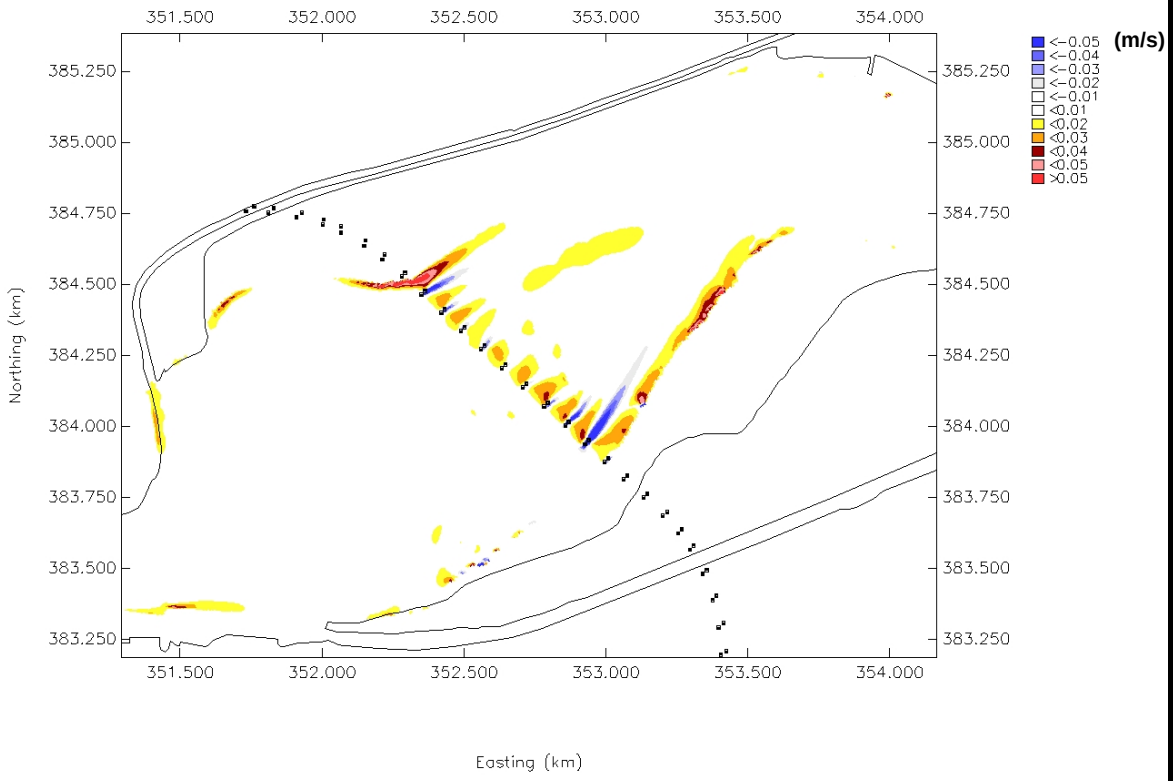


B.

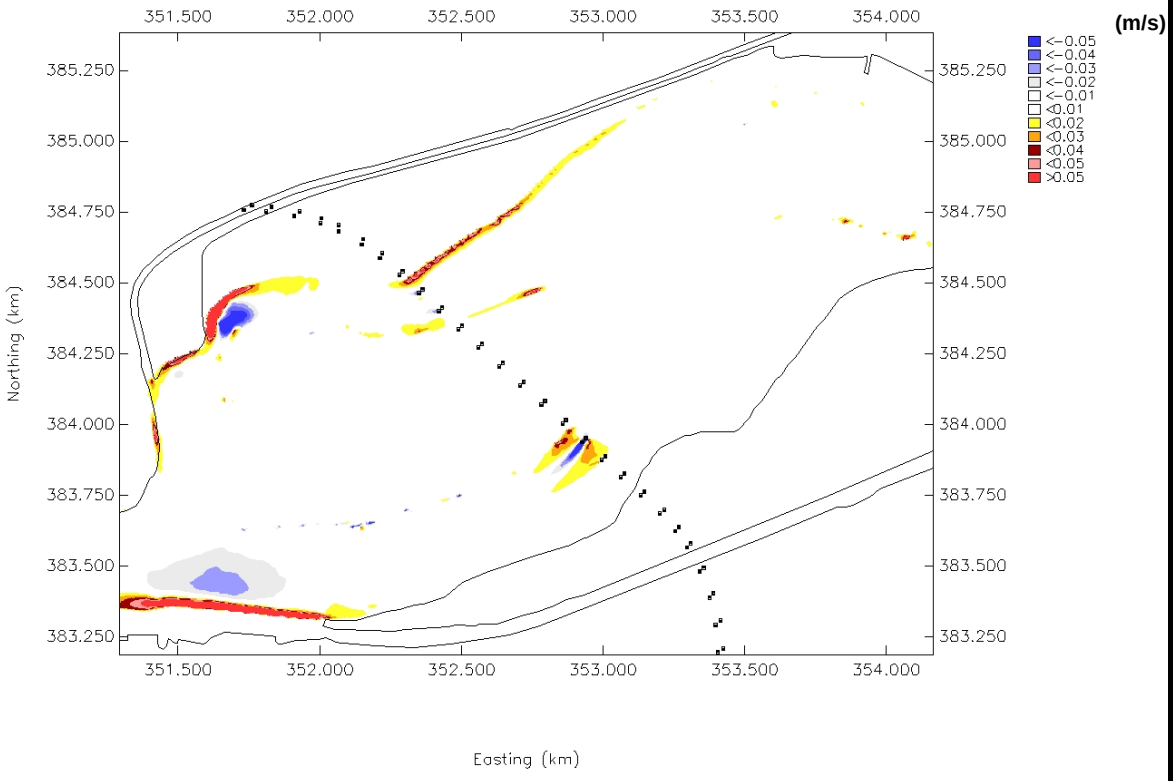


ABP mer marine environmental research	Differences in near-bed speed (m/s) between the proposed bridge scheme Route 3A Short Span revised and the baseline case for low water (A) and peak flood (B) on a spring tide.	Figure C75

A.

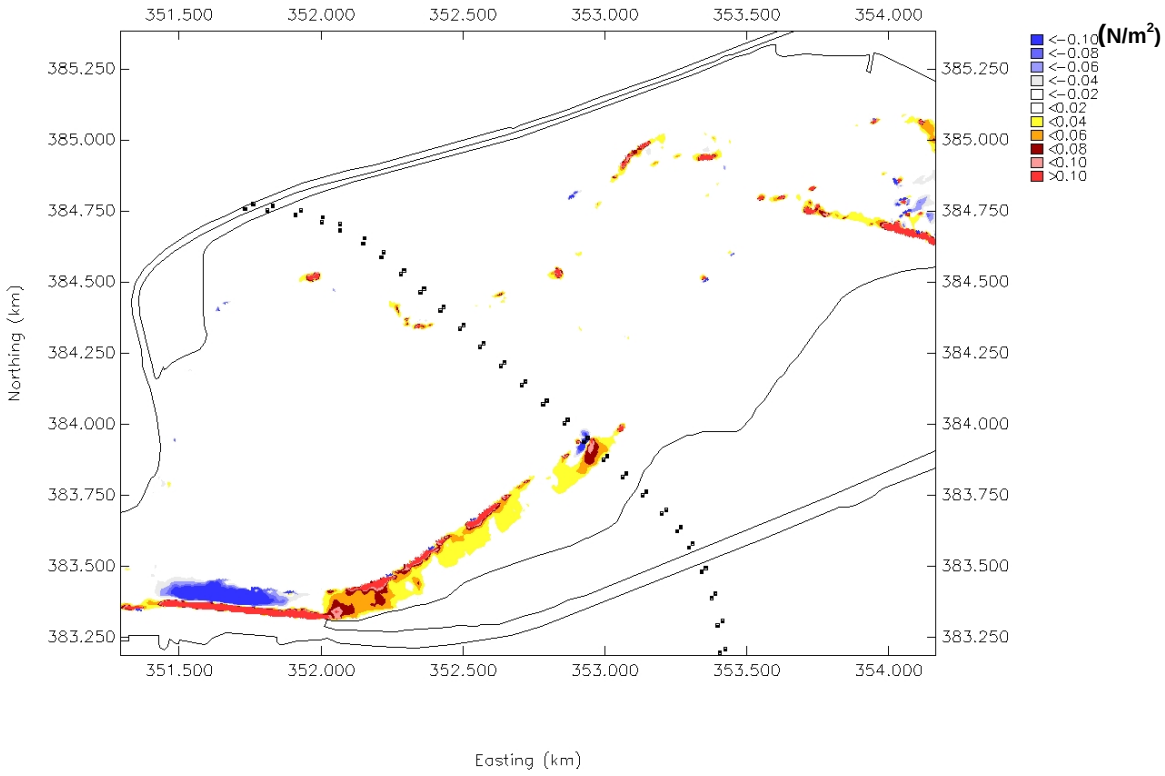


B.

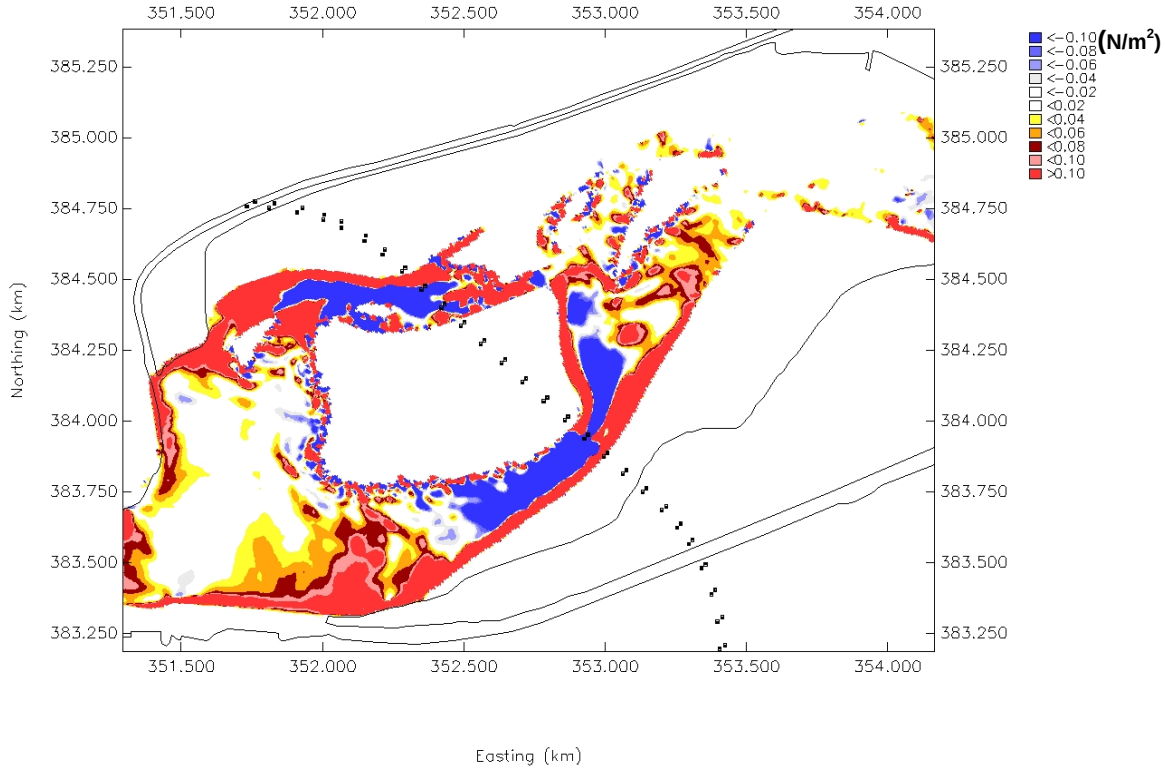


ABP mer marine environmental research	Differences in near-bed speed (m/s) between the proposed bridge scheme Route 3A Short Span revised and the baseline case for high water (A) and peak ebb (B) on a spring tide.	Figure C76

A.



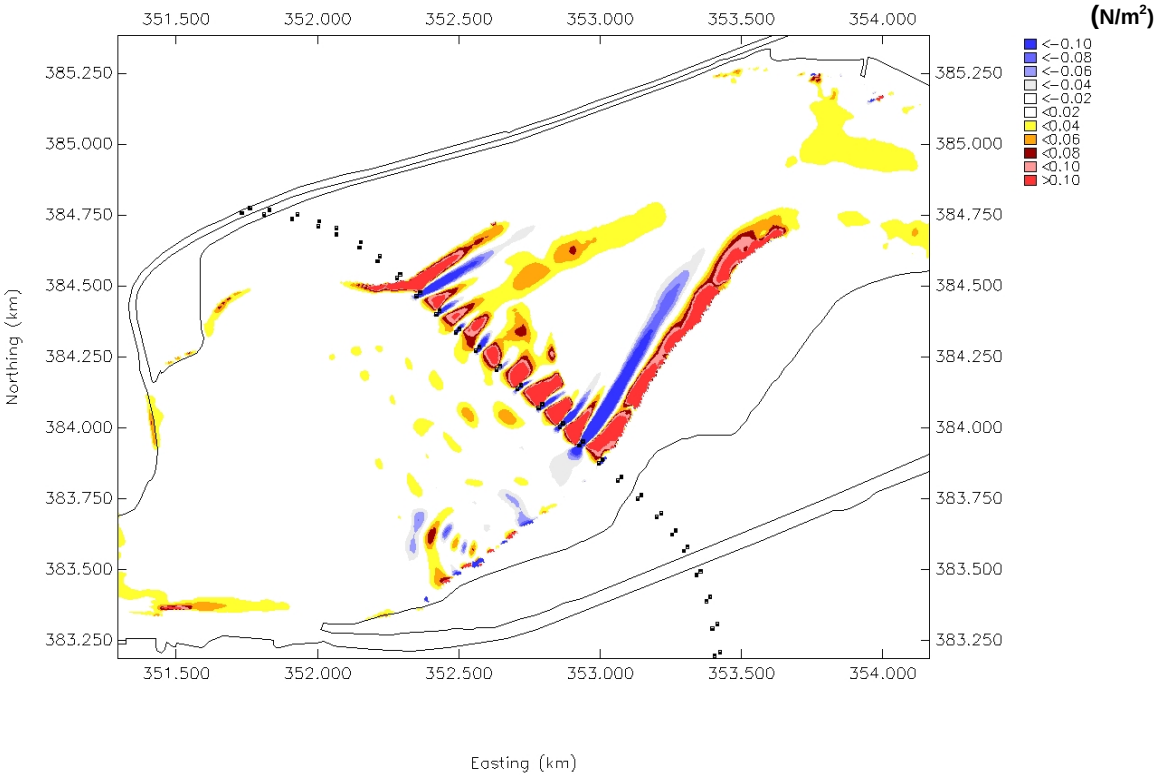
B.



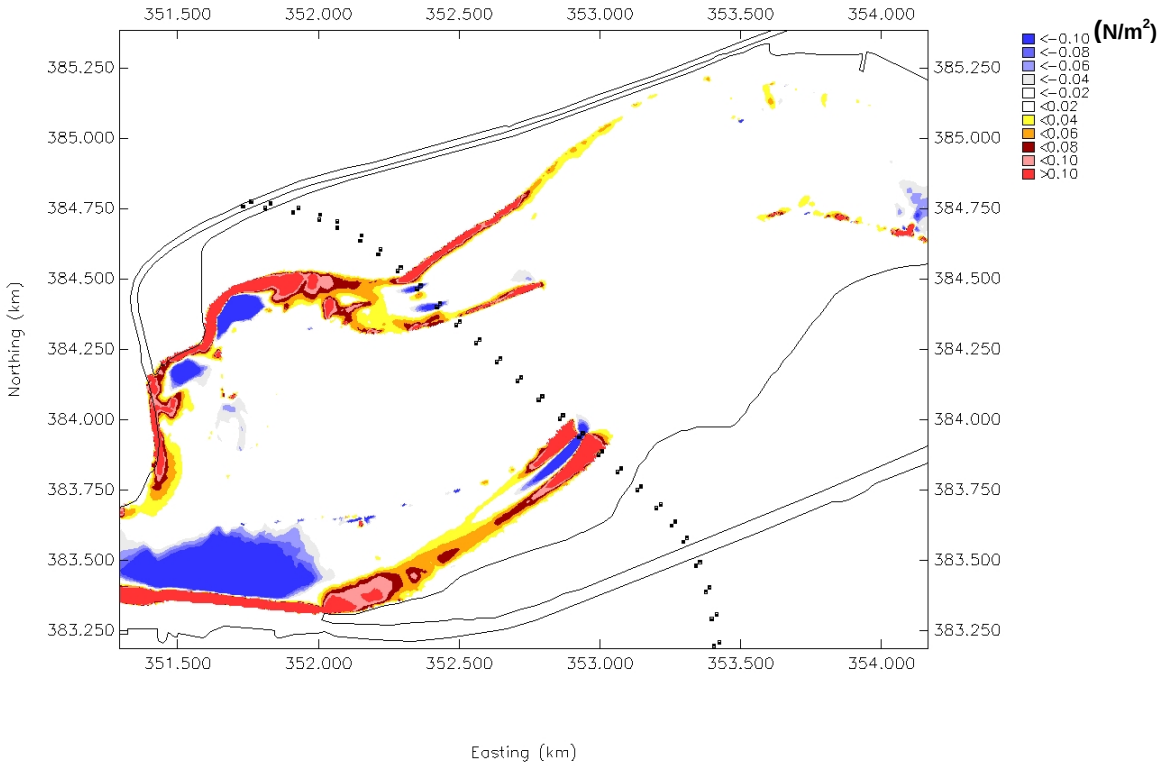
Differences in bed shear stress (N/m²) between the proposed bridge scheme Route 3A Short Span revised and the baseline case for low water (A) and peak flood (B) on a spring tide.

Figure C77

A.



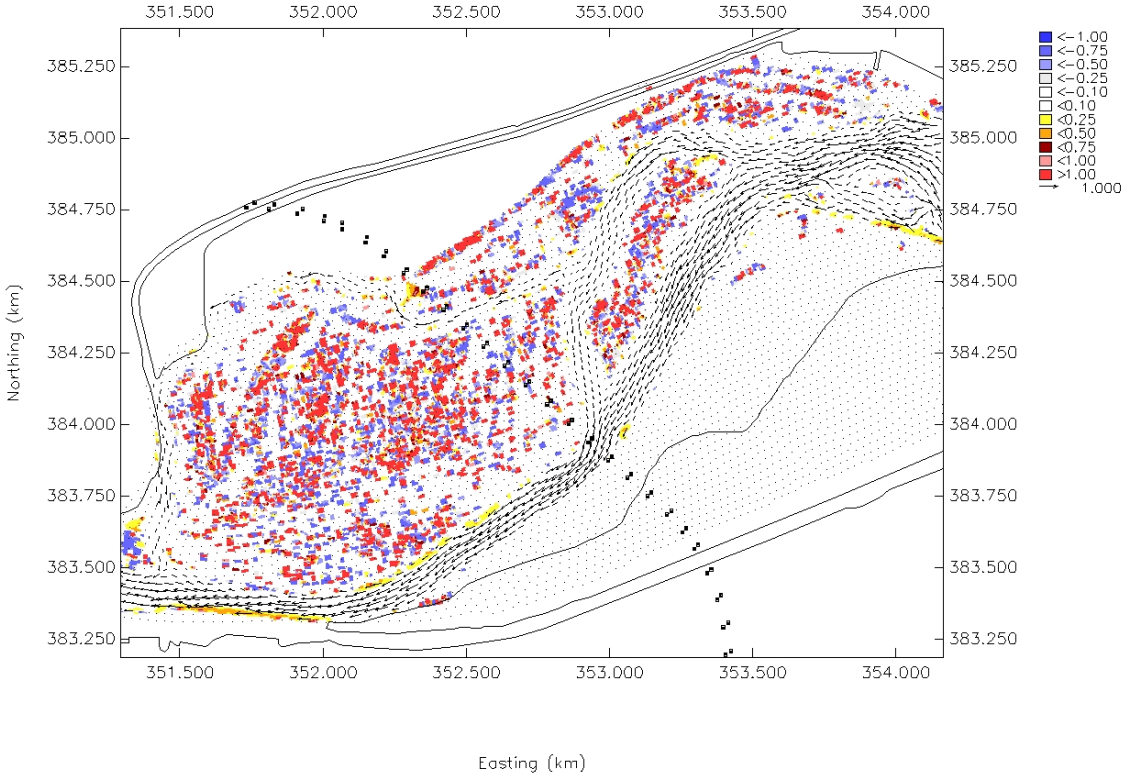
B.



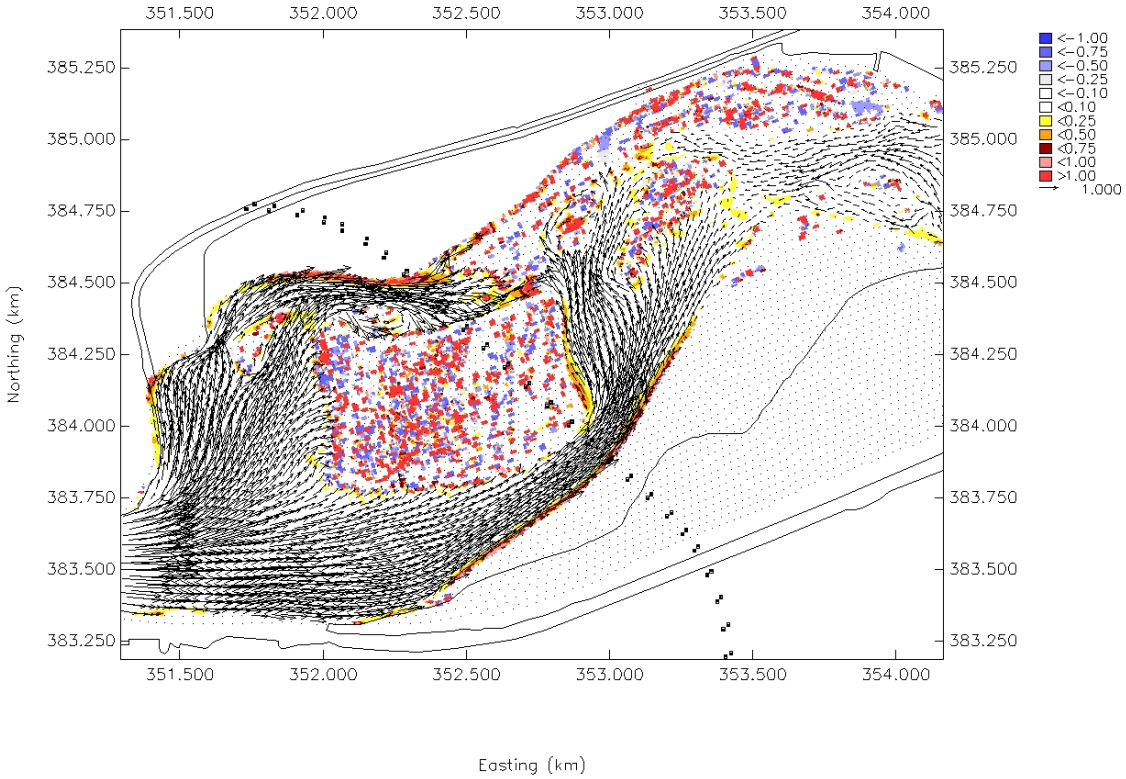
Differences in bed shear stress (N/m²) between the proposed bridge scheme Route 3A Short Span revised and the baseline case for high water (A) and peak ebb (B) on a spring tide.

Figure C78

A.



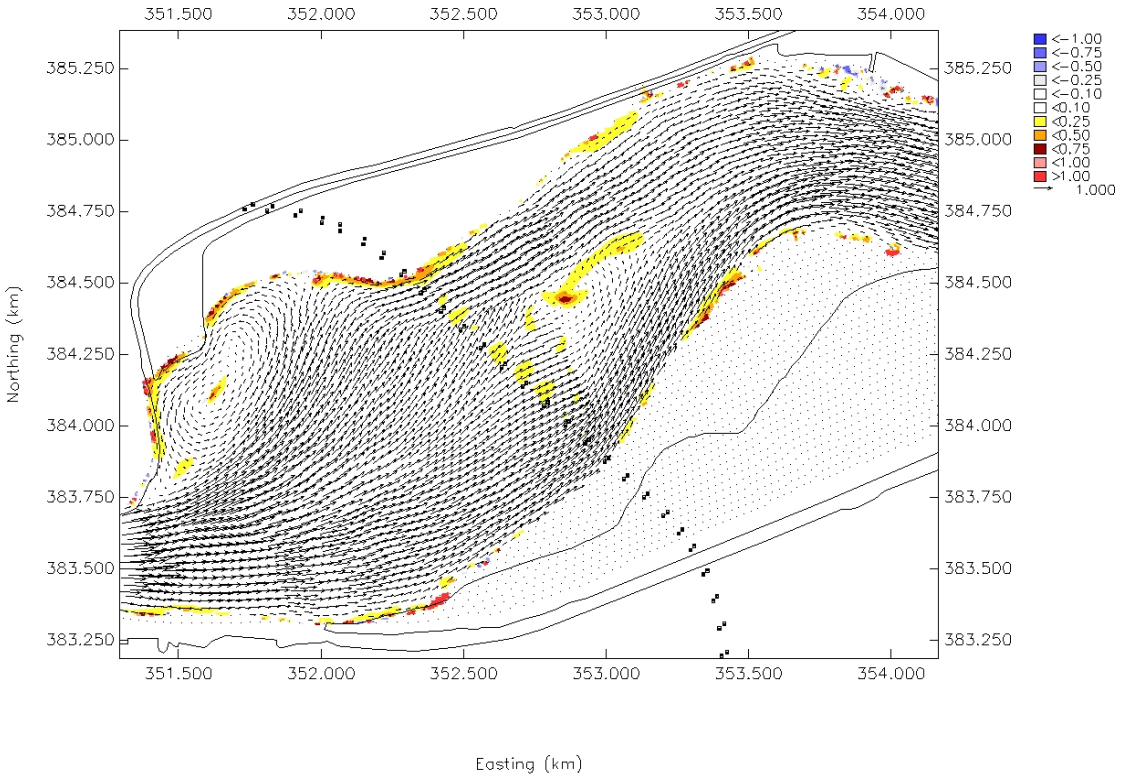
B.



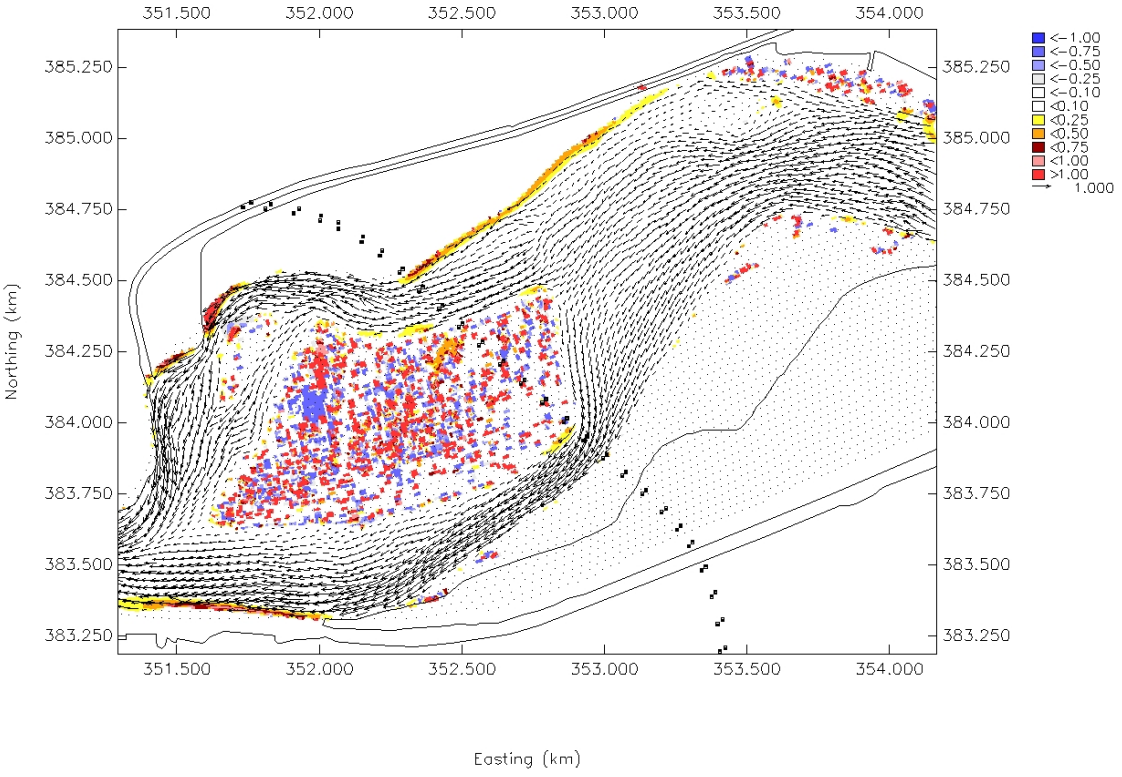
Percentage differences in bed shear stress between the proposed bridge scheme Route 3A Short Span revised and the baseline case for low water (A) and peak flood (B) on a spring tide. (1 = 100%; 0.1 = 10%).

Figure C79

A.

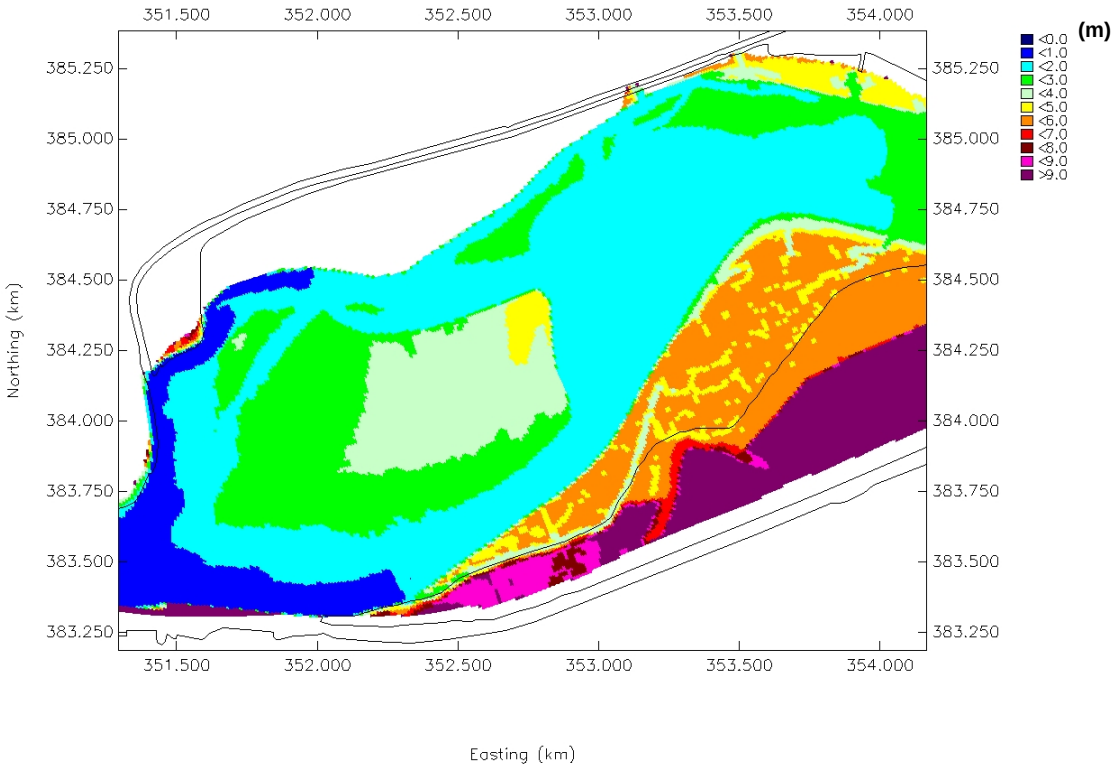


B.

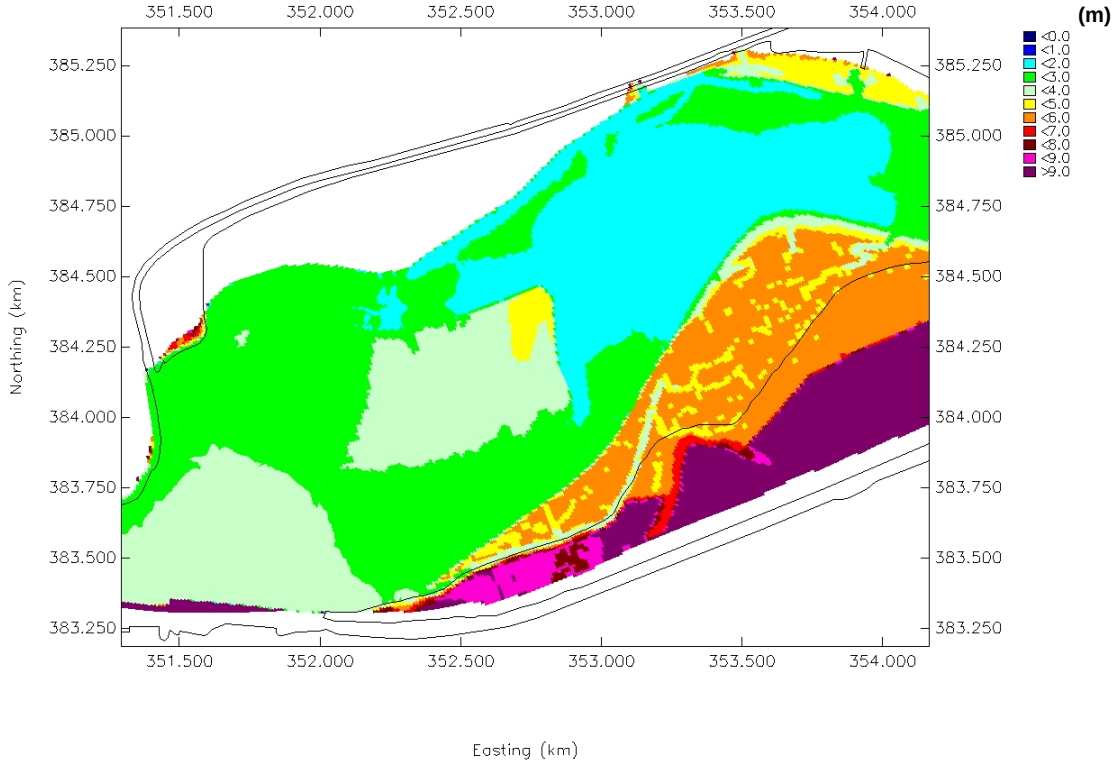


ABP mer marine environmental research	Percentage differences in bed shear stress between the proposed bridge scheme Route 3A Short Span revised and the baseline case for high water (A) and peak ebb (B) on a spring tide. (1 = 100%; 0.1 = 10%).	Figure C80

A.



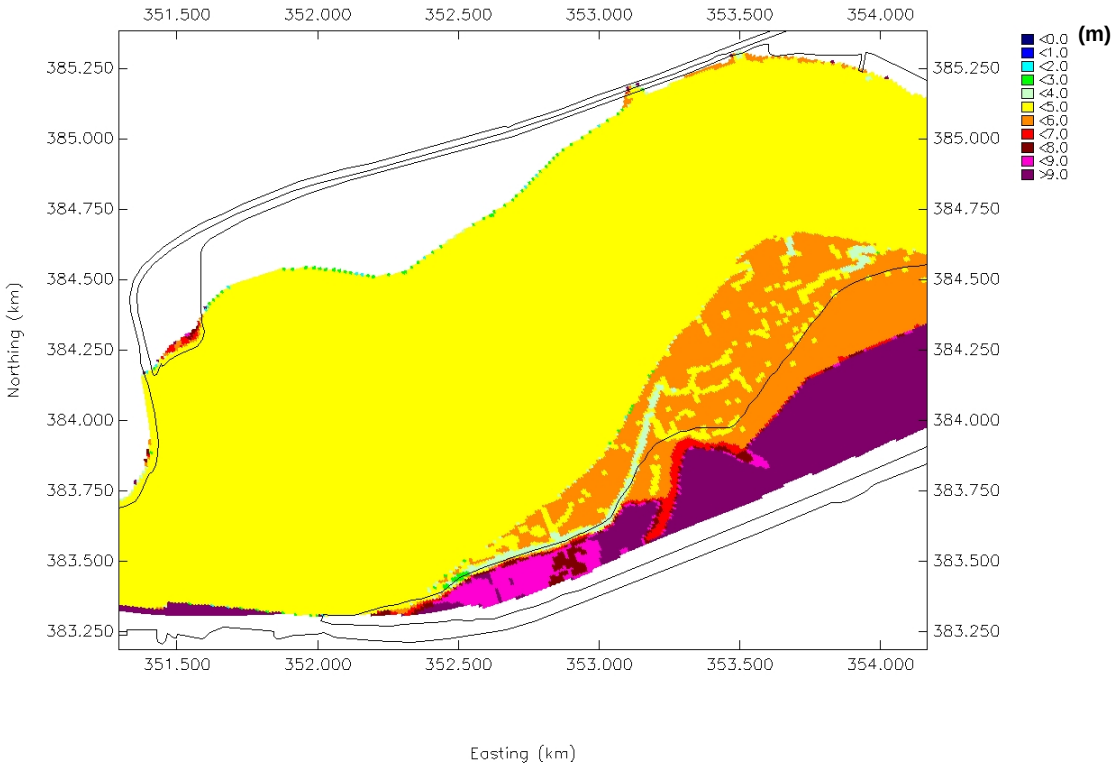
B.



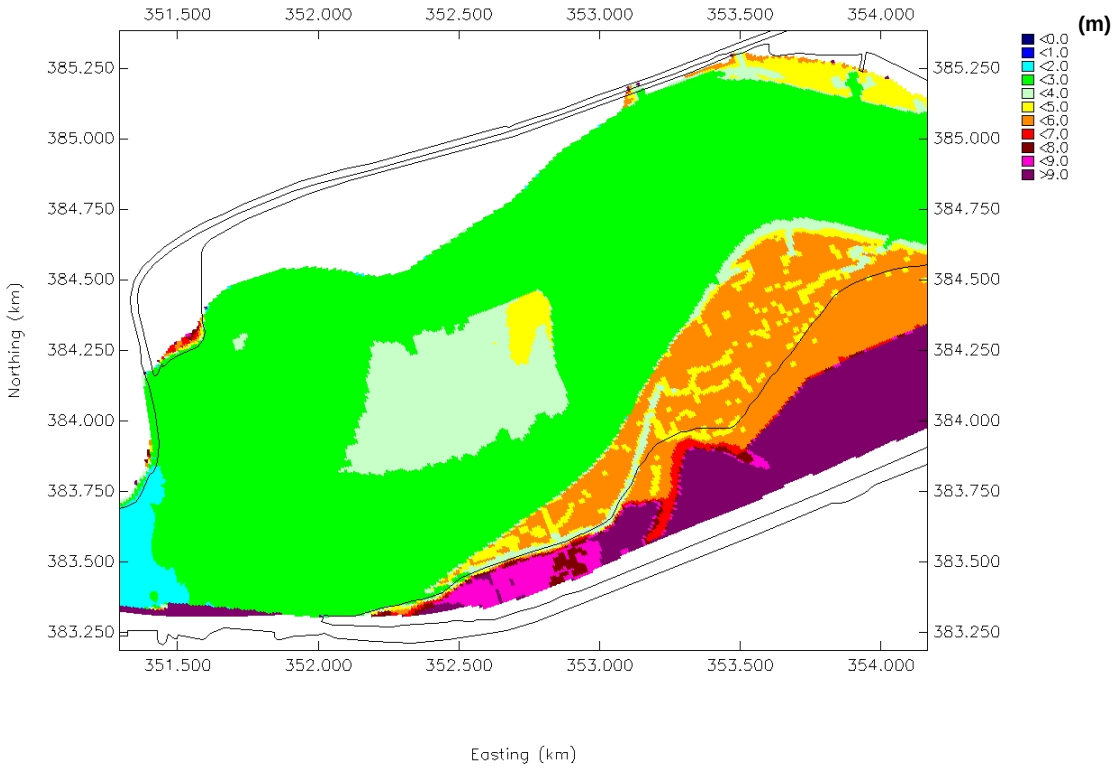
Actual water level (m) in baseline case for low water (A) and peak flood (B) on a spring tide.

Figure C81

A.



B.

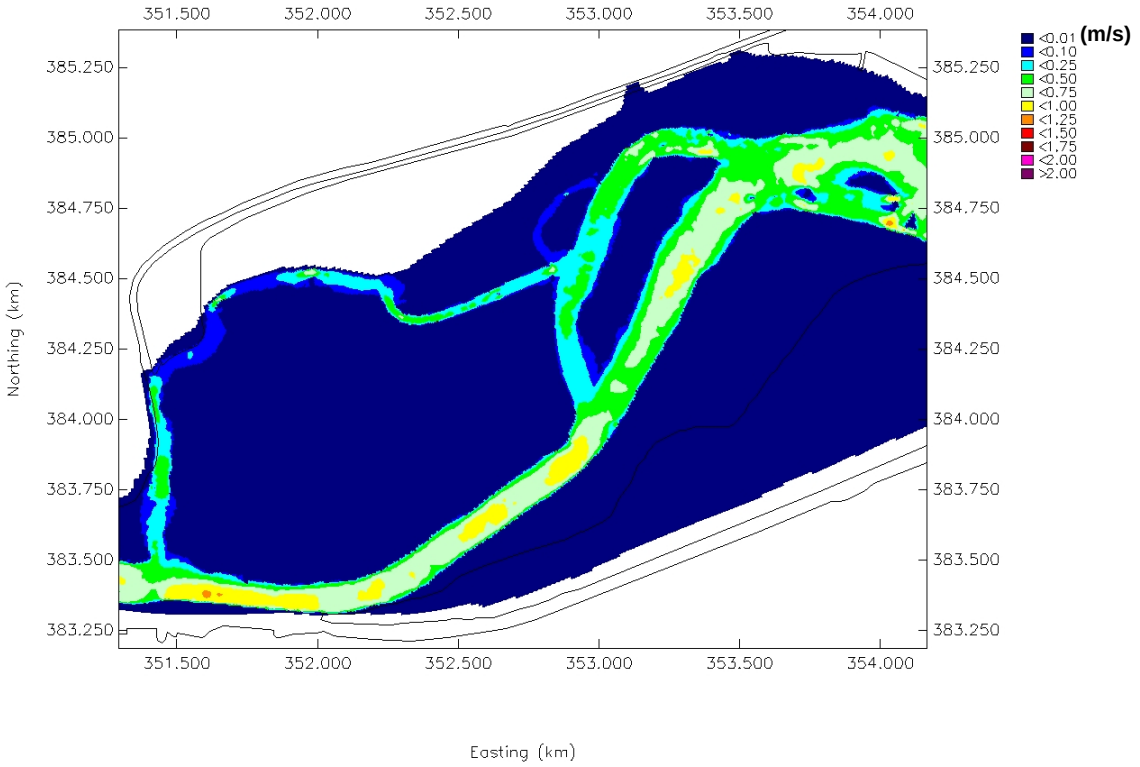


ABP mer marine environmental research

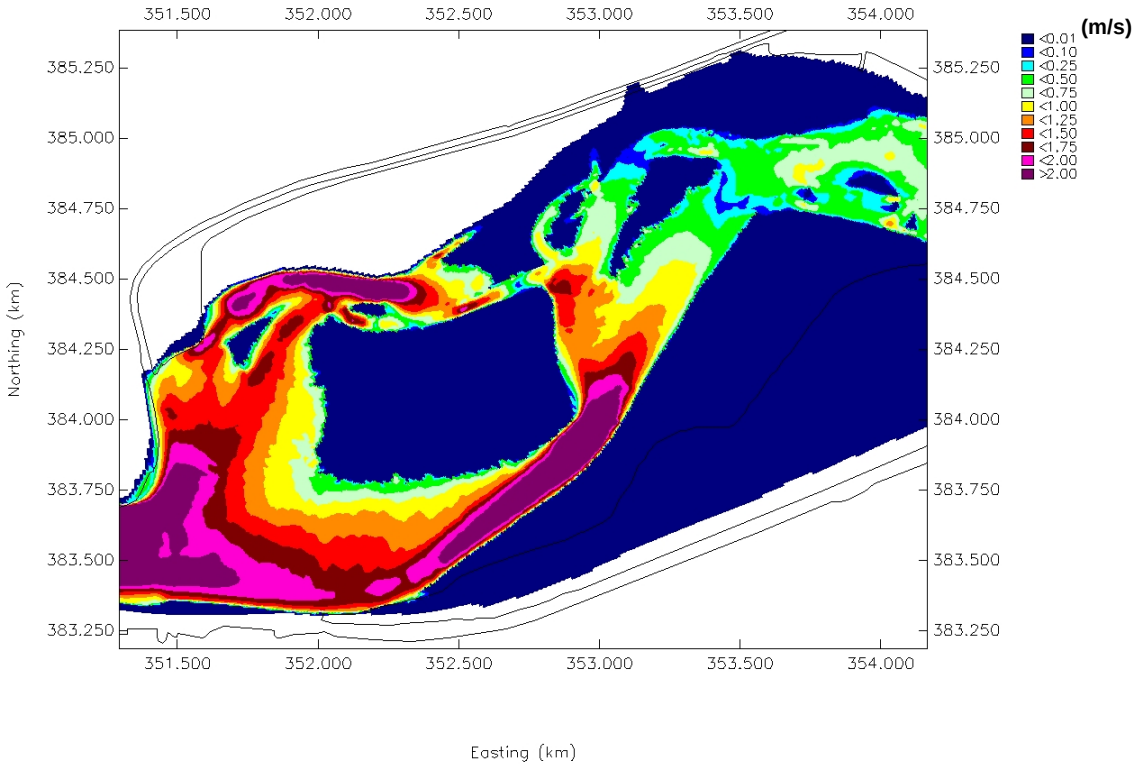
Actual water level (m) in baseline case for high water (A) and peak ebb (B) on a spring tide.

Figure C82

A.



B.

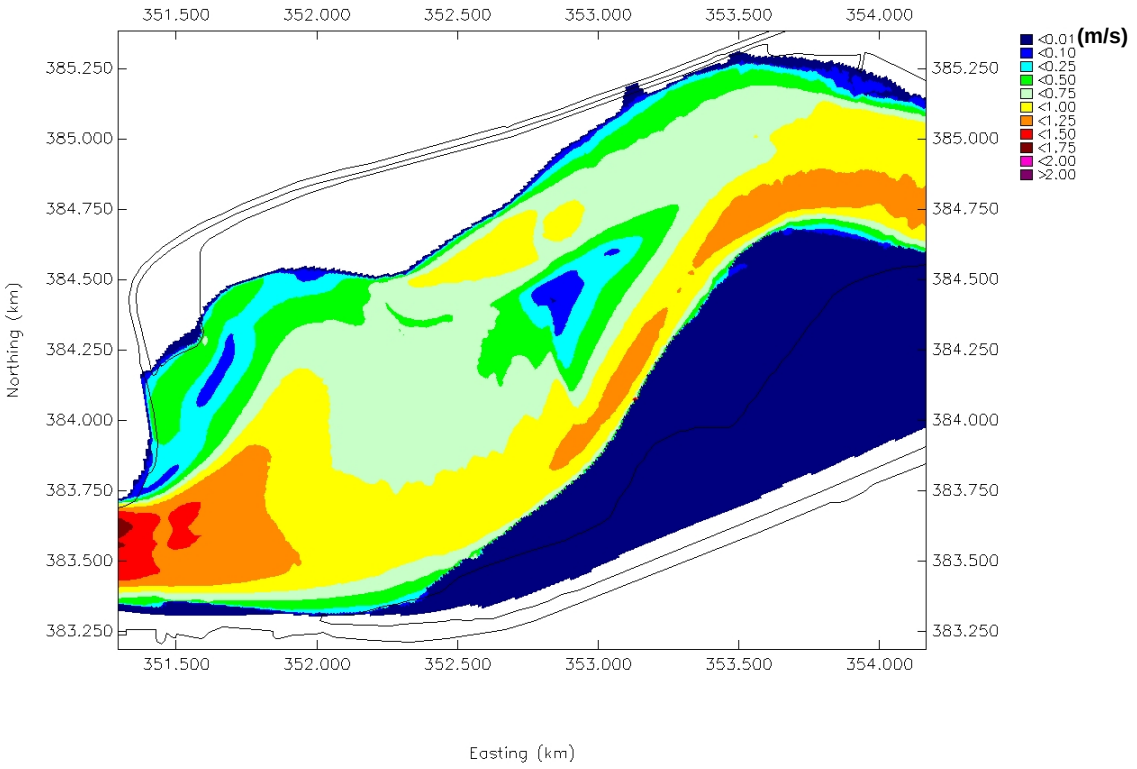


ABP mer marine environmental research

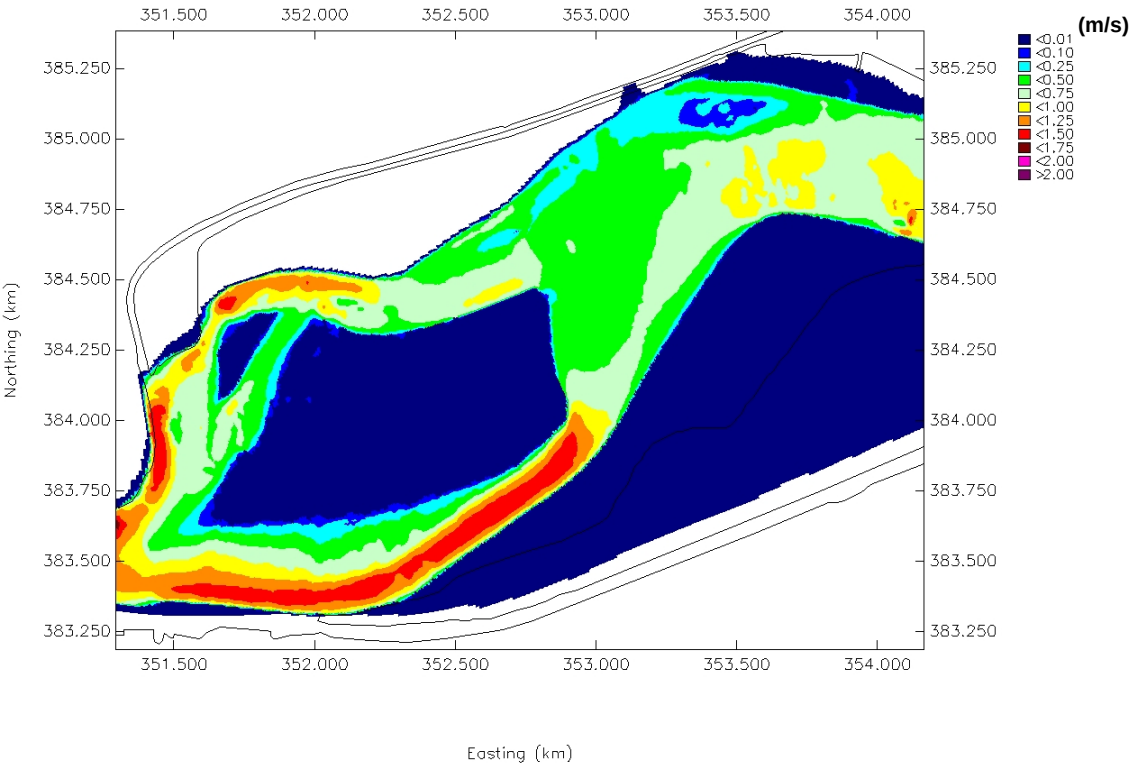
Actual near-surface speed (m/s) in the baseline case for low water (A) and peak flood (B) on a spring tide.

Figure C83

A.



B.

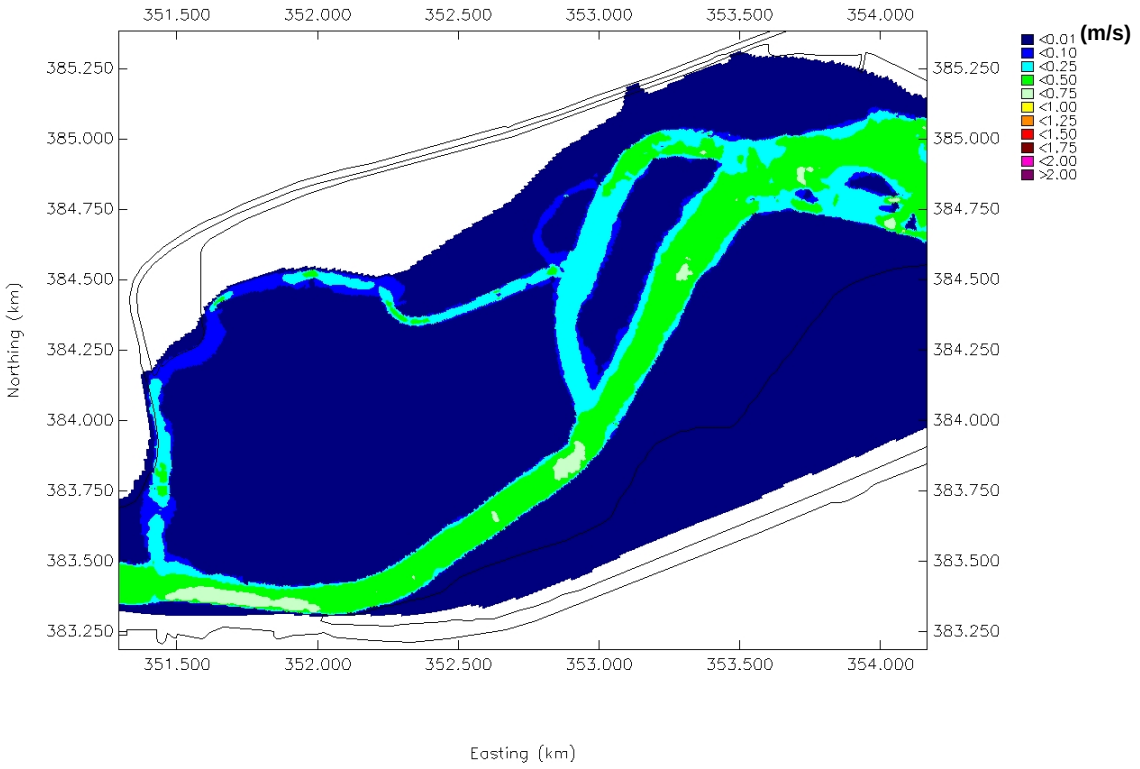


ABP mer marine environmental research

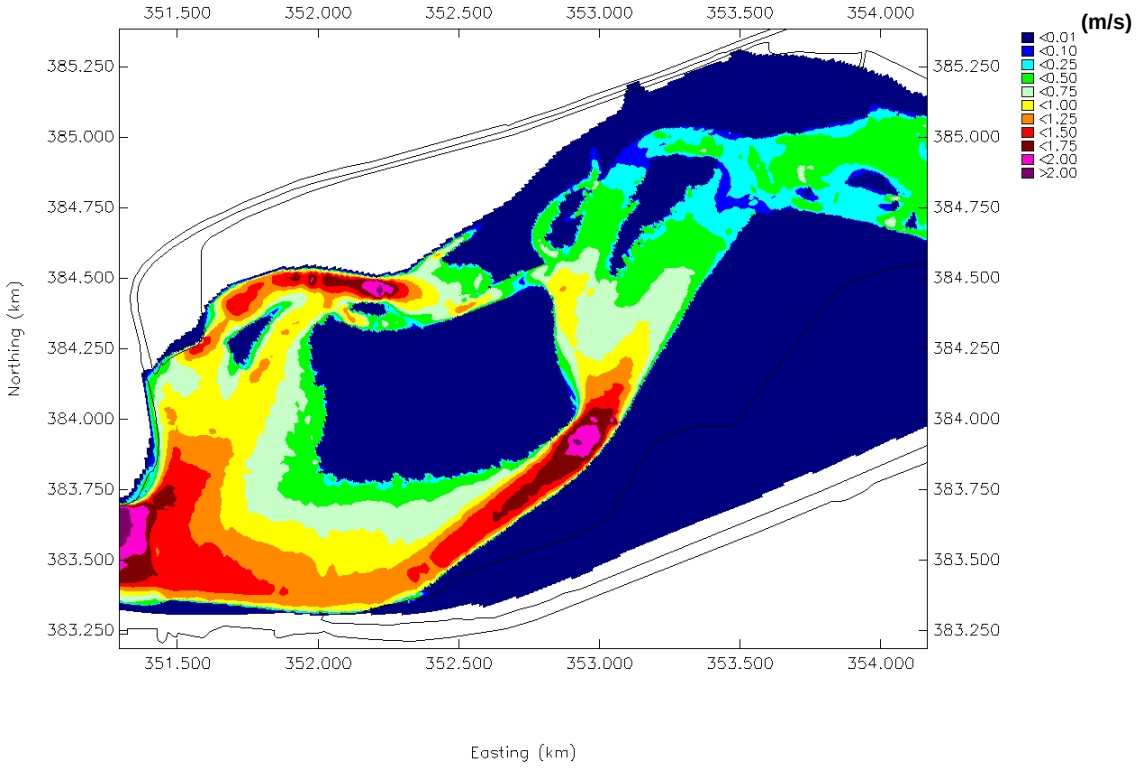
Actual near-surface speed (m/s) in the baseline case for high water (A) and peak ebb (B) on a spring tide.

Figure C84

A.



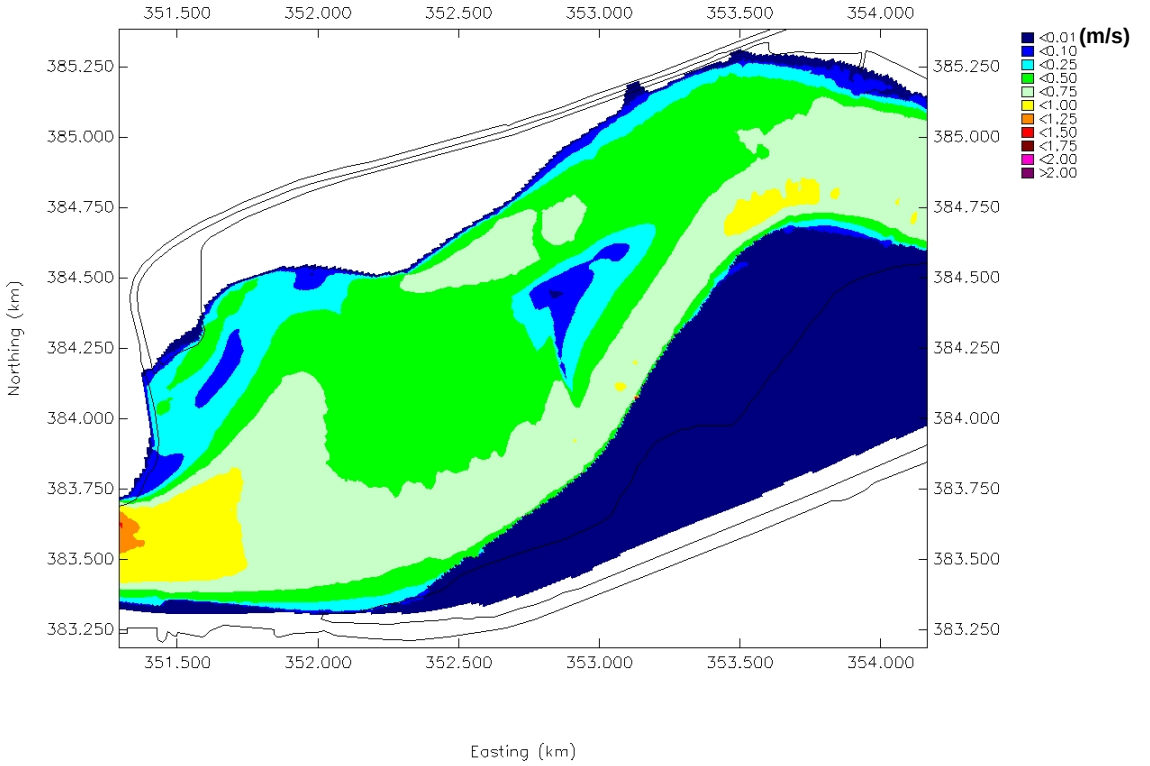
B.



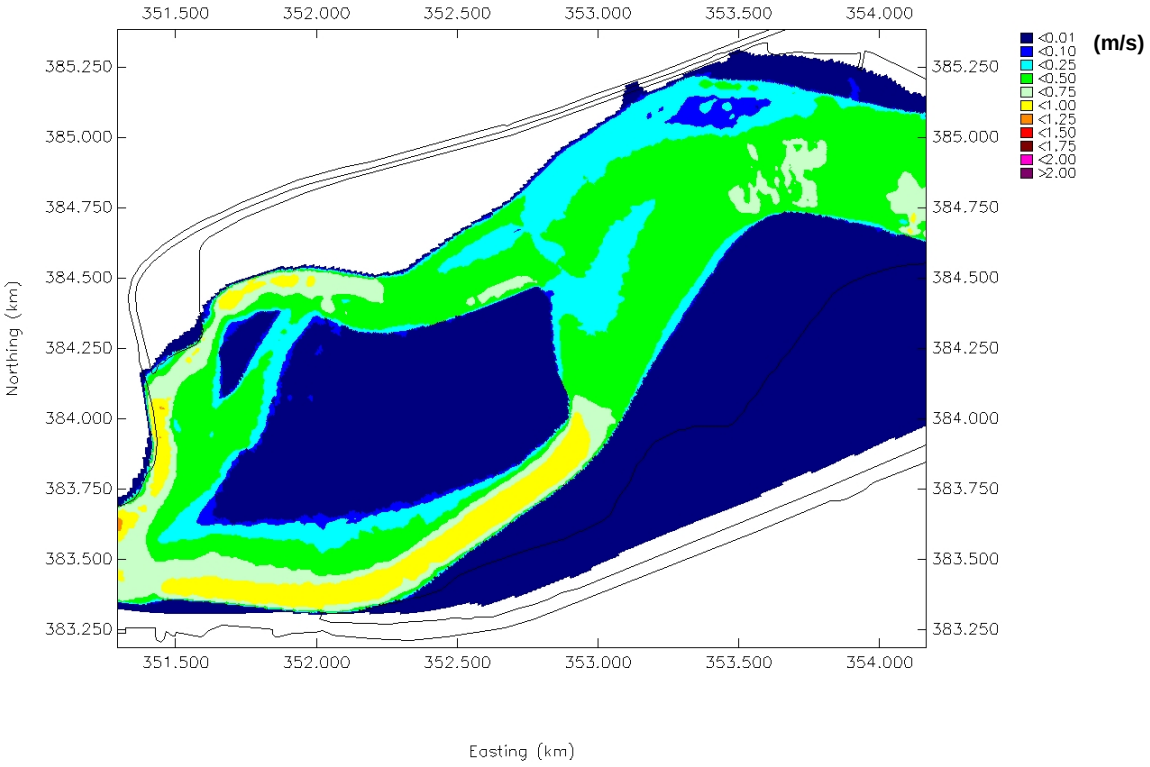
Actual near-bed speed (m/s) in the baseline case for low water (A) and peak flood (B) on a spring tide.

Figure C85

A.



B.

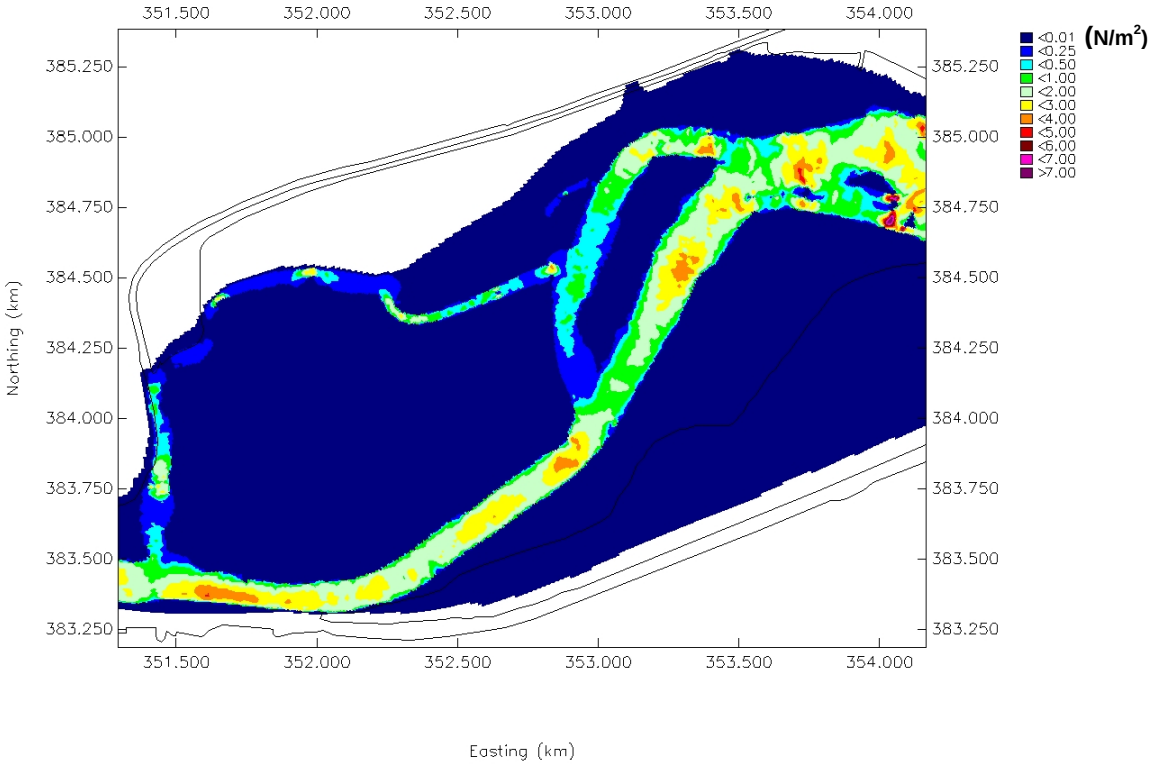


ABP mer marine environmental research

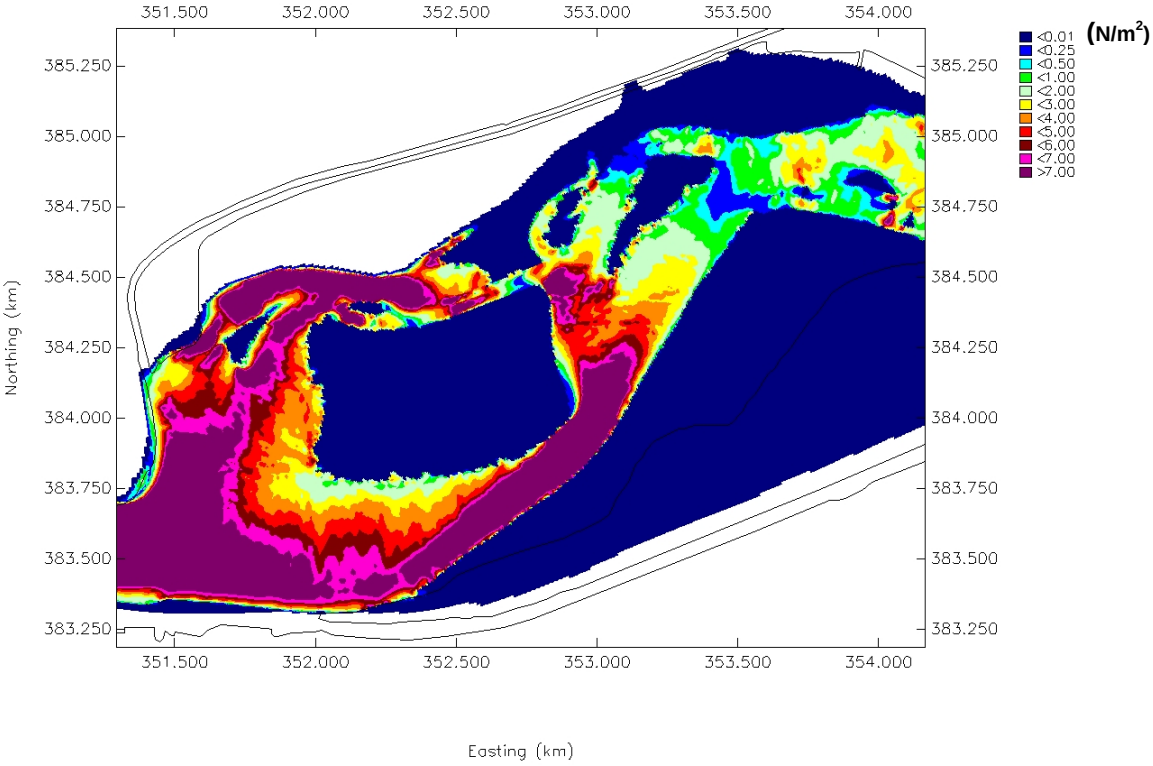
Actual near-bed speed (m/s) in the baseline case for high water (A) and peak ebb (B) on a spring tide.

Figure C86

A.



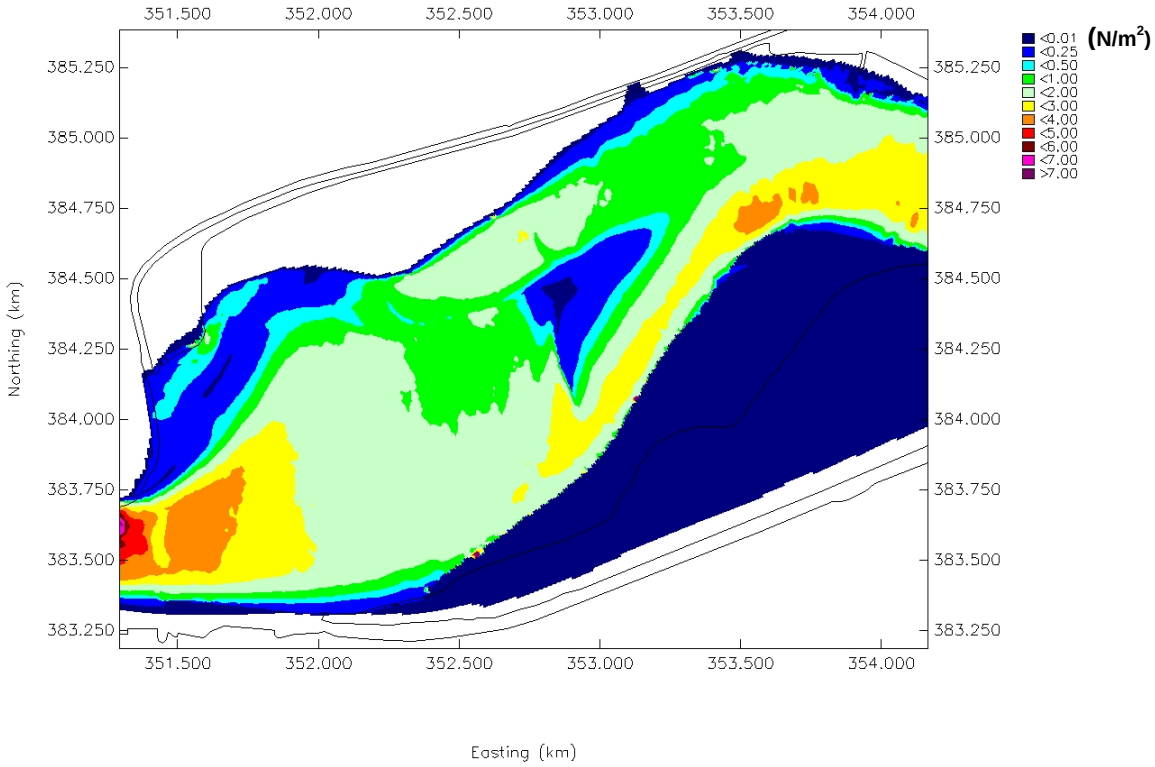
B.



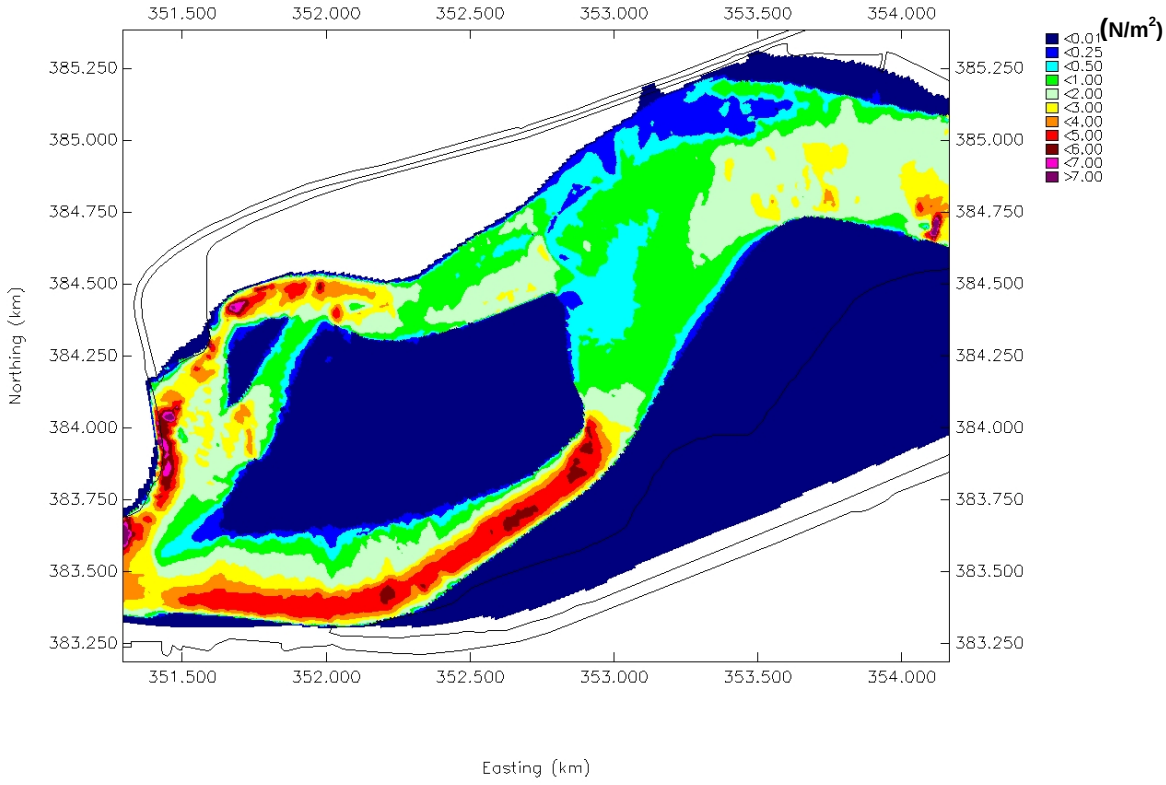
Actual bed shear stress (N/m²) in the baseline case for low water (A) and peak flood (B) on a spring tide.

Figure C87

A.

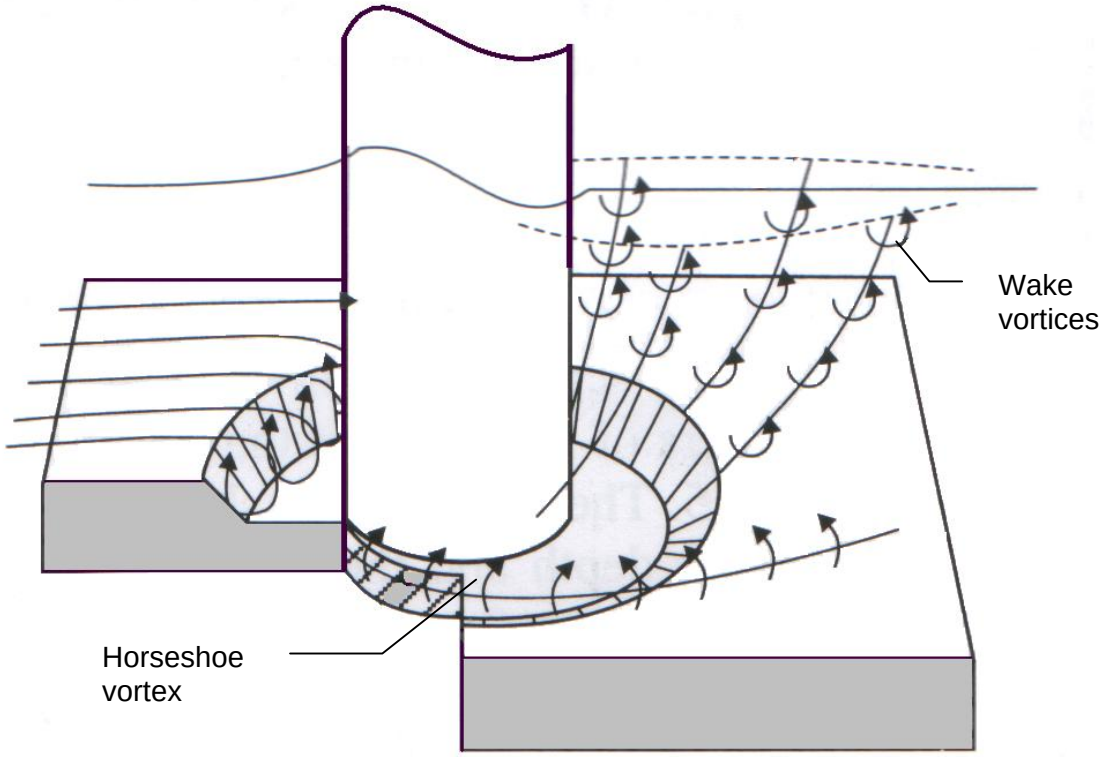


B.

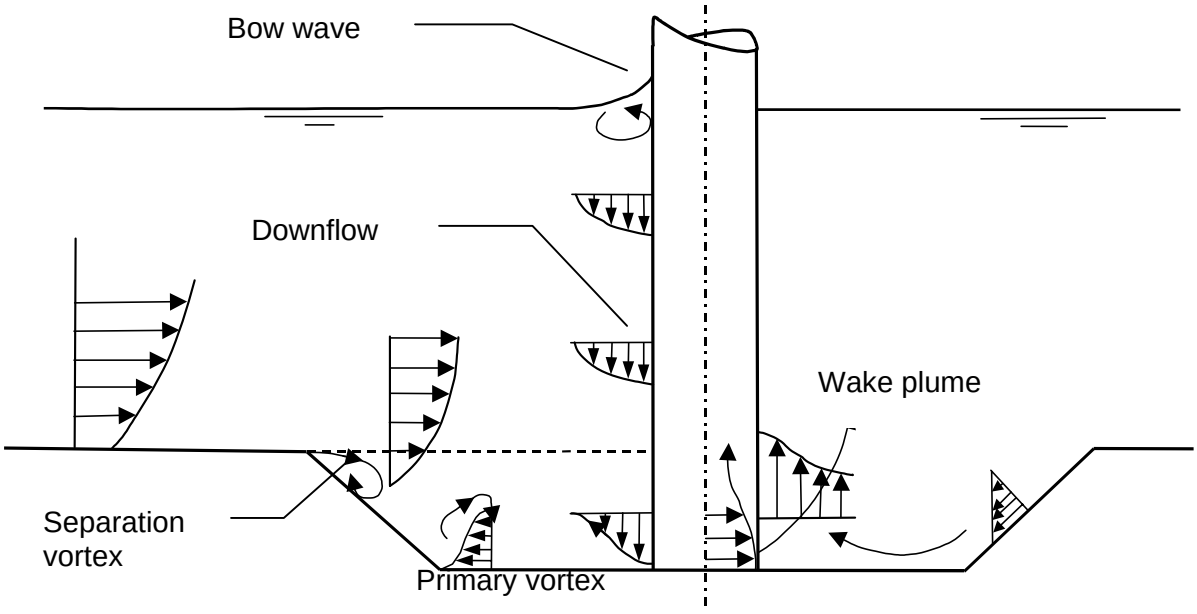


ABP mer marine environmental research	Actual bed shear stress (N/m²) in the baseline case for high water (A) and peak ebb (B) on a spring tide.	Figure C88

A.



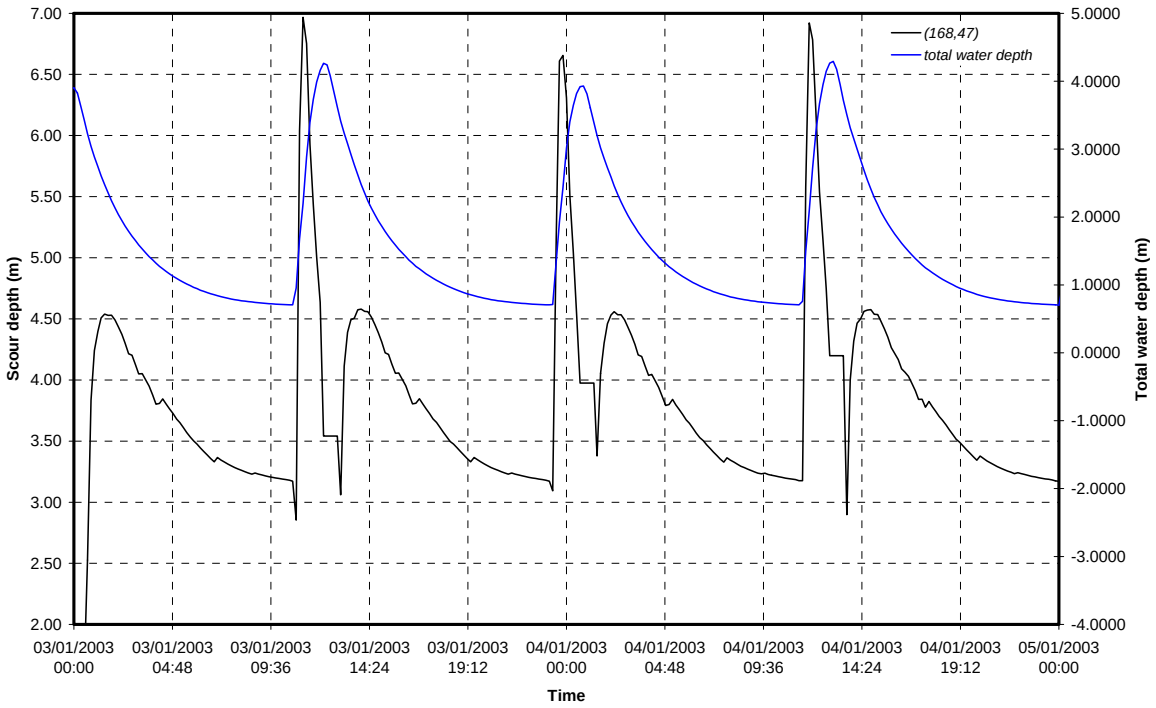
B.



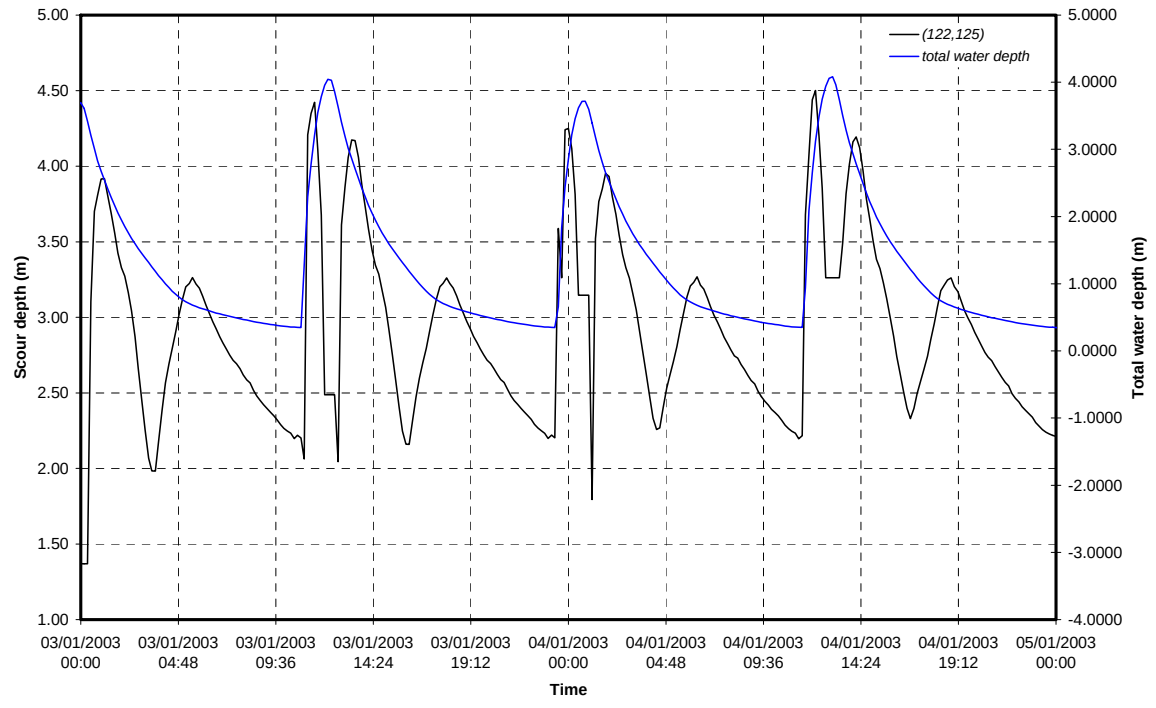
Flow pattern around a cylindrical pile. (after Herbich *et al.* 1984)

Figure C89

A.



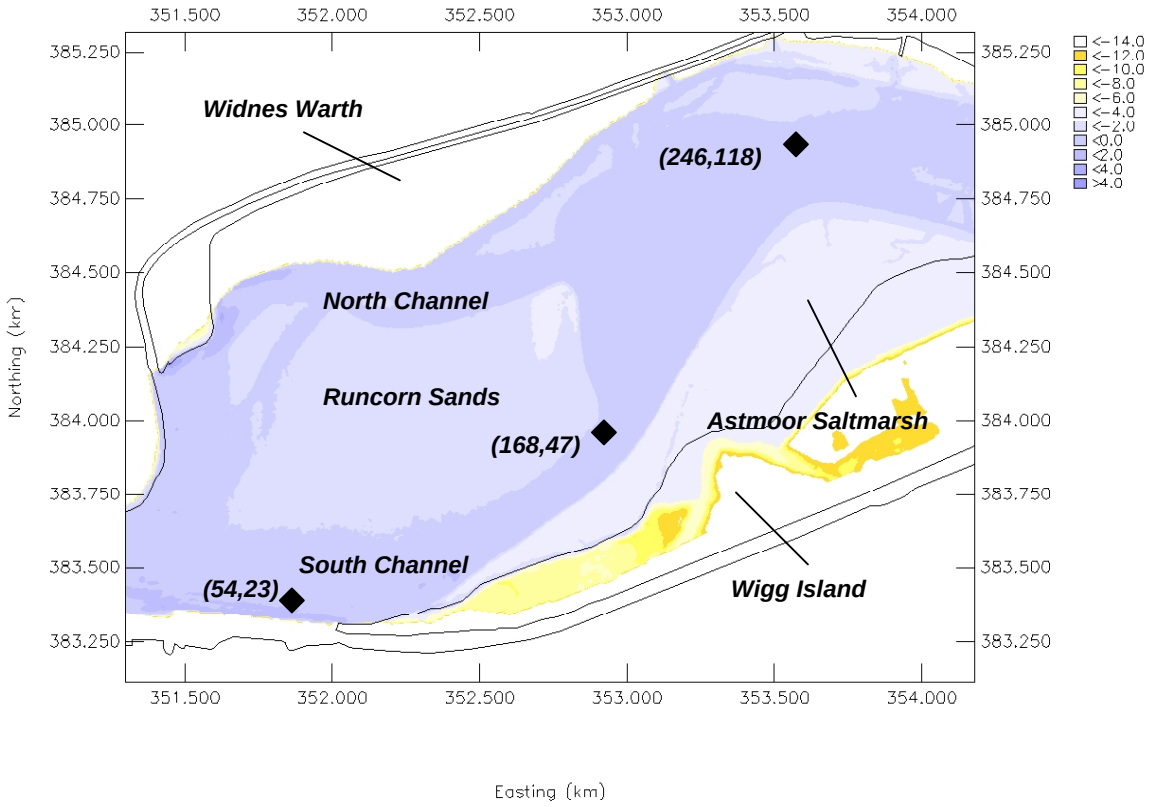
B.



Predicted scour depth through time for piers within the south (A) and north (B) channels for Route 3A Medium Span Original Alignment.

Figure C90

A.



B.

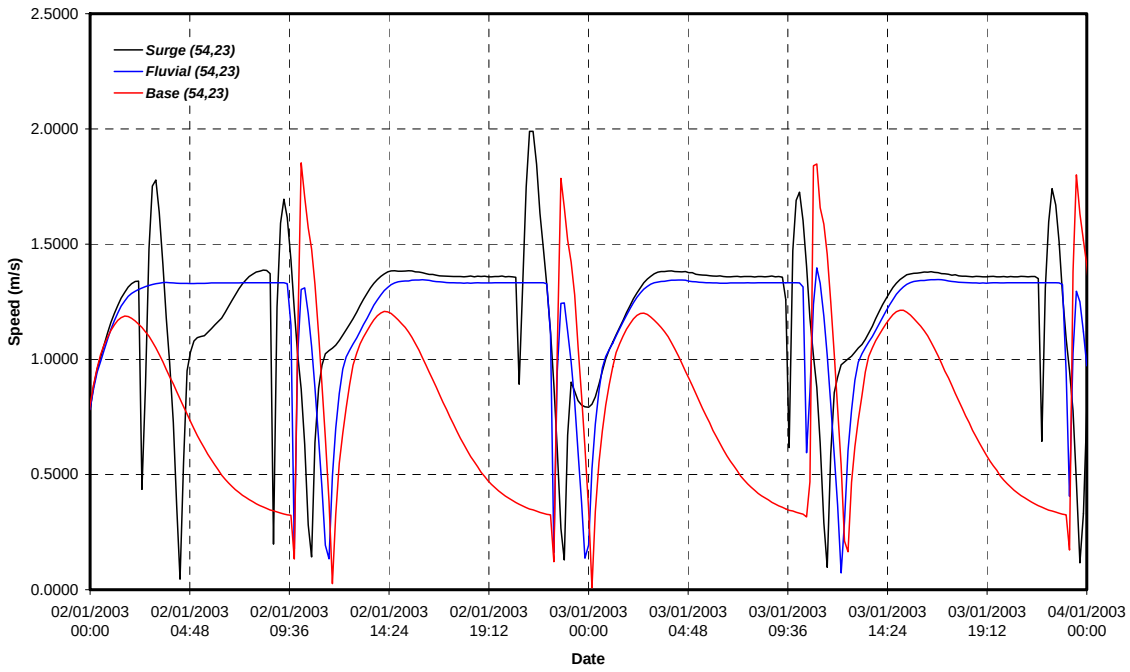
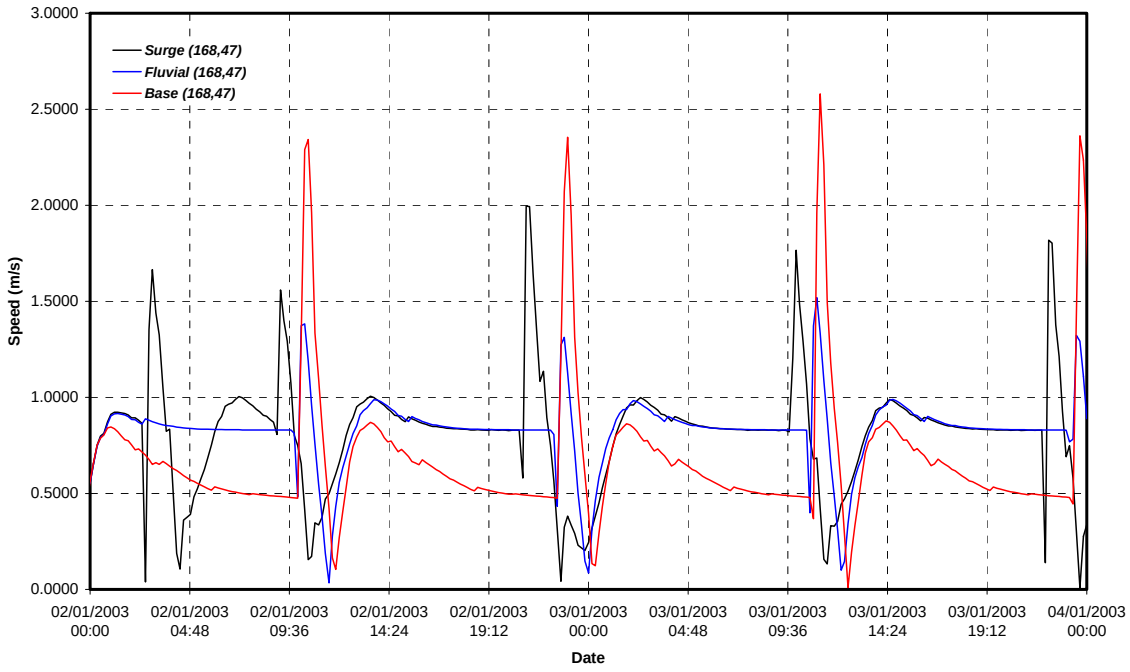


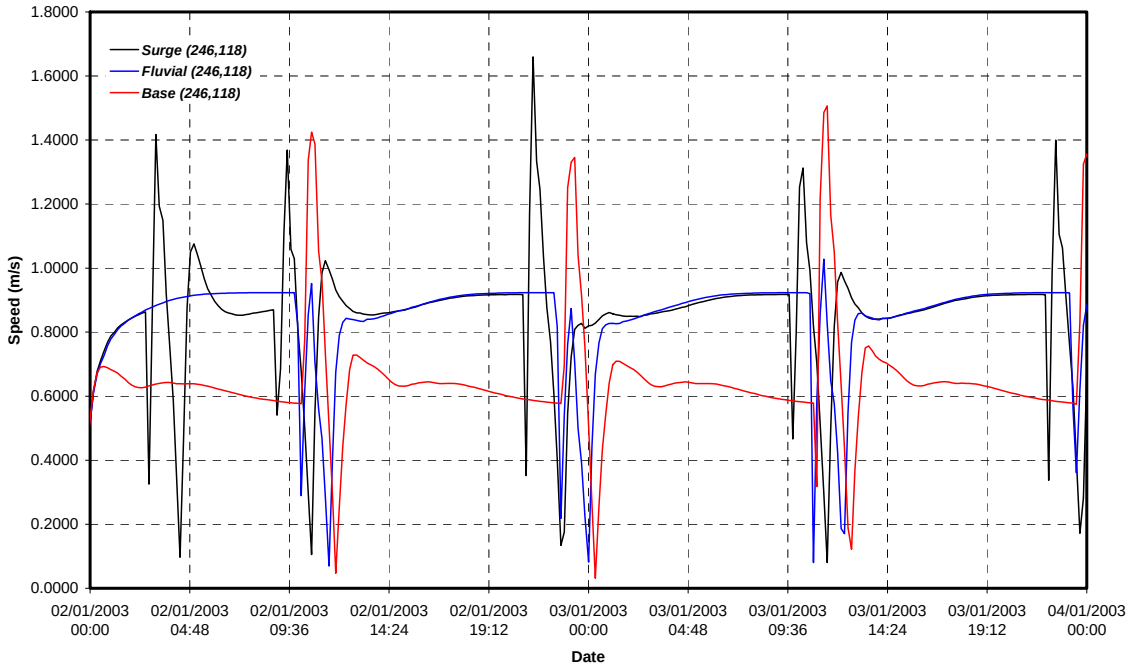
Figure A shows locations of various positions in the study area. Figure B shows the near-surface speed at position (54,23) for baseline, extreme fluvial and extreme surge and fluvial events.

Figure C91

A.

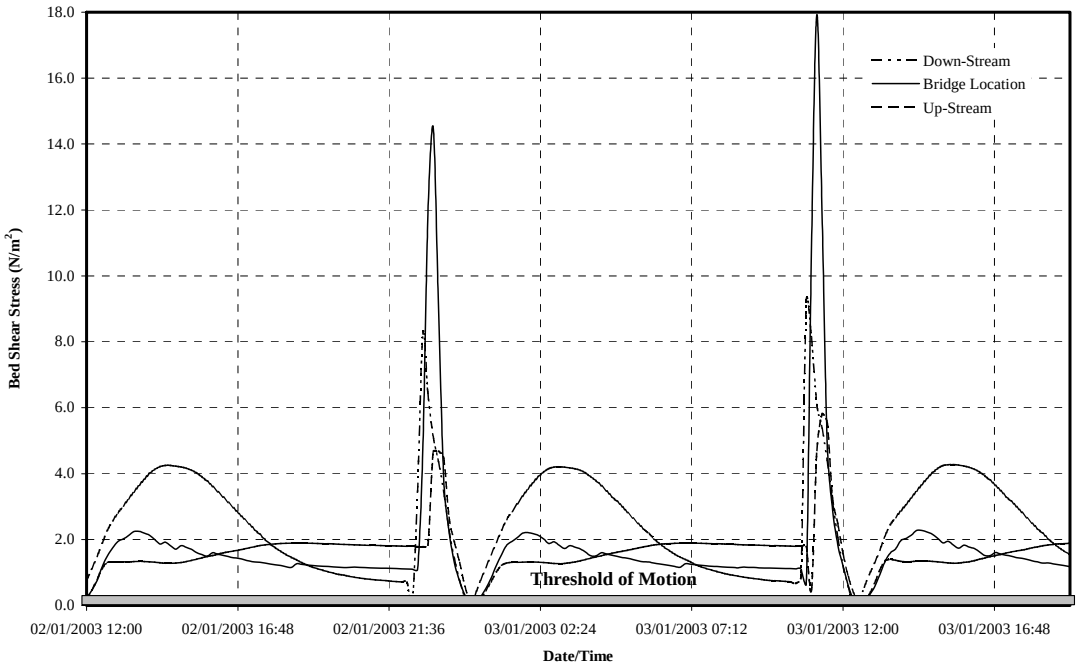


B.

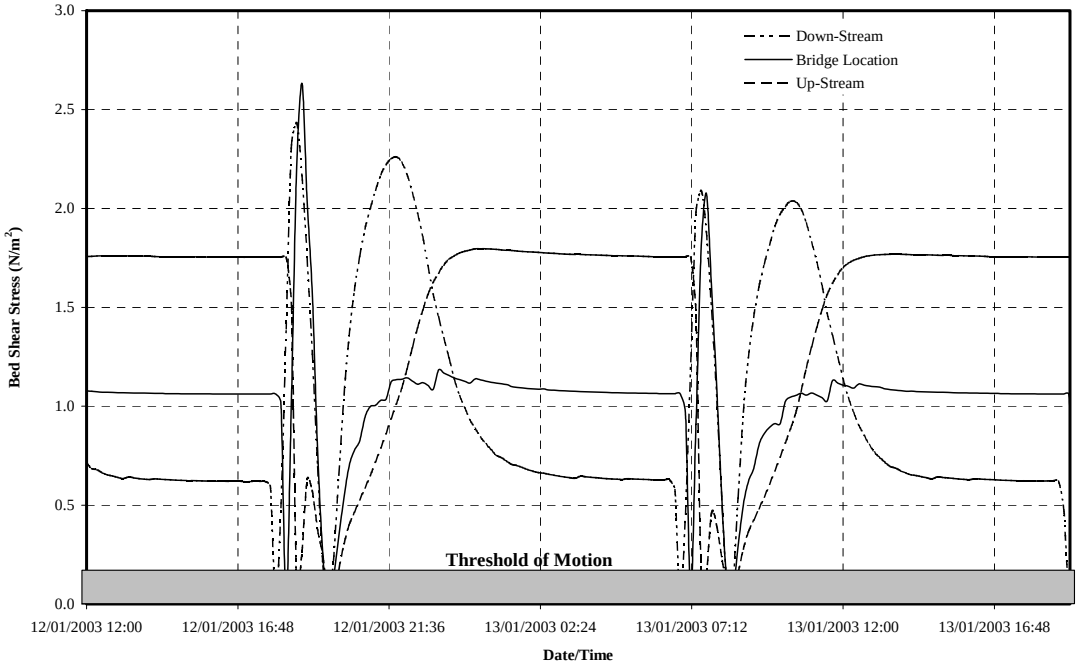


ABP mer marine environmental research	Near-surface speed at positions (168,47) (A) and (246,118) (B) for baseline, extreme fluvial and extreme surge and fluvial events.	Figure C92

A.



B.



ABP mer marine environmental research

Plot of ambient bed shear stress values predicted during the tidal cycle, compared with the anticipated threshold of sediment motion for 150μm grain size over spring (A) and neap (B) tides.

Figure C93

Appendix D

Morphological Modelling

Appendix D. Morphological Modelling

D1. Introduction

In Phase II of the Mersey Crossing study a more detailed numerical model of the Mersey Estuary was constructed to investigate the existing hydrodynamic and sediment transport regimes and the predicted changes brought about by the proposed development of a bridge crossing upstream of Runcorn.

A detailed description of the hydrodynamic model set up, calibration and validation is given in Appendix A. The Mersey Estuary is known to be a highly complex and dynamic system (Price and Kendrick, 1963). To better understand the complex hydrodynamic and morphological processes within the estuary a morphological model was constructed. The model was used to help determine the likely effects the proposed scheme would have on the hydrodynamics and sediment distribution within the estuary.

D2. Online Sediment Module

The Delft3D-Flow module was used to solve the transport equation for a sand fraction representative of sediment within the study area (150μm sand). This allowed for an assessment of the effects of sediment concentration on density, turbulence damping and density currents. Changes in current patterns due to the morphological changes (changes in bathymetry) can be taken into account during the flow computation.

At each time-step, the transport of sediment is calculated by solving the three-dimensional advection-diffusion (mass-balance) equation for the suspended sediment;

$$\frac{\partial c}{\partial t}+\frac{\partial}{\partial x}(uc)+\frac{\partial}{\partial y}(vc)+\frac{\partial}{\partial z}[(w-w_s)c]-\frac{\partial}{\partial x}\left[\varepsilon_{s,x}\frac{\partial c}{\partial x}\right]-\frac{\partial}{\partial y}\left[\varepsilon_{s,y}\frac{\partial c}{\partial y}\right]-\frac{\partial}{\partial z}\left[\varepsilon_{s,z}\frac{\partial c}{\partial z}\right]=0$$

An important aspect of solving this equation is the specification of the local turbulent sediment mixing components. The horizontal components are user specified, the vertical component is taken from the turbulence closure model used to calculate the diffusion of mass and momentum in hydrodynamic calculation. Wave effects are accounted for using the van Rijn (1993) algebraic model. Fall velocity is calculated using the formulations presented by van Rijn (1993) including the effects of hindered settling.

Boundary conditions are also required. At the free surface the vertical diffusion is set to zero and at open lateral boundaries the horizontal diffusion is set to zero. The quantity of sediment advection inward through an open boundary is determined by specifying a vertical concentration profile and, a linear profile was selected. At the bed, a series of sediment source and sink terms are included in the bottom computational layer in order to simulate the exchange of sediment with the bed.

The modified Delft3D-FLOW module also includes the calculation of bed load sediment transport for sand and silt fractions. Activation of the bed-load transport option causes the bed-load transport vector to be calculated at each computational point at each time-step. Spatial gradients in bed-load transport will cause erosion and accretion of the bed. The bed-load sediment transport vector includes an adjustment for the effects of longitudinal and transverse bed slopes. The on-line module can also take into account the effect of an onshore transport component as a result of wave asymmetry.

The bed level is updated during each time-step of the flow computation, taking into account the exchange with the suspended sediment through the vertical and the gradient of the bed load transport. Both terms can be multiplied by a morphological scaling factor and this is also applied at every time-step. The effect of fixed layers can be taken into account, by gradually reducing the vertical exchange and bed load transport terms to zero as the sand layer thickness approaches zero.

D3. Model Set-Up

The morphological model of the Mersey Estuary is based on a three domain calibrated Delft3D-FLOW hydrodynamic model of the Mersey Estuary (see Appendix A). All hydrodynamic parameters are identical to those applied in the more detailed five domain model used to assess hydrodynamic change. The initial bathymetry and sediment distribution map was set up using data provided by the Environment Agency, the British Geological Survey, The University of Southampton, Gifford & Partners and ABPmer.

A spring neap tide was selected covering the period 01/01/2003-16/01/2003. The morphological scaling factor was set at 25, which means that the sedimentation and erosion rates during the simulation are multiplied by a factor of 25. Therefore, the morphological results represent a 1 year period, approximately (28 tides multiplied by 25 = 705 tides $\approx$ 1 year). The initial period of adjustment “spin-up” of the simulation was 15 days. During this period the bed level was updated without any morphological scale factor. The resulting changes in bed elevation were then applied to the 1-year simulation.

The computational grid of the hydrodynamic model consisted of 8 layers through the vertical. The turbulence closure model used was a k-ε turbulence model. Due to the addition of the sediment fraction and morphological updating the computational time-step was reduced to 0.3 min for stability purposes.

The model utilizes the domain decomposition module of Delft3D allowing a model grid to be sub-divided into several smaller model domains (sub-domains). The sub-division is based on the horizontal and vertical model resolution required for adequately simulating the key physical processes under consideration. Domain decomposition allows for local grid refinement in both the horizontal and vertical directions. 3 grids were chosen with a constant vertical resolution. The middle grid had the finest horizontal resolution of typically 20-30m. The coarse resolution in the outer and inner grids allowed for a significant increase in run times (see Appendix A, Figure A3).

The dominant sediment type was chosen based on particle size analysis from the field survey and borehole data. A sand fraction with a d_{50} grain size of 150 μm was applied in the morphological modelling (see also ABPmer, 2003a).

D4. Sediment Sources

The Mersey has always been thought of as an accretionary estuary and up until very recently there has been significant accretion taking place within most sections. However, HR Wallingford (1999) and Thomas (2000) suggest that the estuary may be entering a new state of morphological equilibrium with little overall estuary capacity change. HR Wallingford (1999) also noted that although capacity change has stabilised, there is a substantial amount of sediment redistribution particularly within the Middle Mersey around Ince and Stanlow Banks and Dungeon Bay. In these areas, post 1956 surveys indicate periods of significant erosion and accretion.

The two principal sources of sediment in the Mersey Estuary are;

- Marine sources from the glacial and fluvial glacial deposits covering large parts of the eastern Irish Sea seafloor; and
- Fluvial sources from the freshwater rivers

Previous work indicates that the marine sources are the most significant, with O'Connor (1987) estimating that over 1Mm^3 /year of sediment has been delivered to the estuary since the turn of the century. Price and Kendrick (1963) identified that the mechanism for bringing in sediment from these offshore sources was by the density gradients that exist, which lead to a net landward movement of sediment in the near-bed layer of the water column.

Although the fluvial sources are believed to be small compared with offshore sources, the magnitude and duration of freshwater inputs may affect the lateral migration of low water channels in the Inner and Middle Mersey (see section 2.9; McDowell and O'Connor, 1977). Additionally, localised erosion of the Ince Banks region and Dungeon Bay has provided a recent source of sediment, although this is very small compared to marine sources (HR Wallingford, 1999).

D5. Sediment Transport

For riverbeds consisting of sands (non-cohesive sediments) the movement of these particles depends on the physical properties of the individual grains, such as size, shape and density. For riverbeds made up of silty and muddy materials, the cohesive forces between the sediment particles become important, leading to a significant increase in sediment resistance to erosion. Flocculation of sediment particles is the result of particles adhering together as they come into contact with each other and the resulting aggregations are called flocs. Biological activity at the bed may also influence the critical shear stress values required to initiate sediment movement (Appendix C ABPmer, 2003a). Seasonal variations in sedimentation are considered sufficiently small to be masked by the variances arising from the acknowledged limitations of sediment transport models.

The other important factor relating to the erodibility of cohesive sediments is the consolidation rate. Mud recently deposited consists of low-density mud flocs possessing a relatively loose structure. The cohesive forces in this deposit are not very strong at this early stage. If the deposit is not eroded again, then the density will increase gradually, as the interstitial water (water between the flocs) is expelled from the deposit as a result of its own weight. As the deposit is compacted so its resistance to erosion increases.

In order to initiate transport of sediments, the fluid stresses have to overcome the inertia of the particles on the seabed/riverbed. Once particles are in motion they can move in several ways, which can be generalised as bedload and suspended load. The behaviour of cohesive sediment in suspension is important for water quality. The turbidity and its effect on the ability of light to penetrate the water column is a significant factor in algae growth and algae act to stabilize the sediment. The greater the amount of sediment in suspension, the greater the attenuation of light in the water column. Also, contaminants in the water column are closely linked to the suspended solids due to their large adsorption capacities.

The bed shear stress is an important factor in determining whether or not deposition of suspended particles or erosion of bed sediments will occur. Deposition takes place when the bed shear stress drops below a critical value, whilst resuspension occurs when the bed shear stress exceeds a critical value. In cohesive sediment transport other bed processes such as consolidation and bioturbation also influence movement.

Based on the complexity of sediment transport as discussed above, the results from the morphological model need to be interpreted with care, taking into account the various factors affecting sediment movement, and considering the effects of processes not included as parameters within the model (for example biological activity).

D6. Bed Material

As described earlier, the initial sediment distribution was established using data obtained from a combination of sources. The resulting distribution pattern was then used to establish the locations for the sediment types used in the morphological simulations.

The distribution of material within the Mersey Estuary can be divided, generally, into; sands, silts and rock. Within the Narrows (seaward end of the estuary) the bed consists of a large area of rock, with a small amount of sand at the estuary mouth. Within the inner and upper Estuary much of the bed is made up of sand material with small patches of mud mainly dispersed along the shoreline intertidal region. Beyond Fiddler's Ferry the estuary bed begins to be dominated by fine silts, however, data in this region is scarce.

After the initial model simulation some areas of the model show areas of large erosion and deposition (greater than +/- 10m). A possible explanation for this is related to the initial distribution of sediment. Areas given an unrealistic thickness of sediment will under the hydrodynamic conditions scour or deposit material that in reality would not be there. Alternatively, the differences seen may be due to numerical differences occurring at the boundary of the nested grids. During the calibration procedure, sediment seen to erode/accrete significantly within the simulation period was removed as it was assumed that this material would have eroded and hence should not be included.

Initial thickness of the sand layer was set at approximately 1m. This is based on the assumption of an inerodible sediment layer below the surface. Subsequent borehole data provided by Gifford & Partners and the British Geological Survey (BGS) indicated that the depth of the sand material along some areas of the intertidal is in excess of 4m.

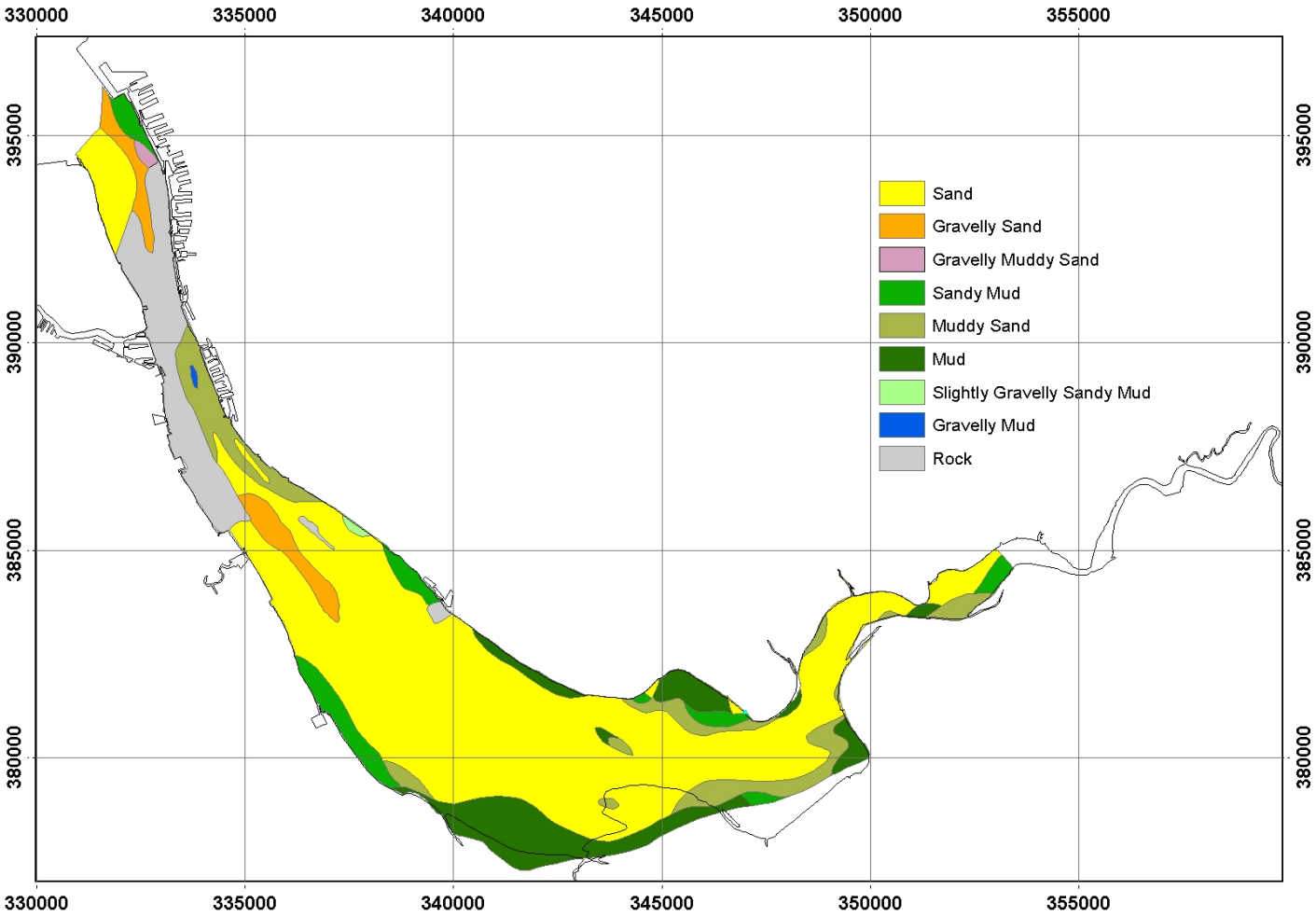


Figure D1. Mersey Sea Bed Sediment Map - Reproduced from the British Geological Society Map data (Licence 2003/006 British Geological Survey ©NERC)

D7. Boundary Conditions

D7.1 Initial Seaward Boundary Conditions

The initial concentration of sand and silt applied at the seaward boundary was 1kg/m^3. These values were based on field data collected by HRS Wallingford (1983) of suspended sediment concentrations.

D7.2 River Discharge

At the freshwater discharge location at Howley Weir, a sediment concentration of 0.01 kg/m^3 for sand was applied. No measured data of sediment concentrations was available at this location on which the model could be calibrated against. Therefore, the inflow concentrations have been calculated using an iterative approach. The discharge of sediment at the seaward and freshwater boundary was constant throughout the simulation period. However, during periods of high or low freshwater discharge /astronomical tide these transport rates are likely to vary considerably. In the present study mean values were used that provided sensible results in the model calibration. These were determined on the basis of a series of sensitivity tests where these parameters were adjusted. The resulting configuration provided the most realistic calibration results.

Although analysis of flow data was undertaken for this phase of the study (ABPmer 2003 Appendix B), only an annual mean discharge has been applied at Howley Weir, subsequent runs have investigated the sensitivity of an extreme fluvial event and an extreme fluvial and surge event combined.

D8. Morphological Calibration

The morphological model of the Mersey Estuary was calibrated for the period December 2002-January 2003. In this study the influence of waves has not been taken into account due to the upstream location of the study area. The focus of the study is the hydrodynamic and sediment regime brought about by the tidal and freshwater boundary conditions.

The model has been calibrated against measured suspended sediment concentrations at various points within the Narrows and at Fiddler's Ferry. The data used in the study was obtained from measurements in the outer estuary acquired by HRS Wallingford (1983), and at Fiddler's Ferry by the Environment Agency. The measurements within the Narrows, recorded suspended sediment concentrations at both the near-surface and near-bed layers.

D8.1 Hydraulics Research Station Ltd, Wallingford (HRS) - Observations of Suspended Sediment Concentrations 1982

Data was collected by a Rapid Drop Profiler (RDP), using an infra-red probe, which measures the amount of emitted light from one sensor to the other across an 8mm gap. With increasing turbidity there is a reduction in detected infra-red light. The instrument was calibrated using sampling tubes attached to the RDP package.

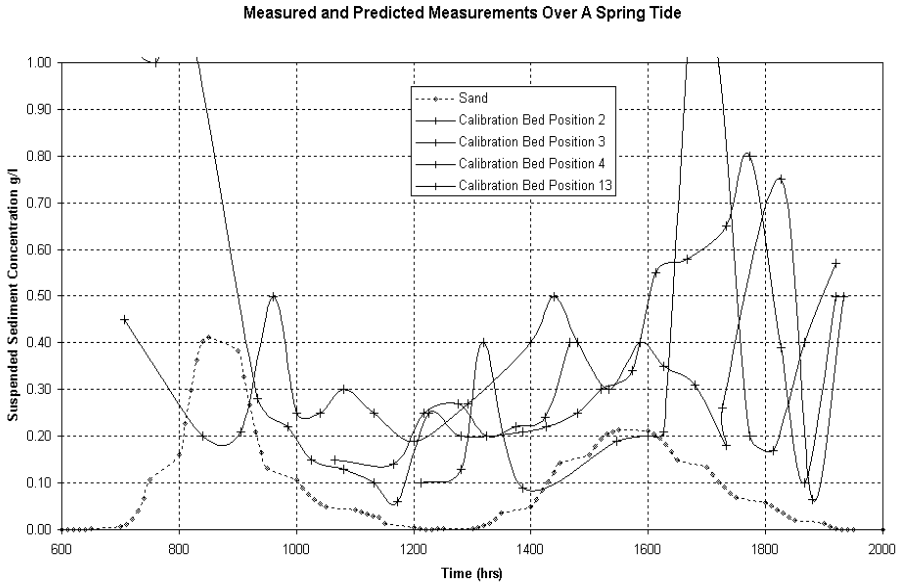


Figure D2. Calibration plot showing measured and modelled suspended sediment concentrations (g/l) at the bed over a spring tide

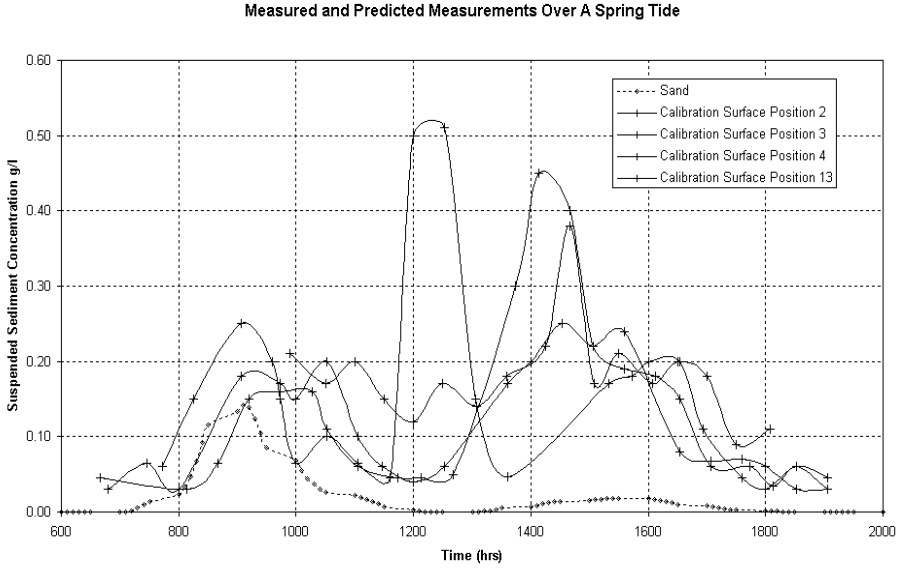


Figure D3. Calibration plot showing measured and modelled suspended sediment concentrations (g/l) at the surface over a spring tide

D8.2 Environment Agency Data

Data collected by the Environment Agency at Fiddlers Ferry was digitised and compared with the results from the Delft3D model for a comparable tidal period. No information has been provided as to how the field measurements have been recorded.

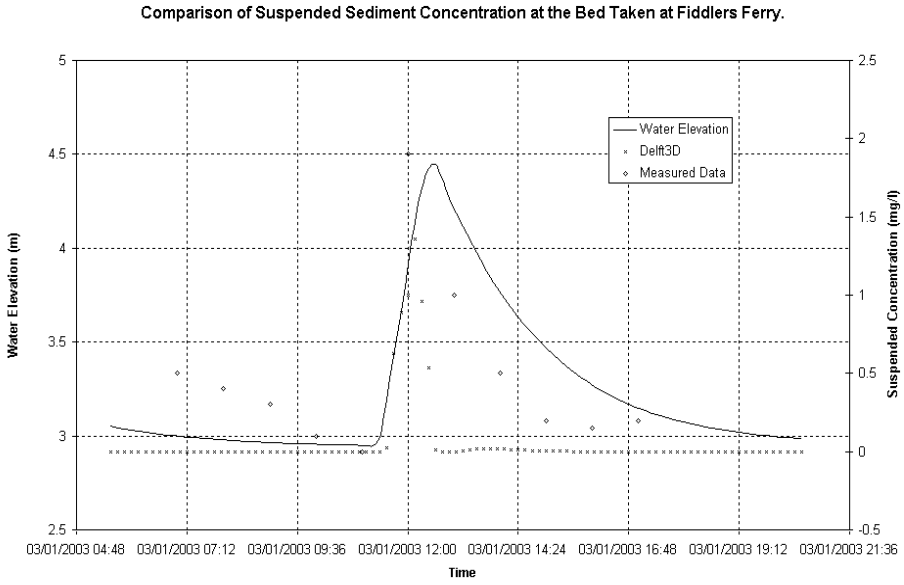


Figure D4. Comparison of measured and modelled suspended sediment concentrations (mg/l) at Fiddler's Ferry

D8.3 Discussion

- HR Wallingford Data:
  The comparison of model data against the data collected by HR Wallingford on a spring tide show reasonable calibration. The measured data shows a higher degree or variability through the water column. The model results show a more consistent suspended sediment concentration both at the surface and bed layers. The degree of variability in the measured data compared to the modelled data is expected and takes into account possible local variations in suspended sediment due to ship movement, local inputs etc.

- Environment Agency Data:
  The area of overlap between the modelled and measured data shows a good agreement. The measured data show a peak in suspended sediment of 2 mg/l. The degree of accuracy of the measured data is not known nor is the methodology and exact location of sampling.

D9. Conclusion

The calibration between the measured data at the sites in the Narrows and at Fiddlers Ferry shows a good fit. The pattern of suspended sediment as well as the concentration is represented well within the morphological model, demonstrating both the upper and lower concentrations seen on the rising and falling tide.

The measured data has only been able to provide a limited view of the suspended sediment concentrations within the Mersey. Ideally, a longer period of measurements in an area more suited to the model would have provided a more ideal calibration (i.e. further away from the boundary). However, given the limitations of the measured data the model is seen to be representing the conditions within the outer section of the Mersey to a reasonable standard.

D10. Modelling Results

The morphological modelling of the Mersey Estuary has been undertaken using the predominant sediment type found across the study area (sand d_{50} = 150 μm). The spatial results are presented as differences between the scheme and baseline conditions. These difference plots (Figure D5 - D15) show changes in the thickness of sediment, and represent the change in actual thickness of sediment on the riverbed. Positive values represent sediment deposition and negative values, sediment erosion. For each scenario two figures are presented at different scales to provide a greater overview of the scale of change. Figures labelled 'A' show 'finer-scale' changes within the limits ±0.05m with a ±0.01 cut-off. Figures labelled 'B' show the larger scale changes within the limits ±1.50m, but also have a ±0.01 cut-off so there is some level of correspondence with the finer-scale figures.

The change in actual thickness of sediment on the riverbed is representative of a 1-year simulation period (28 tides x 25 morphological scale factor). The period of investigation (spring neap cycle) was selected based on high-water to high-water simulation where the high waters were equal in range, approximately.

D11. Existing Conditions

Under a mean spring-neap cycle sediment is deposited within the main channel and along the intertidal areas of the inner estuary. Within the Narrows the modelling results show some erosion to occur but this has been ignored since the BGS data identify this area as consisting of bedrock. The distribution of sediment is consistent with the presence of the flood/ebb channels and residual currents observed within the estuary. Within the Narrows the high current speeds prevent sediment from settling. Within the

wider inner estuary the flow speeds are significantly slower, allowing accretion to occur.

Areas of potential erosion can be seen along the southern bank of the inner estuary and within the flood and ebb channels within the Widnes and Runcorn region. The key findings from the "base-line" simulations after the simulation period were:

- Slow build-up of sediment within the inner basin of the Mersey Estuary.
- Build-up of sediment on the sandbanks within the upper estuary with erosion occurring within the main channel upstream of Runcorn.
- Flood/Ebb channels show some erosion

D12. Route 3A Medium Option - Original Alignment

For the Route 3a Medium Option - Original Alignment there are 3 sets of piers and 4 Towers with footings in the estuary. The bridge layout is shown in Drawing No. B4027/2/B/361. The pier groups are situated on the intertidal area with the remaining structures in the main channel. The bridge piers are octagonal (5m x 5m) and the towers are also octagonal (10m x 10m).

Figures D5a and D5b show the predicted change in sediment distribution across the study area. Downstream of Runcorn and upstream of Fiddlers Ferry, the modelling showed no change in sediment distribution. The results represent the variation in sediment distribution between the scenario and the baseline after a 1 year period.

In the vicinity of the proposed bridge crossing material is eroded from around the bridge tower adjacent to the main South Channel (maximum depth of erosion 0.75m). There is a zone of accretion slightly upstream of this area erosion (depth of accretion 0.10 - 0.20m) which extends into a zone of erosion (0.05 - 0.10m). The largest extent of deposition occurs along the margins of the South Channel and upstream of the pier structures, located towards the margins of the South Channel. Upstream of the proposed bridge crossing an increase in sedimentation of approximately 10-20cm is predicted along the side slopes of the South Channel (Maximum Accretion 1.82m). Along the north bank adjacent to the existing bridge, and along the quay wall, there is a predicted increase in sediment deposition of less than 0.05m. The morphological modelling predicts an increase in bed elevation of approximately 0.5m adjacent to the pier in the North Channel.

A general pattern of increased sedimentation is predicted within the area of the proposed bridge crossing. The pattern of erosion and sedimentation suggests that the placement of the piers has led to an increase in erosion along the margins of the South Channel downstream of the proposed pier positions. The overall pattern upstream of the proposed crossing is of an increase in sediment. This is most likely a result of the

reduced transmission of flows caused by the 'blockage effect' of the structures and the weaker ebb currents. Some localized erosion is seen upstream of the proposed crossing site (0.05 - 0.20m).

D13. Route 3A Medium Option - Modified Alignment

For the Route 3A Medium span Modified alignment there are 3 sets of piers and 4 towers with footings in the estuary. The pier groups are situated on the intertidal area with the remaining structures in the main channel. The bridge piers are octagonal (5m x 5m) and the tower structures are also octagonal (10m x 10m). The modified layout has resulted in minor alignment changes with the bridge towers being moved away from the north and south channels.

Figures D6a and D6b show the change in sediment distribution within the estuary. As in the previous scenario tested the modelling shows no change in sediment distribution downstream of Runcorn and upstream of Fiddlers Ferry. The main area of deposition is observed along the North Channel adjacent to the proposed bridge tower placements (maximum deposition 0.73 m). The modelling shows deposition of sediment occurring between the tower structure and the intertidal area. Upstream and downstream of this deposition are patches of erosion typically 0.05m or less in depth with maximum erosion of 0.15m indicated.

Along the southern side of the channel there is a general increase in sedimentation of less than 0.05m. Immediately adjacent the bridge tower the morphological model predicts erosion to depth of 0.7m, approximately and maximum accretion of 1.32m.

Overall the Route 3A Medium span modified alignment shows a significant improvement in the amount of impact the scheme is causing within the estuary compared to that predicted to occur due to the Route 3A Medium span - original alignment. This effect demonstrates the importance of the placement of the bridge structures within the estuary relative to the main channel positions at least in the short-term.

D14. Route 3A Medium Option - Modified Alignment Extreme Fluvial Event - 1:200 Return Period

The model set-up was modified to account for an extreme fluvial event using a 1: 200 years return period. The return period values were calculated from freshwater flow data obtained from the Environment Agency and the National Flow Archive. A Gumbel distribution was used to determine the return period flows using the annual maxima for each station. The following stations were used in the analysis:

- River Gowy
- River Weaver
- River Mersey
- Sankey Brook
- Ditton Brook

For further details see Appendix B. For comparison purposes it was necessary to re-run the baseline case to include the extreme fluvial event. It should also be noted that the extreme fluvial event and extreme fluvial event with a surge tide have only been run for a spring-neap tidal cycle and not scaled for a year as it was considered a meaningless comparison. Therefore, to assess the impacts of the extreme events the Route 3A Medium Option Modified Alignment was run for a normal spring-neap tidal cycle also without using a morphological scaling factor (Figures D7a and D7b).

The bridge layout is as described above for the Route 3A Medium Option Modified Alignment with 3 sets of piers and 4 towers with footings in the estuary.

The results of the extreme fluvial event morphological run are shown in Figures D8a and D8b. The morphological model suggests that the greatest extent of change occurs within the north channel during an extreme fluvial event. In general there is deposition of sediment upstream and downstream of the tower in the north channel with values of less than 0.05m typically, although there are a couple of patches of deposition up to 0.10m. Immediately adjacent to the tower and left of the tower, when viewed looking towards Runcorn, are areas of erosion (maximum value 0.39m)

Within the south channel the change in sedimentation remains local to the bridge structure. Erosion is indicated to occur between the tower and the intertidal area (-0.47m) with deposition occurring right of this when viewed looking towards Runcorn (0.25m).

The placement of sediment is predominantly downstream of the structures suggesting that there is more ebb dominance in the system as a result of the significantly increased fluvial flows (1:200 years return event).

D15. Route 3A Medium Option - Modified Alignment: Extreme Fluvial and Surge Event - 1:200 Return Period

The model set-up was modified to account for an extreme fluvial and surge event using a 1:200 years return period. The return period values for the freshwater flow were calculated as described above. The extreme surge was determined from an Environment Agency - North West Region report (Environment Agency, 1998). The shape of the surge tide was determined from a surge event recorded at Gladstone Dock. The recorded tidal curve was ‘stretched’ to fit the 1:200 year return event. A

synthetic tidal time-series was then generated and used to provide the driving tidal boundary conditions in the model. Further details are given in Appendix B.

As with the extreme fluvial event, the combined extreme fluvial and surge event has only been run for a spring-neap tidal cycle and no morphological scaling factor has been applied.

Figures D9a and D9b show the morphological results of the combined extreme fluvial and surge event. As observed in the extreme fluvial event the greatest extent of change occurs within the north channel. However, downstream of the bridge structures the higher tidal flows appear to suppress changes in sedimentation compared with the extreme fluvial event. In addition, the higher water levels as a result of the surge lead to changes in sedimentation across the upper areas of the intertidal banks in the vicinity of the two central bridge towers with typical values of deposition less than 0.05m.

Within the north channel the greatest changes occur local to the bridge tower with maximum erosion and deposition of -0.67m and 0.45m, respectively. Along the southern side of the estuary most changes are local to the bridge tower situated towards the south channel. However, the higher water levels result in small changes along the intertidal suggesting that sediment will be deposited (less than 0.05m).

The changes local to the tower in the south channel show maximum deposition of 0.27m and maximum erosion of 0.49m. As observed in the extreme fluvial event, the placement of sediment is still predominantly downstream of the structures suggesting that there is more ebb dominance in the system. This would suggest that the increased fluvial flows (1:200 years return event) are still dominating the flows in the upper estuary despite the significant tidal event.

D16. Route 3A Medium - 3 Tower Option

This section describes the morphological simulation undertaken for the Route 3A medium span layout as shown in Drawing No. B4027/3/B/300. For this modified version of Route 3A Medium Span operational case the number of towers is reduced to 3 and the pier alignments have been modified. The bridge piers are octagonal (5m x 5m) and the towers are also octagonal (10m x 10m). The towers are all located within the main body of the upper estuary whilst the pier groups are located either on or above the intertidal area.

Figures D10a and D10b show the change in sediment distribution within the estuary. The main areas of erosion and deposition are observed immediately adjacent to the bridge structures located in the proximity of the north and south channels (maximum erosion -1.46m, maximum accretion 1.79m). The extent of erosion is approximately

70-100m either side of the bridge towers and piers. In terms of bridge scour the typical width of a scour hole is between 3 and 4 times the pier diameter. Therefore, for the tower structures this would suggest a width of between 30 - 40m. In general, the erosion around the structures appears more elongated and this is most likely an artefact of the tidal forcing.

Along the northern side of the estuary upstream of the proposed bridge structures there is a predicted increase in erosion of between 0.05 - 0.25m. This erosion occurs both along the shoreline and over the intertidal banks. Downstream of the bridge structures deposition of sediment is shown to occur (less than 0.05m) accept for a few small patches of erosion close to Spike Island (< 0.05m).

Along the southern bank, the morphological model predicts erosion to be occurring both upstream and downstream of the bridge structures along the intertidal area adjacent to Wigg Island (typically < 0.05m). Although the bridge tower adjacent to the south channel is away from this channel, the location of the piers on the edge of the intertidal/channel area have a wider influence and result in many of the observed changes along the intertidal area. There is also an area of accretion upstream of the southern bridge tower.

Compared with the Route 3A Medium Option Modified Alignment (4 tower) the Route 3A Medium span 3 tower option performs less well. Despite the reduction in the number of towers placed within the estuary the scenario again demonstrates that poor placement of the bridge structures has a significant impact on the morphological change, at least in the short-term.

D17. Route 3A Medium - 3 Tower Option Revised Alignment

This section describes the morphological simulation undertaken for the Route 3A medium span layout as shown in Drawing No. B4027/3/B/300 Rev A. For this modified version of Route 3A Medium Span operational case the number of towers is reduced to 3 and the pier alignments have been modified. The bridge piers are octagonal (5m x 5m) and the towers are also octagonal (10m x 10m). As with the previous 3 Tower alignment (Drawing No. B4027/3/B/300) the towers are all located within the main body of the upper estuary whilst the pier groups are located either on or above the intertidal area.

Figures D11a and D11b show the morphological results of the Route 3A medium span 3 towers option revised alignment. In general, the changes are local to the tower structures. Moving the position of the towers and piers away from the channels has significantly reduced the impact of the proposed crossing on the system

Away from the bridge structures morphological changes as a result of the scheme are less than ±0.05m. The maximum changes local to the bridge tower adjacent to the north channel are erosion of 1.38m and deposition of 0.29m. Adjacent to the tower situated close to the south channel the maximum deposition is 0.28m and the maximum erosion is 0.68m.

D18. Route 3A Medium - 3 Tower Option Revised Alignment: Extreme Fluvial and Surge Event - 1:200 Return Period

The model set-up was modified to account for an extreme fluvial and surge event using a 1: 200 years return period. The return period values from the freshwater flow are calculated as described in Section D14 and Appendix B. The extreme surge was determined from an Environment Agency – North West Region report (Environment Agency, 1998). The shape of the surge tide was determined from a surge event recorded at Gladstone Dock. Further details are given in Appendix B.

As with the previous extreme events run for the Route 3A Medium span Modified alignment, the combined extreme fluvial and surge event has only been run for a spring-neap tidal cycle and no morphological scaling factor has been applied.

Figures D12a and D12b show the morphological results of the combined extreme fluvial surge event. There is an area of erosion (max ≈ 0.05m) in front and behind the north and south tower. The north tower shows the greatest extent of erosion extending 500m, approximately either side of the tower. The maximum erosion (≈ 1.8m) is predicted to occur adjacent to the north tower, whilst the largest predicted increase in bed elevation of 1.2m occurs either side the north tower (Figure D12b).

Some changes are seen upstream and downstream of the proposed bridge crossing, however, these changes are less than 0.5m and only occur within isolated sections of the study area.

D19. Route 3A Medium - 3 Tower Option Revised Alignment: Recovery

This section describes the morphological simulation undertaken to assess the 'recovery' of the system post construction for the Route 3A medium span 3 towers option revised alignment. The simulation assumes that an aligned jetty approach has been adopted for construction purposes (see ABPmer, 2005). The morphological simulation was run with the construction scheme in place for an extreme fluvial and surge event. At the end of this period the temporary structures related to the construction phase, (for example cofferdams, piles etc) were removed from the model set up and the model then run for a spring-neap-spring cycle scaled to represent one year.

Figures D13a and D13b show the difference in bed elevation after a recovery stage. In general, the changes are local to the tower structures.

Away from the bridge structures morphological changes as a result of the scheme are less than ±0.05m. The maximum changes local to the bridge tower adjacent to the north channel are erosion of 1.37m and deposition of 0.33m.

The results obtained from the recovery scenario are comparable to the revised alignment for the Route 3A medium span 3 towers option (Figures D11a and D11b). The pattern of sediment distribution is very similar with no significant difference in bed elevation. The recovery scenario has demonstrated that from an initial bed elevation, which has been subjected to an extreme event, the system moves back to a condition predicted under normal water levels and fresh water discharges.

D20. Route 3A Medium - 3 Tower Option Revised Alignment: 2005 Bathymetry

In early 2005 a limited survey of the upper estuary local to the proposed crossing was undertaken. This captured the significant movement of the channels between this survey and the previous detailed 2002 survey, the latter survey, which has been used to undertake the modelling to date. The new bathymetry allowed a modelling assessment of the morphological response to the proposed bridge with a completely different channel configuration and to assess the significance of this. This section describes the morphological simulation undertaken for the Route 3A medium span 3 towers option revised alignment with 2005 bathymetry.

Figures D14a and D14b show the predicted change in sediment distribution across the study area. Downstream of Runcorn the modelling showed no change in sediment distribution. The results represent the variation in sediment deposition and erosion between the scenario (with scheme) and the baseline (i.e. no scheme in place) after a 1 year period.

The different channel configuration has created a south channel dominance over that observed for the 2002 bathymetry, which was dominated by flows through the north channel. The greatest extent of change is upstream of the proposed crossing, with accretion predicted to occur along the intertidal shoreline and banks. Downstream of the proposed bridge there is some erosion along the intertidal area adjacent the south bank.

Within the south channel the greatest changes occur local to the bridge tower with maximum erosion and deposition of -1.54m and 0.65m, respectively. Changes within the north channel are limited to the location of the bridge tower and piers.

In general the channel configuration results in a slight increase in bed elevation downstream of the proposed bridge crossing, this increase is localised to the margins of the north channel. The results indicate that no change occurred in bed elevation downstream of the immediate area of the proposed bridge crossing.

D21. Route 3A Short Option

This section describes the hydrodynamic simulation undertaken for the Route 3A Short span layout as shown in Drawing No. B4027/3/B/301. The Route 3A Short Span operational case has modified pier alignments compared to the version tested in Phase I of the modelling study. The bridge piers are octagonal (5m x 5m) and are placed in pairs. There are 11 sets of piers within the channel and intertidal area.

Figures D15a and D15b show the change in sediment distribution within the estuary for the Route 3A short span option. Comparison of the Short Span scenario against the other scheme layouts shows the greatest impact in terms of sediment distribution within the upper Mersey Estuary.

Downstream of the bridge structures the model shows sediment to be eroded along the intertidal area of Wigg Island and downstream of Old Quay Lock (typical changes < 0.15m). Through Runcorn Gap there are patches of erosion and deposition with maximum changes less than 0.20m. Downstream of Runcorn Gap the predicted morphological changes become insignificant.

Upstream of the bridge structures the model shows erosion, predominantly with maximum changes over the intertidal banks of less than 0.20m. Along the intertidal shorelines on the south and north channels the maximum erosion is -0.39m and -1.71m, respectively.

Adjacent to the bridge piers located within or close to the channels the maximum predicted deposition is 1.79m whilst the maximum erosion is 1.48m. In general, the short span option shows that flows are accelerated through the piers on the flood tide leading to increased erosion local to the proposed crossing. The bridge causes a restriction across the channel leading to a build up in the hydraulic head of water at the bridge (backwater effect). This is likely caused by the asymmetry in the tidal curve with a very rapid flood tide (1.5 hours approximately). This increases deposition both upstream and downstream of the crossing over the flood tide due to the increased water levels and the delay in water movement as a result of the backwater effect.

Although the short span option has not been run for any extreme events its is likely that on surge events in particular, this design option will provide an increased restriction to the propagation of the flood tide.

D22. Cross-Section Analysis

Figure D16 shows the position of various cross-sections taken across the upper estuary. Whilst it has been attempted to locate these as close as possible to the position of the cross-section positions used in the Phase I modelling study, the change in the model grid has meant that this is not always practical. This difference in position is to allow for the greatest changes in channel depth to be picked up in the particular cross-section. Table D1 gives a general summary of changes across the cross-sections for the various schemes.

Figure D17 shows the predicted cross-sections A and B. Clearly for all scheme layouts morphological changes are insignificant at the two cross-sections.

Figure D18 shows the bed level changes at cross-sections C and D. At cross-section C most schemes show minor changes in bed elevation over the section with some deposition within the south channel and on across the central bank area. Changes are typically less than 0.04m in depth. The exception is the Route 3A short span, which shows erosion over the central bank area with a maximum change of 0.2m approximately and deposition in the south channel of 0.07m, maximum change.

At cross-section D again the changes are minor for most schemes (typically < 0.03). Route 3A short span shows the greatest change with some erosion in the south channel (max ≈ 0.09m) and deposition within the north channel (max ≈ 0.03m).

Figure D19 shows the bed level changes at cross-sections E and F. At cross-section E the greatest change occurs in the south channel. The Route 3A Medium span 4 Tower option shows significant deposition within the south channel (max ≈ 1.82m) with a narrowing of the channel for this scheme. Changes for the Route 3A Medium span 4 Tower modified option and 3 Tower revised option are small across the section. The Route 3A Medium span 3 Tower option shows both erosion and deposition in the north channel (see Table D1) and Route 3A Medium span 4 Tower option shows deposition (max ≈ 0.60m).

At cross-section F the largest changes in bed level occur in the north channel. For the Route 3A short span and Medium span 3 Tower scenarios there is significant erosion (1.1m – 1.5m maximum) as a result of the position of bridge structures combined with accretion (max ≈ 0.3m). The Medium span 4 Tower scenarios show little change in the north channel and changes across the channel at this location are relatively small, in general.

Within the south channel there is some deposition along the shoreline side of the channel. The greatest changes are observed for the Route 3A Medium span - original alignment and the Route 3A short span case with maximum increases in sediment of between 0.10 - 0.20m.

Figure D20 shows the cross-sections G and H. At cross-section G all the scheme options except the Route 3A Medium span 3 Tower revised alignment show erosion in the south channel with maximum changes of about 0.3m (see Table D1).

Within the north channel only the short span case and the Route 3A Medium span 3 Tower option show any discernible change with maximum erosion and deposition of 0.43m and 0.36m, respectively (see Table D1).

At cross-section H the largest predicted change is seen to occur with the Route 3A short span case. The short span case shows erosion and deposition on the sides of the southern channel, maximum changes 0.45m and 0.28m, respectively. Route 3A Medium span (4 Tower) shows deposition in the south channel (max $\approx$ 0.1m) and erosion on the channel side (max $\approx$ 0.3m).

Figure D21 shows the bed level changes at cross-sections I and J. The greatest change in section I is shown for the short-span and 4 Tower option. The short span option appears to show a movement of the south channel northwards. Route 3A Medium span (4 Tower) shows erosion in the south channel (max $\approx$ 0.2m) Within the north channel the schemes all show varying degrees of change in bed level with maximum changes in deposition of 0.27m, approximately (short span option).

In cross-section J the Route 3A short span option also appears to show movement of the southern channel and bank northwards. As with cross-section I there is some deposition in the north channel with a maximum increase of about 0.20m.

Figure D22 shows the bed level changes at cross-sections K and L. In both cross-sections changes are small with very little discernible change in section L. In cross-section K the greatest decrease in bed level is about 0.11m and the greatest increase in deposition is about 0.35m, both for the short span option.

Similarly in section L the greatest changes are seen for the short span option with maximum changes in accretion of about 0.09m. Table D1 summarises the associated changes to each cross-section for the Route 3A scenarios (excluding extreme events).

For the modelling undertaken for the Route 3A Medium span modified alignment under extreme fluvial and combined surge and fluvial conditions it is not possible to compare cross-sections taken from these runs with those described above as they have only been run for a spring neap cycle. Scaling these results to represent a year would be meaningless. Therefore, an additional series of cross-sections have been extracted.

Figures D23 -D28 show the cross-sectional changes for the extreme Fluvial and the combined extreme surge and fluvial events. A comparison between the corresponding base line conditions (identical simulation set-up but without bridge structures) and the scenario are shown. Also illustrated is the existing condition for a typical spring neap event.

With the exception of cross-section G under combined extreme surge and fluvial conditions all cross-sections show no discernible change compared with their respective baseline condition. The change observed in cross-section G is attributed to the immediate effect of the bridge structure. It is not immediately obvious why the bridge has such a small impact on the morphology under extreme conditions. However, the answer may lie in the overall change on the system as a whole under extreme events. Table D2 summarises the associated changes to each cross-section for the Route 3A Medium extreme events (Fluvial plus Surge, Fluvial scenarios).

A comparison against the 'existing' base-line condition, which is representative of conditions under an average spring-neap tide and mean fluvial flow, shows significant variation in channel layout. These large-scale channel changes may actually mask out some of the changes associated with placing structures in the upper estuary. Generally, the changes observed as a result of the extreme events include an increase in erosion within the main south and north channels. Generally, an increase in deposition along the margins of the south and north channels is observed. Under extreme conditions the channels exhibit significant movement, particularly at sections K and L.

The morphological changes are driven by the increased velocities on the ebb tide. These increased speeds are not transient changes but represent a change in shape of the current profile through time with a sustained velocity on the ebb lasting the whole of the ebb tide period. The magnitude of these speeds can be in excess of 1m/s over spring tides. These changes reflect switch in dominance from a flood to ebb dominated system and this is very significant in driving morphological change in the upper estuary.

There is very little variation between the fluvial event and the combined surge and fluvial event except that with the surge tide the flow speed is higher than that obtained with only enhanced fluvial flow. In fact during the fluvial event the higher fluvial discharges suppress the flood tide velocities. However, the results demonstrate that the fluvial flow is the dominant mechanism for morphological change in the upper estuary.

Table D1. Summary of cross-sectional bed level changes for the various schemes. Description of changes compared against the existing 'baseline' condition

Cross-Section	Scenario				
	Route 3A Medium - Original	Route 3A Medium - Modified	Route 3A Medium - 3 Tower	Route 3A Medium - 3 Tower Revised	Route 3A - Short
A	No change	No change	No change	No change	No change
B	No change	No change	No change	No Change	No Change
C	Minor changes in elevation over cross-section (max ≈ 0.04m)	Minor changes in elevation over cross-section (max ≈ 0.01m)	Minor changes in elevation over cross-section (max ≈ 0.02m)	Minor changes in elevation over cross-section (max ≈ 0.01m)	Some deposition in south channel (max ≈ 0.07m) and erosion over bank (max ≈ 0.18m).
D	Some minor deposition over cross-section (max ≈ 0.03m)	Minor changes in elevation over cross-section (max ≈ 0.02m)	Minor changes in elevation over cross-section (max ≈ 0.02m)	Minor changes in elevation over cross-section (max ≈ 0.01m).	Some erosion in south channel (max ≈ 0.09m) and deposition within north channel (max ≈ 0.03m)
E	Deposition in south channel (max ≈ 1.82m) and north channel (max ≈ 0.60m)	Minor erosion in south channel (max ≈ 0.01m) and deposition within north channel (max ≈ 0.05m)	Some erosion in south channel (max ≈ 0.03m) and erosion (max ≈ 0.19m) and deposition (max ≈ 0.13m) in north channel	Minor changes in elevation over cross-section (max ≈ 0.02m)	Erosion in south channel (max ≈ 0.07m) and deposition within north channel (max ≈ 0.08m)
F	Erosion in south channel (max ≈ 0.13m) deposition in north channel (max ≈ 0.05m)	Minor erosion in south channel (max ≈ 0.02m) and deposition within north channel (max ≈ 0.04m)	Significant erosion and deposition in north channel, max ≈ 1.46m and 0.34m, respectively.	Significant erosion and deposition in north channel, max ≈ 1.38m and 0.29m, respectively.	Significant erosion and deposition in north channel, max ≈ 1.10m and 0.34m, respectively.
G	Some erosion in south channel (max ≈ 0.31m) deposition in north channel (max ≈ 0.09m)	Some erosion in south channel (max ≈ 0.03m) deposition in north channel (max ≈ 0.10m)	Some erosion in south channel (max ≈ 0.07m) deposition in north channel (max ≈ 0.32m)	Deposition in north channel (max ≈ 0.06m)	Erosion in south channel (max ≈ 0.18m) Erosion and deposition in north channel max ≈ 0.43m and 0.36m, respectively.
H	Erosion in south channel (max ≈ 0.11m) and deposition on sides of channel (max ≈ 0.28m). Deposition in north channel (max ≈ 0.06m)	Erosion in south channel (max ≈ 0.08m) and deposition on sides of channel (max ≈ 0.02m). Deposition in north channel (max ≈ 0.07m)	Erosion in south channel and on sides of channel (max ≈ 0.44m). Deposition in north channel (max ≈ 0.18m)	Erosion and deposition on sides of channel max ≈ 0.29m and 0.09m, respectively.	Erosion and deposition on sides of channel max ≈ 0.45m and 0.28m, respectively. Deposition in north channel (max ≈ 0.20m)
I	Erosion and deposition on southern side of channel max ≈ 0.22m and 0.05m, respectively.	General deposition over cross-section (max ≈ 0.06m)	General deposition over cross-section (max ≈ 0.13m)	General deposition over cross-section (max ≈ 0.06m)	Erosion and deposition on southern side of channel max ≈ 0.14m and 0.88m, respectively. Deposition in north channel (max ≈ 0.27m)
J	Erosion and deposition in south channel max ≈ 0.16m and 0.17m, respectively. Over remaining section erosion and deposition (max ≈ 0.08m)	General deposition over cross-section (max ≈ 0.06m). Some erosion over central banks (max ≈ 0.05m)	Generally deposition over cross-section (max ≈ 0.14m) with some erosion over sides of central bank (max ≈ 0.03m)	General deposition over cross-section (max ≈ 0.04m). Some erosion over central banks (max ≈ 0.03m)	Erosion and deposition on southern side of channel max ≈ 0.20m and 0.45m, respectively. Deposition in north channel (max ≈ 0.20m)
K	Erosion and deposition over central banks max ≈ 0.02m and 0.15m, respectively. Deposition in north channel (max ≈ 0.02m)	Deposition in north channel (max ≈ 0.02m)	Generally deposition over cross-section (max ≈ 0.07m) with some erosion over sides of central bank (max ≈ 0.03m)	Generally deposition over cross-section (max ≈ 0.03m) with some localized erosion over sides banks (max ≈ 0.01m)	Erosion and deposition in south channel max ≈ 0.11m and 0.35m, respectively. General deposition over remaining cross-section (max ≈ 0.27m)
L	Deposition over central banks and north channel (max ≈ 0.07m)	Some minor deposition and erosion on north side of channel (max ≈ 0.01m)	Generally deposition over cross-section (max ≈ 0.03m) with some erosion over sides of central bank (max ≈ 0.01m)	Minor changes in elevation over cross-section (max ≈ 0.01m)	General deposition over cross-section (max ≈ 0.09m).

Table D2. Summary of cross-sectional bed level changes for the extreme schemes for the Route 3A 4 Tower modified alignment. Description of changes compared against the corresponding existing condition (without bridge structures)

Cross-Section	Scenario	
	Route 3A Medium Modified Alignment - Fluvial with Surge	Route 3A Medium Modified Alignment - Fluvial
A	No Change	No Change
B	No Change	No Change
C	No Change	No Change
D	No Change	No Change
E	No Change	No Change
F	Slight increase in erosion along the margin of the south channel	No Change
G	No Change	No Change
H	No Change	No Change
I	No Change	No Change
J	No Change	No Change
K	No Change	No Change
L	No Change	No Change

D22.1 Route 3A 3 Tower Revised Alignment – Extreme Fluvial and Surge

Figures D29 – D34 show the various cross-sections for the Route 3A Medium Span 3 Tower revised alignment for an extreme fluvial and surge event. The positions of the cross-sections remain as shown in Figure D16. A summary of the changes is given in Table D3.

Figure D29 shows the cross-sections at A and B. At cross-section A there are no predicted changes. At cross-section B there is some deposition of sediment in the bottom of the central channel (max ≈ 0.04m), whilst towards the northern side there is erosion on the shoulder of the bank (max ≈ 0.03m).

Figure D30 shows the cross-sections at C and D. At section C there is some deposition of sediment over the central part of the channel (max ≈ 0.02m) in addition to some erosion (max ≈ 0.06m).

At cross-section D there is some erosion in the bottom of the southern channel (max ≈ 0.01m) and some deposition part way up the side of the intertidal bank (max ≈ 0.05m). Over the central part of the intertidal bank there is no significant change predicted. In the northern channel there both some erosion (max ≈ 0.04m) and deposition (max ≈ 0.02m) at its bottom.

The changes at cross-sections E and F are shown in Figure D31. At section E there are minor changes in the southern channel with some predicted deposition of sediment (max ≈ 0.01m). There is no predicted change over the central intertidal bank, although there is some erosion (max ≈ 0.08m) on the side of this bank adjacent to the northern channel. Within the northern channel there is sediment accretion predicted (max ≈ 0.23m).

Table D3. Summary of cross-sectional bed level changes for the Route 3A 3 Tower revised alignment for an extreme fluvial and surge event. Description of changes compared against the corresponding existing condition (without bridge structures)

Cross-Section	Scenario Route 3A Medium 3 Tower Revised Alignment - Fluvial with Surge
A	No change
B	Erosion in bottom of central channel (max ≈ 0.04m). Erosion on shoulder of bank towards northern side (max ≈ 0.03m).
C	Some deposition (max ≈ 0.02m) and erosion (max ≈ 0.06m) over central part of channel.
D	Slight erosion in southern channel (max ≈ 0.01m) and deposition on side of intertidal bank (max ≈ 0.05m). Erosion in northern channel (max ≈ 0.04m) as well as some deposition (max ≈ 0.02m).
E	Minor changes in southern channel, deposition (max ≈ 0.01m). In northern channel some erosion on side of intertidal bank (max ≈ 0.08m) and deposition within channel (max ≈ 0.23m).
F	Minor changes in southern channel deposition (max ≈ 0.01m). In northern channel both erosion (max ≈ 1.79m) and deposition (max ≈ 0.86m).
G	Slight erosion (max ≈ 0.03m) and deposition within southern channel. Within northern channel both erosion (max ≈ 0.01m – 0.48m) and deposition (max ≈ 0.01m – 0.59m).
H	Erosion and deposition within southern channel (max ≈ ±0.02m). Some deposition on southern side of intertidal bank (max ≈ 0.04m). Erosion (max ≈ 0.07m) and deposition (max ≈ 0.11m) on shoulder of intertidal bank. In northern channel some erosion (max ≈ 0.08m) and deposition (max = 0.03m).
I	Some erosion and accretion in southern channel (max ≈ ±0.02m). Slight erosion and deposition over central intertidal banks (max ≈ ±0.01m). Towards northern channel areas of erosion (max ≈ 0.04m) and deposition (max ≈ 0.03m).
J	Minor erosion (max ≈ 0.01m) and some deposition (max ≈ 0.02m) in southern channel. Some erosion (max ≈ 0.01m) and deposition (max ≈ 0.02m) over central intertidal banks. Some accretion (max ≈ 0.01m) and erosion (max ≈ 0.02m) towards the northern channel.
K	Within the southern channel there is some erosion (max ≈ 0.01m) and deposition (max ≈ 0.02m). Some deposition (max ≈ 0.01m) across the central channel and banks. Towards the northern bank there is some erosion and deposition (max ≈ ±0.01m).
L	Some erosion and deposition within southern channel (max ≈ ±0.02m). Over central banks and channels there is some erosion and deposition (max ≈ ±0.02m). Towards the northen channel there is erosion (max ≈ 0.02m) and deposition (max ≈ 0.01m).

At cross-section F there is some deposition of sediment in the southern channel (max ≈ 0.01m). However, the greatest changes are predicted to occur in the northern channel with both erosion (max ≈ 1.79m) and deposition (max ≈ 0.86m) of sediment as a response to the proximity of the bridge tower in the northern channel.

Figure D32 shows the cross-sections at G and H. At cross-section G there is both erosion (max ≈ 0.03m) and deposition of sediment within the southern channel. There is no predicted change over the intertidal bank. In the northern channel there is a

change in the bed profile, with reshaping and deepening of the channel adjacent to the intertidal bank (max ≈ 0.48m). In the central part of the northern channel there is deposition of sediment (max ≈ 0.59m). This is material scoured from around the bridge tower within the northern channel and deposited upstream of the structure. Towards the shoreward side of the channel there is both erosion and accretion of sediment.

At section H within the southern channel there is some deposition and erosion of sediment with maximum predicted changes of the order of ±0.02m. There is deposition of sediment on the lower slope of the southern side of the intertidal bank (max ≈ 0.04m). On the shoulder of the bank there is some erosion (max ≈ 0.07m) and deposition (max ≈ 0.11m) of sediment. In the northern channel there is some erosion (max ≈ 0.04m) and deposition (max ≈ 0.03m) of sediment.

Figure D33 shows the cross-sections I and J. At section I there is both erosion and accretion of sediment in the southern channel (max ≈ ± 0.02m). There is some erosion and deposition (max ≈ ±0.01m) of sediment over the central part of the intertidal bank. Towards the northern channel there are areas of erosion (max ≈ 0.04m) and deposition (max ≈ 0.03m).

Figure D33 shows the changes at cross-section J with some erosion (max ≈ 0.01m) and accretion (max ≈ 0.02m) of sediment within the southern channel. There are small changes in sedimentation over the central parts of the intertidal bank with both erosion (max ≈ 0.01m) and deposition (max ≈ 0.02m) predicted. Towards the northern channel there is also some accretion (max ≈ 0.01m) and erosion (max ≈ 0.02m).

Figure D34 shows the variations in cross-sectional form at positions K an L. At section K there is both erosion (max ≈ 0.01m) and deposition (max ≈ 0.02m) predicted to occur in the southern channel. There is some deposition (max ≈ 0.01m) of sediment across the central intertidal banks and central channel. Towards the northern shoreline there is both erosion and deposition of sediment predicted (max ≈ ±0.01m).

At cross-section L there is some erosion and deposition within the southern channel (max ≈ ±0.02m), whilst over the central banks and channels there is also erosion and accretion of sediment (max ≈ ±0.02m). Towards the northern channel there is erosion (max ≈ 0.02m) and some deposition of sediment (max ≈ 0.01m).

D22.2 Route 3A 3 Tower Revised Alignment – Recovery Scenario

As previously, Figure D16 shows the positions of the various cross-sections taken across the upper estuary. Figures D35 – D40 show the various cross-sections for the Route 3A Medium Span 3 Tower revised alignment for a simulated 'recovery' sceanrio. A summary of the changes is given in Table D4.

Table D4. Summary of cross-sectional bed level changes for the Route 3A 3 Tower revised alignment recovery scenario. Description of changes compared against the corresponding existing condition (without bridge structures)

Cross-Section	Scenario
	Route 3A Medium 3 Tower Revised Alignment - Recovery
A	No change
B	No change
C	Some erosion and deposition (max ≈ ±0.01m) over intertidal banks.
D	Towards northern channel some erosion and deposition over intertidal banks (max ≈ ±0.01m). Within the northern channel there is some deposition (max ≈ 0.03m).
E	Limited changes within southern channel with some minor erosion (max ≈ 0.01m). Within the northern channel there is some erosion and deposition (max ≈ ±0.02m).
F	Changes limited to northern channel, with both erosion (max ≈ 1.37m) and deposition (max ≈ 0.29m).
G	Some changes in southern channel and over central intertidal banks (max ≈ ±0.01m). Within the northern channel some deposition (max ≈ 0.06m) and some erosion (max ≈ 0.01m).
H	Some deposition in southern channel (max ≈ 0.02m). Some erosion (max ≈ 0.29m) and deposition (max ≈ 0.09m) on shoulder of intertidal bank. In north channel some erosion and deposition (max ≈ ±0.03m).
I	Some deposition in southern channel (max ≈ 0.01m). Deposition over central area (max ≈ 0.06m) together with some erosion (max ≈ 0.01m). Deposition within northern channel (max ≈ 0.03m).
J	Some erosion and deposition within southern channel and on adjacent intertidal bank (max ≈ ±0.01m). Within central bank area there is some erosion (max ≈ 0.03m) and deposition (max ≈ 0.02m). Within the northern channel there is deposition (max ≈ 0.04m).
K	Some erosion and deposition within southern channel (max ≈ ±0.01m) and on adjacent intertidal bank (max deposition ≈ 0.02m; max erosion ≈ 0.01m). Towards northern side of estuary some erosion (max ≈ 0.01m) and deposition (max ≈ 0.03m).
L	Little change over whole cross-section. Some erosion towards southern side (max ≈ 0.01m) and both deposition and erosion towards northern side (max ≈ ±0.01m).

Figure D35 shows the cross-sections at positions A and B. There is no discernible change in bed elevation between the baseline case and the recovery scenario for each cross-section.

Figure D36 shows the cross-sections at positions C and D. At cross-section C there is some erosion and deposition of sediment over the intertidal banks (max ≈ ±0.01m). At section D, towards the northern channel, there is some erosion and deposition over the intertidal banks (max ≈ ±0.01m). Within the northern channel itself there is some deposition of sediment (max ≈ 0.03m).

Figure D37 shows the cross-sections at positions E and F. At cross-section E there are small changes within the southern channel with some erosion (max ≈ 0.01m). Within the northern channel there is both erosion and deposition of sediment (max ≈ ±0.02m). At section F changes in the profile are confined to the northern channel with both erosion (max ≈ 1.37m) and deposition (max ≈ 0.29m) of sediment.

Changes in profile along cross-sections G and H are shown in Figure D38. At cross-section G there are some changes within the southern channel and over the central intertidal banks with both erosion and accretion of sediment predicted (max ≈ 0.01m).

Within the northern channel there is some deposition (max ≈ 0.06m) and erosion (max ≈ 0.01m) of sediment.

Figure D38 shows cross-section H with some predicted accretion of sediment within the southern channel (max ≈ 0.02m). There is some erosion (max ≈ 0.29m) and deposition (max ≈ 0.09m) on the shoulder of the intertidal bank, whilst in the northern channel there is both erosion and deposition of sediment (max ≈ ±0.03m).

Figure D39 shows the cross-sections at positions I and J. At section I there is some localised deposition in the southern channel (max ≈ 0.01m), whilst over the central area there is deposition (max ≈ 0.06m) and some erosion (max ≈ 0.01m) of sediment. Within the northern channel sediment is deposited (max ≈ 0.04m).

At cross-section J there is erosion and deposition within the southern channel and on the adjacent edge of the intertidal bank (max ≈ 0.01m). Within the area of the central banks and channels there is some erosion (max ≈ 0.03m) and deposition (max ≈ 0.02m) of sediment. In the northern channel sediment is being deposited (max ≈ 0.09m).

Changes in profile along cross-sections K and L are shown in Figure D40. At cross-section K there is some erosion and deposition within the southern channel with maximum changes of ±0.01m, approximately. On the intertidal bank adjacent to the south channel there is both deposition (max ≈ 0.02m) and erosion predicted (max ≈ 0.01m). Towards the northern side of estuary there is some erosion (max ≈ 0.01m) and deposition (max ≈ 0.03m).

At cross-section L there is little change over the whole cross-section. There is some erosion towards the southern side (max ≈ 0.01m) and both deposition and erosion towards the northern side (max ≈ ±0.01m).

D22.3 Route 3A 3 Tower Revised Alignment – 2005 Bathymetry

As in the previous analysis, Figure D16 shows the positions of the various cross-sections taken across the upper estuary. Figures D41 – D46 show the various cross-sections for the Route 3A Medium Span 3 Tower revised alignment for the 2005 bathymetry. A summary of the changes is given in Table D5.

Figure D41 shows the cross-sections at positions A and B. There is no discernible change in bed elevation between the baseline case and the scenario for cross-section A. At cross-section B there is some deposition on the southern bank (max ≈ 0.01m) and erosion in central channel (max ≈ 0.01m). Towards the northern side of the channel there is some erosion predicted.

Figure D42 shows the cross-sections at positions C and D. At cross-section C there is deposition predicted in the southern channel (max ≈ 0.01m) and erosion over the intertidal bank (max ≈ 0.01m). Towards the north bank there is some deposition (max ≈ 0.01m). some erosion and deposition of sediment over the intertidal banks (max ≈ ±0.01m). At section D, there is no discernible change in bed elevation between the baseline case and the scenario.

Table D5. Summary of cross-sectional bed level changes for the Route 3A 3 Tower revised alignment – 2005 bathymetry. Description of changes compared against the corresponding existing condition (without bridge structures)

Cross-Section	Scenario
	Route 3A Medium 3 Tower Revised Alignment – 2005 bathymetry
A	No change
B	Some deposition on southern bank (max ≈ 0.01m). Erosion in central channel (max ≈ 0.01m). Some erosion towards northern side.
C	Deposition in southern channel (max ≈ 0.01m). Erosion over intertidal bank (max ≈ 0.01m). Some deposition towards north bank (max ≈ 0.01m).
D	No change
E	Deposition in southern channel (max ≈ 0.03m) together with some erosion (max ≈ 0.01m). Some deposition on intertidal bank (max ≈ 0.01m). Deposition (max ≈ 0.05m) and erosion (max ≈ 0.04m) in northern channel.
F	Erosion and deposition in southern channel (max ≈ ±0.02m). Erosion and deposition over intertidal bank (max ≈ ±0.02m). Within northern channel there is deposition (max ≈ 0.35m) and erosion (max ≈ 1.01m).
G	Erosion in southern channel on side closest to intertidal bank (max ≈ 0.04m). Some deposition on 'hump' bisecting channel (max ≈ 0.01m) with erosion on other side of channel (max ≈ 0.06m). Erosion (max ≈ 0.36m) and deposition (max ≈ 0.21m) over intertidal bank. Deposition in northern channel (max ≈ 0.11m).
H	Erosion (max ≈ 0.06m) and deposition (max ≈ 0.04m) in southern channel. Erosion (max ≈ 1.39m) and deposition (max ≈ 0.58m) on side of intertidal bank. Over top of bank there is some erosion (max ≈ 0.04m). There is erosion in northern channel (max ≈ 0.04m).
I	Erosion (max ≈ 0.10m) and deposition (max ≈ 0.18m) in south channel. Erosion (max ≈ 0.26m) and deposition (max ≈ 0.20m) over southern side of intertidal bank. Some erosion in northern channel (max ≈ 0.03m).
J	Erosion (max ≈ 0.04m) and deposition (max ≈ 0.29m) in southern channel. Over southern side of intertidal bank there is erosion (max ≈ 0.04m) and deposition (max ≈ 0.14m). Some erosion and deposition in northern channel (max ≈ ±0.01m).
K	Deposition in southern channel (max ≈ 0.09m). Some erosion (max ≈ 0.01m) and deposition (max ≈ 0.13m) over southern side of intertidal bank. Some deposition in northern channel (max ≈ 0.01m).
L	Deposition in southern channel (max ≈ 0.18m). Deposition over southern side of intertidal bank (max ≈ 0.07m). Some erosion and deposition in north channel (max ≈ ±0.01m) .

The changes at cross-sections E and F are shown in Figure D43. At section E there is deposition predicted to occur in the southern channel (max ≈ 0.03m) together with some erosion (max ≈ 0.01m). There is also some deposition on the intertidal bank (max ≈ 0.01m). Within the northern channel there is both deposition (max ≈ 0.05m) and erosion (max ≈ 0.04m) predicted.

At cross-section F there is erosion and deposition within the southern channel (max ≈ ±0.02m) as well as over the intertidal bank (max ≈ ±0.02m). In the northern channel there is deposition (max ≈ 0.35m) and erosion (max ≈ 1.01m) predicted. These larger changes predicted to occur in the northern channel are as a response to the proximity of the bridge tower in the channel.

Changes in profile along cross-sections G and H are shown in Figure D44. At cross-section G there is erosion in the southern channel on the side closest to the intertidal bank (max ≈ 0.04m). There is some deposition on the 'hump' bisecting the south channel (max ≈ 0.01m) with erosion on the other side of the channel (max ≈ 0.06m). Over the intertidal bank there is erosion (max ≈ 0.36m) and deposition (max ≈ 0.21m) predicted to occur. In the northern channel there is deposition (max ≈ 0.11m).

At section H there is erosion (max ≈ 0.06m) and deposition (max ≈ 0.04m) in the southern channel. On the side of the intertidal bank adjacent to the southern channel erosion (max ≈ 1.39m) and deposition (max ≈ 0.58m) is predicted to occur. These predicted changes are a response to the proximity of the bridge tower in the channel. Over the top of the bank there is some erosion of sediment (max ≈ 0.04m). There is also erosion of sediment in the northern channel (max ≈ 0.04m).

Figure D45 shows the cross-sections at positions I and J. At section I there is erosion (max ≈ 0.10m) and deposition (max ≈ 0.18m) of sediment in the south channel. There is also some erosion (max ≈ 0.26m) and deposition (max ≈ 0.20m) of sediment over the southern side of the intertidal bank. Within the northern channel there is some erosion (max ≈ 0.03m).

At cross-section J there is erosion (max ≈ 0.04m) and deposition (max ≈ 0.29m) predicted to occur in the southern channel. Over the southern side of the intertidal bank there is also erosion (max ≈ 0.04m) and deposition (max ≈ 0.14m) of sediment. In the northern channel there is also erosion and deposition (max ≈ ±0.01m)of sediment predicted.

Figure D46 shows the variations in cross-sectional form at positions K an L. At section K deposition of sediment is predicted in the southern channel (max ≈ 0.09m). Over the southern side of the intertidal bank there is some erosion (max ≈ 0.01m) and deposition (max ≈ 0.13m) predicted. In the northern channel the modelling predicts deposition to occur (max ≈ 0.01m).

At cross-section L there is deposition of sediment predicted in the southern channel (max ≈ 0.18m) and over the southern side of the intertidal bank (max ≈ 0.07m). There is some erosion and deposition of sediment in the north channel (max ≈ ±0.01m).

An additional series of runs were undertaken to assess the impact of placing structures in the upper estuary over longer time-scales. Figures D47 and D48 show the predicted changes in bed elevation after a simulated 2 years period for the Route 3A Medium span - Modified alignment and the Route 3A Medium 3 Tower scenario. The results shown are a difference between the bed elevations taken from the end of year 1 and the end of year 2. The plots show small changes $\pm$ 0.02m along the margins of the south channel and inter-tidal regions. The results suggest that within a relatively short period after placing structures in the upper estuary the system appears to have achieved a new equilibrium. If the figures had shown significantly larger changes in bed elevation this would have suggested that the system was still trying to adjust to the placement of the structures.

D.20 Conclusion

The morphological modelling of the Mersey Estuary using the newly developed Domain Decomposition model has allowed an assessment of morphological change to be made as a result of placing bridge structures in the upper estuary. The refined grid has demonstrated the effect the proposed bridge placements can have not only within the main flood/ebb channels, but also the detailed change on the inter-tidal and channel margin areas.

Of all the Route 3A variants tested, the results show that the Modified 4 Tower alignment and the revised 3 Tower alignment have the least impact on the system. Between these two scenarios the revised 3 Tower alignment has the least impact in terms of the extent of change although in terms of magnitude the Modified 4 Tower alignment shows less change.

Under extreme fluvial and combined surge and fluvial conditions the morphological changes are driven by the increased velocities on the ebb tide. These increased speeds are not transient changes but represent a change in shape of the current profile through time with a sustained velocity on the ebb lasting the whole of the ebb tide period. The magnitude of these speeds can be in excess of 1m/s over spring tides. These changes reflect a switch in dominance from a flood to ebb dominated system and this is very significant in driving morphological change in the upper estuary.

The results from the morphological model have to be interpreted with care, taking into account the natural variability of the system, which is a more stochastic process than the modelling allows for.

D.20 References

ABPmer (2003). *New Mersey Crossing*. May, Rep. No. R.1007.

Environment Agency (1998). *Extreme Sea levels for Section 105 Surveys*. Final report, JBA Ltd., July, 9pp (+Tables and Figures).

HR Wallingford (1999). *Analysis of bathymetric surveys of the Mersey Estuary*. Report IT 469, October, 18pp (+ Figures).

HRS Wallingford (1983). *Observations of tidal currents, salinities and suspended solids concentrations during a spring tidal cycle*. Report No. EX 1171.

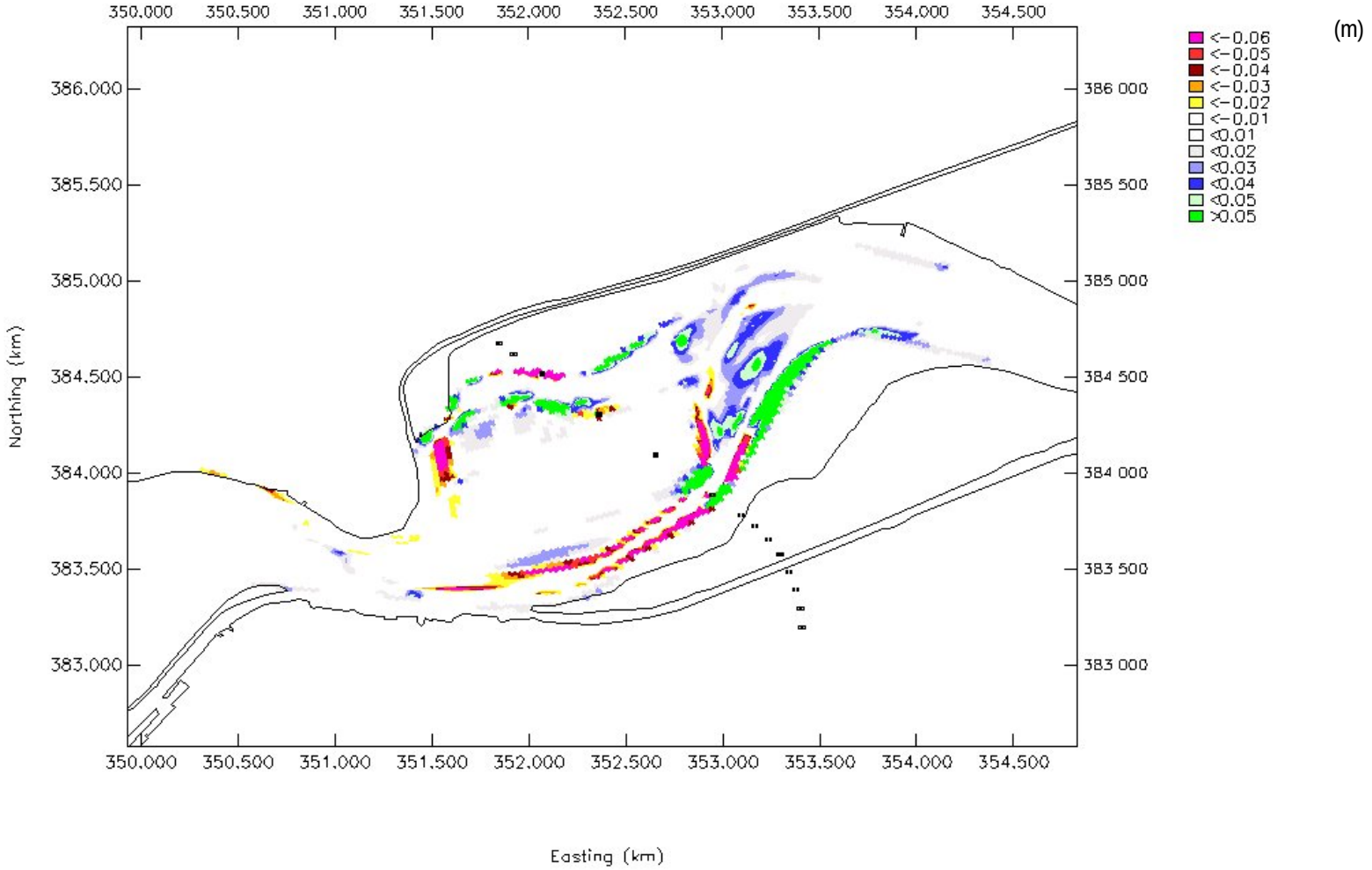
McDowell, D.M. and O'Connor, B.A. (1977). T*he hydraulic behaviour of estuaries*. Macmillan Press Ltd., London, 292pp.

O'Connor, B. A. (1987). Short and long term changes in estuary capacity. J. of Geological Soc., London, Vol. 144, pp. 187 - 195.

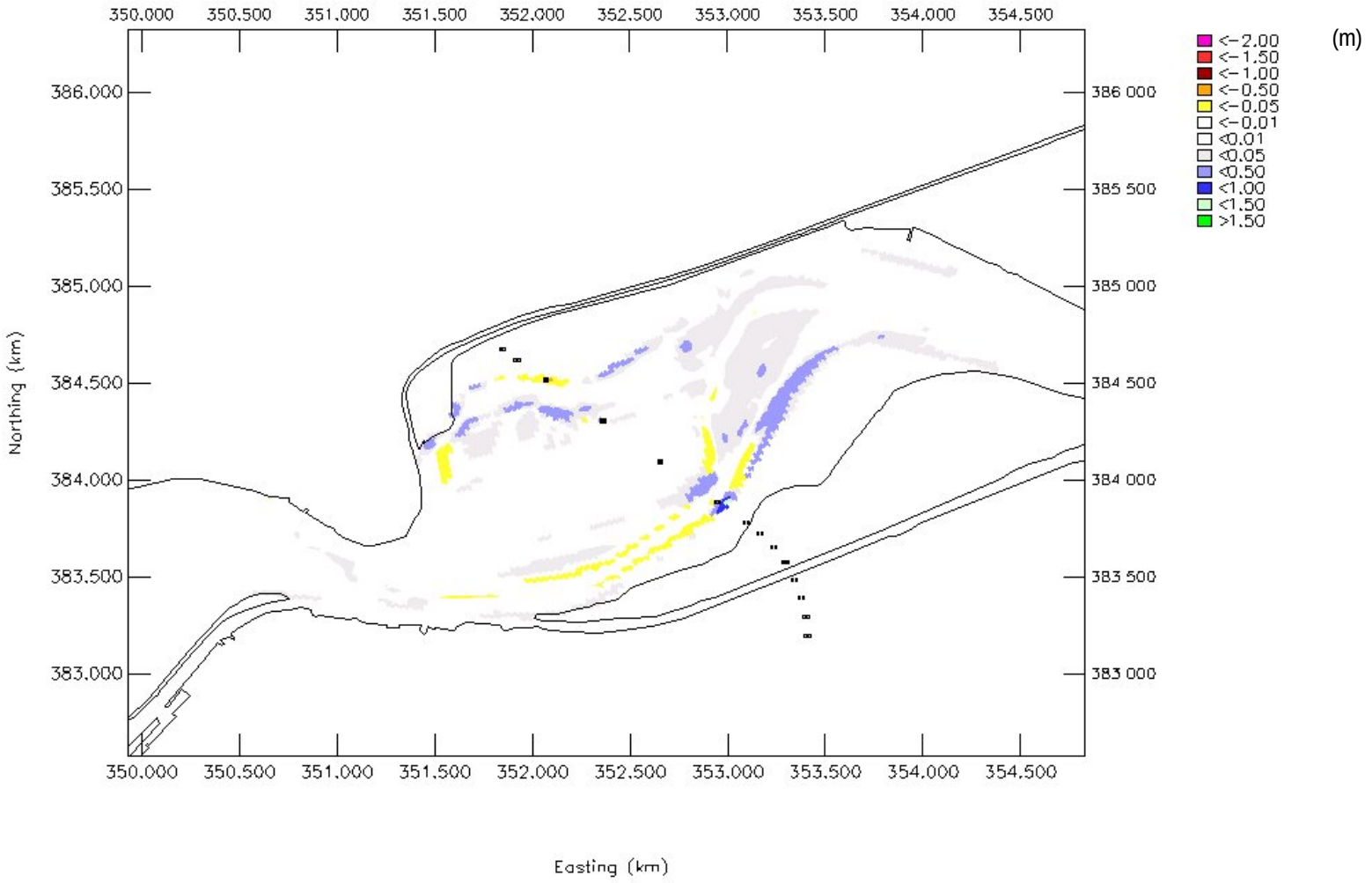
Price, W.A. and Kendrick, M.P. (1963). Field and model investigation into the reasons for siltation in the Mersey Estuary. *Proc. Inst. Civil Engrs*., April, Vol 24, pp 473-518.

Thomas, C. (1999). Analysis of bathymetric surveys of the Mersey Estuary. HR Wallingford, Report IT 469, October, 18pp. + Figures.

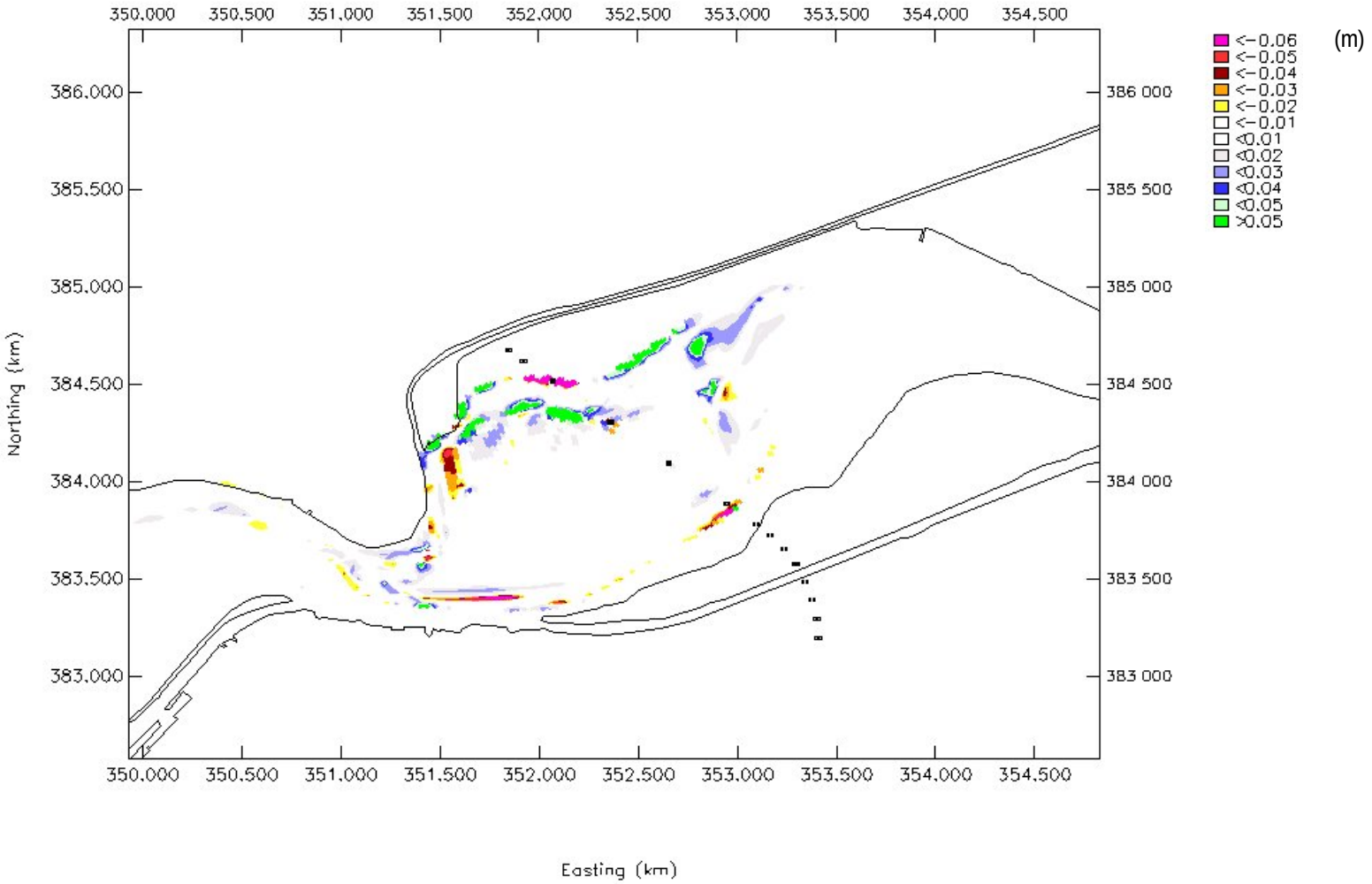
Van Rijn, L.C. (1993). *Principles of Sediment Transport in Rivers, Estuaries and Coastal Seas*. Aqua Publications, Amsterdam.



ABP mer marine environmental research	Morphological change (m) after 1 year. Route 3A Medium Span – Original Alignment Scenario (4 Towers). Differences shown using a fine scale.	Figure D5a

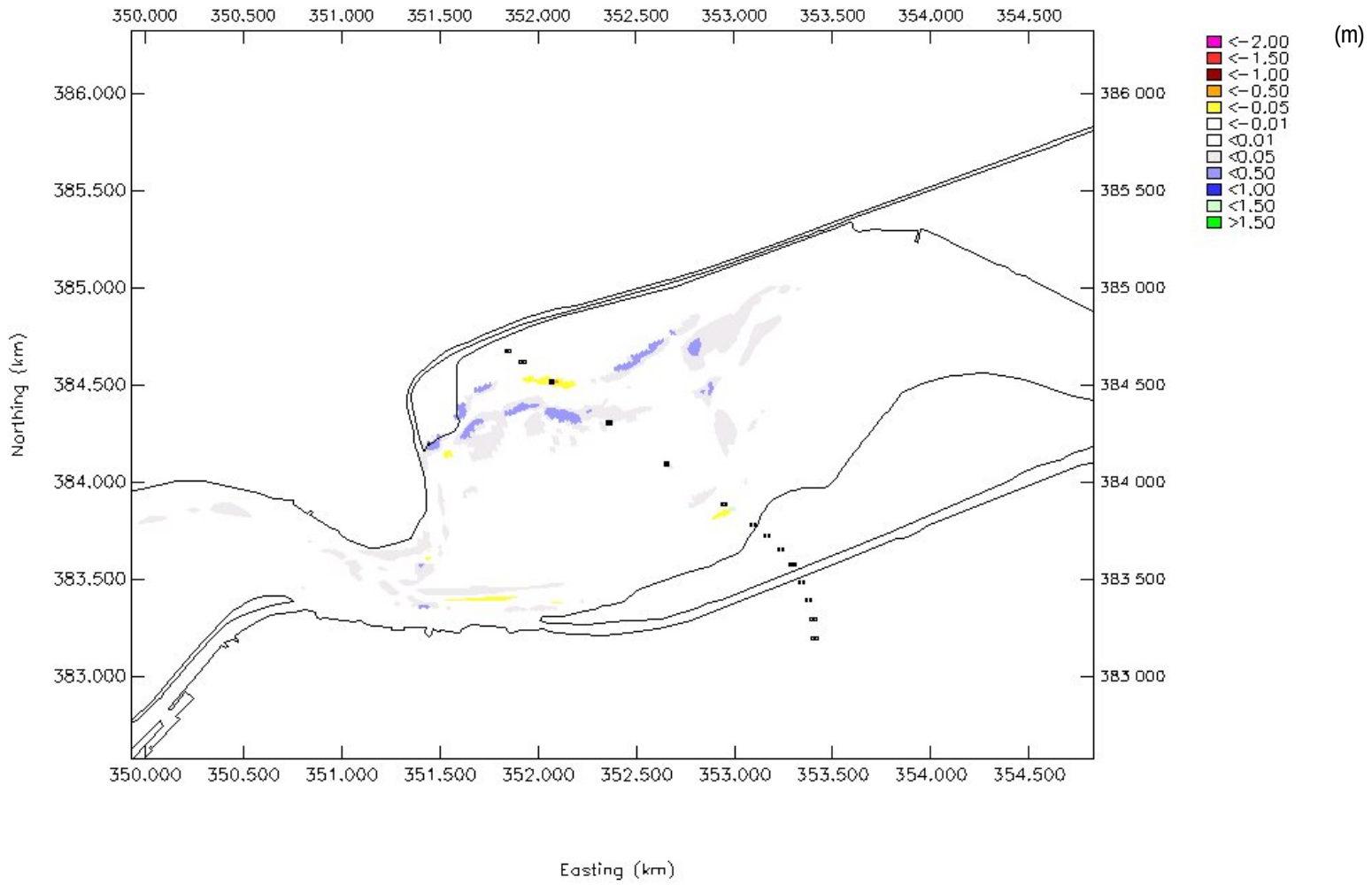


ABP mer marine environmental research	Morphological change (m) after 1 year. Route 3A Medium Span – Original Alignment Scenario (4 Towers). Differences shown using a coarse scale.	Figure D5b

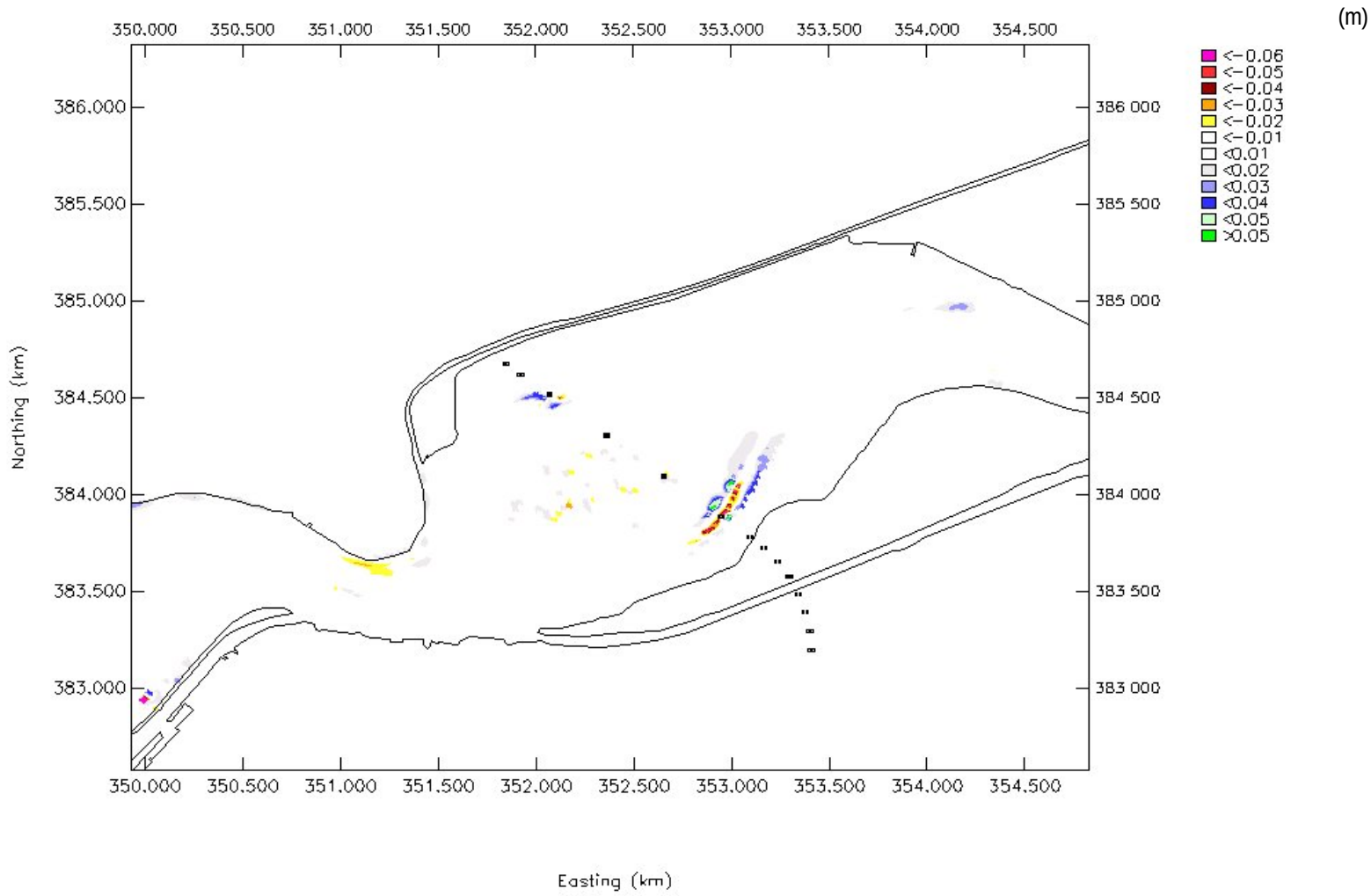


Morphological change (m) after 1 year. Route 3A Medium Span – Modified Alignment Scenario (4 Towers). Differences shown using a fine scale.

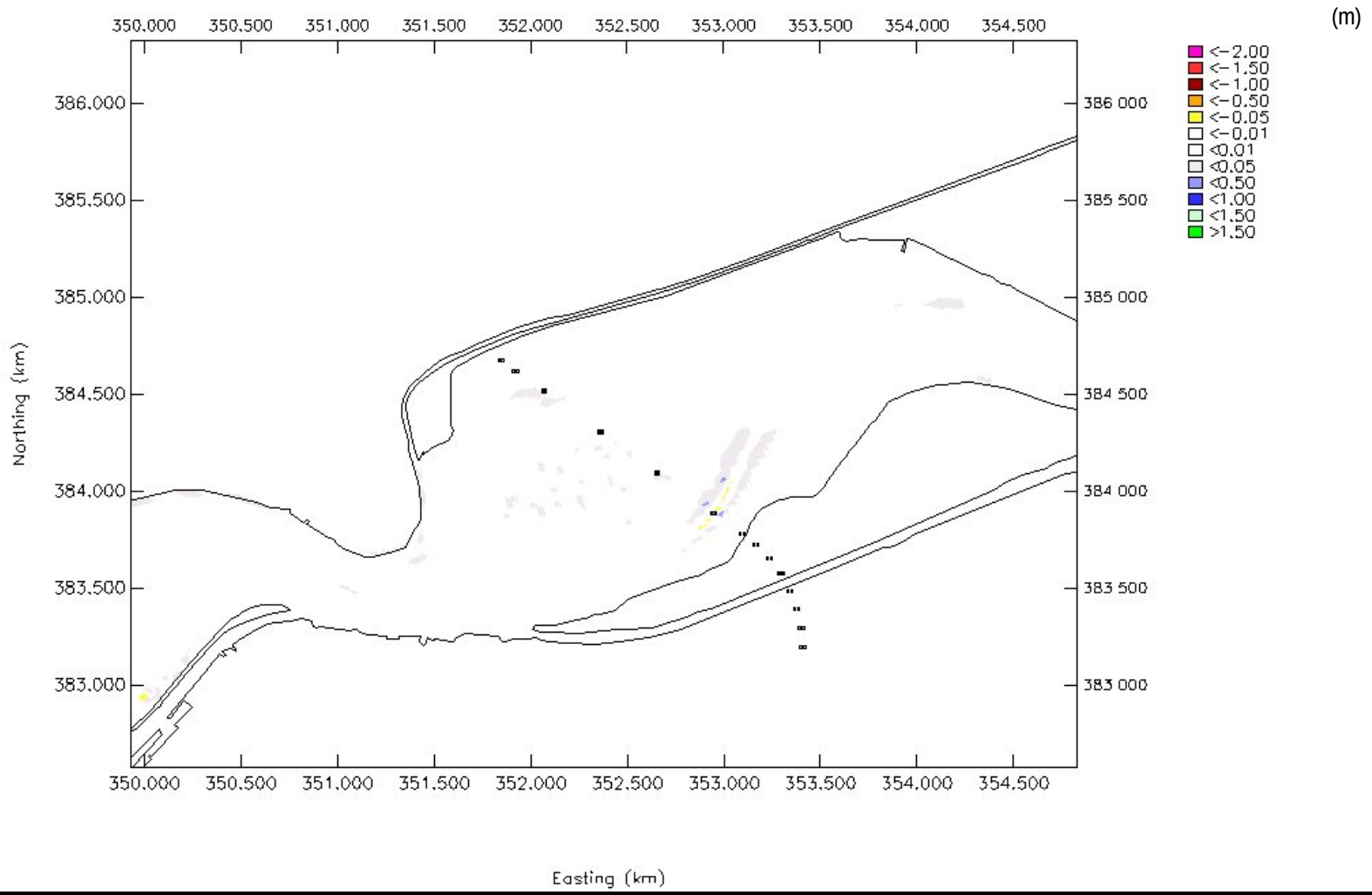
Figure D6a



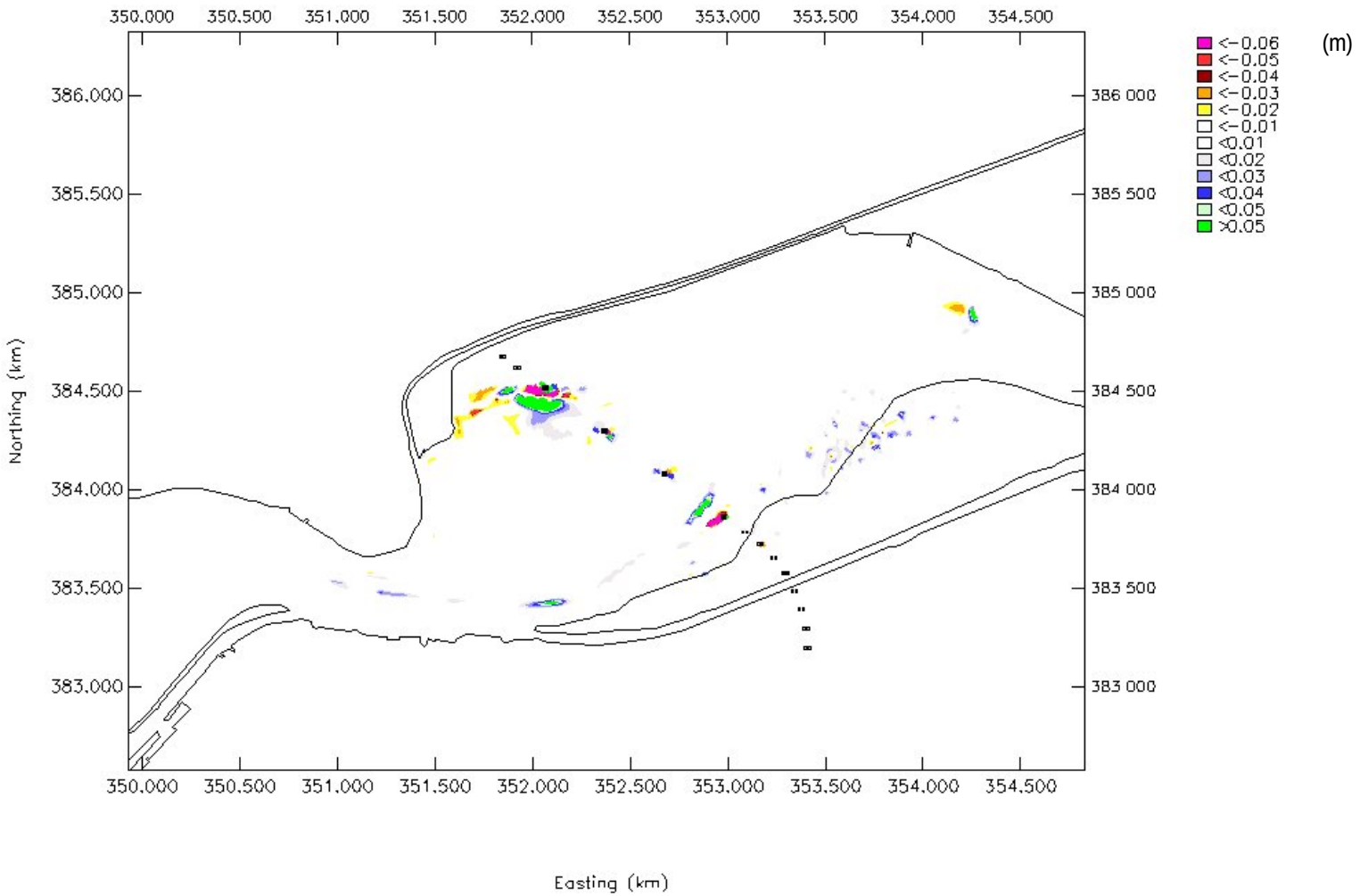
ABP mer marine environmental research	Morphological change (m) after 1 year. Route 3A Medium Span – Modified Alignment Scenario (4 Towers). Differences shown using a coarse scale.	Figure D6b



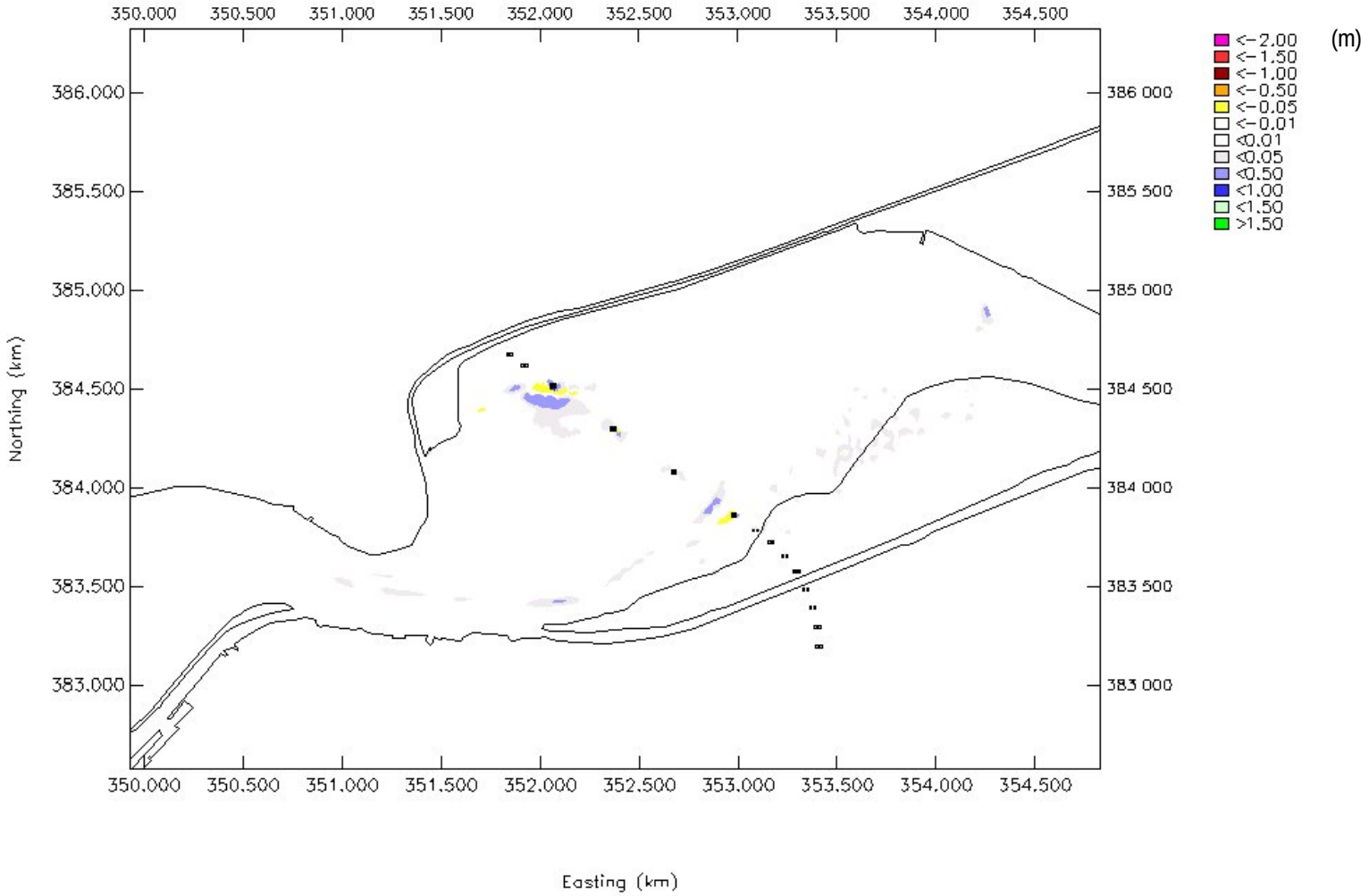
ABP mer marine environmental research	Morphological change (m) after Spring/Neap (15days) period. Medium Span – Modified Alignment Scenario (4 Towers). Differences shown using a fine scale.	Figure D7a



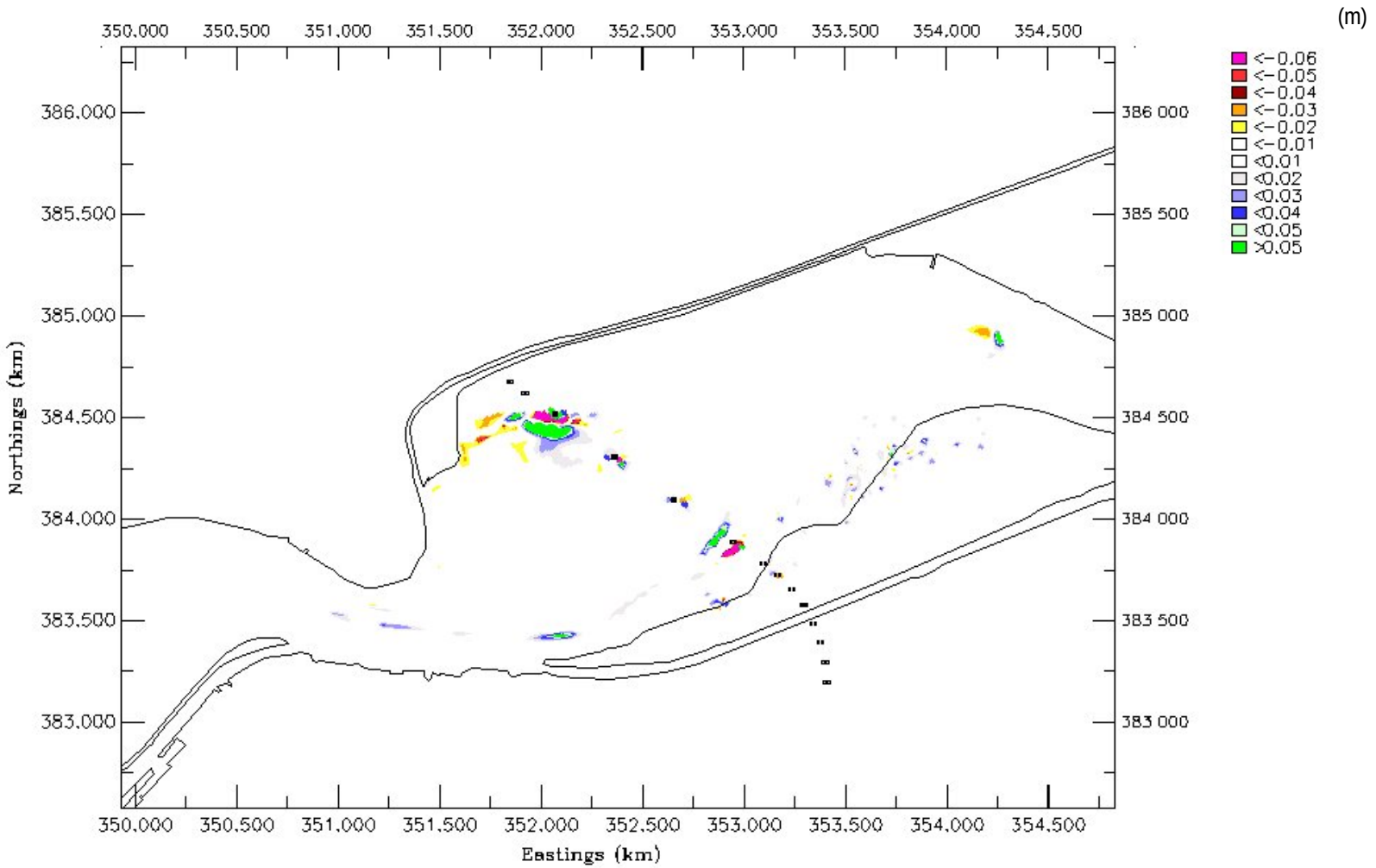
ABP mer marine environmental research	Morphological change (m) after Spring/Neap (15days) period. Medium Span – Modified Alignment Scenario (4 Towers). Differences shown using a coarse scale.	Figure D7b



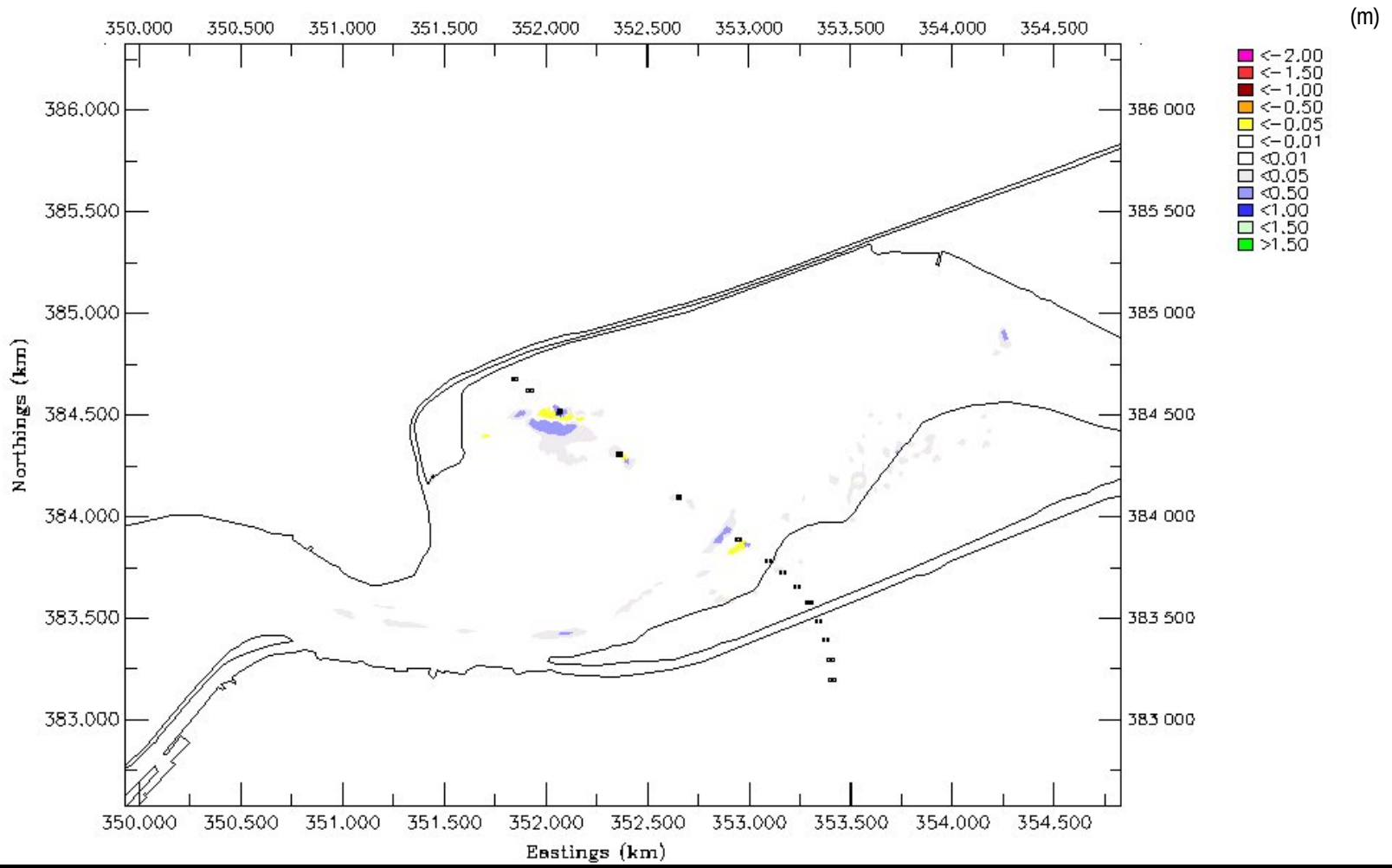
ABP mer marine environmental research	Morphological change (m) after Spring/Neap (15days) period. Medium Span – Modified Alignment Scenario (4 Towers) – Extreme fluvial event. Differences shown using a fine scale.	Figure D8a



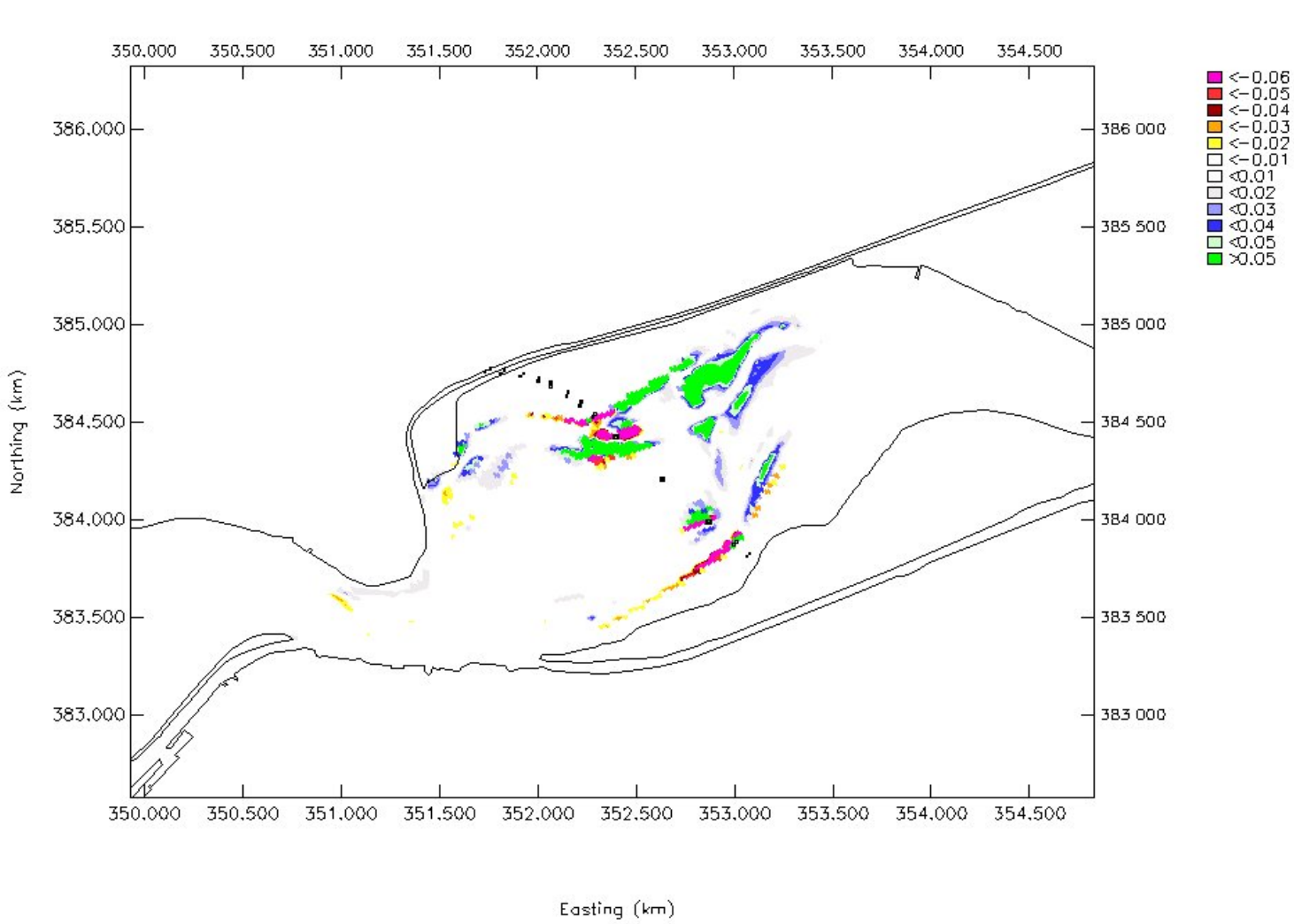
ABP mer marine environmental research	Morphological change (m) after Spring/Neap (15days) period. Medium Span – Modified Alignment Scenario (4 Towers) – Extreme fluvial event. Differences shown using a coarse scale.	Figure D8b



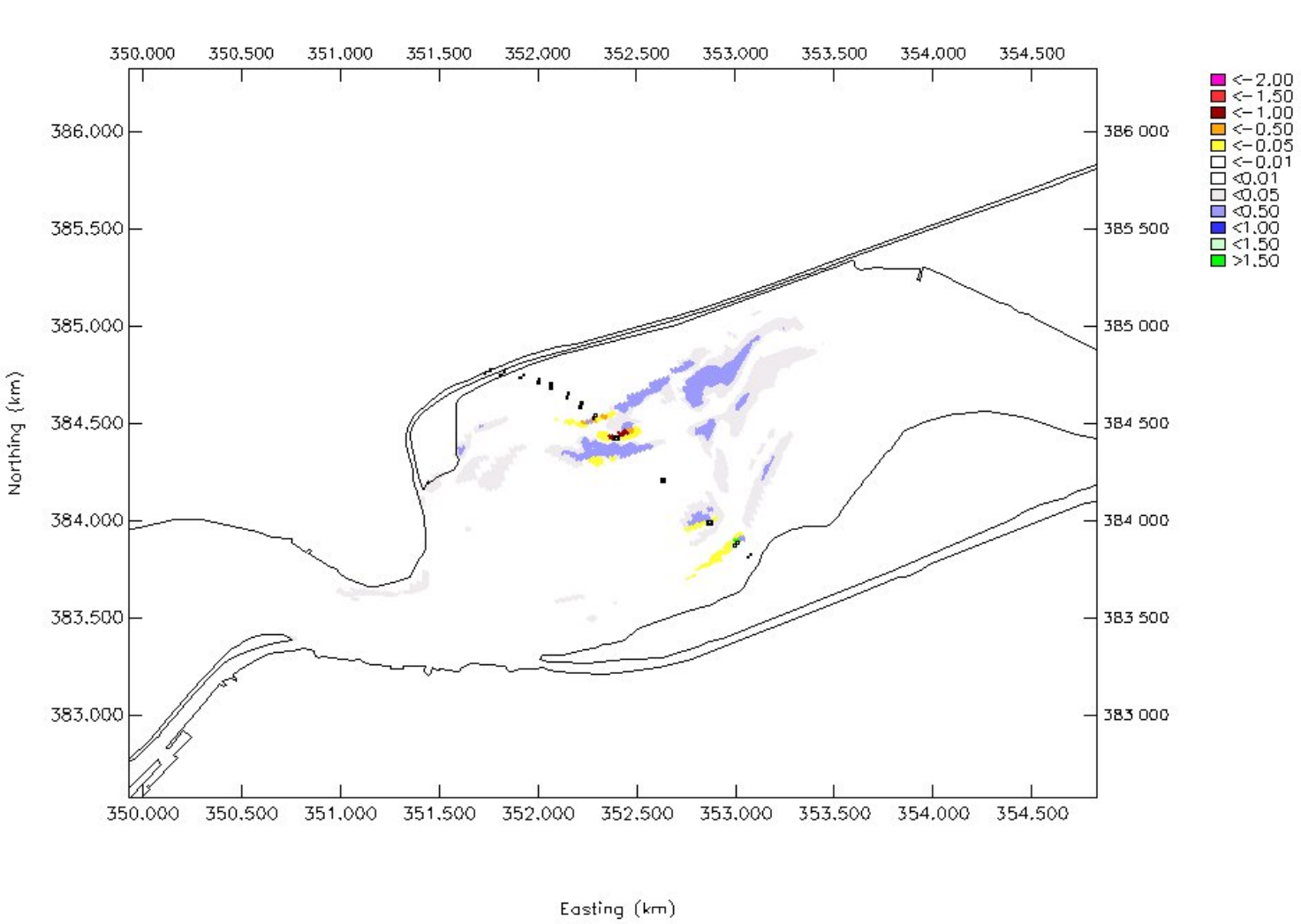
ABP mer marine environmental research	Morphological change (m) after (15 days) during a spring tidal period plus extreme surge tide and fluvial event. Medium Span – Modified Alignment Scenario (4 Towers) – Surge. Differences shown using a fine scale.	Figure D9a



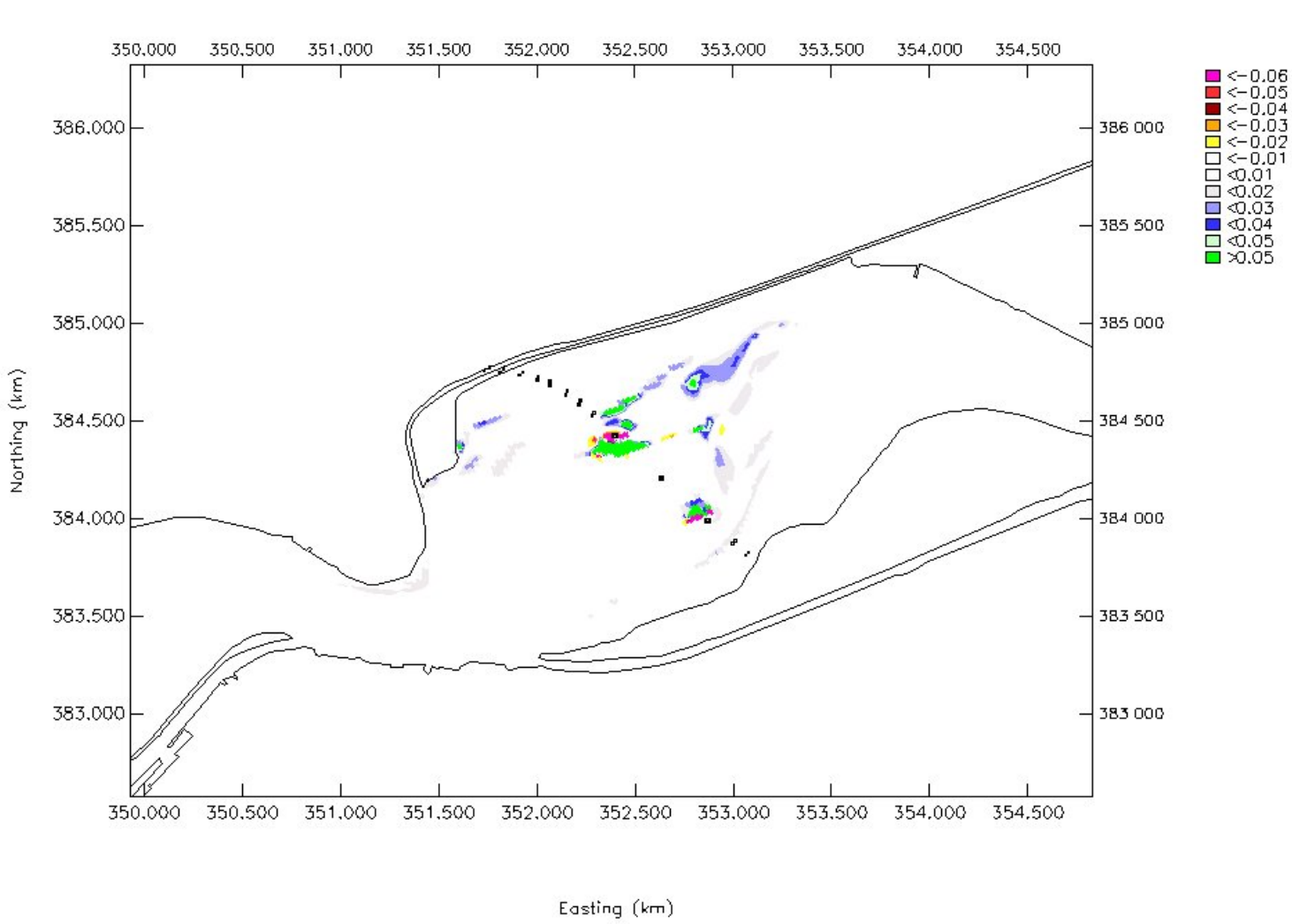
ABP mer marine environmental research	Morphological change (m) after (15 days) during a spring tidal period plus extreme surge tide and fluvial event. Medium Span – Modified Alignment Scenario (4 Towers) – Surge. Differences shown using a coarse scale.	Figure D9b



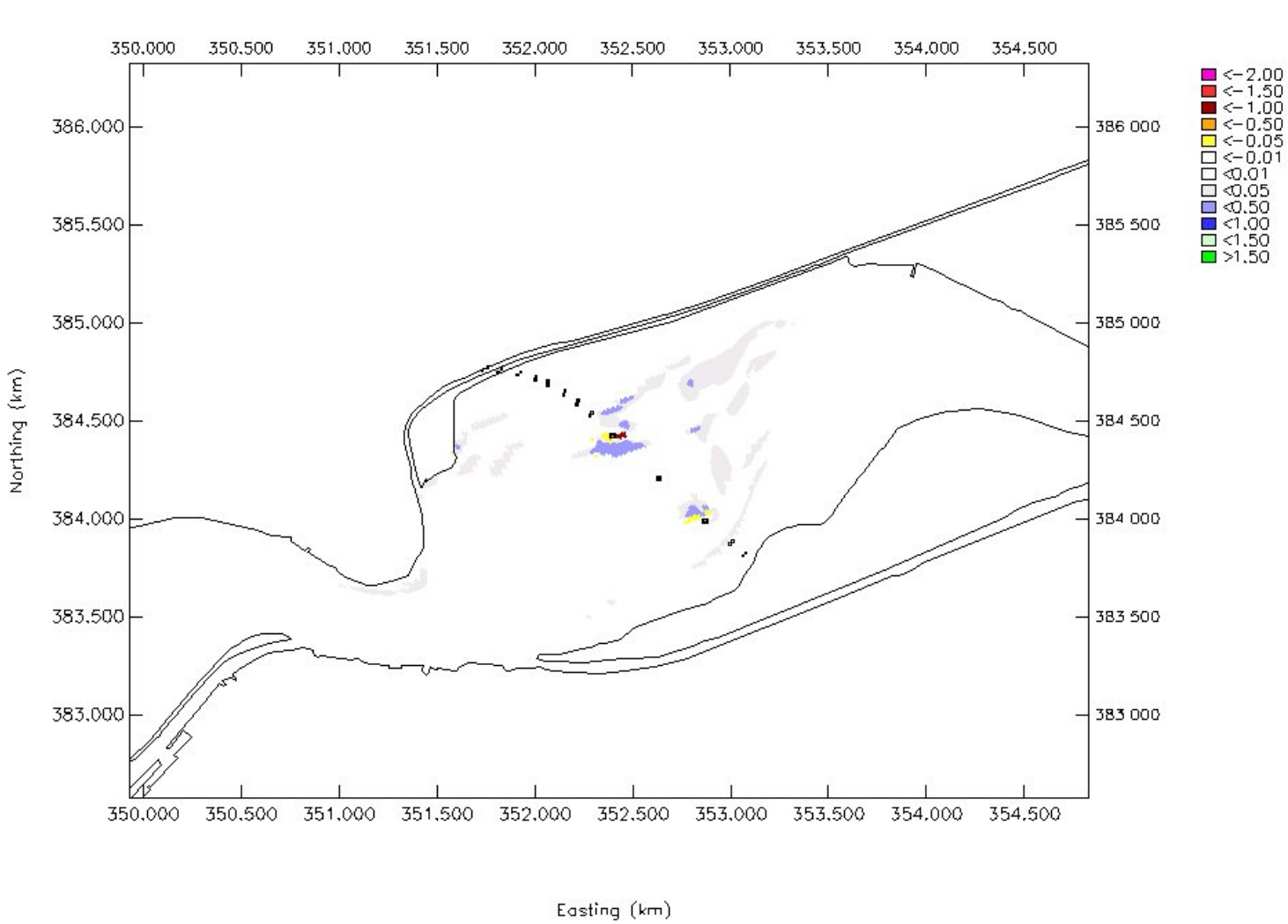
ABP mer marine environmental research	Morphological change (m) after 1 year. Route 3A Medium Span – 3Tower Alignment Scenario. Differences shown using a fine scale.	Figure D10a



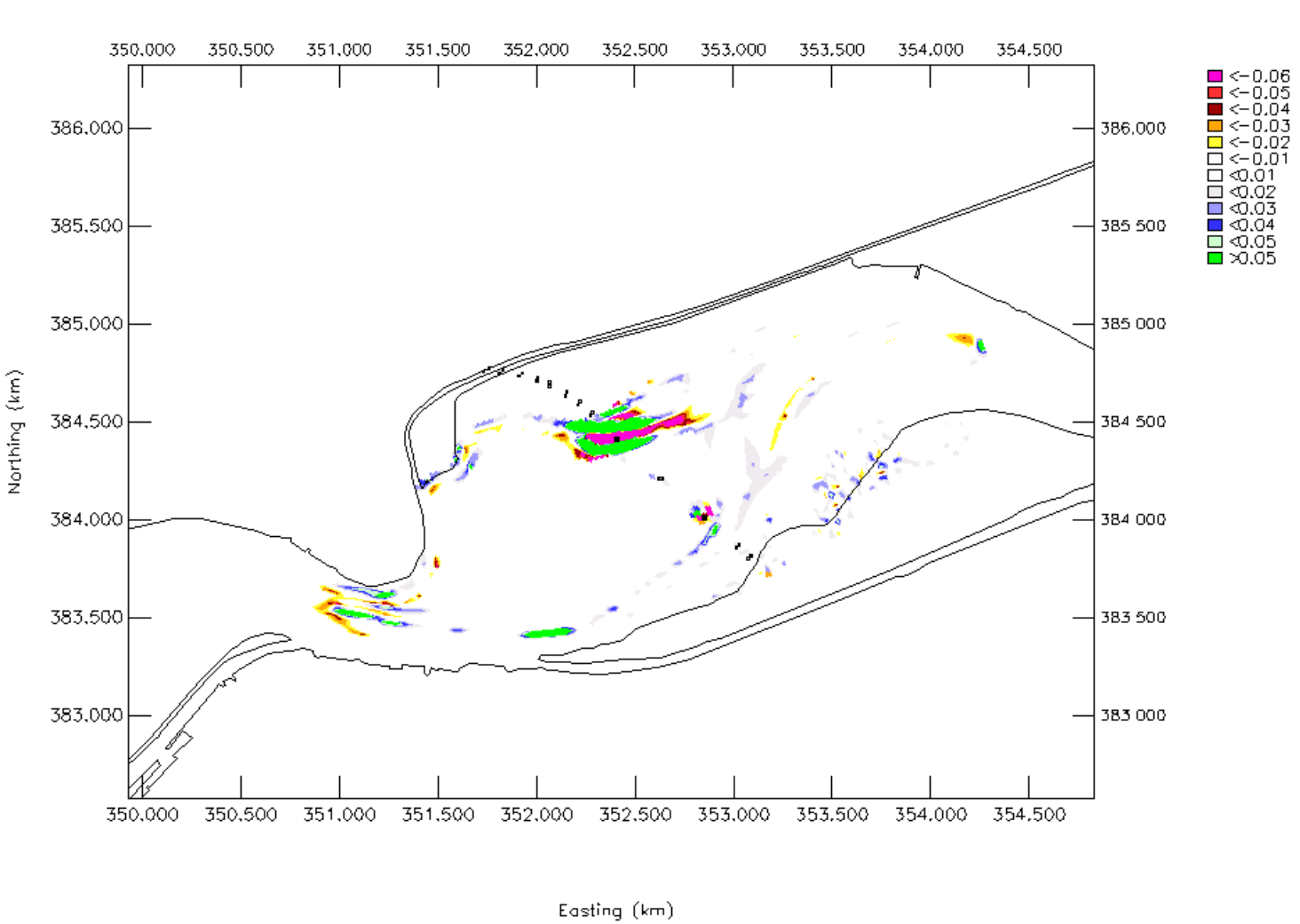
ABP mer marine environmental research	Morphological change (m) after 1 year. Route 3A Medium Span – 3Tower Alignment Scenario. Differences shown using a coarse scale.	Figure D10b



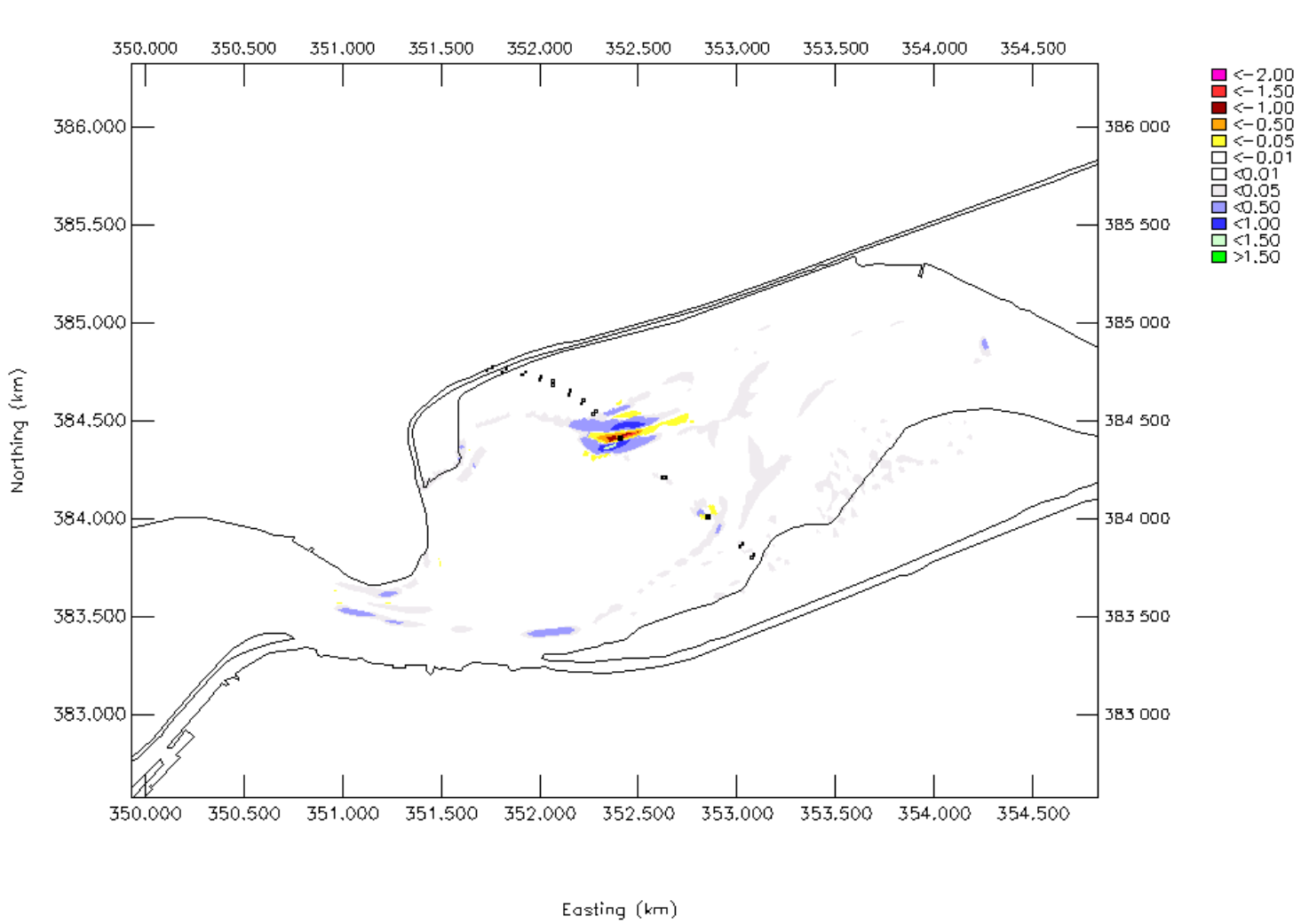
ABP mer marine environmental research	Morphological change (m) after 1 year. Route 3A Medium Span – 3Tower Revised Alignment Scenario. Differences shown using a fine scale.	Figure D11a



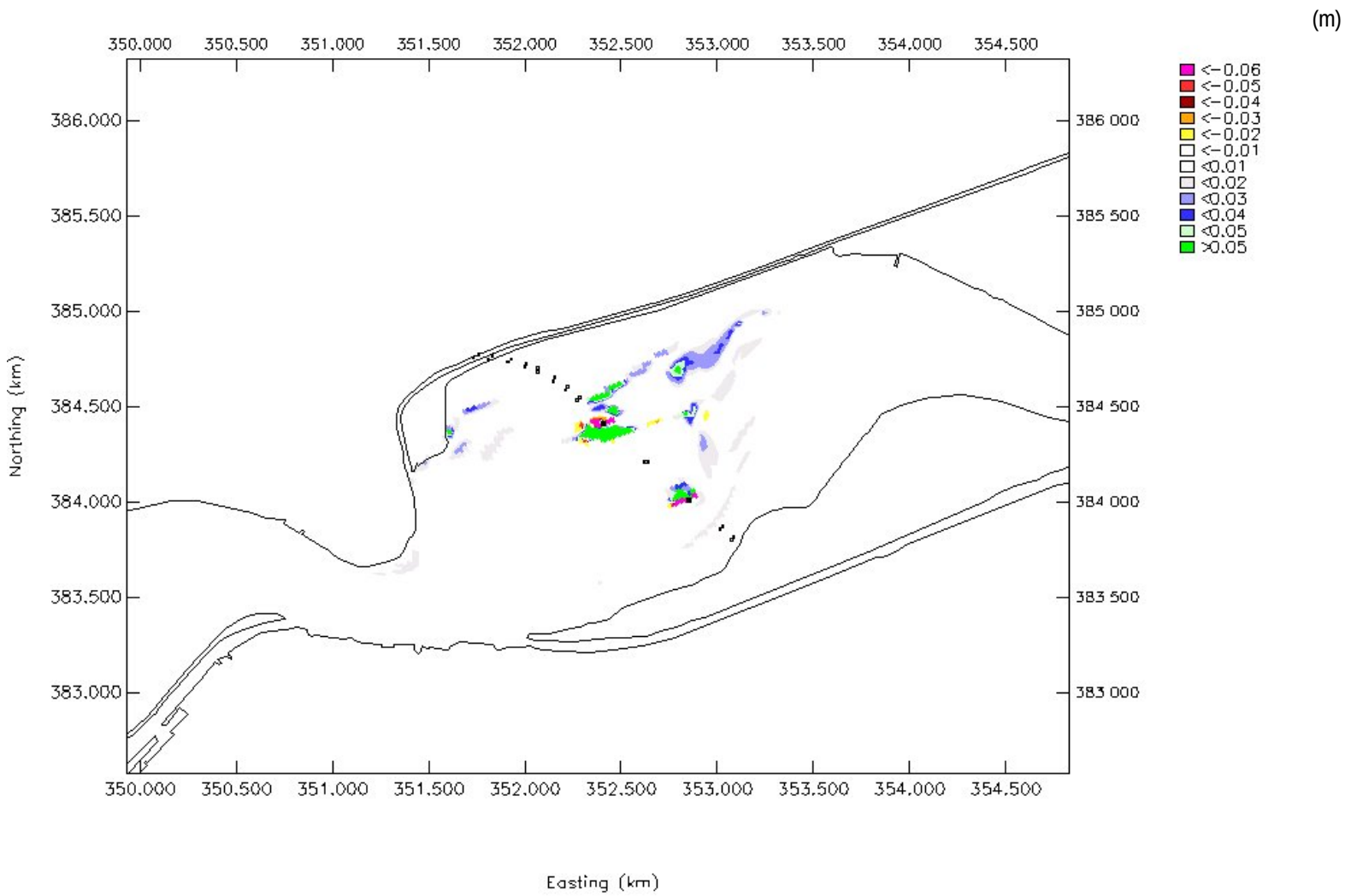
ABP mer marine environmental research	Morphological change (m) after 1 year. Route 3A Medium Span – 3Tower Revised Alignment Scenario. Differences shown using a coarse scale.	Figure D11b



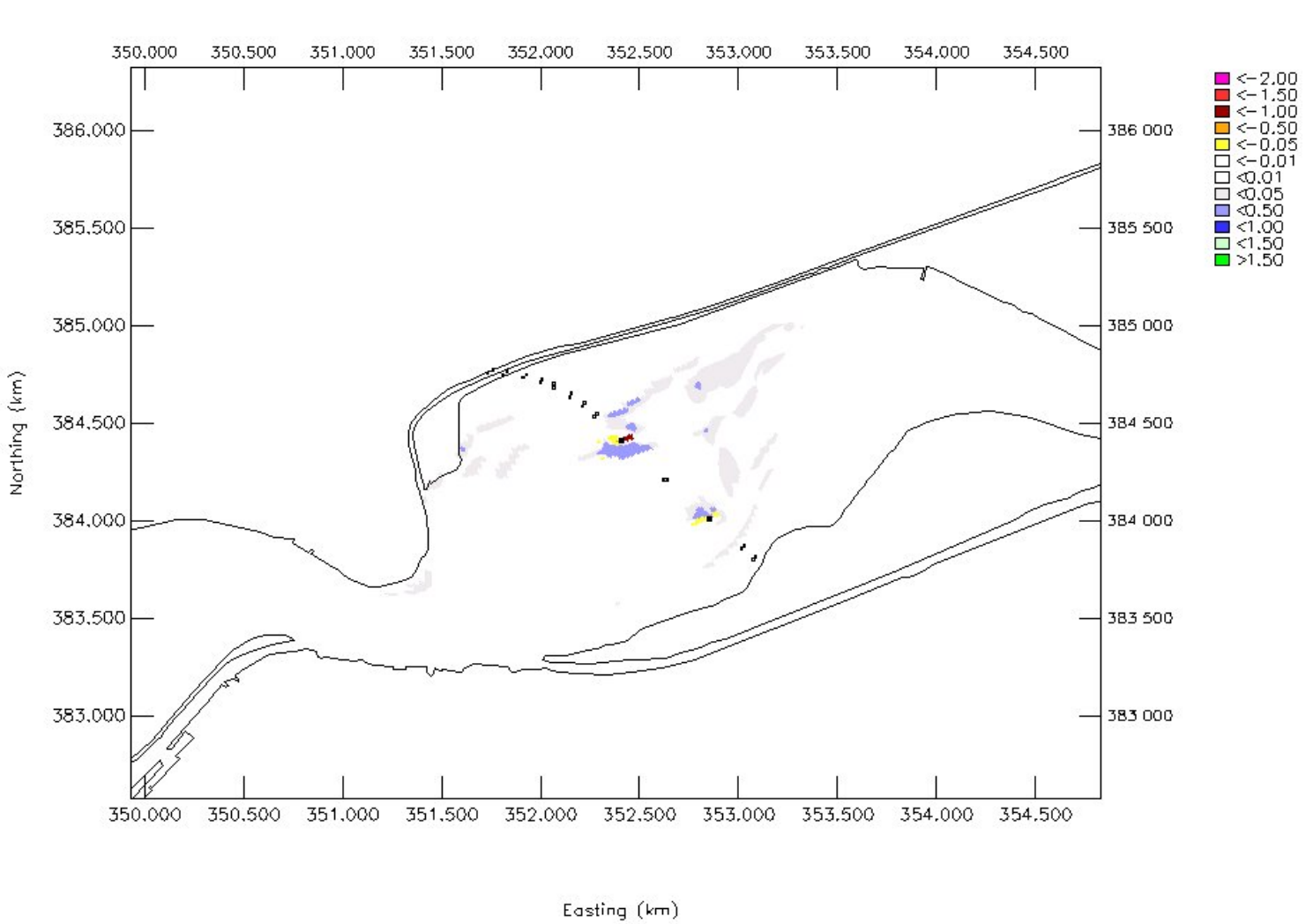
ABP mer marine environmental research	Morphological change (m) after (15 days) spring neap tidal period plus extreme surge tide and fluvial event. Route 3A Medium Span – 3Tower Revised Alignment. Differences shown using a fine scale.	Figure D12a



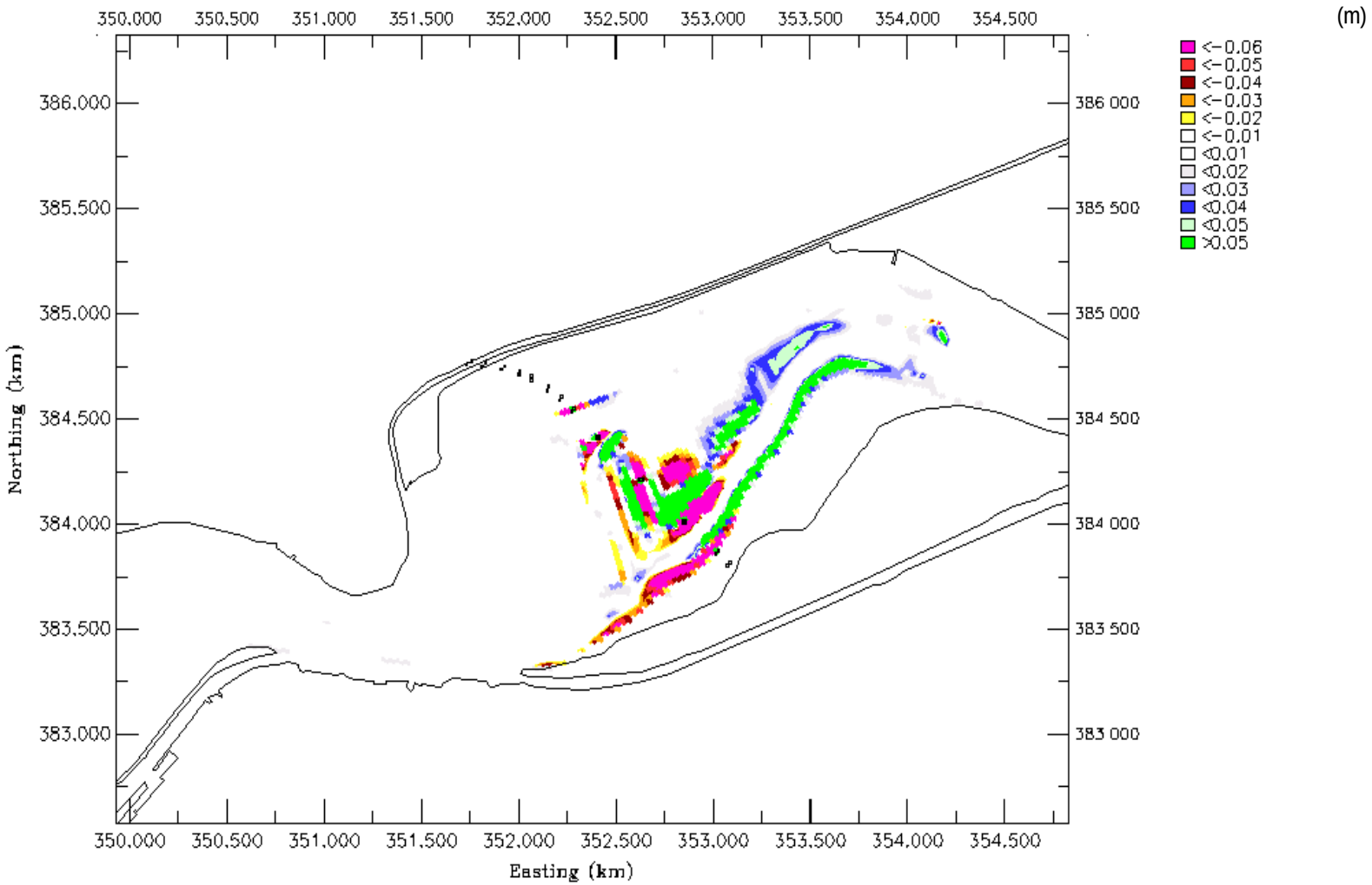
ABP mer marine environmental research	Morphological change (m) after (15 days) spring neap tidal period plus extreme surge tide and fluvial event. Route 3A Medium Span – 3Tower Revised Alignment. Differences shown using a coarse scale.	Figure D12b



ABP mer marine environmental research	Morphological change (m) after 1 year. Route 3A Medium Span – 3Tower Revised Alignment recovery scenario. Differences shown using a fine scale.	Figure D13a

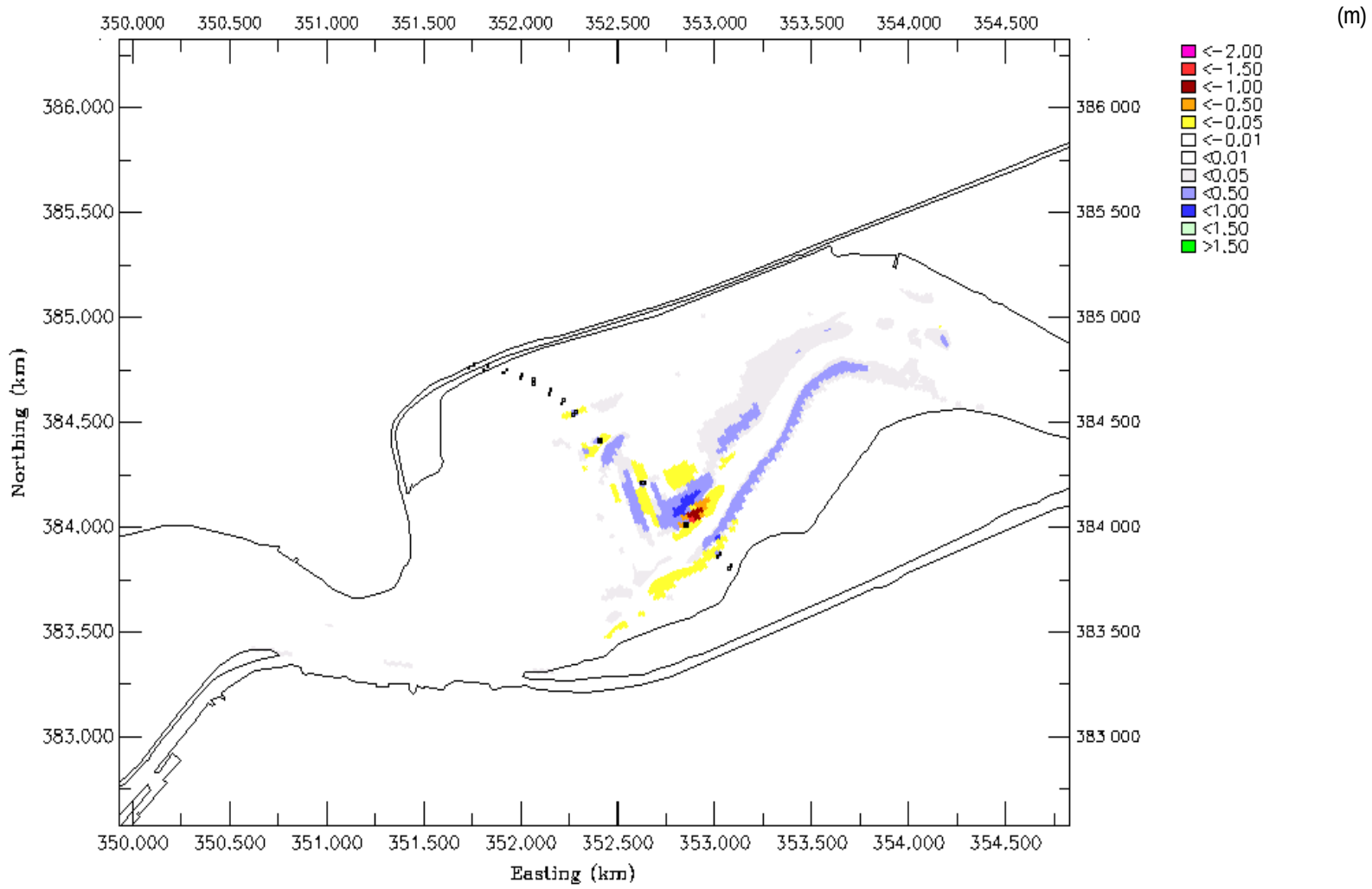


ABP mer marine environmental research	Morphological change (m) after 1 year. Route 3A Medium Span – 3Tower Revised Alignment recovery scenario. Differences shown using a coarse scale.	Figure D13b

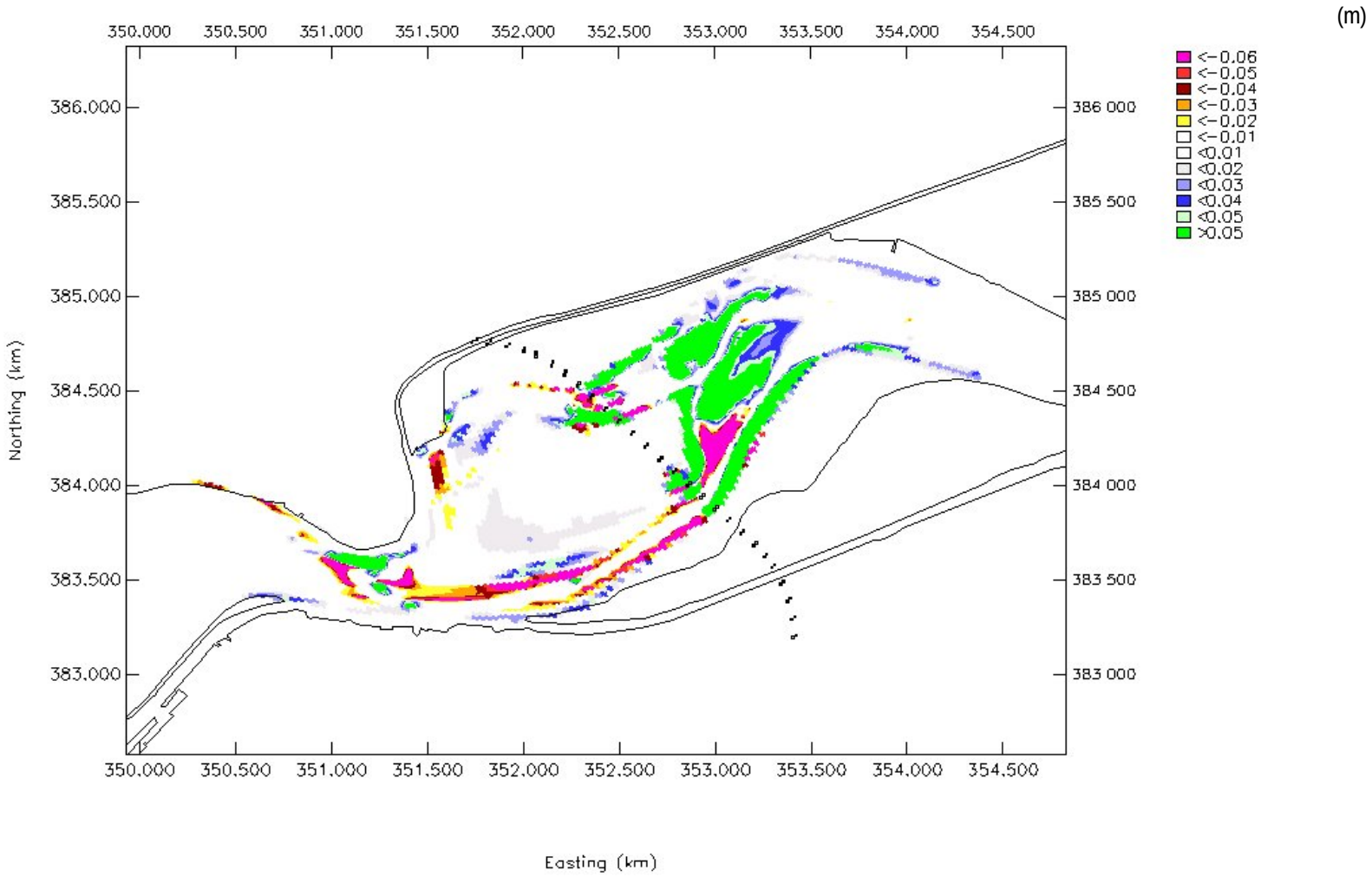


Morphological change (m) after 1 year. Route 3A Medium Span – 3Tower Revised Alignment – 2005 bathymetry. Differences shown using a fine scale.

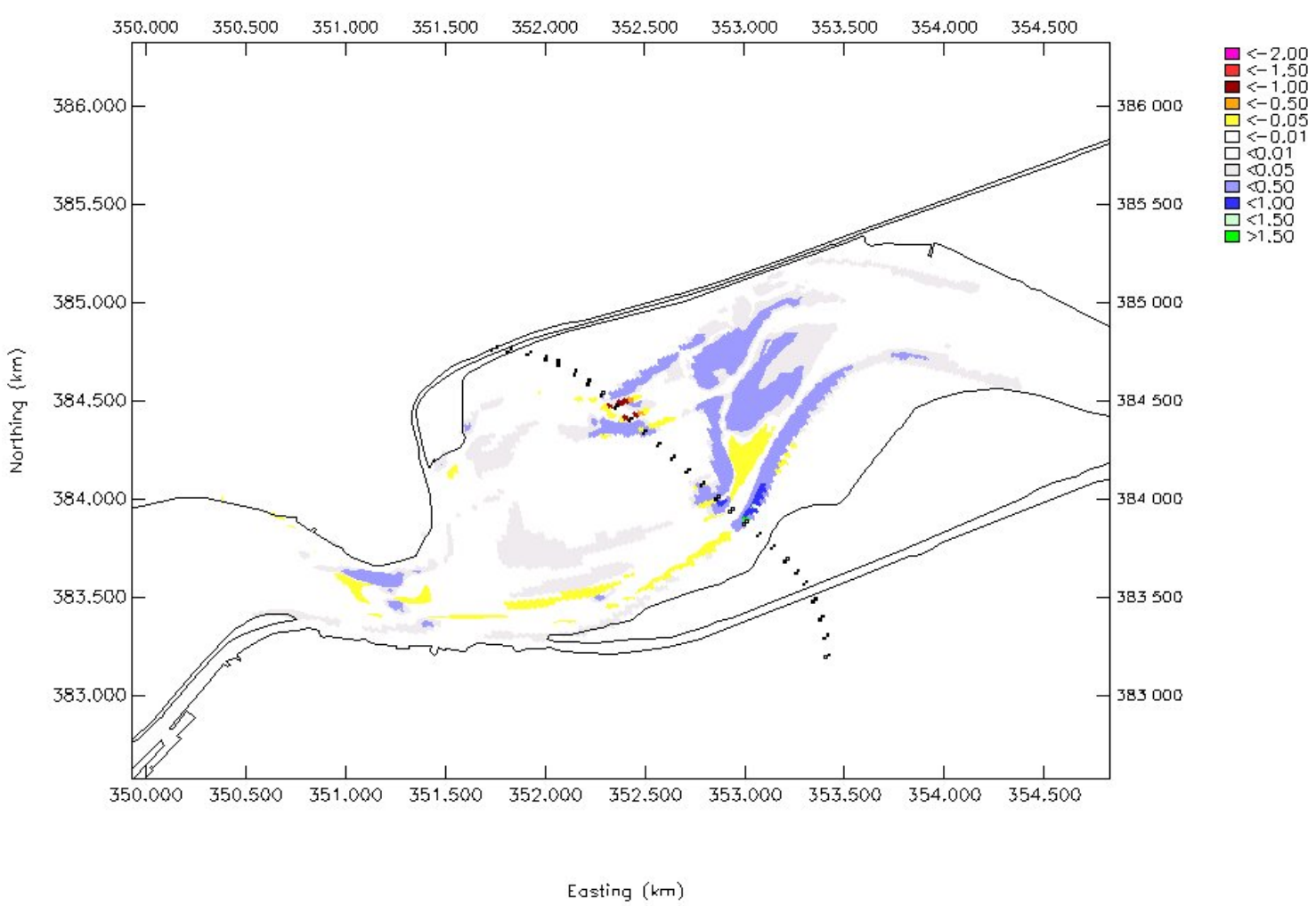
Figure D14a



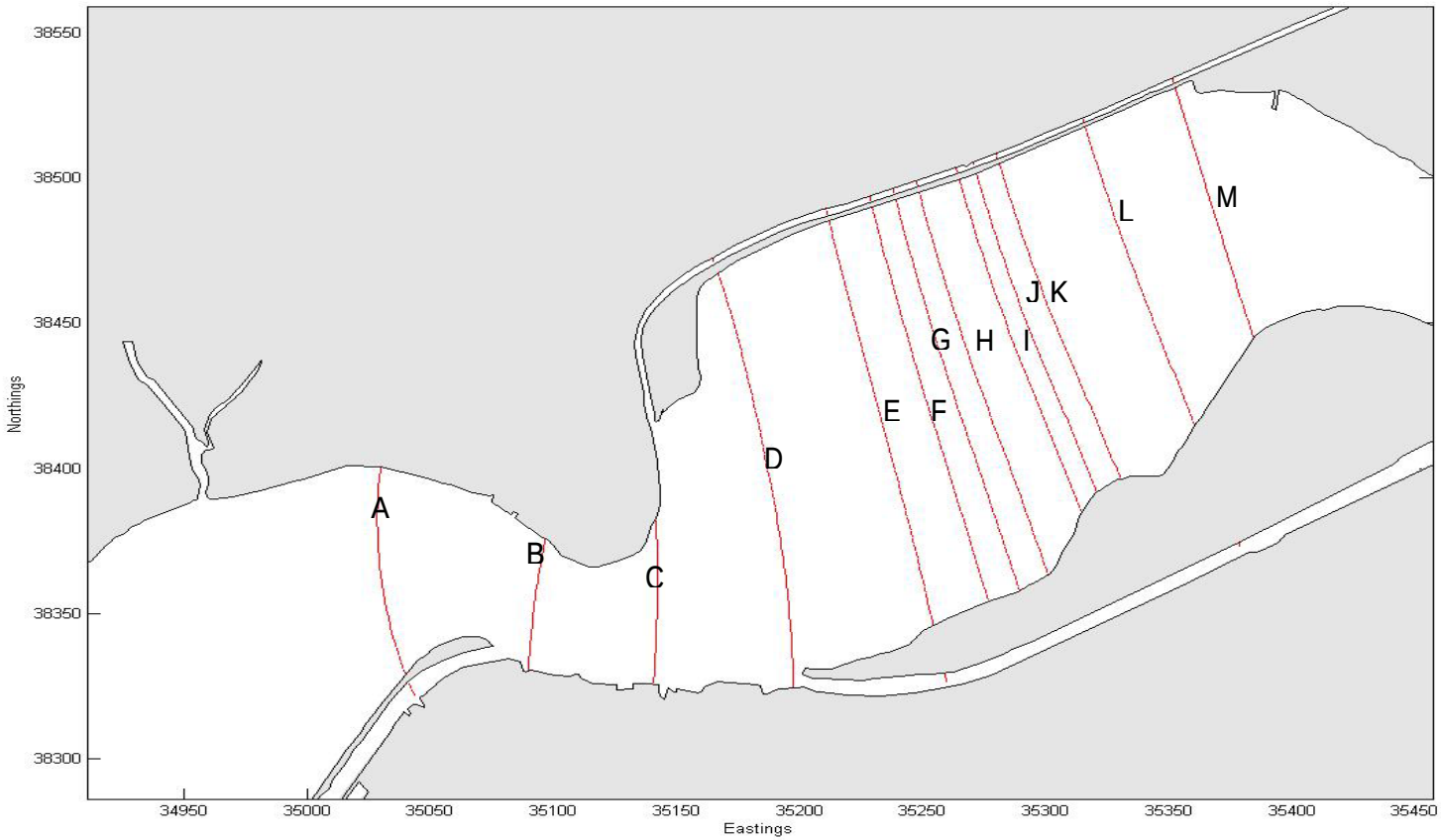
ABP mer marine environmental research	Morphological change (m) after 1 year. Route 3A Medium Span – 3Tower Revised Alignment – 2005 bathymetry. Differences shown using a coarse scale.	Figure D14b



ABP mer marine environmental research	Morphological change (m) after 1 year. Route 3A Short Span Scenario. Differences shown using a fine scale.	Figure D15a

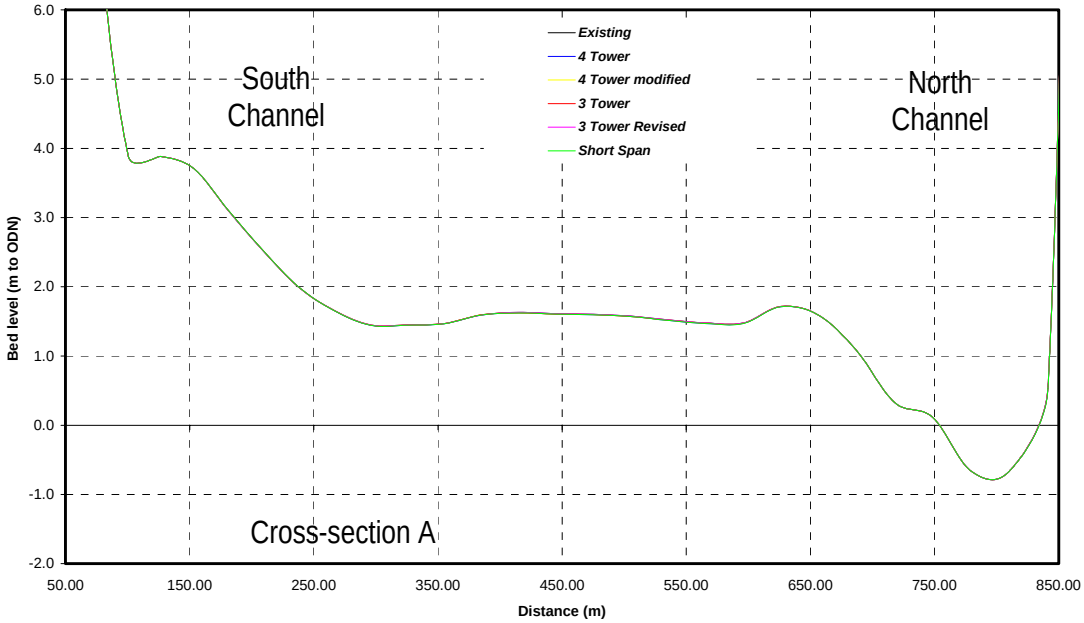


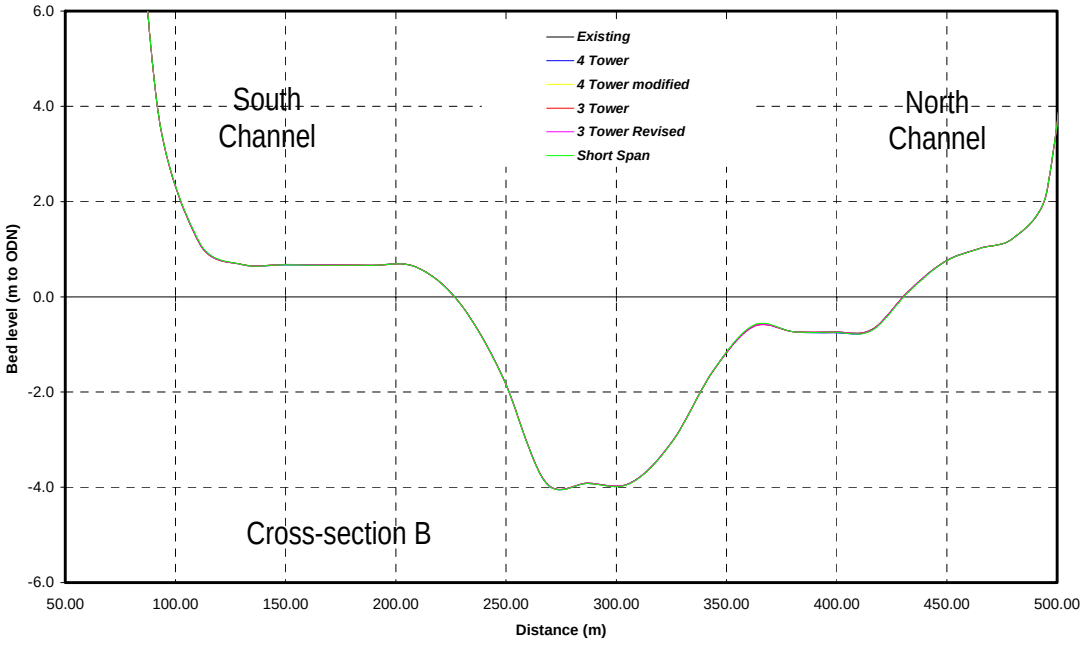
ABP mer marine environmental research	Morphological change (m) after 1 year. Route 3A Short Span Scenario. Differences shown using a coarse scale.	Figure D15b



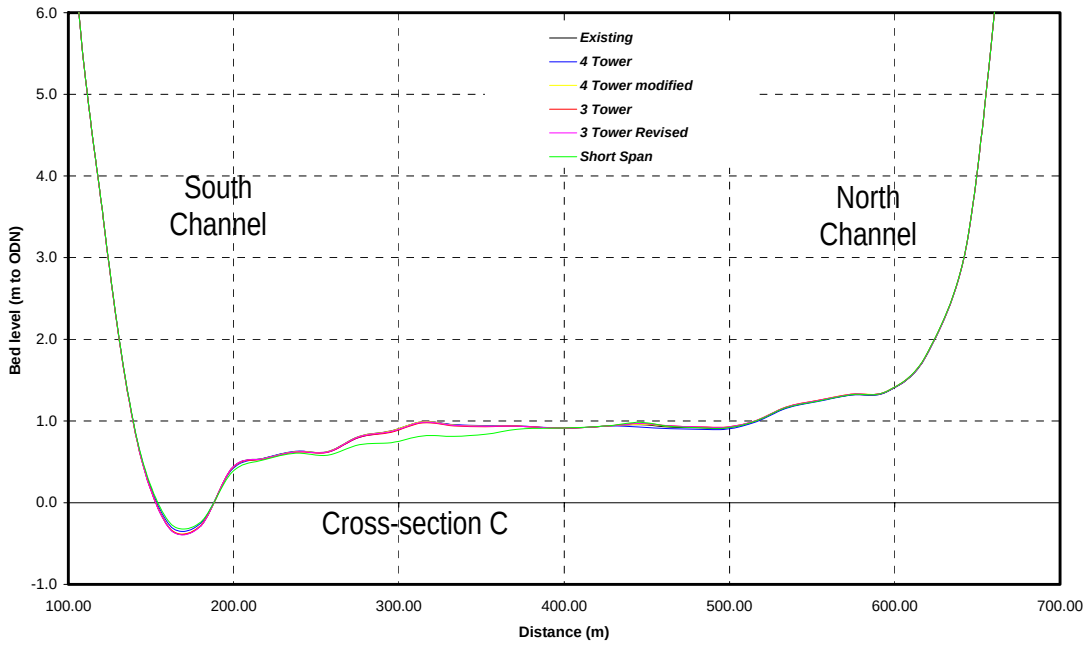
Locations of cross sections examined from the morphological model.

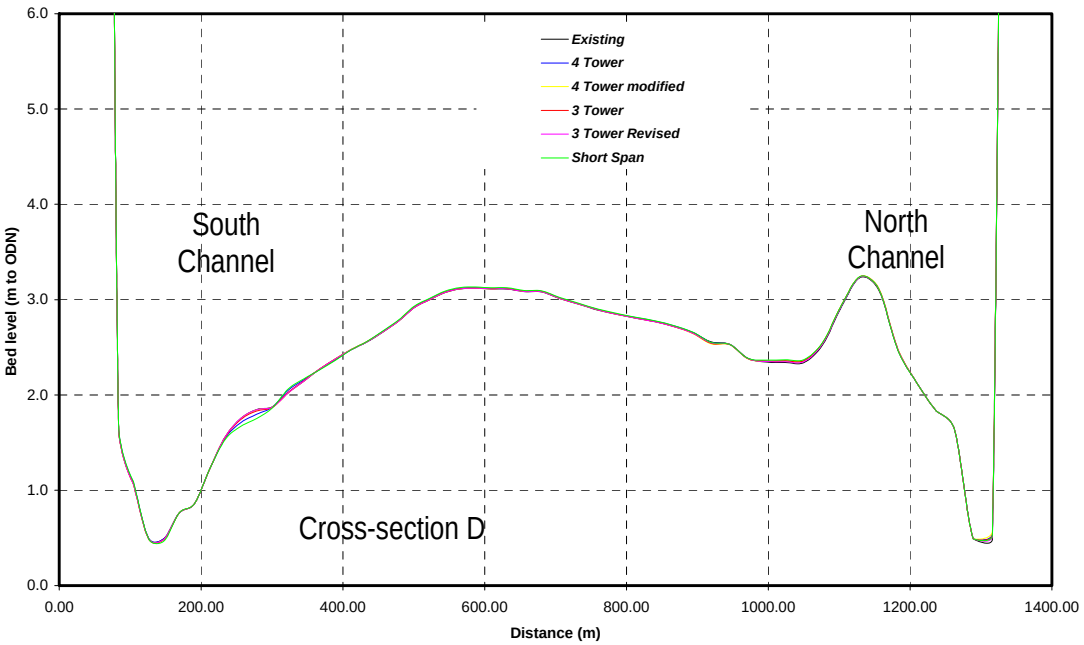
Figure D16



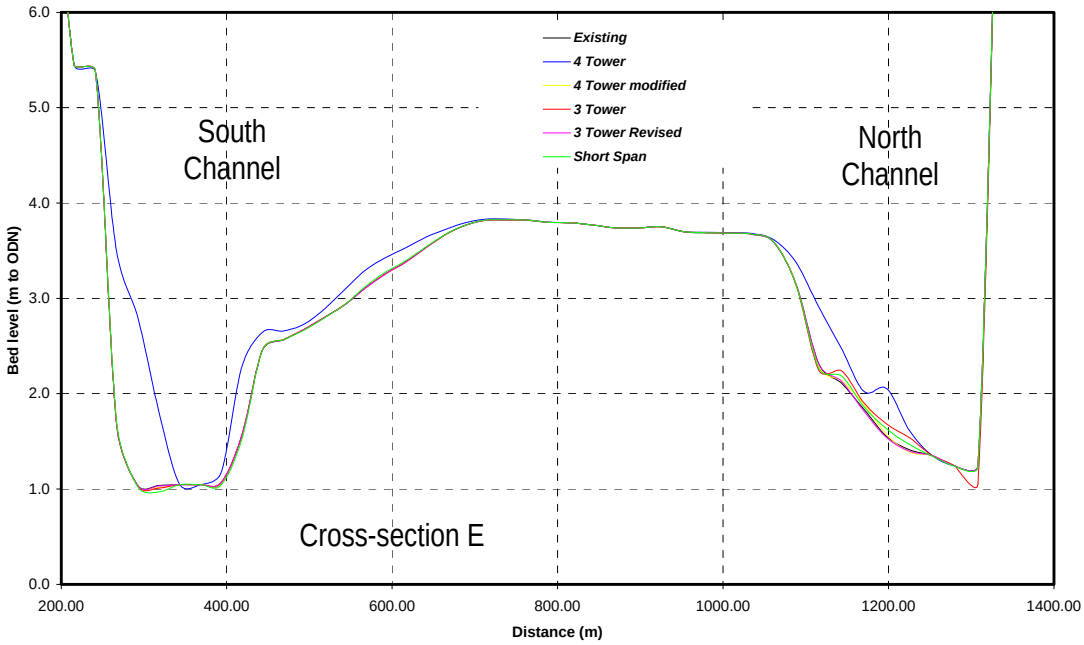


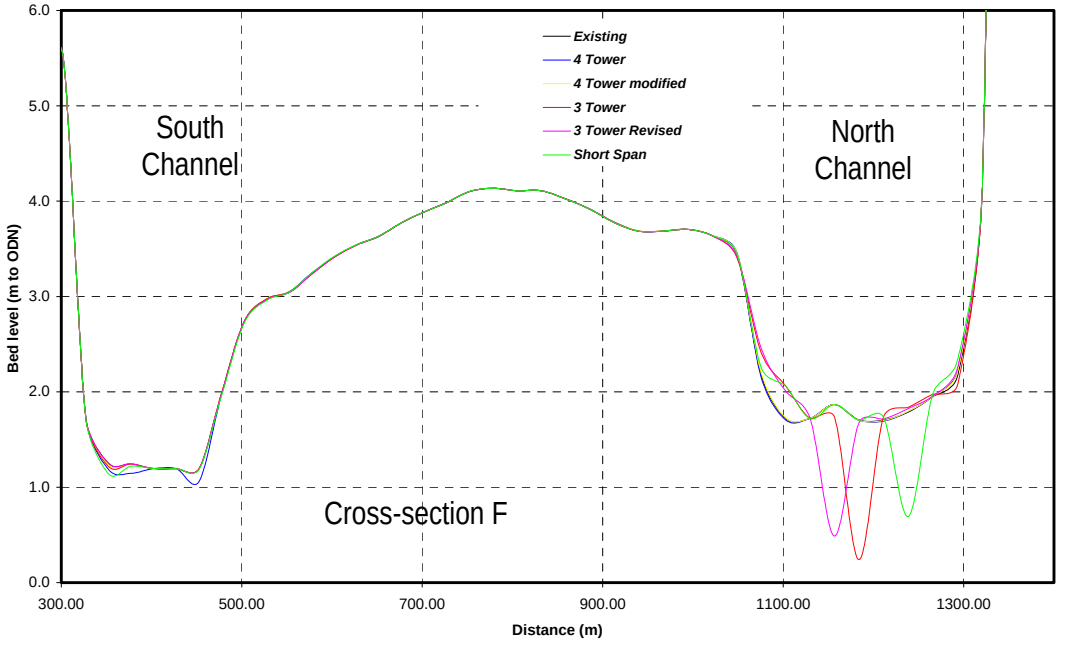
ABP mer marine environmental research	Cross – Sections A and B	Figure D17



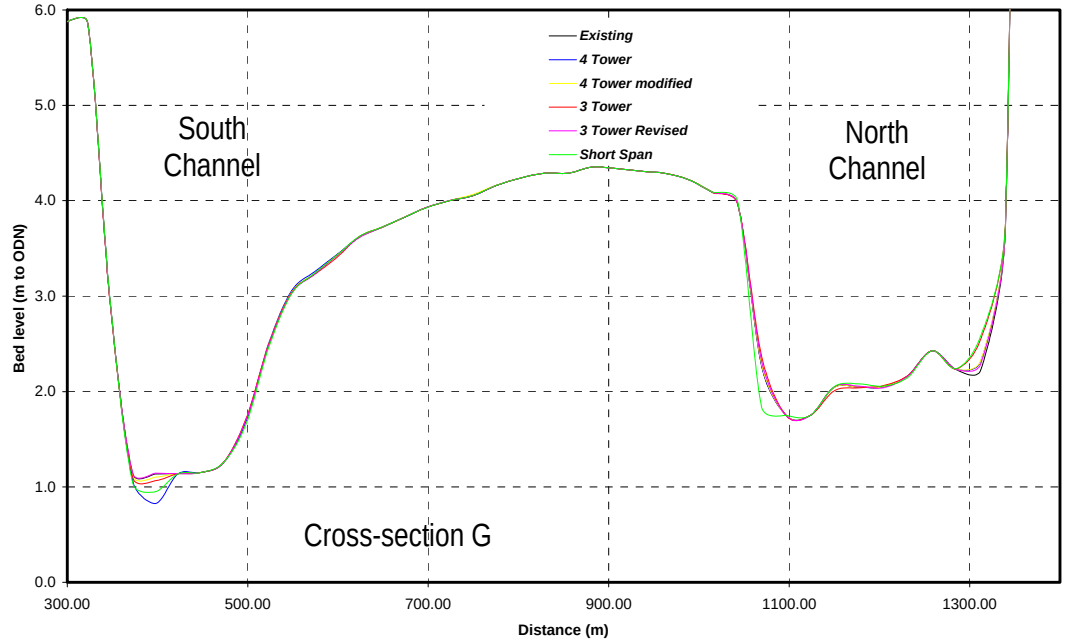


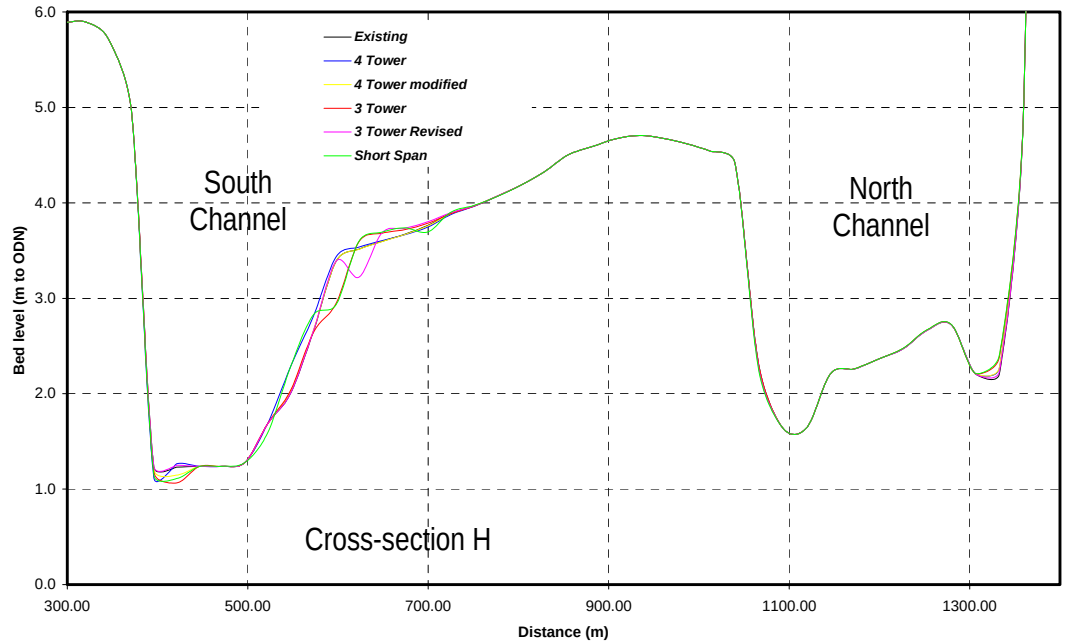
ABP mer marine environmental research	Cross – Sections C and D	Figure D18



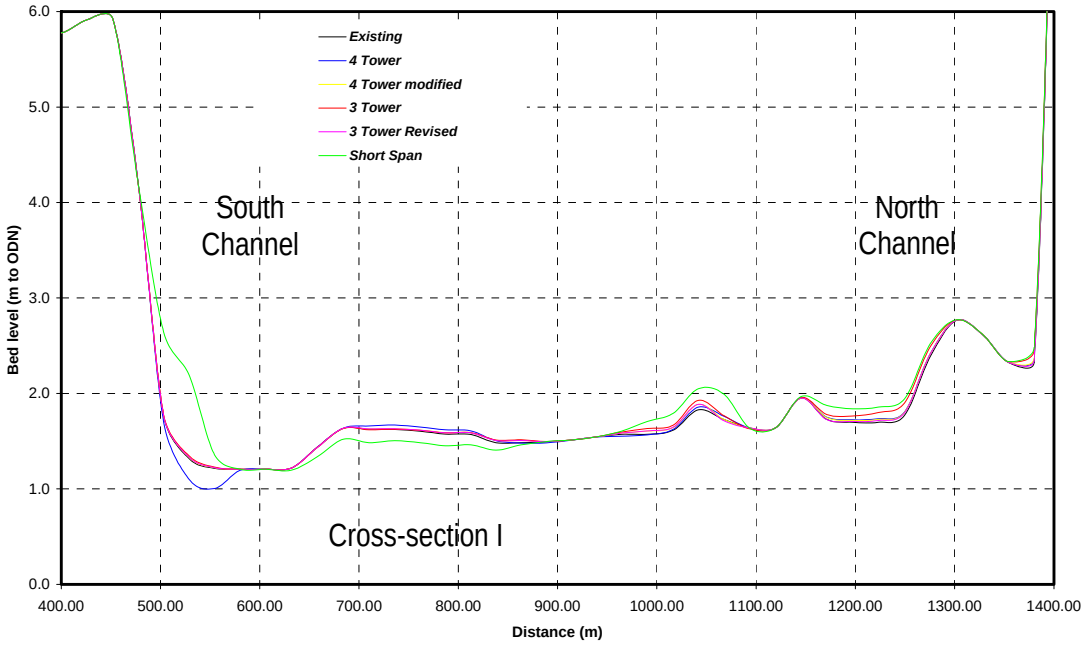


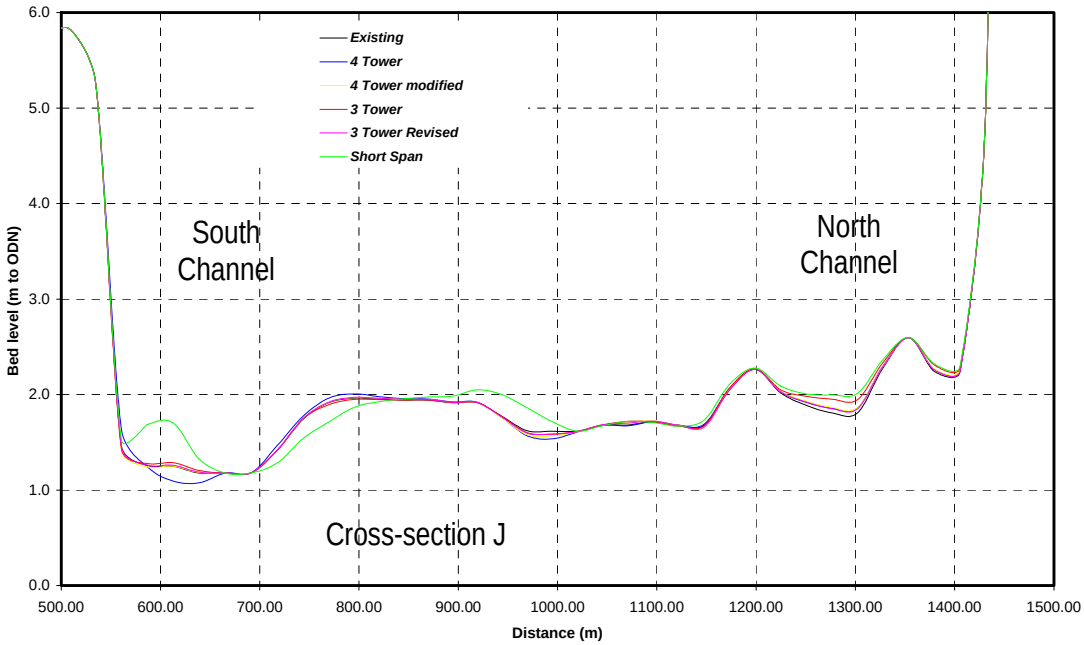
ABP mer marine environmental research	Cross – Sections E and F	Figure D19



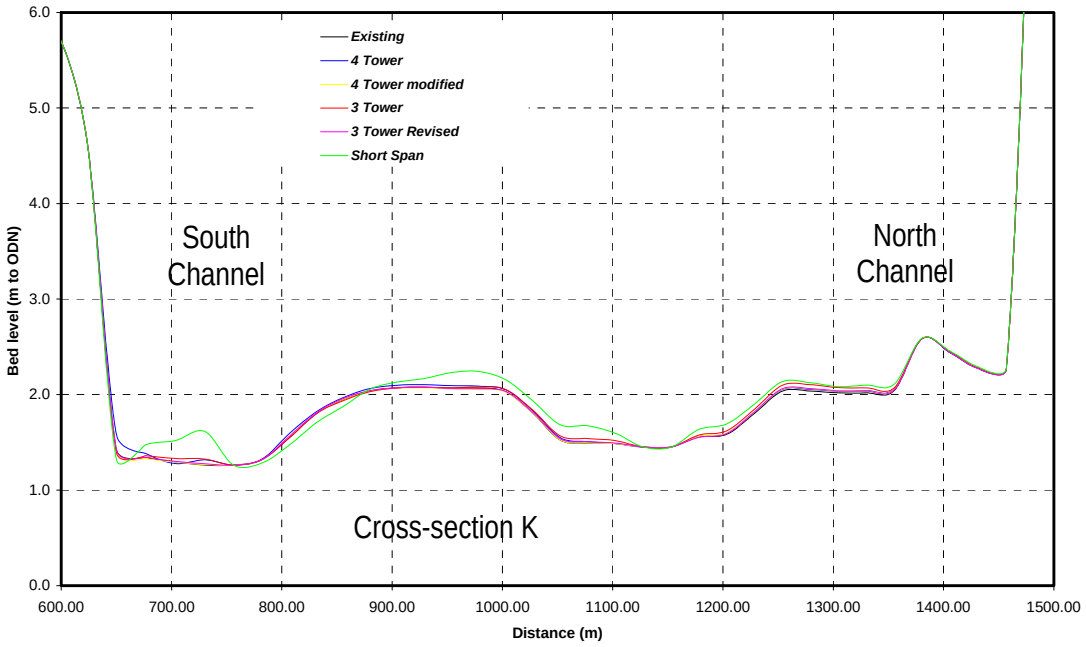


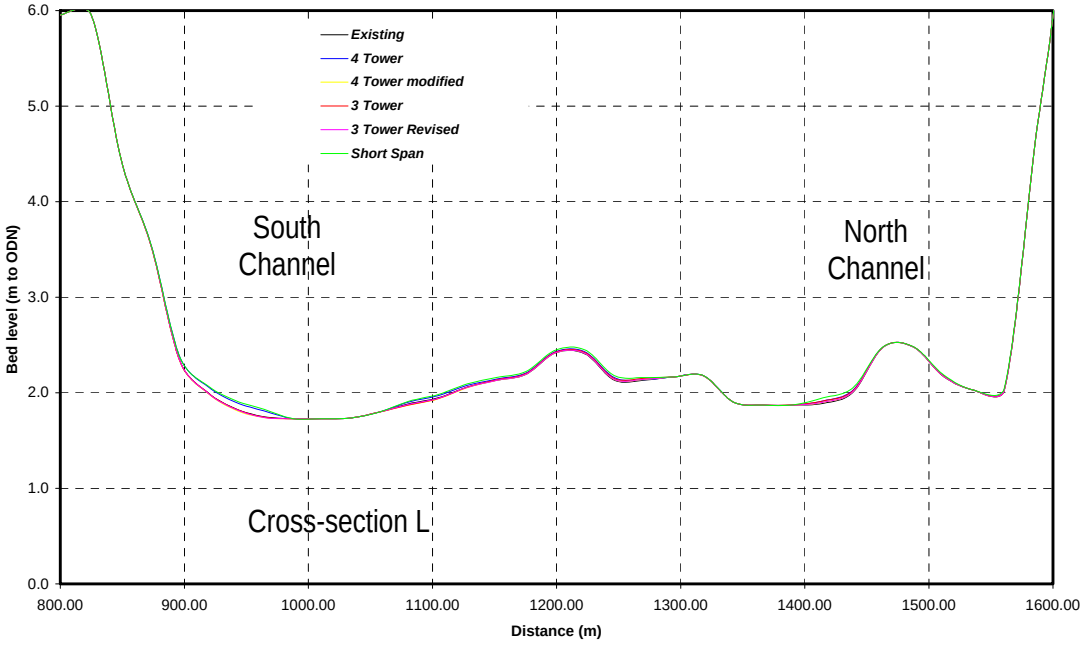
ABP mer marine environmental research	Cross – Sections G and H	Figure D20



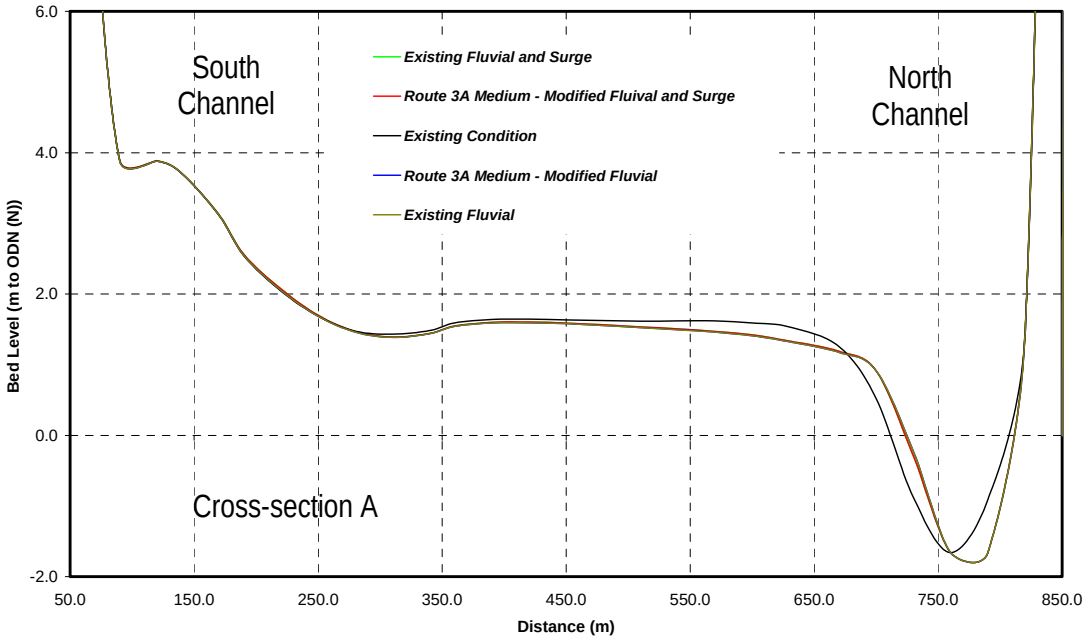


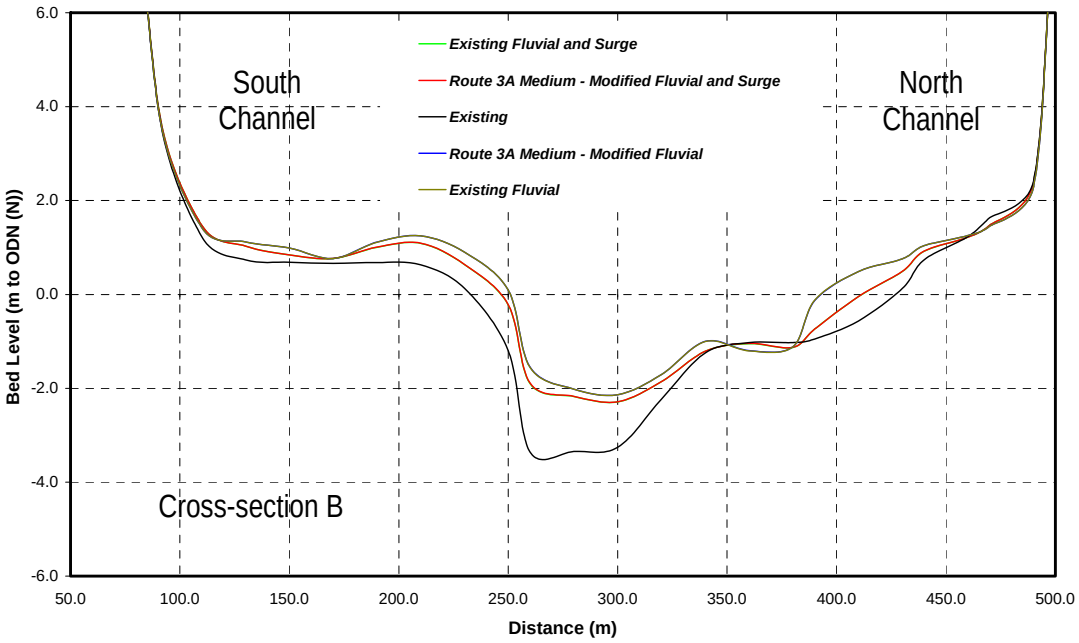
ABP mer marine environmental research	Cross – Sections I and J	Figure D21



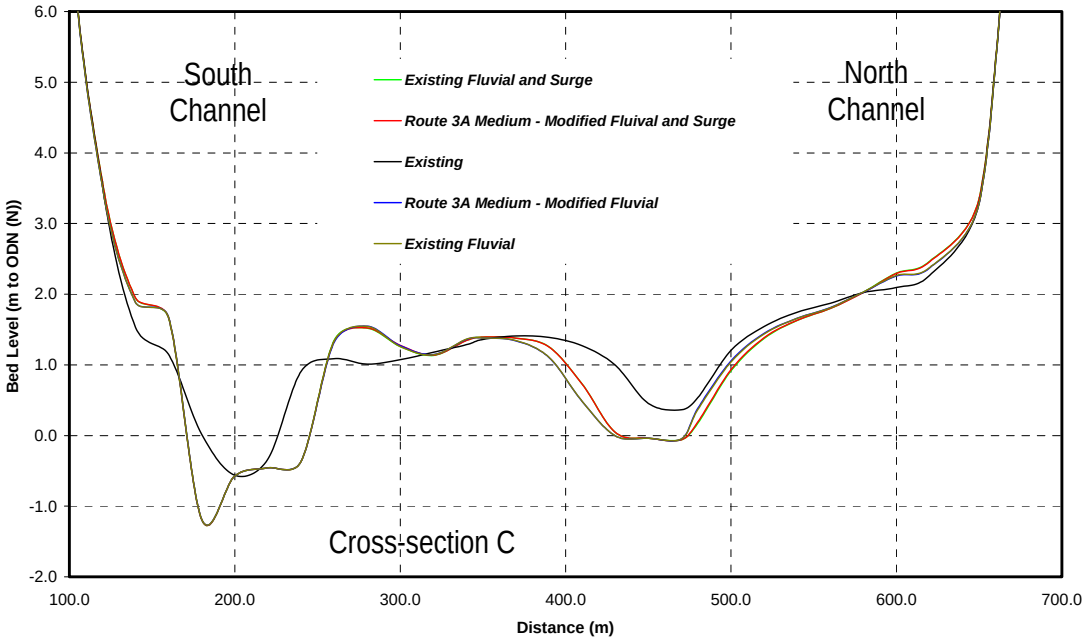


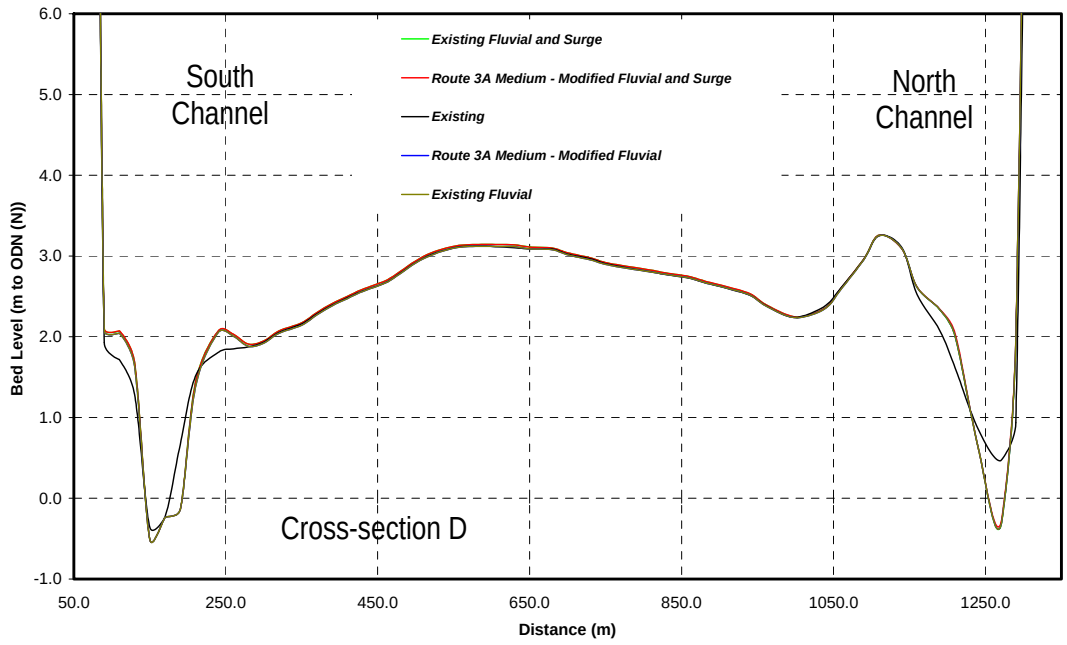
ABP mer marine environmental research	Cross – Sections K and L	Figure D22



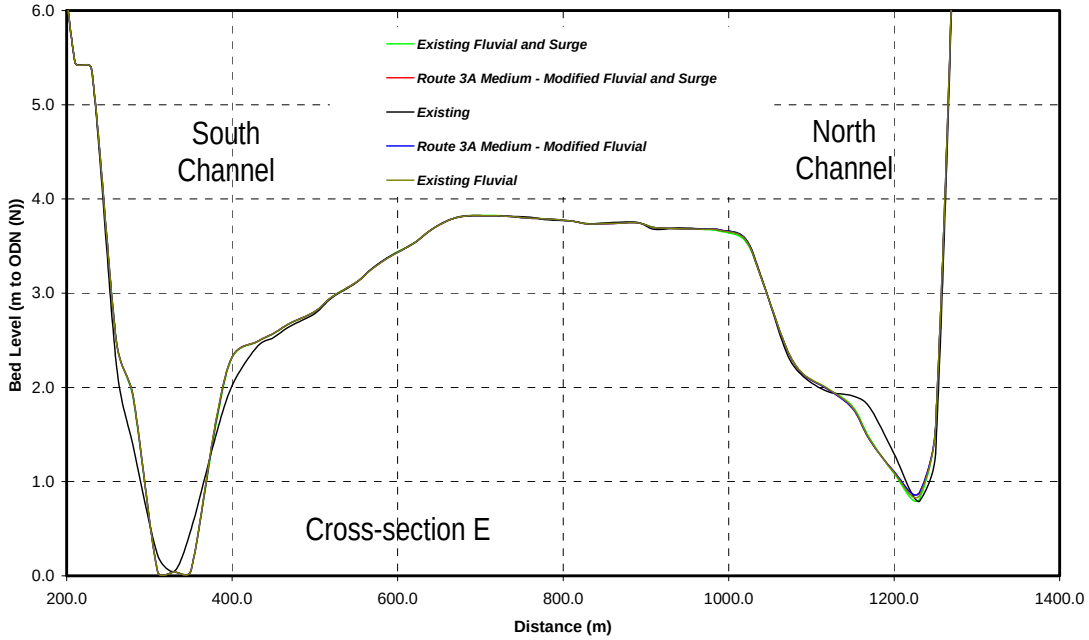


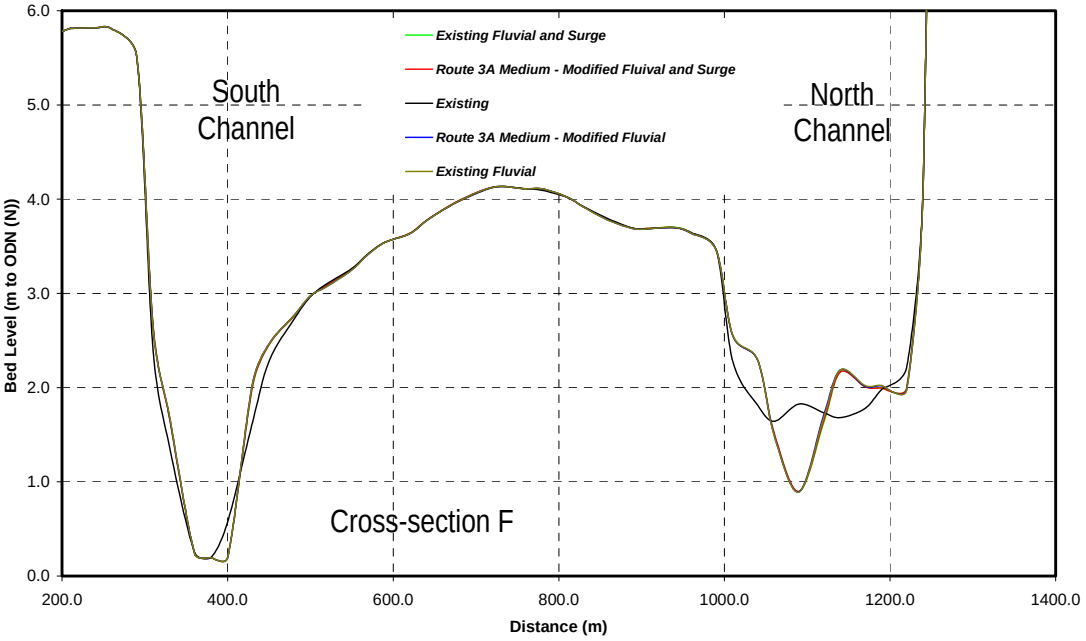
ABP mer marine environmental research	Cross – Sections A and B	Figure D23



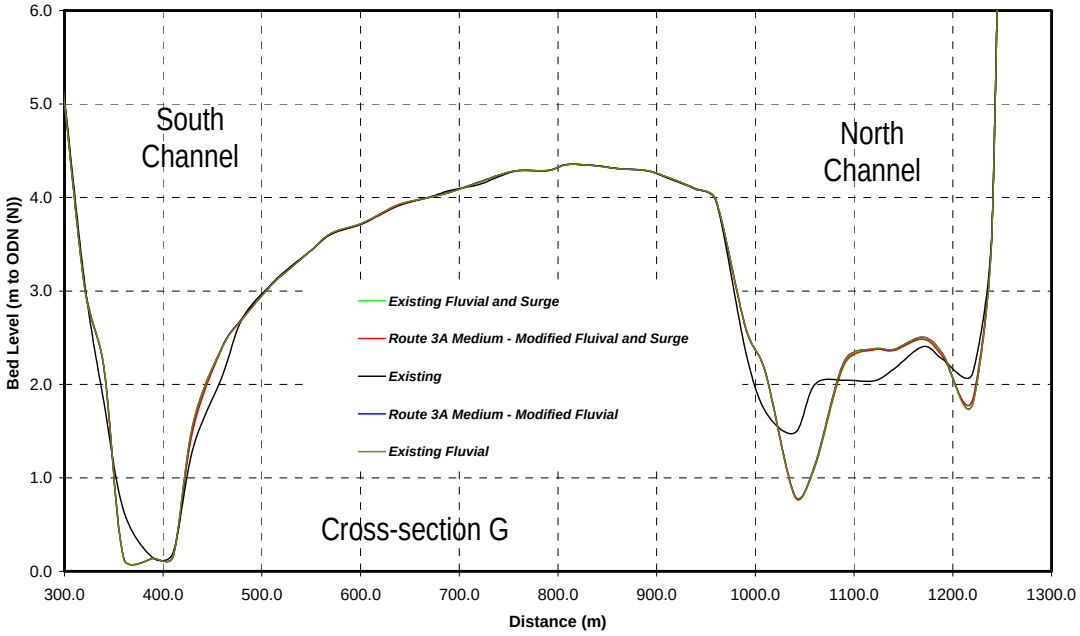


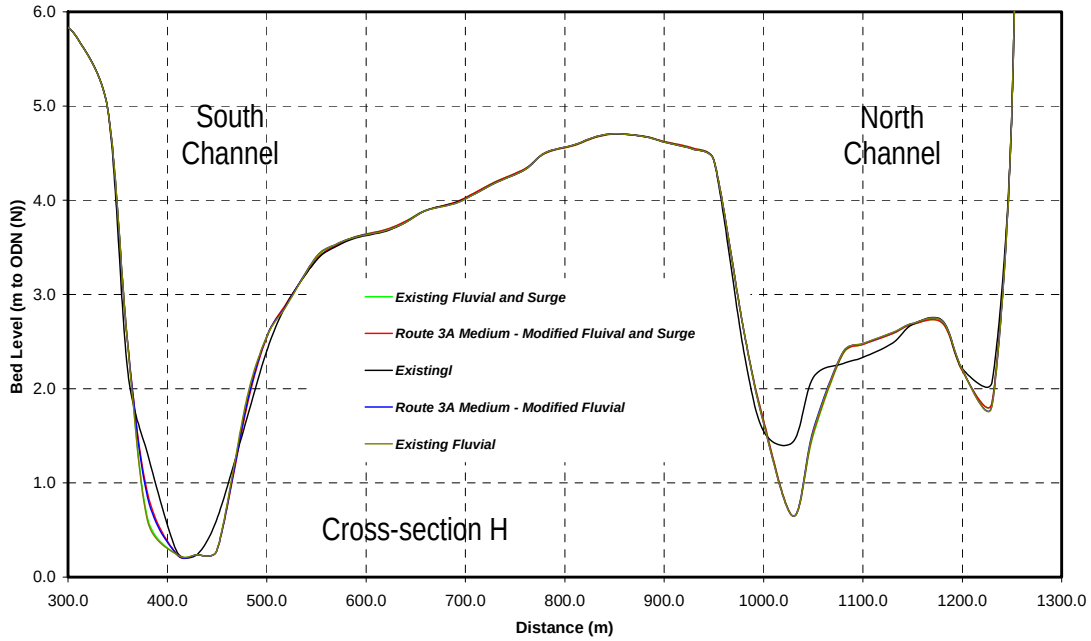
ABP mer marine environmental research	Cross – Sections C and D	Figure D24



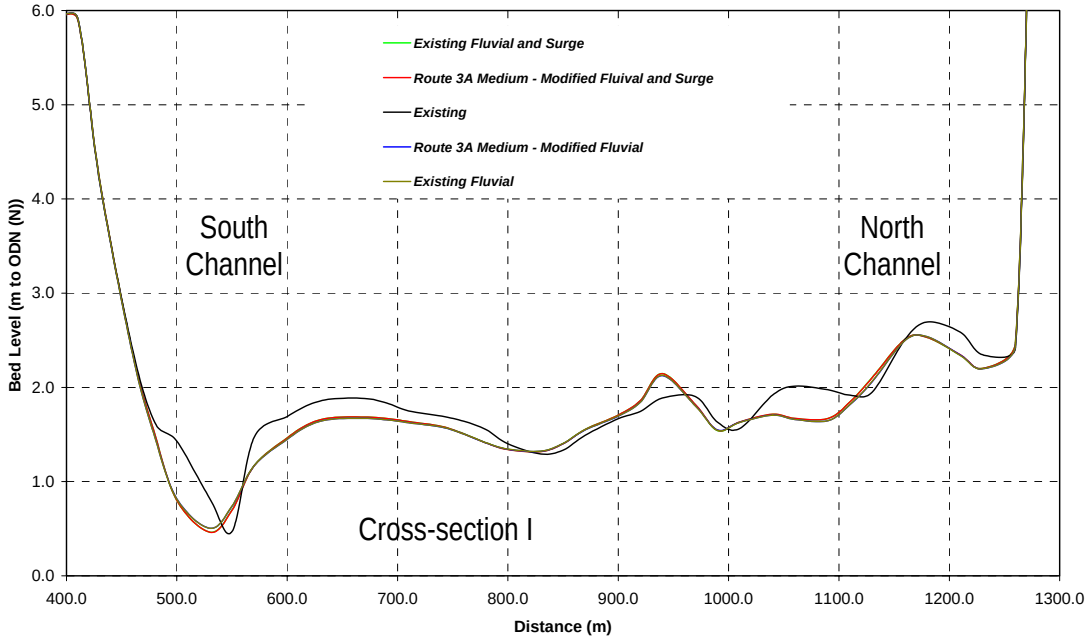


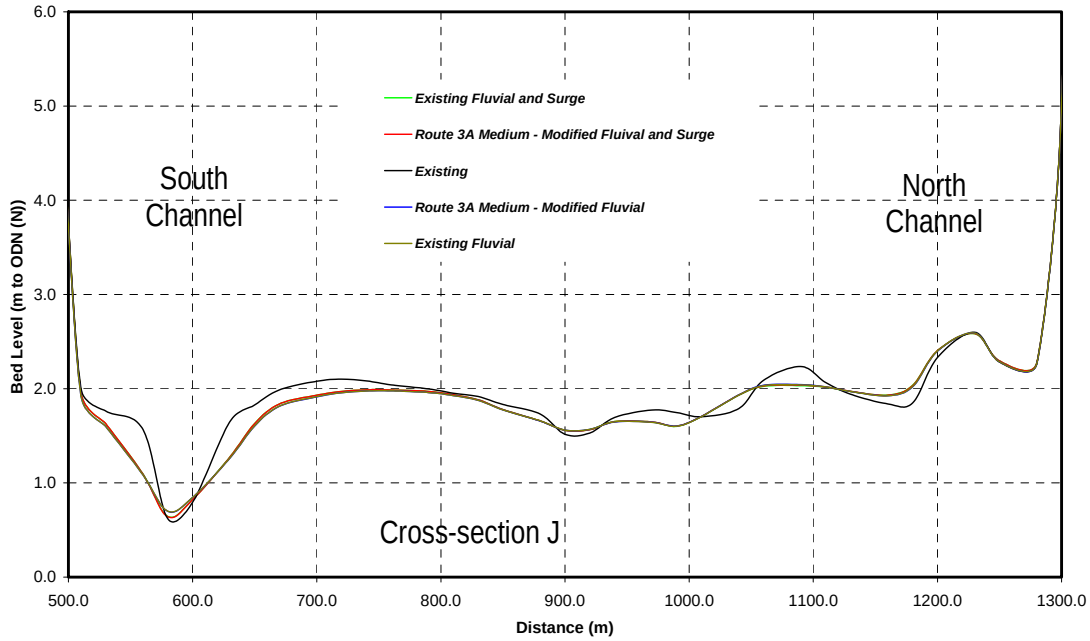
ABP mer marine environmental research	Cross – Sections E and F	Figure D25



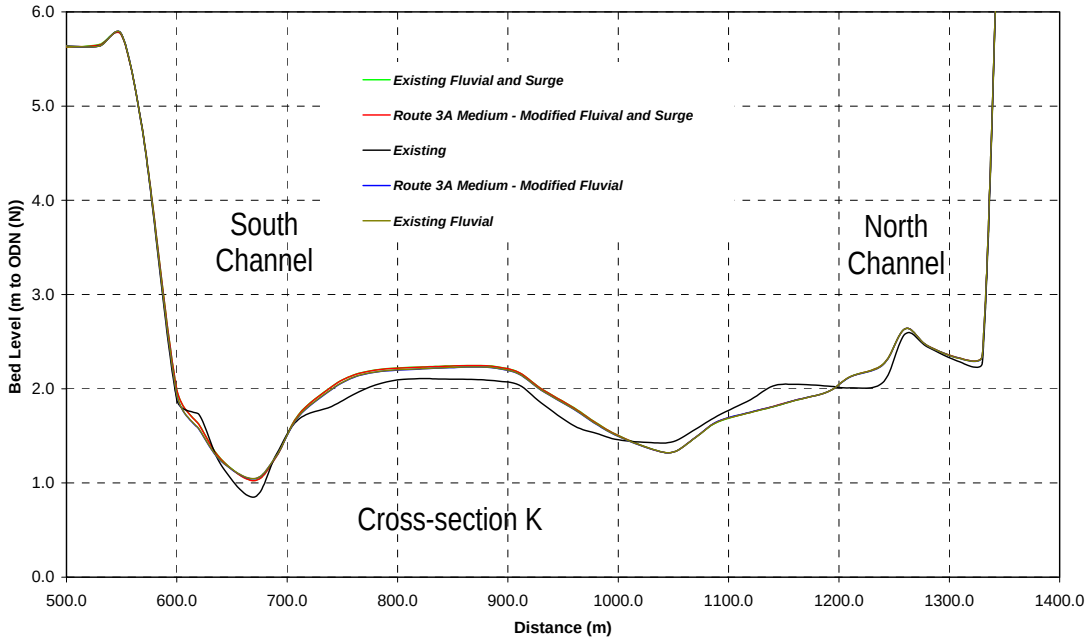


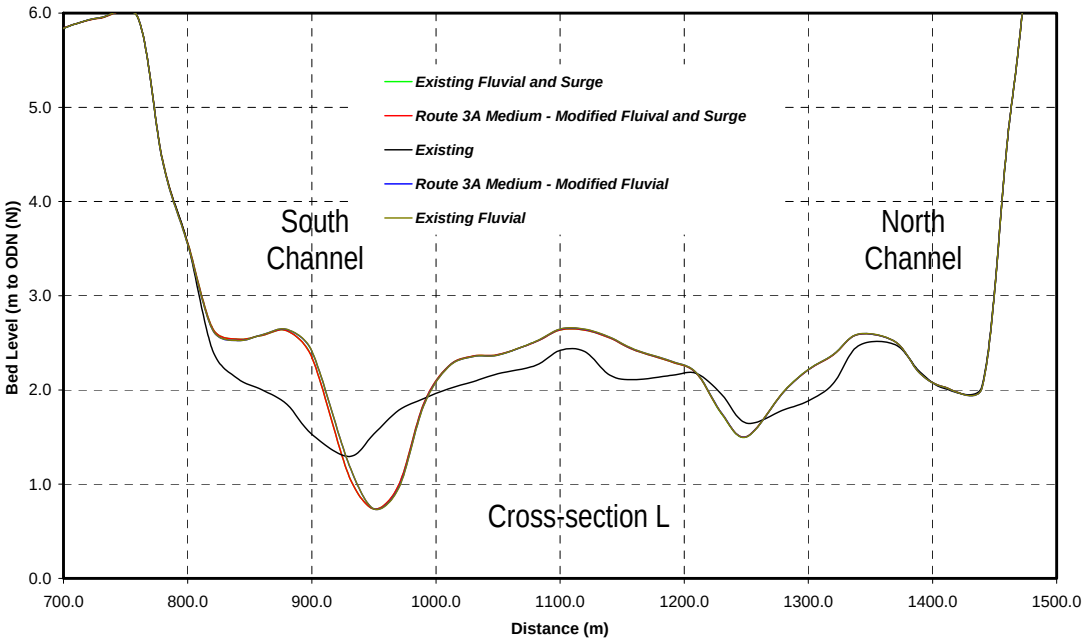
ABP mer marine environmental research	Cross – Sections G and H	Figure D26



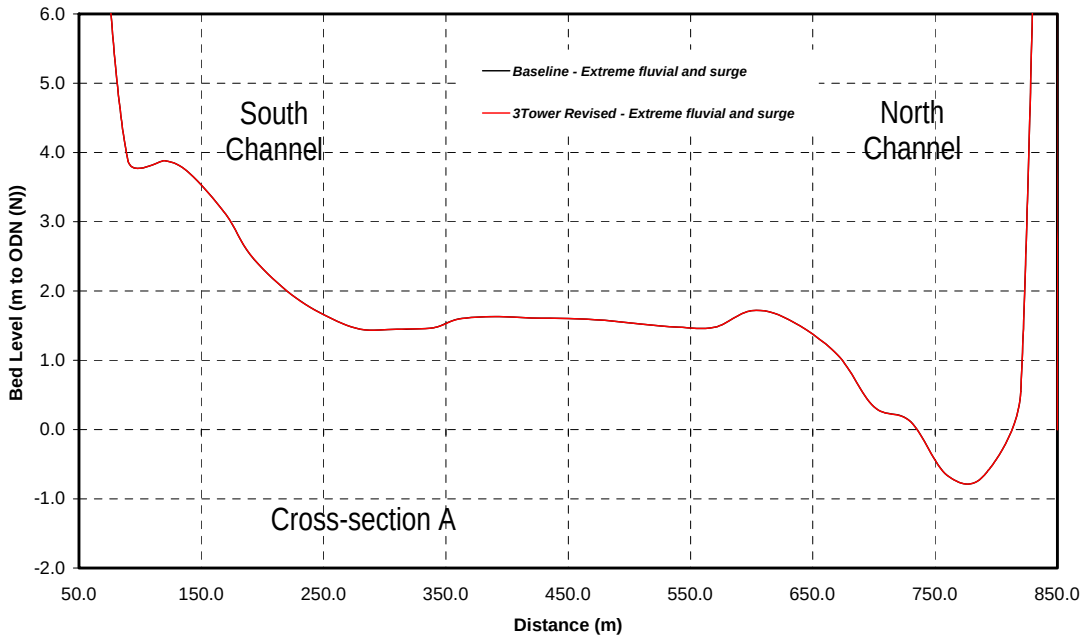


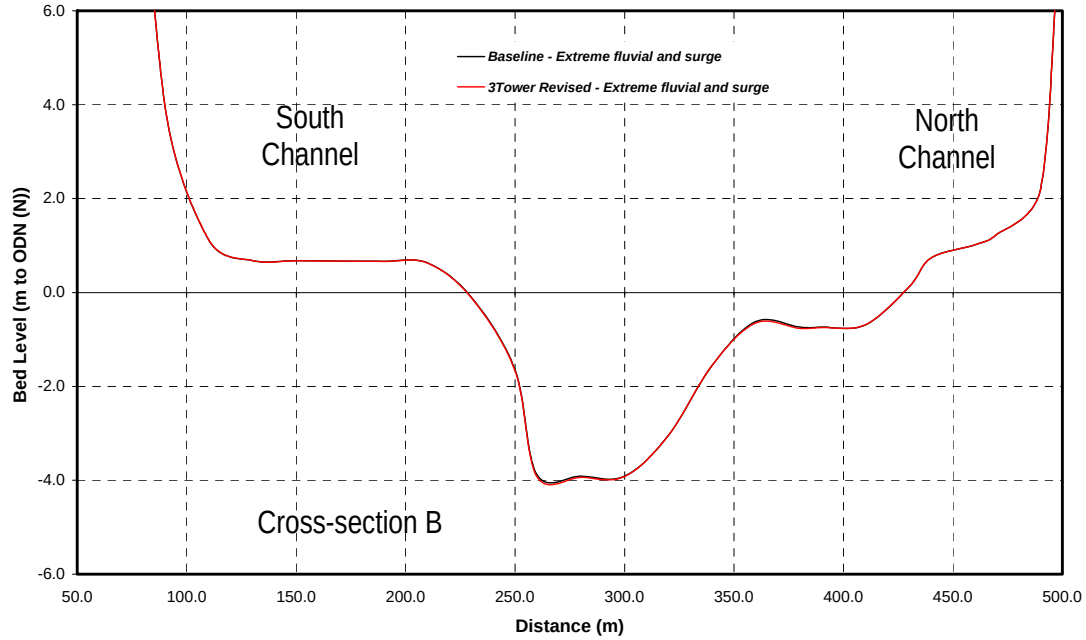
ABP mer marine environmental research	Cross – Sections I and J	Figure D27



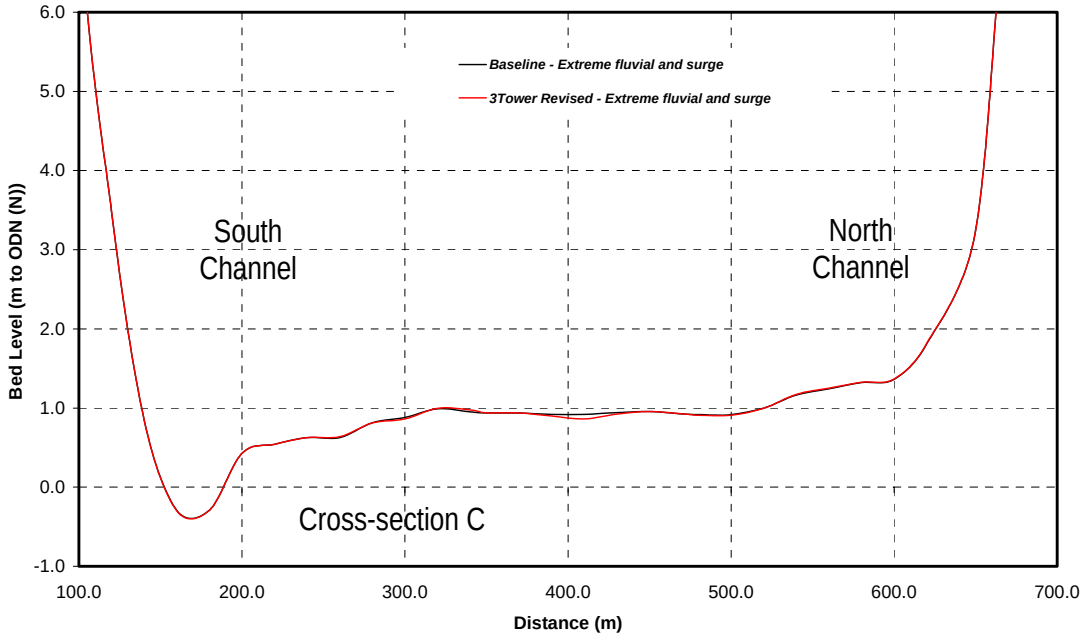


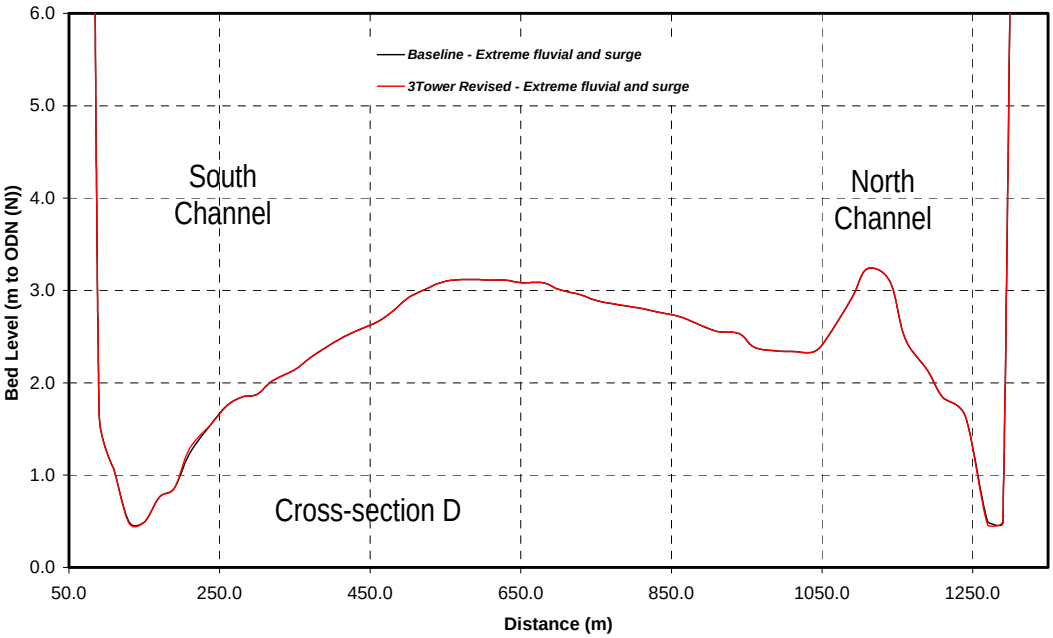
ABP mer marine environmental research	Cross – Sections K and L	Figure D28



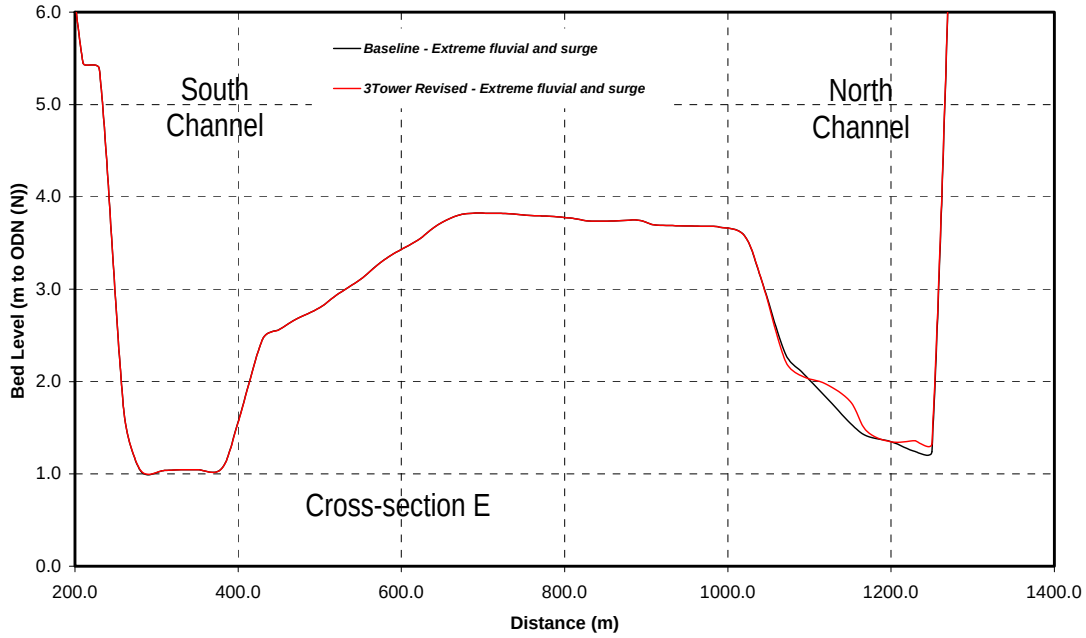


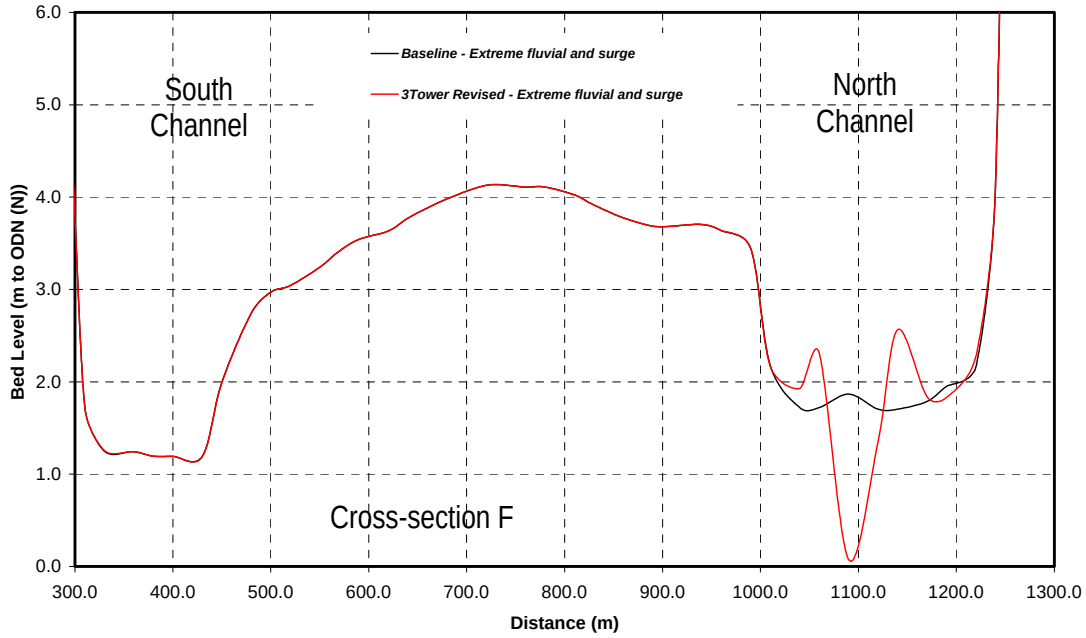
ABP mer marine environmental research	Cross – Sections A and B	Figure D29



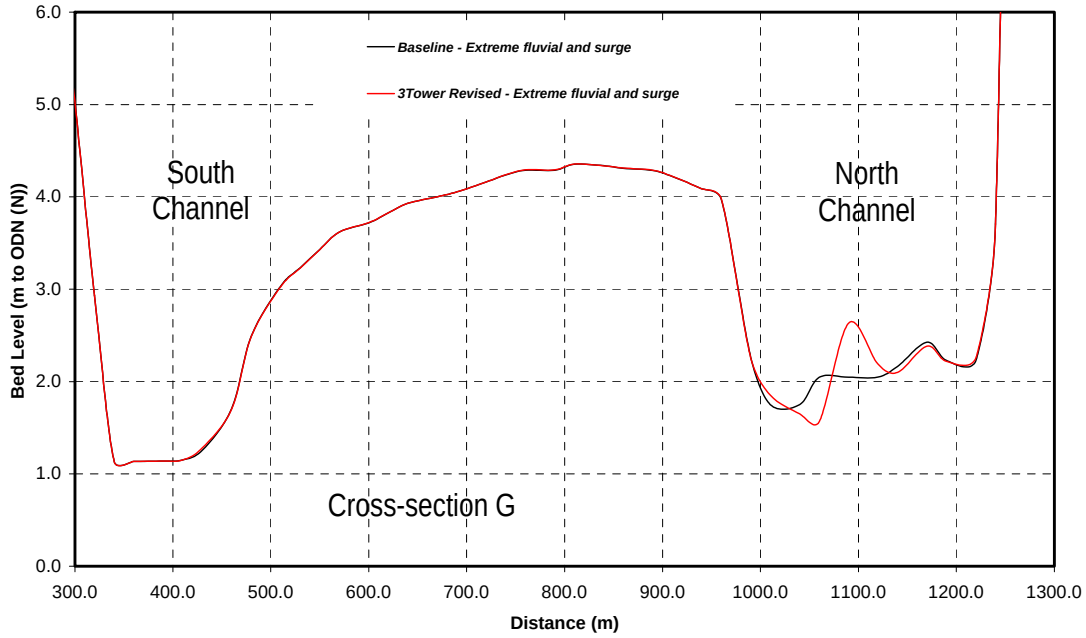


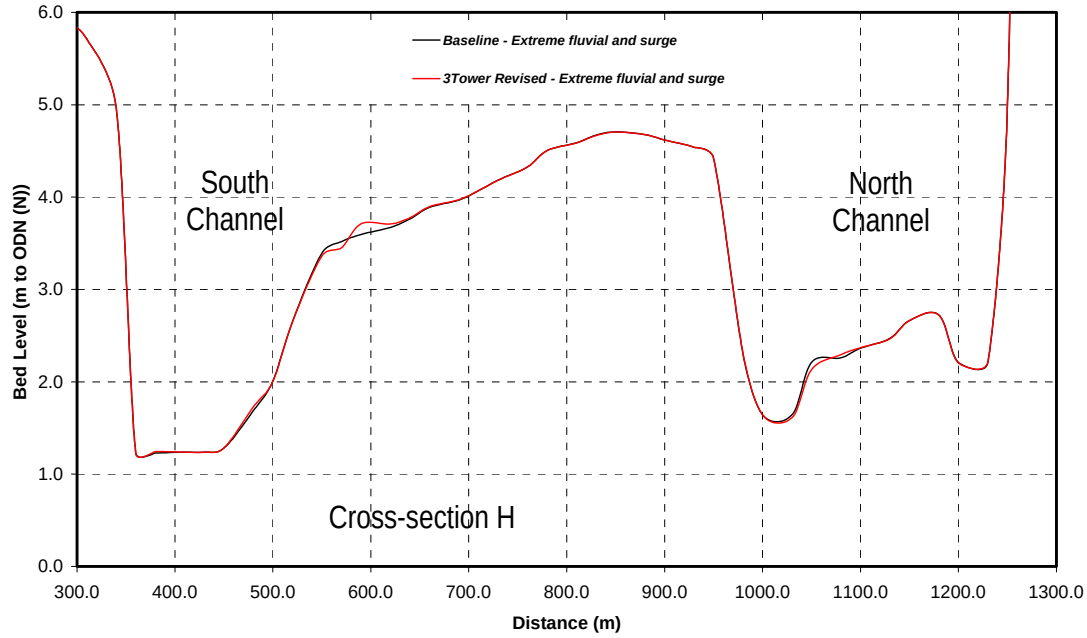
ABP mer marine environmental research	Cross – Sections C and D	Figure D30



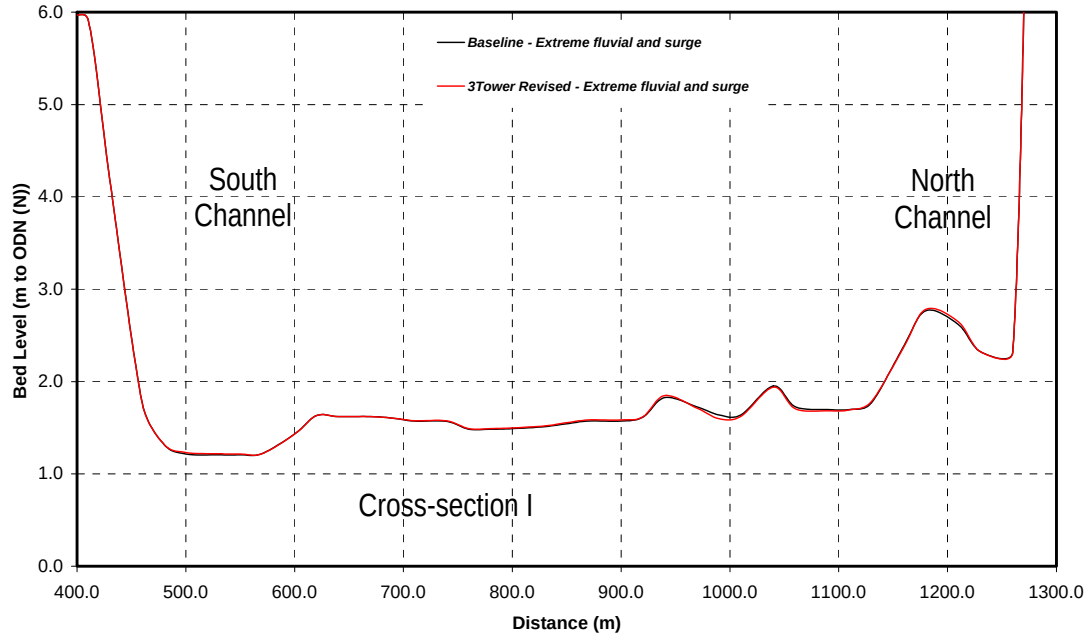


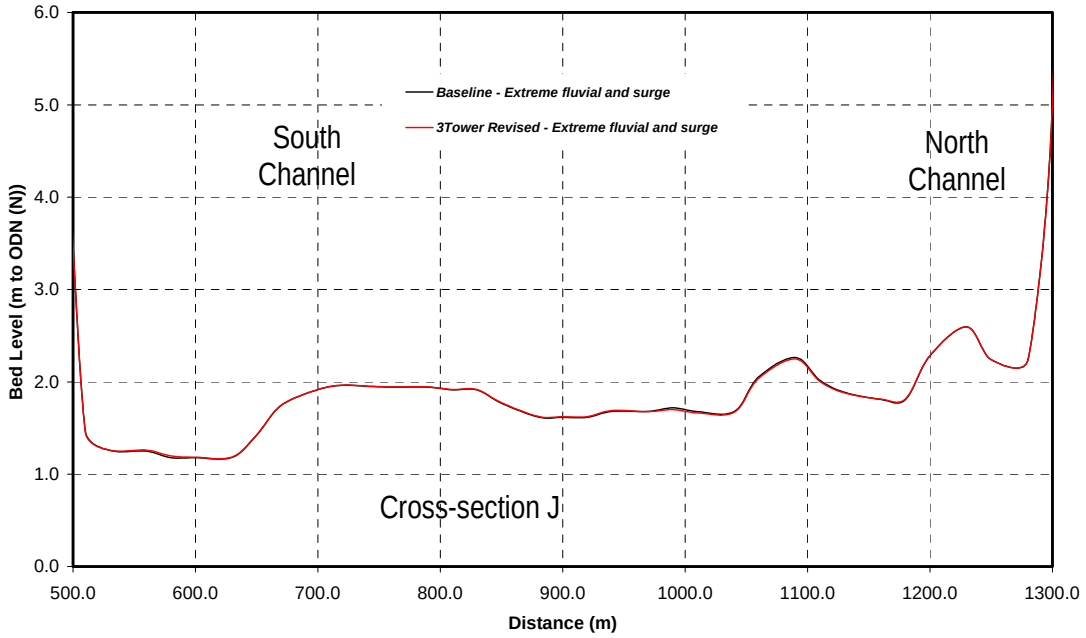
ABP mer marine environmental research	Cross – Sections E and F	Figure D31



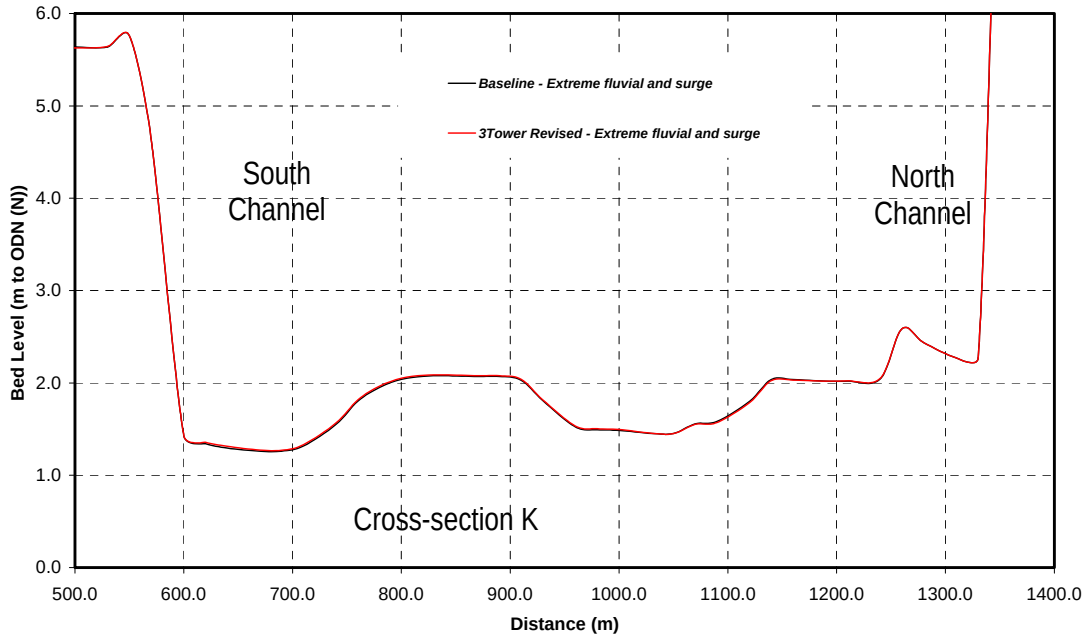


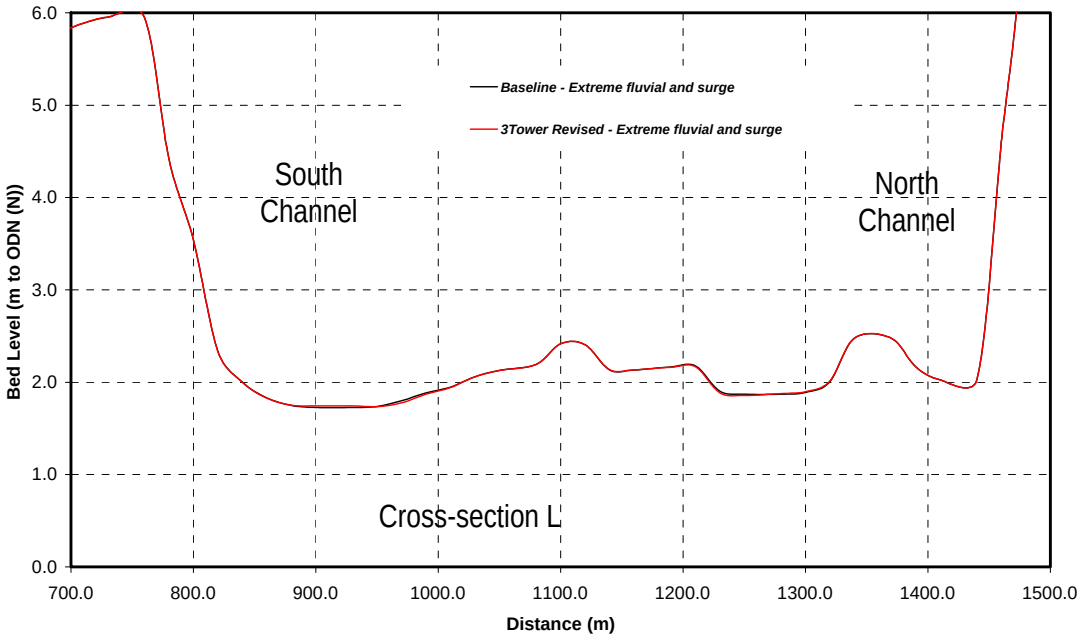
ABP mer marine environmental research	Cross – Sections G and H	Figure D32



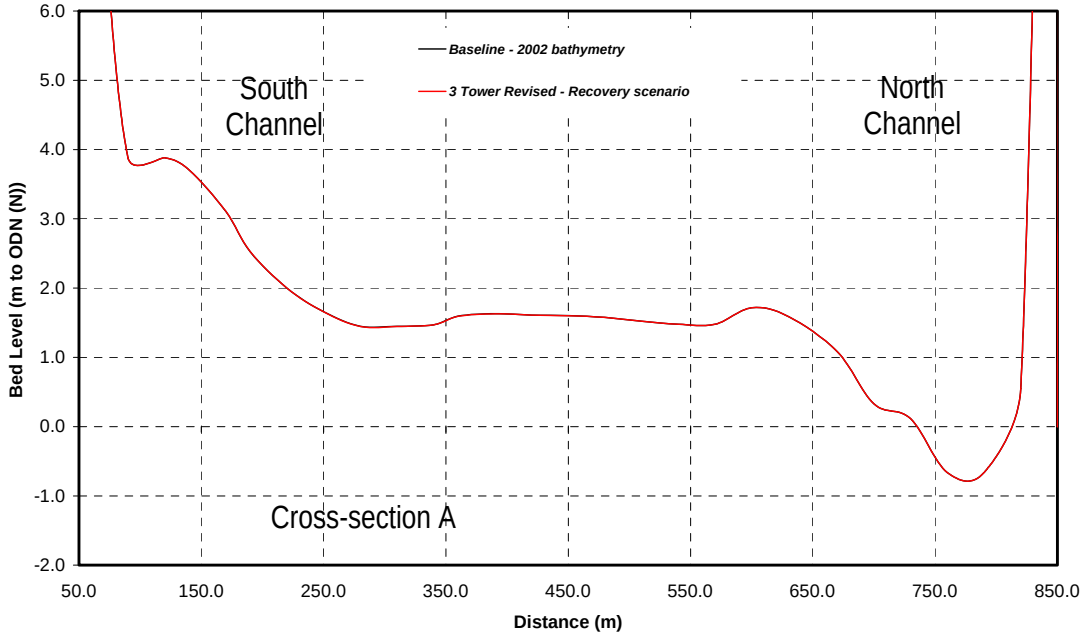


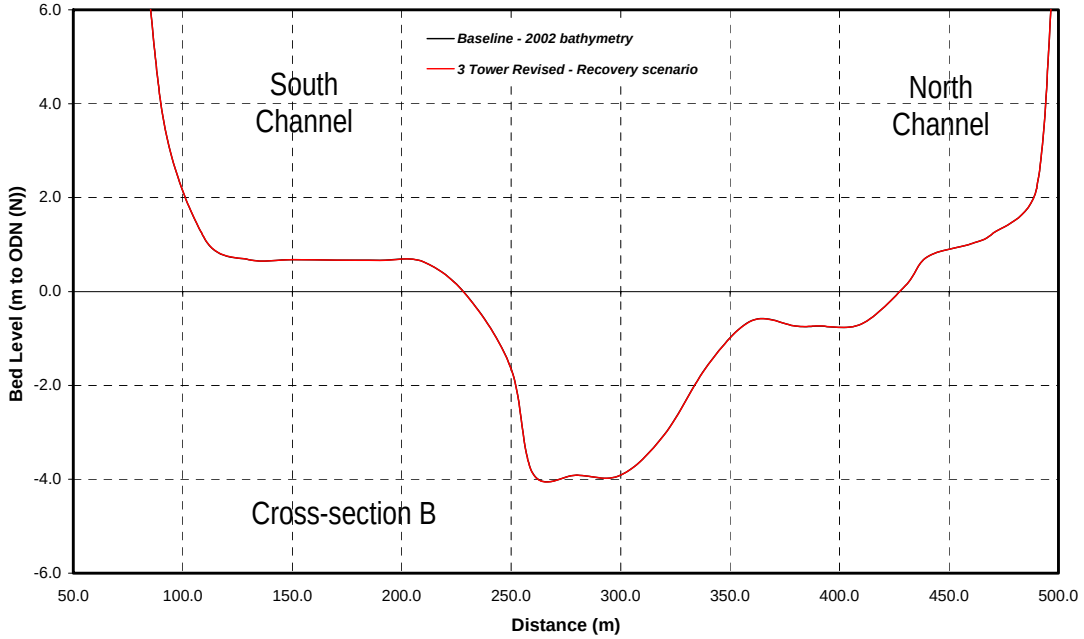
ABP mer marine environmental research	Cross – Sections I and J	Figure D33



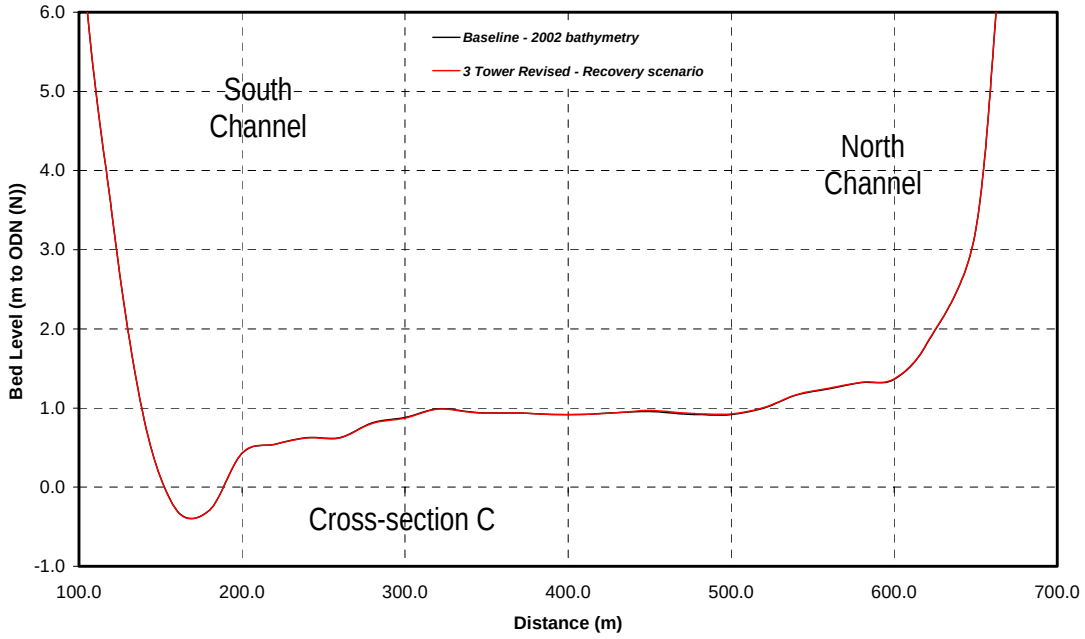


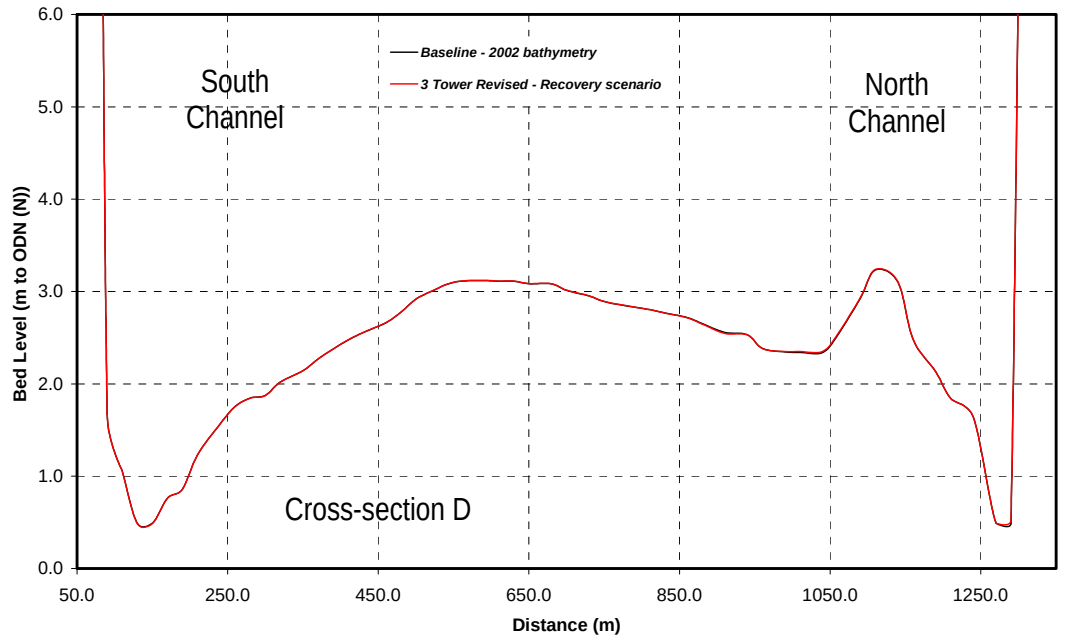
ABP mer marine environmental research	Cross – Sections K and L	Figure D34



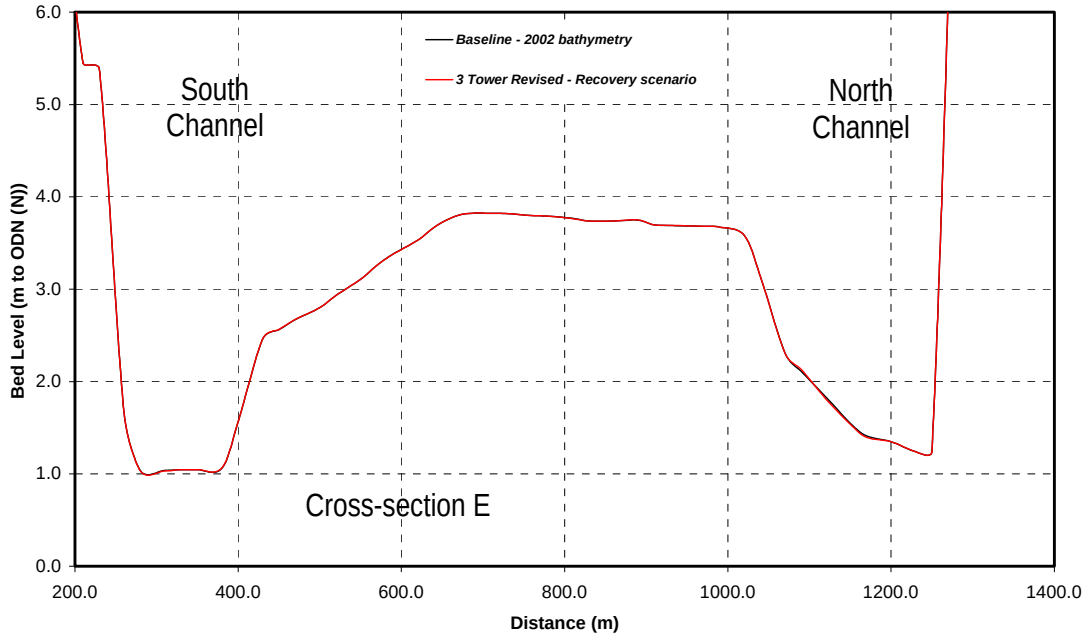


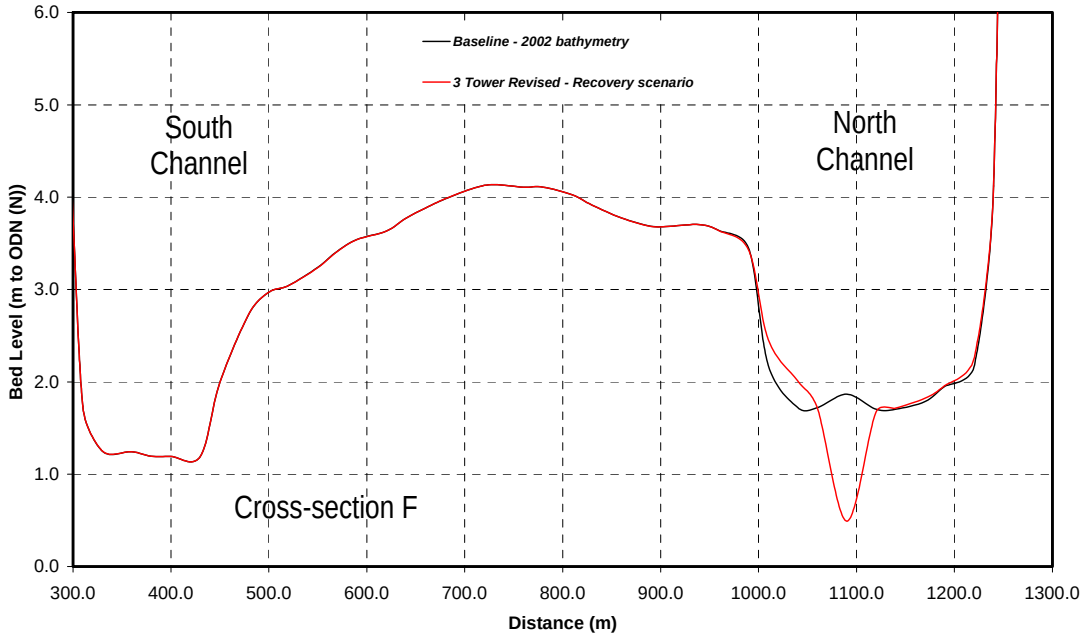
ABP mer marine environmental research	Cross – Sections A and B	Figure D35



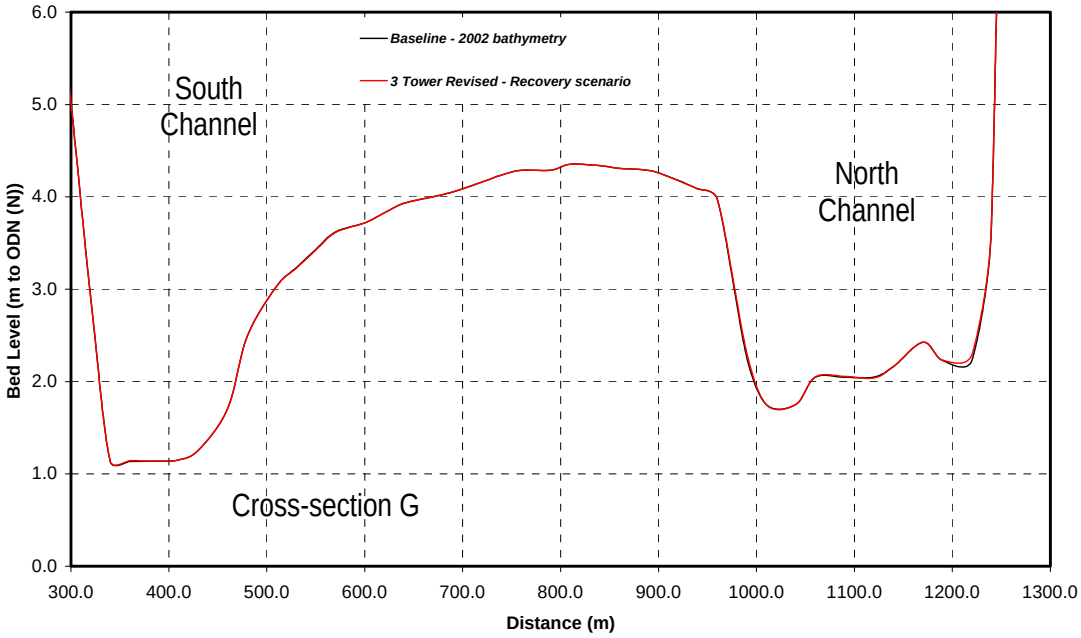


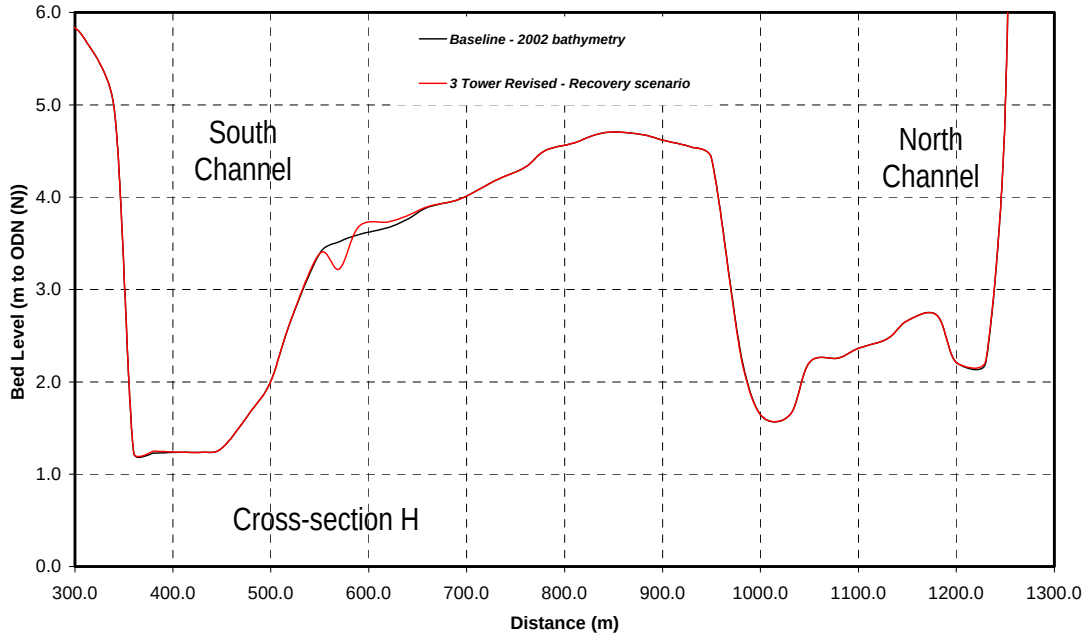
ABP mer marine environmental research	Cross – Sections C and D	Figure D36



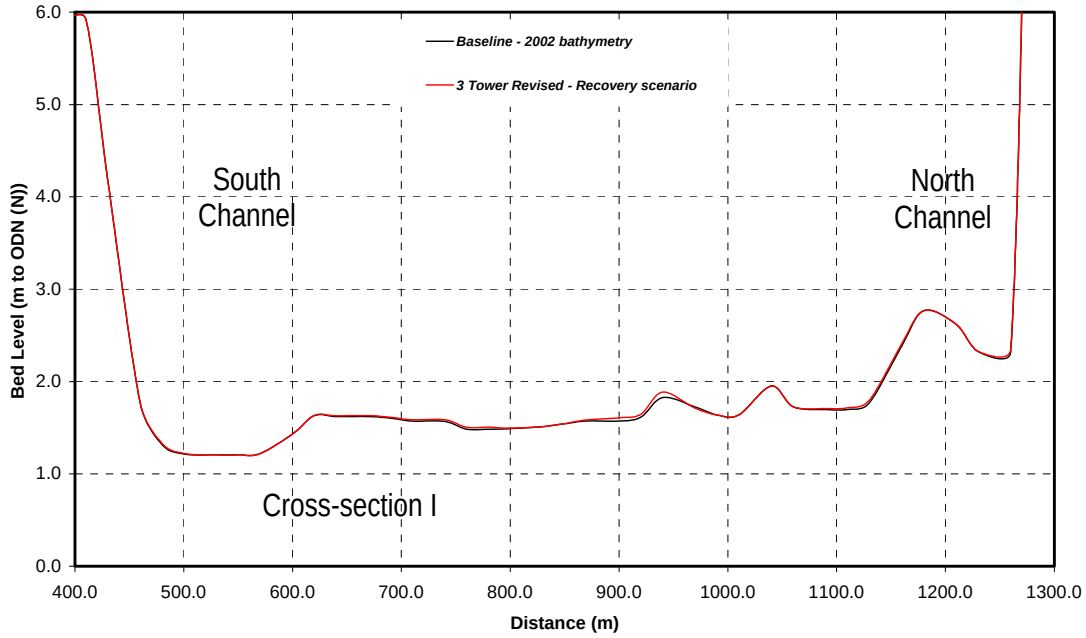


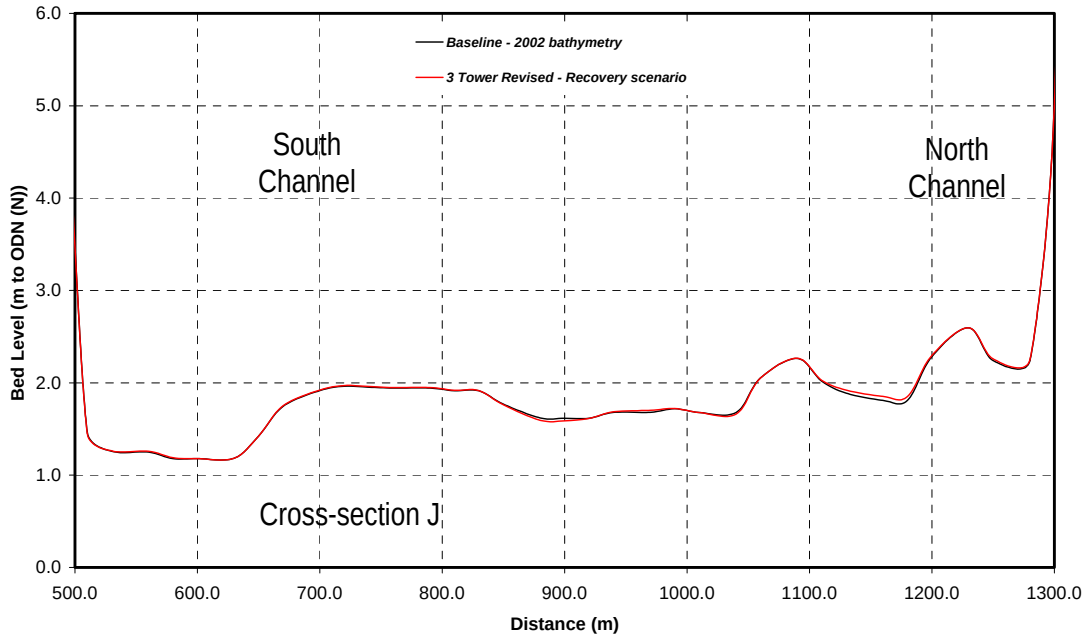
ABP mer marine environmental research	Cross – Sections E and F	Figure D37



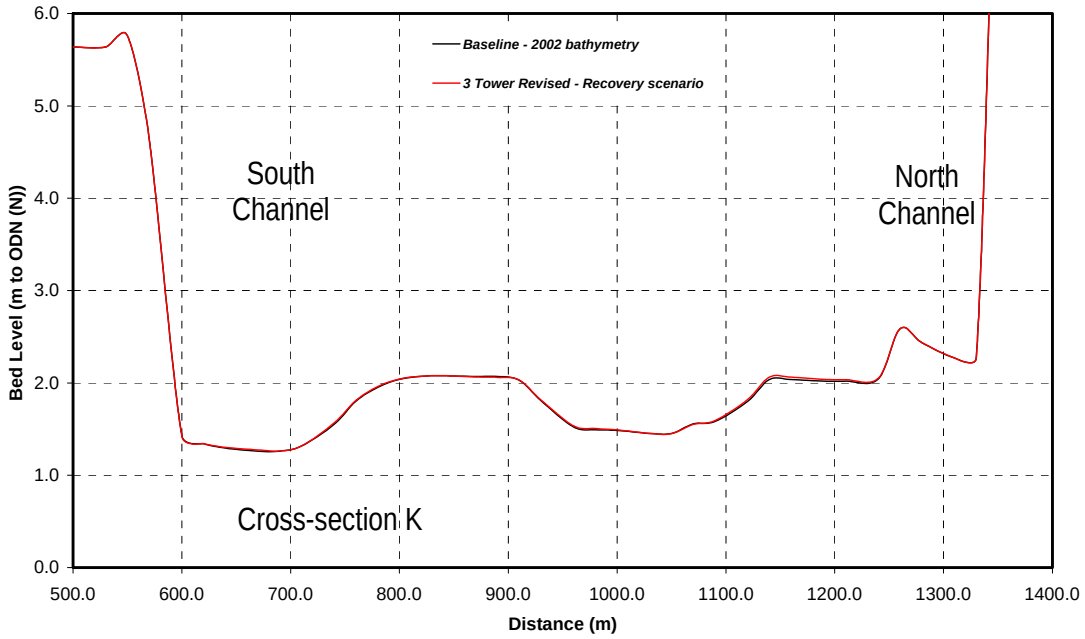


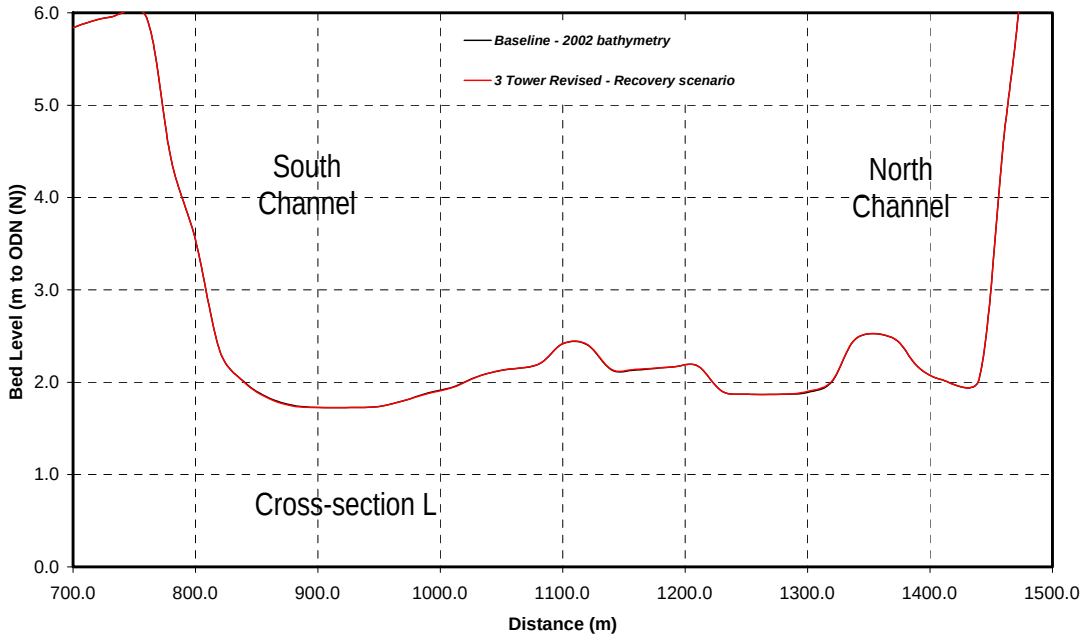
ABP mer marine environmental research	Cross – Sections G and H	Figure D38



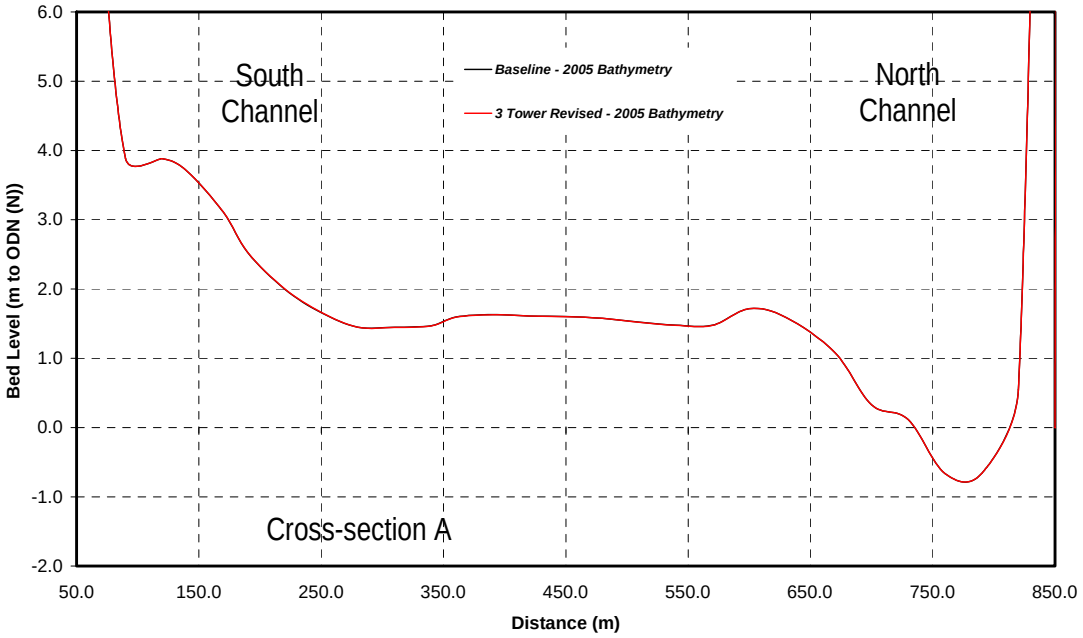


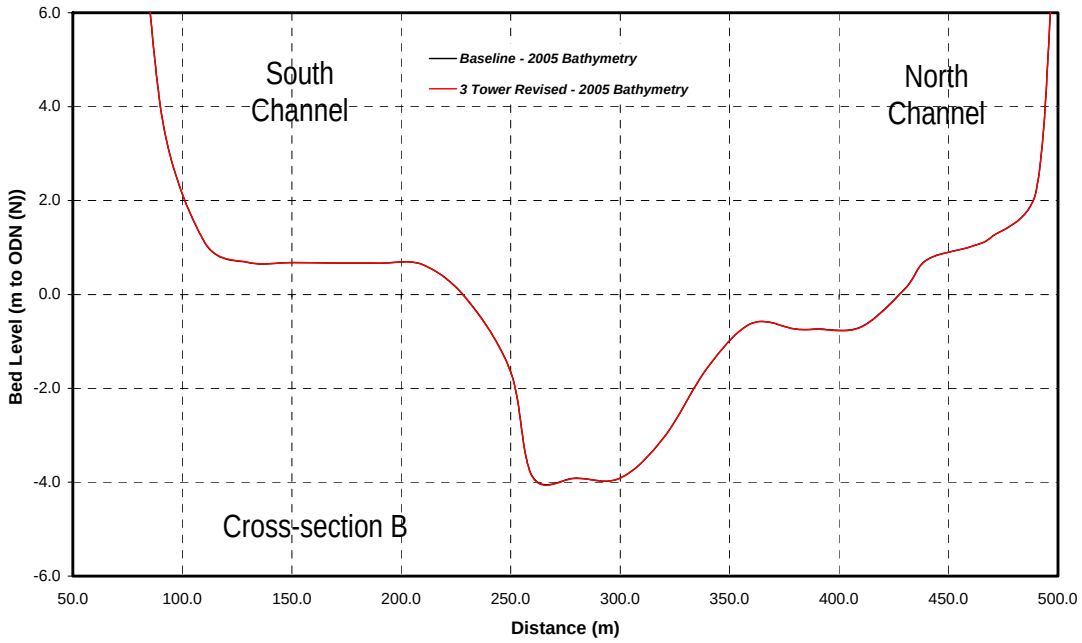
ABP mer marine environmental research	Cross – Sections I and J	Figure D39



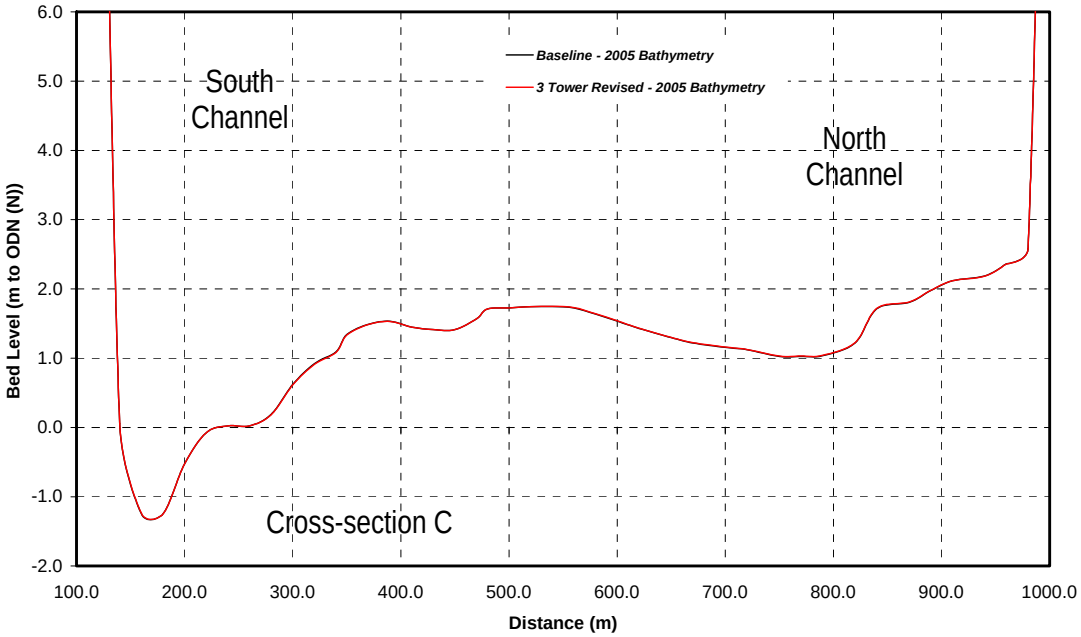


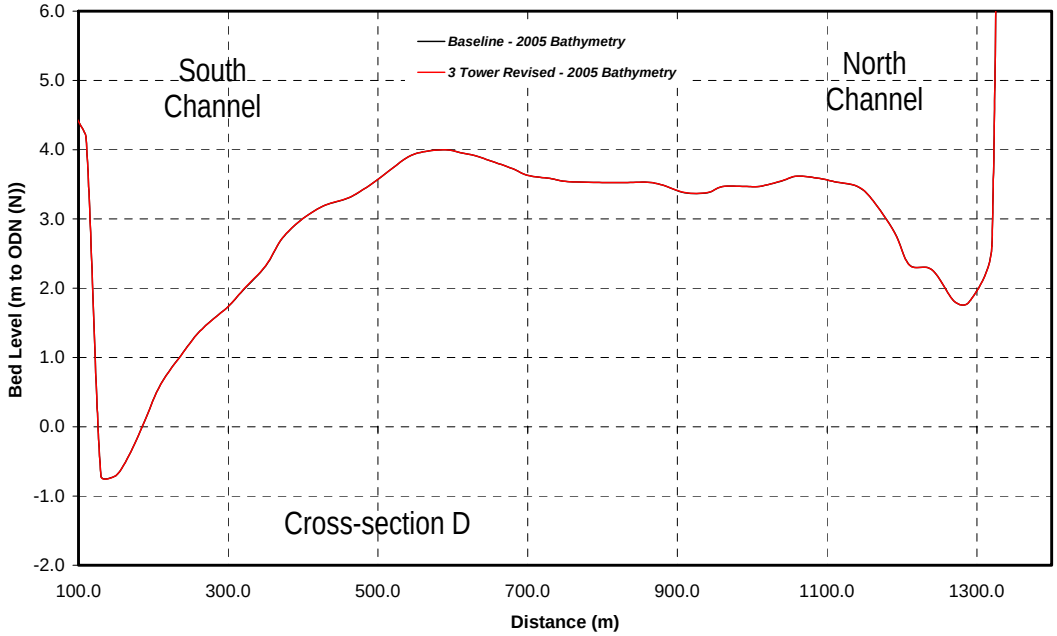
ABP mer marine environmental research	Cross – Sections K and L	Figure D40



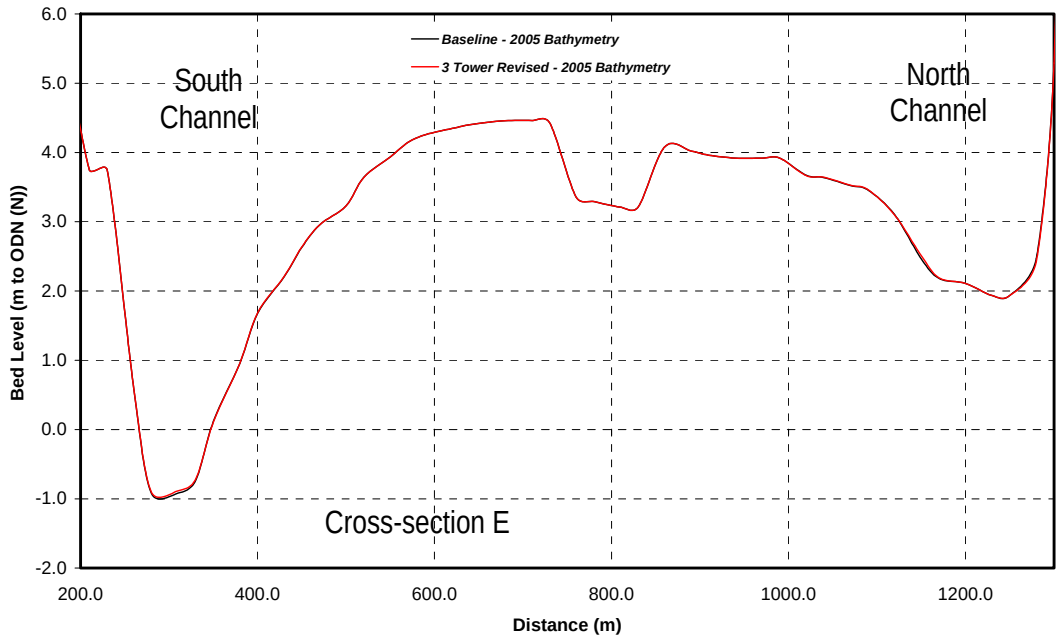


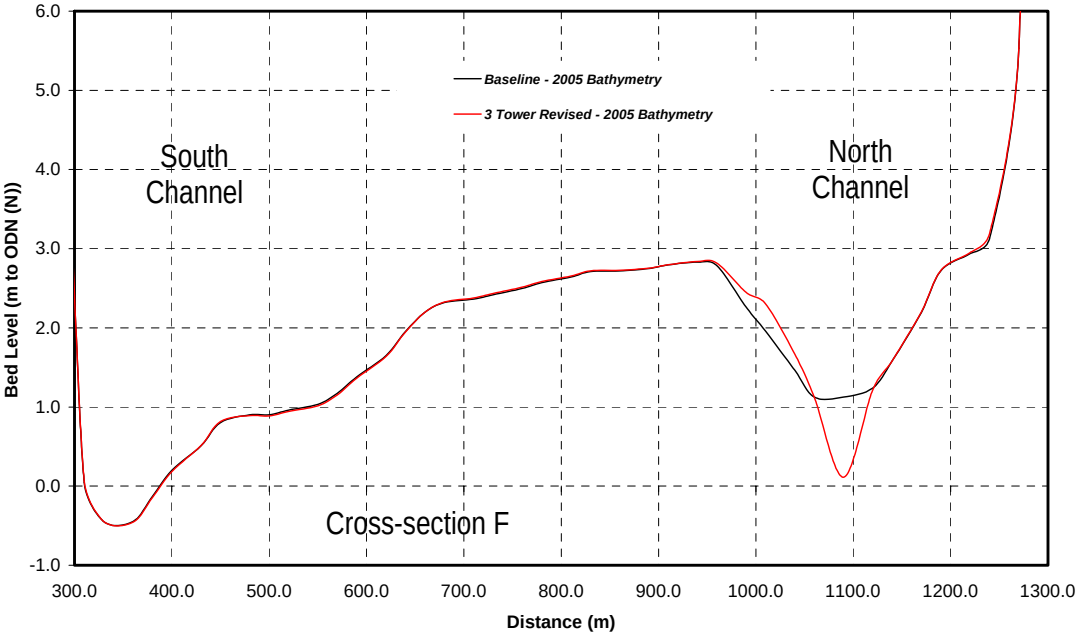
ABP mer marine environmental research	Cross – Sections A and B	Figure D41



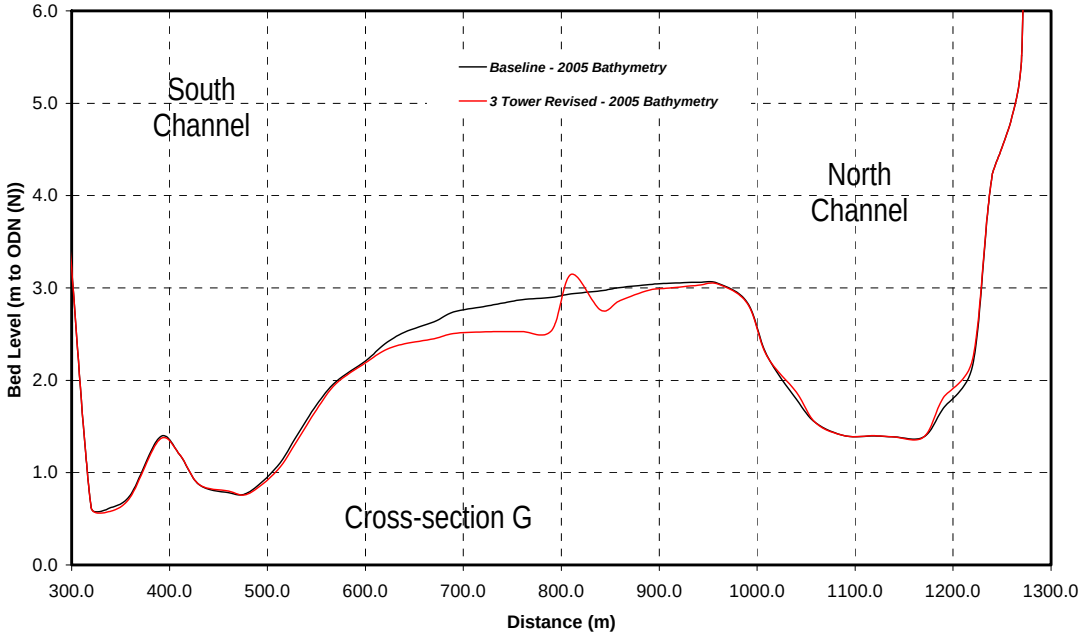


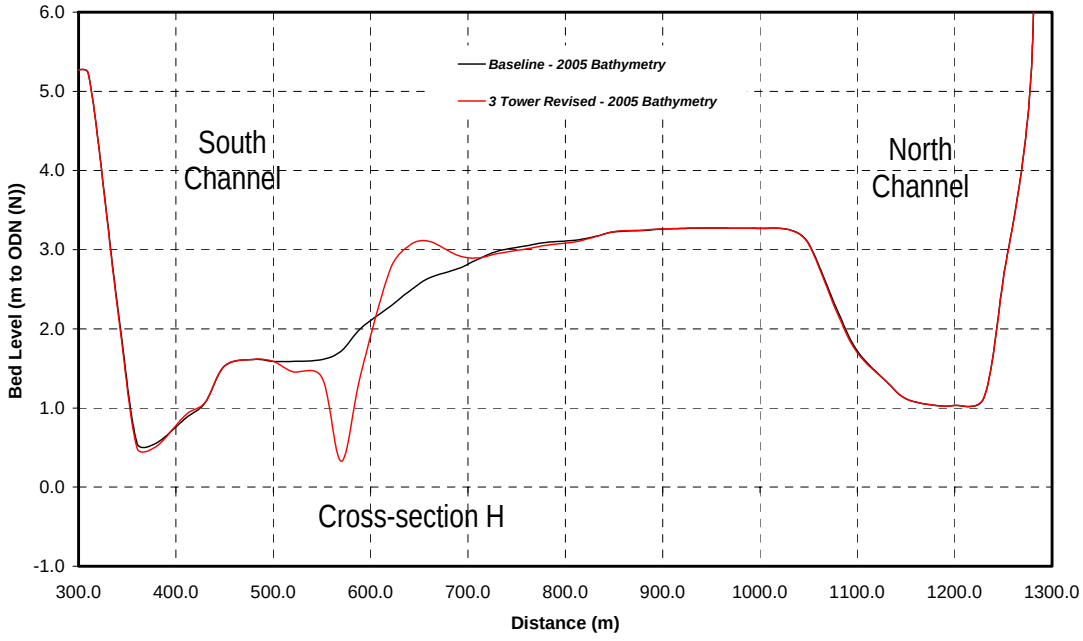
ABP mer marine environmental research	Cross – Sections C and D	Figure D42



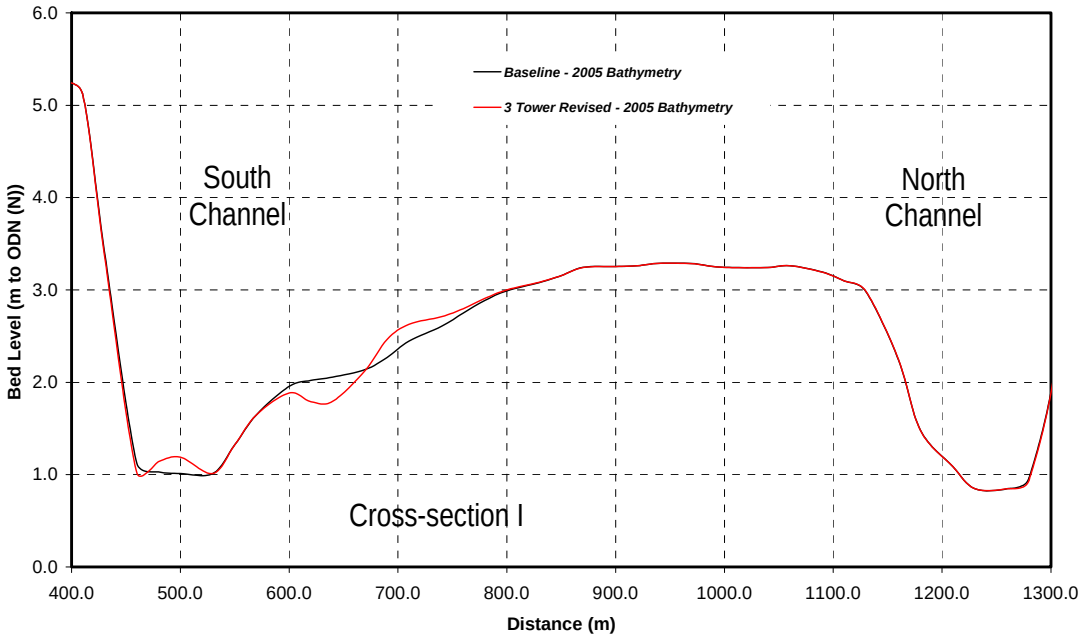


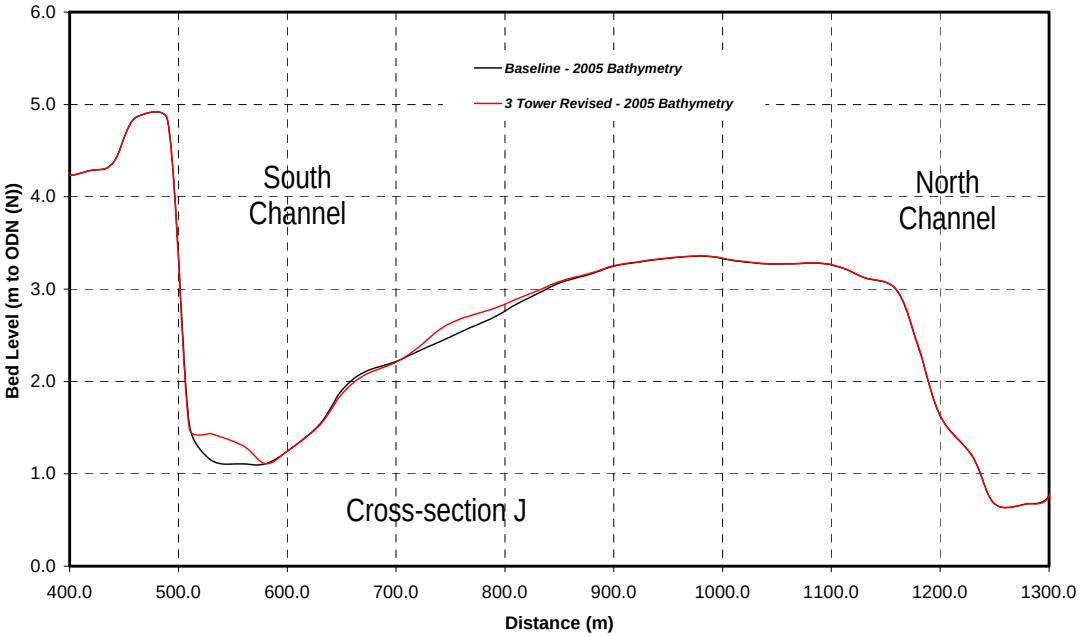
ABP mer marine environmental research	Cross – Sections E and F	Figure D43



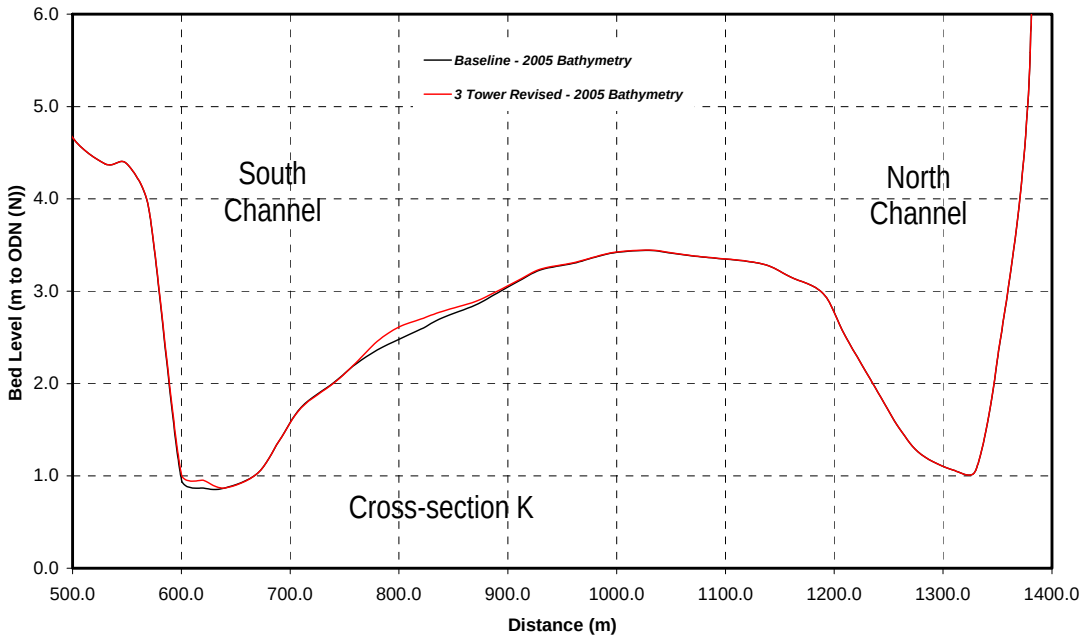


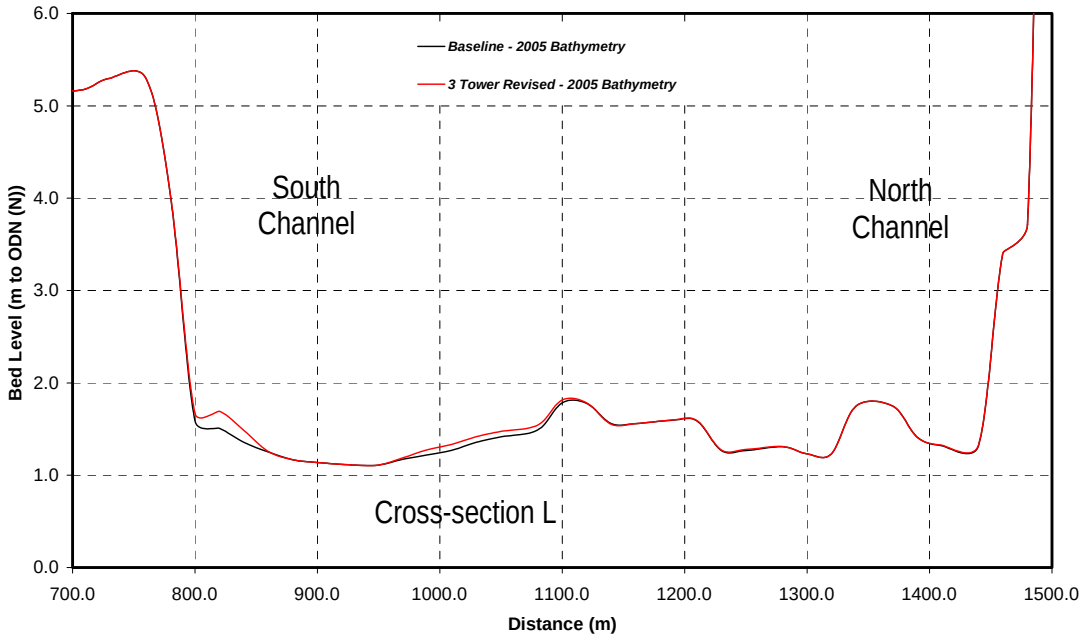
ABP mer marine environmental research	Cross – Sections G and H	Figure D44



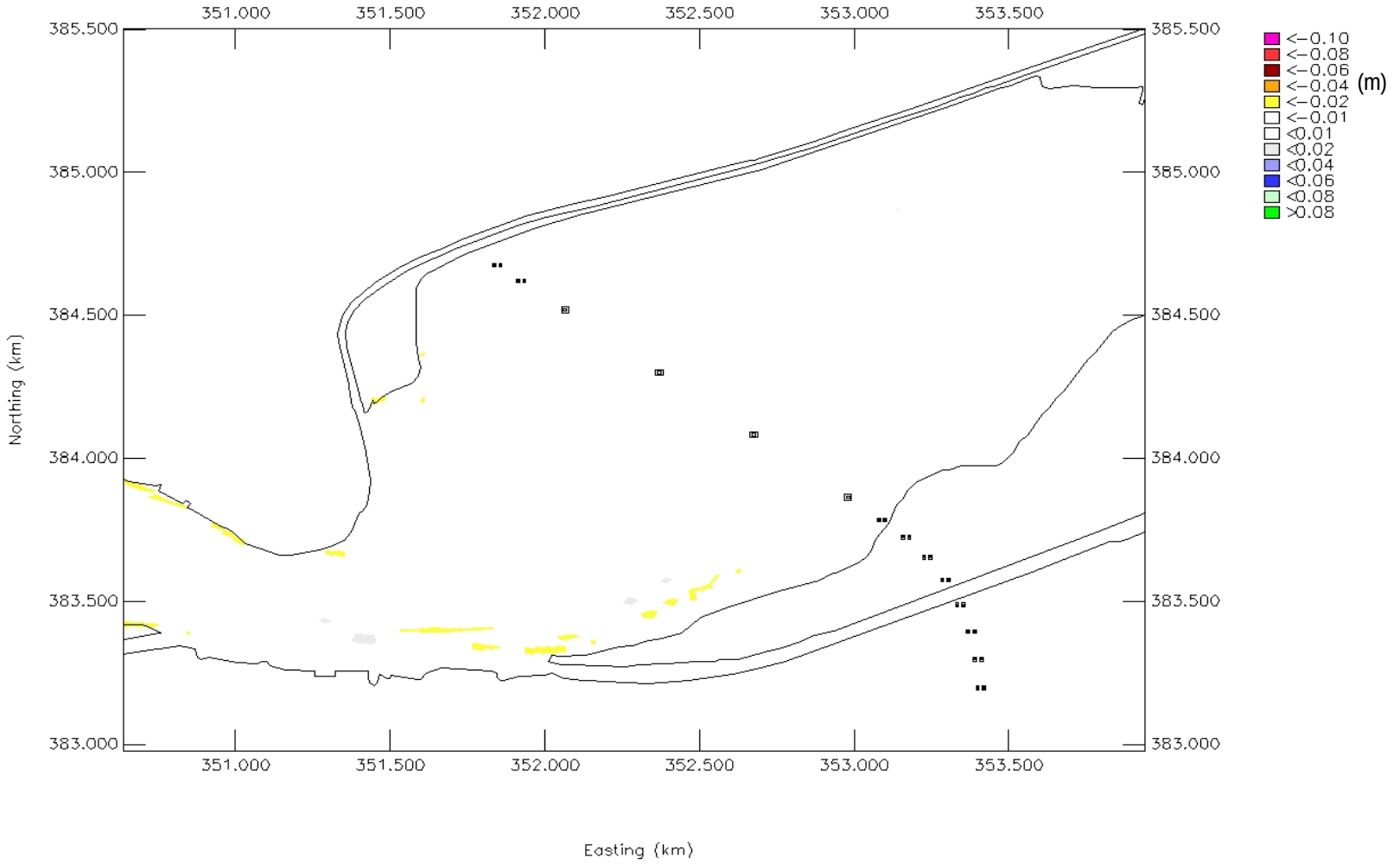


ABP mer marine environmental research	Cross – Sections I and J	Figure D45



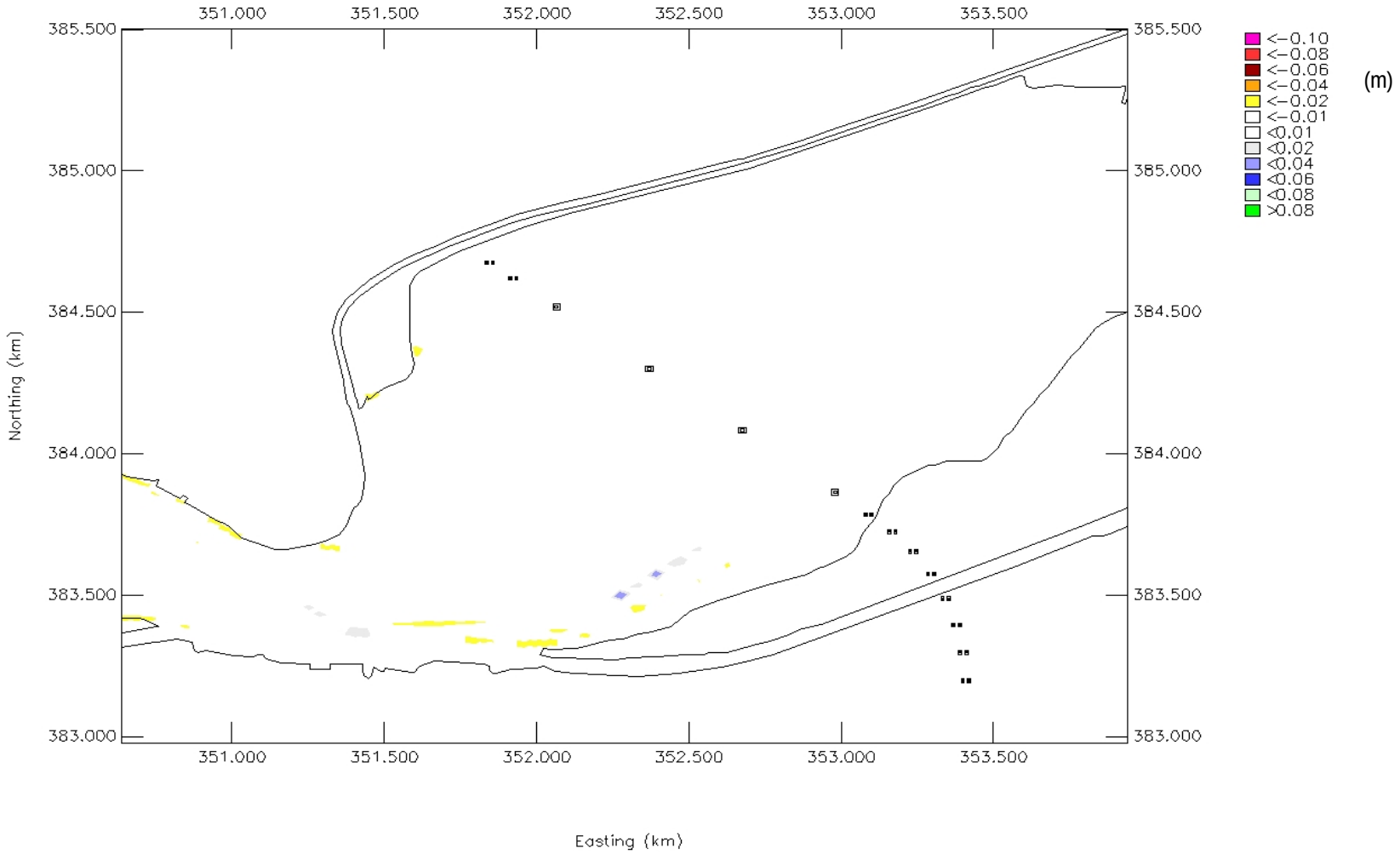


ABP mer marine environmental research	Cross – Sections K and L	Figure D46



Morphological change (m) after 2 years.
Route 3A Medium Span – Modified Alignment Scenario.

Figure D47



Morphological change (m) after 2 years.
Route 3A Medium Span – 3Tower Alignment Scenario.

Figure D48

ABP Marine Environmental Research Ltd
Suite B, Waterside House
Town Quay
Southampton
Hampshire SO14 2AQ

Tel: +44 (0)23 8071 1840
Fax: +44 (0)23 8071 1841
Email: enquiries@abpmer.co.uk

www.abpmer.co.uk